ZooKeys 1217: 1–45 (2024)
DOI: 10.3897/zookeys.1217.126626

Research Article

The era of cybertaxonomy: X-ray microtomography reveals cryptic diversity and concealed cuticular sculpture in *Aphanerostethus* Voss, 1957 (Coleoptera, Curculionidae)

Jake H. Lewis[1,2], Hiroaki Kojima[3], Miyuki Suenaga[4], Dimitrios Petsopoulos[4], Yusuke Fujisawa[5], Xuan Lam Truong[6], Dan L. Warren[4,7]

1 *Environmental Science and Informatics Section, Okinawa Institute of Science and Technology Graduate University, 1919-1 Tancha, Onna-son, Kunigami-gun, Okinawa, 904-0495 Japan*
2 *Department of Natural History, New Brunswick Museum, 277 Douglas Avenue, Saint John, New Brunswick, E2K 1E5, Canada*
3 *Laboratory of Entomology, Tokyo University of Agriculture, 1737 Funako, Atsugi, Kanagawa, 243-0034, Japan*
4 *Biodiversity and Biocomplexity Unit, Okinawa Institute of Science and Technology Graduate University, 1919-1 Tancha, Onna-son, Kunigami-gun, Okinawa, 904-0495, Japan*
5 *Shonan Fujisawa Junior and Senior High School, Keio University, 5466 Endo, Fujisawa, Kanagawa Prefecture, 252-0816 Japan*
6 *Institute of Ecology & Biological Resources, Vietnamese Academy of Science & Technology, 18 Hoang Quoc Viet Road, Cau Giay, Ha Noi, Vietnam*
7 *Gulbali Institute for Applied Ecology, Charles Sturt University, Albury, NSW, 2640, Australia*
Corresponding author: Jake H. Lewis (jake-lewis@oist.jp)

Academic editor:
Miguel Alonso-Zarazaga
Received: 1 May 2024
Accepted: 26 September 2024
Published: 29 October 2024

ZooBank: https://zoobank.org/2B699BE7-7D73-4E62-BB4C-7B6090DC7568

Citation: Lewis JH, Kojima H, Suenaga M, Petsopoulos D, Fujisawa Y, Truong XL, Warren DL (2024) The era of cybertaxonomy: X-ray microtomography reveals cryptic diversity and concealed cuticular sculpture in *Aphanerostethus* Voss, 1957 (Coleoptera, Curculionidae). ZooKeys 1217: 1–45. https://doi.org/10.3897/zookeys.1217.126626

Abstract

Weevils represent one of the most speciose and economically important animal clades, but remain poorly studied across much of the Oriental Region. Here, an integrative revision of the Oriental, flightless genus *Aphanerostethus* Voss, 1957 (Curculionidae: Molytinae) based on X-ray microtomography, multi-gene DNA barcoding (CO1, Cytb, 16S), and traditional morphological techniques (light microscopy, dissections) is presented. Twelve new species, namely, *A. armatus* Lewis & Kojima, **sp. nov.**, *A. bifidus* Kojima & Lewis, **sp. nov.**, *A. darlingi* Lewis, **sp. nov.**, *A. decoratus* Lewis & Kojima, **sp. nov.**, *A. falcatus* Kojima, Lewis & Fujisawa, **sp. nov.**, *A. incurvatus* Kojima & Lewis, **sp. nov.**, *A. japonicus* Lewis & Kojima, **sp. nov.**, *A. magnus* Lewis & Kojima, **sp. nov.**, *A. morimotoi* Kojima & Lewis, **sp. nov.**, *A. nudus* Lewis & Kojima, **sp. nov.**, *A. spinosus* Lewis & Kojima, **sp. nov.**, and *A. taiwanus* Lewis, Fujisawa & Kojima, **sp. nov.** are described from Japan, Taiwan, Vietnam, and Malaysia. A neotype is designated for *A. vannideki* Voss, 1957. The hitherto monotypic genus *Darumazo* Morimoto & Miyakawa, 1985, **syn. nov.** is synonymized under *Aphanerostethus* based on new morphological data and *Aphanerostethus distinctus* (Morimoto & Miyakawa, 1985), **comb. nov.** is transferred accordingly. X-ray microtomography is successfully used to explore for stable interspecific differences in cuticular, internal and micro morphology. Remarkable species-specific sexual dimorphism in the metatibial uncus is described in seven of the newly described *Aphanerostethus* species and the evolution of this character is discussed.

Key words: Biodiversity, DNA barcoding, integrative taxonomy, µCT, micro-ct, sexual selection, species discovery, weevil

Introduction

Weevils (Coleoptera: Curculionoidea) represent one of the most diverse animal groups (ca 62,000 species) and include many economically important pest species (Oberprieler et al. 2014). The great diversity of weevils has been attributed to their co-evolution with Angiosperms (McKenna et al. 2009; Winter et al. 2017), and they have not only evolved to feed on living plants, but also dead plants, fungi, and even mammal dung (Jordal and Cognato 2012; Oberprieler et al. 2014; Escalona et al. 2023). Although many generalists with wide host-plant ranges exist, highly specialized species only feed on one plant species or genus (Anderson 1993; Young et al. 2008). Specialist weevil species are at risk when their host plant is threatened as they lack the ability to switch to other food sources. This has led to presumed extinctions in weevils, such as the Greater Chestnut Weevil *Curculio caryatrypes* (Boheman, 1843) which fed only on American Chestnut (*Castanea dentata* (Marsh.) Borkh.) before the introduced fungal pathogen *Cryphonectria parasitica* (Murrill) M.E.Barr decimated chestnut populations across the United States (Charles and McKenna 2023). Weevil conservation relies most heavily on a solid understanding of host plant preferences, which often differ significantly between species even belonging to the same genus (e.g., Wibmer 1981; Yoshihara 2016; Lewis and Anderson 2022). For this reason, accurate species delineation of weevils (and their host plants) is essential to the discovery of interspecific differences in host plant, and is one of the most fundamental components of conservation biology.

As a tropical mountainous archipelago, Southeast Asia is remarkable for its weevil diversity and high rates of endemism (Setliff 2007; Tanzler et al. 2014; Sprick and Floren 2018). The complex geologic history of southeast Asia has positively influenced weevil speciation rates (Tänzler et al. 2016; Tseng et al. 2017; Letsch et al. 2023), and the loss of flight (common in weevils) undoubtedly contributed further to this radiation (Ikeda et al. 2012; Tänzler et al. 2014). Furthermore, some evidence exists suggesting that tropical *Curculio* are more specialized in host-plant usage than species in temperate zones (Peguero et al. 2017), and this has been suggested as another explanation of the great diversity of phytophagous insects in tropical zones (Forister et al. 2014). Unfortunately for conservation and taxonomy, southeast Asia is also experiencing extreme deforestation (Estoque et al. 2019), and satellite data suggests that one of its most biodiverse regions, Borneo and Sumatra, experienced especially high rates of forest loss from 2000 to 2010 (Achard et al. 2014). Weevil species richness (and beetle species richness in general) is negatively correlated with logging activity and anthropogenic disturbance (Su et al. 2011; Hagge et al. 2019; Sharp et al. 2019), which is certainly at least partially attributable to decreases in plant diversity. Natural history collections and especially those with a focus on tropical fauna have never been more valuable as windows into the past. Important to the preservation of natural history collections is the development and use of non-destructive techniques such as X-ray microtomography and BOMB DNA extraction (Oberacker et al. 2019), which allow for analyses of specimens without sacrificing precious type, historical, or rare material. Such non-destructive methods will be increasingly valuable going forward, as specimen acquisition is impeded by species loss due to habitat destruction and a greater prevalence of opaque biodiversity protection laws.

The oriental, flightless weevil genus *Aphanerostethus* Voss, 1957 was described based on a single species, *A. vannideki*, from West Java, Indonesia, and has been distinguished from similar apterous genera by their daruma doll (hence the name *Darumazo* Morimoto & Miyakawa, 1985, syn. nov.) to bulb-like shape, the six-articled funicle, a canaliculate prosternum, erect scales between eyes ("eye-lashed" appearance), and large eyes (Voss 1957; Morimoto and Miyakawa 1985; Morimoto 2011). The genus is ecologically poorly studied; however, one species, *A. distinctus* (Morimoto & Miyakawa, 1985), has been reared from the galls of *Asteralobia sasakii* (Monzen, 1937) (Diptera: Cecidomyiidae) on *Ilex crenata* Thunb. var. *hachijoensis* Nakai (Aquifoliaceae), and *Ilex integra* Thunb. (Fujii et al. 2012; Kojima 2013), suggesting that (at least) *A. distinctus* may have a highly specialized cecidophagous lifestyle. Although cecidophagy has been reported in a number of lineages (e.g., Yamazaki and Sugiura 2001; Wilson 2012; Prena 2021), it is relatively uncommon in weevils. Here, *Aphanerostethus* Voss, 1957 (= *Darumazo* Morimoto & Miyakawa, 1985, syn. nov.) (Coleoptera: Curculionidae: Molytinae) is revised using a combination of X-ray microtomography, multi-gene DNA barcoding (CO1, Cytb, 16S), and traditional morphological techniques (light microscopy, dissections). Twelve new species of *Aphanerostethus* are described based on specimens collected in Japan, Taiwan, Vietnam, and Malaysia, and seven of these exhibit stunning sexual dimorphism and species-specific variation in the metatibial unci. X-ray microtomography (hereafter X-ray μCT) has become a widely used tool in entomology and has broad applications including enhancing analysis of insects enclosed in amber (Kundrata et al. 2020; Kypke and Solodovnikov 2020), examination of internal morphology (Alba-Alejandre et al. 2019; Aibekova et al. 2022), and for taxonomic character discovery (Garcia et al. 2017; Lewis 2023). The great advantage of X-ray μCT is that it allows for a complete three-dimensional viewing of minute internal and external structures, including those obscured by musculature, dirt and debris, or scales, and that 3D models can be uploaded to online databases for viewing by anyone with access to a computer. X-ray μCT is ideal when working with primary type material, precious fossils, or rare species, as it does not require dissection or intrusive manipulation. As is common in many weevil groups, most *Aphanerostethus* species are covered in a dense mat of appressed scales which obscure the underlying cuticle. By removing scales during the segmentation process, Lewis (2023) found apparent interspecific differences in cuticular sculpturing in the weevil genus *Karekizo* Morimoto, 1962, but was severely limited in sample size (one specimen of each species). As such, it was impossible to ascertain whether these hidden cuticular characters were intraspecifically stable and thereby useful for taxonomy and phylogenetics. We use the same method of Lewis (2023) to search for interspecific differences in pronotal and elytral surface structure as well as internal morphology (hindwing reduction), and investigate the stability of these characters by expanding the sample size to five specimens per species to account for any intraspecific variation. We also use X-ray μCT to examine and visualize the minute metatibial unci of *Aphanerostethus*, which are less than 50 μm in length and frequently obscured by scales and hairs.

Materials and methods

Specimen acquisition and general methodology

Specimens were examined from the following collections:

CMNC	Canadian Museum of Nature, Gatineau, Canada
ELKU	Entomology Lab of Kyushu University, Fukuoka, Japan
FFPRI	Forestry and Forest Products Research Institute, Tsukuba, Japan
HUM	Hokkaido University Museum, Sapporo, Japan
KUM	Kyushu University Museum, Fukuoka, Japan
NMNST	National Museum of Natural Science, Taichung, Taiwan
OIST	Okinawa Institute of Science and Technology, Tancha, Japan
PCHY	Private Collection of H. Yoshitake, Tsukuba, Japan
RMNH	Naturalis Biodiversity Centre, Leiden, Netherlands
RUMC	Ryukyu University Museum Collection, Nishihara, Japan
SFDK	Sarawak Forestry Department, Kuching, Malaysia
TARI	Taiwan Agricultural Research Institute, Taichung, Taiwan
TUA	Tokyo University of Agriculture, Atsugi, Japan
ZMH	Zoological Museum Hamburg, Hamburg, Germany

All examined specimens without institutional Unique Specimen Identifier (USI) labels were assigned labels that read in the form: JHLHY_DAR_###. Specimens were dissected following standard procedures and genitalia were cleared in a solution of KOH and water. Genitalia were photographed with a Nikon DS-Fi3 camera through a Nikon SMZ18 stereomicroscope using NIS-Elements D (v. 5.41.00) (Nikon Corporation, Yokohama, Japan), and were subsequently placed in a small tube of glycerin which was pinned with the dissected specimen. All other images were taken under a Leica M205 C microscope with a Leica DMC 5400 camera and stacked using Leica Application Suite (Leica Microsystems, Wetzlar, Germany). Figures were arranged in Adobe Photoshop (v. 24.3.0).

X-ray microtomography

X-ray μCT scanning was performed using a ZEISS Xradia 510 Versa with ZEISS Scout and Scan Control System software (v. 14.0.14829). For scans of the metatibia, a hind leg was removed and glued to paper point and fixed to a secure mount. To compare interspecific differences in cuticle and hindwing morphology (full body scans), five specimens (when available) varying in size and collection locality were chosen in an effort to encapsulate any potential intraspecific variation. All characters presented here are those which were determined to be stable within the five-specimen sample. Obscuring scales were virtually removed from specimens by varying the threshold during segmentation and also by viewing cross-sections of the body using the *scissors* function in 3D Slicer (v. 5.0.3). All interspecific differences were confirmed by examining worn and dissected specimens. Specimens were rotated 360 degrees throughout the scan run and with 2001 projections. Reconstructions were performed using Zeiss Scout-and-Scan Control System Reconstructor (v. 14.0.14829) and saved in DICOM format. The DICOM files were loaded into 3D Slicer and 3D models were generated in the *Segment Editor* module. The 3D weevil models were cleaned to remove "noise particles" (i.e., remaining bits of scales and background noise) using the *islands* function (*Segment Editor* module) and any leftover particles were removed using the *scissors* function (*Segment Editor* module). Model shading (Cook-Torrance.gdp) was enhanced in MeshLab (v. 2022.02). Individual full body scan and metatibia scan settings for the species are found in Table 1.

DNA barcoding

To complement morphology-based taxonomic hypotheses and to help with associating females with males (not trivial in the Vietnamese species), a maximum likelihood (hereafter ML) tree including eight of the 14 *Aphanerostethus* species was constructed. The Molytine weevils *Deretiosus albicaudatus* Morimoto, 1988 (Sophrorhinini Lacordaire, 1865), *Colobodes ornatoideus* Morimoto, 1988 (Sophrorhinini Lacordaire, 1865), *Protacallodes ryukyuensis* Morimoto, 2011 (Ithyporini Lacordaire, 1865), *Protacallodes* sp. 1, *Ectatorhinus adamsii* Pascoe, 1871 (Ithyporini Lacordaire, 1865), and Tylodina (tribe) sp. 1 (Cryptorhynchini Schoenherr, 1825) were used as outgroup taxa (see Alonso-Zarazaga et al. 2023 for tribal placement). DNA was extracted from the whole specimen non-destructively using the methods of Oberacker et al. (2019). When used exclusively, cytochrome c oxidase subunit I (CO1) can fail to delineate closely related weevil species (Lewis and Anderson 2023; Schutte et al. 2023); as such, we sequenced ~300 bp long fragments from three mitochondrial genes, namely, 16S rRNA, CO1, and cytochrome b (Cytb). Primers and thermal profiles used are presented in Suppl. material 1. General library preparation methodology is outlined in Kennedy et al. (2023; see Section 2.3). Pooled products were sequenced with Illumina MiSeq at OIST using 600-cycle v3 kits. Sample demultiplexing within individual libraries was conducted using Cutadapt (v. 1.18; Martin 2011). Processing of DNA sequence data (de-novo assembly, trimming) was performed in Geneious Prime (v. 11.0.14.1; Dotmatics, Boston, Massachusetts, United States of America). After de-novo assembly all sequence data were run through BLAST to ensure that non-beetle DNA had not been amplified. As a final check that non-target sequence data was not erroneously incorporated into the analyses, a separate neighbor-joining tree was built for each gene to confirm that members of the same species (determined by morphology earlier in the study) clustered together as expected. DNA extraction sample codes read in the form EGP#######. All DNA sequence data were uploaded to GenBank: CO1, accession numbers PP110442–PP110480; Cytb, accession numbers PP115961–PP115995; 16S, accession numbers PP109310–PP109347. DNA sequence data was aligned using MUSCLE (v. 3.8.425 with default settings; Edgar 2004) using default settings for CO1 and Cytb, and quality-controlled by examining translated amino-acid alignments. A structural alignment algorithm (Q-INS-i with default settings; Rozewicki et al. 2019) was used to align 16S sequence data. The CO1, Cytb, and 16S fragments were concatenated into an 872 base pair long alignment which was used in the phylogenetic analysis. Except for EGP0160H08 (16S / CO1 only), EGP0160C07 (16S / CO1 only), EGP0160E02 (16S / CO1 only), and EGP0160F03 (CO1 only), all specimens had full sequence data. Partition model selection was performed

Table 1. X-ray μCT scan settings for species of *Aphanerostethus*. An asterisk (*) beside the species name indicates that the scan was taken of the metatibia, as opposed to the full body.

Species	USI	Magnification (×)	Expo-sure (s)	Source distance (mm)	Detector distance (mm)	Volt-age (kV)	Power (W)
Aphanerostethus armatus	JHLHY_DAR_078	4	0.7	13.12	10.33	50	4
*A. bifidus**	JHLHY_DAR_102	20	7	11.53	8	50	4
A. bifidus	JHLHY_DAR_092	4	0.8	14.02	8.52	50	4
A. bifidus	JHLHY_DAR_101	4	0.7	11.60	6.88	50	4
A. bifidus	JHLHY_DAR_103	4	0.7	12.61	6.88	50	4
A. darlingi	JHLHY_DAR_125	4	0.7	13.04	8.01	50	4
A. darlingi	JHLHY_DAR_126	4	0.7	12.53	8.01	50	4
A. decoratus	JHLHY_DAR_079	4	1	16.02	13.40	60	4
*A. distinctus**	OKENT0087658	20	5	11.07	8.04	50	4
A. distinctus	JHLHY_DAR_011	4	0.9	13.52	15.52	50	4
A. distinctus	JHLHY_DAR_062	4	0.6	11.64	7.55	60	4
A. distinctus	JHLHY_DAR_071	4	0.6	12.19	8.16	60	4
A. distinctus	OKENT0089414	4	0.7	11.53	7.57	50	4
A. distinctus	JHLHY_DAR_146	4	0.7	10.01	7.72	50	4
*A. falcatus**	JHLHY_DAR_099	20	5	11.04	7.52	60	4
A. falcatus	JHLHY_DAR_091	4	0.7	12.03	8.52	50	4
A. falcatus	JHLHY_DAR_167	4	0.7	10.53	8.72	50	4
A. falcatus	JHLHY_DAR_172	4	0.7	10.53	8.22	50	4
A. falcatus	JHLHY_DAR_170	4	0.7	10.53	7.73	50	4
A. falcatus	JHLHY_DAR_094	4	0.7	10.53	8.23	50	4
*A. incurvatus**	JHLHY_DAR_100	20	7	12.02	8.01	50	4
A. incurvatus	JHLHY_DAR_100	4	0.7	12.03	9.02	50	4
A. incurvatus	JHLHY_DAR_095	4	0.7	10.52	7.72	50	4
A. incurvatus	JHLHY_DAR_104	4	0.7	12.16	7.39	50	4
A. japonicus	JHLHY_DAR_051	4	1.3	16.58	15.97	60	4
A. japonicus	JHLHY_DAR_041	4	0.6	11.46	7.53	60	4
A. japonicus	JHLHY_DAR_052	4	0.65	12.08	7.54	60	4
A. japonicus	OKENT0055168	4	0.6	11.54	7.57	60	4
A. japonicus	OKENT0055232	4	0.65	11.13	7.39	50	4
*A. magnus**	JHLHY_DAR_075	20	5	12.05	8.02	50	4
A. magnus	JHLHY_DAR_029	4	1.3	18.53	15.52	50	4
A. magnus	JHLHY_DAR_035	4	1	17.54	7.02	60	4
A. magnus	JHLHY_DAR_027	4	1	16.54	7.02	60	4
A. magnus	JHLHY_DAR_032	4	1	17.45	7.52	60	4
A. magnus	JHLHY_DAR_108	4	0.7	10.59	7.37	50	4
*A. morimotoi**	JHLHY_DAR_113	20	7	11.03	8.51	50	4
A. morimotoi	JHLHY_DAR_093	4	0.7	11.52	9.03	50	4
A. morimotoi	JHLHY_DAR_188	4	0.7	11.03	7	50	4
A. morimotoi	JHLHY_DAR_189	4	0.7	11.04	7.51	50	4
A. morimotoi	JHLHY_DAR_114	4	0.7	12.13	8.14	60	4
A. morimotoi	JHLHY_DAR_115	4	0.7	11.56	7.51	50	4
*A. nudus**	JHLHY_DAR_012	20	5	16.05	7.53	50	4
A. nudus	JHLHY_DAR_014	4	1.5	14.58	19.97	60	4
A. nudus	JHLHY_DAR_074	4	0.6	11.55	7.57	60	4
A. nudus	JHLHY_DAR_012	4	0.6	11.57	7.57	60	4
A. nudus	JHLHY_DAR_015	4	0.6	12.08	7.57	60	4
A. nudus	JHLHY_DAR_013	4	0.6	11.59	7.57	60	4
*A. spinosus**	JHLHY_DAR_077	20	6	10.52	7.51	50	4

Species	USI	Magnification (×)	Expo-sure (s)	Source distance (mm)	Detector distance (mm)	Volt-age (kV)	Power (W)
A. taiwanus	JHLHY_DAR_018	4	0.7	12.01	7.51	60	4
A. taiwanus	JHLHY_DAR_021	4	0.6	11.53	7.51	60	4
A. taiwanus	JHLHY_DAR_070	4	0.6	11.54	7.52	60	4
A. taiwanus	JHLHY_DAR_084	4	0.6	11.66	7.65	60	4
A. taiwanus	JHLHY_DAR_086	4	0.6	12.14	7.65	60	4
A. vannideki	JHLHY_DAR_081	4	0.7	13.67	7.65	60	4
A. vannideki	JHLHY_DAR_082	4	0.7	11.01	7.41	50	4
A. vannideki	ZMH 841853	4	0.7	12.1	8.04	60	4
A. vannideki	ZMA.INS.5117698	4	0.7	11.61	8.04	60	4
A. vannideki	ZMN.INS.5117696	4	0.7	12.62	8.04	60	4

in IQ-TREE (v. 1.6.12; Nguyen et al. 2015) using ModelFinder (command: -m TESTMERGE; Kalyaanamoorthy et al. 2017; Chernomor et al. 2016) to allow for separate models to be applied to the three marker fragments (CO1 / Cytb: GTR+F+I+G4; 16S: GTR+F+G4) separately. The ML analysis was performed in IQ-TREE with a heuristic search of 100,000 initial trees and standard nonparametric bootstrap (hereafter BS) values were calculated from 1000 replicates. To supplement the ML analysis, a Bayesian Inference (hereafter BI) tree was also constructed in Mr. Bayes (v. 3.2.7a; Ronquist et al. 2012) using the same partition model with the following settings (ngen: 2000000, samplefreq: 1000, nruns: 2, nchains: 4, burninfrac: 0.25). Tracer (v. 1.7.2; Rambaut et al. 2018) was used to confirm convergence of the BI analysis (ESS > 800 for all parameter values; ASDFS < 0.005). The tree presented in this paper was visualized in iTOL (v. 6.8.1; Letunic and Bork 2021) and is the ML tree with bootstrap and posterior probability (hereafter PP) values displayed at the nodes.

Results

General remarks

We found strong morphological and molecular evidence that warrants the description of twelve new species, namely, *A. armatus* sp. nov., *A. bifidus* sp. nov., *A. darlingi* sp. nov., *A. decoratus* sp. nov., *A. falcatus* sp. nov., *A. incurvatus* sp. nov., *A. japonicus* sp. nov., *A. magnus* sp. nov., *A. morimotoi* sp. nov., *A. nudus* sp. nov., *A. spinosus* sp. nov., and *A. taiwanus* sp. nov. from Japan, Taiwan, Vietnam, and Malaysia. Including the previously described *A. vannideki* Voss, 1957 and *A. distinctus* (Morimoto & Miyakawa, 1985), this brings the total number of known species of *Aphanerostethus* to fourteen. In addition to differences in the male genitalia, the species are also separable by external morphology. Important external characters include the presence (vs absence) of a prominent prosternal canal, the presence (vs absence) of ventral femoral teeth, patterning of erect elytral scales, the elytra bearing erect scales (vs recumbent scales), the shape of the male metatibial uncus, the presence (vs reduction) of the scutellum, overall size, and color. Sexual dimorphism in the metatibial uncus is particularly remarkable; females all have simple metatibial unci, whereas the metatibial unci in the males of some species are modified in shape and species-specific (see Figs 1, 2). With the exception of *A. taiwanus* and *A. distinctus*, the molecular results (Fig. 3) strongly support the monophyly of all the species analyzed (BS: 100, PP: 1). Although *A. taiwanus* was consistently placed in the same clade as *A. distinctus* (BS: 100, PP: 1) as expected, its presumed basal position (i.e., sister to *A. distinctus*) is only weakly supported (BS: 55, PP: 0.84; see the Comments section in *A. taiwanus* species profile). Notably, the close phylogenetic relationship of *A. magnus* and *A. bifidus* is strongly supported (BS: 95, PP: 1), a finding which was expected based on morphology.

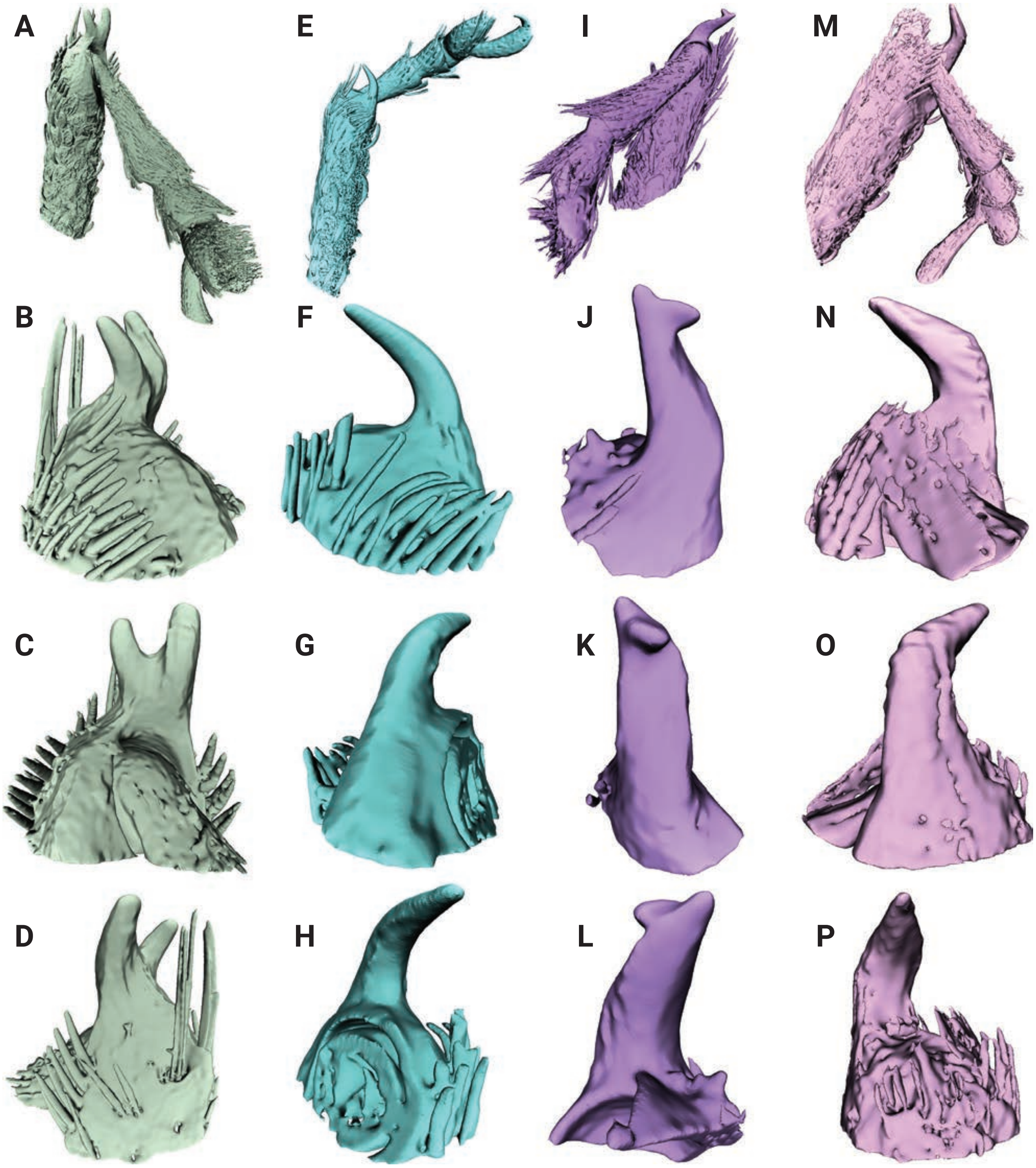

Figure 1. Metatibial unci in *Aphanerostethus* (males) **A–D** *A. bifidus* sp. nov. (JHLHY_DAR_102) **E–H** *A. distinctus* (Morimoto & Miyakawa, 1985) (OKENT0087658) **I–L** *A. falcatus* sp. nov. (JHLHY_DAR_099) **M–P** *A. incurvatus* sp. nov. (JHLHY_DAR_100).

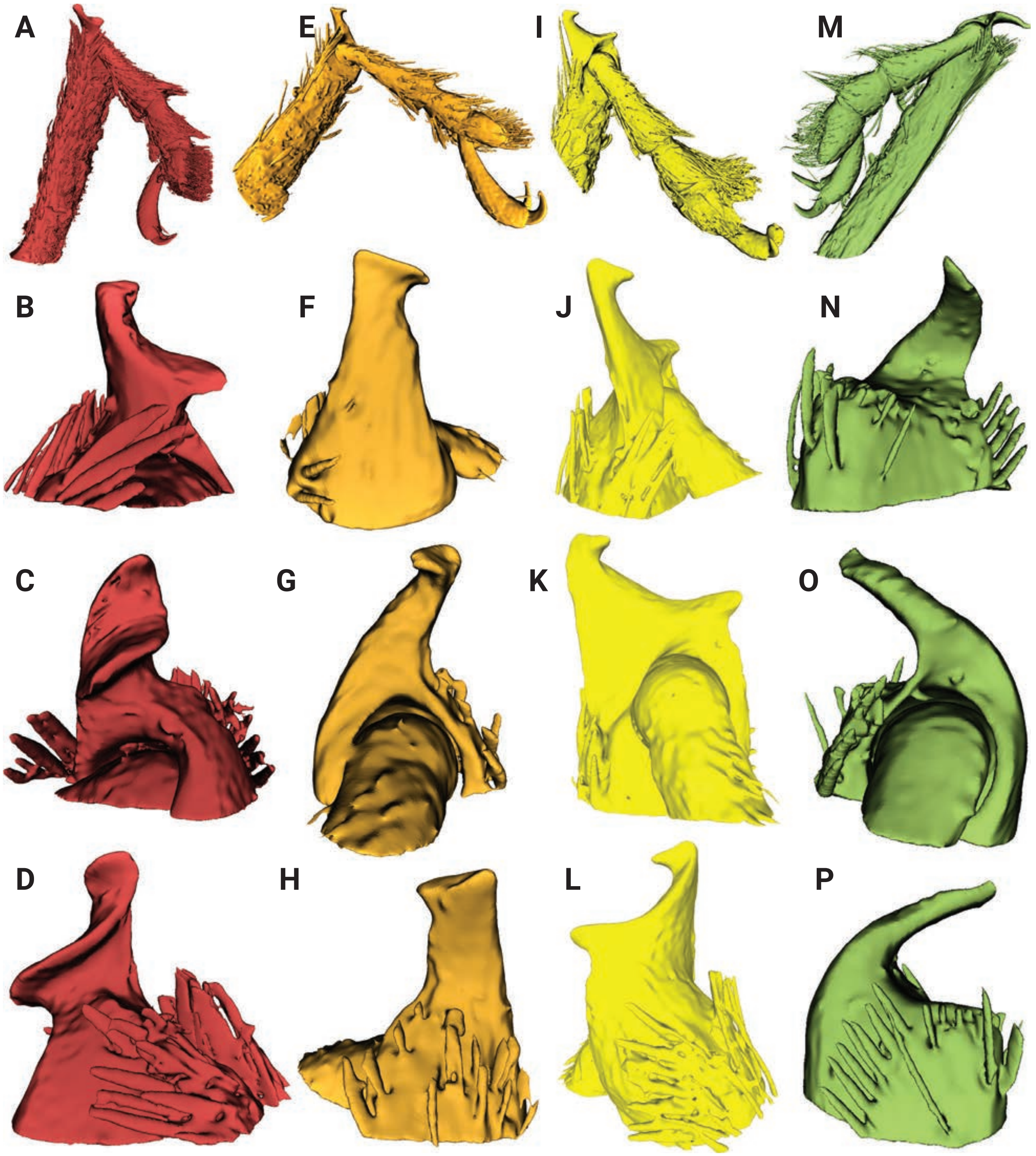

Figure 2. Metatibial unci in *Aphanerostethus* (males) **A–D** *A. magnus* sp. nov. (JHLHY_DAR_075) **E–H** *A. morimotoi* sp. nov. (JHLHY_DAR_113) **I–L** *A. spinosus* sp. nov. (JHLHY_DAR_077) **M–P** *A. nudus* sp. nov. (JHLHY_DAR_012).

X-ray microtomography

Metatibial unci

Remarkable species-specific sexual dimorphism in the metatibial uncus occurs in seven of the fourteen *Aphanerostethus* species examined here, namely, *A. bifidus* (Y-shaped, bifid uncus; Fig. 1A–D), *A. falcatus* (sickle-shaped uncus; simple, but with lateral projection; Fig. 1I–L), *A. incurvatus* (incurved uncus; Fig. 1M–P), *A. magnus* (ear-shaped uncus; Fig. 2A–D), *A. morimotoi* (boot-shaped uncus;

truncated at apex, but with lateral projection; Fig. 2E–H), *A. spinosus* (complex uncus shape; large C-shaped plate with apical inward-facing projection; Fig. 2I–L), and *A. nudus* (weak inward spiral-shaped uncus; Fig. 2M–P).

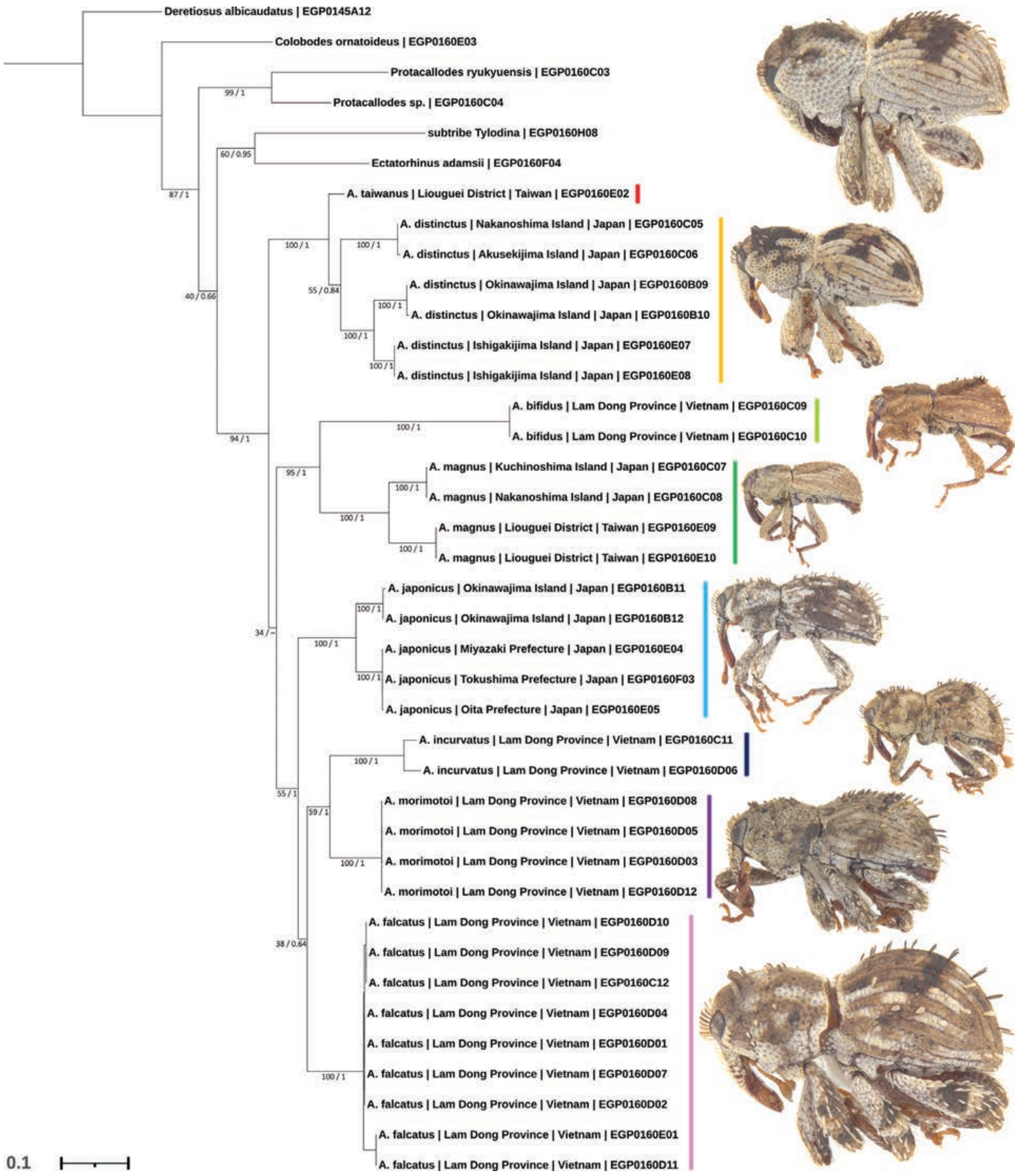

Figure 3. Maximum likelihood tree of *Aphanerostethus* species based on an 872 base-pair long concatenated DNA matrix (CO1, Cytb, 16S) with gene-wise partition modelling (CO1 / Cytb: GTR+F+I+G4; 16S: GTR+F+G4) constructed in IQ-TREE v. 1.6.12. Branch support values represent standard nonparametric bootstraps (1000 replicates) and posterior probabilities. The symbol "–" indicates a posterior probability less than 50 (i.e., collapsed nodes in the Bayesian Inference tree). EGP codes represent DNA extraction codes and serve also as unique specimen identifiers. Associated *Aphanerostethus* weevil figures on the right of the tree are not to scale. Note that, except for *A. distinctus* and *A. taiwanus* (see Comments under the *A. taiwanus* species profile), the monophyly of all *Aphanerostethus* species is strongly supported (BS: 100, PP: 1).

Pronotal morphology

Significant and stable interspecific differences in puncture shape and orientation were discovered after removing scales obscuring the dorsal region of the pronotum (in dorsal view; Figs 4–9). Punctures can be longitudinally elongate (*A. bifidus* (Fig. 4B–D), *A. magnus* (Fig. 7A–C)), C-shaped (*A. decoratus* (Fig. 4E), transversally elongate (*A. distinctus* (Fig. 5A–C), *A. spinosus* (Fig. 4F), *A. taiwanus* (Fig. 8D–F), *A. vannideki* (Fig. 9A–D), *A. darlingi* (Fig. 9E–F)), or approximately circular in shape (*A. armatus* (Fig. 4A), *A. falcatus* (Fig. 5D–F), *A. incurvatus* (Fig. 6A, B), *A. japonicus* (Fig. 6C–F), *A. morimotoi* (Fig. 7D–F), *A. nudus* (Fig. 8A–C)).

Tenth elytral stria

In most species (*A. bifidus*, *A. darlingi*, *A. decoratus*, *A. falcatus*, *A. incurvatus*, *A. japonicus*, *A. magnus*, *A. morimotoi*, *A. spinosus*) the tenth elytral stria extends from the base of the elytra to the apex, and includes 14–21 punctures (Fig. 10A–D). However, in *A. distinctus* and *A. taiwanus*, the tenth stria ends at the middle or slightly past the middle of the elytra, and includes ten punctures at most (Fig. 10E, F).

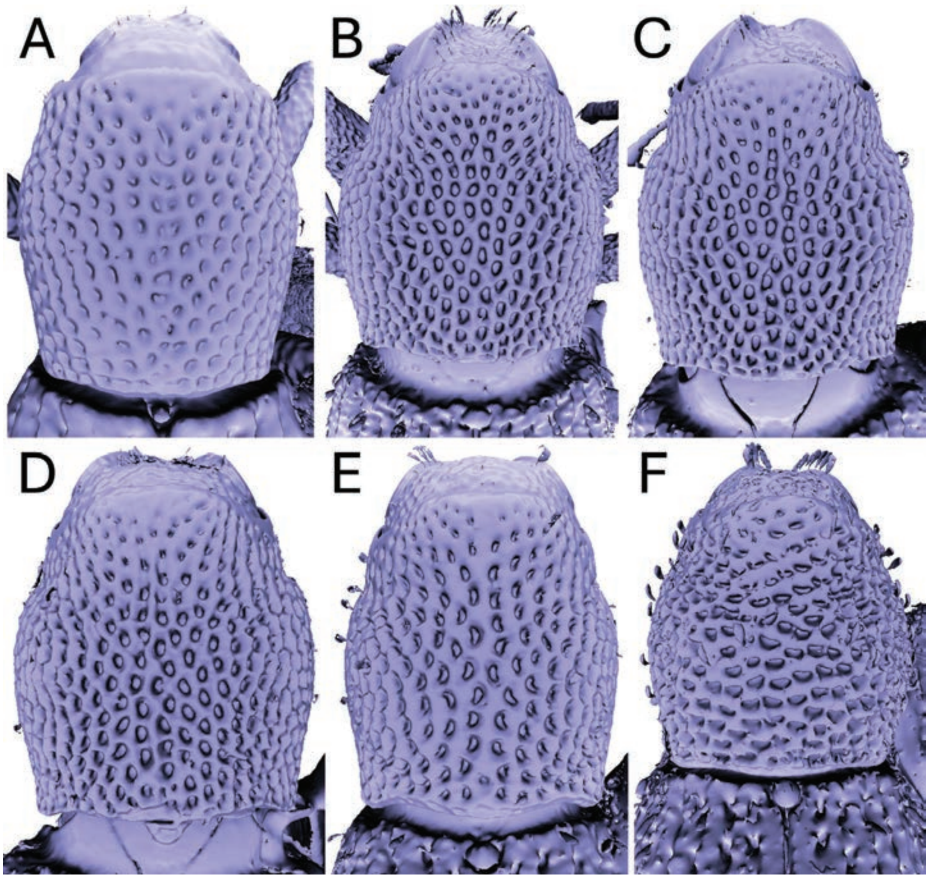

Figure 4. X-ray microtomography generated 3D models of *Aphanerostethus* pronota with scales removed, revealing otherwise hidden differences in underlying puncture morphology **A** *Aphanerostethus armatus* sp. nov. (JHLHY_DAR_078) **B–D** *Aphanerostethus bifidus* sp. nov. (JHLHY_DAR_092, 101, and 103, respectively) **E** *Aphanerostethus decoratus* sp. nov. (JHLHY_DAR_079) **F** *Aphanerostethus spinosus* sp. nov. (JHLHY_DAR_077).

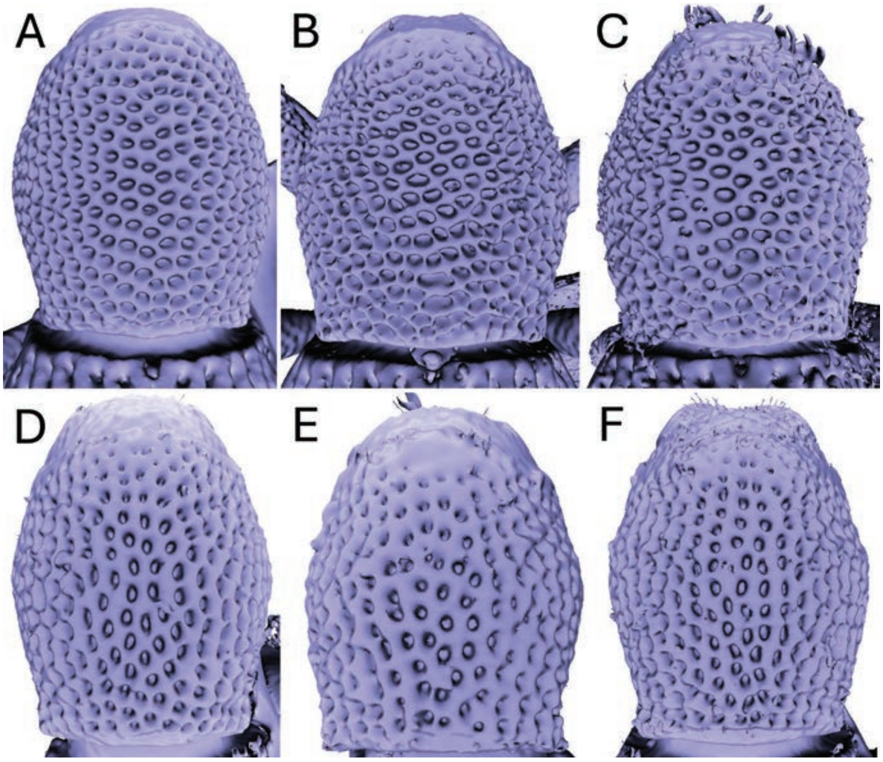

Figure 5. X-ray microtomography generated 3D models of *Aphanerostethus* pronota with scales removed, revealing otherwise hidden differences in underlying puncture morphology **A–C** *Aphanerostethus distinctus* (Morimoto & Miyakawa, 1985) (OKENT0089414, JHLHY_DAR_071, and 062, respectively) **D–F** *Aphanerostethus falcatus* sp. nov. (JHLHY_DAR_167, 170, and 172, respectively).

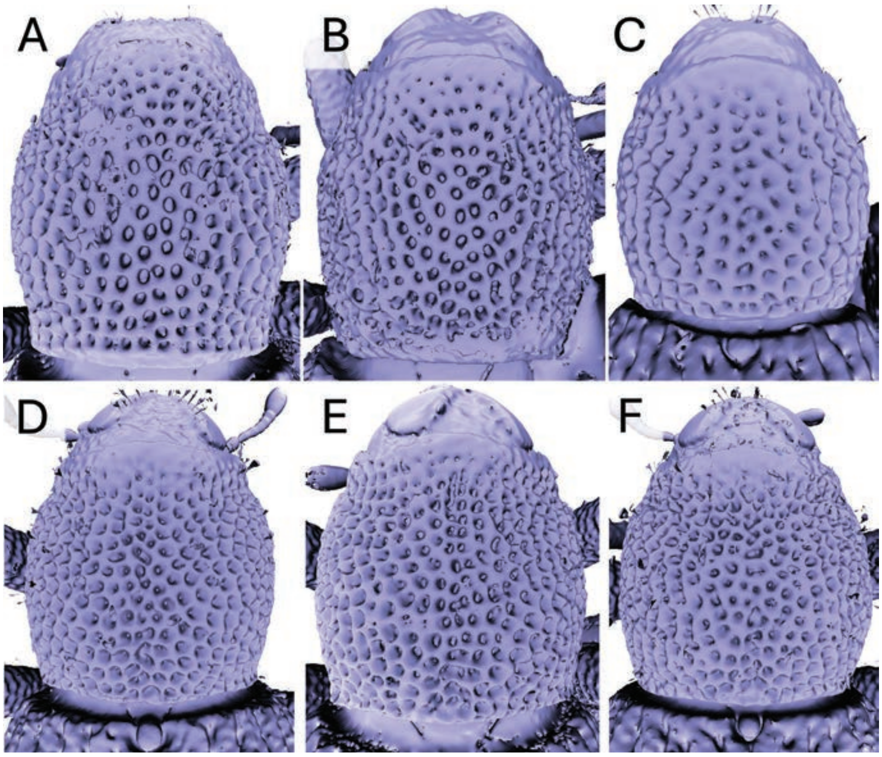

Figure 6. X-ray microtomography generated 3D models of *Aphanerostethus* pronota with scales removed, revealing otherwise hidden differences in underlying puncture morphology **A, B** *Aphanerostethus incurvatus* sp. nov. (JHLHY_DAR_095, 104) **C–F** *Aphanerostethus japonicus* sp. nov. (OKENT0055232, JHLHY_DAR_051, 052, 041).

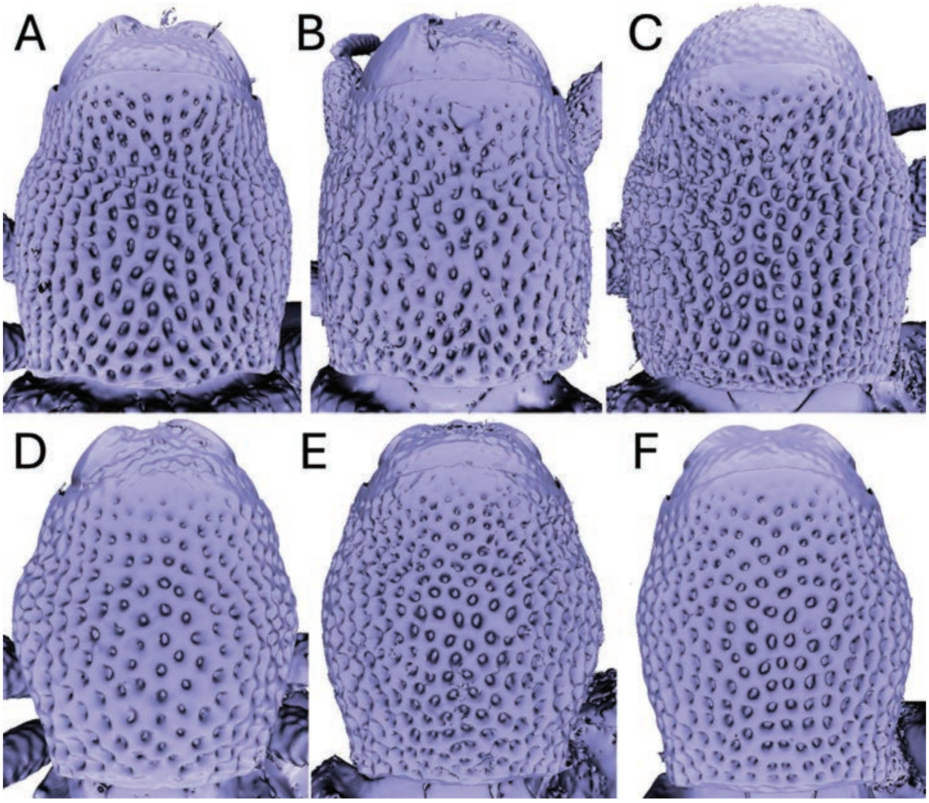

Figure 7. X-ray microtomography generated 3D models of *Aphanerostethus* pronota with scales removed, revealing otherwise hidden differences in underlying puncture morphology **A–C** *Aphanerostethus magnus* sp. nov. (JHLHY_DAR_029, 035, and 108, respectively) **D–F** *Aphanerostethus morimotoi* sp. nov. (JHLHY_DAR_189, 144, and 115, respectively).

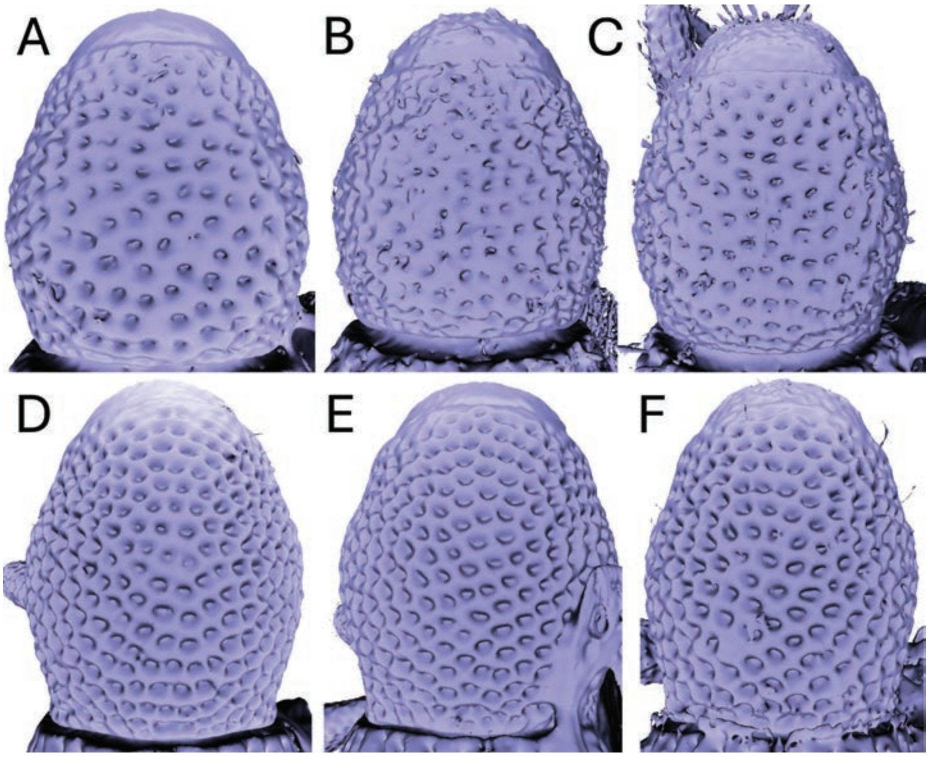

Figure 8. X-ray microtomography generated 3D models of *Aphanerostethus* pronota with scales removed, revealing otherwise hidden differences in underlying puncture morphology **A–C** *Aphanerostethus nudus* sp. nov. (JHLHY_DAR_012, 013, and 014, respectively) **D–F** *Aphanerostethus taiwanus* sp. nov. (JHLHY_DAR_070, 021, and 086, respectively).

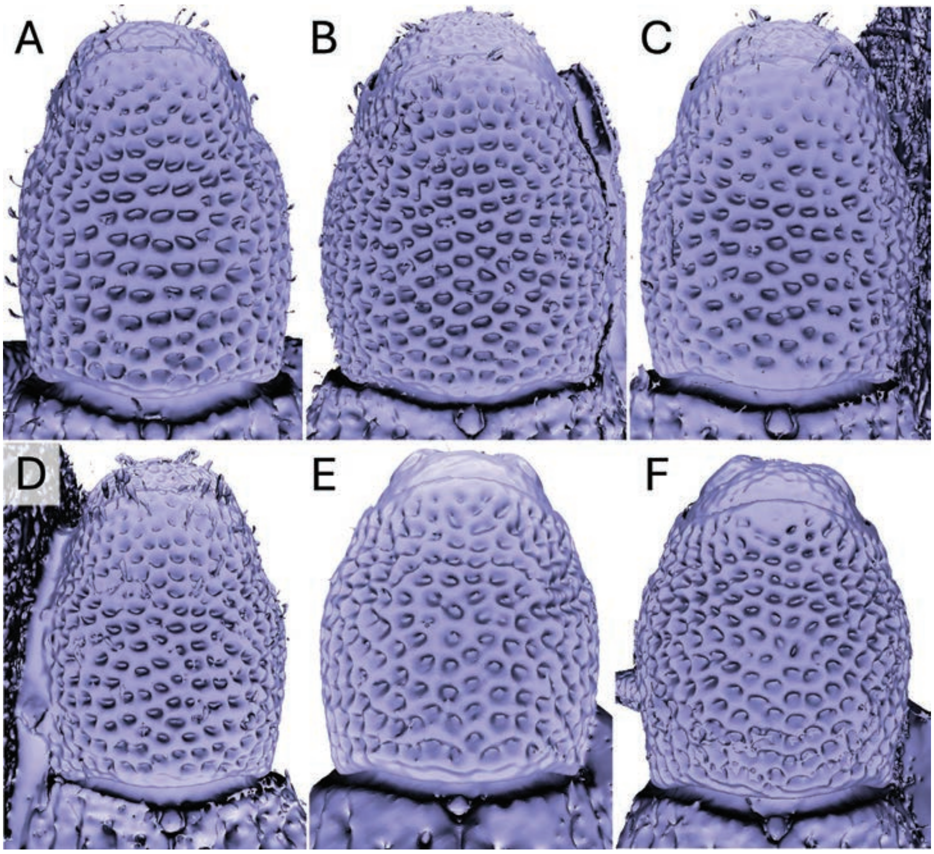

Figure 9. X-ray microtomography generated 3D models of *Aphanerostethus* pronota with scales removed, revealing otherwise hidden differences in underlying puncture morphology **A–D** *Aphanerostethus vannideki* Voss, 1957 (JHLHY_DAR_082 (A), ZMA_5517696 (B), ZMH_841853 (C), and ZMA_5517698 (D), respectively) **E, F** *Aphanerostethus darlingi* sp. nov. (JHLHY_DAR_125, JHLHY_DAR_126).

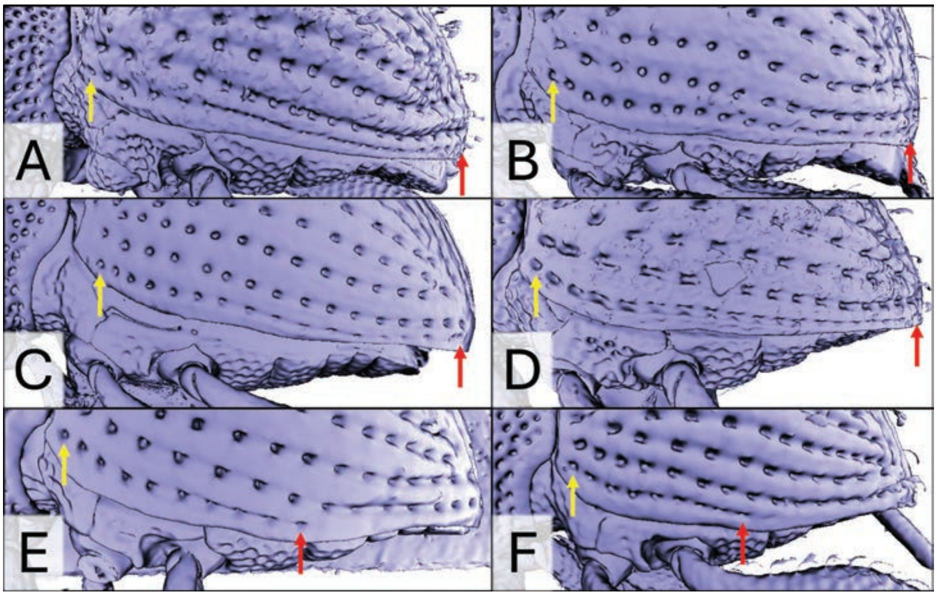

Figure 10. X-ray microtomography generated 3D models of *Aphanerostethus* elytra with scales removed, revealing differences in the length of the 10th elytral stria. The yellow and red arrows indicate the base and apex of the 10th elytral stria, respectively **A** *Aphanerostethus bifidus* sp. nov. (JHLHY_DAR_092) **B** *A. falcatus* sp. nov. (JHLHY_DAR_172) **C** *A. morimotoi* sp. nov. (JHLHY_DAR_115) **D** *A. decoratus* sp. nov. (JHLHY_DAR_079) **E** *A. distinctus* (Morimotoi & Miyakawa, 1985) (OKENT0089414) **F** *A. taiwanus* sp. nov. (JHLHY_DAR_070).

Hind wings

All known *Aphanerostethus* species are flightless; however, the amount of hindwing reduction in the genus varies interspecifically (Fig. 11). The degree of hindwing reduction can be classified into four categories: (1) only a minute stub of hindwing remains (*A. distinctus*, *A. taiwanus*, and *A. nudus*); (2) the hindwing remnants are elongate in shape but not reaching the middle of the elytra (*A. falcatus*, *A. japonicus* (Fig. 11C), *A. spinosus*); (3) the hindwing remnants are long, thin, and reaching past the middle of the elytra (*A. darlingi*, *A. incurvatus*, *A. magnus* (Fig. 11D), *A. morimotoi*, *A. vannideki*); (4) the hindwing remnants are long (reaching past the middle of the elytra), wide, and still clearly show the remains of longitudinal wing venation (*A. bifidus*, Fig. 11A; *A. decoratus*, Fig. 11B).

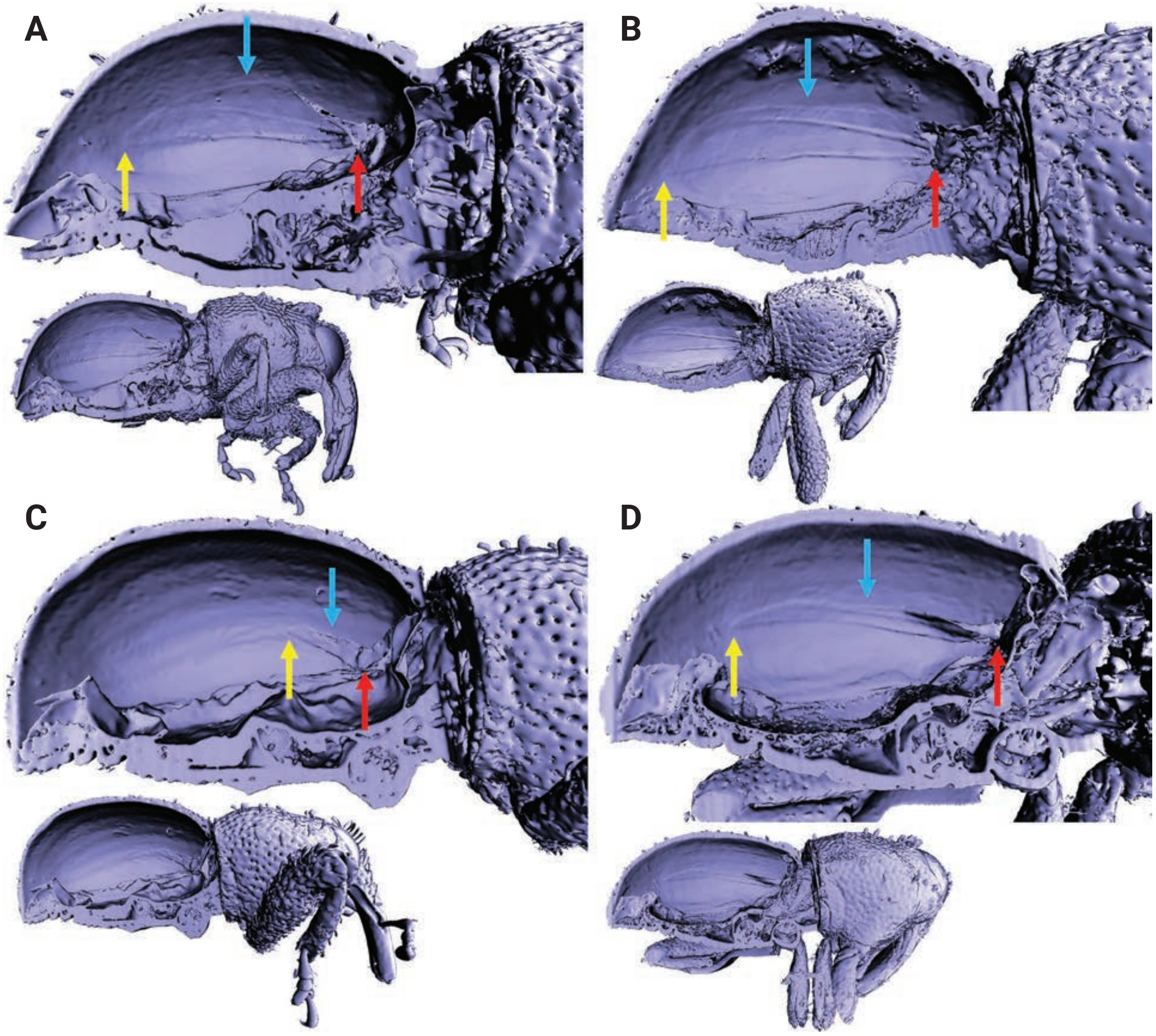

Figure 11. X-ray microtomography generated 3D models of *Aphanerostethus* with the right elytron removed, revealing differences in the length, width, and venation of the hindwing (as shown here, the hindwing is affixed to the inner surface of the elytron in most specimens). A lateral view of the full body is shown below each close-up for reference. The red, blue, and yellow arrows indicate the base, midpoint, and apex of the hindwing, respectively **A** *Aphanerostethus bifidus* sp. nov. (JHLHY_DAR_092) **B** *A. decoratus* sp. nov. (JHLHY_DAR_079) **C** *A. japonicus* sp. nov. (JHLHY_DAR_041) **D** *A. magnus* sp. nov. (JHLHY_DAR_032).

Taxonomy

Genus *Aphanerostethus* Voss, 1957

Darumazo Morimoto & Miyakawa, 1985, syn. nov.

Type species. *Aphanerostethus vannideki* Voss, 1957, by monotypy.

Gender. Masculine.

Redescription. Body length 1.5–3.0 mm. Rounded to bulb-like appearance in lateral view. ***Cuticle*:** Dark to pale red. ***Scale pattern*:** Large flat white, gray, brown, or golden scales covering the body in most species (the cuticle of *A. nudus* is largely exposed); two prominent rows of erect scales ("eyelashes") along inner margin of eye which extends ventrally to basal third to middle of rostrum; pronotum with erect or recumbent scales; erect or recumbent scales always on odd elytral intervals; erect scales on even elytral intervals in some species. ***Head*:** Rostrum punctate, evenly curved; eyes large, ovate; antennae with six-articled funicle (except apparently in *A. armatus* which has five articles). ***Prothorax*:** Densely punctate; margin of prothorax (in lateral view) extending forward, covering part of the eye (or most of it when rostrum fully set into prosternal sulcus); prosternum with strongly or weakly defined prosternal canal. ***Elytra*:** Scutellum prominent or reduced; elytra rounded to bulb-like, with intervals convex; flightless, hind wings reduced to a stub or long filament. ***Abdomen*:** Lateral edge of first abdominal segment contiguous with metanepisternum. ***Legs*:** Femora with or without apico-ventral tooth; unci of fore- and mid-tibiae simple; unci of male hind-tibiae modified (bifid, hooked, or twisted) in some species, simple (evenly curved) in females; third tarsal segment bilobed; tarsal claws simple.

Distribution. *Aphanerostethus* species are known from Japan (Izu Islands, mainland, Nansei Islands), Taiwan, Vietnam (Mt. Lang Biang), Malaysia (Cameron Highlands, Pahang; Sabah, Borneo), and Indonesia (West Java).

Notes. The genus *Darumazo* Morimoto & Miyakawa, 1985 was described based on a single species, *D. distinctus* Morimoto & Miyakawa, 1985, from specimens collected in the Izu Islands, the Nansei Islands, and mainland Japan. Morimoto and Miyakawa (1985) distinguished *Darumazo* from *Aphanerostethus* as the latter have separated fore-coxae as well as toothed femora. However, the twelve new species described here reveal a continuum of forms, relating *A. distinctus* and *A. vannideki* with respect to the above two characters. In particular, although *A. vannideki* has separated fore-coxae and a longer prosternal canal, the related *A. bifidus* possesses weakly separate fore-coxae (contiguous in the related *A. magnus*). Furthermore, the femoral teeth are present but small in *A. morimotoi* (femoral teeth often completely absent) and *A. japonicus*, indicating continuity in this character across the genus as well. We do not feel that a moderate degree of separation in the fore-coxae, nor the presence (vs absence) of femoral teeth is enough to justify the continued recognition of *Darumazo*, especially in light of the continuity of forms newly described here. On the basis of these morphological considerations, we treat *Darumazo*, syn. nov. as a junior synonym of *Aphanerostethus*. The genus *Aphanerostethus* is currently placed in Cryptorhynchini Schoenherr, 1825 and *Darumazo* in Sthereini Hatch, 1971 (Alonso-Zarazaga and Lyal 1999; Alonso-Zarazaga et al. 2023). We are currently working on a molecular phylogeny of *Aphanerostethus* and some undescribed, related genera and hope that this reveals the tribal placement of the genus. Until that work is completed, we treat the genus as Molytinae incertae sedis.

Aphanerostethus species profiles

Aphanerostethus armatus Lewis & Kojima, sp. nov.

https://zoobank.org/6B31DB80-5F3E-48D6-82F1-1EAF13CBCE3B
Figs 4A, 12A, B, 13A, B, E

Specimens examined. ***Holotype***: **Malaysia:** • Perak, Taiping, Bukit Larut, 7.I.1990, T. Yasunaga, deposited in KUM, JHLHY_DAR_078.

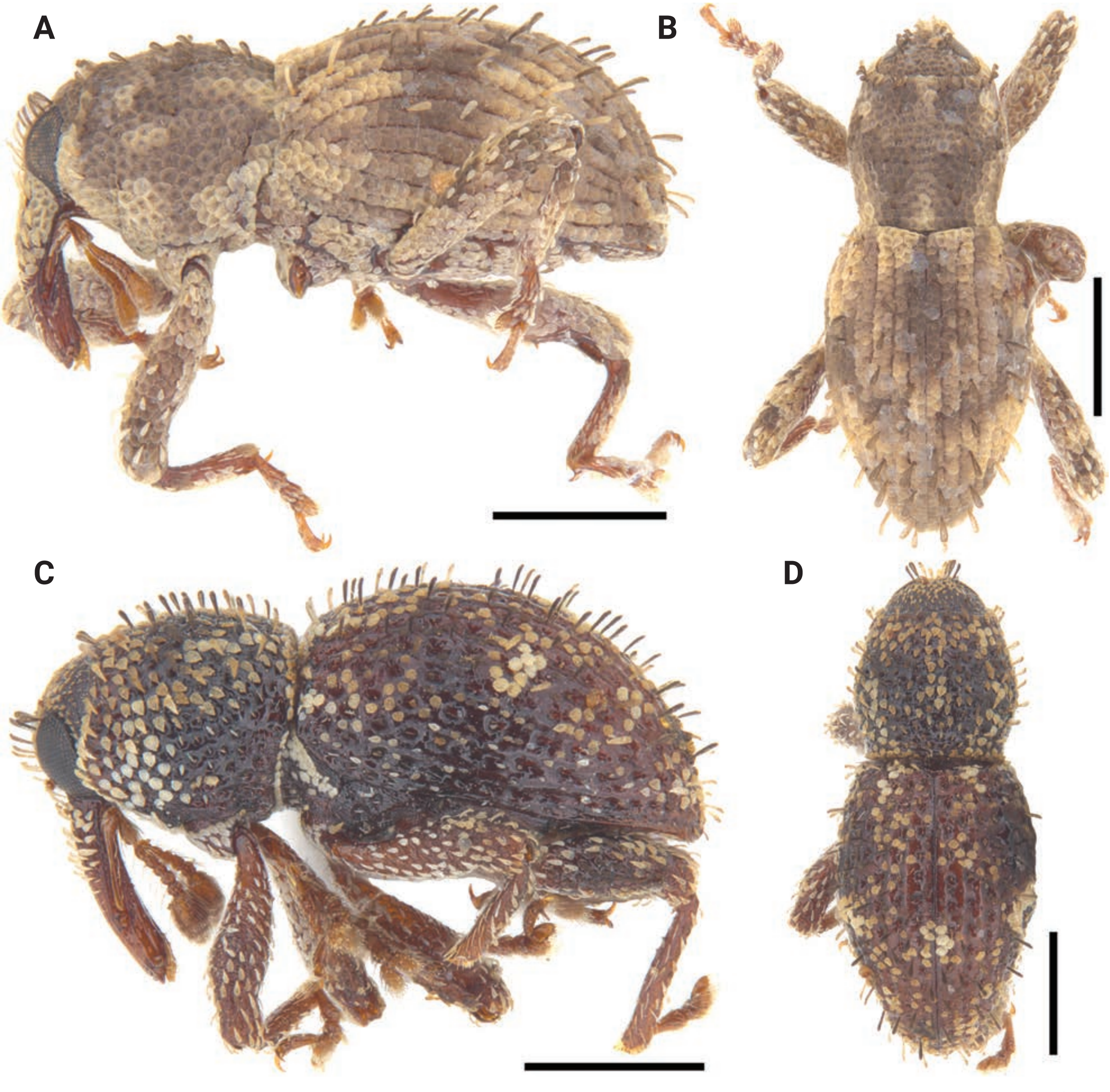

Figure 12. Lateral and dorsal photographs of *Aphanerostethus* species **A, B** *Aphanerostethus armatus* sp. nov. (JHLHY_DAR_078) **C, D** *Aphanerostethus nudus* sp. nov. (JHLHY_DAR_014). Scale bars: 0.5 mm.

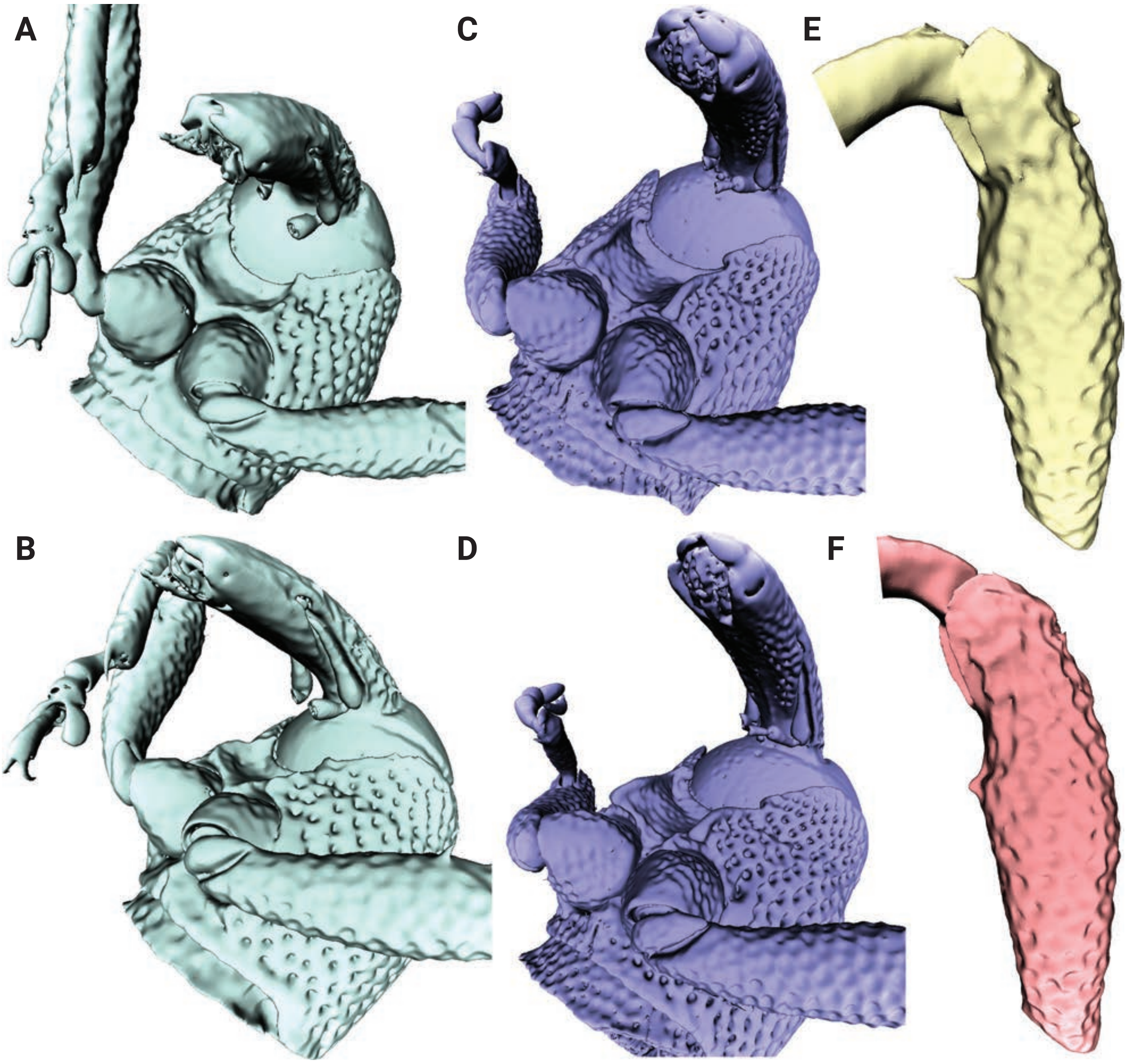

Figure 13. X-ray microtomography generated 3D models of *Aphanerostethus* **A, B** *A. armatus* sp. nov. (JHLHY_DAR_078) shallow prosternal canal **C, D** *A. magnus* sp. nov. (JHLHY_DAR_029) deep prosternal canal **E** *A. armatus* (JHLHY_DAR_078) fore-femur showing elongate, thorn-like ventral tooth **F** *A. japonicus* sp. nov. (JHLHY_DAR_051) fore-femur showing blunt, obtuse ventral tooth.

Diagnosis. Body length 1.7 mm. Cuticle coated in crusty dark, sandy gray, and white scales in weakly defined pattern. Funicle with five articles. Only odd elytral intervals with erect scales. Prosternal cavity very weakly defined and without steep lateral ridges (Fig. 13A, B). Procoxae contiguous. Erect elytral scales evenly distributed, not concentrated in bundle. Scutellum not prominent. Femora each with elongate, thorn-like tooth ventrally (Fig. 13E). Metaventrite flattened between meta- and mesocoxae, without a distinct elevated transverse ridge.

Distribution. This species is currently only known from Perak, Malaysia.

Etymology. The specific name *armatus* is a Latin adjective that refers to the distinctly elongate, sharp tooth on the ventral edge of each femur (see Fig. 13E).

Aphanerostethus bifidus Kojima & Lewis, sp. nov.
https://zoobank.org/F64611EA-ECDE-42DE-B1AF-C77ADC0B5A69
Figs 1A–D, 3, 4B–D, 10A, 11A, 14A, B, 15A, B

Specimens examined. ***Holotype*: Vietnam:** • Lam Dong Province, Mount Lang Biang, 12°02'N, 108°26'E, elevation 1700 m, 18.II.2011, H. Kojima, male deposited in TUA, JHLHY_DAR_092. ***Paratypes*:** • Lam Dong Province, Mount Lang Biang, 12°02'N, 108°26'E, elevation 1700 m, 18.II.2011, H. Kojima, (1, TUA; 1, OIST), JHLHY_DAR_101 (EGP0160C09), JHLHY_DAR_102; • same locality, 26.II.2013, H. Kojima, (1, TUA), JHLHY_DAR_103 (EGP0160C10).

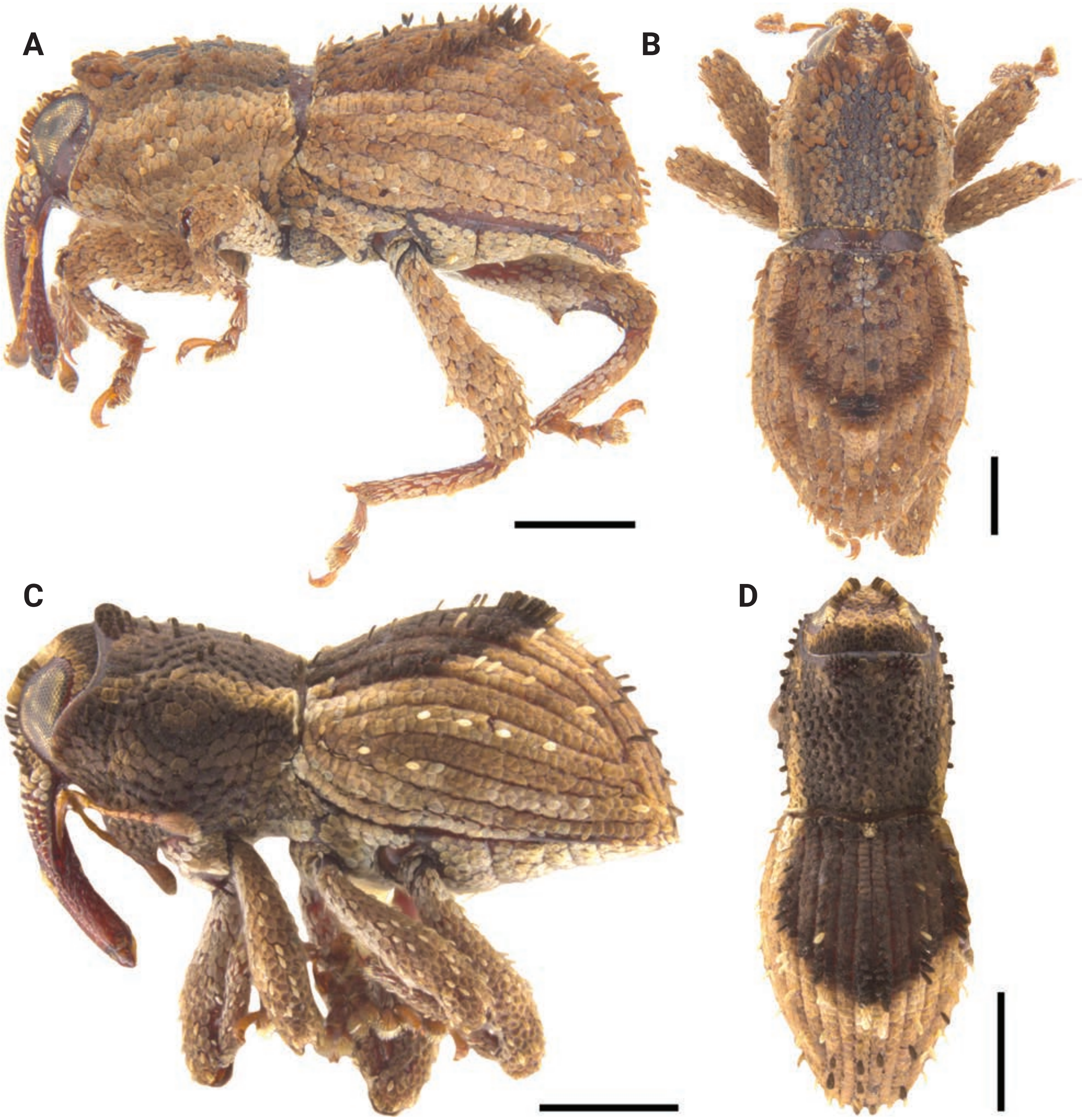

Figure 14. Lateral and dorsal photographs of *Aphanerostethus* species **A, B** *Aphanerostethus bifidus* sp. nov. (JHLHY_DAR_092) **C, D** *Aphanerostethus decoratus* sp. nov. (JHLHY_DAR_079). Scale bars: 0.5 mm.

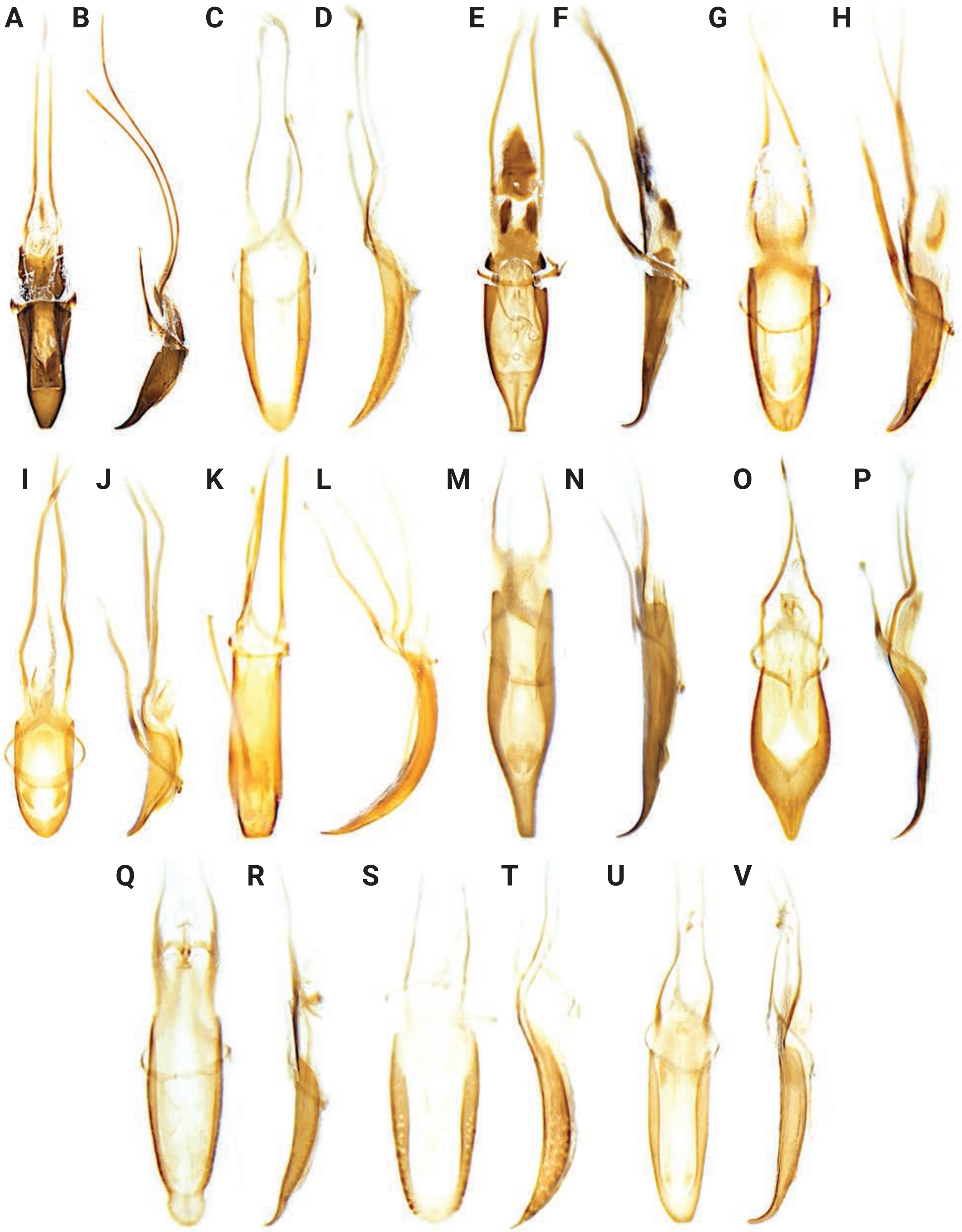

Figure 15. Aedeagi of *Aphanerostethus* species **A, B** *A. bifidus* sp. nov. (JHLHY_DAR_102) **C, D** *A. distinctus* (Morimoto & Miyakawa, 1985) (OKENT87658) **E, F** *A. falcatus* sp. nov. (JHLHY_DAR_099) **G, H** *A. incurvatus* sp. nov. (JHLHY_DAR_100) **I, J** *A. japonicus* sp. nov. (JHLHY_DAR_052) **K, L** *A. magnus* sp. nov. (JHLHY_DAR_022) **M, N** *A. morimotoi* sp. nov. (JHLHY_DAR_113) **O, P** *A. nudus* sp. nov. (JHLHY_DAR_012) **Q, R** *A. spinosus* sp. nov. (JHLHY_DAR_077) **S, T** *A. taiwanus* sp. nov. (JHLHY_DAR_016) **U, V** *A. vannideki* Voss, 1957 (JHLHY_DAR_082).

Diagnosis. Body length 2.7–2.9 mm. Cuticle covered in dark to pale brown scales, with distinct dark, V-shaped band across anterior part of elytra. Funicle with six articles. Prosternal cavity prominent and with steep lateral ridges. Procoxae slightly separated. Second and odd-numbered elytral intervals with erect scales. Erect elytral scales concentrated in bundle on first, third, and fifth interval along V-shaped band. Scutellum prominent. Femora with large ventral tooth at midpoint. Metaventrite with a distinct elevated transverse ridge separating the meta- and mesocoxae. Metatibial uncus bifid in male (Fig. 1A–D). Aedeagus with distinctly long apodemes, and subquadrate in apical half (Fig. 15A, B).

Distribution. This species is currently only known from Mount Lang Biang, Vietnam.

Etymology. The specific name *bifidus* is a Latin adjective in reference to the bifid metatibial uncus observed in males (Fig. 1A–D).

Aphanerostethus darlingi Lewis, sp. nov.

https://zoobank.org/AF2C84EB-9B60-451A-8327-F6A76FE4DD8B

Figs 9E, F, 16A, B

Specimens examined. ***Holotype*: Malaysia: Borneo: Sarawak:** • Gunung Mulu National Park, 1387 m, Camp 3, 4°2.284'N, 114°53.36'E, 27.XI.2009–12.I.2010, malaise trap, D.C. Darling, B. Hubley, deposited in SFDK, ROM_OSU 308049, JHLHY_DAR_126. ***Paratype*: Malaysia: Borneo: Sarawak:** • Gunung Mulu National Park, 1387 m, Camp 3, 4°2.284'N, 114°53.36'E, 24.VII–21.IX.2011, malaise trap, D.C. Darling, (1, CMNC), ROM_OSU 308460, JHLHY_DAR_125.

Diagnosis. Body length 2.0 mm. Cuticle coated in crusty dark, sandy gray, and white scales in weakly defined pattern. Funicle with six articles. Procoxae contiguous. Only odd-numbered elytral intervals with erect scales. Erect elytral scales evenly distributed, not concentrated in bundle. Scutellum not distinct. Femora each with prominent tooth. Prosternal cavity prominent and with steep lateral ridges. Metaventrite with small tubercle between meta- and mesocoxae, not a distinct transverse ridge.

Distribution. This species is currently only known from Gunung Mulu National Park, Borneo, Malaysia.

Etymology. The specific name *darlingi* honors the collector of the type series, Christopher Darling (Royal Ontario Museum), for his contributions to entomology in southeast Asia. It is a genitive, invariable.

Aphanerostethus decoratus Lewis & Kojima, sp. nov.

https://zoobank.org/DDA220E8-BD2E-4EFE-998C-E0848B431F6B

Figs 4E, 10D, 11B, 14C, D

Specimens examined. ***Holotype*: Malaysia:** • Cameron Highlands, 2.IV.1990, J. Mateu, deposited in KUM, JHLHY_DAR_079.

Diagnosis. Body length 2.2 mm. Cuticle covered in dark to pale brown scales, with distinct, dark, V-shaped band across anterior part of elytra. Funicle with six articles. Procoxae contiguous. Prosternal cavity prominent and with steep lateral ridges. Only odd-numbered elytral intervals with erect scales. Elytral scales concentrated in bundle on first interval at midpoint. Scutellum prominent. Femora with large ventral tooth at midpoint. Metaventrite with a distinct elevated transverse ridge separating the meta- and mesocoxae.

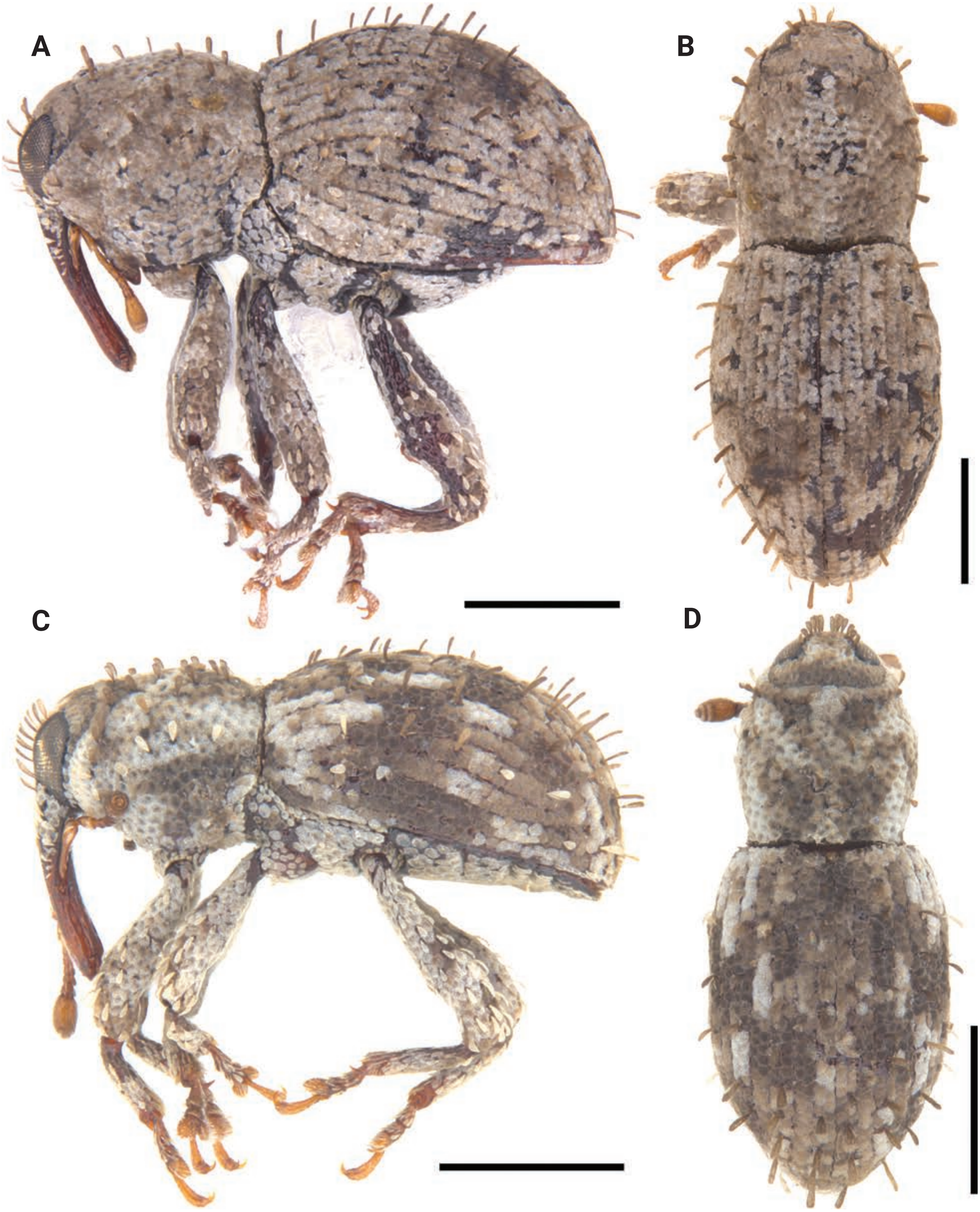

Figure 16. Lateral and dorsal photographs of *Aphanerostethus* species **A, B** *A. darlingi* sp. nov. (JHLHY_DAR_126) **C, D** *A. japonicus* sp. nov. (OKENT0055168). Scale bars: 0.5 mm.

Distribution. This species is currently only known from one specimen collected at Cameron Highlands, Malaysia.

Etymology. The specific name *decoratus* is a Latin participle in reference to the posterior half of the elytra which is adorned with a dense tuft of erect scales.

Aphanerostethus distinctus (Morimoto & Miyakawa, 1985), comb. nov.

Figs 1E–H, 3, 5A–C, 10E, 15C, D, 17A, B, 18A

Darumazo distinctus Morimoto & Miyakawa, 1985.

Specimens examined. ***Holotype*: Japan: Tokyo City:** • Miyake Island, Sabigahama, 2.V.1975, T. Mikage, deposited in ELKU, JHLHY_DAR_002. ***Paratypes*: Japan: Kagoshima Prefecture:** • Akuseki Is., 24.IV.1971, M. Sakai, (1, KUM), JHLHY_DAR_069; • **Nagasaki Prefecture:** Nagasaki City, Mt. Kompira, 25.III.1953, H. Kamiya, (1, KUM), JHLHY_DAR_003; • **Okinawa Prefecture:** Iriomote Is., Ushikumori, 9.III.1964, Y. Miyatake, (1, KUM), JHLHY_DAR_009; • Yonaguni Is., Sonai, 25–29.VIII.1969, H. Makihara, (1, KUM), JHLHY_DAR_010; • **Tokyo City:** Izu Oshima Is., Sashikiji, 3.V.1979, S. Miyakawa, (1, PCHY), JHLHY_DAR_004; • Izu Oshima Is., Mt. Atagoyama, 30.IV.1979, S. Miyakawa, (1, KUM), JHLHY_DAR_005; • Miyake Is., Sabigahama, 2.V.1975, T. Mikage, (1, KUM), JHLHY_DAR_006; • Aogashima Is., Ike no Sawa, 23.V.1979, J. Okuma, (1, KUM), JHLHY_DAR_007; • Hachijo-jima Is., Mihara rindo, 20.IV.1978, S. Miyakawa, (1, KUM), JHLHY_DAR_008; • Miyake Is., Nanto rindo, 27.IV.1978, Jun Okuma, (1, KUM), JHLHY_DAR_068.

Non-type material examined. Japan: Fukui Prefecture: • Mikata-chou, Ongami Is., 5.X.1986, T. Ueno, (1, KUM), JHLHY_DAR_071, JHLHY_DAR_072. **Kagoshima Prefecture:** • Iwayadomari, Kuchinoerabu-jima Island, 28.VII.2013, H. Kojima, on *Boehmeria* sp., (50, TUA), JHLHY_DAR_200 – JHLHY_DAR_249; • Sato, Nakanoshima Is., 7–9.VII.2019, S. Imada, (1, KUM), JHLHY_DAR_067; • Yoriki, Nakanoshima Island, 15.III.2013, H. Kojima, (2, TUA), JHLHY_DAR_105 (EGP0160C05), JHLHY_DAR_143; • Mt. Otake, Nakanoshima Island, 13–16.III.2013, H. Kojima, (3, TUA), JHLHY_DAR_144; • Ookizaki, Nakanoshima Island, 30.IX.2015, H. Kojima, (1, TUA), JHLHY_DAR_145; • Mt. Negamiyama, Akuseki Island, 7–8.III.2013, H. Kojima, (2, TUA), JHLHY_DAR_146, JHLHY_DAR_147; • Mt. Birouyama, Akuseki Island, 6–8.III.2013, H. Kojima, (4, TUA), JHLHY_DAR_106 (EGP0160C06), JHLHY_DAR_148 – JHLHY_DAR_150; **Okinawa Prefecture**: • Kunigami, 20.IV.–12.VI.2006, H. Goto, (1, FFPRI), JHLHY_DAR_011; • Okinawa Is., Kunigami, Oku (26.83604°N, 128.27191°E), 27.V.–10.VI.2016, L. Iha, S. Iriyama, (1, OIST), OKENT0089219, EGP0160B10; • same locality, 8–22.VII.2016, Y. Tamaki, I. Maehira, (4, OIST), OKENT0089411–OKENT0089414, EGP0160B09; • Okinawa Is., Kunigami, Oku (26.83630°N, 128.27051°E), 8–22.VII.2016, Y. Tamaki, I. Maehira, (3, OIST), OKENT0087604–OKENT0087606; • same locality, 22.VII.–5.VIII.2016, T. Kinjo, K. Uekama, (1, OIST), OKENT0087637; • same locality, 5–19.VIII.2016, Y. Tamaki, K. Uekama, (1, OIST), OKENT0087658; • same locality, 19.VIII–2.IX.2016, K. Uekama, T. Yoshida, (1, OIST), OKENT0087677; • Iriomote Is., Funaura, 8.X.1977, S. Azuma, (1, RUMC), JHLHY_DAR_020; • Iheya Is., Koshi-dake, 4.V.1988, T. Ueno, (1, KUM), JHLHY_DAR_060; • Yonaguni Is., Mt. Urabu, 29.XII.1988, T. Ueno,

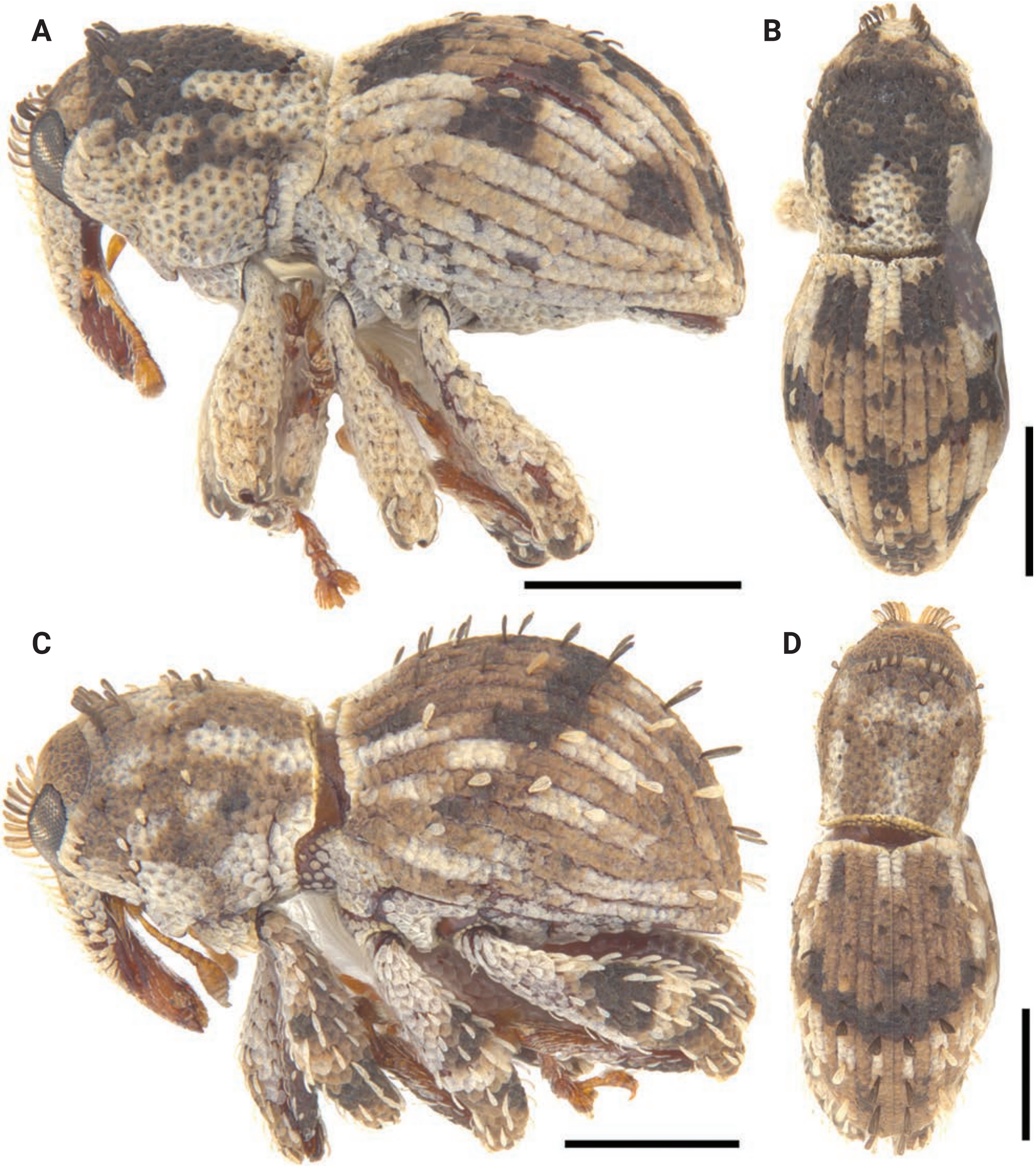

Figure 17. Lateral and dorsal photographs of *Aphanerostethus* species **A, B** *Aphanerostethus distinctus* (Morimoto & Miyakwa, 1985) (OKENT0087605) **C, D** *Aphanerostethus falcatus* sp. nov. (JHLHY_DAR_167). Scale bars: 0.5 mm.

(2, KUM), JHLHY_DAR_061, JHLHY_DAR_073; • Yonaguni Is., Mt. Kubura-dake, 26–31.III.1997, Tadashi Ishikawa, (1, PCHY), JHLHY_DAR_062; • same locality, 6.VII.1993, K. Shigematsu, (2, TUA), JHLHY_DAR_151, JHLHY_DAR_152; • Ishigaki Is., Nosko, Mt. Nosoko-dake, 24.4889°N, 124.2487°E, 16.III.2013, H. Yoshitake, (2, PCHY), JHLHY_DAR_063 (EGP0160E07), JHLDAR_DAR_064 (EGP0160E08); **Tokyo City:** • Hachijo-jima Is., 25.X.1962, R. Aoki, (1, KUM), JHLHY_DAR_128.

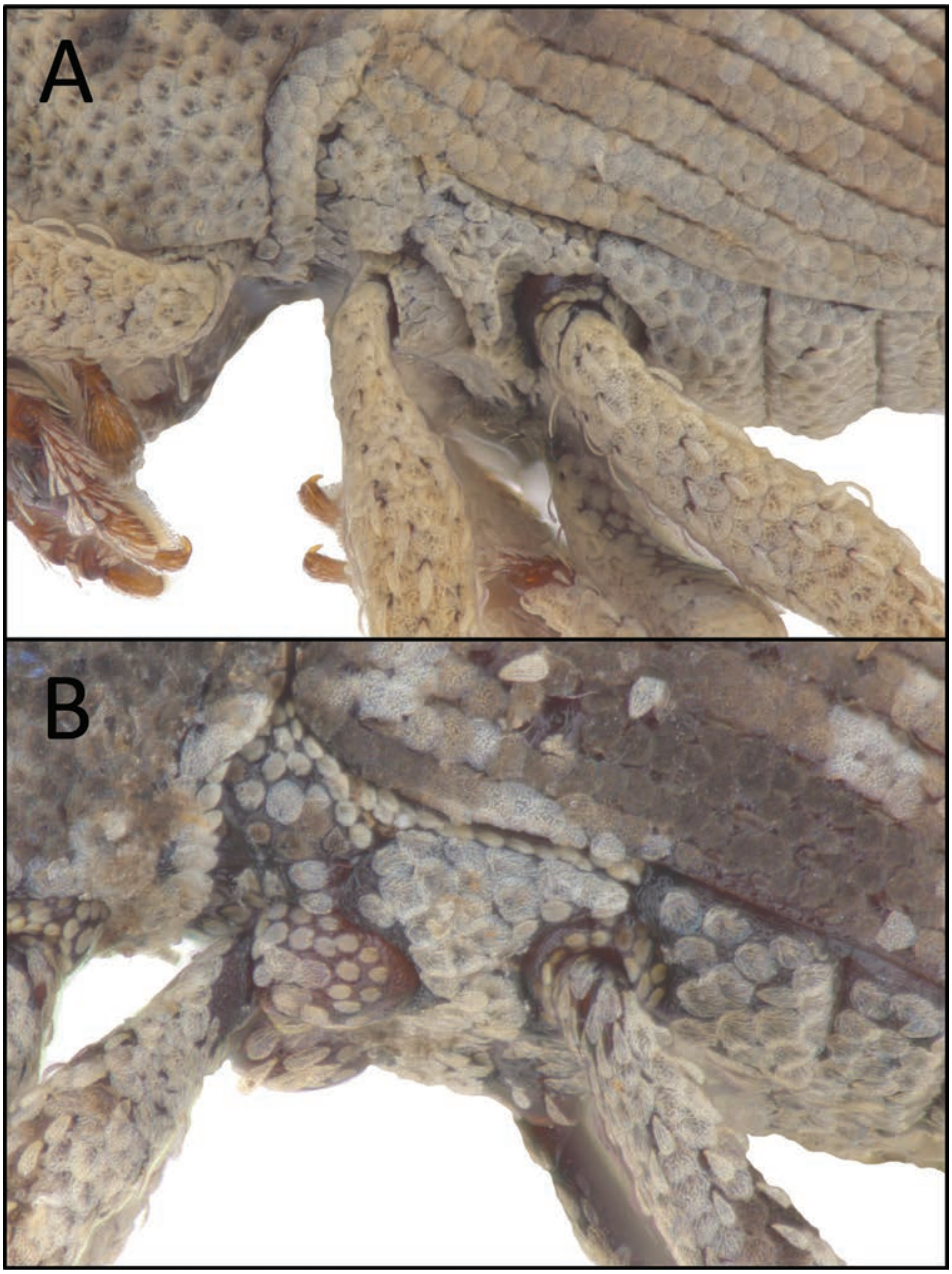

Figure 18 A Prominent ridge between meso- and metacoxae (*Aphanerostethus distinctus* (Morimoto & Miyakawa, 1985), OKENT0087604) **B** No prominent ridge between meso- and metacoxae (*A. japonicus* sp. nov., OKENT0055168).

Diagnosis. Body length 1.5–2.0 mm. Cuticle coated in dark, sandy gray, and white scales in contrasting pattern. Funicle with six articles. Procoxae contiguous. Only odd-numbered elytral intervals with recumbent scales. Erect elytral scales evenly distributed, not concentrated in bundle. Femora without ventral teeth. Scutellum reduced. Aedeagus short, with two sclerotized structures apico-laterally (one on each side) in internal sac. Prosternal cavity prominent and with steep lateral ridges. Metaventrite with a distinct elevated transverse ridge separating the meta- and mesocoxae (Fig. 18A). Metatibial uncus simple in both sexes (Fig. 1E–H). Aedeagus weakly tapering in apical half, and evenly curved in lateral view (Fig. 15C, D). Internal sac lacking prominent basal protruding structure (Fig. 15C, D).

Distribution. This species is currently known from the Izu Islands (Miyake Is., Hachijo-jima Is., Aogashima Is.), Nagasaki Prefecture, Fukui Prefecture, Kagoshima Prefecture (Nakanoshima), and the Ryukyu Islands (Okinawa Is., Ishigaki Is., Yonaguni Is.) (Kojima and Morimoto 2004; Lewis and Yoshitake 2022). The *A. distinctus* records from Taiwan in Alonso-Zarazaga et al. (2023) and Kojima and Morimoto (2004) are more likely *A. taiwanus* as no specimens of *A. distinctus* were encountered in examined collections.

Comments. Fujii et al. (2012) reared *A. distinctus* from the galls of *Asteralobia sasakii* (Monzen, 1937) on *Ilex crenata* Thunb. var. *hachijoensis* Nakai, and Kojima (2013) reared specimens from the galls of *A. sasakii* on *Ilex integra* Thunb. Kojima (2014) also collected 50 specimens from *Boehmeria* sp. on Kuchinoerabu-jima Island. On Okinawa Island, specimens of *A. distinctus* were only collected from Oku, Yambaru National Park (Lewis and Yoshitake 2022) despite several years of continuous, year-long malaise trapping at 24 sites (3 traps per site) across the island. This suggests that *A. distinctus* is sensitive to anthropogenic disturbance and, coupled with the apparent cecidophagous habits of the species, may be the reason for its relative rarity in collections.

Aphanerostethus falcatus **Kojima, Lewis & Fujisawa, sp. nov.**

https://zoobank.org/8C985A03-E302-41EA-9754-B9F58E9B0E01

Figs 1I–L, 3, 5D–F, 10B, 15E, F, 17C, D

Specimens examined. ***Holotype*****: Vietnam: Lam Dong Province:** • Mount Lang Biang, 12°02'N, 108°26'E, elevation 1700 m, 18.II.2011, H. Kojima, male deposited in TUA, JHLHY_DAR_153. ***Paratypes*****: Vietnam: Lam Dong Province:** • Mount Lang Biang, 12°02'N, 108°26'E, elevation 1700 m, 17–18.II.2011, H. Kojima, (21, TUA; 1 OIST), JHLHY_DAR_094, JHLHY_DAR_096 (EGP0160D01), JHLHY_DAR_097, JHLHY_DAR_099, JHLHY_DAR_110 (EGP0160C12), JHLHY_DAR_112 (EGP0160D02), JHLHY_DAR_116 (EGP0160D10), JHLHY_DAR_117 (EGP0160D09), JHLHY_DAR_119 (EGP0160D07), JHLHY_DAR_154 – JHLHY_DAR_166; • near Phi Lieng, Lam Ha, 21.II.2011, H. Kojima, (1, TUA), JHLHY_DAR_118 (EGP0160D11); • Da Knang, Dam Rong District, 23.II.2013, H. Kojima, (1, TUA), JHLHY_DAR_122 (EGP0160E01); • same locality, 2.III.2014, Y. Fujisawa, (1, TUA); • Mount Lang Biang, 12°02'N, 108°26'E, elevation 1700 m, 20–26.II.2013, H. Kojima, (18, TUA; 2, OIST), JHLHY_DAR_091, JHLHY_DAR_109 (EGP0160D04), JHLHY_DAR_168 – JHLHY_DAR_179, JHLHY_DAR_181 – JHLHY_DAR_186.

Diagnosis. Body length 1.7–2.1 mm. Cuticle coated in dark, sandy gray, and white scales in indistinct pattern. Funicle with six articles. Procoxae contiguous. Only odd-numbered elytral intervals with erect scales. Erect elytral scales evenly distributed, not concentrated in bundle. Elytral interval 5 + 6 not distinctly arched at base. Hind femora with distinct tooth along ventral edge. Fore- and mid-femur with minute tooth. Scutellum reduced. Prosternal cavity prominent and with steep lateral ridges. Metaventrite with a distinct elevated transverse ridge separating the meta- and mesocoxae. Metatibial uncus sickle-shaped in male (Fig. 1I–L). Aedeagus tapering over apical half, and swelling at tip (Fig. 15E, F), unevenly curved in lateral view; clearly bent ventrally at apex (Fig. 15E, F). Internal sac with basal protruding structure (Fig. 15E, F).

Distribution. This species is currently only known from Lam Dong Province (Mt. Lang Biang, Phi Lieng, and Da Knang), Vietnam.

Etymology. The specific name *falcatus* is a Latin adjective in reference to the sickle-shaped metatibial uncus of males (Fig. 1I–L).

Aphanerostethus incurvatus Kojima & Lewis, sp. nov.

https://zoobank.org/D8E5DE1D-E198-4A13-99CC-4BBFDE3395BF
Figs 1M–P, 3, 6A, B, 15G, H, 19A, B

Specimens examined. ***Holotype*: Vietnam:** • Lam Dong Province, Mount Lang Biang, 12°02'N, 108°26'E, elevation 1700 m, 17.II.2011, H. Kojima, male deposited in TUA, JHLHY_DAR_095. ***Paratypes*: Vietnam:** • Lam Dong Province, Mount Lang Biang, 12°02'N, 108°26'E, elevation 1700 m, 17.II.2011, H. Kojima, (1, TUA), JHLHY_DAR_104 (EGP0160C11); • same locality, 17.II.2011, H. Kojima, (1, TUA), JHLHY_DAR_100 (EGP0160D06).

Diagnosis. Body length 1.7–2.1 mm. Cuticle coated in dark, sandy gray, and white scales in indistinct pattern. Funicle with six articles. Procoxae contiguous. Only odd-numbered elytral intervals with erect scales. Erect elytral scales concentrated in bundle along third elytral interval at midpoint; evenly distributed along other intervals. Elytral interval 5 + 6 distinctly arched at base. Femora all with large tooth along ventral edge. Scutellum reduced. Prosternal cavity prominent and with steep lateral ridges. Metaventrite with a distinct elevated transverse ridge separating the meta- and mesocoxae. Metatibial uncus curved inwards, and with minute black tubercles at base in males (Fig. 1M–P). Aedeagus evenly curved in lateral half, and in lateral view (Fig. 15G, H). Internal sac with U-shaped, basal protruding structure (Fig. 15G, H).

Distribution. This species is currently only known from Mount Liang Bang, Lam Dong Province, Vietnam.

Etymology. The specific name *incurvatus* is a Latin participle in reference to the incurved metatibial uncus of males (Fig. 1M–P).

Aphanerostethus japonicus Lewis & Kojima, sp. nov.

https://zoobank.org/48E49909-06AB-42CD-AEC0-F3D68AE8D359
Figs 3, 6C–F, 11C, 13F, 15I, J, 16C, D, 18B

Specimens examined. ***Holotype*: Japan: Miyazaki Prefecture:** • Gokase-chou, Shiraiwa-yama, 6.V.2009, Y. Tsutsumiuchi, male deposited in KUM, JHLHY_DAR_052. ***Paratypes*: Japan: Ehime Prefecture:** • Odamiyama, 2.IV.1986, E. Yamamoto, (1, KUM), JHL_SYN_197; **Kagawa Prefecture:** • Shionoe-chou, Ootaki-yama, 11.VII.1992, K. Kume, (1, KUM), JHLHY_DAR_053; **Miyazaki Prefecture:** • Gokase-chou, Shiraiwa-yama, 6.V.2009, Y. Tsutsumiuchi, (3, KUM; 1, OIST), JHLHY_DAR_048 – JHLHY_DAR_051; • Gokase, Mt. Mokouzaka, 17.VI.2017, R. Ito, (4, KUM), JHLHY_DAR_059 (EGP0160E04), JHL_SYN_194 – JHL_SYN_196; • Mt. Goyodake, Hinokage, 15.VII.2018, R. Ito, (1, KUM), JHL_SYN_199; **Oita Prefecture:** • Saiki-shi, Fujigawachi-keikoku, 10.IX.2017, R. Ito, (2, KUM), JHLHY_DAR_054, JHLHY_DAR_055; • Saiki-shi, Fujigawachi-keikoku, 18.V.2018, R. Ito, (3, KUM), JHLHY_DAR_056 – JHLHY_DAR_058, EGP0160E05;

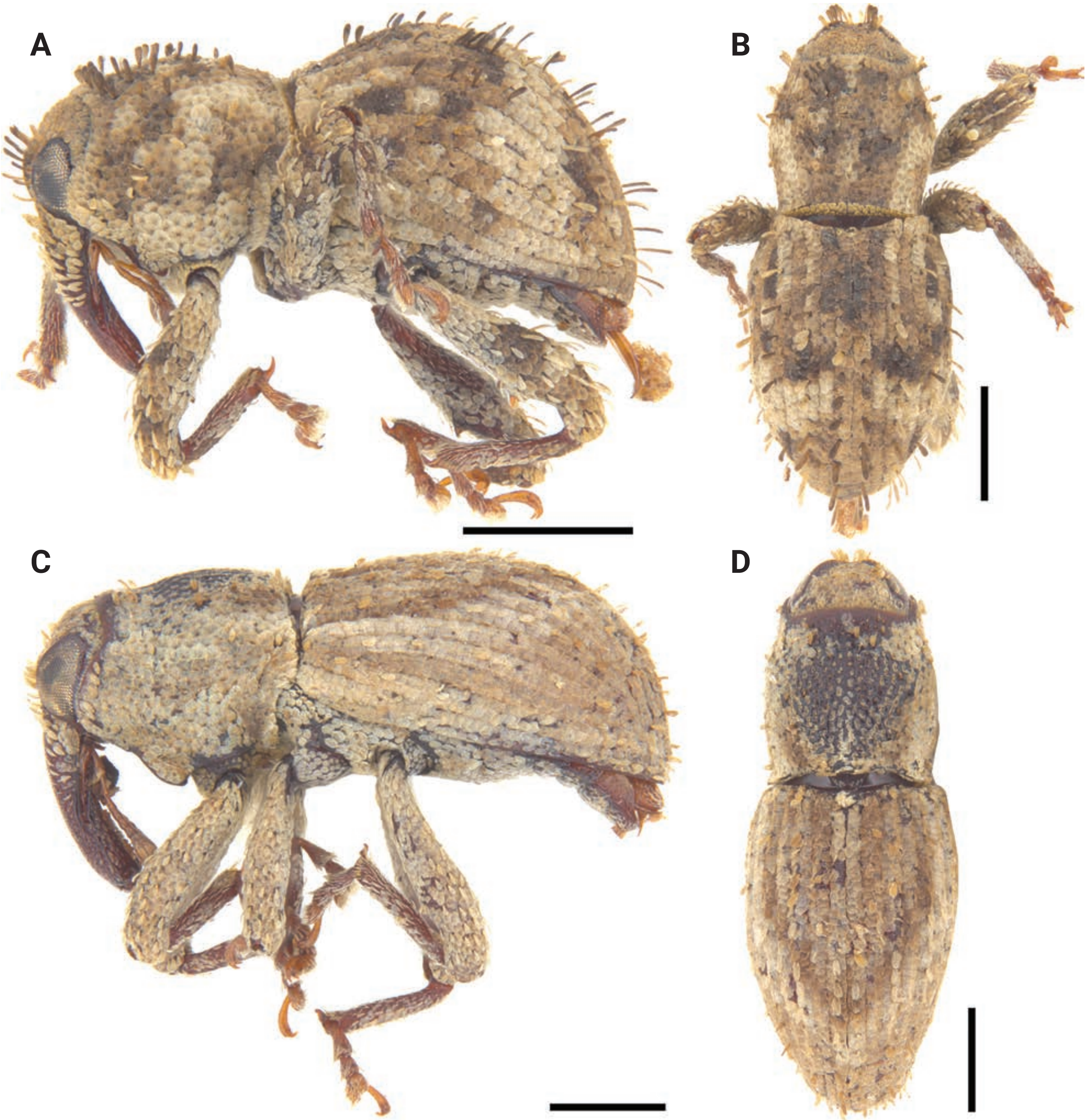

Figure 19. Lateral and dorsal photographs of *Aphanerostethus* species **A, B** *Aphanerostethus incurvatus* sp. nov. (JHLHY_DAR_095) **C, D** *Aphanerostethus magnus* sp. nov. (JHLHY_DAR_023). Scale bars: 0.5 mm.

Okinawa Prefecture: • Okinawa Island, Kunigami, Yona Field (26.73894°N, 128.23720°E), 10–24.VI.2016, L. Iha, T. Kinjo, (1, OIST), OKENT0062435; • Okinawa Island, Kunigami, Yona Field (26.73894°N, 128.23720°E), 5–19.II.2016, L. Iha, T. Kinjo, (1, OIST), OKENT0055232 (EGP0160B12); • Okinawa Island, Kunigami, Yona Field (26.73894°N, 128.23720°E), 22.VII.–5.VIII.2016, T. Kinjo, K. Uekama, (1, OIST), OKENT0055516 (EGP0160B11); • Okinawa Island, Kunigami, Yona Field (26.73894°N, 128.23720°E), 27.XI.–11.XII.2015, Y. Tamaki, S. Iriyama, T. Yoshida, (1, OIST), OKENT0055168; **Tokushima Prefecture:** • Mima-gun, Tsurugi-chou, Ichiu, 33°53'N, 134°4'E, 31.VII.2011, K. Kume, (4, KUM; 1, OIST), JHLHY_DAR_037 – JHLHY_DAR_041; • Mt. Tomaru, Tsurugi-chou, 27.VII.2014, K. Kanno, (1, KUM), JHL_SYN_198; • Nishiiyayama-son, 33°58'N, 133°4'E, 4.VIII.2021, K. Kume, (1, KUM), JHLHY_DAR_042; • Miyoshi-shi, Mikamo-chou, Furonto, 22.VII.2012, K. Kume, (4, KUM; 1, OIST), JHLHY_DAR_043 – JHLHY_DAR_047 (EGP0160F03).

Diagnosis. Body length 1.4–1.7 mm. Cuticle coated in crusty dark, sandy gray, and white scales in weakly defined pattern. Funicle with six articles. Procoxae contiguous. Eyes not dimorphic (separated in both sexes). Only odd-numbered elytral intervals with erect scales. Erect elytral scales evenly distributed, not concentrated in bundle. Scutellum distinct. Femora each with low, obtuse tooth ventrally. Prosternal cavity very weakly defined and without steep lateral ridges. Metaventrite flattened between meta- and mesocoxae, without a distinct elevated transverse ridge. Metatibial uncus simple in both sexes. Aedeagus rounded in lateral half (Fig. 15I, J). Internal sac with basal protruding structure (Fig. 15I, –J).

Distribution. This species is currently only known from Japan, north from Tokushima Prefecture and Kagawa Prefecture, and in the Ryukyu Islands from Okinawa Prefecture (Yambaru National Park).

Etymology. The specific name *japonicus* is a Latin adjective in reference to the country of collection. We also suggest the Japanese common name ニッポンダルマクチカクシゾウムシ [Nippon-daruma-kuchi-kakushi-zômushi], which translates in English to “Japanese daruma cryptorhynchine weevil”.

Variation. Specimens of *A. japonicus* from Okinawa Island are noticeably slenderer than those collected on the mainland, but are otherwise indistinguishable and do not possess any structural characters that would support treating these as different species.

Comments. The exact phylogenetic relationship of *A. japonicus* (along with *A. nudus* and *A. armatus*) to typical *Aphanerostethus* (i.e., those possessing a prominent prosternal canal and ridge between the meso- and metacoxae) remains uncertain given that the molecular data presented here does not clearly suggest whether they represent a lineage nested within or sister to typical *Aphanerostethus* (see Fig. 3). However, the fact that *A. nudus* possesses dimorphic metatibial uncus, a character which occurs sparsely in weevils, is significant and further supports the association of typical *Aphanerostethus* and the *A. nudus* group.

Like *A. distinctus* (see Comments under *A. distinctus*), this species was only collected from one site (Yona, Yambaru National Park) on Okinawa Island despite several years of malaise trapping at twenty-four sites across the island suggesting that it is also sensitive to anthropogenic disturbance.

Aphanerostethus magnus Lewis & Kojima, sp. nov.

https://zoobank.org/CD1F7D2D-F57F-4C51-A6F3-9D971B75A03C

Figs 2A–D, 3, 7A–C, 11D, 13C, D, 15K, L, 19C, D

Specimens examined. ***Holotype*: Japan: Kagoshima Prefecture:** • Nakanoshima Is., 1–2.V.1975, H. Irie, male deposited in KUM, JHLHY_DAR_023. ***Paratypes*: Japan: Kagoshima Prefecture:** • Nakanoshima Is., 1–2.V.1975, H. Irie, (4, KUM; 1, OIST), JHLHY_DAR_022, JHLHY_DAR_024 – JHLHY_DAR_026, JHLHY_DAR_076; • same locality, 7.VII.1974, J. Okuma, (2, KUM), JHLHY_

DAR_027, JHLHY_DAR_028; • same locality, 5.VIII.1989, T. Ueno, (2, KUM; 1, OIST), JHLHY_DAR_029–JHLHY_DAR_031; • same locality, 28.V.1962, M. Sato, (1, KUM), JHLHY_DAR_034; • Nakanoshima, Sato, 7.VII.1974, J. Okuma, (1, KUM), JHLHY_DAR_032; • Nakanoshima, Satsuda, 14.VII.1982, Y. Takai, (1, KUM), JHLHY_DAR_033; • Nakanoshima, 29.IV.1987, S. Nomura, (1, KUM), JHLHY_DAR_075; • Nakanoshima, 14.VII.1986, H. Fujita, (1, HUM), JHLHY_DAR_141; • Nakanoshima, 6.VI.1953, (1, HUM), JHLHY_DAR_142; • Nakanoshima, 21.VII.1969, M. Sakai, (2, KUM), JHLHY_DAR_139, JHLHY_DAR_140; • Nakanoshima, entrance of Mt. Otake-tozandoro, 2.X.2015, H. Kojima, (1, TUA), JHLHY_DAR_108, EGP0160C08; • Kuchinoshima, Seranma, 5.V.2013, H. Kojima, (1, TUA), JHLHY_DAR_107, EGP0160C07; **Kouchi Prefecture**: • Okinoshima Is., 31.VII.1953, K. Morimoto, (1, KUM), JHLHY_DAR_035; **Taiwan: Kaohsiung City:** • Liouguei District, Zhong-Xing-Long Li, near Mt. Taiyuanshan, 19.X.2015, H. Yoshitake, (2, NMNST), JHLHY_DAR_065 (EGP0160E09), JHLHY_DAR_066 (EGP0160E10).

Diagnosis. Body length 2.6–3.0 mm. Cuticle covered in dark to pale brown scales, with dark, V-shaped band across anterior part of elytra. Procoxae contiguous. Funicle with six articles. Second and odd-numbered elytral intervals with erect scales. Erect elytral scales variably concentrated in bundle on first elytral interval at apex of V-shaped band. Scutellum prominent and bulging. Elytral intervals moderately convex. Femora all with ventral tooth along ventral edge at midpoint. Prosternal cavity prominent and with steep lateral ridges. Metaventrite with a distinct elevated transverse ridge separating the meta- and mesocoxae. Metatibial uncus C-shaped in male (Fig. 2A–D). Aedeagus tapering in lateral half and weakly subquadrate at apex (Fig. 15K, L). Internal sac lacking prominent basal protruding structure (Fig. 15K, L).

Distribution. This species is known from Nakanoshima Is. (Kagoshima Prefecture) and Okinoshima Is. (Kouchi Prefecture), Japan, as well as Zhong-Xing-Long Li (Liouguei District), Taiwan.

Etymology. The specific name *magnus* is a Latin adjective in reference to the distinctly large body size and elongate aedeagus of this species. We suggest the Japanese common name オオダルマクチカクシゾウムシ [Oo-daruma-kuchi-kakushi-zômushi], which translates in English to “Big daruma cryptorhynchine weevil”.

Comments. This species is closely allied with *A. bifidus*, a phylogenetic hypothesis which is also strongly supported by our molecular phylogenetic analysis (BS: 95, PP: 1). Both *A. bifidus* and *A. magnus* exhibit the same distinctive brown scaling pattern, similarity in metatibial uncus morphology, and general appearance. *Aphanerostethus magnus* is present in the Osumi and Tokara Islands and Taiwan, but apparently absent from the more southern Nansei Island groups such as the Amami Islands, the Okinawa Islands, and the Sakishima Islands. This peculiar distributional pattern occurs in a number of other weevil species, such as *Acicnemis sauteri* Hubenthal, 1917, *Dendropemon japonicus* (Morimoto, 1979), *Orychodes planicollis* (Walker, 1859), and *Stiboderes impressus* (Jordan, 1912) (Kojima and Morimoto 2004), and possibly is explained by climatic and floristic differences between these regions as there are few large mountains in the Nansei Islands south of the Tokara Islands that could harbor high-altitude or more northerly distributed species.

Aphanerostethus morimotoi Kojima & Lewis, sp. nov.

https://zoobank.org/CA175CD9-FD04-45A7-A32C-3B71D07D11C0
Figs 2E–H, 3, 7D–F, 10C, 15M, N, 20A, B

Specimens examined. ***Holotype*: Vietnam:** • Lam Dong Province, Mount Lang Biang, 12°02'N, 108°26'E, elevation 1700 m, 27.II.2011, H. Kojima, male deposited in TUA, JHLHY_DAR_093. ***Paratypes*: Vietnam:** • Lam Dong Province, Mount Lang Biang, elevation 1640–2000 m, 21–27.II.2013, H. Kojima, (2, TUA; 1, OIST;

Figure 20. Lateral and dorsal photographs of *Aphanerostethus* species **A, B** *Aphanerostethus morimotoi* sp. nov. (JHLHY_DAR_093) **C, D** *Aphanerostethus spinosus* sp. nov. (JHLHY_DAR_077). Scale bars: 0.5 mm.

1, KUM), JHLHY_DAR_113 – JHLHY_DAR_115 (EGP0160D03, EGP0160D08, EGP0160D12), JHLHY_DAR_187; • Lam Dong Province, Mount Lang Biang, 12°02'N, 108°26'E, elevation 1700 m, 17–18.II.2011, H. Kojima, (3, TUA; 1, OIST), JHLHY_DAR_111 (EGP0160D05), JHLHY_DAR_188 – JHLHY_DAR_190.

Diagnosis. Body length 1.8–2.0 mm. Cuticle coated in dark, sandy gray, and white scales in indistinct pattern. Funicle with six articles. Procoxae contiguous. Only odd-numbered elytral intervals with erect scales. Erect elytral scales evenly distributed along intervals. Elytral interval 5 + 6 not distinctly arched at base. Femora with or without extremely minute tubercle or tooth along ventral edge. Scutellum reduced. Prosternal cavity prominent and with steep lateral ridges. Metaventrite with a distinct elevated transverse ridge separating the meta- and mesocoxae. Metatibial uncus in male curved inwards, and with minute black tubercles at base (Fig. 2E–H). Aedeagus sinuate near midpoint, and tapering prominently in lateral half (Fig. 15M, N), unevenly curved, but rather bent ventrally at apex (Fig. 15M, N). Internal sac with roughened basal protruding structure (Fig. 15M, N).

Distribution. This species is currently only known from Mount Liang Bang, Lam Dong Province, Vietnam.

Etymology. This eponym is dedicated to the late Dr. Katsura Morimoto, who pioneered the field of weevil taxonomy and amassed an invaluable specimen collection (at KUM) which we humbly make use of in this study.

Aphanerostethus nudus Lewis & Kojima, sp. nov.

https://zoobank.org/009FEE4B-6E20-47AD-AA5E-F8FDC817F490
Figs 2M–P, 8A–C, 12C, D, 15O, P

Specimens examined. ***Holotype*: Malaysia: Brinchang:** • 17.V.1973, S. Miyakawa, male deposited in KUM, JHLHY_DAR_014. ***Paratypes*: Malaysia: Brinchang:** • 17.V.1973, S. Miyakawa, (3, KUM; 1, OIST), JHLHY_DAR_012, JHLHY_DAR_013, JHLHY_DAR_015, JHLHY_DAR_074; • Pahang, Cameron Highlands, Brinchang, 18–31.VII.1992, C.W. & L.B. O’Brien, (2, OIST; 8, KUM), JHLHY_DAR_127, JHLHY_DAR_130 – JHLHY_DAR_138.

Diagnosis. Body length 1.7–1.9 mm. Cuticle dark red and largely bare; covered unevenly with yellow scales. Funicle with six articles. Procoxae contiguous. Eyes dimorphic (connected at base of rostrum in male; separated in female). All elytral intervals with erect scales. Erect elytral scales evenly distributed, not concentrated in bundle. Scutellum reduced. Femora without ventral tubercle or tooth. Prosternal cavity very weakly defined and without steep lateral ridges. Metaventrite flattened between meta- and mesocoxae, without a distinct elevated transverse ridge. Metatibial uncus weakly spiral-shaped in male (Fig. 2M–P). Aedeagus wide at midpoint, and tapering near apex (Fig. 15O, P). Internal sac with basal protruding structure (Fig. 15O, P).

Distribution. This species is currently only known from Malaysia (Brinchang).

Etymology. The specific name *nudus* is a Latin adjective that refers to the distinctly naked (unscaled) cuticle of this species.

Aphanerostethus spinosus **Lewis & Kojima, sp. nov.**

https://zoobank.org/7D1FBE1A-4F4B-423B-82D1-57D3ADE821F7

Figs 2I–L, 4F, 15Q, R, 20C, D

Specimens examined. ***Holotype*: MALAYSIA:** • Borneo Island, Sabah, Kinabalu Park Headquarters, alt. 1800–2500 m, 15.III.1993, H. Hiratate, male deposited in KUM, JHLHY_DAR_077.

Diagnosis. Body length 1.9 mm. Cuticle coated in dark, sandy gray, and white scales in indistinct pattern. Funicle with six articles. Procoxae contiguous. Second and odd-numbered elytral intervals with erect scales. Erect elytral scales concentrated in small bundles of two or three along second elytral interval at midpoint; evenly distributed along other intervals. Elytral interval 5 + 6 not distinctly arched at base. Femora all with large, acute tooth along ventral edge. Scutellum distinct, bulging, and covered in white scales. Prosternal cavity prominent and with steep lateral ridges. Metaventrite with a distinct elevated transverse ridge separating the meta- and mesocoxae. Metatibial uncus of male claw-shaped (Fig. 2I–L). Aedeagus with diagnostic, laterally expanded apex (Fig. 15Q, R). Internal sac with M-shaped, basal protruding structure (Fig. 15Q, R).

Distribution. This species is only known from one site in Kinabalu Park, Borneo.

Etymology. This specific name *spinosus* is a Latin adjective in reference to the distinctly acute, elongate tooth on the ventral side of the femora.

Comments. Although the female is unknown it is likely the case that the metatibial uncus is sexually dimorphic as in other closely related *Aphanerostethus* species.

Aphanerostethus taiwanus **Lewis, Fujisawa & Kojima, sp. nov.**

https://zoobank.org/61696EC1-39CD-4745-B798-04456E89B9A6

Figs 3, 8D–F, 10F, 15S, T, 21A, B

Specimens examined. ***Holotype*: TAIWAN:** • Tainan Hsein, Kuanzruling, 6.IV.1965, S. Ueno, male deposited in KUM, JHLHY_DAR_016. ***Paratypes*: TAIWAN:** • Taipei Hsein, Kuanzruling, Yangmingshan, 28.III.1965, Y. Hirashima (1, KUM), JHLHY_DAR_017; • Ping Tung Hsein, Kenting, 23.IV.1965, S. Miyamoto, (1, KUM), JHLHY_DAR_018; • Kaohsiung City, Liouguei District, Zhong-Xing-Long Li (near Mt. Taiyuanshan), 19.X.2015, H. Yoshitake, (1, NMNST), JHLHY_DAR_019 (EGP0160E02); • Pingtung Hsein, Kenting, 4.IV.1965, T. Saigusa (2, KUM; 1, OIST), JHLHY_DAR_021, JHLHY_DAR_036, JHLHY_DAR_070; • Pingtung City, Shan Shimen village, Mt. Kao-shih-fo, 14.VII.2014, Y. Komeda, (1, KUM), JHLHY_DAR_129; • Mudan Township, Pingtung County, 22°06'13.46"N, 120°47'33.88"E, 5.III.2016, Y. Fujisawa, (1, TUA), JHLHY_DAR_600; • Mudan Township, Pingtung County, 22°08'21.71"N, 120°51'31.23"E, 9.III.2016, Y. Fujisawa, (1, TUA), JHLHY_DAR_601; • Mudan Township, Pingtung County, 22°05'23"N, 120°47'58"E, 6.III.2016, Y. Fujisawa & S. Shimizu, (2, TUA), JHLHY_DAR_602, JHLHY_DAR_603; • Pingtung Hsein, Kenting, 22–26.II.1982, T. Lin and S.C. Lin, (8, TARI), JHLHY_DAR_083–JHLHY_DAR_090.

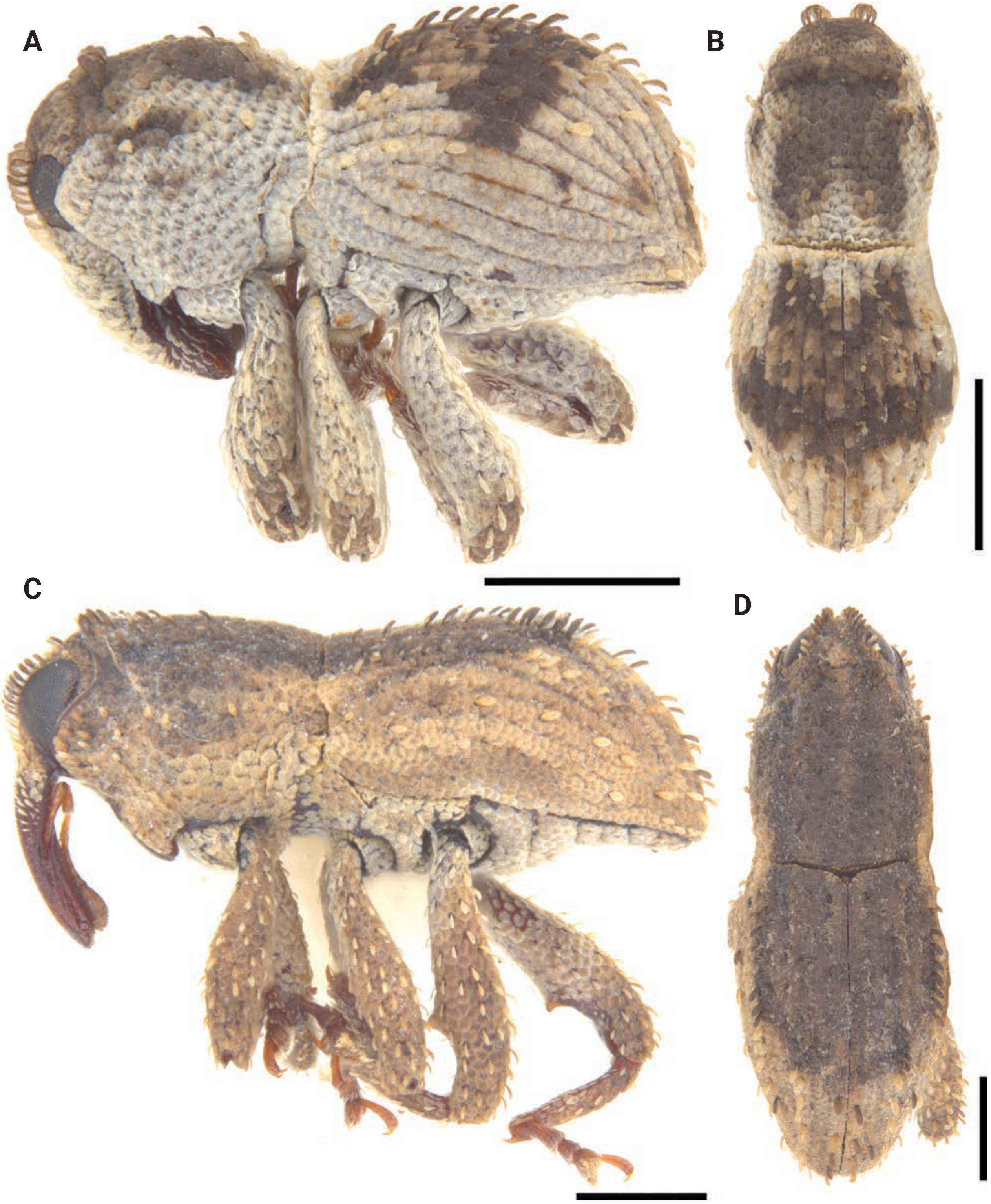

Figure 21. Lateral and dorsal photographs of *Aphanerostethus* species **A, B** *Aphanerostethus taiwanus* sp. nov. (JHLHY_DAR_084) **C, D** *Aphanerostethus vannideki* Voss, 1957 (JHLHY_DAR_081). Scale bars: 0.5 mm.

Diagnosis. Body length 1.7–1.9 mm. Cuticle coated in dark, sandy gray, and white scales in contrasty pattern. Funicle with six articles. Procoxae contiguous. Second and odd-numbered elytral intervals with sub-erect scales. Erect elytral scales evenly distributed, not concentrated in bundle. Femora without ventral teeth. Scutellum reduced. Prosternal cavity prominent and with steep lateral ridges. Metaventrite with a distinct elevated transverse ridge separating the meta- and mesocoxae. Metatibial uncus simple in both sexes. Aedeagus evenly curved at apex, and in lateral view (Fig. 15S, T). Internal sac without prominent basal protruding structure (Fig. 15S, T).

Distribution. This species is known from a few sites in Taiwan (Kuanzruling, Kenting, Zhong-Xing-Long Li).

Etymology. The specific name is an adjective in reference to the collection locality of the species.

Comments. Our ML analysis (Fig. 3) consistently clustered *A. taiwanus* with *A. distinctus* (BS: 100); however, the presumed basal position of *A. taiwanus* (i.e., sister to *A. distinctus*) was only weakly supported (BS: 55, PP: 0.84). Here, we separate *A. taiwanus* from *A. distinctus* based not on this weak molecular evidence, but primarily on consistent differences in morphology and biogeography. In particular, *A. taiwanus* possesses an oblique row of erect scales on the pronotum (*A. distinctus* with at most 4 or 5 recumbent scales), sub-erect scales on the odd and second elytral intervals (*A. distinctus* with recumbent scales only on odd elytral intervals), differences in male genitalia, and apparently non-overlapping geographic range (*A. taiwanus* only known from Taiwan; *A. distinctus* only known from Japan).

Aphanerostethus vannideki **Voss, 1957**

Figs 9A–D, 15U, V, 21C, D

Type material examined. ***Neotype*** **(designated here): Indonesia: West Java:** • Depok, 18.XII.1948, C. Van Nidek, (1, RMNH), ZMAN type COLE.1673.1, JHLHY_DAR_191, bears red label reading "PARATYPUS" as well as new, red neotype label. ***Paratypes*****: Indonesia: West Java:** • Depok, 29.II.1948, C. Van Nidek, (1, ZMH), ZMH 841850, bears red label reading "PARATYPUS"; • Depok, 12.IX.1948, C. Van Nidek, (1, ZMH), ZMH 841852, bears original red label reading "PARATYPUS".

Notable historical material examined. Indonesia: West Java: • Depok, 31.VII.1948, C. Van Nidek, (1, ZMH), ZMH 841853, bears red label reading "PARATYPUS"; • Depok, 12.I.1949, C. Van Nidek, (1, ZMH), ZMH 841851, bears red label reading "PARATYPUS".

Non-type material examined. Indonesia: West Java: • Depok, X–XII.1949, C. Van Nidek, (5, RMNH), ZMA.INS.5117697 – ZMA.INS.5117700; **Malaysia:** • Santubon, Kuching, Sarawak, 8.V.1997, T. Takano, (1, KUM), JHLHY_DAR_001; • Sepilok, Sandakan, Sabah, 23.VII–4.VIII.1981, K. Morimoto, (1, KUM), JHLHY_DAR_082; • Sabah, 10.5 miles from Keningau, 6–10.III.1993, H. Kojima, (1, KUM), JHLHY_DAR_081.

Diagnosis. Body length 2.1–2.4 mm. Cuticle covered in dark to pale brown scales, with dark, V-shaped band across anterior part of elytra. Funicle with six articles. Prosternal cavity prominent and with steep lateral ridges. Procoxae separated, and bordered posteriorly by two large projections which receive the rostrum in repose. Femora with prominent ventral teeth. Metaventrite with a distinct elevated transverse ridge separating the meta- and mesocoxae. Metatibial uncus simple in both sexes. Aedeagus tapering at apex, and abruptly curved ventrally at apex in lateral view (Fig. 15U, V).

Distribution. This species is known from Indonesia (West Java) and Malaysia (Sabah, Sarawak).

Comments. Voss (1957) mentions four type specimens in his original description, three of which (ZMH 841852, ZMH 841850, ZMAN type COLE.1673.1) were examined here, as the collection dates / locality / collector data matches the specimens listed in Voss's description. These three specimens bear red labels reading "PARATYPUS", suggesting that there is also a holotype; however, no holotype is mentioned in Voss's paper and we could not locate the holotype. Two additional specimens in the ZMH collection (ZMH 841853, ZMH 841851) with identical locality and collector data (Depok, C. Van Nidek) bear the same red paratype labels, but have the collection dates "31-7-48" and "12-1-49" which do not appear in Voss's original description. As no holotype was clearly designated, and as we were unable to locate any holotype, we hereby fix the identity of *A. vannideki* by designating one of Voss's date-verified paratypes (ZMAN type COLE.1673.1, JHLHY_DAR_191) as a neotype for this species.

Key to the species of *Aphanerostethus*

*The characters listed in this key are either clearly visible under a light microscope (i.e., external) or genital (requires dissection) in nature, and do not require the use of X-ray microtomography.

1 Prosternal cavity weak and lacking prominent lateral ridges (Fig. 13A,B); metaventrite at anterior margin of metacoxae without a distinct transverse ridge separating the meta- and mesocoxae (Fig. 18B)..................... **2**

– Prosternal cavity prominent and defined by protruding lateral ridges (Fig. 13C, D); metaventrite at anterior margin of metacoxae with a distinct transverse ridge separating the meta- and mesocoxae in most species (Fig. 18A) **4**

2 Body largely naked (dark red cuticle), except for scattered yellow and brown scales (Fig. 12C, D); erect scales on all elytral intervals; eyes dimorphic (contiguous in males, separated in females); metatibial uncus weakly spiral-shaped in male (Fig. 2M–P) .... ***A. nudus* sp. nov.**

– Body covered entirely in pale to dark gray, white, and yellowish scales (Figs 12A, B, 16C, D); erect scales only on odd elytral intervals; eyes separated to same extent in both sexes; metatibial uncus simple in both sexes **3**

3 Tooth along ventral edge of femora low and obtuse (Fig. 13F; often obscured by scales); scutellum visible; funicle with six articles .... ***A japonicus* sp. nov.**

– Tooth along ventral edge of femora elongate and thorn-like (Fig. 13E); scutellum reduced, barely visible; funicle with five articles......................... ....***A. armatus* sp. nov.**

4 Fore coxae separate; posterior edge of prosternum with large projections that receive the rostrum in repose .... ***A. vannideki* Voss, 1957**

– Fore coxae contiguous in most species (slightly separated in *A. bifidus*); posterior edge of prosternum lacking projections that receive the rostrum in repose **5**

5 Elytra with erect, sub-erect or recumbent scales on odd intervals and at least a few on second interval (worn off in some specimens) **6**

– Elytra with erect, sub-erect, or recumbent scales on odd intervals only **9**

6 Scutellum reduced and indistinct; without ventral tooth on hind femur; metatibial uncus simple (unmodified) in males .... ***A. taiwanus*** **sp. nov.**

– Scutellum large and distinct; with prominent ventral tooth on hind femur; metatibial uncus modified in males **7**

7 Smaller (1.9 mm), gray-scaled, and rounded species; metatibial uncus of male forming a large plate with a distinct apical hook (Fig. 2I–L)............... .... ***A. spinosus*** **sp. nov.**

– Larger (2.6–3.0 mm), brown-scaled, and elongate species; metatibial uncus of males bifid or ear-shaped (Figs 1A–D, 2A–D)................................. **8**

8 Metatibial uncus of male ear-shaped (Fig. 2A–D); pronotum approximately 50% the length of elytra; aedeagus (Fig. 15K–L) parallel-sided (in dorsal view), quadrate at apex, and evenly curved (in lateral view)......................... .... ***A. magnus*** **sp. nov.**

– Metatibial uncus of male bifid (Fig. 1A–D); pronotum approximately 60% the length of elytra; aedeagus (Fig. 15A, B) not parallel sided (in dorsal view), tapering at apex, and not evenly curved (in lateral view) .... ***A. bifidus*** **sp. nov.**

9 Hind-femur without ventral tooth; standing scales on odd elytral intervals curled back towards body and recumbent; metatibial uncus of male simple (unmodified) .... ***A. distinctus*** **(Morimoto & Miyakawa, 1985)**

– Hind femur with ventral tooth (minute or absent in some *A. morimotoi*); standing scales on odd elytral intervals sub-erect or erect; metatibial uncus modified in known males.. **10**

10 Larger (2.2 mm), dark brown scaled species; fore-femur with large, prominent ventral tooth; first elytral interval with prominent, dense cluster of erect scales at midpoint ....***A. decoratus*** **sp. nov.**

– Smaller (1.7–2.1 mm), grayish-scaled species; fore-femur with or without prominent ventral tooth; first elytral interval with erect scales more or less evenly distributed across elytral length **11**

11 Third elytral interval with prominent, dense cluster of 8–10 erect scales near midpoint; fore-femur with prominent ventral tooth; fifth elytral interval distinctly arched laterally at elytral base; metatibial uncus of male abruptly curved inwards at midpoint and lacking knob-like projection at apex (Fig. 1M–P)...***A. incurvatus*** **sp. nov.**

– Third elytral interval with erect scales more or less evenly distributed across elytral length; fore-femur with or without prominent ventral tooth; fifth elytral interval not arched laterally at elytral base; metatibial uncus of male unknown or not abruptly curved inwards at midpoint and with knob-like projection at apex **12**

12 Hind-femur with minute ventral tooth or small swelling; metatibial uncus of male truncated at apex and with lateral projection (Fig. 2E–H); standing scales of first and third elytral intervals short, round, sub-erect in anterior half of elytra and elongate and erect in posterior half of elytra; apex of aedeagus elongate and tapering (Fig. 15M, N) .... ***A. morimotoi*** **sp. nov.**

– Hind femur with prominent ventral tooth; standing scales of first and third elytral intervals erect throughout elytral length; apex of aedeagus tapering over apical half, and swelling at tip (Fig. 15E, F) (aedeagus unknown in *A. darlingi*) **13**

13 Metaventrite at anterior margin of metacoxae with a prominent transverse ridge separating the meta- and mesocoxae; possesses dark and pale, warm brown scales ....***A. falcatus* sp. nov.**

– Metaventrite at anterior margin of metacoxae with a minute tubercle separating the meta- and mesocoxae; with only pale gray and white scales ... .***A. darlingi* sp. nov.**

Concluding remarks

X-ray microtomography was effectively used to examine minute (< 50 µm), frequently obscured metatibial unci in fine detail, and to find stable interspecific differences in cuticle sculpturing and internal (hindwing) morphology in *Aphanerostethus* weevils. Some of these *cryptic* characters are synapomorphies for particular clades (e.g., 10th stria reduction in the *A. distinctus* / *A. taiwanus* clade), and are therefore not only useful for diagnostic purposes, but also for phylogenetics. X-ray µCT adds new dimensions (literally) to the character discovery process, and much like DNA barcoding, will inevitably become standard practice in taxonomy and phylogenetics as the technology becomes more accessible (through outsourcing for most institutions), cheaper, and faster (see van de Kamp et al. 2013). Remarkably, four new *Aphanerostethus* species described here occurred sympatrically on the same Vietnamese mountain (Mt. Lang Biang) and are currently only known from that region. Given that pockets of hitherto undescribed *Aphanerostethus* diversity like this exist, we suspect that the knowledge of *Aphanerostethus* diversity is still in the early stages and that further species will likely be uncovered in other regions. Additionally, seven of the fourteen known *Aphanerostethus* species show species-specific sexual dimorphism in the metatibial uncus (modified in males, simple in females). Many weevils (including Molytinae) possess a simple, straight or curved tooth at the apex of the metatibiae; however, in most groups the shape of this tooth does not vary significantly between sexes or species. Metatibial uncus variation has, however, been documented in several unrelated lineages and exhibit varying degrees of sexual dimorphism, interspecific variation, or both. Documented groups in which such variation occurs includes *Anthonomus* Germar, 1817 (Curculionidae: Curculioninae: Anthonomini) (Eller 1995), *Conotrachelus* Dejean, 1835 (Curculionidae: Molytinae: Conotrachelini) (Schoof 1942), *Lignyodes* Dejean, 1835 (Curculionidae: Curculioninae: Tychiini) (Clark 1980a, b; Clark and Lodos 1981), *Lissorhoptrus* (Curculionidae: Brachycerinae: Tanysphyrini) (Kuschel 1951; O'Brien and Haseeb 2014), *Plocetes* LeConte, 1876 (Curculionidae: Curculioninae: Tychiini) (Clark 1980c, 1982), *Proctorus* LeConte, 1876 (Curculionidae: Curculioninae: Ellescini) (Lewis and Anderson 2022), and *Tyloderma* Say, 1832 (Curculionidae: Molytinae: Cryptorhynchini) (Wibmer 1981). Although the independent evolution of species-specific metatibial unci in multiple weevil lineages has not been formally investigated, we suspect that, as the metatibial unci would be positioned near the rear (i.e., genitalia) of the female during copulation (Fig. 22), the unci may be used to stimulate the female (sexual selection). This selection mechanism would explain why metatibial uncus variation is apparently more common than pro- and mesotibial unci variation. Alternatively, they may provide additional gripping function during copulation (see Haley and Gray (2011) (coercion) and Harari et al. (2003) (mate

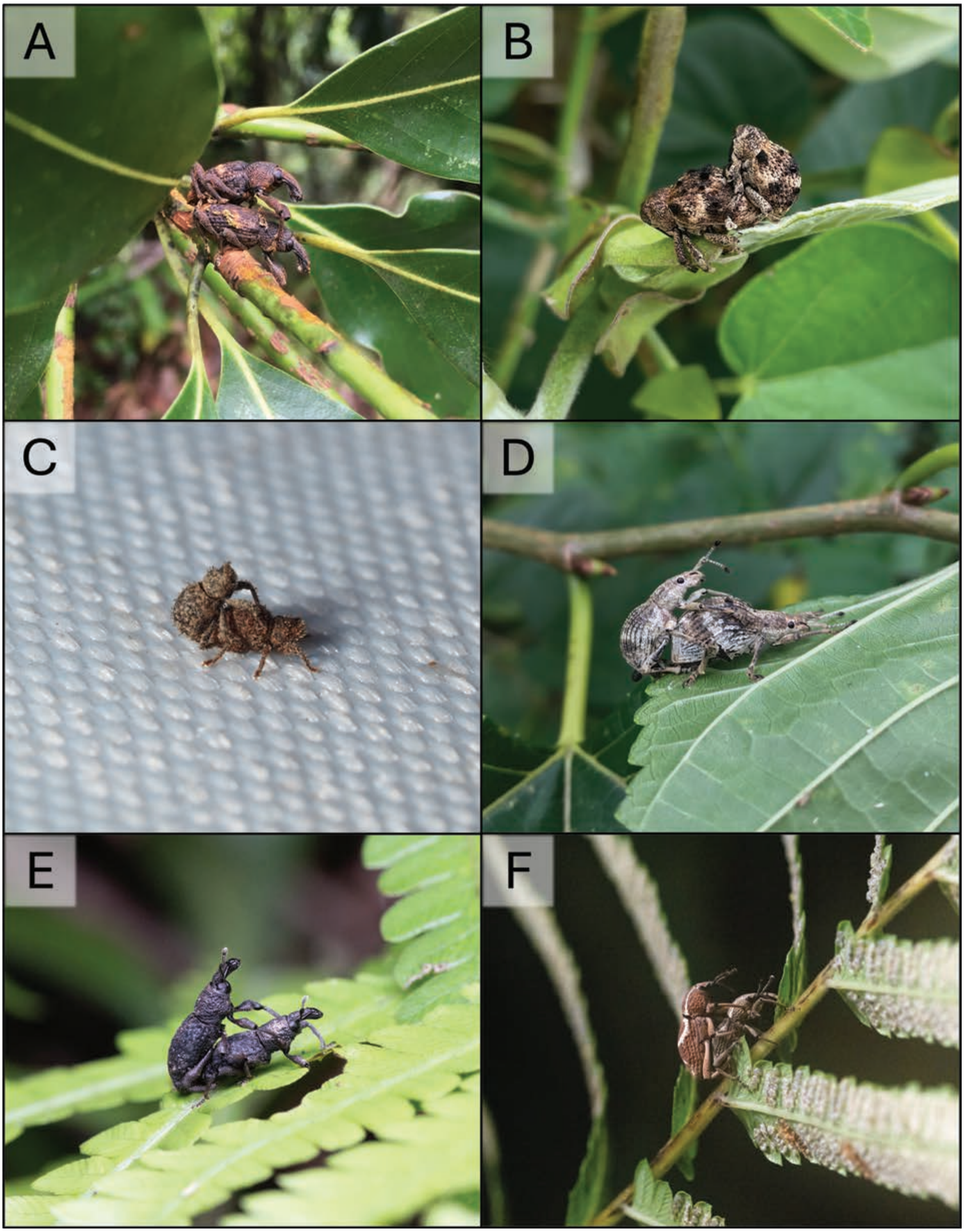

Figure 22. Weevils in copula **A** *Pimelocerus hylobioides* (Desbrochers, 1891) (Molytinae) (photo credit: JHL) **B** *Desmidophorus crassus* Hubenthal, 1917 (Brachycerinae) (photo credit: JHL) **C** *Microcryptorhynchus* sp. (Molytinae) (photo credit: HK) **D** *Episomus mori* Kono, 1928 (Entiminae) (photo credit: JHL) **E** *Euthycus* sp. (Molytinae) (photo credit: JHL) **F** *Cryptoderma kuniyoshii* Morimoto, 1978 (Dryophthorinae) (photo credit: JHL). Males often use their hindlegs to grip females from behind, and the metatibiae are usually positioned along the females ventrites or near her genitalia during copulation. The independent evolution of modified, species-specific metatibial unci in males in many weevil lineages may be explained by sexual selection (as they may be used to stimulate females) or as they provide additional gripping function during copulation.

guarding)). Careful observation of weevil mating behavior comparing lineages with and without modified metatibial unci would be lucrative and help confirm the above hypothesis.

Acknowledgements

We thank M. Maruyama, T. Mita, N. Tsuji, S. Imada (ELKU, KUM), M. Ohara (HUM), C-F. Lee (TARI), T. Sasaki (RUMC), O. Vorst, W. van Bohemen (RMNH), D. Żyła (ZMUH), H. Yoshitake (Tsukuba City), R. Anderson, A. Smith, and F. Genier (CMNC) for their assistance in preparing loans of specimens used in this project. JHL is grateful to the CMNC for providing a Beaty Centre for Species Discovery travel grant which facilitated a trip to their collection. JHL also gratefully acknowledges funding from the Natural Sciences and Engineering Research Council of Canada (NSERC PGS-D). We thank M. Alonso-Zarazaga, A. Riedel, and C. Lyal for reviewing the manuscript.

Additional information

Conflict of interest

The authors have declared that no competing interests exist.

Ethical statement

No ethical statement was reported.

Funding

No funding was reported.

Author contributions

JHL conceptualized and wrote the manuscript; HK, YF, JHL, and XLT collected specimens; MS and DP produced raw DNA sequence data; JHL performed the phylogenetic and X-ray μCT analyses; JHL and HK revised the manuscript; JHL and DLW secured funds for the project.

Author ORCIDs

Jake H. Lewis https://orcid.org/0000-0001-5147-7237
Dimitrios Petsopoulos https://orcid.org/0000-0002-4408-0458
Yusuke Fujisawa https://orcid.org/0009-0007-1758-7599
Xuan Lam Truong https://orcid.org/0000-0002-1758-903X
Dan L. Warren htt https://orcid.org/0000-0002-8747-2451 ps

Data availability

All of the data that support the findings of this study are available in the main text or Supplementary Information.

References

Achard F, Beuchle R, Mayaux P, Stibig HJ, Bodart C, Brink A, Carboni S, Desclee B, Donnay F, Eva HD, Lupi A, Rasi R, Seliger R, Simonetti D (2014) Determination of tropical deforestation rates and related carbon losses from 1990 to 2010. Global Change Biology 20(8): 2540–2554. https://doi.org/10.1111/gcb.12605

Aibekova L, Boudinot BE, Beutel RG, Richter A, Keller RA, Hita-Garcia F, Economo EP (2022) The Skeletomuscular System of the Mesosoma of *Formica rufa* Workers (Hymenoptera: Formicidae). Insect Systematics and Diversity 6(2): 1–26. https://doi.org/10.1093/isd/ixac002

Alba-Alejandre I, Alba-Tercedor J, Vega FE (2019) Anatomical study of the coffee berry borer (*Hypothenemus hampei*) using micro-computed tomography. Scientific Reports 9: 17150. https://doi.org/10.1038/s41598-019-53537-z

Alonso-Zarazaga MA, Lyal CHC (1999) A World Catalogue of Families and Genera of Curculionoidea (Insecta: Coleoptera) (excepting Scolytidae and Platypodidae). Entomopraxis, Barcelona, 315 pp.

Alonso-Zarazaga MA, Barrios H, Borovec R, Bouchard P, Caldara R, Colonnelli E, Gúltekin L, Hlavá P, Korotyaev B, Lyal CHC, Machado A, Meregalli M, Pierotti H, Ren L, Sánchez- Ruiz M, Sforzi A, Silfverberg H, Skuhrovec J, Trýzna M, Velázquez de Castro AJ, Yunakov NN (2023) Cooperative Catalogue of Palearctic Coleoptera Curculionoidea. Monografías electrónicas SEA 8. Sociedad Entomológica Aragonesa S.E.A, Zaragoza, 780 pp.

Anderson R (1993) Weevils and plants: Phylogenetic versus ecological mediation of evolution of host plant associations in Curculioninae (Coleoptera: Curculionidae). Memoirs of the Entomological Society of Canada 125(165): 197–232. https://doi.org/10.4039/entm125165197-1

Charles MA, McKenna DD (2023) Did the Functional Extinction of the American Chestnut, *Castanea dentata*, Result in the Extinction of the Greater Chestnut Weevil, *Curculio caryatrypes*? Northeastern Naturalist 30(4): 511–520. https://doi.org/10.1656/045.030.0413

Chernomor O, von Haeseler A, Minh BQ (2016) Terrace aware data structure for phylogenomic inference from supermatrices. Systematic Biology 65(6): 997–1008. https://doi.org/10.1093/sysbio/syw037

Clark WE (1980a) Revision of nearctic weevils of the genus *Lignyodes* Dejean (Coleoptera: Curculionidae). Transactions of the American Entomological Society 106(3): 273–326. https://www.jstor.org/stable/25078266

Clark WE (1980b) Revision of the weevil genus *Neotylopterus* Hustache (Coleoptera: Curculionidae). Annals of the American Entomological Society 73(2): 216–230. https://doi.org/10.1093/aesa/73.2.216

Clark WE (1980c) Additions to the neotropical weevil genus *Rosella* Whitehead (Coleoptera: Curculionidae): *R. triophori* (Gyllenhal), n. comb., transferred from *Lignyodes* Dejean, and *R. arcuata*, n. sp. The Coleopterists Bulletin 34(3): 299–304. https://www.jstor.org/stable/4000068

Clark WE (1982) Classification of the weevil tribe Lignyodini (Coleoptera, Curculionidae, Tychiinae), with revision of the genus *Plocetes*. Transactions of the American Entomological Society 108(1/2): 11–151.

Clark WE, Lodos N (1981) Notes on Turkish *Lignyodes* Dejean (Coleoptera: Curculionidae) with description of a new species. The Coleopterists Bulletin 35(3): 311–315. https://www.jstor.org/stable/4007903

Edgar RC (2004) MUSCLE: multiple sequence alignment with high accuracy and high throughput. Nucleic Acids Research 32: 1792–1797. https://doi.org/10.1093/nar/gkh340

Eller FJ (1995) A previously unknown sexual character for the Pepper Weevil (Coleoptera: Curculionidae). Florida Entomologist 78(1): 180–144. https://doi.org/10.2307/3495683

Escalona HE, Jennings D, Oberprieler R (2023) Dung-Beetle Impostor: Revision of the Australian weevil genus *Tentegia* Pascoe and the dung-rolling behaviour of *Tentegia stupida* (Fabricius) (Curculionidae: Molytinae: Cryptorhynchini). Annales Zoologici 73(1): 111–151. https://doi.org/10.3161/00034541ANZ2023.73.1.010

Estoque RC, Ooba M, Avitabile V, Hijioka Y, DasGupta R, Togawa T, Maruyama Y (2019) The future of Southeast Asia's forests. Nature Communications 10: 1829. https://doi.org/10.1038/s41467-019-09646-4

Forister ML, Novotny V, Panorska AK, Baje L, Basset Y, Butterill PT, Cizek L, Coley PD, Dem F, Diniz IR, Drozd P, Fox M, Glassmire AE, Hazen R, Hreck J, Jahner JP, Kaman O, Kozubowski TJ, Kursar TA, Lewis OT, Lill J, Marquis RJ, Miller SE, Morais HC, Murakami M, Nickel H, Pardikes NA, Ricklefs RE, Singer MS, Smilanich AM, Stureman JO, Villamarin-Cortez S, Vodka S, Volf M, Wagner DL, Walla T, Weiblen GD, Dyer LA (2014) The global distribution of diet breadth in insect herbivores. Proceedings of the National Academy of Sciences 112(2): 442–447. https://doi.org/10.1073/pnas.1423042112

Fujii T, Yoshitake H, Matsuo K, Tokuda M (2012) Collection records of *Darumazo distinctus* (Coleoptera, Curculionidae) from galls induced by *Asteralobia sasakii* (Diptera, Cecidomyiidae) on the Izu Islands, Japan. Japanese Journal of Systematic Entomology 18: 253–256.

Garcia FH, Fischer G, Liu C, Audisio TL, Economo EP (2017) Next-generation morphological character discovery and evaluation: an X-ray micro-CT enhanced revision of the ant genus *Zasphinctus* Wheeler (Hymenoptera, Formicidae, Dorylinae) in the Afrotropics. ZooKeys 693: 33–93. https://doi.org/10.3897/zookeys.693.13012

Hagge J, Seibold S, Gruppe A (2019) Beetle biodiversity in anthropogenic landscapes with a focus on spruce plantations, Christmas tree plantations and maize fields. Journal of Insect Conservation 23: 565–572. https://doi.org/10.1007/s10841-019-00146-w

Haley EL, Gray DA (2011) Mating behavior and dual-purpose armaments in a camel cricket. Ethology 118(1): 49–56. https://doi.org/10.1111/j.1439-0310.2011.01985.x

Harari AR, Lanbdolt PJ, O'Brien CW, Brockman HJ (2003) Prolonged mate guarding and sperm competition in the weevil *Diaprepes abbreviatus* (L.). Behavioral Ecology 14(1): 89–96. https://doi.org/10.1093/beheco/14.1.89

Ikeda H, Nishikawa M, Sota T (2012) Loss of flight promotes beetle diversification. Nature Communication 3: 648. https://doi.org/10.1038/ncomms1659

Jordal BH, Cognato AI (2012) Molecular phylogeny of bark and ambrosia beetles reveals multiple origins of fungus farming during periods of global warming. BMC Evolutionary Biology 12: 133. https://doi.org/10.1186/1471-2148-12-133

Kalyaanamoorthy S, Minh B, Wong T, Haeseler A, Jermiin LS (2017) ModelFinder: fast model selection for accurate phylogenetic estimates. Nature Methods 14: 587–589. https://doi.org/10.1038/nmeth.4285

Kennedy S, Calaor J, Zurápiti Y, Hans J, Yoshimura M, Choo J, Andersen JC, Callaghan J, Roderick GK, Krehenwinkel H, Rogers H, Gillespie RG, Economo EP (2023) Richness and resilience in the Pacific: DNA metabarcoding enables parallelized evaluation of biogeographic patterns. Molecular Ecology 32: 6710–6723. https://doi.org/10.1111/mec.16575

Kojima H (2013) A new host record for a cecidophagous molytine weevil, *Darumazo distinctus* (Coleoptera, Curculionidae). Elytra 3: 185–186.

Kojima H (2014) Distributional records of weevils new to the fauna of Kuchinoerabu-jima Island, the Osumi Islands, southwest Japan (Coleoptera, Curculionoidea). Elytra 4: 1–2.

Kojima H, Morimoto K (2004) An online checklist and database of the Japanese weevils (Insecta: Coleoptera: Curculionoidea) (excepting Scolytidae and Platypodidae). http://de05.digitalasia.chubu.ac.jp/index.html [accessed 3 Oct 2022]

Kundrata R, Bukejs A, Prosvirov AS, Hoffmannova J (2020) X-ray micro-computed tomography reveals a unique morphology in a new click-beetle (Coleoptera, Elateridae) from the Eocene Baltic amber. Scientific Reports 10: 20158. https://doi.org/10.1038/s41598-020-76908-3

Kuschel G (1951) Revisión de *Lissorhoptrus* LeConte y géneros vecinos de América (Ap. 11 de Coleoptera Curculionidae). Revista Chilena de Entomología 1: 23–74.

Kypke JL, Solodovnikov A (2020) Every cloud has a silver lining: X-ray micro-CT reveals *Orsunius* rove beetle in Rovno amber from a specimen inaccessible to light microscopy. Historical Biology 32(7): 940–950. https://doi.org/10.1080/08912963.2018.1558222

Letsch H, Balke M, Kusy D, McKenna DD, Narakusumo RD, Sagata K, Toussaint EFA, White LT, Riedel A (2023) Beetle evolution illuminates the geological history of the world's most diverse tropical archipelago. Ecography 12: e06898. https://doi.org/10.1111/ecog.06898

Letunic I, Bork P (2021) Interactive Tree Of Life (iTOL) v. 5: an online tool for phylogenetic tree display and annotation. Nucleic Acids Research 49(1): 293–296. https://doi.org/10.1093/nar/gkab301

Lewis JH (2023) A new species of *Karekizo* Morimoto, 1962 (Coleoptera: Curculionidae: Molytinae) from the Alishan Mountains of Taiwan and a first record of *Karekizo impressicollis* outside Japan. Zootaxa 5277(2): 381–387. https://doi.org/10.11646/zootaxa.5277.2.8

Lewis JH, Anderson RS (2022) A revision of the North American genus *Proctorus* (Coleoptera, Curculionidae, Ellescini) with descriptions of two new species. ZooKeys 1131: 135–153. https://doi.org/10.3897/zookeys.1131.90392

Lewis JH, Anderson RS (2023) A review of *Ellescus* (Coleoptera: Curculionidae) in North America: new species and synonyms revealed through integrative taxonomy. The Canadian Entomologist 155(e15): 1–27. https://doi.org/10.4039/tce.2023.2

Lewis JH, Yoshitake H (2022) New records of weevils (Coleoptera, Curculionidae) from Okinawajima Island, Japan. Elytra 12: 146–150.

Martin M (2011) Cutadapt removes adapter sequences from high-throughput sequencing reads. EMBnet journal 17.1: 10–12. https://doi.org/10.14806/ej.17.1.200

McKenna DD, Sequeira AS, Marvaldi AE, Farrell BD (2009) Temporal lags and overlap in the diversification of weevils and flowering plants. PNAS 106(17): 7083–7088. https://doi.org/10.1073/pnas.0810618106

Morimoto K (2011) Weevils of the genus *Protacalles* and its allies in Japan (Coleoptera: Curculionidae: Molytinae) (Part 1). Masumushi – Special Publication of the Japanese Society of Scarabaeoidology 1: 325–336.

Morimoto K, Miyakaw S (1985) Weevil fauna of the Izu Islands. Mushi 50(3): 19–85.

Nguyen L-T, Schmidt HA, von Haeseler A, MinhBQ (2015) IQ-TREE: A fast and effective stochastic algorithm for estimating maximum likelihood phylogenies. Molecular Biology and Evolution 32: 268–274. https://doi.org/10.1093/molbev/msu300

O'Brien CW, Haseeb M (2014) Revision of the "rice water weevils" genus *Lissorhoptrus* LeConte (Coleoptera: Curculionidae) in North America north of Mexico. The Coleopterists Bulletin 68(2): 163–186. https://doi.org/10.1649/0010-065X-68.2.163

Oberacker P, Stepper P, Bond DM, Hohn S, Focken J, Meyer V, Schelle L, Sugrue VJ, Jeunen G, Moser T, Hore SR, Meyenn F, Hipp K, Hore TA, Jurkowski TP (2019) Bio-On-Magnetic-Beads (BOMB): Open platform for high- throughput nucleic acid extraction and manipulation. PLOS Biol 17(1): e3000107. https://doi.org/10.1371/journal.pbio.3000107

Oberprieler RG, Anderson RS, Marvaldi AE (2014) 3. Curculionoidea Latreille, 1802: Introduction, Phylogeny. In: Leschen RAB and Beutel RG (Eds) Handbook of Zoology (Coleoptera, Beetles), Morphology and Systematics, Vol. 3. De Gruyter, Berlin, 285–300. https://doi.org/10.1515/9783110274462.285

Peguero G, Bonal R, Sol D, Munoz A, Sork VL, Espelta JM (2017) Tropical insect diversity: evidence of greater host specialization in seed-feeding weevils. Ecology 98(8): 2180–2190. https://doi.org/10.1002/ecy.1910

Prena J (2021) *Acythopeus glyptorhis*, a new gall-inducing weevil (Coleoptera, Curculionidae, Baridinae) damaging gac vines in Southeast Asia. Zootaxa 4981(2): 388–392. https://doi.org/10.11646/zootaxa.4981.2.10

Rambaut A, Drummond AJ, Xie D, Baele G and Suchard MA (2018) Posterior summarisation in Bayesian phylogenetics using Tracer 1.7. Systematic Biology 67(5): 901–904. https://doi.org/10.1093/sysbio/syy032

Ronquist F, Teslenko M, van der Mark P, Ayres DL, Darling A, Höhna S, Larget B, Liu L, Suchard MA, Huelsenbeck JP (2012) MRBAYES 3.2: Efficient Bayesian phylogenetic inference and model selection across a large model space. Systematic Biology 61(3): 539–542. https://doi.org/10.1093/sysbio/sys029

Rozewicki J, Li S, Amada KM, Standley DM, Katoh K (2019) MAFFT-DASH: integrated protein sequence and structural alignment. Nucleic Acids Research 47(1): 5–10. https://doi.org/10.1093/nar/gkz342

Schoof HF (1942) The genus *Conotrachelus* Dejean (Coleoptera: Curculionidae) in the north central United States. Illinois biological monographs 19(3): 1–170. https://doi.org/10.5962/bhl.title.50123

Schutte A, Stuben PE, Astrin JJ (2023) Molecular Weevil Identification Project: A thoroughly curated barcode release of 1300 Western Palearctic weevil species (Coleoptera, Curculionoidea). Biodiversity Data Journal 11: e96438. https://doi.org/10.3897/BDJ.11.e96438

Setliff GP (2007) Annotated checklist of weevils from the Papuan region (Coleoptera, Curculionoidea). Zootaxa 1536: 1–296. https://doi.org/10.11646/zootaxa.1536.1.1

Sharp AC, Barclay MVL, Chung AYC, Ewers RM (2019) Tropical logging and deforestation impacts multiple scales of weevil beta-diversity. Biological Conservation 234: 172–179. https://doi.org/10.1016/j.biocon.2019.03.024

Sprick P, Floren A (2018) Diversity of Curculionoidea in Humid Rain Forest Canopies of Borneo: A Taxonomic Blank Spot. Diversity 10(4): 116. https://doi.org/10.3390/d10040116

Su Z, Zhang R, Qiu J (2011) Decline in the diversity of willow trunk-dwelling Weevils (Coleoptera: Curculionoidea) as a result of urban expansion in Beijing, China. Journal of Insect Conservation 15(3): 367–377. https://doi.org/10.1007/s10841-010-9310-6

Tänzler R, Toussaint EFA, Suhardjono YR, Balke M, Riedel A (2014) Multiple transgressions of Wallace's Line explain diversity of flightless *Trigonopterus* weevils on Bali. PNAS 281: 1782. https://doi.org/10.1098/rspb.2013.2528

Tänzler R, Van Dam M, Toussaint E, Suhardjono YR, Balke M, Riedel A (2016) Macroevolution of hyperdiverse flightless beetles reflects the complex geological history of the Sunda Arc. Scientific Reports 6: 18793. https://doi.org/10.1038/srep18793

Tseng H, Huang W, Jeng M, Villaneuva RJT, Nuneza OM, Lin C (2017) Complex inter-island colonization and peripatric founder speciation promote diversification of flightless *Pachyrhynchus* weevils in the Taiwan–Luzon volcanic belt. Journal of Biogeography 45(1): 1–12. https://doi.org/10.1111/jbi.13110

van de Kamp T, Ershov A, Rolo TS, Riedel Am Baumbach T (2013) Insect imaging at the ANKA synchrotron radiation facility. Entomologie heute 25: 147–160.

Voss E (1957) Neue und bekannte, vorwiegend indonesische Curculioniden (Coleoptera). Treubia 24(1): 7–63.

Wibmer GJ (1981) Revision of the new world weevil genus *Tyloderma* in American north of Mexico (Coleoptera: Curculionidae: Cryptorhynchinae). The Southwestern Entomologist 3: 1–95.

Wilson LF (2012) Life History and Some Habits of the Pine Gall Weevil, *Podapion gallicola* Riley, in Michigan. The Canadian Entomologist 97(9): 962–969. https://doi.org/10.4039/Ent97962-9

Winter S, Friedman ALL, Astrin, JJ, Gottsberger B, Letsch H (2017) Timing and host plant associations in the evolution of the weevil tribe Apionini (Apioninae, Brentidae, Curculionoidea, Coleoptera) indicate an ancient co-diversification pattern of beetles and flowering plants. Molecular Phylogenetics and Evolution 107: 179–190. https://doi.org/10.1016/j.ympev.2016.10.015

Yamazaki K, Sugiura S (2001) Bionomics of the gall-parasitic flea weevil *Rhynchaenus hustachei* (Coleoptera: Curculionidae). Entomological Science 4(2): 239–242.

Yoshihara K (2016) The Insects of Japan (Vol. 6) – Coleoptera, Curculionidae, Baridinae. Touka Shobo Co. Ltd., Fukuoka, 171 pp.

Young LM, Marris JWM, Pawson SM (2008) Back from extinction: rediscovery of the Canterbury knobbled weevil *Hadramphus tuberculatus* (Pascoe 1877) (Coleoptera: Curculionidae), with a review of its historical distribution. New Zealand Journal of Zoology 35: 323–330. https://doi.org/10.1080/03014220809510129

Supplementary material 1

Primer and thermocycler settings for *Aphanerostethus* barcoding

Author: Miyuki Suenaga

Data type: xlsx

Copyright notice: This dataset is made available under the Open Database License (http://opendatacommons.org/licenses/odbl/1.0/). The Open Database License (ODbL) is a license agreement intended to allow users to freely share, modify, and use this Dataset while maintaining this same freedom for others, provided that the original source and author(s) are credited.

Link: https://doi.org/10.3897/zookeys.1217.126626.suppl1

ZooKeys 1217: 47–78 (2024)
DOI: 10.3897/zookeys.1217.115627

Research Article

Adelphomyia crane flies (Diptera, Limoniidae) of Korea with identification key for all Palaearctic species

Sigitas Podenas[1,2], Sun-Jae Park[3], Changhwan Bae[4]

1 Nature Research Centre, Akademijos str. 2, LT-08412 Vilnius, Lithuania
2 Life Sciences Centre of Vilnius University, Sauletekio str. 7, LT-10257 Vilnius, Lithuania
3 Climate Change and Environmental Biology Research Division, National Institute of Biological Resources, Incheon 404-708, Republic of Korea
4 Species Diversity Research Division, National Institute of Biological Resources, Incheon 404-708, Republic of Korea
Corresponding author: Sigitas Podenas (sigitas.podenas@gamtc.lt)

Abstract

Limnophilinae crane flies belonging to the genus *Adelphomyia* Bergroth, 1891 of the Korean Peninsula were studied starting from 1937, but only one species *A. macrotrichiata* (Alexander, 1923) has been recorded from North Korea so far. The genus was unknown from South Korea. Four species were found during our studies on the Peninsula, one of them from Jeju Island described as new, *Adelphomyia jejuana* Podenas, **sp. nov.** Three species are recorded from both northern and southern parts of the Peninsula. Specimens on which was based the record of *A. macrotrichiata* from North Korea was misidentified and no more specimens were collected; therefore, *A. macrotrichiata* is deleted from the Korean species list. Habitat, elevation range, and seasonality data is presented for each species. Images of taxonomically important morphological characters, and an identification key for all Palaearctic species of the genus *Adelphomyia* are presented. Distribution maps are presented for all Korean species.

Key words: East Palaearctic, habitat, key, Limnophilinae, taxonomy

Academic editor: Xiao Zhang
Received: 11 November 2023
Accepted: 15 April 2024
Published: 30 October 2024

ZooBank: https://zoobank.org/E14C2EA8-236A-4EAE-80CB-7163AF04D4DA

Citation: Podenas S, Park S-J, Bae C (2024) *Adelphomyia* crane flies (Diptera, Limoniidae) of Korea with identification key for all Palaearctic species. ZooKeys 1217: 47–78. https://doi.org/10.3897/zookeys.1217.115627

Introduction

Crane flies belonging to the genus *Adelphomyia* Bergroth, 1891 are easily recognised by the densely trichiated distal wing cells and nearly translucent wings with greatly reduced dark pattern except the distinct stigma. Adults fly in shaded places close to streams (Salmela and Härmä 2004), but larvae and other preimaginal stages are still unknown for the genus. Adults usually are collected together with other Limoniidae crane flies that prevail in wet areas under tree canopies. Despite many *Adelphomyia* specimens were collected in 1937–1939, only one species, *A. macrotrichiata* (Alexander, 1923) was recorded from the north of the Korean Peninsula and no species were known from South Korea. Our studies of the museum specimens and of specimens collected by ourselves in 2012–2019 revealed four species of *Adelphomyia*. Three of them are widely distributed in North and South Koreas, and one species from Jeju Island is new. Despite many specimens collected during field trips, *A. macrotrichiata* was not found in South Korea, it was not found also in additional material available from the museum collections.

Materials and methods

Despite the many museum collections that were examined, *Adelphomyia* crane flies from the Korean Peninsula were found only at the National Institute of Biological Resources (**NIBR**), Incheon, South Korea; The Snow Entomological Museum, University of Kansas, Lawrence, KS, USA (**SMEK**); and at the National Museum of Natural History, Smithsonian Institution, Washington, DC, USA (**USNM**). Comparative material from Lithuania for *A. punctum* (Meigen, 1818) was used from the collections of the Nature Research Centre (**NRC**), Vilnius, Lithuania.

Adults were collected in various ways, including by insect nets, with Malaise traps, LED light traps, black light traps, Mosquito Magnet® traps (Pro Model, Woodstream Corp., Lititz, PA), New Jersey (NJ) traps, and at light sources. The collected specimens were dry mounted laterally on paper points. Wet specimens were preserved in 96% ethanol (EtOH). Some male wings were slide-mounted in Euparal and photographed. Dissected male genitalia were cleared in 10% KOH and preserved in microvials with glycerol.

Information on the examined material is given according to the journal requirements, thus altitudes are given in metric system regardless of the system applied for the label. For specimens collected by SP and his colleagues, the date on the label is followed by a number in brackets, the number referring to locality: different localities where insects were collected on the same date were given separate numbers and all information from those localities, whether in the field notes, database, photographs, and other locality information, were marked with this specific number. Specimens are arranged according to the collecting date.

Specimens were examined with an Olympus SZX10 dissecting microscope and Nikon Eclipse Ti microscope. Photographs were taken with a Canon R5 camera through a Canon MP-E 65 mm macro lens and through Mitutoyo M Plan apo 10× lens mounted on the same camera at Nature Research Centre, Vilnius, Lithuania.

The terminology of adult morphological features generally follows that of Cumming and Wood (2017), while terminology of wing venation follows de Jong (2017).

Taxonomy

Adelphomyia **Bergroth, 1891**

Adelphomyia Bergroth, 1891: 134; Savchenko and Krivolutskaya 1976: 57; Savchenko 1983: 49; Savchenko 1986: 273–275; Savchenko 1989: 76–79.
Limnophila (*Tricholimnophila*) Alexander, 1928: 476–477.
Limnophila (*Adelphomyia*): Alexander 1938: 324; Ishida 1959: 2.

Type species. *Adelphomyia helvetica* Bergroth, 1891 (= *punctum* Meigen, 1818) (West and East Palaearctic).

Type locality. Weissenburg, Canton Bern, Switzerland.

Description. Medium-sized crane flies with body length 3.9–8.4 mm and wing length 5.5–8.8 mm. Colouration varies from pale yellow to dark brown or black (Figs 25, 40, 44).

Head. Rounded posteriorly. Antenna with 14-segmented flagellum. Flagellomeres slightly elongate or oval, covered with short pubescence, verticils variable, up to 2.5× as long as respective segment.

Thorax. Frontal margin of pronotum straight. Mesonotal prescutum with distinct tubercular pits and pseudosutural fovea. Katepisternum bare, without setae. Meron small. Middle and posterior coxae close to each other. Wing (Figs 1, 5, 9, 12, 15, 17, 22, 24, 27, 29, 34, 36, 38, 41, 45) comparatively wide, no pattern or with darkening surrounding only cross-veins except stigma. *Arculus* present, vein *Sc* reaching wing margin slightly before branching point of *Rs*, *sc-r* approximately its own length before tip of *Sc*. R_1 elongate, R_2 2–3× its own length before tip of R_1. Radial sector long, cell r_3 long with short stem. Cell m_1 usually long, but sometimes missing completely (e.g., one wing of *A. satsumicola* (Alexander, 1930) holotype). Discal cell always present, usually elongate. Cross-vein *m-cu* far beyond branching point of *M*. Anal vein reaching wing margin at approximately same level as base of *Rs*. Anal angle wide. Distal wing cells always with macrotrichiae. Frontal tibia with single spur, tibiae of second and third pairs of legs with two spurs each.

Abdomen. Tergites with two transverse indentations frontally. Male terminalia approximately as wide as rest abdominal segments. Epandrium (ninth tergum) with two small lobes at the middle of posterior margin. Gonocoxite simple: elongate with no additional lobes, two pairs of elongate, narrow gonostyles. According to Savchenko (1986) interbases are missing, still the structure is present (Figs 7, 20, 32, 43), in addition, Ribeiro (2008) showed the structure is clearly noticeable in Limnophilinae. Aedeagus long, narrow, one pair of elongate parameres, but length varies widely depending on species. Ovipositor (Figs 8, 21, 33, 46) with long, narrow cercus and hypogynial valve.

Twenty-five species of *Adelphomyia* are known worldwide (Oosterbroek 2024), 13 of them occur in Oriental Region and 12 (one of them with two subspecies) in East Palaearctic. Only *A. punctum* (Meigen, 1818) has a wide distribution, occurring in East and West Palaearctic.

List of Palaearctic *Adelphomyia* species (species from Korean Peninsula marked with asterisk)

Adelphomyia acicularis acicularis (Alexander, 1954) (Figs 1–3)
**Adelphomyia acicularis bidens* Savchenko, 1983 (Figs 4–8)
Adelphomyia biacus (Alexander, 1954) (Figs 9–11)
Adelphomyia breviramus (Alexander, 1924) (Figs 12–14)
Adelphomyia caesiella (Alexander, 1929) (Figs 15, 16)
**Adelphomyia flavella* (Alexander, 1920) (Figs 17–21)
(*)*Adelphomyia macrotrichiata* (Alexander, 1923) (record from North Korea based on misidentification) (Figs 22, 23)
Adelphomyia pilifer (Alexander, 1919) (Figs 24–26)
Adelphomyia prionolaboides (Alexander, 1934) (Figs 27, 28)
**Adelphomyia punctum* (Meigen, 1818) (Figs 29–33)
Adelphomyia saitamae (Alexander, 1920) (Figs 34, 35)
Adelphomyia satsumicola (Alexander, 1930) (Figs 36, 37)
Adelphomyia simplicistyla (Alexander, 1940b) (Figs 38, 39)
**Adelphomyia jejuana* Podenas, sp. nov. (Figs 40–46)

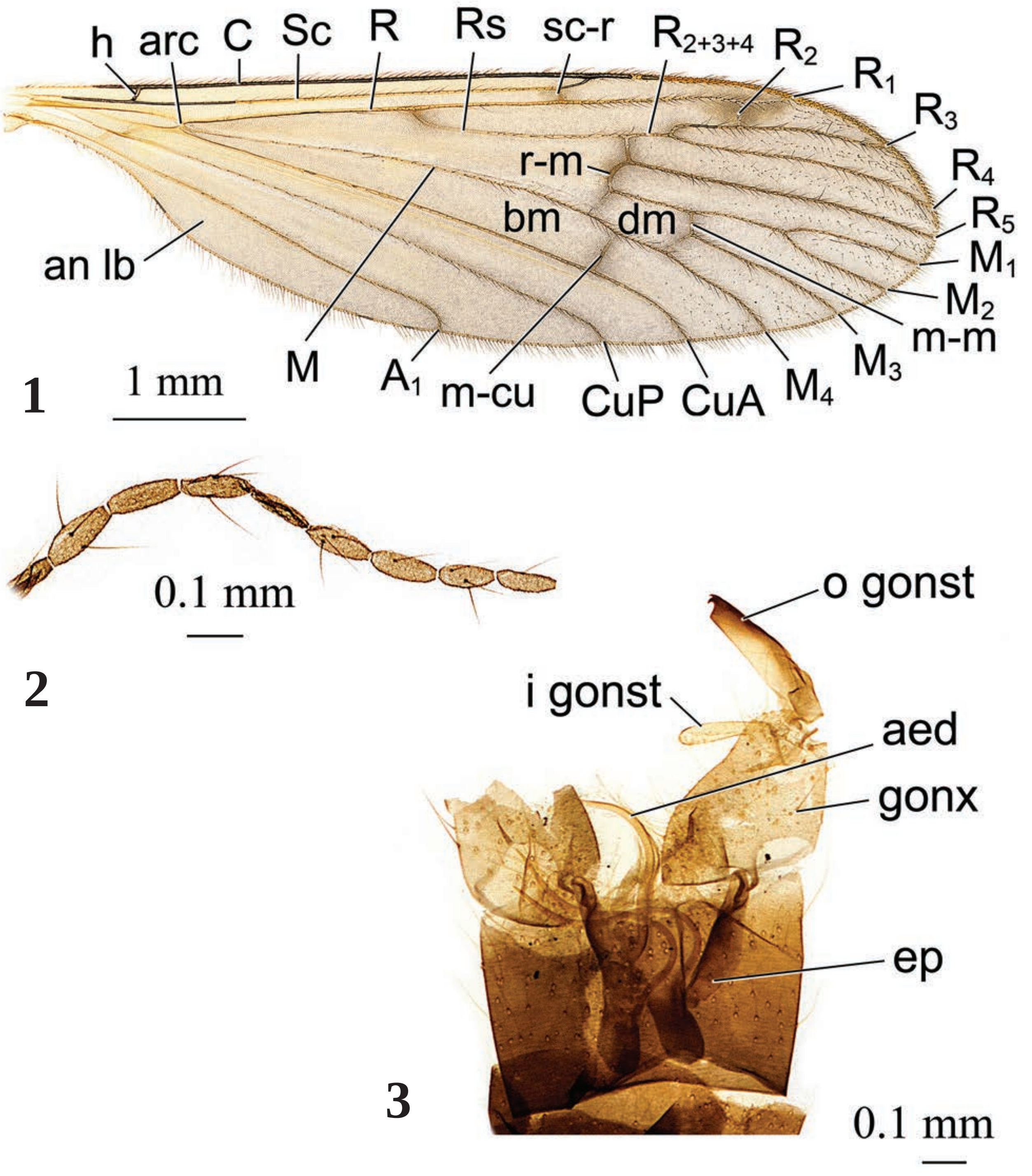

Figures 1–3. *Adelphomyia acicularis acicularis* (Alexander, 1954), male **1** wing, paratype **2** fragment of antennal flagellum, paratype **3** genitalia, dorsal view, holotype. Abbreviations: A_1 – first branch of anal vein; aed – aedeagus; an lb – anal lobe; *arc* – arculus; *bm* – basal medial cell; *C* – costal vein; *CuA* – anterior branch of cubital vein; *CuP* – posterior branch of cubital vein; *dm* – discal medial cell; ep – epandrium (ninth tergite); gonx – gonocoxite; *h* – humeral vein; i gonst – inner gonostylus; *M* – medial vein, or media; M_1 – first branch of media; M_2 – second branch of media; M_3 – third branch of media; M_4 – fourth branch of media; *m-cu* – medial-cubital cross-vein; *m-m* – medial cross-vein; o gonst – outer gonostylus; *R* – radius, or radial vein; R_1 – anterior branch of radius; R_2 – second branch of radius; R_{2+3+4} – stem of radial branches R_2, R_3 and R_4; R_3 – lower branch of second branch of radius; R_4 – upper branch of third branch of radius; R_5 – lower branch of third branch of radius; *r-m* – radio-medial cross-vein; *Rs* – radial sector; *Sc* – subcostal vein; *sc-r* – subcostal-radial cross-vein.

Key to Palaearctic species of the genus *Adelphomyia*

1 Main body colour, including thorax and abdomen, dark (dark grey, brown, or black) (Fig. 25) **2**

– Main body colour, including thorax and abdomen, pale (yellow, brownish yellow or pale brown) (Figs 40, 44) **8**

2 Entire mesonotum dull grey or brown **3**

– Mesonotum polished black anteriorly............. ***A. pilifer* (Alexander, 1919)**

3 Dark areas surrounding cross-veins restricted but evident (Figs 1, 5, 15, 27) **4**

– Dark areas surrounding cross-veins missing (Fig. 12) or indistinct (Fig. 36) **7**

4 Head dark grey, thorax dark grey, abdomen brown, femur obscure yellow **5**

– Head pale grey, thorax grey or brownish grey with black stripes, abdomen black, femur yellow with widely darkened tip **6**

5 Medial lobes of epandrium parallel-sided, notch between them U-shaped (Fig. 3) ....***A. acicularis acicularis* (Alexander, 1954)**

– Medial lobes of epandrium diverging distally, notch between them V-shaped (Fig. 6) ....***A. acicularis bidens* Savchenko, 1983**

6 Thorax grey, antenna pale brown .... ***A. caesiella* (Alexander, 1929)**

– Thorax brownish grey with black stripes, antenna brown to dark brown .... ***A. prionolaboides* (Alexander, 1934)**

7 Thorax reddish brown, abdomen dark brown, femur obscure yellow, head dark grey, antenna pale brown (Fig. 13), macrotrichiae covering nearly entire cell r_3 (Fig. 12), medial lobes of epandrium diverging distally, notch between them shallowly U-shaped (Fig. 14).. .... ***A. breviramus* (Alexander, 1924)**

– Thorax grey, abdomen brownish grey, femur yellow with narrowly dark tip, head grey, antenna dark brown, macrotrichiae covering only outer end of cell r_3 (Fig. 36), medial lobes of male epandrium parallel-sided, notch between them widely U-shaped (Fig. 37)...***A. satsumicola* (Alexander, 1930)**

8 Complete body, including thorax, abdomen, head, antennae (Fig. 10), legs, and wings (Fig. 9), yellow or pale yellow......... ***A. biacus* (Alexander, 1954)**

– Thorax or abdomen grey or brownish (Figs 40, 44) **9**

9 Wing pattern indistinct or missing (Figs 17, 22, 38, 41, 45)...................... **10**

– Wing pattern restricted but evident (Figs 29, 34) **13**

10 Thorax brown. Macrotrichiae covering outer ends of cells r_2 to m_4 (Fig. 38) ....***A. simplicistyla* (Alexander, 1940b)**

– Thorax brownish yellow. Macrotrichiae covering nearly entire or only outer ends of cells r_2 to m_4 (Figs 17, 22, 41, 45).. **11**

11 Abdominal tergites brownish yellow. Notch between medial lobes of male epandrium V-shaped (Figs 18, 42) **12**

– Abdominal tergites brown. Notch between medial lobes of male epandrium U-shaped (Fig. 23).........................***A. macrotrichiata* (Alexander, 1923)**

12 Head brownish yellow with yellow antennae. Macrotrichiae covering nearly entire cells r_2 to m_4 (Fig. 17) .... ***A. flavella* (Alexander, 1920)**

– Head greyish brown with pale brown antennae. Macrotrichiae covering only outer ends of cells r_2 to m_4 (Figs 41, 45)........... ***A. jejuana* Podenas, sp. nov.**

13 Head brownish yellow, tips of femora not darkened. Medial lobes of male epandrium diverging distally, notch between them V-shaped (Fig. 35)....... ....***A. saitamae* (Alexander, 1920)**

– Head grey, tips of femora narrowly darkened. Medial lobes of male epandrium acute, notch between them narrow, parallel-sided (Fig. 30)............. ....***A. punctum* (Meigen, 1818)**

Adelphomyia acicularis bidens Savchenko, 1983
Figs 4–8

Adelphomyia acicularis bidens Savchenko, 1983: 53.

Examined material. (Fig. 47) **NORTH KOREA** • 2 ♂ (pinned); Ompo; alt. 122 m; 29 May 1938; A. M. Yankovsky leg.; USNM • 3 ♂ (pinned); Seren Mts.; alt. 1067 m; 22 June 1938; A. M. Yankovsky leg.; USNM; **SOUTH KOREA** • 1 ♂ (in ethanol); Gangwon-do, Pyeongchang-gun, Daegwallyeong-myeon, Yongsan-ri, Mt. Balwangsan; 19 July 2008; J. D. Yeo, M. J. Jeon and K. G. Kim leg.; Malaise trap; NIBR • 1 ♀ (in ethanol); Gangwon-do, Jeongseon-gun, Imgye-myeon, Dojeon-ri; 37.53583°N, 128.90278°E; alt. 762 m; 24 May – 23 June 2011; H.-W. Byun et al. leg.; Malaise trap; NIBR • 1 ♂ (in ethanol); Gyeongsangnam-do, Hadong-gun, Hwagae-myeon, Beomwang-ri; 35.27360°N, 127.61121°E; alt. 369 m; 8 May 2013 (2); S. Podenas leg.; NIBR • 1 ♂ (in ethanol); Jeollanam-do, Gurye-gun, Toji-myeon, Naedong-ri; 35.26580°N, 127.58128°E; alt. 378 m; 10 May 2013; S. Podenas leg.; NIBR • 1 ♂ (in ethanol); Jeollanam-do, Gurye-gun, Toji-myeon, Naedong-ri; 35.26580°N, 127.58128°E; alt. 378 m; 11 May 2013; S. Podenas leg.; at light; NIBR • 1 ♂ (pinned); Jeollanam-do, Gurye-gun, Toji-myeon, Naeseo-ri, Piagol valley; 35.25825°N, 127.58208°E; alt. 310 m; 26 April 2015 (2); S. Podenas leg.; NIBR • 2 ♂ (in ethanol); Jeollanam-do, Gurye-gun, Toji-myeon, Naeseo-ri, Jirisan National Park, Piagol valley; 35.27448°N, 127.56378°E; alt. 593 m; 1 May 2015 (1); S. Podenas leg.; at light; NIBR • 1 ♂ (pinned); Jeollanam-do, Gurye-gun, Toji-myeon, Naeseo-ri, Jirisan National Park, Piagol valley; 35.27177°N, 127.57146°E; alt. 490 m; 2 May 2015 (1); S. Podenas leg.; NIBR • 2 ♂ (in ethanol); Jeollanam-do, Gurye-gun, Toji-myeon, Naeseo-ri, Jirisan National Park, Piagol valley; 35.25825°N, 127.58208°E; alt. 310 m; 2 May 2015 (2); S. Podenas leg.; NIBR • 1 ♂ (pinned); Jeollanam-do, Gurye-gun, Toji-myeon, Naeseo-ri, Jirisan National Park, Piagol valley; 35.26590°N, 127.58096°E; alt. 446 m; 2 May 2015 (4); S. Podenas leg.; at light; NIBR • 2 ♂ (in ethanol); Jeollanam-do, Gurye-gun, Toji-myeon, Naeseo-ri, Jirisan National Park, Piagol valley; 35.26590°N, 127.58096°E; alt. 446 m; 3 May 2015 (3); S. Podenas leg.; at light; NIBR • 1 ♂ (in ethanol); Jeollanam-do, Gurye-gun, Toji-myeon, Naeseo-ri, Jirisan National Park, Piagol valley; 35.26590°N, 127.58096°E; alt. 446 m; 27 June 2015 (2); S. Podenas leg.; at light; NIBR • 2 ♂ (in ethanol); Gyeonggi-do, Yangpyeong, Cheongun-myeon, Dowon-ri; 37.54507°N, 127.79483°E; alt. 224 m; 28 May 2017; S. Podenas leg.; at light; NIBR.

Redescription. General body colouration brown to dark brown densely covered with grey pruinosity. Body length of male 5.6–8.4 mm, of female 8.0 mm. Wing length of male 6.3–8.7 mm, of female 8.4 mm.

Head. Dark brown, dusted with grey, pale grey pruinose frontally and along eye margin. Eyes widely separated in both sexes, distance between them at

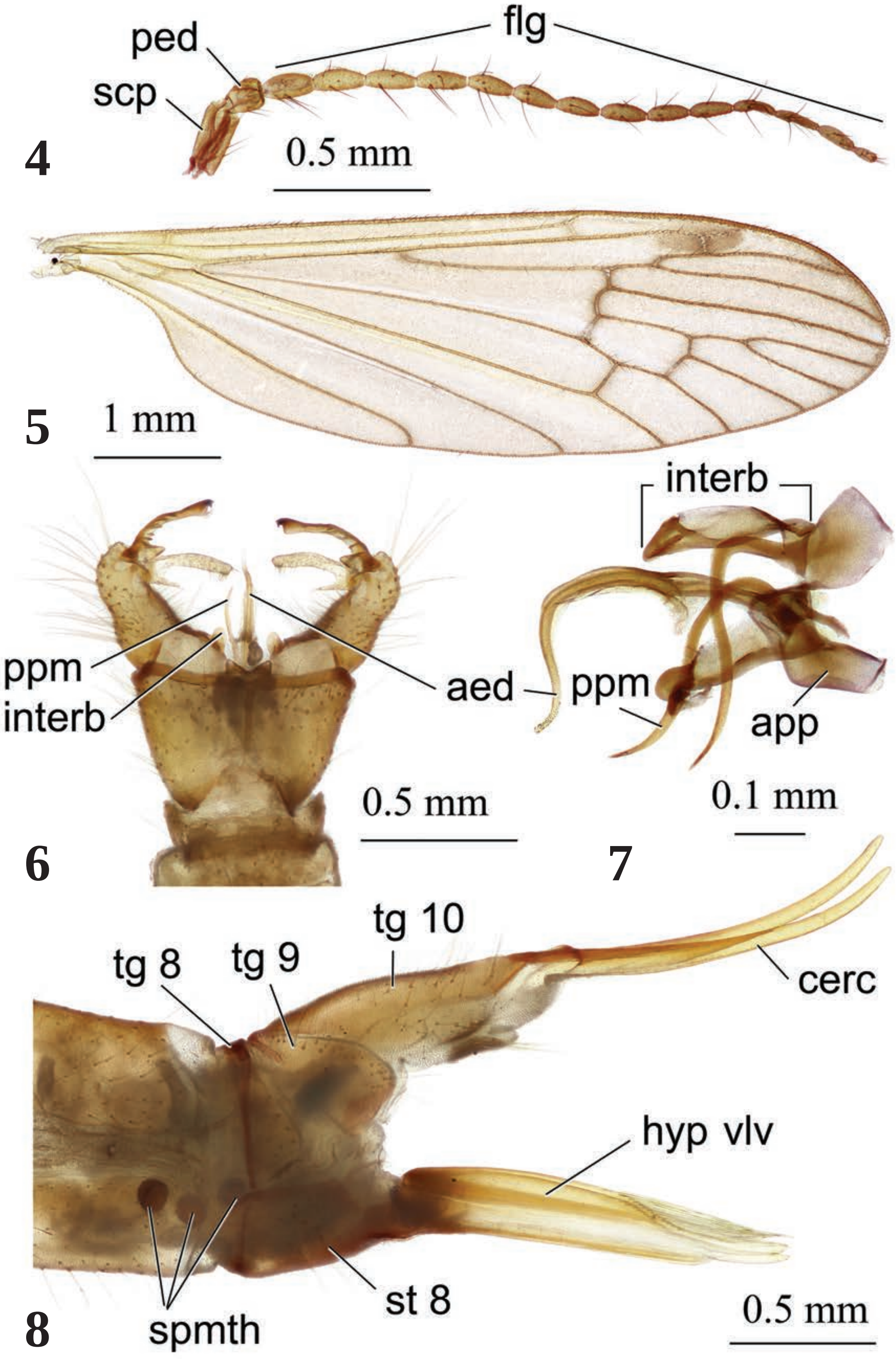

Figures 4–8. *Adelphomyia acicularis bidens* Savchenko, 1983 **4** male antenna **5** male wing **6** male genitalia, dorsal view **7** aedeagal complex, lateral view **8** ovipositor, lateral view. Abbreviations: aed – aedeagus; app – anterior part of paramere; cerc – cercus; flg – flagellum; hyp vlv – hypogynial valve ; interb – interbase; ped – pedicel; ppm – posterior part of paramere; scp – scape; spmth – spermatheca; st – sternite; tg – tergite.

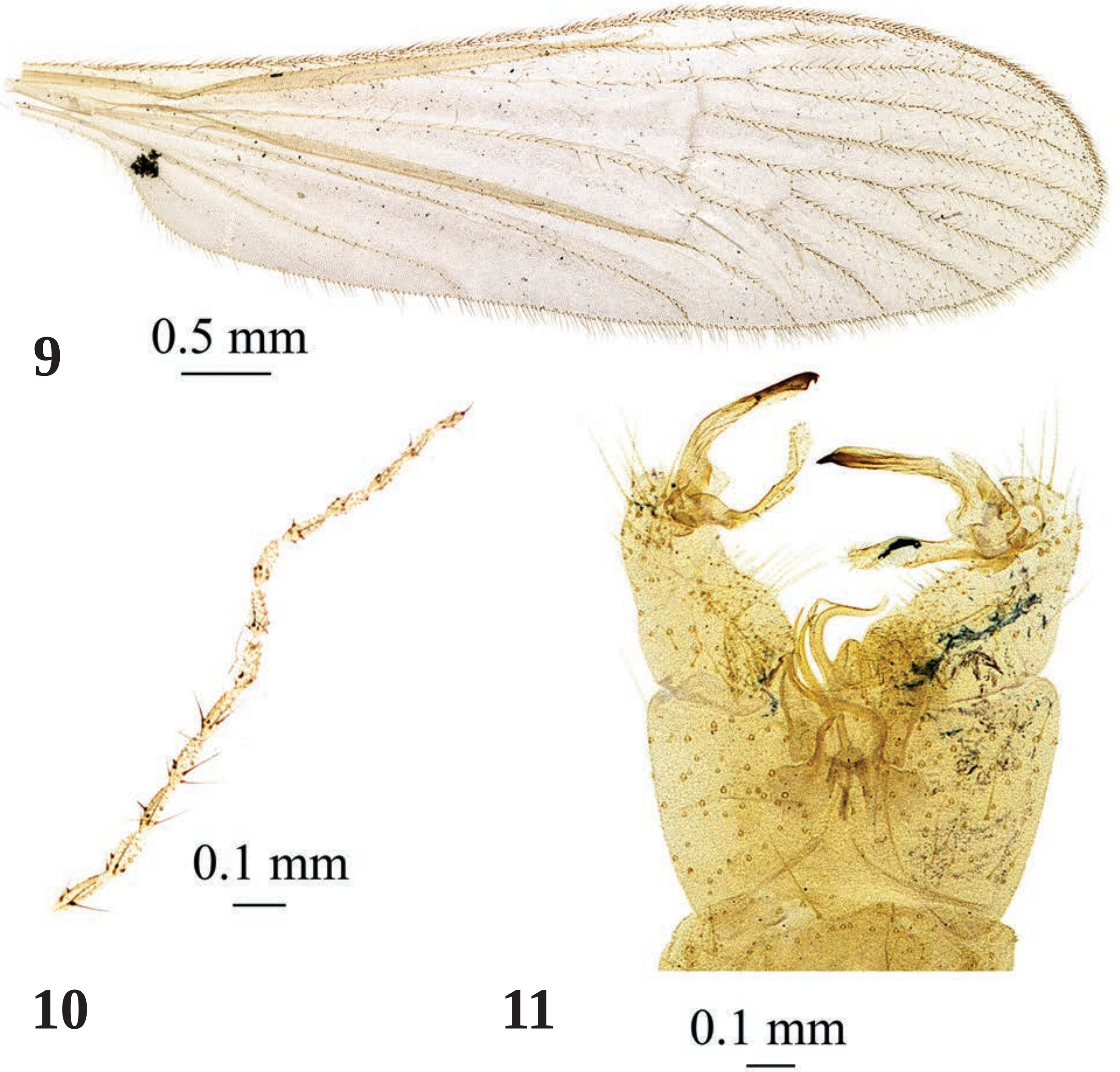

Figures 9–11. *Adelphomyia biacus* (Alexander, 1954), male, holotype **9** wing **10** antenna **11** genitalia, dorsal view.

base of antennae exceeds length of scape. Antenna (Fig. 4) 1.7–2.8 mm long in male, 1.7 mm in female, extending beyond wing base if bent backward. Scape greyish brown, elongate, nearly cylindrical, 2× as long as pedicel, pedicel pear-shaped. Flagellum yellow basally, slightly darkened distally. Flagellomeres elongate, longest at middle, apical flagellomere slightly smaller than penultimate. Verticils brownish, longest verticils ~ 1.5× as long as respective segments. Rostrum dark brown dusted with grey, palpus and labellum dark brown.

Thorax. Cervical sclerites brown to dark brown. Pronotum pale brown to dark brown, depending on specimen, covered with sparse erect long yellowish setae dorsally. Presutural scutum brown, dusted with grey, without stripes or with indistinct darker median stripes on the anterior half. Tubercular pit small, polished-brown at frontal margin of sclerite, prescutal pit distinct, polished-brown, surrounded by grey area. Scutal lobe and scutellum brown, dusted with grey, area between scutal lobes pale brown, mediotergite brown, dusted with grey

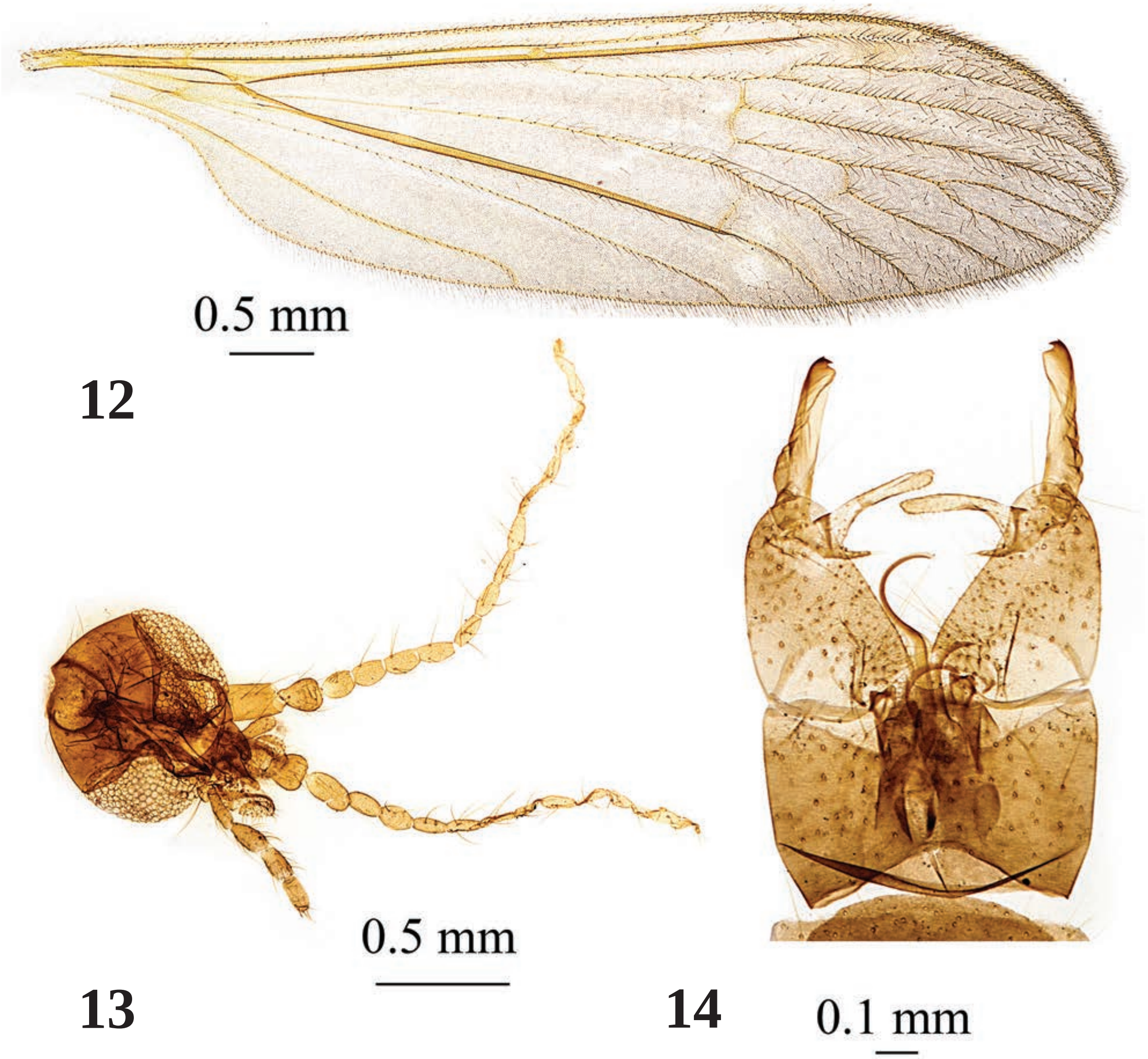

Figures 12–14. *Adelphomyia breviramus* (Alexander, 1924), male **12** wing, holotype **13** head, dorsal view **14** genitalia, dorsal view, holotype.

along middle, yellowish brown laterally. Pleuron uniformly brown, densely covered with brown pruinosity. Wing (Fig. 5) brownish. Stigma elongate, from pale brown to brown. Cross-veins and branching points of veins narrowly surrounded by indistinct darker areas in some specimens, in other specimens darker areas missing. Veins brownish, yellowish at wing base. Macrotrichiae more abundant in radial cells and cell m_1, also present in other marginal cells along postero-apical wing margin, few macrotrichiae present also in cell *cua* at wing margin. Venation: *Sc* long, reaching slightly before branching point of *Rs*, *sc-r* less than its own length from tip of *Sc*. *Rs* long, slightly arched at base. Free end of R_1 longitudinal, R_2 transverse, indistinct, 3× its own length from tip of R_1, R_3, and R_4 slightly diverging towards wing margin, cell r_3 with short stem. Cross-vein *r-m* distinct, at base of discal cell. Discal cell slightly more than 2× as long as wide. Cross-vein *m-cu* slightly before middle of discal cell. Anal vein

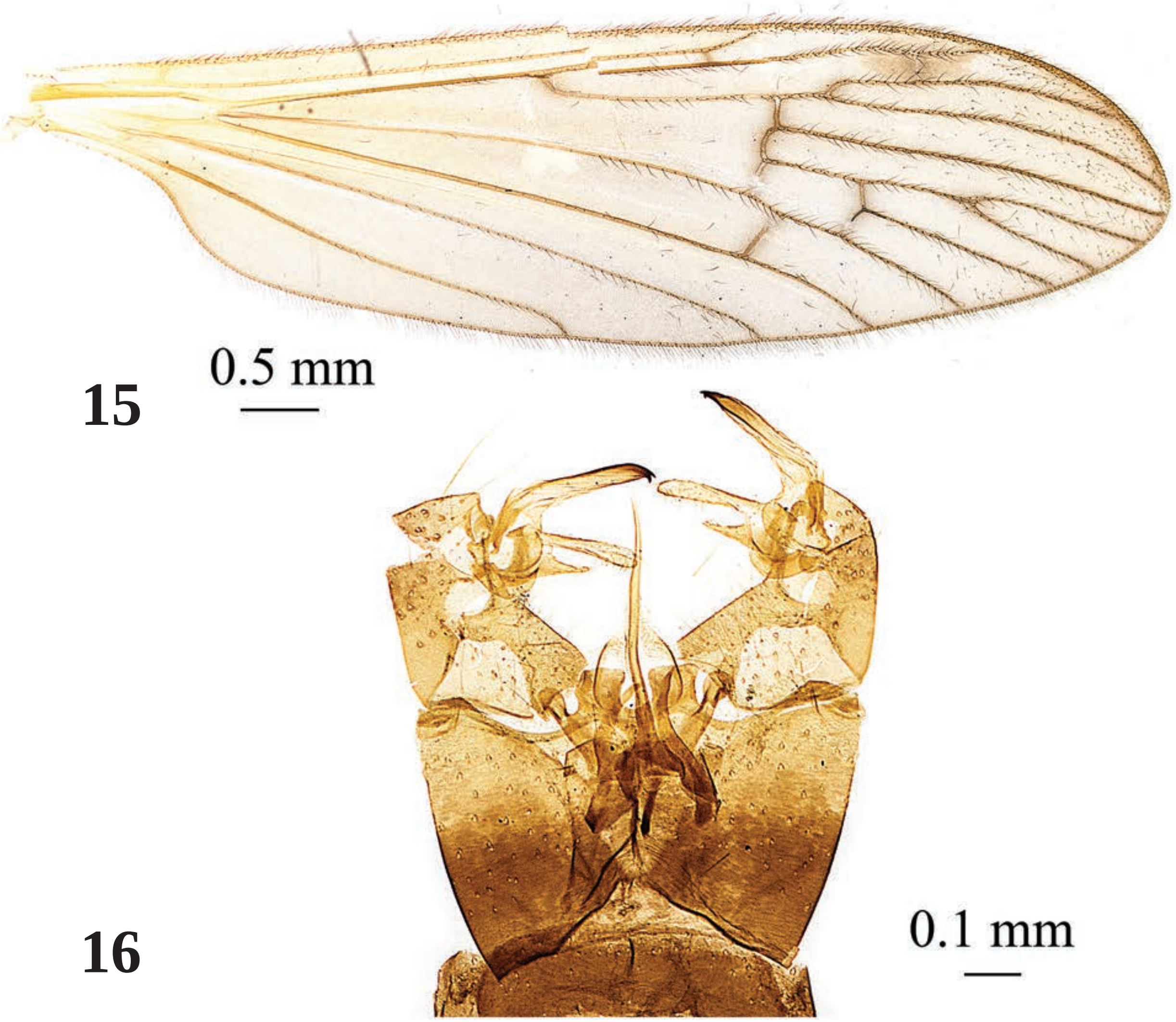

Figures 15, 16. *Adelphomyia caesiella* (Alexander, 1929), male **15** wing **16** genitalia, dorsal view.

slightly arched at apex, reaching wing margin at the level of *Rs* base. Anal angle widely rounded. Length of male halter 1.0–1.5 mm, of female 1.2 mm. Halter pale yellowish, knob slightly infuscate. Coxae yellow, only fore coxa brownish at base. Trochanters pale yellow. Femora yellow with indistinctly darkened apices, tibiae yellow with darker distal ends. Basal tarsomeres pale brown, remaining tarsomeres dark brown. Male femur I: 4.1–5.2 mm long, II: 4.0–5.4 mm, III: 4.5–6.0 mm, tibia I: 5.3–6.5 mm, II: 4.8–5.9 mm, III: 6.0–6.5 mm, tarsus I: 5.1–6.2 mm, II: 5.0–5.6 mm, III: 4.6–5.0 mm. Female femur II: 4.7 mm long, tibia II: 4.7 mm, tarsus II: 4.3 mm. Claw simple, without spines.

Abdomen. Tergites brown, dusted with grey, sternites yellowish brown, paler at base of abdomen. Male terminalia (Fig. 6) yellow. Ninth tergite with two diverging triangle-shaped lobes at the middle of posterior margin and wide V-shaped indentation between them. Gonocoxite elongate, wider at base, narrower beyond middle, without additional lobe. Outer gonostylus with long, narrow, slightly arched outer branch that has few transverse ridges on basal half and small triangle-shaped lobe at base. Outer branch with sclerotised distal part and blackened apex, two small apical hook-shaped teeth curved medially.

Inner gonostylus large, fleshy, setose, two-branched. Outer branch long, narrow, inner branch short, very narrow, reaching to ~ 1/3 of outer branch. Aedeagus (Fig. 7) strongly curved ventrally at ~ 2/3 length, distal part at ~ 90^0 angle to basal part (clearly visible in lateral view). Paramere darkened, posteriorly long, narrow, rod-shaped, nearly as long as aedeagus, strongly curved at ~ 1/6 length; basal part extends parallel to main body axis, distal part directed exactly downwards. Interbase nearly oblong with tip rounded. Ovipositor (Fig. 8) brownish yellow. Cercus long, narrow, apical part slightly raised upwards, apex obtuse. Hypogynial valve long, straight, wide at base, apical part distinctly narrower, apex reaching beyond middle of cercus, dorsal margin at ~ 1/3 length from tip with long straight setae.

Elevation range. From 100 m to 1100 m.

Period of activity. From end of April through middle of July.

Habitat. Slopes to small mountainous streams densely covered with deciduous trees and shrubs, moss tufts on rocks. Species is attracted to light.

General distribution. The nominotypical subspecies is known only from Shikoku island, Japan, subspecies *A. acicularis bidens* only from southern part of the Far East of Russia. Species and subspecies recorded from the Korean Peninsula for the first time.

Adelphomyia flavella (Alexander, 1920)

Figs 17–21

Limnophila (*Lasiomastix*) *flavella* Alexander, 1920: 12.
Adelphomyia flavella: Oosterbroek 2024.

Type material examined. **JAPAN** • **Paratype** ♂ (as *Limnophilla flavella*), wing and genitalia slide-mounted; Tokio; 5 May 1919; R. Takahashi leg.; USNM.

Other examined material. (Fig. 48) **NORTH KOREA** • 6 ♀ (pinned); Ompo; alt. 37 m; 15 June 1937; A. M. Yankovsky leg.; USNM • 1 ♀ (pinned); Ompo; alt. 122 m; 3 June 1938; A. M. Yankovsky leg.; USNM • 2 ♀ (pinned); Ompo; alt. 107 m; 11 June 1938; A. M. Yankovsky leg.; USNM • 3 ♂ (pinned); Kankyo Nando, Puksu Pyaksan; alt. 1219 m; 9 June 1939; A. M. Yankovsky leg.; USNM • 1 ♂ (pinned); Kankyo Nando, Puksu Pyaksan; alt. 1280 m; 6 June 1939; A. M. Yankovsky leg.; USNM • 1 ♂ (pinned); Kankyo Nando, Puksu Pyaksan; alt. 1433 m; 6 June 1939; A. M. Yankovsky leg.; USNM • 1 ♂ (pinned); Kankyo Nando, Puksu Pyaksan; alt. 1463 m; 6 June 1939; A. M. Yankovsky leg.; USNM • 1 ♂, 1 ♀ (pinned); Kankyo Nando, Puksu Pyaksan; alt. 1676 m; 8 June 1939; A. M. Yankovsky leg.; USNM; **SOUTH KOREA** • 1 ♂, 5 ♀ (pinned); #8, Central National Forest, 29 km NE Seoul; alt. 122–152 m; 28 May 1954; George W. Byers leg.; 2 ♀ USNM; 1 ♂, 3 ♀ SMEK • 3 ♂, 1 ♀ (pinned); #9, Central National Forest, 29 km NE Seoul; alt. 122–152 m; 29 May 1954; George W. Byers leg.; SMEK • 1 ♂ (pinned); #12, Hwy. #20, 13 km SW Kangnung; 37.70000°N, 128.78333°E; alt. 587 m; 8 June 1954; George W. Byers leg.; SMEK • 1 ♂ (pinned); #17, Central National Forest, 29 km NE Seoul; alt. 107–152 m; 20 June 1954; George W. Byers leg; SMEK • 1 ♀ (in ethanol); Gangwon-do, Pyeongchang-gun, Yongpyeong-myeon, Nodong-ri, Mt. Gyebang-san; 19 July – 12 August 2008; H. Y. Seo & K. G. Kim leg.; Malaise trap; NIBR • 1 ♂ (in ethanol); Haanmi-ri, Daehwa-myeon, Pyeongchang-gun, Gangwon-do,

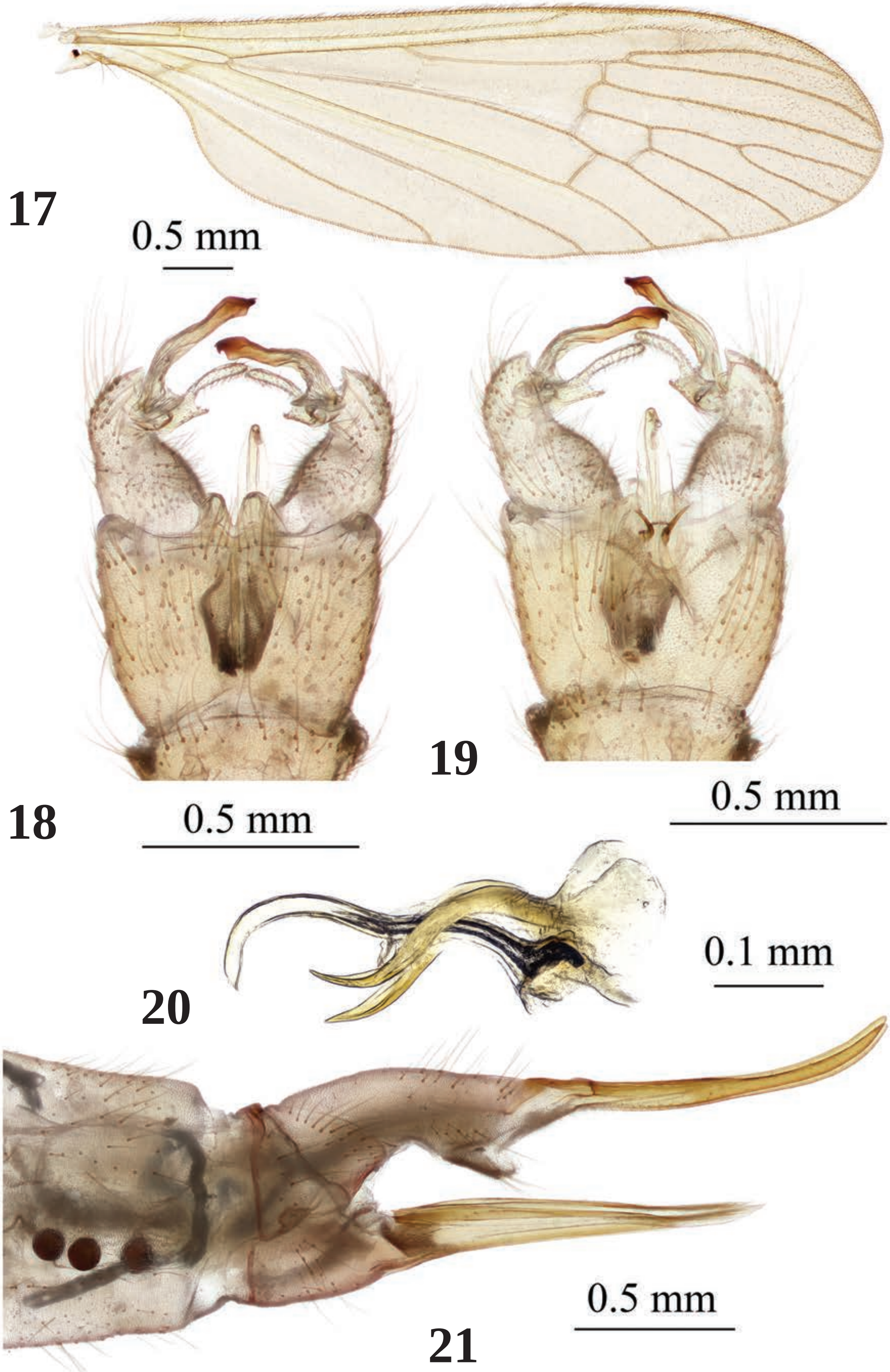

Figures 17–21. *Adelphomyia flavella* (Alexander, 1920) **17** male wing **18** male genitalia, dorsal view **19** male genitalia, ventral view **20** aedeagal complex, lateral view **21** ovipositor, lateral view.

Mt. Gariwangsan; 37.45028°N, 128.50306°E; 13 May – 3 June 2009; W. Y. Choi et al. leg.; NIBR • 1 ♂ (in ethanol); Gangwon-do, Pyeongchang-gun, Jinbu-myeon, Jangjeon-ri, Mt. Gariwangsan; 37.48778°N, 128.54528°E; alt. 693 m; 4 –17 June 2009; J. D. Yeo, J. D. Yoon leg.; Malaise trap; NIBR • 1 ♀ (in ethanol); Jeollanam-do, Gurye, Toji-myeon, Naedong-ri; 35.26580°N, 127.58128°E; alt. 378 m; 11 May 2013; S. Podenas leg.; at light; NIBR • 1 ♂ (in ethanol); Jeollanam-do, Gurye-gun, Toji-myeon, Naedong-ri; 35.26580°N, 127.58128°E; alt. 378 m; 12 May 2013; S. Podenas leg.; NIBR • 4 ♂, 1 ♀ (in ethanol); Jeollanam-do, Gurye-gun, Toji-myeon, Naeseo-ri, Piagol valley; 35.25257°N, 127.58981°E; alt. 304 m; 29 April 2015 (1); S. Podenas leg.; NIBR • 3 ♂, 2 ♀ (in ethanol); Jeollanam-do, Gurye-gun, Toji-myeon, Naeseo-ri, Piagol valley; 35.25825°N, 127.58208°E; alt. 310 m; 2 May 2015 (2); S. Podenas leg.; NIBR • 2 ♂ (in ethanol); Jeollanam-do, Gurye-gun, Toji-myeon, Naeseo-ri, Piagol valley; 35.26590°N, 127.58096°E; alt. 446 m; 3 May 2015 (3); S. Podenas leg.; at light; NIBR • 1 ♀ (in ethanol); Jeollanam-do, Gurye-gun, Toji-myeon, Naeseo-ri, Piagol valley; 35.27448°N, 127.56378°E; alt. 593 m; 1 July 2015 (1); V. Podeniene leg.; NIBR • 1 ♂ (in ethanol); Gangwon-do, Yangyang-gun, Seo-myeon, Garapi-ri; 38.07933°N, 128.52042°E; alt. 160 m; 7 July 2015 (1); S. Kim, S. Podenas leg.; NIBR • 1 ♀ (in ethanol); Gangwon-do, Hongcheon-gun, Duchon-myeon, Cheonhyeon-ri, near Mt. Garisan; 37.84840°N, 127.98879°E; alt. 304 m; 8 July 2015 (3); S. Kim, S. Podenas leg.; NIBR • 2 ♂, 2 ♀ (in ethanol); Gyeongsangbuk-do, Gyeongju-si, Jinhyeon-dong, Tohamsan (Mt.), 1.3 km southeast from Seokgulam; 35.78797°N, 129.33919°E; alt. 297 m; 27 May 2016; S. Podenas, H.M. Baek leg.; NIBR • 1 ♀ (in ethanol); Jeollanam-do, Gurye-gun, Toji-myeon, Naeseo-ri, Piagol valley; 35.27177°N, 127.57146°E; alt. 490 m; 3 June 2016 (2); S. Podenas leg.; NIBR • 1 ♂ (in ethanol); Jeollanam-do, Gurye-gun, Toji-myeon, Naeseo-ri, Piagol valley; 35.26586°N, 127.58090°E; alt. 448 m; 3 June 2016 (4); S. Podenas leg.; at light; NIBR • 2 ♂ (in ethanol); Gyeonggi-do, Yangpyeong, Cheongun-myeon, Dowon-ri; 37.54507°N, 127.79483°E; alt. 224 m; 28 May 2017 (1); S. Podenas leg.; with net and at light; NIBR • 1 ♂ (in ethanol); Gyeonggi-do, Dongducheon, Tapdong-dong, Casey; 37.87845°N, 127.14566°E; alt. 503 m; 20 June 2017; T. A. Klein, H.-C. Kim leg.; NJ trap; NIBR • 2 ♂ (in ethanol); Gyeonggi-do, Dongducheon, Tapdong-dong, Casey; 37.87845°N, 127.14566°E; alt. 503 m; 26 June 2017; T. A. Klein, H.-C. Kim leg.; NJ trap; NIBR • 1 ♂ (in ethanol); Gyeonggi-do, Dongducheon-si, Gwangam-dong, Hovey; 37.90044°N, 127.10319°E; alt. 353 m; 26 June 2017; T. A. Klein, H.-C. Kim leg.; NJ trap; NIBR • 1 ♂, 1 ♀ (pinned); Jeollanam-do, Gurye-gun, Toji-myeon, Naeseo-ri, Piagol valley; 35.27333°N, 127.56924°E; alt. 546 m; 25 June 2019 (1); S. Podenas leg.; NIBR.

Redescription. General body colouration brownish yellow. Body length of male 4.2–6.7 mm, of female 5.3–7.9 mm. Wing length of male 5.5–7.3 mm, of female 5.7–7.7 mm.

Head. Brownish greyish yellow, pale grey pruinose frontally and along eye margin. Eyes widely separated in both sexes, distance between them at base of antennae exceeds lengths of scape and pedicel combined. Antenna 1.2–2.1 mm long in male, 0.9–1.7 mm in female, reaching to the wing base if bent backward. Both basal antennomeres yellow, scape slightly dusted with grey basally, elongate, nearly cylindrical, 2× as long as pedicel, pedicel pear-shaped. Flagellum yellow basally, slightly darkened distally. Flagellomeres elongate, longest at middle, apical flagellomere smaller than penultimate. Verticils brownish, longest verticils approximately as long as respective segments. Rostrum pale brown, palpus darker brown, mouth parts pale brown.

Thorax. Cervical sclerites yellow. Pronotum pale brown dorsally, yellow laterally, covered with long, sparse, erect, yellow setae dorsally. Mesonotal prescutum uniformly brownish yellow, without stripes, sparsely dusted with grey. Tubercular pit indistinct, pseudosutural fovea concolourous with presutural scutum. Scutal lobes and scutellum brownish yellow, mediotergite yellow to brownish yellow. Pleuron yellow dorsally, pale yellow ventrally, sparsely dusted with greyish yellow. Wing (Fig. 17) semi-translucent, pale yellow, without darker areas except stigma. Stigma indistinct, brownish. Veins pale brown, yellowish at wing base and in costal area. Macrotrichiae more abundant in radial cells and cell m_1, also present in other marginal cells along postero-apical wing margin, few macrotrichiae present in cell *cua* at wing margin. Venation: *Sc* long, reaching slightly before branching point of *Rs*, *sc-r* ~ 3× its own length from tip of *Sc*. *Rs* long, slightly arched at base. Free end of R_1 longitudinal, R_2 transverse, indistinct, 3.3× its own length from tip of R_1, R_3, and R_4 slightly arched and diverging towards wing margin, cell r_3 with short stem. Cross-vein *r-m* distinct, at base of discal cell. Discal cell 1.8× as long as wide. Cross-vein *m-cu* at middle of discal cell. Anal vein slightly arched at wing margin, ending beyond base of *Rs*. Anal angle widely rounded. Length of male halter 0.8–1.2 mm, of female 0.8–1.6 mm. Halter pale, knob slightly infuscate. Coxae and trochanters yellow to pale yellow. Femur and tibia yellow, tibia slightly infuscate at apex. Basal tarsomere pale brown, remaining tarsomeres dark brown. Male femur I: 3.6–4.3 mm long, II: 4.0–4.8 mm, III: 3.9–5.0 mm, tibia I: 4.5–5.4 mm, II: 3.9–4.9 mm, III: 4.0–5.2 mm, tarsus I: 4.6–5.5 mm, II: 4.2–5.0 mm, III: 3.3–4.2 mm. Female femur I: 3.3–4.0 mm long, II: 3.1–4.4 mm, III: 3.4–4.9 mm, tibia I: 3.9–4.4 mm, II: 3.0–4.0 mm, III: 3.2–4.6 mm, tarsus I: 3.6–4.1 mm, II: 3.2–5.0 mm, III: 3.0–3.6 mm. Claw simple, without spines.

Abdomen. Tergites brownish yellow, sternites yellow. Male terminalia (Figs 18, 19) yellow. Ninth tergite with two triangle-shaped lobes at the middle of posterior margin and V-shaped indentation between them. Gonocoxite elongate, distinctly wider at base, narrower beyond middle, without additional lobe. Outer gonostylus with long, narrow, slightly sinuous outer branch and small triangle-shaped lobe at base. Outer branch with sclerotised distal part and blackened apex, two small apical hook-shaped teeth curved medially. Inner gonostylus large, fleshy, setose, two-branched. Outer branch long and narrow, inner branch short, reaching to ~ 1/3 of outer branch. Aedeagus (Fig. 20) strongly curved at ~ 2/3 length, distal part at ~ 90 ^{0} angle to basal part (clearly visible in lateral view). Paramere posteriorly short, narrow, rod-shaped with darkened distal part, reaching just slightly beyond base of gonocoxite (best visible in ventral view). Interbase with tip rounded. Ovipositor (Fig. 21) pale yellow. Cercus very long, narrow, distal part slightly raised upwards. Hypogynial valve long, wedge-shaped, pointed apex reaching slightly beyond middle of cercus. Spermatheca small, rounded.

Elevation range. From the sea level to nearly 1700 m.

Period of activity. From the end of April through late July.

Habitat. Mountainous river margins covered with deciduous trees and shrubs.

General distribution. Species was known only from Honshu island, Japan. Recorded from the Korean Peninsula for the first time.

Adelphomyia macrotrichiata **(Alexander, 1923)**
Figs 22, 23

Limnophila (*Lasiomastix*) *macrotrichiata* Alexander, 1923: 65–66.
Limnophila (*Adelphomyia*) *macrotrichiata*: Alexander 1940a: 49, 75, pl. 1, fig. 7.
Adelphomyia macrotrichiata: Savchenko 1983: 52–53; Oosterbroek 2024.

Type material examined. Japan • Holotype ♂; wing and genitalia slide-mounted; Hokkaido, Teshio; 3 July 1916; T. Issiki leg.; USNM.

Other examined material. (all these specimens are *A. punctum* but misidentified as *A. macrotrichiata*). **North Korea** • 1 ♂ (wing and genitalia slide-mounted); Ompo; alt. 37 m; 15 June 1937; A. M. Yankovsky leg.; C. P. Alexander det.; USNM • 1 ♀ (pinned); Ompo; alt. 61 m; 20 May 1938; A. M. Yankovsky leg.; C. P. Alexander det.; USNM • 1 ♀ (pinned); Ompo; alt. 61 m; 24 May 1938; A. M. Yankovsky leg.; C. P. Alexander det.; USNM • 1 ex. (pinned, wing and tip of abdomen missing); Ompo; alt. 61 m; 28 May 1938; A. M. Yankovsky leg.; C. P. Alexander det.; USNM • 1 ♂ (pinned); Ompo; alt. 152 m; 28 May 1938; A. M. Yankovsky leg.; C. P. Alexander det.; USNM • 1 ♂ (pinned); Ompo; alt. 91 m; 29 May 1938; A. M. Yankovsky leg.; C. P. Alexander det.; USNM • 2 ♀ (pinned); Ompo; alt. 122 m; 29 May 1938; A. M. Yankovsky leg.; C. P. Alexander det.; USNM.

Redescription. Body semi-polished brownish yellow with darker abdomen. Male body length 5.5–6.8 mm, female 7.7–9.2 mm, male wing length 6.2–9.1 mm, female 7.6–8.5 mm.

Head. Pale bluish grey because of dense pruinosity, covered with long, semi-erect, brownish yellow setae. Eyes widely separated in both sexes, distance between eyes at base of antenna exceeds length of scape. Antenna rather long, approximately reaching to base of halter if bent backwards. Male antenna 1.4 mm long, that of female 1.1–1.6 mm. Scape elongate, nearly cylindrical, obscure yellow, turning brownish towards apex, covered with sparse greyish pruinosity. Pedicel obscure yellow to brown, depending on specimen, wider distally. Few basal flagellomeres yellow to greyish yellow, distal flagellomeres greyish brown. Basal flagellomeres oval, distal segment spindle-shaped. Rostrum brownish, sparsely dusted with grey dorsally, palpus brown.

Thorax. Pronotum pale grey, covered with short erect yellow setae, postpronotum obscure yellow. Presutural scutum semi-polished, uniformly brownish yellow medially, yellowish along frontal and lateral margins, without stripes. Scutal lobe brownish yellow with paler margins. Area between scutal lobes yellow. Scutellum greyish yellow. Mediotergite greyish with yellowish lateral and posterior margins. Pleuron pale brown, sparsely covered with bluish grey pruinosity. Wing (Fig. 22) semi-translucent, yellowish. Stigma oval, pale brown. Indistinct darker areas surround cord, distal margin of discal cell and *m-cu*. Veins pale brown, yellowish at wing base. Venation: *Sc* comparatively long, reaching costal vein slightly before branching point of *Rs*, *sc-r* ~ 3× its own length from tip of *Sc*. *Rs* long, slightly arched at base. Free end of R_1 longitudinal, R_2 oblique, 2.8× its own length from tip of R_1. R_3 and R_4 slightly arched and diverging towards wing margin, cell r_3 with short stem, veins R_4 and R_5 converging towards wing margin. Cross-vein *r-m* distinct, at base of discal cell. Discal cell 2.2× as long as wide. Cell m_1 2.2× as long as its stem. Cross-vein *m-cu* slightly before middle of discal cell. Anal vein distinctly arched at wing margin, ending beyond

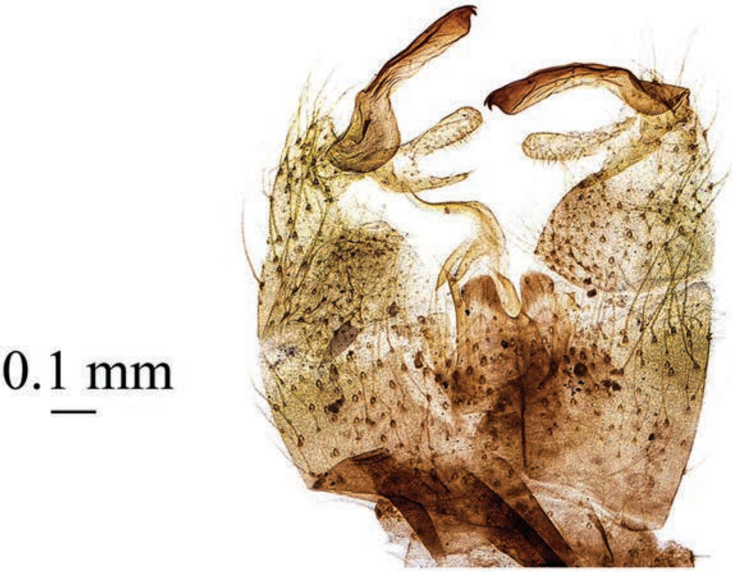

Figures 22, 23. *Adelphomyia macrotrichiata* (Alexander, 1923), male, holotype **22** wing **23** genitalia, dorsal view.

base of *Rs*. Anal angle widely rounded. Distal radial and medial wing cells with abundant macrotrichiae, covering mostly distal half of each cell, and missing or nearly missing on basal half. Length of male halter 1.0 mm, of female 0.9–1.2 mm. Halter pale, base, and knob slightly infuscate. Coxae obscure yellow, dusted with grey, fore coxa brownish at base. Trochanters pale yellow. Femur pale yellow with slightly darkened brownish apex, tibia yellow with slightly infuscate tip, first tarsomere yellowish brown at base, brown at distal half, remaining tarsomeres brown to dark brown. Male femur I: 4.1–4.4 mm long, II: 5.2 mm, III: 4.3 mm, tibia I: 4.4–5.3 mm, II: 3.8 mm, III: 4.2 mm, tarsus I: 4.5–5.4 mm, II: 4.4 mm, III: 3.9 mm. Female femur I: 4.0–4.5 mm long, II: 4.4 mm, III: 4.6 mm, tibia I: 4.4–4.5 mm, II: 3.7 mm, III: 5.0 mm, tarsus I: 4.0–4.7 mm, II: 4.1 mm, III: 4.2 mm. Claw simple, black, without spines.

Abdomen. Tergites brown, pregenital tergite dark brown. Four basal sternites yellow to pale yellow, remaining sternites brown, pregenital sternite darker. Male terminalia (Fig. 23) with base of ninth segment darker brown. Distal margin of ninth segment, gonocoxites and gonostyli yellow except blackened distal part of outer gonostylus. Epandrium with two apically blunt lobes at the middle of posterior margin and narrow U-shaped indentation between them. Gonocoxite distinctly wider at base, narrower beyond middle, without addition-

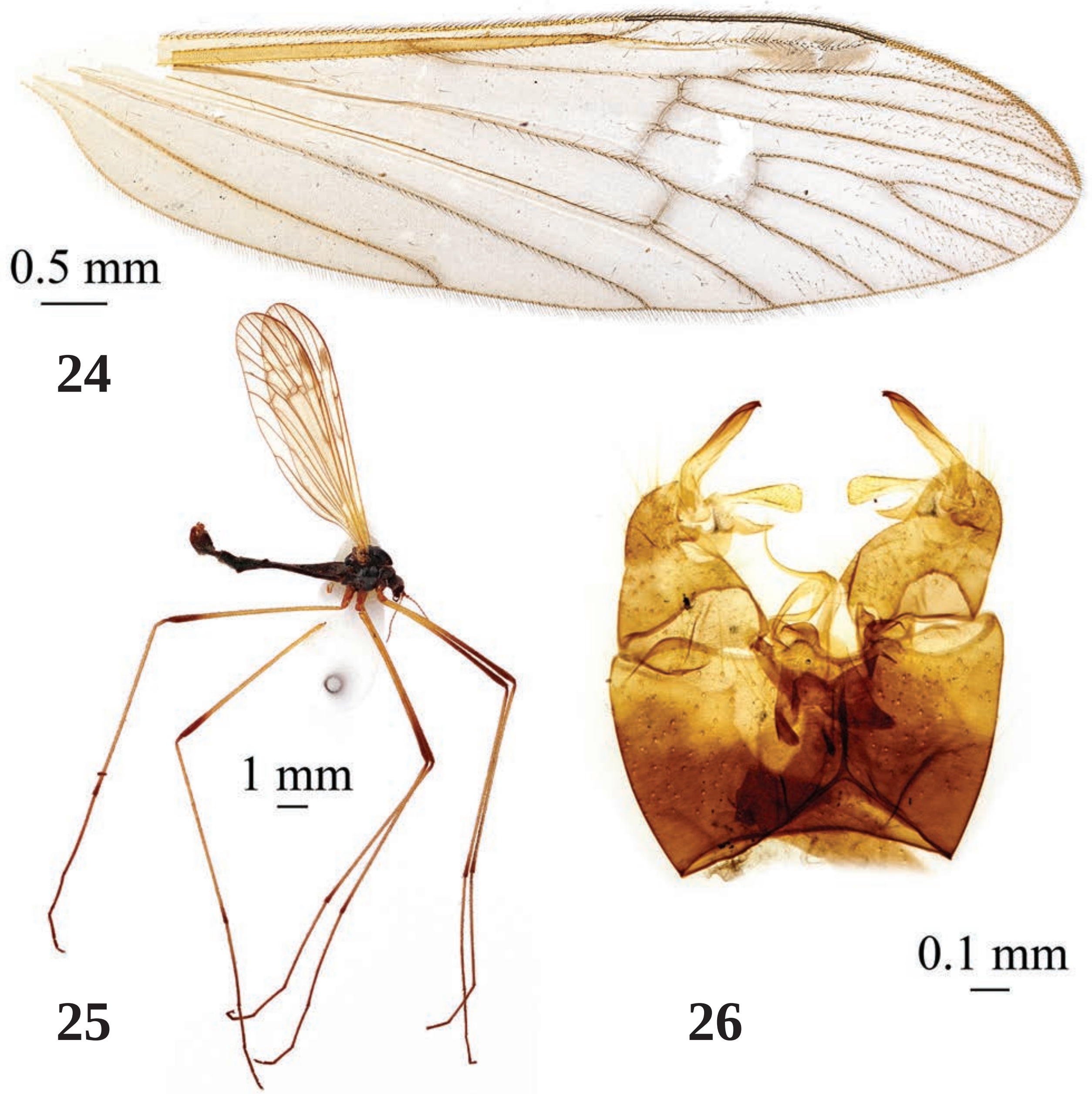

Figures 24–26. *Adelphomyia pilifer* (Alexander, 1919), male **24** wing, paratype **25** general view **26** genitalia, dorsal view, paratype.

al lobe. Outer gonostylus with long, narrow, slightly curved outer branch, and subbasal widening; widened part rounded, but not extended into separate lobe. Outer branch with sclerotised distal part and blackened apex, two small, apical, hook-shaped teeth at tip of outer margin. Inner gonostylus two-branched, outer branch long, narrow, blunt apex knob-shaped, inner branch short, narrow, reaching to approximately middle of outer branch. Aedeagus long, narrow, strongly curved ventrally, distal part at ~ 90° angle to basal part (clearly visible in lateral view). Paramere posteriorly narrow, rod-shaped. Ovipositor obscure yellow. Cercus very long, narrow, distal part slightly raised upwards. Hypogynial valve long, spine-shaped, apex reaching distinctly beyond middle of cercus.

Elevation range. Unknown.

27

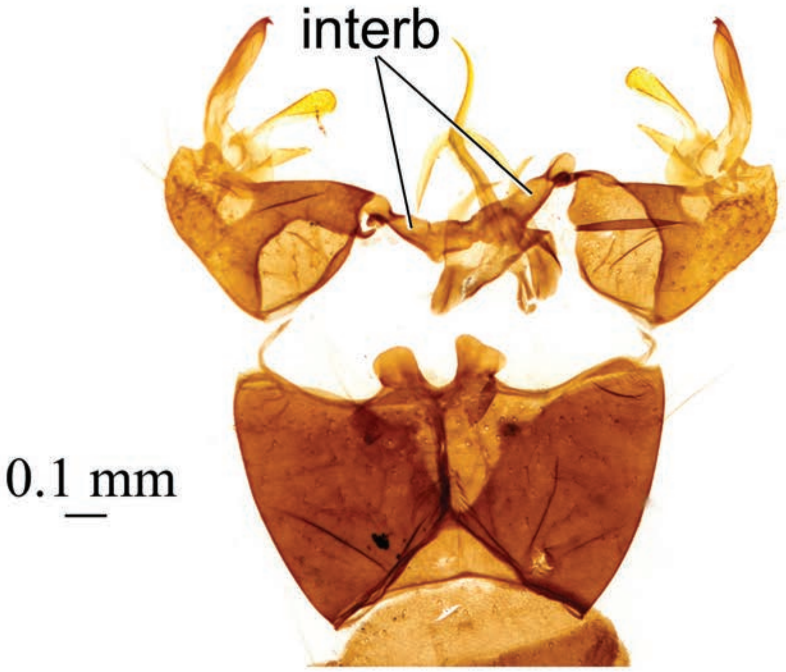

28

Figures 27, 28. *Adelphomyia prionolaboides* (Alexander, 1934), male **27** wing **28** genitalia, dorsal view. Abbreviation: interb – interbases.

Period of activity. Adults were collected only during first two weeks of July in Japan and the Far East of Russia.

Habitat. Adults are flying among dense grassy vegetation along margins of streams and rivers surrounded by wet broad-leaved forests in South Primorye close to the border with Korea (Savchenko 1983).

General distribution. Species was described from Japan (Hokkaido Island), it is recorded from the Far East of Russia (Primorsky Kray).

Remarks. Wing illustrated in Alexander (1940a: pl. 1, fig. 7) does not belongs to the genus *Adelphomyia* or even to the subfamily Limnophilinae. *Adelphomyia macrotrichiata* wing venation is probably shown in pl. 1 fig. 15. Savchenko (1983: 52) wrote that macrotrichiae nearly completely cover distal radial and medial cells in the specimens from the Far East of Russia (in 'Key for identification of regional species'), while North Korean specimens have macrotrichiae mostly at distal half of each cell, basal half bare. Because of that character, North Korean specimens could be identified as *A. punctum* in Savchenko's key for the Far Eastern *Adelphomyia*. Specimens from the Far East have trichiation more similar to the specimens from Japan and to holotype. Savchenko also mentions a large variability of wing venation, especially in the position of R_2, comparative length of cell m_1 and position of *m-cu*. Shape of *A. macrotrichiata* aedeagus is very different from that of *A. punctum*. Aedeagus of *A. macrotrichiata* is long and strongly curved with distal part at right angle to the basal part when aedeagus of *A. punctum* is short and nearly straight. Genitalia of all specimens on which was based the record of *A. macrotrichiata* from North Korea were examined and all of them were identified as *A. punctum*. No *A. macrotrichiata* was found in additional material from the same locality, and the species was not found among other *Adelphomyia* specimens from Korea. Based on this we delete *A. macrotrichiata* from Korean species list. On the other hand, *A. macrotrichiata* was found in the Far East of Russia close to the border with Korea and we expect this species at least in the northern part of the Peninsula.

Adelphomyia punctum **(Meigen, 1818)**

Figs 29–33

Limnobia punctum Meigen, 1818: 128.
Limnophila punctum: Verrall 1886: 200; Meijere 1921: 65, 81; Pierre 1924: 121, 126; Nielsen 1925: 75; Lackschewitz 1940: 85.
Adelphomyia helvetica: Bergroth 1891: 134–135; Pierre, 1924: 115.
Limnophila (*Adelphomyia*) *punctum*: Alexander 1938: 324.
Adelphomyia punctum: Savchenko 1986: 275; Savchenko 1989: 79.

Examined material. (Fig. 49) **North Korea** • 2 ♂ (pinned); Ompo; alt. 76 m; 19 May 1937; Yankovsky leg.; USNM • 1 ♀ (pinned); Ompo; alt. 76 m; 9 June 1937; Yankovsky leg.; USNM • 1 ♂, 8 ♀ (pinned); Ompo; alt. 37 m; 15 June 1937; Yankovsky leg.; USNM • 1 ♂, 1 ex. (broken, pinned); Ompo; alt. 183 m; 23 June 1937; Yankovsky leg.; USNM • 1 ♂ (pinned); Ompo; alt. 274 m; 12 May 1938; Yankovsky leg.; USNM • 1 ♂ (pinned); Ompo; alt. 305 m; 13 May 1938; Yankovsky leg.; USNM • 1 ♂ (pinned); Ompo; alt. 46 m; 25 May 1938; A. Yankovsky leg.; USNM • 1 ♂ (pinned); Ompo; alt. 122 m; 27 May 1938; Yankovsky leg.; USNM • 1 ♂, 1 ♀ (pinned); Ompo; alt. 91 m; 29 May 1938; Yankovsky leg.; USNM • 1 ♂, 5 ♀ (pinned); Ompo; alt. 122 m; 3 June 1938; Yankovsky leg.; USNM • 1 ♀ (pinned); Ompo; alt. 91 m; 9 June 1938; Yankovsky leg.; USNM • 1 ♂, 3 ♀ (pinned); Ompo; alt. 91 m; 10 June 1938; Yankovsky leg.; USNM • 3 ♀ (pinned); Ompo; alt. 107 m; 11 June 1938; Yankovsky leg.; USNM • 3 ♂, 2 ♀ (pinned); Seren Mts.; alt. 762 m; 14 June 1938; A. Yankovsky leg.; USNM • 2 ♂ (pinned); Seren Mts.; alt. 853 m; 15 June 1938; Yankovsky leg.; USNM • 1 ♂ (pinned); Seren Mts.; alt. 914 m; 22 June 1938; A. Yankovsky leg.; USNM • 2 ♂, 1 ex. (broken, pinned); Seren Mts.; alt. 1067 m; 22 June 1938; A. Yankovsky leg.; USNM • 1 ♂ (pinned); Seren Mts.; alt. 1219 m; 22 June 1938; A. M. Yankovsky leg.; USNM • 1 ♀ (pinned); Seren Mts.; alt. 1524–1829 m; 25 June 1938; A. M. Yankovsky leg.; USNM • 1 ♀ (pinned); Seren Mts.; alt. 1676 m; 25 June 1938; A. Yankovsky leg.; USNM • 2 ♂, 1 ♀ (pinned); Seren Mts.; alt. 1829 m; 25 June 1938; A. Yankovsky leg.; USNM • 1 ♂ (pinned); Seren Mts.; alt. 914 m; 30 June 1938; A. Yankovsky leg.; USNM • 1 ♂ abdomen (pinned); Kankyo Nando Puksu Pyaksan; alt. 1829 m; 15 June 1939; Yankovsky leg.; USNM • 1 ♂ (pinned, genitalia dissected in microvial with glycerol on same pin); Kankyo Nando, Puksu Pyaksan; alt. 1676 m; 17 July 1939;

A. Yankovsky leg.; USNM • 1 ♂, 1 ♀ (pinned); Kankyo Nando, Puksu Pyaksan; alt. 1829 m; 24 July 1939; A. Yankovsky leg.; USNM • 1 ♂, 2 ♀ (pinned); Kankyo Nando, Puksu Pyaksan; alt. 1524 m; 3 August 1939; A. Yankovsky leg.; USNM; **South Korea** • 1 ♂ (in ethanol); Gangwon-do, Pyeonchang-gun, Odaesan National Park; 37.74913°N, 128.57723°E; alt. 726 m; 22 June 2012; S. Kim, S. Podenas leg.; NIBR • 2 ♂ (in ethanol); Jeollabuk-do, Namwon, Unbong-eup, Hwasu-ri; 35.45345°N, 127.57759°E; alt. 509 m; 6 May 2013 (01); S. Podenas leg.; NIBR • 1 ♂ (in ethanol); Gyeongsangnam-do, Hamyang, Macheon-myeon, Samjeong-ri; 35.36713°N, 127.65228°E; alt. 406 m; 11 May 2013 (5); S. Podenas leg.; NIBR • 2 ♂ (in ethanol); Gyeonggi-do, Paju-si, Gunnae-myeon, Jeomwon-ri, Gate (South-MDL); 37.93430°N, 126.72097°E; alt. 39 m; 20 May 2016; T. E. Klein, H.-C. Kim leg.; Mosquito Magnet; NIBR • 1 ♀ (in ethanol); Jeollanam-do, Gurye-gun, Toji-myeon, Naeseo-ri, Piagol valley; 35.27333°N, 127.56924°E; alt. 546 m; 3 June 2016 (3); S. Podenas leg.; NIBR • 1 ♀ (in ethanol); Jeollanam-do, Gurye-gun, Toji-myeon, Naeseo-ri, Piagol valley; 35.27123°N, 127.57133°E; alt. 534 m; 4 June 2016 (1); V. Podeniene leg.; NIBR • 2 ♂ (in ethanol); Gyeonggi-do, Paju-si, Gunnae-myeon, Jeomwon-ri, Gate (South-MDL); 37.93431°N, 126.72096°E; alt. 39 m; 17 May 2019; T. E. Klein, H.-C. Kim leg.; Mosquito Magnet; NIBR.

Comparative material examined. **Lithuania** • 1 ♂ (genitalia in microvial with glycerol); Raseiniai district, Sargeliai; 55.4762°N, 23.4563°E; 5–13 June 2009; NRC • 1 ♂, 1 ♀ (pinned); Moletai distr., river Skardis; 55.29132°N, 025.45485°E; alt. 150 m; 26 May 2012; S. Podenas leg.; NRC.

Redescription. General body colouration varies from yellowish brown to greyish brown. Body length of male 3.9–8.2 mm, female 6.4–7.2 mm. Male wing: 6.1–8.8 mm; female wing: 6.1–8.3 mm.

Head. Slightly extended posteriorly, grey, brownish grey postero-laterally, pale grey frontally, covered with long, sparse, yellowish setae, longest of which nearly as long as both basal antennomeres combined. Eyes widely separated in both sexes, distance between them at base of antennae nearly same as length of both basal antennomeres together. Length of male antenna 0.9–1.8 mm, reaching wing base if bent backward; female 1.1–1.3 mm. Scape brown dusted with grey, elongate, nearly cylindrical, 2.2× as long as wide and 2× as long as pedicel. Pedicel oval, brown, covered with few short setae. Flagellum 14-segmented, brown, distal flagellomeres darker. Flagellomeres oval with short apical pedicels, apical segment nearly as long as preceding. Verticils up to 2.5× as long as respective segments. Short erect pubescence, covering segments pale. Rostrum, palpi, and mouth parts dark brown to blackish.

Thorax. Cervical sclerites brown, dark brown ventrally, covered with grey pruinosity. Thorax yellowish brown to brown covered with sparse grey pruinosity. Pronotum pale brown to brown, dusted with grey, dorso-laterally covered with sparse erect long setae. Mesonotal prescutum semi-polished, pale brown, sparsely dusted with grey, yellowish laterally, covered with sparse erect setae, longitudinal stripes absent or very indistinct in some specimens. Tubercular pit small, brown, close to frontal margin of sclerite, pseudosutural fovea distinct dark brown. Scutal lobe frontally concolourous with presutural scutum, laterally and posteriorly brownish yellow. Area between scutal lobes greyish. Scutellum brownish at the middle, yellow laterally. Mediotergite yellow with narrow indistinct greyish brown median line. Pleuron bare, without setae, brownish yellow, sparsely dusted with grey; posterior basal area brown. Wing (Fig. 29) semi-trans-

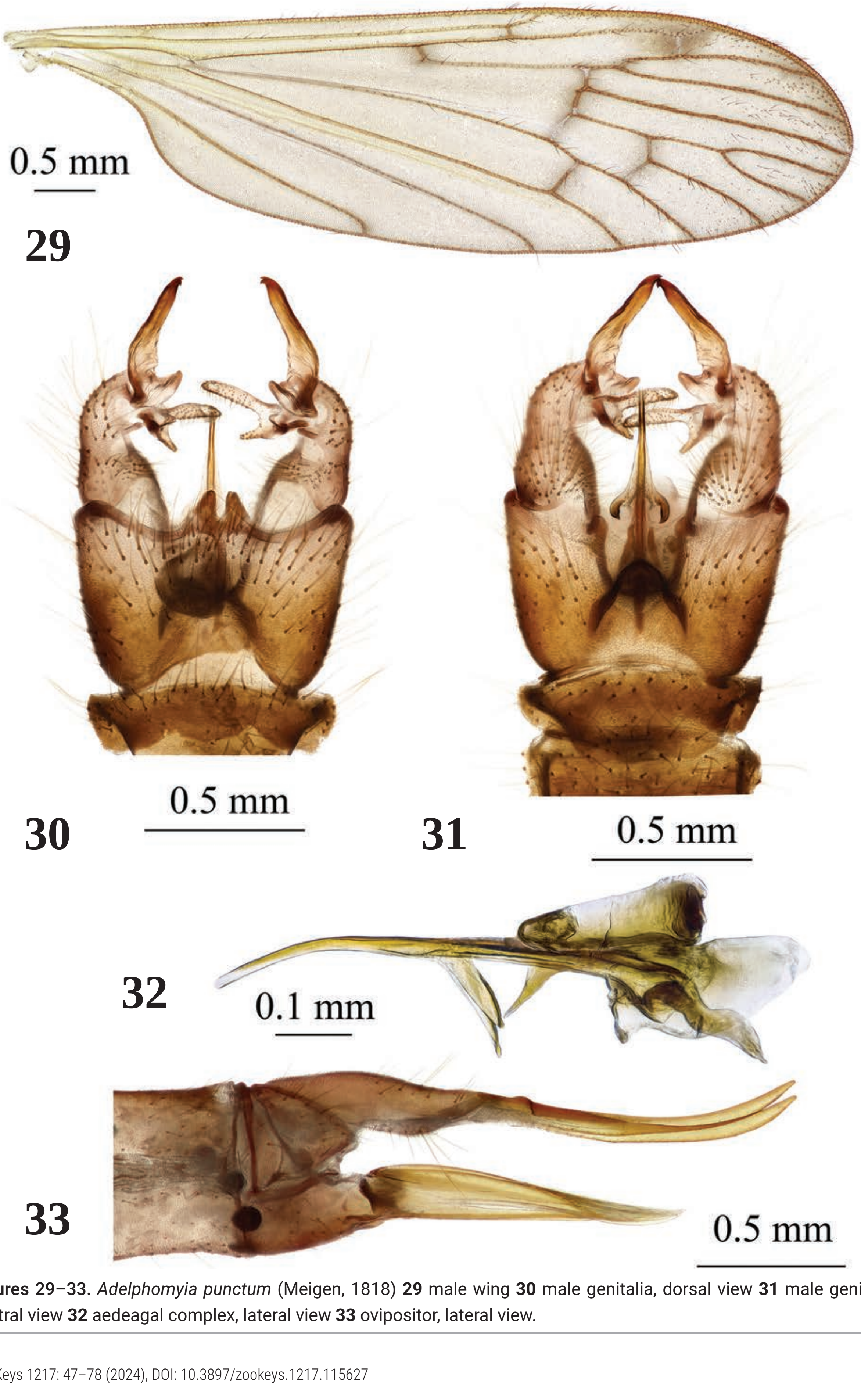

Figures 29–33. *Adelphomyia punctum* (Meigen, 1818) **29** male wing **30** male genitalia, dorsal view **31** male genitalia, ventral view **32** aedeagal complex, lateral view **33** ovipositor, lateral view.

lucent, with indistinct darkening surrounding cross-veins and apices of all longitudinal veins at wing margin, some specimens without such darkening. Stigma elongate, brownish. Veins brown, yellowish at wing base and in costal area. Macrotrichiae more abundant in radial cells and cell m_1, present also in other marginal cells along postero-apical wing margin. Venation: *Sc* long, but not reaching branching point of *Rs*, *sc-r* ~ 3× its own length from tip of *Sc*. *Rs* long, slightly arched or angulate at base, with or without short spur. Free end of R_1 longitudinal, R_2 transverse, indistinct, ~ 2× its own length from tip of R_1, R_3, and R_4 slightly diverging towards wing margin, cell r_3 with short stem. Cross-vein *r-m* distinct, at base of discal cell. Discal cell 2× as long as wide. Cross-vein *m-cu* slightly before middle of discal cell. Anal vein slightly arched at wing margin, ending slightly before base of *Rs*. Anal angle widely rounded. Male halter 0.9–1.7 mm long, female 0.8–1.3 mm. Halter pale brownish, knob slightly infuscate distally. Frontal coxa pale brown frontally, yellow posteriorly, remaining coxae yellow, slightly dusted with grey, covered with long erect yellowish setae. Trochanters yellow to brownish yellow. Femur yellow, darkened at apex, tibia yellowish brown with darkened distal part, tarsomeres dark brown, only base of basal tarsomeres yellowish. Male femur I: 3.9–5.0 mm, II: 4.2–5.2 mm, III: 4.2–6.2 mm, tibia I: 5.7–5.9 mm, II: 4.8–5.5 mm, III: 4.5–6.2 mm, tarsus I: 5.7–6.4 mm, II: 5.4–5.9 mm, III: 3.9–5.3 mm. Female femur I: 3.6 mm long, II: 3.8–4.2 mm, III: 4.1–4.7 mm, tibia I: 4.1 mm, II: 3.5–4.0 mm, III: 4.0–5.0 mm, tarsus I: 3.9–4.0 mm, II: 3.5–3.8 mm, III: 3.1–3.7 mm long. Claw simple without subbasal spines or teeth.

Abdomen. Semi-polished brownish yellow to brown. Two pregenital segments darkened in male, concolourous with the rest abdominal segments in female. Tergites with narrowly darkened lateral margins, with two transverse narrow indentations frontally and slightly paler posterior margin in both sexes. Male terminalia (Figs 30, 31) brownish yellow. Ninth tergite with two triangle-shaped lobes at the middle of posterior margin. Gonocoxite elongate, distinctly wider at base, narrower beyond middle, without additional lobe. Outer gonostylus with long narrow outer branch and small rounded lobe at base. Outer branch with sclerotised distal part and blackened apex, two small apical hook-shaped teeth curved medially. Inner gonostylus large, fleshy, setose, two-branched. Outer branch long and narrow, inner branch narrowly triangle-shaped reaching approximately to middle of outer branch. Aedeagus (Fig. 32) long and nearly straight, paramere posteriorly short, slightly arched, reaching before middle of aedeagus. Ovipositor (Fig. 33) yellow with very long, narrow cercus and hypovalva. Distal part of cercus slightly turned upwards, dorsal margin brownish, apex point-shaped. Hypogynial valve long, straight, wide at base, narrowing towards apex, distal part distinctly narrower, apex reaching beyond middle of cercus, dorsal margin at ~ 1/4 length from apex with long dense setae.

Elevation range. From the lowest elevations in Korea to more than 1800 m.

Period of activity. Adults on wing from beginning of May through early August.

Habitat. Wet places near streams and ponds surrounded by deciduous trees and in wet places of deciduous and mixed forests.

General distribution. Species has widely disjunct area, it is widely distributed in Europe, recorded also from eastern part of East Palaearctic. Recorded from the Korean Peninsula for the first time.

Remarks. Some specimens from North Korea are distinctly darker than specimens from Europe, their wings lack any pattern except stigma. At the moment, it is difficult to say if that is variation or colour change due to long preservation.

34

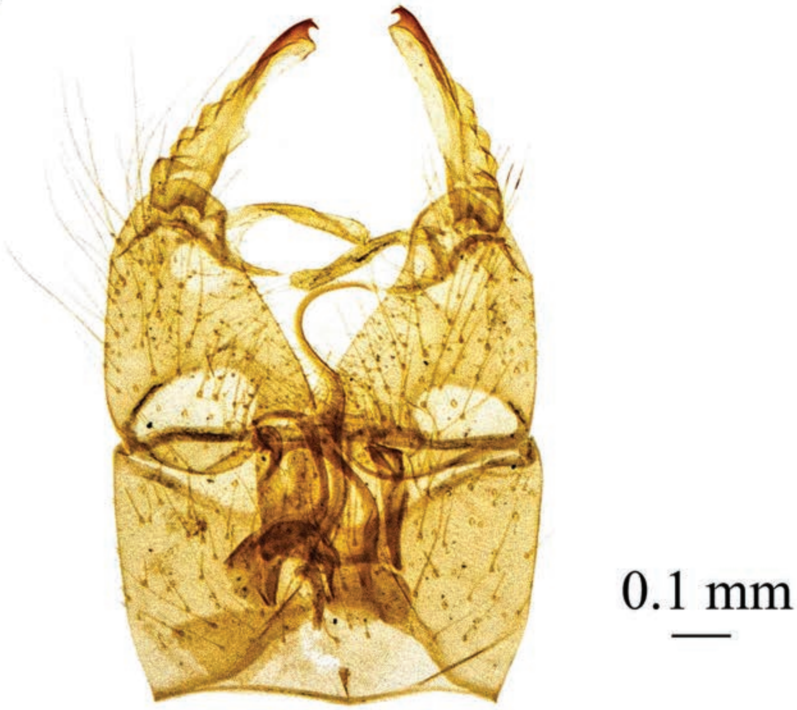

35

Figures 34, 35. *Adelphomyia saitamae* (Alexander, 1920), male **34** wing **35** genitalia, dorsal view.

North Korean specimens were collected 80 years ago. We examined male genitalia of these specimens and compared them with "typical" specimens from Europe and South Korea, but no differences were observed.

Adelphomyia jejuana Podenas, sp. nov.

https://zoobank.org/5EA7A898-2697-49FE-B459-C68920F6C199

Figs 40–46

Type material examined. South Korea • Holotype ♂ (pinned, wing slide-mounted, genitalia in microvial with glycerol on same pin); Jeju-do, Jeju-si, Hallasan National Forest; 33.43222°N, 126.59776°E; alt. 577 m; 24 May 2017 (1); S. Podenas leg.; NIBR. **Paratypes** • 1 ♀ (pinned, wing slide-mounted); same data as holotype, topotypic; NIBR • 1 ♀ (in ethanol); Jeju-do, Seogwipo-si, Saekdal-dong; 33.36044°N, 126.46275°E; alt. 1103 m; 19 June 2019 (1); S. Podenas leg.; NIBR.


36


37

Figures 36, 37. *Adelphomyia satsumicola* (Alexander, 1930), male, holotype **36** wing **37** genitalia, dorsal view.

Diagnosis. Reddish brown species ~ 4–7 mm long (Figs 40, 44). Head greyish brown, thorax pale brown, prescutal stripes missing. Wing brownish, no pattern with indistinct stigma. Abdomen yellow, dorsally slightly darker than ventrally. Ninth tergite of male genitalia with two point-apexed triangle-shaped lobes at posterior margin. Gonocoxite elongate. Outer gonostylus with long narrow outer branch and small angulate lobe at base. Outer branch with longitudinal wrinkles, sclerotised distal part and blackened apex. Distal part with widely rounded medial edge and two small apical hook-shaped teeth curved medially. Inner gonostylus large, fleshy, setose, two-branched. Aedeagus comparatively short, slightly arched, paramere narrowly rod-shaped, slightly arched, reaching to ~ 2/3 of aedeagus length. Ovipositor yellow with very long, narrow cercus and hypovalva. Apical part of cercus slightly turned upwards.

Etymology. Species is named after its type locality, Jeju Island, Korea.

Description. General body colour reddish brown (Figs 40, 44). Body length of male ~ 4 mm, female 5.3–6.8 mm. Male wing: 6.2 mm, female wing: 6.7 mm.

Head. Greyish brown, posteriorly pale brown, pale grey along eye margin, with few yellowish setae dorsally. Eyes widely separated in both sexes, distance between them at base of antennae same as length of scape. Length of female antenna 1.2 mm, reaching wing base if bent backwards. Scape brown dusted with grey, elongate, nearly cylindrical, 2× as long as wide, and 2× as long as pedicel. Pedicel rounded, brown, covered with few short setae. Flagellum

38

39

Figures 38, 39. *Adelphomyia simplicistyla* (Alexander, 1940b), male, holotype **38** wing **39** genitalia, dorsal view.

14-segmented, pale brown. Flagellomeres oval with short apical pedicels, apical segment as long as preceding. Verticils 2× as long as respective segments. Short erect pubescence, covering segments pale. Rostrum, palpi, and mouth parts brown sparsely dusted with grey.

Thorax. Brownish yellow, covered with sparse brownish grey pruinosity. Cervical sclerites and pronotum brown sparsely dusted with grey. Pronotum elongate with extended postero-lateral angle. Mesonotal prescutum semi-polished, brownish yellow with sparse grey pruinosity, frontal margin slightly darkened, stripes missing. Scutal lobes, scutellum, and mediotergite uniformly brownish yellow. Pleuron brownish yellow indistinctly darker above coxae. Wing (Figs 41, 45) translucent with weak brownish tint, slightly yellowish at base. No darkening along cross-veins or branching points of veins. Stigma indistinct, nearly missing. Veins pale brown. Wing venation: vein *Sc* long, apex reaching wing margin slightly before branching point of radial sector, *sc-r* 2× its own length before apex of *Sc*, *Rs* long, nearly straight, just slightly arched at base, R_2 4× its own length before apex of R_1, cell r_1 slightly widened at wing margin; R_3 and R_4 slightly diverging towards wing margin, cell r_3 with short stem. Cross-vein *r-m* distinct, at base of discal cell. Discal cell 2.3× as long as wide. Cross-vein *m-cu* slightly before middle of discal cell. Anal vein slightly arched at wing margin, ending at the level of *Rs* base in male, slightly beyond base of *Rs* in female. Anal angle widely rounded. Male halter 0.8 mm long, female 1.0 mm. Halter brownish

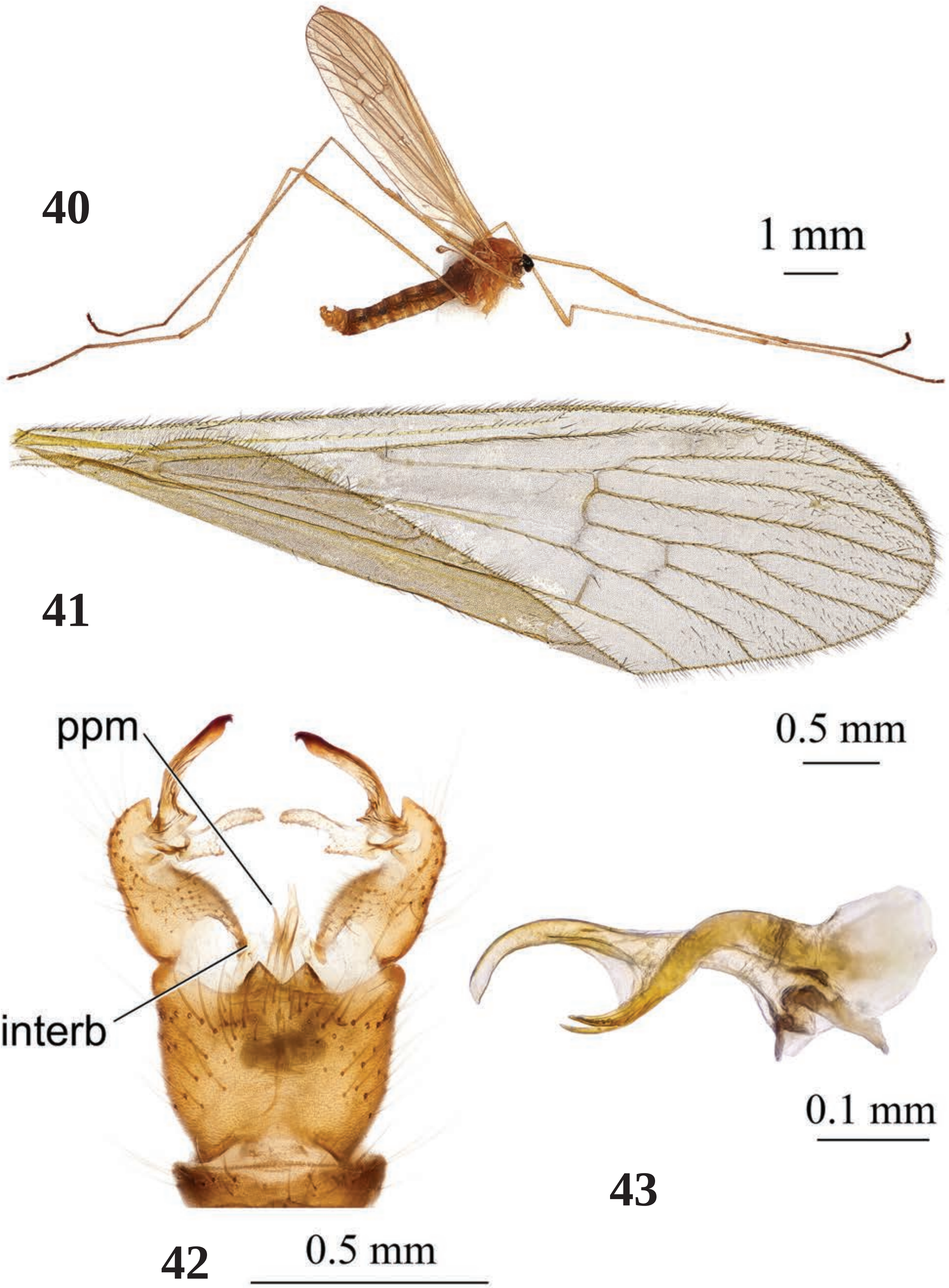

Figures 40–43. *Adelphomyia jejuana* Podenas, sp. nov., holotype, male **40** general view **41** wing **42** genitalia, dorsal view **43** aedeagal complex, lateral view. Abbreviations: interb – interbase; ppm – posterior part of paramere.

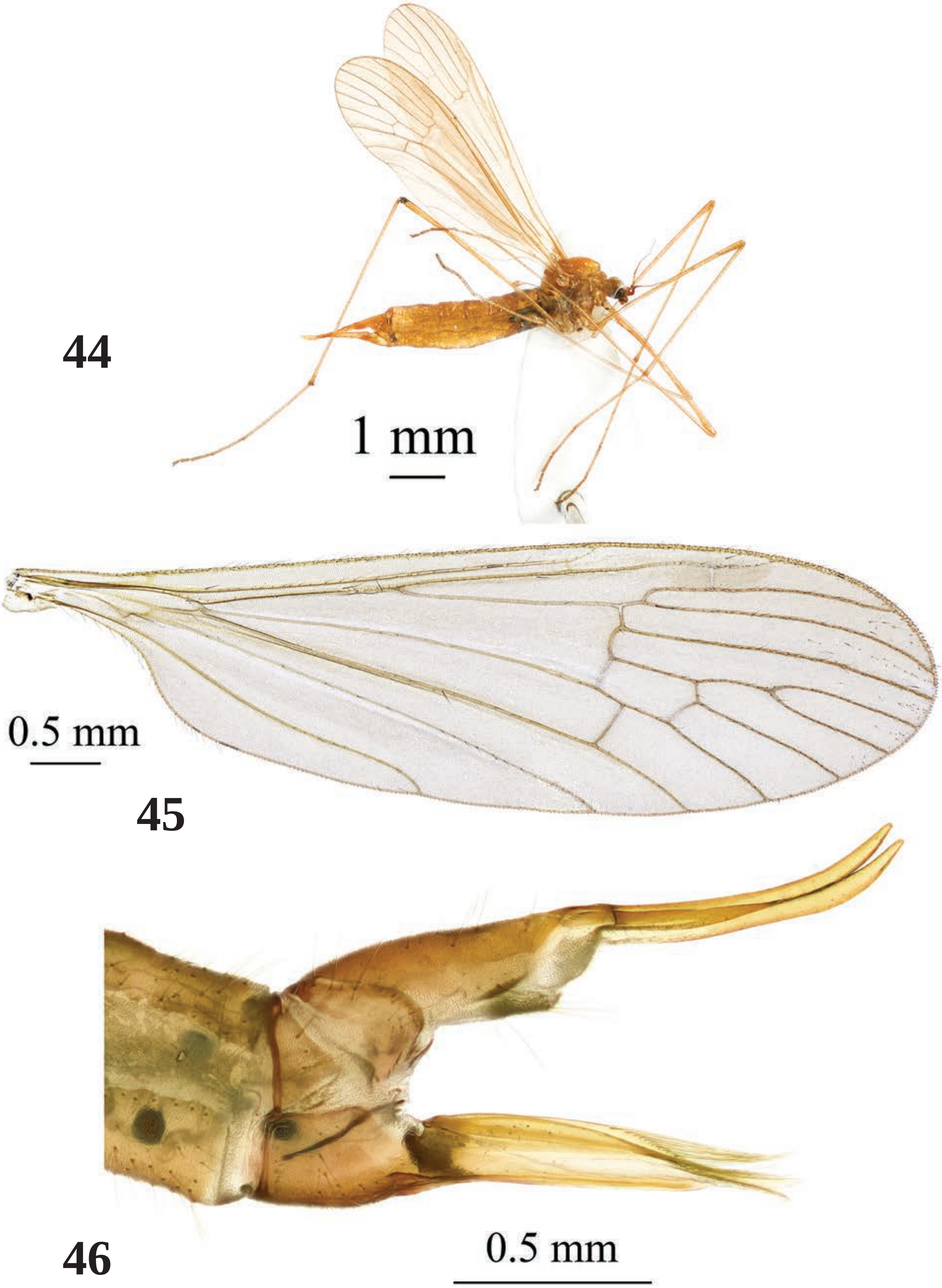

Figures 44–46. *Adelphomyia jejuana* Podenas, sp. nov., paratype, female **44** general view **45** wing **46** ovipositor, lateral view.

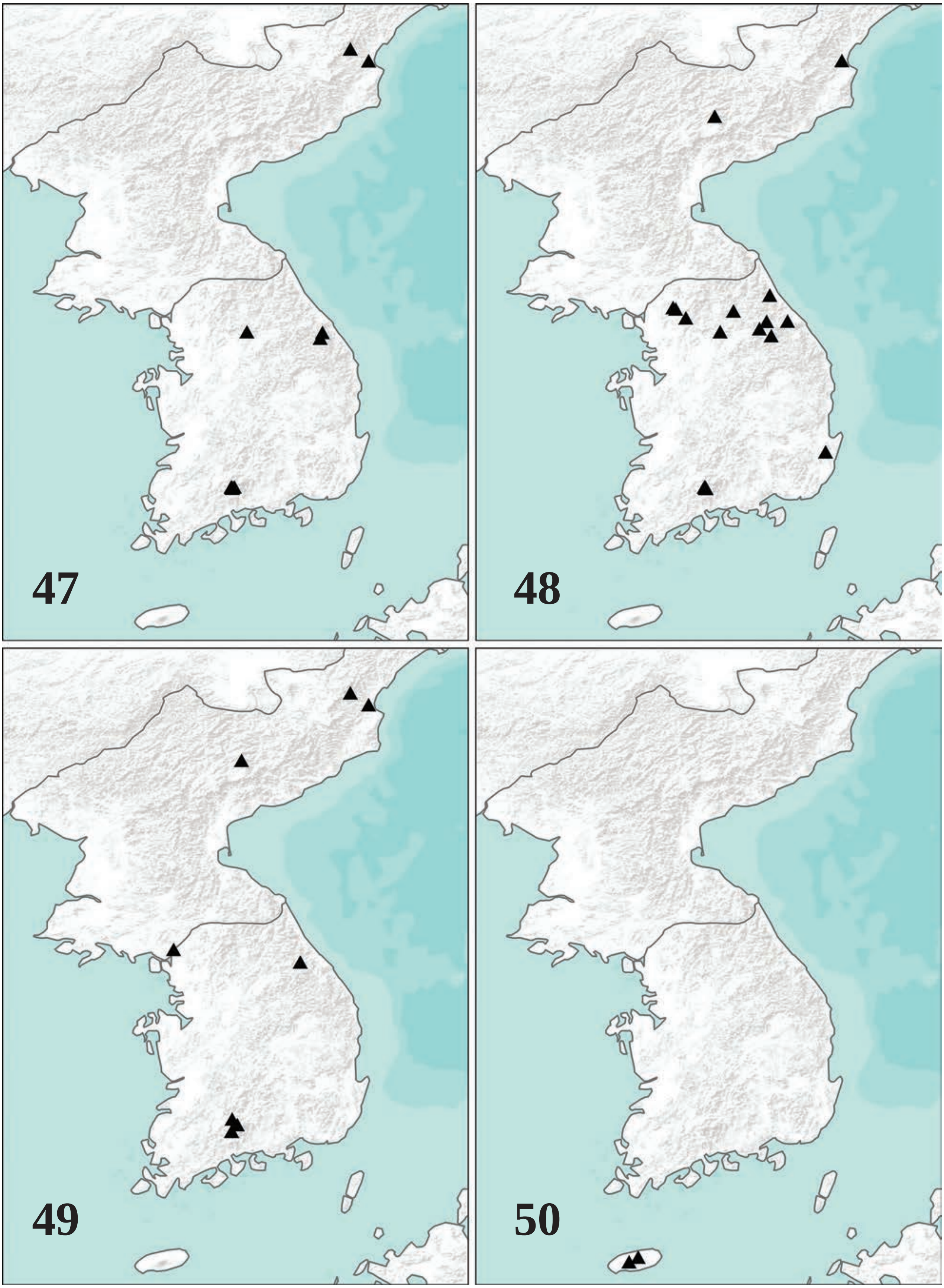

Figures 47–50. Sampling localities of Korean *Adelphomyia* **47** *A. acicularis bidens* Savchenko, 1983 **48** *A. flavella* (Alexander, 1920) **49** *A. punctum* (Meigen, 1818) **50** *A. jejuana* Podenas, sp. nov.

yellow, knob with greyish tinge. Coxae and trochanters brownish yellow, legs yellow with brownish distal tarsomeres. Male femur I: 3.6 mm, III: 4.5 mm, tibia I: 4.7 mm, III: 4.6 mm, tarsus I: 4.7 mm, III: 4.0 mm. Female femur I: 3.7 mm long, II: 3.5 mm, III: 4.2 mm, tibia I: 4.0 mm, II: 3.5 mm, III: 4.2 mm, tarsus I: 4.0 mm, II: 3.5 mm, III: 3.5 mm long. Claw simple without subbasal spines or teeth.

Abdomen. Tergites brownish yellow, sternites yellow. Male terminalia (Fig. 42) yellow. Ninth tergite with two sharply apexed triangle-shaped lobes at the middle of posterior margin and wide V-shaped emargination between them. Gonocoxite elongate, wider at base, narrower beyond two thirds of length, without additional lobe. Outer gonostylus with long, narrow outer branch and small angulate lobe at base. Outer branch with longitudinal wrinkles, sclerotised distal part and blackened apex. Distal part with widely rounded medial edge and two small apical hook-shaped teeth curved medially. Inner gonostylus large, fleshy, setose, two-branched. Outer branch long, narrow, inner branch short triangle-shaped reaching to ~ 1/4 of outer branch length. Aedeagus (Fig. 43) comparatively short, slightly arched, paramere narrowly rod-shaped, slightly arched, reaching to ~ 2/3 of aedeagus. Distal part of interbase pale yellow, rounded. Ovipositor (Fig. 46) yellow with very long narrow cercus and hypovalva. Apical part of cercus slightly raised upwards. Hypogynial valve wide at base, apical part distinctly narrower, dorso-apical margin covered with long setae. Apex of hypogynial valve reaches slightly beyond middle of cercus.

Distribution. Currently known only from Jeju Island, South Korea (Fig. 50).

Habitats. Small valley of temporary stream covered with deciduous trees and shrubs, moss-covered rocks; small swampy meadow on the edge of small stream surrounded by deciduous forest.

Elevation. From less than 600 m to 1100 m.

Period of activity. Adults on wing from late May through middle of June.

Remarks. *Adelphomyia jejuana* Podenas, sp. nov., having unpatterned wings and pale body colouration, resembling *A. flavella* but differs from it by details of male terminalia and darker body colouration. Ninth tergite of *A. jejuana* Podenas, sp. nov., especially lobes on posterior margin, resemble that of *A. acicularis bidens*, but in *A. jejuana* Podenas, sp. nov. they are distinctly wider at base and point-apexed. Subapical angle of outer gonostylus is low and widely rounded in *A. jejuana* Podenas, sp. nov., when that in most other Palaearctic species is very distinct and nearly right-angled. Aedeagus of *A. jejuana* Podenas, sp. nov. is shorter than that in *A. flavella*, just slightly extending beyond apices of parameres, when that in *A. flavella* is very long and distinctly curved. Aedeagus in *A. acicularis bidens*, *A. saitamae*, *A. macrotrichiata*, *A. breviramus*, *A. biacus*, and *A. flavella* is strongly curved at nearly right angle, straight in *A. punctum*, *A. casiella*, and *A. satsumicola*, but slightly arched in *A. jejuana* Podenas, sp. nov. Paramere of *A. jejuana* Podenas, sp. nov. is similar to that of *A. flavella*.

Other examined material from Palaearctic

Adelphomyia acicularis acicularis (Alexander, 1954) (Figs 1–3). **Japan** • **Holotype** ♂; as *Limnophilla* (*Adelphomyia*) *acicularis*; wing, leg, and genitalia slide-mounted; Shikoku, Mt. Tsurugi-Awa; 1 June 1950; Issiki-Ito leg.; USNM; • **Paratype** ♂; head, wing, leg, and genitalia slide-mounted; Shikoku, Imanoyama, Tosa; alt. 865 m; 12 May 1951; Issiki-Ito leg.; USNM.

Adelphomyia biacus (Alexander, 1954) (Figs 9–11). **Japan** as *Limnophila* (*Adelphomyia*) *biacus*; • **Holotype** ♂; slide–mounted; Shikoku, Mt. Isizuti; June 10, 1950; Issiki-Ito leg.; USNM; • **Paratype** ♂; slide-mounted; Shikoku, Omogokei; June 6, 1952; T. Yano leg.; USNM.

Adelphomyia breviramus (Alexander, 1924) (Figs 12–14). **Japan** as *Limnophila* (*Lasiomastix*) *breviramus*; • **Holotype** ♂; slide-mounted; Yumoto; alt. 1774 m; 23 July 1923; T. Esaki leg.; USNM; • **Metatype** ♂; slide-mounted; Shikoku, Mt. Ishizuchi-Iyo; 9 June 1950; Issiki Ito leg.; USNM; as *Limnophila* (*Adelphomyia*) *brevirama*; • **Metatype** ♂; slide-mounted; Hida, Ontake; 26 July 1959; T. Mishima leg.; USNM.

Adelphomyia caesiella (Alexander, 1929) (Figs 15, 16). **Japan** as *Limnophila* (*Tricholimnophila*) *caesiella*; • **Metatype** ♂; slide-mounted; Kiushiu, Mt. Kirishima; alt. 762 m; 3 May 1929; S. Issiki leg.; USNM.

Adelphomyia pilifer (Alexander, 1919) (Figs 24–26). **Japan** • **Paratopotype** ♂; as *Limnophila* (*Lasiomastix*) *pilifer*; slide-mounted wing and genitalia; Tokyo, Meguro; 9 April 1919; R. Takahashi leg.; USNM • 1 ♂; pinned; Hokkaido, near Sapporo, Maruyama; 31 May 1953; S. Kuwayama leg.; USNM • 2 ♂, 1 specimen with broken abdomen; pinned; Hokkaido, Prov. Ishikari, Nopporo; 18 June 1953; Y. Nishio leg.; USNM.

Adelphomyia prionolaboides (Alexander, 1934) (Figs 27, 28). **Japan** as *Limnophila* (*Adelphomyia*) *prionolaboides*; • **Metatype** ♂; slide-mounted; Mino, Sakauchi; 4 May 1958; T. Mishima leg.; USNM.

Adelphomyia saitamae (Alexander, 1920) (Figs 34, 35). **Japan** as *Limnophila saitamae*; • **Metatype** ♂; slide-mounted; Honshu, Tyuzenzi; 22 June 1932; S. Issiki leg.; USNM.

Adelphomyia satsumicola (Alexander, 1930) (Figs 36, 37). **Japan** as *Limnophila* (*Tricholimnophila*) *satsumicola*; • **Holotype** ♂; slide-mounted; Shiroyama hill, city-oz Kagoshima; 27 April 1929; S. Issiki leg.; USNM; • **Paratype** ♂; slide-mounted, Shiroyama hill, Kagoshima city; 27 April 1929; S. Issiki leg.; USNM.

Adelphomyia simplicistyla (Alexander, 1940b) (Figs 38, 39). **China** as *Limnophila simplicistyla*; • **Holotype** ♂; slide-mounted; Szechwan [Sichuan], Omei, Nwa Ien Ting Temple; alt. 1981 m; 15 June 1938; Tsen leg.; USNM.

Acknowledgements

Our warmest thanks to all Korean friends and colleagues who helped us during our visits to South Korea. We are very grateful for Dr F. Shockley and Dr T. Dikow (USNM) and Dr J. K. Gelhaus (Academy of Natural Sciences of Drexel University, U. S. A.) for the use of specimens from the USNM collections, Dr T. A. Klein and Dr H.-C. Kim (Force Health Protection and Preventive Medicine, Medical Department Activity-Korea (MEDDAC-K)/65th Medical Brigade, Unit 15281, APO AP 96271) for their specimens and two anonymous reviewers for their comments and improvements of the text.

Additional information

Conflict of interest

The authors have declared that no competing interests exist.

Ethical statement

No ethical statement was reported.

Funding

This work was supported by a grant from the National Institute of Biological Resources (NIBR), funded by the Ministry of Environment (MOE) of the Republic of Korea (NIBR202203104).

Author contributions

All authors have contributed equally.

Author ORCIDs

Sun-Jae Park https://orcid.org/0000-0003-3759-6517
Sigitas Podenas https://orcid.org/0000-0002-2597-566X

Data availability

All of the data that support the findings of this study are available in the main text.

References

Alexander CP (1919) Undescribed species of Japanese crane-flies (Tipulidae, Diptera). Annals of the Entomological Society of America 12(4): 327–348. https://doi.org/10.1093/aesa/12.4.327

Alexander CP (1920) New or little-known crane-flies from Japan (Tipulidae, Diptera). Transactions of the American Entomological Society 46: 1–26.

Alexander CP (1923) Undescribed species of Japanese crane-flies (Tipulidae, Diptera). Part III. Annals of the Entomological Society of America 16(1): 57–76. https://doi.org/10.1093/aesa/16.1.57

Alexander CP (1924) New or little-known Tipulidae (Diptera). XXVI. Palaearctic species. Annals & Magazine of Natural History 15(9): 65–81. https://doi.org/10.1080/00222932508633181

Alexander CP (1928) New or little-known Tipulidae from eastern Asia (Diptera). II. Philippine Journal of Science 35: 455–489. https://doi.org/10.5962/bhl.part.25391

Alexander CP (1929) New or little-known Tipulidae from eastern Asia (Diptera). V. Philippine Journal of Science 40: 519–547.

Alexander CP (1930) New or little-known Tipulidae from eastern Asia (Diptera). VII. Philippine Journal of Science 42: 507–535.

Alexander CP (1934) New or little-known Tipulidae from eastern Asia (Diptera). XVIII. Philippine Journal of Science 53: 267–300.

Alexander CP (1938) New or little-known Tipulidae from eastern Asia (Diptera). XXXVIII. Philippine Journal of Science 66: 309–342.

Alexander CP (1940a) New or little-known Tipulidae from eastern Asia (Diptera). XLI. Philippine Journal of Science 71: 39–76.

Alexander CP (1940b) New or little-known Tipulidae from eastern Asia (Diptera). XLII. Philippine Journal of Science 71: 169–204.

Alexander CP (1954) Records and descriptions of Japanese Tipulidae (Diptera). Part III. The crane-flies of Shikoku. III. Philippine Journal of Science 82: 263–308.

Bergroth EE (1891) Beitrag zur Tipuliden-Fauna der Schweiz. Mitteilungen der Naturforschenden Gesellschaft in Bern 1890: 129–138.

Cumming JM, Wood DM (2017) Adult morphology and terminology. In: Kirk-Spriggs AH, Sinclair BJ (Eds) Manual of Afrotropical Diptera. Volume 1. Introductory chapters and keys to Diptera families. Suricata 4. South African National Biodiversity Institute, Pretoria, 107–151.

de Jong H (2017) 14. Limoniidae and Tipulidae (crane flies). In: Kirk-Spriggs AH, Sinclair BJ (Eds) Manual of Afrotropical Diptera. Volume 2. Nematocerous Diptera and lower Brachycera. Suricata 5. South African National Biodiversity Institute, Pretoria, 427–477.

Ishida H (1959) The catalogue of the Japanese Tipulidae, with the keys to the genera and subgenera (Diptera). V. Limoniinae, Tribe Hexatomini. Science Report of the Hyogo University of Agriculture, Serie. Nature and Science 4(1): 3–11.

Lackschewitz P (1940) Die palaarktischen Limnophilinen, Anisomerinen und Pediciinen des Wiener Naturhistorischen Museums. Annalen des Naturhistorischen Museums in Wien 50: 68–122.

Meigen JW (1818) Systematische Beschreibung der bekannten europaischen zweiflugeligen Insekten. F.W. Forstmann, Aachen, 333 pp. https://doi.org/10.5962/bhl.title.13731

Nielsen P (1925) Stankelben. Danmarks Fauna. G. E. C. Gads Forlag, Copenhagen 28: 165 pp.

Oosterbroek P (2024) Catalogue of the Craneflies of the World (CCW). https://ccw.naturalis.nl/index.php [last update 23 Mar. 2024]

Pierre C (1924) Dipteres: Tipulidae. Faune de France. Paul Lechevalier, Paris, 8: 159 pp.

Ribeiro GC (2008) Phylogeny of the Limnophilinae (Limoniidae) and early evolution of the Tipulomorpha (Diptera). Invertebrate Systematics 22(6): 627–694. https://doi.org/10.1071/IS08017

Salmela J, Härmä O (2004) *Adelphomyia punctum* (Meigen, 1818) found from Finland (Diptera, Limoniidae). Sahlbergia 9: 141–143.

Savchenko EN (1983) Limoniidae of South Primorye. Akademiya Nauk Ukrainskoy SSR, I. I. Schmalhausen Institute of Zoology of Academy of Sciences of Ukraine, Naukova Dumka, Kiev, 156 pp. [in Russian]

Savchenko EN (1986) Short-palped crane flies. (General description, subfamilies Pediciinae and Hexatominae). Fauna Ukrainy. Akademiya Nauk Ukrainskoy SSR, I. I. Schmalhausen Institute of Zoology of Academy of Sciences of Ukraine, Naukova Dumka, Kiev 14(2): 380 pp. [in Russian]

Savchenko EN (1989) Limoniidae fauna of the USSR. Determination tables of superspecies taxa with catalogue survey of species. Akadimiya Nauk Ukrainian SSR, I. I. Schmalhausen Institute of Zoology of Academy of Sciences of Ukraine, Naukova Dumka, Kiev, 377 pp. [in Russian]

Savchenko EN, Krivolutskaya GO (1976) Limoniidae of the south Kuril Islands and south Sakhalin. Akademiya Nauk Ukrainskoy SSR, I. I. Schmalhausen Institute of Zoology of Academy of Sciences of Ukraine, Naukova Dumka, Kiev, 160 pp. [in Russian]

Verrall GH (1886) A hundred new British species of Diptera. Entomologist's Monthly Magazine 22: 179–182, 199–202, 230–234.

ZooKeys 1217: 79–100 (2024)
DOI: 10.3897/zookeys.1217.132351

Research Article

A century later: a new species of *Mastigoceras* Handschin, 1924 (Collembola, Orchesellidae), with morphological and systematic updates on the genus

Iandra Vitória Bezerra Rodrigues[1], Paolla Gabryelle Cavalcante de Souza[1,2], Rudy Camilo Nunes[3], Nerivânia Nunes Godeiro[4], Bruno Cavalcante Bellini[1]

1 *Department of Botany and Zoology, Biosciences Center, Federal University of Rio Grande do Norte, Natal, Rio Grande do Norte, Brazil*
2 *Graduate Program of Biological Sciences (Zoology),Centre of Exact Sciences and Nature (CCEN), Federal University of Paraíba (UFPB), João Pessoa, Paraíba, Brazil*
3 *Biodiversity and Biotechnology Research Group of North Center Piaui, Federal Institute of Education, Science and Technology of Piaui, Pedro II, Piaui, Brazil*
4 *Natural History Research Center, Shanghai Natural History Museum, Shanghai Science and Technology Museum, Shanghai, 200041, China*
Corresponding author: Bruno Cavalcante Bellini (entobellini@gmail.com)

Abstract

Mastigoceras camponoti Handschin, the sole member of its genus and the Mastigocerini tribe, exhibits unusual dorsal chaetotaxy compared to other Orchesellidae. This includes a reduction in dorsal macrochaetotaxy and a secondary covering of fusiform scales intermixed with ciliate microchaetae. Despite three redescriptions, *Mastigoceras* chaetotaxy remains poorly understood, with no data on tergal sensilla patterns or dorsal macrochaetae homology. Here, the genus is revisited by describing a new Brazilian species a century after the original description of *M. camponoti*, based on morphological depiction combined with the use of DNA barcoding, *Mastigoceras handschini* Rodrigues, Souza & Bellini, **sp. nov.** The two species are differentiated by a few and unusual aspects of the dorsal chaetotaxy, especially scales distribution, and may be considered as pseudocryptic taxa. Our study of tergal sensilla formula, scales morphology, and distribution in *Mastigoceras* reveals no clear morphological support for placing Mastigocerini within Heteromurinae.

Key words: Cryptic diversity, Entomobryoidea systematics, Heteromurinae, integrative taxonomy, S-chaetotaxy

Academic editor: Louis Deharveng
Received: 17 July 2024
Accepted: 10 September 2024
Published: 30 October 2024

ZooBank: https://zoobank.org/2D9F30D6-A5A6-45EA-8BCD-3BE4FA3D7E71

Citation: Rodrigues IVB, de Souza PGC, Nunes RC, Nunes Godeiro N, Bellini BC (2024) A century later: a new species of *Mastigoceras* Handschin, 1924 (Collembola, Orchesellidae), with morphological and systematic updates on the genus. ZooKeys 1217: 79–100. https://doi.org/10.3897/zookeys.1217.132351

Introduction

Mastigoceras Handschin, 1924 is a monotypic genus of Orchesellidae only recorded from Brazil (Mari-Mutt and Bellinger 1990, 1996; Mari-Mutt et al. 1996–2021; Zeppelini et al. 2024). Its sole species, *Mastigoceras camponoti* Handschin, 1924, has a unique morphology compared with other Orchesellidae, especially regarding its very long, somewhat whip-like, five-segmented antennae, hyaline fusiform scales on the dorsal trunk, scales absent on the appendages, dorsal macrochaetotaxy reduced, sixth abdominal segment sexually dimorphic, and mucro bidentate with the basal spine (Mari-Mutt 1978; Cassagnau and Oliveira 1992). The systematic position of *Mastigoceras* has been debated by many authors, and it was considered as: an intermediate form between Entomobryinae, Paronellinae, and Orchesellidae (Handschin 1924); part of Entomobryidae (Salmon 1964); a tribe, Mastigocerini, without clear positioning within the Orchesellidae (Mari-Mutt 1978, 1980a); or as an ingroup of Heteromurinae, likely as the sister group of Heteromurini (Soto-Adames et al. 2008; Zhang and Deharveng 2015; Zhang et al. 2019; Godeiro et al. 2023).

Many aspects of the dorsal chaetotaxy of *Mastigoceras* are unusual compared to other Orchesellidae, like the reduction or absence of macrochaetae on the anterior, medio-ocellar and sutural series of the head, overall reduction of the trunk macrochaetae, including in the mesothoracic collar, and adult specimens secondary coverage composed by pointed fusiform scales together with plentiful microchaetae, putting the genus in an intermediate position between scaled and unscaled taxa (Mari-Mutt 1978; Cassagnau and Oliveira 1992; Soto-Adames et al. 2008). The dorsal macrochaetotaxy of *Mastigoceras* itself is unmatched compared to all other Orchesellidae (Mari-Mutt 1978).

Many advances in the systematics of the Entomobryoidea were recently published based on molecular markers and endorsed by some extent in the morphology. The groundbreaking studies of Zhang and Deharveng (2015) and Zhang et al. (2015) better delimited the suprageneric systematics of the Entomobryoidea, and were followed by subsequent studies which were able to corroborate or better outline the natural groups within the superfamily (like Zhang et al. 2019; Godeiro et al. 2021, 2023). One of the main contributions of Zhang and Deharveng (2015) study was to suggest the trunk sensilla pattern as a reliable complementary tool to assign species and genera to Entomobryoidea subfamilies. However, so far, *Mastigoceras* was not included in any molecular or morphological phylogenetic study, and its recent incorporation in Heteromurinae was proposed mostly based on the presence of body scales (Soto-Adames et al. 2008; Zhang and Deharveng 2015; Zhang et al. 2019). In fact, even after three redescriptions (Cassagnau 1963; Mari-Mutt 1978; Cassagnau and Oliveira 1992), the detailed chaetotaxy of *Mastigoceras camponoti* is not well understood, and there is no data on its tergal sensilla pattern or dorsal macrochaetae homology. Additionally, there is limited information on the actual distribution of body scales clearly capable of linking the species to the Heteromurini.

The use of DNA barcoding to complement species description and delimitation, thereby allowing for better species characterization, has been previously applied to many genera of Collembola, such as *Deutonura* Cassagnau, 1979 (Porco et al. 2010), *Heteromurus* Wankel, 1860 (Lukić et al. 2015), *Homidia* Börner, 1906 (Pan 2015), *Lepidobrya* Womersley, 1937 (Zhang et al. 2017), *Protaphorura* Absolon, 1901 (Sun et al. 2017), *Tomocerus* Nicolet, 1842 (Zhang et al. 2014a; Yu et al. 2017), and *Thalassaphorura* Bagnall, 1949 (Sun et al. 2018). Among groups of closely related populations with unclear taxonomic status, DNA-based methods are thought to be highly effective instruments for species delimitation. In this sense, mitochondrial markers with more than 3% of divergence between two or more studied populations strongly support their separation into different species (Hebert et al. 2003a). Even so, the degree of divergence across congeneric species differs on each invertebrate group. For instance, insects often exhibit smaller interspecific divergences compared to non-winged arthropods, and average DNA barcode genetic distances between congeneric species range from 7% to 8% in Holarctic Lepidoptera (Hebert and

Landry 2010; Hausmann et al. 2011), 9.3% in Diptera (Hebert et al. 2003b), 11.5% in Hymenoptera, and 13.9% in North American Ephemeroptera (Webb et al. 2012). In contrast, studies on Collembola describe a substantially greater divergence in COI sequences amongst congeneric species, with reported values usually ranging from 16.35% to 24.55% (Porco et al. 2012; Yu et al. 2016; Sun et al. 2018). A remarkable exception regards a study of two intertidal *Thalassaphorura* species from Europe, which are well-defined taxa regarding morphology but show a inter-specific COI divergence of only 4.3% (Sun et al. 2018).

Here we revisit *Mastigoceras* describing in detail a new species from Brazil. We also provide an updated diagnosis to the genus, and notes on Mastigocerini morphology, structures homology and systematics. Complete mitochondrial Cytochrome Oxidase I (COI) sequences of the new species and *Mastigoceras camponoti* were obtained and compared, and the genetic distance between them was calculated to better support the new species status.

Materials and methods

Individuals of the new species were collected at the Urubu-Rei waterfall, Pedro II municipality, Piauí State, Brazil (Fig. 1). Specimens were sampled with pitfall traps and entomological aspirators, and were preserved in 70% ethanol. They were later sorted, cleaned in Nesbitt's and Arlé's solutions, following Arlé and Mendonça (1982) and Jordana et al. (1997) procedures, and mounted in glass slides in Hoyer's medium. The detailed morphological study was conducted in a DM750 optical microscope with phase contrast and a drawing tube. Habitus of the new species was photographed in 70% ethanol under LAS v. 4.12 software, using a Leica EC4 camera attached to a S8APO stereomicroscope. Photographs of smaller structures were taken with a Leica MC170 HD camera attached to a DM750 microscope, also using LAS software. The type locality map was created in QGIS software v.3.10.4 (QGIS.org 2024) using raw shapefiles from IBGE's map database (IBGE 2024). Photographs and raw drawings were digitally improved and labeled using ADOBE ILLUSTRATOR software.

One specimen of *Mastigoceras handschini* sp. nov. from Piauí state and one of *M. camponoti* from the southern region of Minas Gerais state, Mariana municipality, both in Brazil, were sent to China for DNA extraction, sequencing, and posterior bioinformatic analysis. A TIANamp MicroDNA Extraction Kit (Tiangen Co., Ltd., China) was used to extract the DNA, and a KAPA Hyper Prep Kit (Roche, Basel, Switzerland) was used to construct the DNA libraries. Shanghai Yaoen Biotechnology Co., Ltd. (China) performed all molecular experiments and sequenced 10G bp data of paired-end reads from each sample using an Illumina NovaSeq 6000 platform.

The data produced was enough to assemble the mitogenomes of both species, but for the present study we used only the COI gene to analyze the genetic distance between them. A coming study will describe in detail the mitochondrial DNA of *Mastigoceras* spp. together with other Orchesellidae. Both mitogenomes were assembled and annotated using MITOZ v.3 (Meng et al. 2019). After annotation, we firstly aligned the entire COI sequences of *Mastigoceras handschini* sp. nov., *M. camponoti*, and saved as a first file. A second alignment file was created with the addition of *Orchesella cincta* (Linnaeus, 1758) partial COI sequence. We trimmed the *Mastigoceras* sequences at its same size, 658

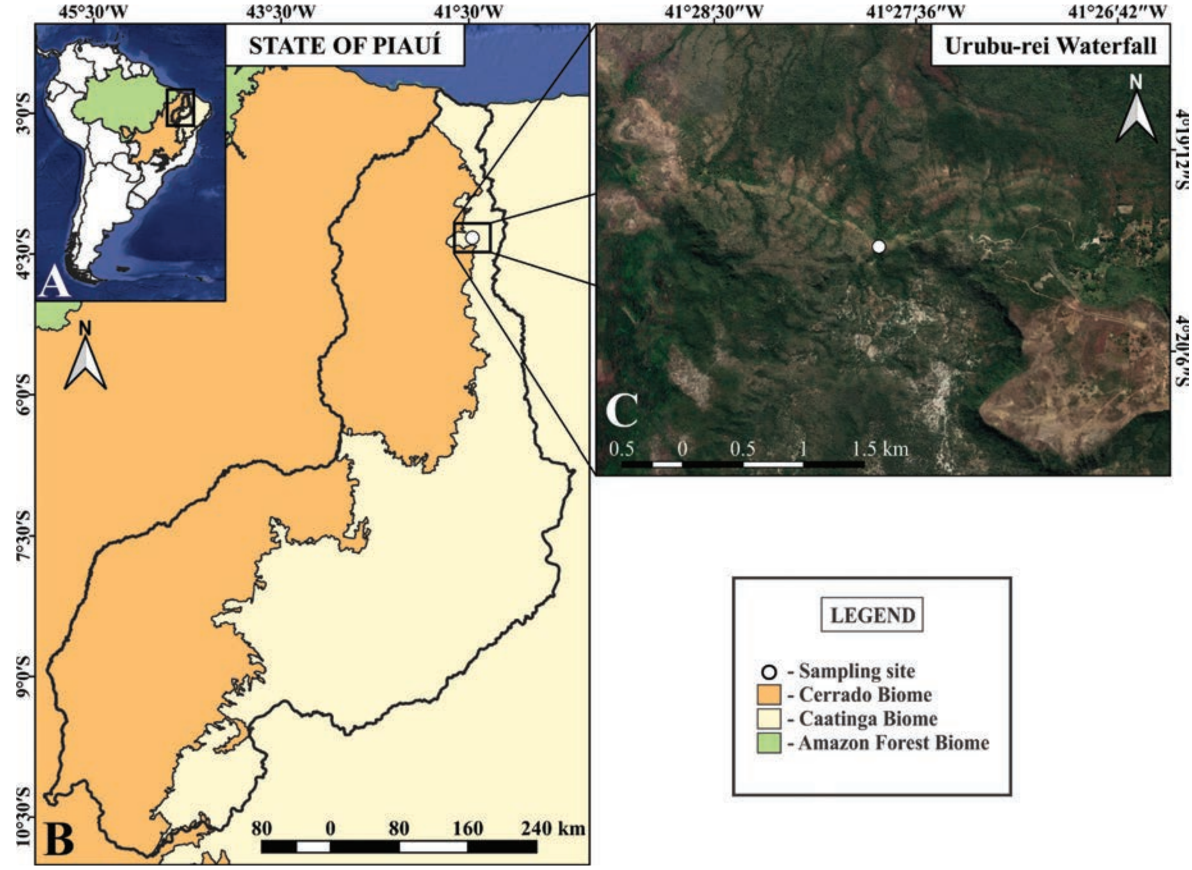

Figure 1. Type locality of *Mastigoceras handschini* sp. nov. **A** South America map highlighting Brazil and the sampling region **B** Piauí state map, showing the Caatinga-Cerrado transitional area **C** profile of the surrounding areas of the sampling site of the new species, Urubu-Rei waterfall.

nucleotides, and the sequence of *O. cincta* was excluded, whereas the remaining two sequences were realigned. The genetic distances of both entire and partial COI of the *Mastigoceras* species were calculated under the model Kimura 2 Parameter (K2P) and p-distance using MEGA v. X (Kimura 1980; Kumar et al. 2018; Stecher et al. 2020). We applied a bootstrap of 1000 replicates, codon positions included were 1st+2nd+3rd+Noncoding, and all ambiguous positions were removed. To know the exact number of dissimilarities between the two sequences we used BLASTn, available at https://blast.ncbi.nlm.nih.gov/. The resulting COI sequences were deposited at GenBank (NCBI), and their accession numbers are available in the end of this paper.

The terminology used in the morphological description follows: Gisin (1967) for labial chaetotaxy; Fjellberg (1999) for labial palp papillae and guards; Cipola et al. (2014) for labral chaetotaxy; Mari-Mutt (1979) for dorsal head chaetotaxy, with additions of Soto-Adames (2008), and following Bellini et al. (2022) as a base model; Szeptycki (1972) for tergal sensilla formula (S-chaetotaxy), with additions of Zhang and Deharveng (2015); and Szeptycki (1979) for dorsal chaetotaxy, with additions of Jordana and Baquero (2005), Soto-Adames (2008), Zhang and Deharveng (2015) and Zhang et al. (2019). For a better depiction of *Mastigoceras* dorsal chaetotaxy homology, we compared it with *Capbrya brasiliensis* Nunes, Santos-Costa & Bellini, 2020 in Nunes et al. (2020), *Dicranocentrus abestado* Siqueira, Bellini & Cipola, 2020 in Bellini et al. (2020), and *Australotomurus* Stach, 1947 *sensu* Bellini et al. (2022).

Abbreviations used in the description and/or drawings are **Ant.**—antennal segment(s); **PAO**—postantennal organ; **Th.**—thoracic segment(s); **Abd.**—abdominal segment(s); **mac**—macrochaeta(e); **mes**—mesochaeta(e); **mic**—microchaeta(e). Ant. I subdivisions are **a**—to proximal subarticle; **b**—to distal subarticle. Depository abbreviation: **CC/UFRN**—Collembola Collection of the Biosciences Center of the Federal University of Rio Grande do Norte, Natal, Brazil.

The main symbols used in the drawings are listed in Fig. 2. Chaetae of uncertain homology are followed by a question mark (?). Chaetae labels, eye lenses, and labial papillae are given in bold in the text. The taxonomic description and comparisons are based on half body, except for labral and prelabral chaetae.

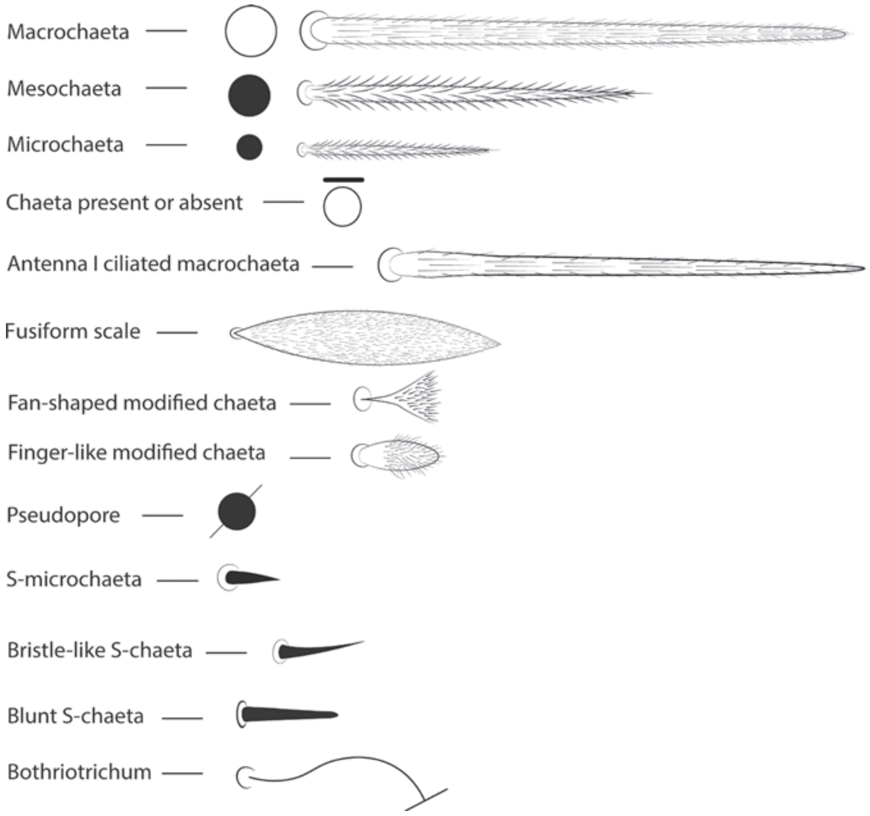

Figure 2. Symbols used in the chaetotaxy description of *Mastigoceras handschini* sp. nov.

Results

Taxonomic account

Family Orchesellidae Börner, 1906 *sensu* Godeiro et al. 2023
Subfamily Heteromurinae Absolon & Kseneman, 1942 *sensu* Zhang and Deharveng, 2015
Tribe Mastigocerini Mari-Mutt, 1980a *sensu* Zhang and Deharveng, 2015

Genus *Mastigoceras* Handschin, 1924

Type species. *Mastigoceras camponoti* Handschin, 1924.

Diagnosis. Fusiform small hyaline ciliate scales, without ribs, present at least in dorso-anterior Th. III–Abd. III, present or absent on dorsal head, Th. II, and Abd. IV; antennae, legs, ventral tube, tenaculum and furca scaleless. Body also densely covered by secondary ciliate mic; dorsal macrochaetotaxy reduced. Antennae very long, 2–4× the body length; antennae with five segments, Ant. I subdivided, Ant. II stiff or weakly annulated, Ant. III–IV longer than other segments, annulated and whip-like; Ant. IV apical bulb absent. Eyes 8+8, PAO present. Tergal sensilla and microsensilla formulae of Th. II–Abd. V as 1,1|0,3,3,+,9 and 1,0|1,0,1,0,0, respectively. Th. II anterior (**a**) series, including the collar, with up to 17 mac. Abd. IV less than 1.5× the length of Abd. III in the midline. Abd. VI of males short and rounded; of females long and conical. Trochanteral organ variably developed. Tenaculum without chaetae. Manubrium dorsally with one or two bothriotrichum-like chaetae; dens crenulate, without spines; mucro bidentate with the basal spine (adapted and updated from Handschin 1924; Cassagnau 1963; Mari-Mutt 1978; Cassagnau and Oliveira 1992).

Remarks. Our updated diagnosis adds the tergal sensilla and microsensilla formulae to *Mastigoceras*, details on the distribution of body scales, and outlines the presence of the PAO. This last feature was overlooked in the original description of *M. camponoti* (Handschin 1924), along with its subsequent redescriptions (Cassagnau 1963; Mari-Mutt 1978; Cassagnau and Oliveira 1992). However, we could confirm the presence of this structure in a specimen of *M. camponoti* from the type locality (Mariana municipality, south of Minas Gerais state, Brazil), as well as in *Mastigoceras handschini* sp. nov. In Mari-Mutt (1978: 46, fig. 8), there is a SEM picture of the right eyepatch of *M. camponoti* showing the PAO as a small cuticle fold in front of **A** eye lens.

The overall morphology of *Mastigoceras* species resembles other Entomobryoidea in several aspects. These shared features include the presence of a trochanteral organ and post-ocular bothriotricha, dorsal body covered with abundant secondary ciliate mic, alongside some larger ciliate mes and blunt mac, Abd. II–IV bothriotricha formula 2,3,2, and dens crenulate with a bidentate mucro holding the basal spine (Soto-Adames et al. 2008). Even so, the disposition of Abd. IV bothriotricha in *Mastigoceras* is quite unusual, being posteriorly displaced (see Figs 4E, 6F; Cassagnau and Oliveira 1992: 30, fig. 2b). This condition does not relate with other Orchesellidae or Entomobryoidea (Szeptycki 1979; Zhang et al. 2019; Nunes et al. 2020) and makes it difficult to understand the homology of the lateral chaetae on the same tergite.

Mastigoceras handschini **Rodrigues, Souza & Bellini, sp. nov.**

https://zoobank.org/7E0F9978-400C-49EA-8B0B-03C2688EFF10
Figs 3–7, Table 1

Type material. ***Holotype*:** Brazil • 1 male, 1.65 mm; Piauí state, Pedro II municipality, Urubu-rei waterfall; 4°19'37.90"S, 41°27'45.89"W; 06 Nov. 2019; E.P. Santos leg.; soil surface/entomological aspirators; GenBank: PP960563; deposited at CC/UFRN, *Mastigoceras handschini*. ***Paratypes*:** • 4 females and 4 males in slides, same data of holotype • 2 juveniles in slides, same data as holotype, except 10 Oct. 2019, pitfall traps. • 4 females and 4 juveniles in slides, same data of holotype, except 24 May 2019. All material deposited at CC/ UFRN.

Diagnosis. Fusiform scales present on anterior region of Th. III–Abd. III, rarely on Th. II posterior region, scales absent on head and Abd. IV–VI; sutural cephalic series with one mac (**S1**); labial basomedian field **m1** chaeta usually smooth, rarely

Figure 3. *Mastigoceras handschini* sp. nov. habitus in ethanol, lateral view (Ant. III–IV missing).

Table 1. Comparison between *Mastigoceras* species.

Species/Features	*M. camponoti*$^{1-5}$	*M. handschini* sp. nov.^{5}
Head		
Dorsal scales	present^{2,5}	absent
Sutural cephalic mac	0^{4}, 1^{5} or 2^{2}	1
Trunk		
Th. II anterior and medial scales	present^{5}	absent
Th. II **a** series mac	11–12^{3,5}	17
Abd. III internal mac	1^{1,5}, 2^{2,4}	1
Abd. IV finger-shaped **T3**	absent^{4,5}	present
Abd. IV scales	present^{4}	absent
Abd. VI male apical papilla	present^{4}	absent
Distribution in Brazil (states)	Minas Gerais*, São Paulo, Rio de Janeiro, Paraná, Amazonas, Ceará, Pará**	Piauí

Legends: '*' type locality; '**' originally written as "Pava" (see Mari-Mutt 1978, pg. 44), but likely Pará state. Data based on: ^{1}Cassagnau 1963; ^{2}Mari-Mutt 1978; ^{3}Mari-Mutt 1980a; ^{4}Cassagnau and Oliveira 1992; ^{5}this study.

ciliate; Th. II **a** series with 17 mac, 15 on the collar plus **a2** and **a5**; Abd. III with one internal mac (**a2?**); Abd. VI of males without the apical papilla; trochanteral organ with 26–31 spine-like smooth chaetae; ventral tube lateral flap with ~ 4 ciliate and 26 smooth chaetae; manubrial plate with three pseudopores and 5–7 chaetae.

Description. Body length (head + trunk) of the type series ranging from 1.32 to 2.22 mm (*n* = 10). Holotype body length 1.65 mm. Specimens with dark purple pigment on antennae, on head as lateral bands and with an anterior spot between the antennal bases, on trunk as a lateral band from Th. II to Abd. V (sometimes missing on Abd. II) and some dorso-internal spots and/or stripes on the segments; and on femora and tibiotarsi as 1 and 2 axial stripes, respectively; furca lacking pigments (Fig. 3). Hyaline ciliate fusiform scales present on dorsal anterior region of Th. III–Abd. III, rarely on Th. II posterior region (only in two specimens) (Figs 2, 4D, 6H), scales absent on head and Abd. IV–VI; dorsal head and trunk covered by plentiful ciliate secondary mic.

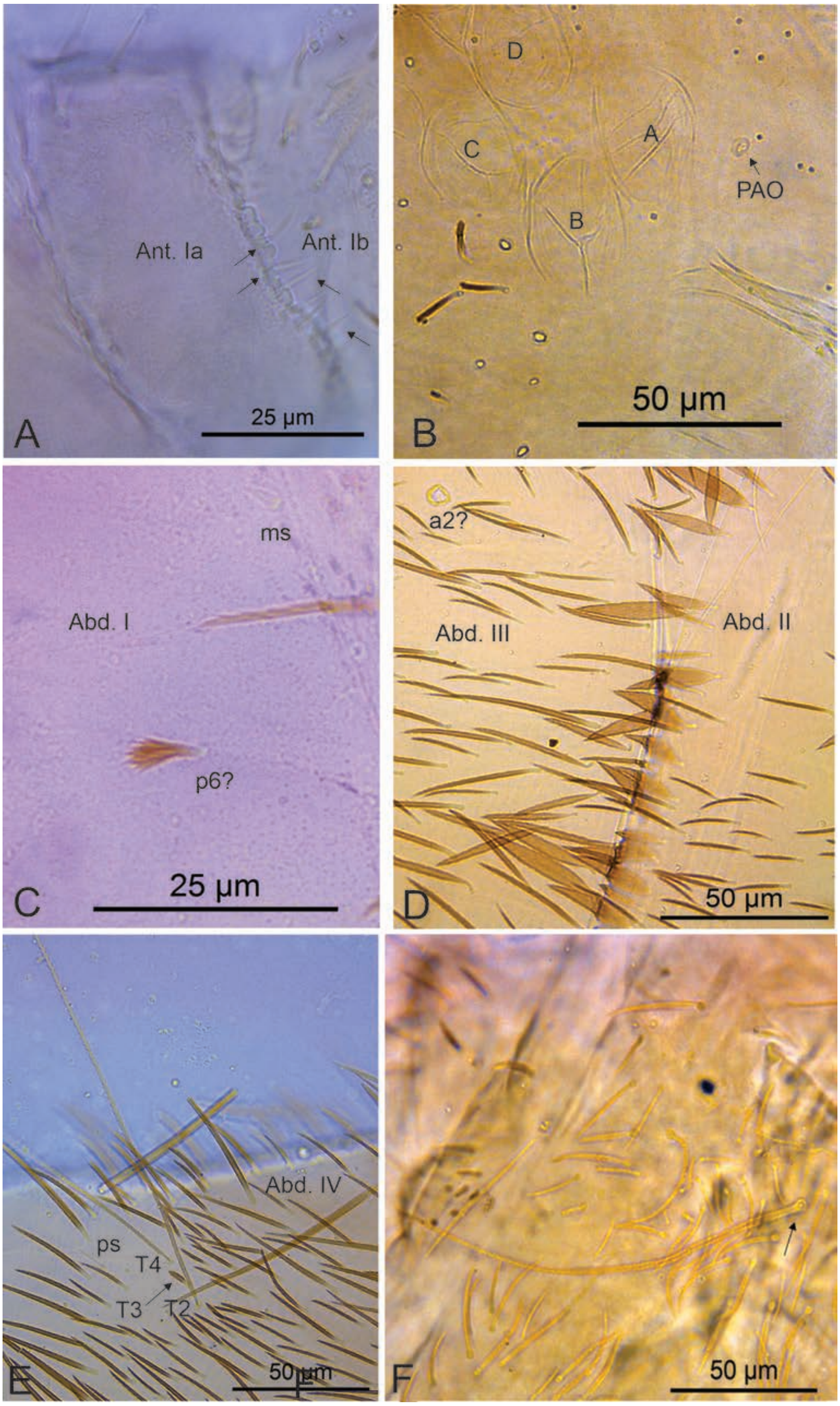

Figure 4. *Mastigoceras handschini* sp. nov. overall morphology **A** Ant. Ia apex, arrows point to small smooth mic at the apex **B** head, showing frontal eyes and PAO **C** Abd. I with modified fan-shaped **p6?** and **ms** microsensillum **D** Abd. III anteriorly (Abd. II tergum covering the most anterior region of Abd. III), with a transversal line of fusiform scales, both Abd. II and III with plentiful secondary mic **E** Abd. IV distal region, showing **T2** and **T4** bothriotricha, **T3** finger-like chaeta and **ps** sensillum **F** Dorsal (anterior) manubrium, arrow points to a bothriotrichum-like chaeta.

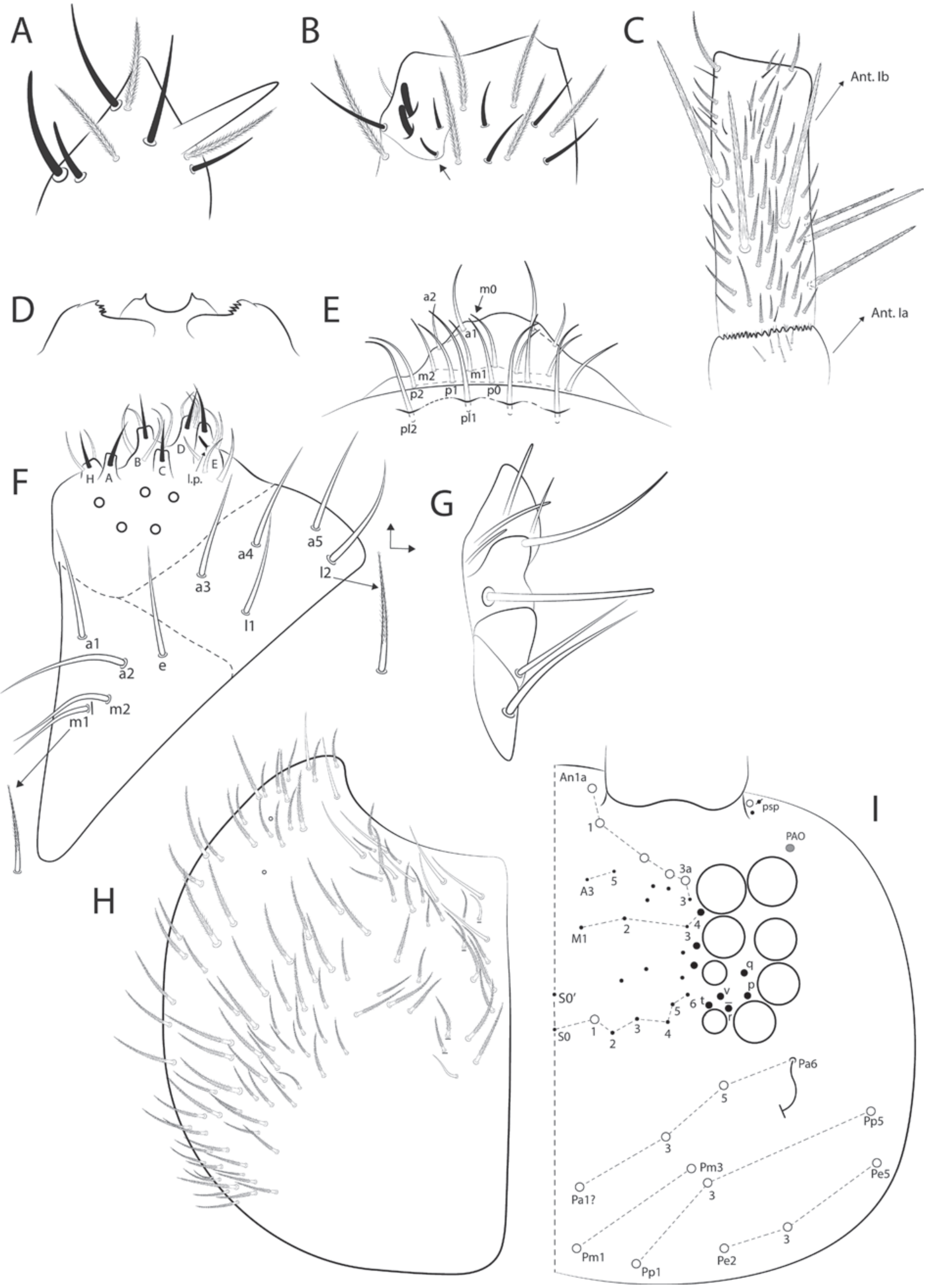

Figure 5. *Mastigoceras handschini* sp. nov. head **A** apex of right Ant. IV, dorsal view **B** left Ant. III sense organ and surrounding chaetae, ventral view, the arrow indicates the blunt guard sensillum **C** right Ant. I, dorsal view **D** labral ornamentations **E** prelabral and labral chaetotaxy **F** labium, right side, **l.p.** = lateral process of labial papilla E **G** right outer maxillary lobe and sublobal plate, including the oral fold **H** post-labial chaetotaxy, left side **I** Dorsal head chaetotaxy, eyes, and PAO.

Head (Figs 4A, B, 5). Antennae 3–4× longer than body length, with five segments (Ant. I subdivided), Ant. IV and III apparently fused in most specimens, possibly due to antennal regeneration. Antennal ratio Ant. Iab–IV of one paratype: 1:4:30:5.6:43.3 (Ant. III broken, basal part lost). Ant. IV long and annulated, with at least three types of chaetae: blunt sensilla, acuminate sensilla and ciliate chaetae, with a prominent subapical pin projection (Fig. 5A). Ant. III long and annulated, apical sense organ with two sensory rods, three guard sensilla (one of them smaller and blunt) and at least five extra surrounding sensilla (Fig. 5B). Ant. II flexible, weakly annulated; Ant. I subdivided, with several small smooth mic at the apex of segment Ia (Fig. 4A), Ant. Ib with six slightly ciliate stiff mac (Fig. 5C). Labral apical papillae absent, labral ornamentation as in Fig. 5D. Four prelabral smooth chaetae, labral chaetotaxy formula as 5(**p**), 5(**m**), 4(**a**), all smooth, **a1** larger than **a2** (Fig. 5E). Clypeal chaetae unclear. Labial palp with five proximal subequal chaetae, labial papillae short, formula of papillae and guards as: **H**(2), **A**(0), **B**(5), **C**(0), **D**(4), **E**(5) + a finger-shaped lateral process, not reaching the base of papilla **E** (Fig. 5F). Labial basomedian and basolateral fields chaetae formula as **a1**–**5**/**m1**–**2el1**–**2**, **m2**, **e** and **l1** always smooth, **m1** and **l2** usually smooth, rarely ciliate (only in 2 specimens) or **m1** absent, **r** chaeta absent (Fig. 5F). Maxillary outer lobe apical appendage slightly longer than the blunt basal chaeta, sublobal plate with four chaetae-like appendages, the three internal blunt, oral fold with two chaetae (Fig. 5G). Ventral post-labial chaetotaxy with ~ 100 ciliate and 11 or 12 smooth chaetae, cephalic groove with five ciliate and two or three smooth chaetae surrounding it (Fig. 5H). Eyes 8+8, **A**–**B** larger, **C**–**F** subequal, and **G**–**H** smaller than others, with four or five interocular mes (**r** present or absent); PAO as a small circular fold next to **A** lens, anterior pseudopore next to the antennal base (Figs 4B, 5I). Dorsal chaetotaxy with five antennal (**An1a**–**3a**), one sutural (**S1**), three postoccipital anterior (**Pa1**?, **Pa3**, **Pa5**), two post-occipital medial (**Pm1**, **Pm3**), three post-occipital posterior (**Pp1**, **Pp3**, **Pp5**), and three post-occipital external (**Pe2**, **Pe3**, **Pe5**) mac, dorsal head mic and mes homology as in Fig. 5I.

Trunk (Figs 4C–E, 6). Tergal sensilla and microsensilla formulae of Th. II–Abd. V as 1,1|0,3,3,+,9 and 1,0|1,0,1,0,0, respectively; Th. II–Abd. IV central mac formula, excluding the mesothoracic collar, as: 5,3|1,1–2,1,3–4; lateral mac formula as 1,0|0,1,2,0; bothriotricha formula as 0,0|0,2,3,2 (Fig. 6A–G). Th. II with 17 anterior mac, **a2** and **a5** detached from the anterior collar, more posteriorly displaced (Fig. 6A). Abd. I **p6?** as a fan-shaped modified chaeta (Figs 4C, 6C). Abd. III with one internal mac (**a2?**) (Figs 4D, 6E); Abd. IV **T3** as a finger-shaped chaeta (Figs 4D, 6F). Abd. V lateral chaetae as mes or bothriotricha-like chaetae (Figs 6G). Detailed homology of the main dorsal trunk chaetae presented in Fig. 6. Ratio Abd. III–IV in the midline of the holotype as: 1:1.27.

Trunk appendages (Figs 4F, 7). Trocantheral organ with 26–31 spine-like smooth chaetae (Fig. 7A). Tibiotarsus III with one smooth distal chaeta near the unguiculus, pretarsus with one posterior and one anterior short chaetae; ungues with four inner teeth: two paired basal, one unpaired medial and one reduced unpaired apical; lateral and external teeth present; unguiculi lanceolate, with the postero-external lamella with a small proximal tooth; tenent hairs slightly ciliate and capitate (Fig. 7B); empodial complex of leg III ratio of smooth chaeta, unguiculus, unguis and tenent-hair of holotype as 1:1:1.7:2.2. Ventral tube anterior side with 14 or 15 ciliate chaetae plus one distal mac (Fig. 7C);

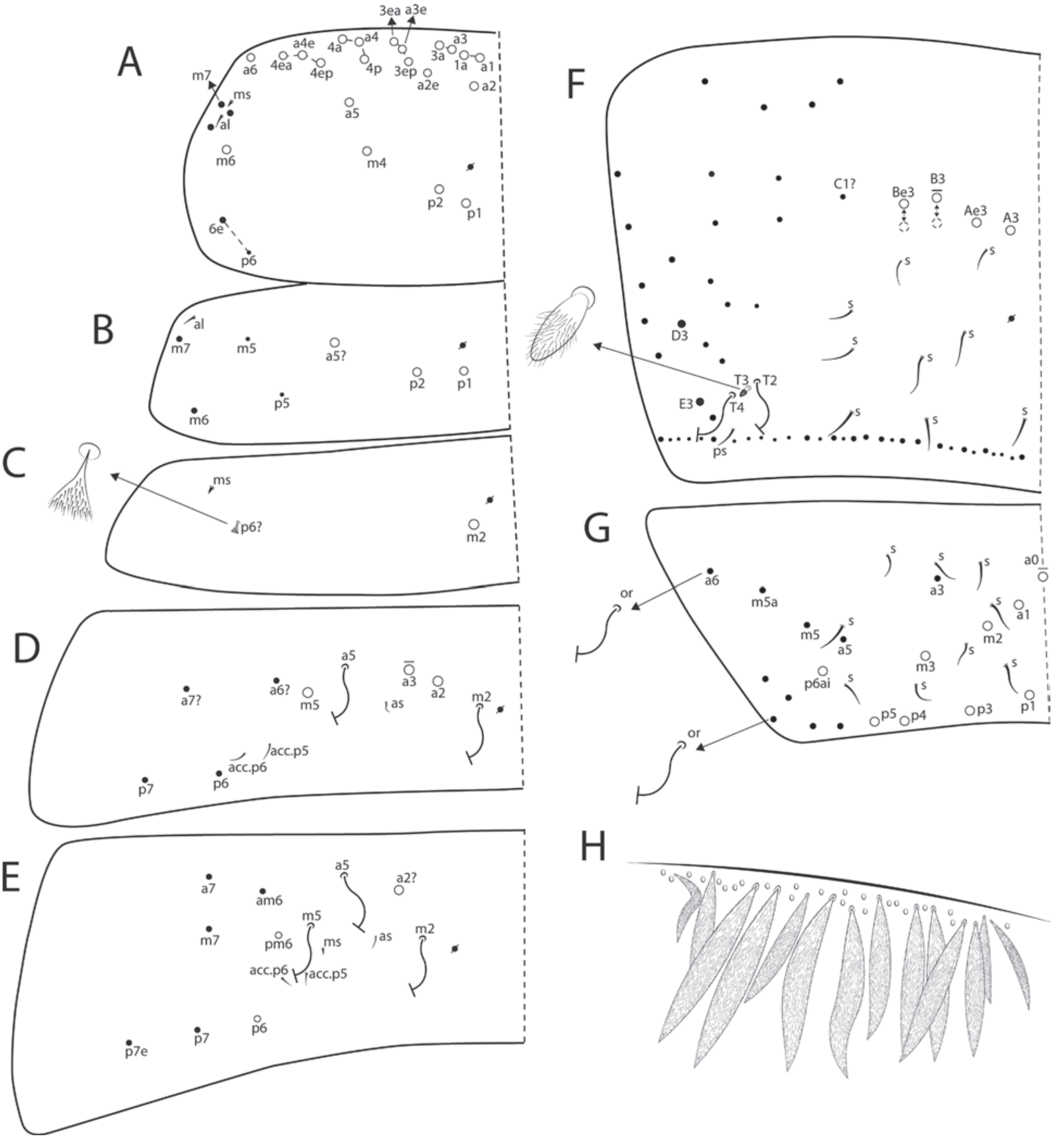

Figure 6. *Mastigoceras handschini* sp. nov. dorsal trunk chaetotaxy, left side **A** Th. II **B** Th. III **C** Abd. I, arrow indicates a small fan-shaped modified chaeta **D** Abd. II **E** Abd. III **F** Abd. IV, arrow indices a finger-shaped ciliate chaeta (**T3**) between the bothriotricha, dotted mac alveoli represent different positions to the same chaetae **G** Abd. V, arrows pointing to lateral mes which can also be bothriotricha-like chaetae **H** transversal row of anterior scales on Abd. II. Other primary chaetae may be present in terga as mic, but are obscured by the dense microchaetal covering of the specimens.

posterior side with at least 64 ciliate and eight smooth chaetae in total (Fig. 7D); lateral flap with ~ 4 ciliate and 26 smooth chaetae (Fig. 7E). Tenaculum rami with four teeth, corpus without chaetae (Fig. 7F). Manubrium dorsally with 1+1 or 2+2 long bothriotricha-like chaetae (Fig. 4F). Manubrial plate with three pseudopores and 5–7 chaetae (Fig. 7G). Dens without spines. Mucro bidentate, apical tooth larger than basal one, mucronal spine reaching the apex of basal tooth (Fig. 7H). Ratio manubrium: mucrodens of the holotype as 1:1.88.

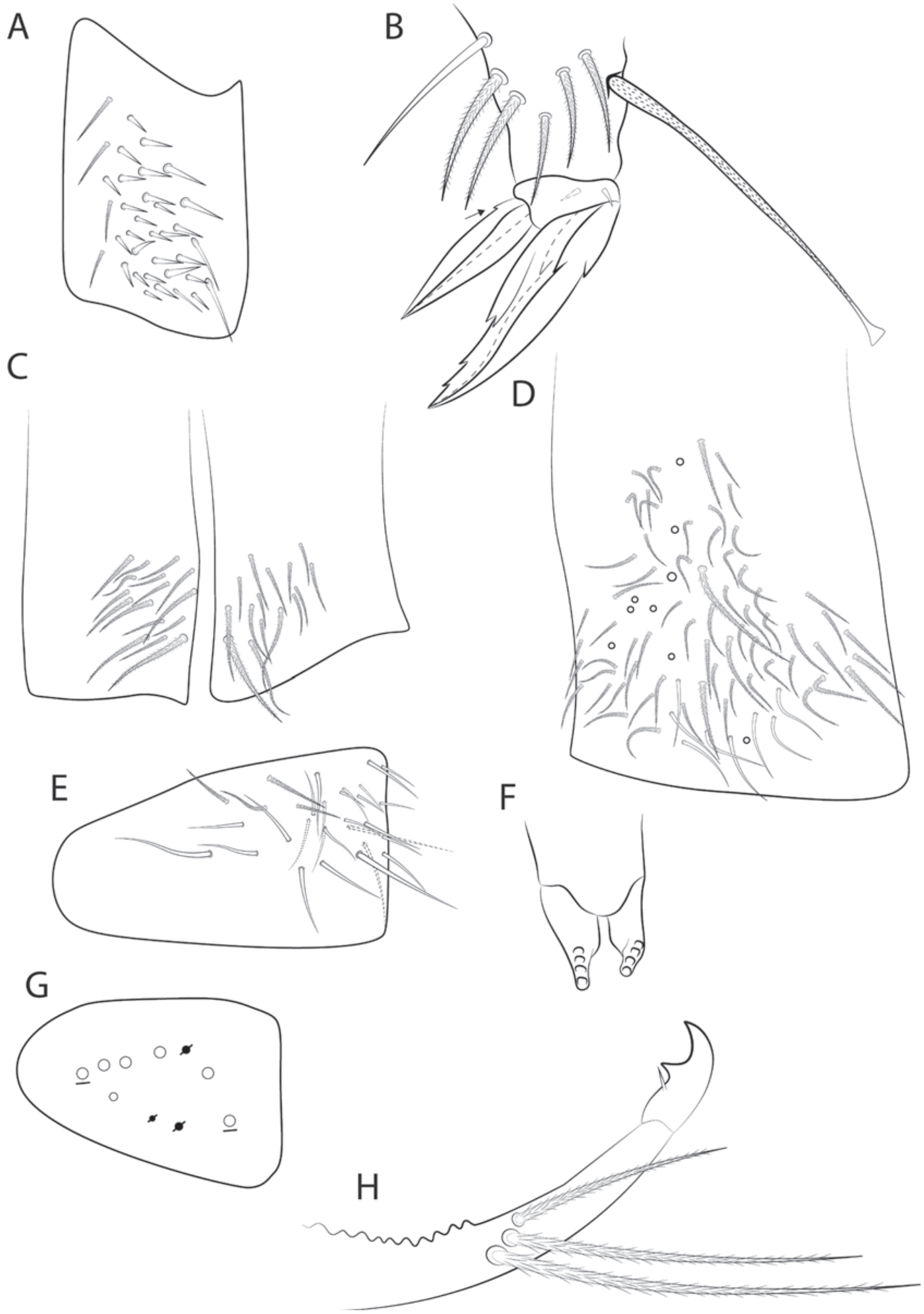

Figure 7. *Mastigoceras handschini* sp. nov. trunk appendages **A** trochanteral organ **B** empodial complex III and distal tibiotarsus (posterior view), arrow indicates the small posterior tooth on unguiculus **C** ventral tube anterior side **D** ventral tube posterior side **E** right lateral flap **F** tenaculum **G** left manubrial plate **H** distal dens and mucro, lateral view.

Results of COI species delimitation. Comparing the whole mitochondrial COI gene of *Mastigoceras handschini* sp. nov. with *M. camponoti*, the sequence length is the same in both species, with 1539 bp. However, the p-distance (number of base differences per site from between sequences) is 17%, and the

K2P interspecific distance between them is 19.2%, enough to separate them as independent species. Considering the partial COI (658 pb), the p-distance is 16.3%, and the K2P interspecific distance between them is 18.6%. As previously discussed, earlier studies have found that the interspecific distance for Collembola species usually ranges from 16.35% to 24.55%. (Porco et al. 2012; Yu et al. 2016; Sun et al. 2018).

Etymology. The species honors Dr. Eduard Handschin (1894–1962), who described the genus *Mastigoceras* and its single species, *M. camponoti*.

Distribution and habitat. *Mastigoceras* is only found in Brazil, with previous records from the Amazon and Atlantic forests and the Caatinga biomes (Cassagnau 1963; Cassagnau and Oliveira 1992; Mendonça et al. 2009; Bellini 2014; Cipola et al. 2019; Zeppelini et al. 2024). Handschin's (1924) original description does not list the municipality where the type material was sampled, mentioning only "south of Minas" (southern region of Minas Gerais state). Thus, it is unclear if his specimens of *Mastigoceras* were previously sampled from the Cerrado biome. The record of *Mastigoceras handschini* sp. nov. from a transitional zone between the Caatinga and Cerrado biomes represents the second record of the genus from the northeastern region of Brazil, with *M. camponoti* having been previously recorded from the state of Ceará (Bellini 2014; Zeppelini et al. 2024).

The new species was found at "Cachoeira do Urubu-Rei" (Urubu-Rei waterfall), located in the rural region of Pedro II municipality, Piauí state, Brazil. The region has minimum of 23.1 °C and maximum temperatures of 29.3 °C, with a hot and humid tropical rainy climate classified as "As" according to the Köppen-Geiger system (Kottek et al. 2006). The collection site is located at an altitude of 603 m above sea level and is covered by riparian forest vegetation following a perennial watercourse, featuring evergreen broadleaf plants, bryophytes, and pteridophytes. Unlike the type material of *M. camponoti*, which was sampled from ant nests, specimens of *Mastigoceras handschini* sp. nov. were sampled above the leaf litter using pitfall traps and entomological aspirators (Fig. 8).

Remarks. We could revise one female specimen of *M. camponoti* from the southern region of Minas Gerais state, Mariana municipality, but the quality of the slide prevented us from redescribing it this time and draw further comparisons between the species. Even so, we could confirm its dorsal macrochaetotaxy is mostly the same of *Mastigoceras handschini* sp. nov., with the exception of the anterior collar on Th. II. The morphology of this specimen matches Mari-Mutt's 1980a observation of *M. camponoti*, who stated Mastigocerini has nine or ten mac in the collarette (Mari-Mutt 1980a, pg. 457). Our revised specimen has ten anterior mac on the collar plus **a2** and **a5** more posteriorly¸ totaling 12 mac on Th. II **a** series. We could observe in *M. camponoti* the distribution of body scales, also present on head (only a few were observed), as noted by Mari-Mutt (1978), and on anterior and medial regions of Th. II (tergum densely covered by scales). Other features which would be useful to compare the species like ventral tube, manubrial plate and trochanteral organ chaetotaxy could not be clearly analyzed due to the slide quality.

Mastigoceras handschini sp. nov. is remarkably similar to *M. camponoti* in color pattern, size of antennae and overall chaetotaxy. However, it differs from the latter species especially by: scales absent on dorsal head, Th. II anterior and medial regions, and Abd. IV (vs. present in *M. camponoti*), Th. II **a** series

Figure 8. Environmental characteristics of Urubu-Rei waterfall and its surroundings, where specimens of *Mastigoceras handschini* sp. nov. were collected **A** pitfall traps covered by plastic plates used to collect the specimens from the leaf litter **B** riparian forest vegetation, with the presence of evergreen broadleaf plants **C** sampling site, highlighting the rocky floor and vegetation adapted to the site's humid conditions **D** view of Urubu-Rei waterfall.

with 17 mac, including the collar (up to 12 in *M. camponoti*), Abd. IV with a finger-shaped **T3** (absent in *M. camponoti*), and Abd. VI not papillate in males (vs. with an apical papilla in *M. camponoti*). Details on *Mastigoceras* species comparative morphology and their distribution are summarized in Table 1. For further discussion on the genus and tribe morphology, see the next section.

Discussion

Mastigoceras distribution, habitat, and species morphology

Mastigoceras has a wide distribution in Brazil, occurring across various biomes and in widely separated regions (Cassagnau 1963; Cassagnau and Oliveira 1992; Mendonça et al. 2009; Bellini 2014; Cipola et al. 2019; Zeppelini et al. 2024). Its presence in the southernmost region of the Atlantic Forest (Cipola et al. 2019) and the northwestern region of the Amazon Rainforest (Cassagnau and Oliveira 1992) suggests that the genus may also occur in other South American countries. Regarding its preferred habitat, most *Mastigoceras* samples were collected directly from leaf litter or soil top, using pitfall traps or entomological aspirators (Mendonça et al. 2009; Bellini 2014; Cipola et al. 2019). However, its occurrence inside nests of the ant *Camponotus rufipes* (Fabricius), as reported by Handschin (1924), is quite intriguing. The very long antennae of *Mastigoceras*, along with the dense coverage of chaetae and scales, presence of all eyes, long furca, and pigmented body, suggest an epiedaphic or atmobiotic lifeform, which aligns with the aforementioned collection methods. It is unlikely that *M. camponoti* is actually a myrmecophilous species, and we believe Handschin's specimens were found within such nests accidentally.

Mastigoceras camponoti and *Mastigoceras handschini* sp. nov. can be considered as pseudocryptic species, as their main differences are few, unusual for the current Entomobryoidea taxonomy, and discrete, and only a detailed morphological review combined with another investigation tool, in this case the use of a genetic marker, could elucidate their distinct biological identities (Knowlton 1993; Lajus et al. 2015). Regarding the morphological differences between *M. camponoti* and *Mastigoceras handschini* sp. nov., they are also limited partly because, even though the first species has been redescribed three times before (Cassagnau 1963; Mari-Mutt 1978; Cassagnau and Oliveira 1992), such descriptions did not provide detailed information on other chaetotaxic features currently used in Entomobryoidea taxonomy to differentiate species. These features include the chaetotaxy of the ventral head (other than the labial one), trochanteral organ, ventral tube and manubrial plate, as well as a detailed depiction of scales distribution, as this last characteristic varies within *Mastigoceras* (see Table 1). It is worth noting that the depictions of *M. camponoti* provided by Cassagnau (1963), Mari-Mutt (1978), and Cassagnau and Oliveira (1992) have some differences, and were based on specimens from different regions and biomes of Brazil. Since the overall morphology of *Mastigoceras* species appears to be quite conserved, as our data suggest, it is likely that the slightly different depictions of *M. camponoti* provided by these authors, based on populations from distinct regions of the country, may actually hide a complex of species. In this scenario, the use of molecular markers such as mitochondrial COI, combined with a more detailed study of the morphology of different populations, should be employed to verify this hypothesis.

Is Mastigocerini a tribe of Heteromurinae?

Soto-Adames et al. (2008) considered Mastigocerini as closely related to Heteromurini due to the presence of body scales, a classification followed by subsequent revisions of the Entomobryoidea (Zhang and Deharveng 2015; Zhang et al. 2019; Godeiro et al. 2023). Even so, it was clear to the authors that the secondary coverage of adult *Mastigoceras* was atypical compared to Heteromurini, due to the presence of plentiful mic on the terga (Soto-Adames et al. 2008). This morphology somewhat resembles the condition of *Heteromurus peyerimhoffi* Denis, 1937, which also has a dorsal covering mixing secondary mic and scales (Mari-Mutt 1980ab). However, *H. peyerimhoffi* has many features that place it within *Heteromurus*, and thus in Heteromurini, such as the dorsal trunk, tibiotarsal and manubrial chaetotaxy comparable with other *Heteromurus* species, as well as the morphology of body scales, which are apically rounded or truncated (Mari-Mutt 1980b; Cipola et al. 2016). In this sense, the heterogeneous dorsal coverage of *H. peyerimhoffi* is likely an autapomorphy of the species within *Heteromurus*. On the other hand, *Mastigoceras*, the sole genus of Mastigocerini, has a main dorsal coverage composed by mic, with scales being scarce and only present in some terga, mostly in the anterior region of Th. III–Abd. III as a single row on each tergum, being variably present in the posterior head, Th. II and near the bothriotricha of Abd. IV (Cassagnau 1963; Mari-Mutt 1978; Cassagnau and Oliveira 1992; see also Table 1). More importantly, the shape of these scales does not match those of Heteromurinae, as they are small, narrow, and pointed, resembling flattened mic (Fig. 4D). Such scales are also completely absent from the appendages in Mastigocerini. Scales have emerged more than once in the Entomobryidae (Szeptycki 1979; Zhang and Deharveng 2015; Zhang et al. 2014b, 2015), and the comparison between Mastigocerini and Heteromurini suggests the same among the Orchesellidae. For now, there is no clear evidence that the scales of the Mastigocerini relate to the structures seen in Heteromurini, neither in morphology nor in body distribution.

Another feature that differentiates Mastigocerini from Heteromurini is the tergal sens pattern (S-chaetotaxy) of Th. II to Abd. V, which is 1,1|0,3,3,+,9 in the former and 2,2|1,3,3,+,3–7 in the latter (Zhang and Deharveng 2015; Cipola et al. 2016; Zhang et al. 2019, 2020; Bellini et al. 2020). Considering the first three terga (Th. II to Abd. I), the pattern seen in Mastigocerini (1,1|0) matches that of Capbryini and Bessoniellini, while the pattern of Heteromurini (2,2|1) is the same as that of Orchesellini, Nothobryini, and Corynothrichini (Zhang and Deharveng 2015; Cipola et al. 2016; Zhang et al. 2019, 2020; Nunes et al. 2020). Since the S-chaetotaxy is a significant feature for supporting suprageneric groups of Entomobryoidea (Zhang and Deharveng 2015; Zhang et al. 2015, 2019), this observation may advocate for dismissing the current Heteromurinae. In fact, the entire tergal sens pattern and reduced dorsal macrochaetotaxy of *Mastigoceras*, especially in the mesothoracic collar, are unique features of Mastigocerini that distinguish it from all other Orchesellidae (Mari-Mutt 1980a) (Table 2).

Table 2. Comparison between the tribes of Orchesellidae.

Tribes/features	Nothobryini[2,8]	Capbryini[2,8]	Orchesellini[2,3,5,8]	Corynothrichini[2,3,5,8]	Bessoniellini[*,1,3,5]	Heteromurini[3–7]	Mastigocerini[9]
Secondary coverage by	chaetae	chaetae	chaetae	chaetae	chaetae	scales**	chaetae and scales
Scale shape	-	-	-	-	-	large R or T	small F
Scale distribution	-	-	-	-	-	head, trunk, antennae, legs, furca**	head (+/-), posterior Th. II–Abd. II, Abd. IV (+/-)
Tergal ms formula***	1,0|1,0,1	1,0|1,0,0–1	1,0|1,0,1	1,0|1,0,1	0,0|0,0,0	1,0|1,0,1	1,0|1,0,1
Tergal sens formula****	2,2|1,6,6,+,4	1,1|0,2–3,2,2,3	2,2|1,>3,>3,+,>4	2,2|1,>3,>4,-,9	1,1|0,2,4,3,3	2, 2|1,3,3,+,3–7	1,1|0,3,3,+,9
Antennal segments	4–6	4	5–6	4	5	5–6	5
Ant. IV apical bulb	-	+	+/-	-	-	+/-	-
Ant. IV pin projection	+	-	+/-	+	+	+/-	+
PAO	+	+	+/-	-	-	+/-	+
Trochanteral organ chaetae	3–15	3–6	>10	8–20	~10	>12	26–31
Tenaculum chaetae	2–4	1–2	1–15	2–5	0	0–16	0
Mucronal teeth	1	1	2	2	3	2	2
Mucronal spine	-	-	+/-	+	-	+/-	+

Legends: '*' as the equivalent of Bessoniellinae; '**' excluding *Heteromurus peyerimhoffi* Denis, 1937 from glacial caves of Algeria, which also have secondary plurimicrochaetosis on dorsal head and body, and absence of scales on legs; '***' Th. II–Abd. III; '****' Th. II–Abd. V; '-' absent; '+' present; '/' or; '~' approximately; '>' or more; 'ms' microsensilla; 'sens' sensilla; 'R' apically rounded; 'T' apically truncate; 'F' fusiform. Data based on: [1]Deharveng and Thibaud 1989; [2]Soto-Adames et al. 2008; [3]Zhang and Deharveng 2015; [4]Cipola et al. 2016; [5]Zhang et al. 2019; [6]Zhang et al. 2020; [7]Bellini et al. 2020; [8]Nunes et al. 2020; [9]this study. Classification based on Godeiro et al. 2023.

Our survey of *Mastigoceras*, including additional data based on the description of *Mastigoceras handschini* sp. nov., and of other Orchesellidae does not support a clear relationship between the Heteromurini and Mastigocerini (see Table 2 for a detailed comparison between the Orchesellidae lineages). However, it is also not clear to which other tribe(s) Mastigocerini is related. The internal relationships and systematics of the Orchesellidae are far from being resolved, and the possibility that the family is polyphyletic cannot be ruled out (Zhang et al. 2019; Godeiro et al. 2021, 2023; Bellini et al. 2023). Morphology suggests that Mastigocerini may actually represent an independent subfamily of Orchesellidae; or even a family itself. However, we could not provide a phylogeny of the basal Entomobryoidea at this time, so we will consider changing the status of Mastigocerini in a future study, aiming to resolve at least partially the many uncertainties regarding the internal relationships of the Orchesellidae.

Conclusions

Mastigoceras, the sole genus of Mastigocerini, is a very intriguing group of Orchesellidae, showing many peculiar traits compared to members of other tribes within the family. In this study we describe a second species of *Mastigoceras*, *Mastigoceras handschini* sp. nov., based on morphological and molecular evidence. Through detailed analysis of this new species, we identified for the first time the presence of the PAO and tergal sensilla and microsensilla formulae for the genus. There is little, if any, evidence that Mastigocerini is closely related to Heteromurini. However, we expect to provide a more comprehensive phylogeny of Orchesellidae in a future study to better understand the relationships among its tribes and to shed light on the external relationships of Mastigocerini.

Acknowledgements

We thank our dear friends Dr. Rodrigo Lopes Ferreira for supplying us with two specimens of *M. camponoti* from Minas Gerais; Edson Peres dos Santos for helping in the sampling of *Mastigoceras handschini* sp. nov. specimens; Dr. Nikolas Gioia Cipola for sharing the template of some chaetal symbols used in the drawings; and MSc. Nathália Michelly da Cunha Santos for her assistance in revising one of these specimens. We also thank the anonymous referees for their suggestions and corrections to improve this manuscript.

Additional information

Conflict of interest

The authors have declared that no competing interests exist.

Ethical statement

No ethical statement was reported.

Funding

This research was funded by the National Council for Scientific and Technological Development (CNPq), grant number #309114/2021-7—Bruno Cavalcante Bellini; and grant number #133624/2023-4—Iandra Vitória Bezerra Rodrigues; Fundação de

Apoio à Pesquisa do Estado da Paraíba (FAPESQ/PB), PhD scholarship, grant number #07/2021-SEECT—Paolla Gabryelle Cavalcante de Souza; and the National Science Foundation of China, research fund for international young scientists, grant number #32350410418—Nerivânia Nunes Godeiro.

Author contributions

Conceptualization: NNG, RCN, BCB. Data curation: PGCS, IVBR, BCB. Formal analysis: PGCS, RCN, IVBR. Funding acquisition: BCB. Investigation: NNG, BCB, PGCS, IVBR. Methodology: IVBR, BCB, NNG, PGCS. Project administration: BCB. Resources: BCB. Software: IVBR, NNG, PGCS. Supervision: BCB, RCN. Validation: BCB, RCN, NNG. Visualization: PGCS, BCB. Writing - original draft: IVBR, PGCS, BCB. Writing - review and editing: PGCS, RCN, BCB, IVBR.

Author ORCIDs

Iandra Vitória Bezerra Rodrigues https://orcid.org/0000-0002-4838-1151
Paolla Gabryelle Cavalcante de Souza https://orcid.org/0000-0003-0612-8438
Rudy Camilo Nunes https://orcid.org/0000-0002-3140-9146
Nerivânia Nunes Godeiro https://orcid.org/0000-0002-1669-6124
Bruno Cavalcante Bellini https://orcid.org/0000-0001-7881-9436

Data availability

The resulting COI sequences of Mastigoceras spp. can be accessed at https://www.ncbi.nlm.nih.gov/, with the following numbers: PP960562 and PP960563, respectively for *M. camponoti* and *Mastigoceras handschini* sp. nov.

References

Absolon K (1901) Weitere Nachricht über europäische Höhlencollembolen und über die Gattung Aphorura A. D. MacG. Zoologischer Anzeiger 24: 385–389.

Absolon K, Ksenemann M (1942) Troglopedetini. Vergleichende Studie über eine altertümliche höhlenbewohnende Kollembolengruppe aus den dinarischen Karstgebieten. Studien aus dem Gebiete der allgemeinen Karstforschung, der wissenschaftlichen Höhlenkunde, der Eiszeitforschung und den Nachbargebieten 16: 5–57.

Arlé R, Mendonça C (1982) Estudo preliminar das espécies de *Dicranocentrus* Schött, 1893, ocorrentes no Parque Nacional da Tijuca, Rio de Janeiro (Collembola). Revista Brasileira de Biologia 42: 41–49.

Bagnall RS (1949) Contributions toward a knowledge of the Onychiuridae (Collembola-Onychiuroidea)V–X. Annals and Magazine of Natural History 12: 498–511. https://doi.org/10.1080/00222934908654001

Bellini BC (2014) Fauna de Collembola (Arthropoda) em áreas úmidas do semiárido. *In*: Bravo F and Calor A (Eds) Artrópodes do Semiárido, Biodiversidade e Conservação, Feira de Santana, 57–68.

Bellini BC, Cipola NG, Siqueira OJR (2020) A Survey of the Brazilian *Dicranocentrus* Schött (Collembola, Orchesellidae, Heteromurini) with the Description of a New Species and notes on the Genus. Insects 11: 709. https://doi.org/10.3390/insects11100709

Bellini BC, Greenslade P, Baquero E, Jordana R, Souza PGC (2022) A synthesis of the current knowledge on the Australian Orchesellidae (Collembola, Entomobryoidea). Zootaxa 5115: 221–257. https://doi.org/10.11646/zootaxa.5115.2.3

Bellini BC, Zhang F, Souza PGC, Santos-Costa RC, Medeiros GS, Godeiro NN (2023) The Evolution of Collembola Higher Taxa (Arthropoda, Hexapoda) Based on Mitogenome Data. Diversity 15: 1–24. https://doi.org/10.3390/d15010007

Börner C (1906) Das System der Collembolen-nebst Beschreibung neuer Collembolen des Hamburger Naturhistorischen Museums. Mitteilungen aus dem Naturhistorischen Museum in Hamburg 23: 147–188.

Cassagnau P (1963) Collemboles d'Amerique du Sud, II. Orchesellini, Paronelline, Cyphoderinae. In: Deboutteville CD, Rapoport E (Eds) Biologie de L'Amérique Australe. V.II Études sur la faune du sol, Paris, 127–148.

Cassagnau P (1979) Les Collemboles Neanuridae des Pays Dinaro-Balkaniques: leur interêt phylogénétique et biogéographique. Biologia Gallo-Hellenica 8: 185–203.

Cassagnau P, Oliveira E (1992) Sur *Mastigoceras camponoti* Handschin, Collembole Orchesellinae d'Amazonie. Bulletin de la Société d'histoire naturelle d, Toulouse 128: 27–31.

Cipola NG, Morais JW, Bellini BC (2014) A new species of *Seira* (Collembola: Entomobryidae: Seirini) from Northern Brazil, with the addition of new chaetotaxic characters. Zoologia 31: 489–495. https://doi.org/10.1590/S1984-46702014000500009

Cipola NG, Oliveira FGL, Morais JW, Bellini BC (2016) The Heteromurini Absolon & Ksenemann (Collembola, Entomobryidae): a review of the genera status and diagnoses, keys for species of *Alloscopus* Börner and *Heteromurtrella* Mari Mutt and description of a new species. Zootaxa 4084: 151–186. https://doi.org/10.11646/zootaxa.4084.2.1

Cipola NG, Zequi JAC, Bellini BC (2019) Collembola (Hexapoda). In: Zequi JAC, Orsi ML and Shibatta LS (Eds) Fauna e flora do Parque Estadual Mata São Francisco: norte do Paraná, Londrina, 105–119.

Deharveng L, Thibaud JM (1989) *Bessoniella procera* n. g., n. sp., nouvel Orchesellidae cavernicole relictuel des Pyrénées (Insecta, Collembola). Bulletin du Muséum National d'Histoire Naturelle. Paris 4 (ser 11): 397–405. https://doi.org/10.5962/p.288296

Denis JR (1937) Sur les Collemboles d'Afrique du Nord. Bullertin de la Societé d'Histoire Naturelle de l'Afrique du Nord 26: 85–87.

Fjellberg A (1999) The labial palp in Collembola. Zoologischer Anzeiger 237: 309–330.

Gisin H (1967) Especes nouvelles et lignées évolutives de *Pseudosinella* endogés. Memórias e Estudos do Museu Zoologico da Universidade de Coimbra 301: 5–25.

Godeiro NN, Bellini BC, Ding N, Xu C, Ding Y, Zhang F (2021) A mitogenomic phylogeny of the Entomobryoidea (Collembola): A comparative perspective. Zoologica Scripta 50: 658–666. https://doi.org/10.1111/zsc.12487

Godeiro NN, Ding Y, Cipola NG, Jantarit S, Bellini BC, Zhang F (2023) Phylogenomics and systematics of Entomobryoidea (Collembola): marker design, phylogeny and classification. Cladistics 39: 101–115. https://doi.org/10.1111/cla.12521

Handschin E (1924) Neue myrmecophile und termitophile Collembolenformen aus Sud-Amerika. Neue Beiträge zur Systematischen Insektenkunde, Berlim 3: 13–26.

Hausmann A, Haszprunar G, Segerer AH, Speidel W, Behounek G, Hebert PDN (2011) Now DNA-barcoded: the butterflies and larger moths of Germany. Spixiana 34: 47–58.

Hebert PDN, Landry JF (2010) DNA barcodes for 1/1000 of the animal kingdom. Biology Letters 6: 359–362. https://doi.org/10.1098/rsbl.2009.0848

Hebert PDN, Ratnasingham S, De Waard JR (2003a) Barcoding animal life: cytochrome c oxidase subunit 1 divergences among closely related species. Proceedings of the Royal Society B: Biological Sciences 270(Suppl_1): S96–S99. https://doi.org/10.1098/rsbl.2003.0025

Hebert PDN, Cywinska A, Ball SL, De Waard JR (2003b) Biological identifications through DNA barcodes. Proceedings of the Royal Society B: Biological Sciences 270: 313–321. https://doi.org/10.1098/rspb.2002.2218

IBGE Instituto Brasileiro de Geografia e Estatística (2024) Portal de Mapas. https://portaldemapas.ibge.gov.br/portal.php#homepage [Acessed on 12 June 2024].

Jordana R, Baquero E (2005) A proposal of characters for taxonomic identification of *Entomobrya* species (Collembola, Entomobryomorpha), with description of a new species. Abhandlungen und Berichte des Naturkundemuseums Görlitz 76: 117–134.

Jordana R, Arbea JL, Simón C, Luciáñez MJ (1997) Fauna Iberica: Collembola Poduromorpha. Museo Nacional de Ciencias Naturales, Madrid 8, 642–807.

Kimura M (1980) A simple method for estimating evolutionary rate of base substitutions through comparative studies of nucleotide sequences. Journal of Molecular Evolution 16: 111–120. https://doi.org/10.1007/BF01731581

Knowlton N (1993) Sibling species in the sea. Annual Review of Ecology and Systematics 24: 189–216. https://doi.org/10.1146/annurev.es.24.110193.001201

Kottek M, Grieser J, Beck C, Rudolf B, Rubel F (2006) World map of the Köppen-Geiger climate classification updated. Meteorologische Zeitschrift 15: 259–263. https://doi.org/10.1127/0941-2948/2006/0130

Kumar S, Stecher G, Li M, Knyaz C, Tamura K (2018) MEGA X: Molecular Evolutionary Genetics Analysis across computing platforms. Molecular Biology and Evolution 35: 1547–1549. https://doi.org/10.1093/molbev/msy096

Lajus D, Sukhikh N, Alekseev V (2015) Cryptic or pseudocryptic: can morphological methods inform copepod taxonomy? An analysis of publications and a case study of the *Eurytemora affinis* species complex. Ecology and Evolution 5: 2374–2385. https://doi.org/10.1002/ece3.1521

Linnaeus C (1758) Systema naturæ per regna tria naturæ, secundum classes, ordines, genera, species, cum characteribus, differentiis, synonymis, locis, 10th edn. Impensis Direct. Laurentii Salvii, Stockholm, 824 pp. https://doi.org/10.5962/bhl.title.542

Lukić M, Porco D, Bedos A, Deharveng L (2015) The puzzling distribution of *Heteromurus* (*Verhoeffiella*) *absoloni* Kseneman, 1938 (Collembola: Entomobryidae: Heteromurinae) resolved: Detailed redescription of the nominal species and description of a new species from Catalonia (Spain). Zootaxa 4039: 249–275. https://doi.org/10.11646/zootaxa.4039.2.3

Mari-Mutt JA (1978) A Review of the Genus *Mastigoceras* with remarks on its Systematic Position (Collembola: Entomobryidae). The Pan-Pacific Entomologist 54: 43–47.

Mari-Mutt JA (1979) A revision of the genus *Dicranocentrus* Schott (Insecta: Collembola: Entomobryidae). Agricultural Experiment Station Bulletin 259: 1–79.

Mari-Mutt JA (1980a) A Classification of the Orchesellinae with a Key to Tribes, Genera and Subgenera (Collembola: Entomobryidae). Annals of the Entomological Society of America 73: 455–459. https://doi.org/10.1093/aesa/73.4.455

Mari-Mutt JA (1980b) A Revision of *Heteromurus* s. str. (Insecta: Collembola: Entomobryidae). Transactions of the Illinois State Academy of Science 72: 29–50.

Mari-Mutt JA, Bellinger PF (1990) A catalog of the Neotropical Collembola. Flora & fauna handbook n° 5. Sandhill Crane Press, Gainesville, Florida, 237 pp.

Mari-Mutt JA, Bellinger PF (1996) Supplement to the catalog of the Neotropical Collembola. Caribbean Journal of Science 32: 166–175.

Mari-Mutt JA, Bellinger PF, Janssens F (1996–2021) Checklist of the Collembola: Supplement to the Catalog of the Neotropical Collembola. http://www.collembola.org/publicat/neotrcat.htm/ [Accessed on 28 June 2024]

Mendonça MC, Fernandes LH, Abrantes EA, Queiroz GC, Bernardo AN, Silveira TC (2009) Fauna Colembológica do Estado do Rio de Janeiro, Brasil. Arquivos do Museu Nacional, Rio de Janeiro 67: 265–274.

Meng G, Li Y, Yang C, Liu S (2019) MitoZ: A toolkit for animal mitochondrial genome assembly, annotation and visualization. Nucleic Acids Research 47: 63. https://doi.org/10.1093/nar/gkz173

Nicolet H (1842) Recherches pour Servir á l'Histoire des Podurelles. Nouvelles Mémoires de la. Société Helvetica Scientiae Naturalis 6: 1–88.

Nunes RC, Santos-Costa RC, Bellini BC (2020) The first Neotropical *Capbrya* Barra, 1999 (Collembola: Orchesellidae: Nothobryinae) and the reinterpretation of Nothobryinae systematics. Zoologischer Anzeiger 288: 24–42. https://doi.org/10.1016/j.jcz.2020.06.009

Pan ZX (2015) Two closely related *Homidia* species (Entomobryidae, Collembola) revealed by morphological and molecular evidence. Zootaxa 3918: 285–294. https://doi.org/10.11646/zootaxa.3918.2.9

Porco D, Bedos A, Deharveng L (2010) Cuticular compounds bring new insight in the post-glacial recolonization of a Pyrenean area: *Deutonura deficiens* Deharveng, 1979 complex, a case study. PLoS ONE 5: e14405. https://doi.org/10.1371/journal.pone.0014405

Porco D, Bedos A, Greenslade P, Janion C, Skarżyński D, Stevens M, van Vuuren BJ, Deharveng L (2012) Challenging species delimitation in Collembola: cryptic diversity among common springtails unveiled by DNA barcoding. Invertebrate Systematics 26: 470–477. https://doi.org/10.1071/is12026

QGIS.org (2024) QGIS Geographic Information System. QGIS Association. http://www.qgis.org [accessed 28 June 2024]

Salmon JT (1964) An index to the Collembola. Royal Society of New Zealand 7: 1–651.

Soto-Adames FN (2008) Postembryonic development of the dorsal chaetotaxy in *Seira dowlingi* (Collembola, Entomobryidae); with an analysis of the diagnostic and phylogenetic significance of primary chaetotaxy in *Seira*. Zootaxa 1683: 1–31. https://doi.org/10.11646/zootaxa.1683.1.1

Soto-Adames FN, Barra JA, Christiansen K, Jordana R (2008) Suprageneric Classification of the Entomobryomorpha Collembola. Annals of the Entomological Society of America 101: 501–513. https://doi.org/10.1603/0013-8746(2008)101[501:SCOCE]2.0.CO;2

Stach J (1947) The Apterygotan Fauna of Poland in Relation to the World-Fauna of this Group of Insects. Family: Isotomidae. Polska Akademia Umiejętności, Acta monographica Musei Historiae Naturalis, Kraków, 488 pp.

Stecher G, Tamura K, Kumar S (2020) Molecular Evolutionary Genetics Analysis (MEGA) for macOS. Molecular Biology and Evolution 37: 1237–1239. https://doi.org/10.1093/molbev/msz312

Sun X, Bedos A, Deharveng L (2017) Two new species of the genus *Thalassaphorura* Bagnall, 1949 (Collembola: Onychiuridae) from south China, with an updated key to world species of the genus. Zootaxa 4338: 319–332. https://doi.org/10.11646/zootaxa.4338.2.6

Sun X, Bedos A, Deharveng L (2018) Unusually low genetic divergence at COI barcode locus between two species of intertidal *Thalassaphorura* (Collembola: Onychiuridae). PeerJ 6: e5021. https://doi.org/10.7717/peerj.5021

Szeptycki A (1972) Morpho-systematic studies on Collembola. III. Body chaetotaxy in the first instars of several genera of the Entomobryomorpha. Acta Zoologica Cracoviensia 17: 341–372.

Szeptycki A (1979) Morpho-systematic studies on Collembola. IV. Chaetotaxy of the Entomobryidae and its phylogenetical significance. Polska Akademia Nauk, Krakow, 1–218.

Wankel H (1860) Beiträge zur fauna der Mäharichen Hohlen. Lotos, Prague 10: 201–206.

Webb JM, Jacobus LM, Funk DH, Zhou X, Kondratieff B, Geraci CJ, DeWalt RE, Baird DJ, Richard B, Phillips I (2012) A DNA barcode library for North American Ephemeroptera: progress and prospects. PLoS ONE 7: e38063. https://doi.org/10.1371/journal.pone.0038063

Womersley H (1937) Collembola (Springtails). Reports of B.A.N.Z. Antarctic Research Expedition 1929–1931 4: 1– 7. https://doi.org/10.26749/SFQG9801

Yu D, Zhang F, Stevens MI, Yan Q, Liu M, Hu F (2016) New insight into the systematics of Tomoceridae (Hexapoda, Collembola) by integrating molecular and morphological evidence. Zoologica Scripta 45: 286–299. https://doi.org/10.1111/zsc.12149

Yu D, Ding Y, Ma Y (2017) Revision of *Tomocerus* similis Chen & Ma, with discussion of the kinoshitai complex and the distal tibiotarsal chaetae in Tomocerinae (Collembola, Tomoceridae). Zootaxa 4268: 395–410. https://doi.org/10.11646/zootaxa.4268.3.5

Zeppelini D, Queiroz GC, Bellini BC, Brito RA, Oliveira JVLC, Lopes BCH, Lima ECA, Ferreira AS, Brito NP (2024) *Mastigoceras* in Catálogo Taxonômico da Fauna do Brasil. PNUD. http://fauna.jbrj.gov.br/fauna/faunadobrasil/18545 [accessed 28 June 2024]

Zhang F, Deharveng L (2015) Systematic revision of Entomobryidae (Collembola) by integrating molecular and new morphological evidence. Zoologica Scripta 44: 298–311. https://doi.org/10.1111/zsc.12100

Zhang F, Yu D, Luo Y, Ho SYW, Wang B, Zhu C (2014a) Cryptic diversity, diversification and vicariance in the two species complexes of *Tomocerus* (Collembola, Tomoceridae) from China. Zoologica Scripta 43: 393–404. https://doi.org/10.1111/zsc.12056

Zhang F, Chen Z, Dong RR, Deharveng L, Stevens MI, Huang YH, Zhu CD (2014b) Molecular phylogeny reveals independent origins of body scales in Entomobryidae (Hexapoda: Collembola). Molecular Phylogenetics and Evolution 70: 231–239. https://doi.org/10.1016/j.ympev.2013.09.024

Zhang F, Sun DD, Yu DY, Wang BX (2015) Molecular phylogeny supports S-chaetae as a key character better than jumping organs and body scales in classification of Entomobryoidea (Collembola). Scientific Reports 5: 1–12. https://doi.org/10.1038/srep12471

Zhang F, Greenslade P, Stevens MI (2017) A revision of the genus *Lepidobrya* Womersley (Collembola: Entomobryidae) based on morphology and sequence data of the genotype. Zootaxa 4221: 523–536. https://doi.org/10.11646/zootaxa.4221.5.2

Zhang F, Bellini BC, Soto-Adames FN (2019) New insights into the systematics of Entomobryoidea (Collembola: Entomobryomorpha): first instar chaetotaxy, homology and classification. Zoological Systematics 44: 249–278. https://doi.org/10.11865/zs.201926

Zhang F, Cipola N, Ding N (2020) New insight into the systematics of Heteromurini (Collembola: Entomobryidae: Heteromurinae) with special reference to *Alloscopus* and *Sinodicranocentrus* gen. n. Arthropod Systematics and Phylogeny 78: 1–16. https://doi.org/10.26049/ASP78-1-2020-01

ZooKeys 1217: 101–117 (2024)
DOI: 10.3897/zookeys.1217.134704

Research Article

150 years after Ferdinand Morawitz: a survey of megachilid bees (Hymenoptera, Megachilidae) of Dagestan, Russia

Alexander V. Fateryga[1], Maxim Yu. Proshchalykin[2]

1 *T.I. Vyazemsky Karadag Scientific Station – Nature Reserve of RAS – Branch of A.O. Kovalevsky Institute of Biology of the Southern Seas of RAS, Nauki Str. 24, Kurortnoye, 298188 Feodosiya, Russia*
2 *Federal Scientific Center of the East Asia Terrestrial Biodiversity, Far Eastern Branch of the Russian Academy of Sciences, 100-let Vladivostoku Ave. 159, 690022 Vladivostok, Russia*
Corresponding author: Alexander V. Fateryga (fater_84@list.ru)

Abstract

A list of 148 species of megachilid bees from 16 genera and five tribes is reported for the Republic of Dagestan. The list is based on more than 2,500 examined specimens and one reliable literature record. Twelve species are new to Russia: *Chelostoma* (*Chelostoma*) *emarginatum* (Nylander, 1856), *C.* (*Foveosmia*) *maidli* (Benoist, 1935), *Hoplitis* (*Alcidamea*) *campanularis* (Morawitz, 1877), *H.* (*A.*) *caucasica* (Friese, 1920), *H.* (*Anthocopa*) *perezi* (Ferton, 1894), *H.* (*Pentadentosmia*) *tringa* (Warncke, 1991), *Osmia* (*Allosmia*) *melanura* Morawitz, 1871, *O.* (*Helicosmia*) *breviata* Warncke, 1988, *O.* (*Osmia*) *scheherazade* Peters, 1978, *O.* (*Pyrosmia*) *saxicola* Ducke, 1899, *Anthidium* (*Anthidium*) *taeniatum* Latreille, 1809, and *Megachile* (*Chalicodoma*) *montenegrensis* Dours, 1873. Nine other species are new to the North Caucasus, and 46 other species are new to Dagestan. Compared to the first list of the bees of Dagestan published by F. Morawitz 150 years ago, the number of species of Megachilidae known from the republic was increased by five times.

Key words: Biodiversity, Caucasus, new record, Palaearctic region

Academic editor: Michael S. Engel
Received: 14 August 2024
Accepted: 11 October 2024
Published: 30 October 2024

ZooBank: https://zoobank.org/4B5A1491-13C2-4EA8-BFFE-646211FAFCD1

Citation: Fateryga AV, Proshchalykin MYu (2024) 150 years after Ferdinand Morawitz: a survey of megachilid bees (Hymenoptera, Megachilidae) of Dagestan, Russia. ZooKeys 1217: 101–117. https://doi.org/10.3897/zookeys.1217.134704

Introduction

The Republic of Dagestan is the most southern region of Russia. The northern half of Dagestan is a part of the Caspian Depression while its southern half is a part of the Greater Caucasus, one of the most important biodiversity hotspots in the world. The area of Dagestan is somewhat more than 50,000 km^2, which is not particularly large but the territory of the republic is elevated from −27 to 4,466 m a.s.l. Therefore, landscapes and habitats are extremely diverse and correspondingly changing from lowland deserts to alpine meadows, with a few forest zones as well. The biodiversity of the Republic of Dagestan is also very high; there are more than 3,500 species of vascular plants and 604 species of vertebrates occurring here, while invertebrates are generally poorly studied (Red Book of the Republic of Dagestan 2020). The Megachilidae is a large family of bees numbering more than 4,000 described species worldwide (Michener 2007; Ascher and Pickering 2024); 220 species are known from Russia (Proshchalykin et al. 2023), while knowledge of megachilid bees of Dagestan is very incomplete.

Ferdinand Morawitz (1827–1896) was one of the leading specialists on the bees (Hymenoptera, Anthophila) at the end of the 19th century (Fig. 1A). He published 64 papers, 44 of them dealing with melittology. In total, Morawitz described five new genera and 725 new species of bees, including 185 species of the family Megachilidae (Pesenko and Astafurova 2003). The vast majority of the species described by him are currently recognized as valid (Schwarz 1980a, 1980b, 1987; Schwarz and Gusenleitner 2002, 2004; Dathe and Proshchalykin 2017; Astafurova and Proshchalykin 2020; Astafurova et al. 2021, 2022). In 1873, Morawitz published the first paper dealing with the bees of Dagestan (Fig. 1B), where he reported 30 species of the family Megachilidae (Morawitz 1873). Six of these species were described as new to science, of which four are currently recognized as valid species (Table 1, Fig. 1C, D). Considering some recently published papers (Fateryga 2017; Fateryga et al. 2019, 2023; Fateryga and Proshchalykin 2020; Litman et al. 2021; Levchenko 2023; Proshchalykin et al. 2023), the number of species of megachilid bees of Dagestan has been increased to 81, which is expected to be still very far from the true number of species occurring in the republic. The purpose of the present contribution is to publish the complete list of all species of megachilid bees known from the Republic of Dagestan to date.

Table 1. Species of the family Megachilidae described from Dagestan by Ferdinand Morawitz.

Species name	Sex	Type locality	Current status	Source
Anthidium alpinum Morawitz, 1873	♂	Kurush	Valid, as *Pseudoanthidium alpinum* (Morawitz, 1873)	Kasparek 2022; Kasparek and Ebmer 2023
Anthidium clypeare Morawitz, 1873	♀	Derbent	Valid, as *Eoanthidium clypeare* (Morawitz, 1873)	Kasparek 2020, 2022
Coelioxys conspersa Morawitz, 1873	♀	Derbent	Junior synonym of *Coelioxys polycentris* Förster, 1853	Schwarz and Gusenleitner 2003; Fateryga et al. 2019
Coelioxys pulchella Morawitz, 1873	♂	Derbent	Junior synonym of *Coelioxys haemorrhoa* Förster, 1853	Schwarz 2001; Schwarz and Gusenleitner 2003
Osmia nana Morawitz, 1873	♂	Derbent	Valid	van der Zanden 1991; Warncke 1992
Osmia viridana Morawitz, 1873	♀, ♂	Derbent	Valid	van der Zanden 1991; Warncke 1992

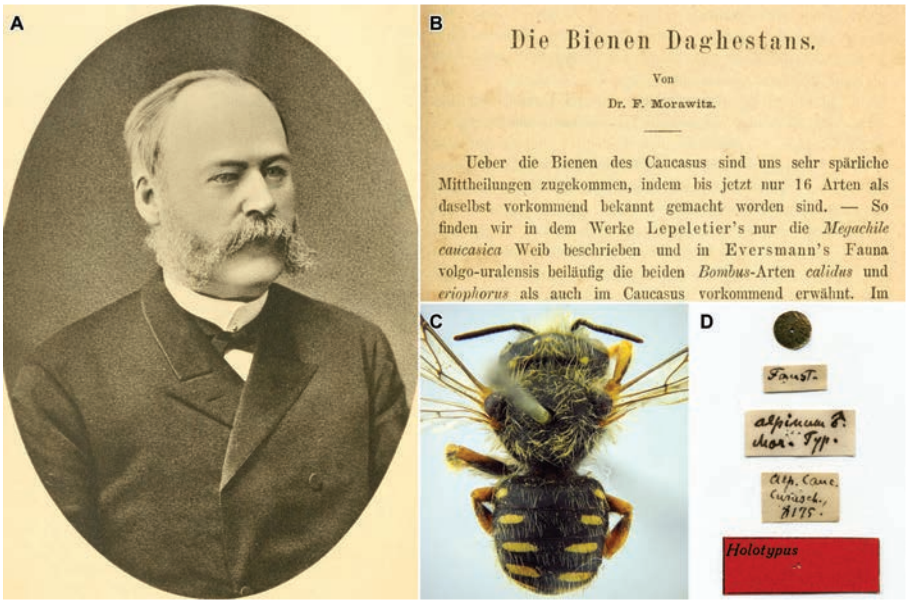

Die Bienen Daghestans.

Von

Dr. F. Morawitz.

Ueber die Bienen des Caucasus sind uns sehr spärliche Mittheilungen zugekommen, indem bis jetzt nur 16 Arten als daselbst vorkommend bekannt gemacht worden sind. — So finden wir in dem Werke Lepeletier's nur die *Megachile caucasica* Weib beschrieben und in Eversmann's Fauna volgo-uralensis beiläufig die beiden *Bombus*-Arten *calidus* und *eriophorus* als auch im Caucasus vorkommend erwähnt. Im

Figure 1. Ferdinand Morawitz and his heritage **A** portrait of F. Morawitz (public domain) **B** beginning of Morawitz's (1873) paper on the bees of Dagestan (public domain) **C, D** male holotype of *Pseudoanthidium alpinum* (Morawitz, 1873) described from Dagestan, dorsal view and labels (photographs by Yu. Astafurova).

Materials and methods

Several field expeditions were made to various districts of the Republic of Dagestan in 2015–2023, where megachilid bees were collected in all types of landscapes and habitats (Figs 2, 3). Collected specimens are deposited mainly in the collections of the Zoological Institute of the Russian Academy of Sciences, Saint Petersburg, Russia [**ZISP**], the Federal Scientific Center of the East Asia Terrestrial Biodiversity of the Far Eastern Branch of the Russian Academy of Sciences, Vladivostok, Russia [**FSCV**], and the research collections of A.V. Fateryga, Feodosiya, Russia [**CAFK**] and T.V. Levchenko, Moscow, Russia [**CTLM**]. Old material deposited in ZISP was also studied. A total of 2,556 specimens of megachilid bees from Dagestan were examined. Selected specimens were sent to be deposited (some of them temporary) in the Entomological Collection of ETH Zurich, Switzerland [**ETHZ**], Muséum d'Histoire Naturelle de Neuchâtel, Switzerland [**MHNN**], and the research collections of M. Kasparek, Heidelberg, Germany [**CMKH**]. Possible literature sources were also studied but the present work is principally based on material directly examined by the authors and does not include data published online that has not otherwise been validated by experts (e.g., observations reported on iNaturalist). The general distributions of species reported as new to Russia are based on Müller (2024) for the tribe Osmiini, as well as Fateryga et al. (2020), Boustani et al. (2021), and Maharramov et al. (2021) for other taxa.

Results

As the result of the study, 2,511 specimens of megachilid bees from Dagestan were identified to 147 species. The remaining 45 specimens represented five species, which identity was unclear. They cannot be identified either without males, as in the case of *Heriades* sp. and *Osmia* (*Pyrosmia*) sp., or in the lack of a comprehensive revision of the corresponding group, as in the case of *Hoplitis* (*Hoplitis*) spp. and *Protosmia* (*Nanosmia*) sp. One more species, *Pseudoanthidium* (*Pseudoanthidium*) *tenellum* (Mocsáry, 1880), was added to the list on the base of a reliable literature record (Litman et al. 2021). A total of 148 species from 16 genera and five tribes were found to occur in Dagestan (Table 2). Full label data of all specimens are represented in Suppl. material 1.

Twelve species are reported here from Russia for the first time; their full label data and general distribution are listed below. Besides them, 55 other species are new to Dagestan and nine of them are also reported for the first time from the North Caucasus as a whole: *Hoplitis* (*Alcidamea*) *praestans* (Morawitz, 1893), *H.* (*A.*) *scita* (Eversmann, 1852), *Osmia* (*Pyrosmia*) *hellados* van der Zanden, 1984, *Stelis* (*Stelidomorpha*) *nasuta* (Latreille, 1809), *S.* (*Stelis*) *odontopyga* Noskiewicz, 1926, *Coelioxys* (*Coelioxys*) *quadridentatus* (Linnaeus, 1758), *C.* (*Paracoelioxys*) *mandibularis* Nylander, 1848, *Megachile* (*Eutricharaea*) *anatolica* Rebmann, 1968, and *M.* (*Megachile*) *lapponica* Thomson, 1872 (Table 2). The record of *Hoplitis scita* is especially remarkable because this species was previously known in Russia only from Siberia and the Far East, while its general distribution includes also Kyrgyzstan, Mongolia, and China (Müller 2024).

Table 2. A list of the megachilid bees of Dagestan (species new to the North Caucasus are indicated with an asterisk; species new to Russia are indicated with two asterisks).

Species name	Literature records	Material examined
Tribe Lithurgini		
Lithurgus chrysurus Fonscolombe, 1834	Fateryga et al. (2019)	43 ♀, 100 ♂
Lithurgus cornutus (Fabricius, 1787)	Morawitz (1873), as *L. monoceros*, partial misidentification of *L. chrysurus*	4 ♀, 1 ♂
Lithurgus tibialis Morawitz, 1875	Fateryga et al. (2019)	2 ♀, 1 ♂
Tribe Osmiini		
Chelostoma (*Chelostoma*) *emarginatum* (Nylander, 1856)**	–	1 ♀, 2 ♂
Chelostoma (*Chelostoma*) *florisomne* (Linnaeus, 1758)	–	2 ♀
Chelostoma (*Foveosmia*) *campanularum* (Kirby, 1802)	Fateryga et al. (2019)	1 ♀, 9 ♂
Chelostoma (*Foveosmia*) *distinctum* (Stöckhert, 1929)	Fateryga et al. (2019)	35 ♀, 24 ♂
Chelostoma (*Foveosmia*) *foveolatum* (Morawitz, 1868)	–	3 ♀, 13 ♂
Chelostoma (*Foveosmia*) *maidli* (Benoist, 1935)**	–	1 ♂
Chelostoma (*Gyrodromella*) *rapunculi* (Lepeletier de Saint-Fargeau, 1841)	–	7 ♀, 34 ♂
Heriades (*Heriades*) *crenulata* Nylander, 1856	–	7 ♀, 38 ♂
Heriades (*Heriades*) *rubicola* Pérez, 1890	–	59 ♀, 19 ♂
Heriades (*Heriades*) *truncorum* (Linnaeus, 1758)	–	8 ♀, 13 ♂
Hoplitis (*Alcidamea*) *acuticornis* (Dufour & Perris, 1840)	–	10 ♀, 1 ♂
Hoplitis (*Alcidamea*) *campanularis* (Morawitz, 1877)**	–	1 ♀, 3 ♂
Hoplitis (*Alcidamea*) *caucasica* (Friese, 1920)**	–	2 ♀
Hoplitis (*Alcidamea*) *curvipes* (Morawitz, 1871)	Fateryga and Proshchalykin (2020); Ivanov et al. (2023)	1 ♀, 5 ♀
Hoplitis (*Alcidamea*) *leucomelana* (Kirby, 1802)	Morawitz (1873), as *Osmia parvula*	26 ♀, 46 ♂
Hoplitis (*Alcidamea*) *ozbeki* Tkalců, 2000	Proshchalykin et al. (2023)	1 ♀, 1 ♂
Hoplitis (*Alcidamea*) *praestans* (Morawitz, 1893)*	–	2 ♀, 4 ♂
Hoplitis (*Alcidamea*) *scita* (Eversmann, 1852)*	–	2 ♀, 5 ♂
Hoplitis (*Alcidamea*) *tridentata* (Dufour & Perris, 1840)	–	16 ♀, 11 ♂
Hoplitis (*Anthocopa*) *caucasicola* Müller, 2012	–	1 ♀
Hoplitis (*Anthocopa*) *jakovlevi* (Radoszkowski, 1874)	Fateryga et al. (2019)	3 ♀, 1 ♂
Hoplitis (*Anthocopa*) *mocsaryi* (Friese, 1895)	Levchenko (2023)	1 ♀, 1 ♂
Hoplitis (*Anthocopa*) *papaveris* (Latreille, 1799)	–	6 ♀, 1 ♂
Hoplitis (*Anthocopa*) *perezi* (Ferton, 1894)**	–	1 ♀, 2 ♂
Hoplitis (*Hoplitis*) *adunca* (Panzer, 1798)	Morawitz (1873), misidentification of *H. manicata*	50 ♀, 43 ♂
Hoplitis (*Hoplitis*) *anthocopoides* (Schenck, 1853)	–	1 ♀, 1 ♂
Hoplitis (*Hoplitis*) *astragali* Fateryga, Müller & Proshchalykin, 2023	Fateryga et al. (2023)	46 ♀, 42 ♂
Hoplitis (*Hoplitis*) *dagestanica* Fateryga, Müller & Proshchalykin, 2023	Fateryga et al. (2023)	6 ♀, 31 ♂
Hoplitis (*Hoplitis*) *linguaria* (Morawitz, 1875)	Proshchalykin et al. (2023)	12 ♀, 4 ♂
Hoplitis (*Hoplitis*) *manicata* Morice, 1901	Fateryga et al. (2019)	11 ♀, 17 ♂
Hoplitis (*Pentadentosmia*) *tringa* (Warncke, 1991)**	–	2 ♀
Osmia (*Allosmia*) *melanura* Morawitz, 1871**	–	10 ♀, 2 ♂
Osmia (*Allosmia*) *rufohirta* Latreille, 1811	–	55 ♀, 5 ♂
Osmia (*Erythrosmia*) *andrenoides* Spinola, 1808	Fateryga (2017)	12 ♀, 5 ♂
Osmia (*Helicosmia*) *aurulenta* (Panzer, 1799)	–	7 ♀, 2 ♂
Osmia (*Helicosmia*) *breviata* Warncke, 1988**	–	1 ♀
Osmia (*Helicosmia*) *caerulescens* (Linnaeus, 1758)	–	29 ♀, 5 ♂
Osmia (*Helicosmia*) *cinerea* Warncke, 1988	Fateryga and Proshchalykin (2020)	3 ♀
Osmia (*Helicosmia*) *dimidiata* Morawitz, 1870	–	2 ♀, 5 ♂
Osmia (*Helicosmia*) *leaiana* (Kirby, 1802)	–	2 ♀
Osmia (*Helicosmia*) *melanogaster* Spinola, 1808	Morawitz (1873), as *O. aterrima*	20 ♀, 9 ♂
Osmia (*Helicosmia*) *niveata* (Fabricius, 1804)	Morawitz (1873), as *O. fulviventris*, misidentification of *O. melanogaster*	26 ♀, 2 ♂
Osmia (*Helicosmia*) *signata* Erichson, 1835	Morawitz (1873), as *O. melanogastra*	9 ♀, 8 ♂
Osmia (*Hoplosmia*) *bidentata* Morawitz, 1875	Fateryga et al. (2019)	5 ♀, 10 ♂
Osmia (*Hoplosmia*) *ligurica* Morawitz, 1868	Fateryga and Proshchalykin (2020)	1 ♀
Osmia (*Hoplosmia*) *scutellaris* Morawitz, 1868	Morawitz (1873)	3 ♀, 1 ♂
Osmia (*Hoplosmia*) *spinulosa* (Kirby, 1802)	Morawitz (1873)	1 ♀, 2 ♂
Osmia (*Metallinella*) *brevicornis* (Fabricius, 1798)	Morawitz (1873), as *O. panzeri*	27 ♀, 9 ♂

Species name	Literature records	Material examined
Osmia (*Osmia*) *apicata* Smith, 1853	Fateryga and Proshchalykin (2020)	8♀, 5♂
Osmia (*Osmia*) *bicornis* (Linnaeus, 1758)	Morawitz (1873)	12♀
Osmia (*Osmia*) *cornuta* (Latreille, 1805)	–	1♀, 2♂
Osmia (*Osmia*) *mustelina* Gerstäcker, 1869	Fateryga and Proshchalykin (2020)	2♀
Osmia (*Osmia*) *scheherazade* Peters, 1978**	–	1♀
Osmia (*Pyrosmia*) *cephalotes* Morawitz, 1870	–	35♀, 12♂
Osmia (*Pyrosmia*) *cyanoxantha* Pérez, 1879	Fateryga and Proshchalykin (2020)	1♀
Osmia (*Pyrosmia*) *hellados* van der Zanden, 1984*	–	4♀, 4♂
Osmia (*Pyrosmia*) *nana* Morawitz, 1873	Morawitz (1873)	1♂
Osmia (*Pyrosmia*) *saxicola* Ducke, 1899**		1♀
Osmia (*Pyrosmia*) *versicolor* Latreille, 1811	Fateryga and Proshchalykin (2020)	10♀, 6♂
Osmia (*Pyrosmia*) *viridana* Morawitz, 1873	Morawitz (1873)	35♀, 3♂
Osmia (*Tergosmia*) *tergestensis* Ducke, 1897	–	6♀, 9♂
Protosmia (*Protosmia*) *glutinosa* (Giraud, 1871)	Fateryga and Proshchalykin (2020)	4♀
Protosmia (*Protosmia*) *tiflensis* (Morawitz, 1876)	Fateryga and Proshchalykin (2020)	7♀
Tribe Anthidiini		
Anthidiellum (*Anthidiellum*) *strigatum* (Panzer, 1805)	Morawitz (1873)	20♀, 32♂
Anthidiellum (*Anthidiellum*) *troodicum* Mavromoustakis, 1949	Proshchalykin et al. (2023)	1♀, 1♂
Anthidium (*Anthidium*) *cingulatum* Latreille, 1809	Fateryga et al. (2019)	11♀, 25♂
Anthidium (*Anthidium*) *dalmaticum* Mocsáry, 1884	Proshchalykin et al. (2023)	2♀, 7♂
Anthidium (*Anthidium*) *diadema* Latreille, 1809	–	1♀
Anthidium (*Anthidium*) *florentinum* (Fabricius, 1775)	–	48♀, 48♂
Anthidium (*Anthidium*) *loti* Perris, 1852	Fateryga et al. (2019)	7♀, 11♂
Anthidium (*Anthidium*) *manicatum* (Linnaeus, 1758)	–	5♀, 2♂
Anthidium (*Anthidium*) *melanopygum* Friese, 1917	Fateryga et al. (2019), as *A. spiniventre*; Kasparek and Fateryga (2023)	6♀, 11♂
Anthidium (*Anthidium*) *punctatum* Latreille, 1809	Fateryga (2017)	10♀, 21♂
Anthidium (*Anthidium*) *taeniatum* Latreille, 1809**	–	1♀, 2♂
Anthidium (*Proanthidium*) *oblongatum* (Illiger, 1806)	–	11♀, 7♂
Eoanthidium (*Eoanthidium*) *clypeare* (Morawitz, 1873)	Morawitz (1873)	1♀
Icteranthidium ferrugineum (Fabricius, 1787)	Fateryga et al. (2019)	9♀, 9♂
Icteranthidium grohmanni (Spinola, 1838)	Fateryga (2017), misidentification of *I. ferrugineum*; Fateryga et al. (2019)	9♀, 4♂
Pseudoanthidium (*Pseudoanthidium*) *alpinum* (Morawitz, 1873)	Morawitz (1873)	1♀, 1♂
Pseudoanthidium (*Pseudoanthidium*) *nanum* (Mocsáry, 1880)	Morawitz (1873), as *Anthidium lituratum*; Litman et al. (2021)	6♀, 10♂
Pseudoanthidium (*Pseudoanthidium*) *stigmaticorne* (Dours, 1873)	Litman et al. (2021)	4♀, 4♂
Pseudoanthidium (*Pseudoanthidium*) *tenellum* (Mocsáry, 1880)	Litman et al. (2021)	–
Pseudoanthidium (*Royanthidium*) *melanurum* (Klug, 1832)	–	1♀, 1♂
Pseudoanthidium (*Royanthidium*) *reticulatum* (Mocsáry, 1884)	Fateryga et al. (2019)	2♂
Stelis (*Protostelis*) *signata* (Latreille, 1809)	Fateryga (2017)	1♀, 3♂
Stelis (*Stelidomorpha*) *nasuta* (Latreille, 1809)*	–	3♀
Stelis (*Stelis*) *breviuscula* (Nylander, 1848)	–	1♂
Stelis (*Stelis*) *odontopyga* Noskiewicz, 1926*	–	1♂
Stelis (*Stelis*) *ornatula* (Klug, 1807)	–	5♀
Stelis (*Stelis*) *phaeoptera* (Kirby, 1802)	Morawitz (1873); Popov (1933), as *S. phaeoptera meridionalis*	1♀, 1♂
Stelis (*Stelis*) *punctulatissima* (Kirby, 1802)	–	2♂
Stelis (*Stelis*) *scutellaris* Morawitz, 1894	–	1♀
Trachusa (*Archianthidium*) *pubescens* (Morawitz, 1872)	Morawitz (1873)	1♀, 10♂
Trachusa (*Paraanthidium*) *integra* (Eversmann, 1852)	–	2♀, 6♂
Tribe Dioxyini		
Aglaoapis tridentata (Nylander, 1848)	Fateryga et al. (2019)	4♀, 4♂
Tribe Megachilini		
Coelioxys (*Allocoelioxys*) *acanthura* (Illiger, 1806)	Fateryga et al. (2019)	3♀, 2♂
Coelioxys (*Allocoelioxys*) *afer* Lepeletier de Saint-Fargeau, 1841	Morawitz (1873), as *C. coronata*	7♀, 16♂
Coelioxys (*Allocoelioxys*) *argenteus* Lepeletier de Saint-Fargeau, 1841	Morawitz (1873), as both *C. constricta* and *C. argentea*; Fateryga et al. (2019)	3♀, 2♂
Coelioxys (*Allocoelioxys*) *brevis* Eversmann, 1852	Morawitz (1873)	6♀, 7♂
Coelioxys (*Allocoelioxys*) *caudatus* Spinola, 1838	Fateryga et al. (2019)	1♀, 2♂
Coelioxys (*Allocoelioxys*) *echinatus* Förster, 1853	Fateryga and Proshchalykin (2020)	1♂

Species name	Literature records	Material examined
Coelioxys (*Allocoelioxys*) *haemorrhoa* Förster, 1853	Morawitz (1873), as *C. pulchella*	3 ♂
Coelioxys (*Allocoelioxys*) *polycentris* Förster, 1853	Morawitz (1873), as *C. conspersa*; Fateryga et al. (2019)	11 ♀, 5 ♂
Coelioxys (*Coelioxys*) *quadridentatus* (Linnaeus, 1758)*	–	3 ♀, 2 ♂
Coelioxys (*Liothyrapis*) *decipiens* (Spinola, 1838)	Fateryga et al. (2019)	1 ♀, 2 ♂
Coelioxys (*Melissoctonia*) *conoideus* (Illiger, 1806)	Morawitz (1873), as *C. conoidea*	1 ♀
Coelioxys (*Paracoelioxys*) *elongatus* Lepeletier de Saint-Fargeau, 1841	Fateryga and Proshchalykin (2020)	1 ♀
Coelioxys (*Paracoelioxys*) *inermis* (Kirby, 1802)	–	1 ♀, 4 ♂
Coelioxys (*Paracoelioxys*) *mandibularis* Nylander, 1848*	–	3 ♀, 1 ♂
Coelioxys (*Rozeniana*) *aurolimbatus* Förster, 1853	Morawitz (1873), as *C. recurva*	8 ♂
Coelioxys (*Rozeniana*) *rufescens* Lepeletier de Saint-Fargeau & Audinet-Serville, 1825	–	7 ♀, 3 ♂
Megachile (*Chalicodoma*) *albocristata* Smith, 1853	Morawitz (1873), as *Chalicodoma lefebvrei* (misidentified); Fateryga and Proshchalykin (2020)	22 ♀, 8 ♂
Megachile (*Chalicodoma*) *albonotata* Radoszkowski, 1886	Fateryga et al. (2019)	14 ♀, 4 ♂
Megachile (*Chalicodoma*) *alborufa* Friese, 1911	–	6 ♀, 2 ♂
Megachile (*Chalicodoma*) *montenegrensis* Dours, 1873**	–	3 ♂
Megachile (*Chalicodoma*) *parietina* (Geoffroy, 1785)	–	10 ♀
Megachile (*Creightonella*) *albisecta* (Klug, 1817)	–	21 ♀, 23 ♂
Megachile (*Eutricharaea*) *anatolica* Rebmann, 1968*	–	4 ♀, 3 ♂
Megachile (*Eutricharaea*) *apicalis* Spinola, 1808	Morawitz (1873), misidentification of *M. versicolor*	12 ♀, 23 ♂
Megachile (*Eutricharaea*) *argentata* (Fabricius, 1793)	–	55 ♀, 41 ♂
Megachile (*Eutricharaea*) *burdigalensis* Benoist, 1940	Fateryga et al. (2019)	5 ♀, 2 ♂
Megachile (*Eutricharaea*) *deceptoria* Pérez, 1890	Fateryga et al. (2019)	24 ♀, 42 ♂
Megachile (*Eutricharaea*) *giraudi* Gerstäcker, 1869	Fateryga et al. (2019)	11 ♀, 4 ♂
Megachile (*Eutricharaea*) *leachella* Curtis, 1828	Fateryga (2017)	29 ♀, 38 ♂
Megachile (*Eutricharaea*) *leucomalla* Gerstäcker, 1869	Fateryga et al. (2019)	4 ♀
Megachile (*Eutricharaea*) *marginata* Smith, 1853	Fateryga et al. (2019)	11 ♀, 4 ♂
Megachile (*Eutricharaea*) *rotundata* (Fabricius, 1787)	–	19 ♀, 13 ♂
Megachile (*Eutricharaea*) *rubrimana* Morawitz, 1893	Fateryga and Proshchalykin (2020)	1 ♀, 1 ♂
Megachile (*Eutricharaea*) *semicircularis* auct. nec van der Zanden, 1996	Fateryga et al. (2019)	5 ♀
Megachile (*Megachile*) *centuncularis* (Linnaeus, 1758)	–	7 ♀, 10 ♂
Megachile (*Megachile*) *lapponica* Thomson, 1872*	–	1 ♀
Megachile (*Megachile*) *ligniseca* (Kirby, 1802)	–	1 ♀
Megachile (*Megachile*) *melanopyga* Costa, 1863	–	9 ♀, 9 ♂
Megachile (*Megachile*) *octosignata* Nylander, 1852	Fateryga and Proshchalykin (2020)	5 ♀
Megachile (*Megachile*) *pilicrus* Morawitz, 1877	–	14 ♀, 27 ♂
Megachile (*Megachile*) *versicolor* Smith, 1844	–	3 ♀, 9 ♂
Megachile (*Pseudomegachile*) *ericetorum* Lepeletier de Saint-Fargeau, 1841	–	18 ♀, 7 ♂
Megachile (*Pseudomegachile*) *flavipes* Spinola, 1838	Fateryga et al. (2019)	32 ♀, 11 ♂
Megachile (*Pseudomegachile*) *saussurei* Radoszkowski, 1874	Fateryga et al. (2019)	1 ♂
Megachile (*Pseudomegachile*) *tecta* Radoszkowski, 1888	Morawitz (1873), as *M. derasa* (misidentified); Fateryga et al. (2019)	16 ♀, 7 ♂
Megachile (*Xanthosarus*) *analis* Nylander, 1852	–	1 ♂
Megachile (*Xanthosarus*) *circumcincta* (Kirby, 1802)	–	7 ♀, 4 ♂
Megachile (*Xanthosarus*) *lagopoda* (Linnaeus, 1761)	–	6 ♀, 11 ♂
Megachile (*Xanthosarus*) *maritima* (Kirby, 1802)	Morawitz (1873), misidentification of *M. lagopoda*	5 ♀, 7 ♂
Megachile (*Xanthosarus*) *willughbiella* (Kirby, 1802)	–	12 ♀, 9 ♂

New species records for Russia

Chelostoma (*Chelostoma*) *emarginatum* (Nylander, 1856)

Material examined. Russia • Dagestan: Vicinity of Tatil, 42°00'01"N, 48°00'17"E, 4.V.2022, 1 ♂, leg. A. Fateryga [CAFK]; • ibid., 8.V.2022, 1 ♂, leg. A. Fateryga [CAFK]; • ibid., 23.V.2022, 1 ♀, leg. M. Proshchalykin [CAFK].

Distribution. Russia (European part: North Caucasus), Western, Southern, and Eastern Europe, Azerbaijan, Turkey, Iraq, Iran, Turkmenistan.

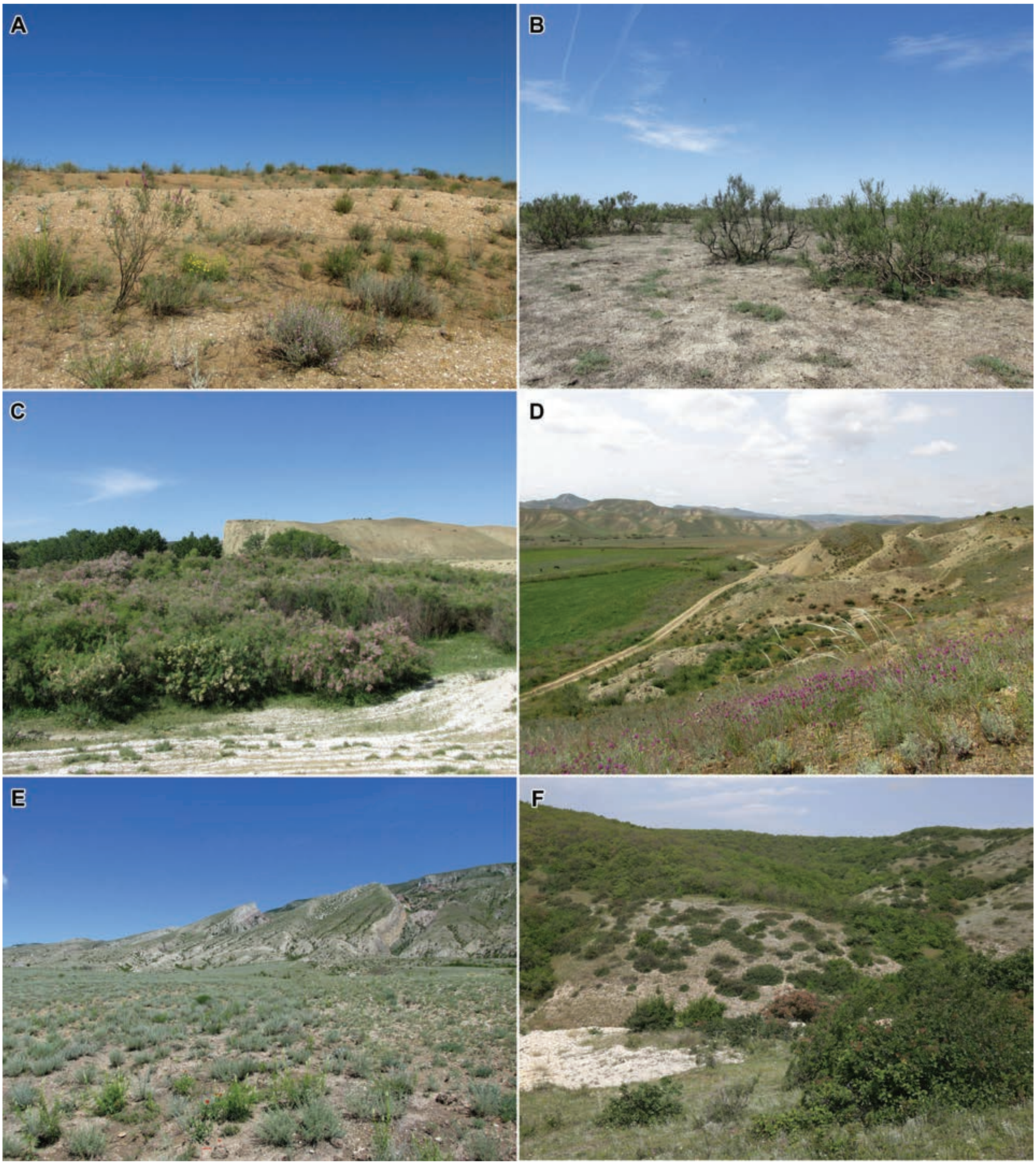

Figure 2. Landscapes of Dagestan **A** coastal dune with flowering *Astragalus hyrcanus* Pall., *A. barbidens* Freyn, and *Gelasia biebersteinii* (Lipsch.) Zaika, Sukhor. & N. Kilian **B** community of *Halostachys caspica* (M. Bieb.) C.A. Mey. in clay desert **C** flowering *Tamarix* spp. in a river valley **D** steppe slope with flowering *Astragalus bungeanus* Boiss. in foothills **E** clay semi-desert with flowering *Reseda globulosa* Fisch. & C.A. Mey. in foothills **F** steppe slope with shrubs at oak forest edge on mountain slope.

Chelostoma **(*Foveosmia*)** ***maidli*** **(Benoist, 1935)**

Material examined. **Russia** • **Dagestan:** Tekipirkent, 41°20'18"N, 47°52'32"E, 29.VI.2023, 1 ♂, leg. A. Fateryga [CAFK].

Distribution. Russia (European part: North Caucasus), Turkey, Syria, Lebanon, Israel.

Figure 3. Landscapes of Dagestan **A** limestone scree on mountain slope **B** beech forest on mountain slope **C** limestone mountain slope with flowering *Bilacunaria microcarpos* (M. Bieb.) Pimenov & V.N. Tikhom. **D** sub-alpine meadow with flowering *Coronilla varia* L., *Galium verum* L., *Libanotis pyrenaica* (L.) Bourg., and other herb species **E** alpine shale scree with flowering *Betonica nivea* Steven on mountain slope **F** alpine meadow.

Hoplitis (*Alcidamea*) *campanularis* (Morawitz, 1877)

Material examined. Russia • Dagestan: Vicinity of Talgi, 42°52'36"N, 47°26'42"E, 21.V.2022, 1 ♂, leg. A. Fateryga [CAFK]; • ibid., 21.V.2022, 1 ♀, 1 ♂, leg. D. Puzanov [CAFK]; • Dubki, Sulak River, 43°01'50"N, 46°49'29"E, 31.V.2023, 1 ♂, leg. T. Levchenko [CTLM].

Distribution. Russia (European part: North Caucasus), Southern and Eastern Europe, North Africa, Georgia, Turkey, Lebanon, Israel.

***Hoplitis* (*Alcidamea*) *caucasica* (Friese, 1920)**

Material examined. Russia • Dagestan: Tsudakhar, 42°19'43"N, 47°09'51"E, 15.VI.2023, 2 ♀, leg. M. Proshchalykin [CAFK, ETHZ].

Distribution. Russia (European part: North Caucasus), Azerbaijan, Turkey.

***Hoplitis* (*Anthocopa*) *perezi* (Ferton, 1894)**

Material examined. Russia • Dagestan: 7 km SE Gedzhykh, 42°03'52"N, 48°05'57"E, 3.VI.2019, 1 ♀, 1 ♂, leg. M. Proshchalykin, V. Loktionov [FSCV]; • Derbent, railroad to the north from the fortress wall, on *Convolvulus arvensis*, 4.VII.2022, 1 ♂, leg. T. Levchenko [CTLM].

Distribution. Russia (European part: North Caucasus), Western, Southern, and Eastern Europe, North Africa, Armenia, Azerbaijan, Turkey, Israel, Iran, Afghanistan, Turkmenistan, Tajikistan, Uzbekistan, Kyrgyzstan, Kazakhstan.

***Hoplitis* (*Pentadentosmia*) *tringa* (Warncke, 1991)**

Material examined. Russia • Dagestan: Tsudakhar, 42°19'43"N, 47°09'51"E, 15.VI.2023, 2 ♀, leg. M. Proshchalykin [CAFK, ETHZ].

Distribution. Russia (European part: North Caucasus), Azerbaijan, Turkey, Iran.

***Osmia* (*Allosmia*) *melanura* Morawitz, 1871**

Material examined. Russia • Dagestan: Gelinbatan, 41°56'30"N, 48°10'41"E, 5.V.2022, 8 ♀, 2 ♂, leg. A. Fateryga [CAFK]; • ibid., on *Onobrychis majorovii*, 5.V.2022, 1 ♀, leg. A. Fateryga [CAFK]; • Kamyshchay River valley, 41°54'33"N, 48°13'47"E, on *Astragalus bungeanus*, 5.V.2022, 1 ♀, leg. A. Fateryga [CAFK].

Distribution. Russia (European part: North Caucasus), Southern and Eastern Europe, Armenia, Azerbaijan, Turkey.

***Osmia* (*Helicosmia*) *breviata* Warncke, 1988**

Material examined. Russia • Dagestan: Khotoch, 42°24'52"N, 46°57'10"E, 17.VI.2023, 1 ♀, leg. M. Proshchalykin [ETHZ].

Distribution. Russia (European part: North Caucasus), Southern Europe, Turkey, Lebanon, Israel, Iran.

Osmia (*Osmia*) *scheherazade* Peters, 1978

Material examined. Russia • Dagestan: 5 km NNW Chirag, 41°52'47"N, 47°23'25"E, 25.VI.2023, 1 ♀, leg. M. Proshchalykin [CAFK].

Distribution. Russia (European part: North Caucasus), Turkey, Iran.

Osmia (*Pyrosmia*) *saxicola* Ducke, 1899

Material examined. Russia • Dagestan: Tsudakhar, 42°19'43"N, 47°09'51"E, 28–29.V.2022, 1 ♀, leg. M. Proshchalykin [CAFK].

Distribution. Russia (European part: North Caucasus), Southern and Eastern Europe, Turkey, Cyprus, Syria, Jordan, Lebanon, Israel, Iraq, Iran, Tajikistan.

Anthidium (*Anthidium*) *taeniatum* Latreille, 1809

Material examined. Russia • Dagestan: Belidzhi, hot spring, 41°54'2"N, 48°26'14"E, on *Lotus corniculatus*, 10.VI.2023, 1 ♀, 2 ♂, leg. T. Levchenko [CTLM].

Distribution. Russia (European part: North Caucasus), Western, Southern, and Eastern Europe, Azerbaijan, Turkey, Lebanon, Israel, Iran, Turkmenistan.

Megachile (*Chalicodoma*) *montenegrensis* Dours, 1873

Material examined. Russia • Dagestan: Vicinity of Gubden, 42°34'23"N, 47°33'01"E, 2.VI.2022, 1 ♂, leg. A. Fateryga [MHNN]; • ibid., 3.VI.2022, 2 ♂, leg. A. Fateryga [CAFK].

Distribution. Russia (European part: North Caucasus), Southern and Eastern Europe, North Africa, Armenia, Azerbaijan, Turkey, Syria, Lebanon, Israel, Iran, Afghanistan, Tajikistan, Uzbekistan.

Discussion

The first paper on the bees of the Republic of Dagestan was published 150 years ago by Morawitz (1873) and it contained 30 species of the family Megachilidae, including a species later synonymized (*Coelioxys constrictus* Förster, 1853 with *C. argenteus* Lepeletier de Saint-Fargeau, 1841); some other species were misidentified (Table 2). Recently published papers (Fateryga 2017; Fateryga et al. 2019, 2023; Fateryga and Proshchalykin 2020; Litman et al. 2021; Levchenko 2023; Proshchalykin et al. 2023) added 52 species, including two species described as new to science (Fateryga et al. 2023). By this way, the total number of species of megachilid bees of Dagestan has increased to 81. The present contribution reports a total of 148 species of megachilid bees known from Dagestan. Compared to the first list published by Morawitz (1873), the number of species known from the republic was increased by five times.

Thirty-two species recorded in Dagestan are widespread in the whole Palaearctic region: *Lithurgus cornutus*, *Chelostoma foveolatum*, *C. rapunculi*, *Heriades truncorum*, *Hoplitis leucomelana*, *H. tridentata*, *Osmia leaiana*, *Anthidiellum strigatum*, *Anthidium florentinum*, *A. punctatum*, *Stelis ornatula*, *Coelioxys afer*, *C. brevis*, *C. conoideus*, *C. elongatus*, *C. haemorrhoa*, *C. inermis*, *C. mandibularis*, *C. quadridentatus*, *C. rufescens*, *Megachile analis*, *M. centuncularis*, *M. circumcincta*, *M. ericetorum*, *M. lagopoda*, *M. lapponica*, *M. ligniseca*, *M. maritima*, *M. melanopyga*, *M. rotundata*, *M. versicolor*, and *M. willughbiella*.

Fifteen species are widespread in West Palaearctic: *Lithurgus chrysurus*, *Chelostoma campanularum*, *C. florisomne*, *Heriades crenulata*, *Hoplitis anthocopoides*, *H. curvipes*, *H. manicata*, *Osmia melanura*, *O. tergestensis*, *Pseudoanthidium alpinum*, *Stelis odontopyga*, *Trachusa integra*, *Megachile burdigalensis*, *M. leachella*, and *M. octosignata*.

Fifty species are distributed in Europe to Caucasus and Central Asia: *Lithurgus tibialis*, *Heriades rubicola*, *Hoplitis acuticornis*, *H. adunca*, *H. jakovlevi*, *H. perezi*, *H. praestans*, *H. papaveris*, *Osmia bicornis*, *O. brevicornis*, *O. caerulescens*, *O. cephalotes*, *O. cornuta*, *O. dimidiata*, *O. spinulosa*, *O. viridana*, *Anthidium cingulatum*, *A. diadema*, *A. loti*, *A. manicatum*, *A. oblongatum*, *A. taeniatum*, *Icteranthidium ferrugineum*, *I. grohmanni*, *Pseudoanthidium tenellum*, *Stelis breviuscula*, *S. nasuta*, *S. phaeoptera*, *S. punctulatissima*, *S. scutellaris*, *S. signata*, *Aglaoapis tridentata*, *Coelioxys acanthura*, *C. aurolimbatus*, *C. argenteus*, *C. caudatus*, *C. decipiens*, *Megachile albisecta*, *M. apicalis*, *M. argentata*, *M. deceptoria*, *M. flavipes*, *M. giraudi*, *M. marginata*, *M. montenegrensis*, *M. parietina*, *M. pilicrus*, *M. rubrimana*, *M. saussurei*, and *M. tecta*.

Nearly a third of the megachilid fauna of Dagestan is formed by species with smaller ranges or endemic distributions. Forty species are distributed from Southern Europe to the Caucasus, or from the Mediterranean to the Middle East and the Caucasus (some species also occur in Iran, north-western Turkmenistan Afghanistan, and Pakistan): *Chelostoma distinctum*, *C. emarginatum*, *C. maidli*, *Hoplitis campanularis*, *H. mocsaryi*, *Osmia andrenoides*, *O. apicata*, *O. aurulenta*, *O. bidentata*, *O. breviata*, *O. cyanoxantha*, *O. hellados*, *O. ligurica*, *O. melanogaster*, *O. mustelina*, *O. nana*, *O. niveata*, *O. rufohirta*, *O. saxicola*, *O. scutellaris*, *O. signata*, *O. versicolor*, *Protosmia glutinosa*, *P. tiflensis*, *Anthidiellum troodicum*, *Anthidium dalmaticum*, *A. melanopygum*, *Eoanthidium clypeare*, *Pseudoanthidium nanum*, *P. melanurum*, *P. reticulatum*, *P. stigmaticorne*, *Trachusa pubescens*, *Coelioxys echinatus*, *C. polycentris*, *Megachile albocristata*, *M. albonotata*, *M. anatolica*, *M. leucomalla*, and *M. semicircularis*. One species has a remarkably disjunctive distribution in the Caucasus and eastern Central Asia to the Far East: *Hoplitis scita*. Ten species are endemic or subendemic to the Caucasus and Turkey (some of them also occur in Iran or north-western Turkmenistan): *Hoplitis astragali*, *H. caucasica*, *H. caucasicola*, *H. dagestanica*, *H. linguaria*, *H. ozbeki*, *H. tringa*, *Osmia cinerea*, *O. scheherazade*, and *Megachile alborufa*; and one of them (*H. dagestanica*) is known only from Dagestan.

Thus, the fauna of Dagestan is very diverse and consists of species with wide Palaearctic or Western Palaearctic ranges, as well as elements of Mediterranean, European, Central Asian faunas and a relatively small number of endemic species.

According to the studied material, *Lithurgus chrysurus*, *Anthidium florentinum*, *Megachile argentata*, *Hoplitis adunca*, *H. astragali*, *Heriades rubicola*, *Hoplitis leucomelana*, *Megachile leachella*, *M. deceptoria*, and *Osmia rufohirta* are the most common species of megachilid bees in Dagestan, with ≥ 60 collected specimens. At the same time, 20 species are known by one specimen each (Table 2). Only 39 species of megachilid bees were recorded in the northern half of Dagestan (a part of the Caspian Depression) and just three of them (*Pseudoanthidium tenellum*, *Coelioxys decipiens*, and *Megachile saussurei*) were recorded only there. In the southern half of the republic (a part of the Greater Caucasus), 145 species were recorded. Among the four major landscape zones of this territory, the richest megachilid-bee fauna was revealed in the belt of foothills (109 species). The belt of so-called Intramountain Dagestan numbered 70 species of megachilid bees, 65 species were revealed in the coastal lowland, and 49 in the high mountain belt.

Twenty-five species of megachilid bees of 148 are kleptoparasitic taxa of the genera *Stelis* Panzer, 1806, *Aglaoapis* Cameron, 1901, and *Coelioxys* Latreille, 1809. The remaining 123 species are nest building. In the curse of our fieldwork in Dagestan, we recorded nests of nine species of megachilid bees. Nests of *Hoplitis adunca*, *Osmia caerulescens*, and *O. dimidiata* were recorded in trap nests made of reed stems. Biology of all three species was well studied previously (summarised by Müller 2024). The nests of *O. caerulescens* were especially numerous. A nest of *Megachile albocristata* was found between stones (Fig. 4A). The nest was subsequently sealed by the female bee with pebbles fastened with leaf pulp (Fig. 4B). A nest of *Megachile flavipes* was found in an abandoned nest hole of *Anthophora* sp. (Hymenoptera, Apidae) on a clay cliff. The nest consisted of two cylindrical mud cells (Fig. 4C). A nest of *Hoplitis mocsaryi* was found in the ground, on horizontal surface. The nest entrance was lined with fragments of petals of *Linum tauricum* Willd. (Fig. 4D, E). This bee species is well known to use flax petals (Ivanov and Filatov 2008; Levchenko 2023). Two nests of *Osmia cornuta* were revealed in abandoned nest cells of *Sceliphron* sp. (Hymenoptera, Sphecidae). This bee species is well known to use various pre-existing cavities for nesting (summarised by Müller 2024). Six nests of *Hoplitis astragali* were revealed on a clay cliff (Fig. 4G); females of this species excavated burrows by themselves and used mud for nest construction. The nests were described in detail by Fateryga et al. (2023). The most remarkable nest found in Dagestan was that of *Hoplitis curvipes*. It consisted of two cells placed side by side under a stone; the cells were constructed from leaf fragments, which were imbricately arranged, forming a cone-like structure; each leaf fragment consisted of a basal part that was masticated to leaf pulp and an apical part that protruded freely from the cell wall (Fig. 4H). The nest of this species was described in detail by Ivanov et al. (2023). Males of *Hoplitis curvipes* were recorded sleeping in inflorescences of *Allium rotundum* L. s. l. (Fig. 4I).

The megachilid-bee fauna of Dagestan is rich. Almost 2/3 of all species known from Russia (232 according to Proshchalykin et al. 2023 and present data) occur in Dagestan, while the area of Dagestan is about 0.3% of the area of Russia. The megachilid-bee fauna of Dagestan is less diverse but still comparable to that of neighbouring Azerbaijan, which has 175 species of megachilid bees (Maharramov et al. 2023; Fateryga et al. 2023), while the area of Azerbaijan is more than one and a half times more than that of Dagestan. A comparison of the list of megachilid bees of Azerbaijan (compiled from Fateryga et al. 2020; Proshchalykin and Maharramov 2020; Maharramov et al. 2021, 2023; Fateryga et al. 2023) with that of Dagestan revealed that 109 species (51%) occur in both territories. Our results also show that the knowledge of the family Megachilidae of Dagestan is still incomplete. Despite the reached progress,

Figure 4. Biology of megachilid bees from Dagestan **A** female of *Megachile albocristata* Smith, 1853 at her nest entrance **B** same nest sealed with pebbles **C** nest cell of *Megachile flavipes* Spinola, 1838 extracted from the substrate **D** female of *Hoplitis mocsaryi* (Friese, 1895) at her nest entrance **E** same nest entrance from above **F** dissected old nest cell of *Sceliphron* sp. with a cell of *Osmia cornuta* (Latreille, 1805) containing a cocoon **G** female of *Hoplitis astragali* Fateryga, Müller & Proshchalykin, 2023 closing her nest with a plug of mud **H** nest of *Hoplitis curvipes* (Morawitz, 1871) extracted from the substrate **I** male of *H. curvipes* sleeping in an inflorescence of *Allium rotundum* L. s. l.

several species remained unidentified, and this problem may be solved only in the curse of special taxonomic investigations of particular subgenera and groups of species. Biology of many species occurring in Dagestan is unknown and should be also studied during further research.

Acknowledgements

We thank Ramazan Murtazaliev and Maxim Mallaliev (Makhachkala, Russia) for their kind help during our research trips to Dagestan. We also thank Yulia Astafurova (Saint Petersburg, Russia) for her help during our work in ZISP. We are also indebted to Timofey Levchenko (Moscow, Russia) for making the material collected by him in Dagestan available to our study. We are especially grateful to Andreas Müller (Zurich, Switzerland) for his kind help in the identification of the bees of the tribe Osmiini. Max Kasparek (Heidelberg, Germany), Yulia Astafurova, and an anonymous reviewer provided helpful suggestions to improve the manuscript.

Additional information

Conflict of interest

The authors have declared that no competing interests exist.

Ethical statement

No ethical statement was reported.

Funding

The research was carried out within the state assignments of the Ministry of Science and Higher Education of the Russian Federation, No. 124030100098-0 (for A.F.) and No. 124012400285-7 (for M.P.).

Author contributions

All authors have contributed equally.

Author ORCIDs

Alexander V. Fateryga https://orcid.org/0000-0002-5346-3477
Maxim Yu. Proshchalykin https://orcid.org/0000-0001-7870-8226

Data availability

All of the data that support the findings of this study are available in the main text or Supplementary Information.

References

Ascher JS, Pickering J (2024) Discover Life bee species guide and world checklist (Hymenoptera: Apoidea: Anthophila). http://www.discoverlife.org/mp/20q?guide=Apoidea_species [Accessed 08.08.2024]

Astafurova YuV, Proshchalykin MYu (2020) The bees of the family Halictidae (Hymenoptera) described by Ferdinand Morawitz from the collection of Aleksey Fedtschenko. ZooKeys 994: 35–104. https://doi.org/10.3897/zookeys.994.58441

Astafurova YuV, Proshchalykin MYu, Sidorov DA, Osytshnjuk AZ (2021) The type specimens of bees (Hymenoptera, Apoidea) deposited in the Zoological Institute of the Russian Academy of Sciences, St. Petersburg. Contribution IV. Family Andrenidae, genus *Andrena* Fabricius, 1775, species described by F. Morawitz. Zootaxa 5037(1): 1–78. https://doi.org/10.11646/zootaxa.5037.1.1

Astafurova YuV, Proshchalykin MYu, Sidorov DA (2022) The bees of the genus *Andrena* Fabricius, 1775 (Hymenoptera, Andrenidae) described by Ferdinand Morawitz from the collection of Aleksey Fedtschenko. ZooKeys 1120: 105–176. https://doi.org/10.3897/zookeys.1120.90206

Boustani M, Rasmont P, Dathe HH, Ghisbain G, Kasparek M, Michez D, Müller A, Pauly A, Risch S, Straka J, Terzo M, Van Achter X, Wood TJ, Nemer N (2021) The bees of Lebanon (Hymenoptera: Apoidea: Anthophila). Zootaxa 4976(1): 1–146. https://doi.org/10.11646/zootaxa.4976.1.1

Dathe HH, Proshchalykin MYu (2017) Type revision of Asiatic bees of the genus *Hylaeus* F. described by Ferdinand Morawitz (Hymenoptera: Apoidea, Colletidae). Zootaxa 4227(1): 1–48. https://doi.org/10.11646/zootaxa.4227.1.1

Fateryga AV (2017) New data on megachilid bees (Hymenoptera: Megachilidae) of the European part of Russia. Proceedings of the Russian Entomological Society 88(2): 86–90. https://doi.org/10.47640/1605-7678_2017_88_2_86

Fateryga AV, Proshchalykin MYu (2020) New records of megachilid bees (Hymenoptera: Megachilidae) from the North Caucasus and the South of European Russia. Caucasian Entomological Bulletin 16(2): 225–231. https://doi.org/10.23885/181433262020162-225331

Fateryga AV, Proshchalykin MYu, Astafurova YuV, Popov IB (2019) [2018] New records of megachilid bees (Hymenoptera, Megachilidae) from the North Caucasus and neighboring regions of Russia. Entomological Review 98(9): 1165–1174. https://doi.org/10.1134/S0013873818090026

Fateryga AV, Proshchalykin MYu, Maharramov MM (2020) Bees of the tribe Anthidiini (Hymenoptera, Megachilidae) of Nakhchivan Autonomous Republic of Azerbaijan. Entomological Review 100(3): 323–336. https://doi.org/10.1134/S0013873820030069

Fateryga AV, Müller A, Proshchalykin MYu (2023) Two new *Hoplitis* species of the subgenus *Hoplitis* Klug, 1807 (Hymenoptera, Megachilidae) and the nesting biology of *H. astragali* sp. nov. in Dagestan. Journal of Hymenoptera Research 96: 641–656. https://doi.org/10.3897/jhr.96.109255

Ivanov SP, Filatov MA (2008) Nest cells construction of wild bees *Megachile albisecta*, *Hoplitis mocsaryi* and *Osmia tergestensis* (Hymenoptera: Apoidea: Megachilidae). Kharkov Entomological Society Gazette 15(1–2): 109–116. [In Russian]

Ivanov SP, Fateryga AV, Müller A (2023) Brood cells like conifer cones: the peculiar nesting biology of the osmiine bee *Hoplitis* (*Alcidamea*) *curvipes* (Morawitz, 1871) (Hymenoptera, Megachilidae). Journal of Hymenoptera Research 96: 735–750. https://doi.org/10.3897/jhr.96.109587

Kasparek M (2020) Variation in *Eoanthidium judaeense* (Mavromoustakis, 1945) and *E. clypeare* (Morawitz, 1874) (Apoidea: Megachilidae: Anthidiini) in the Middle East: semispecies or cases of geographic dimorphism? Zoology in the Middle East 66(2): 145–166. https://doi.org/10.1080/09397140.2020.1729563

Kasparek M (2022) The resin and wool carder bees (Anthidiini) of Europe and Western Turkey. Identification – distribution – biology. Chimaira, Frankfurt am Main, 290 pp.

Kasparek M, Ebmer AW (2023) The wool carder bee *Pseudoanthidium alpinum* (Morawitz, 1873): identity of the enigmatic type species of the genus *Pseudoanthidium* (Hymenoptera: Megachilidae: Anthidiini). Osmia 11: 39–50. https://doi.org/10.47446/OSMIA11.7

Kasparek M, Fateryga AV (2023) DNA barcoding confirms the validity of *Anthidium melanopygum* Friese, 1917 stat. nov. (Hymenoptera: Megachilidae) as a distinct species of Western Asia. Zootaxa 5346(5): 567–580. https://doi.org/10.11646/zootaxa.5346.5.4

Levchenko TV (2023) *Hoplitis* (*Anthocopa*) *mocsaryi* (Friese, 1895) – a new for Middle Russia species of megachilid bees (Hymenoptera: Megachilidae) from the Kulikovo Field. In: Burova OV, Volkova EM, Shvets OV (Eds) Problems of study and recovering of landscapes of forest-steppe zone: historical-cultural and nature territories (Iss. 5). Kulikovo Pole State Museum-Reserve & Russian Geographical Society, Tula, 74–79. [In Russian]

Litman JR, Fateryga AV, Griswold TL, Aubert M, Proshchalykin MYu, Le Divelec R, Burrows S, Praz CJ (2021) Paraphyly and low levels of genetic divergence in morphologically distinct taxa: revision of the *Pseudoanthidium scapulare* (Latreille, 1809) complex of carder bees (Apoidea, Megachilidae, Anthidiini). Zoological Journal of the Linnean Society 195(4): 1287–1337. https://doi.org/10.1093/zoolinnean/zlab062

Maharramov MM, Fateryga AV, Proshchalykin MYu (2021) Megachilid bees (Hymenoptera: Megachilidae) of the Nakhchivan Autonomous Republic of Azerbaijan: tribes Lithurgini, Dioxyini, and Megachilini. Far Eastern Entomologist 428: 12–24. https://doi.org/10.25221/fee.428.3

Maharramov MM, Fateryga AV, Proshchalykin MYu (2023) New records of megahilid bees (Hymenoptera: Megachilidae) from the Nakhchivan Autonomous Republic of Azerbaijan. Far Eastern Entomologist 472: 18–24. https://doi.org/10.25221/fee.472.2

Michener CD (2007) The Bees of the World (2nd edn). Johns Hopkins University Press, Baltimore, [xvi +] 953 pp. [+ 20 pls]

Morawitz F (1873) [1874] Die Bienen Daghestans. Horae Societatis Entomologicae Rossicae 10(2–4): 129–189.

Müller A (2024) Palaearctic Osmiine Bees, ETH Zürich. http://blogs.ethz.ch/osmiini [Accessed 08.08.2024]

Pesenko YuA, Astafurova YuV (2003) Annotated bibliography of Russian and Soviet publications on the bees (Hymenoptera: Apoidea; excluding *Apis mellifera*): 1771–2002. Denisia 11: 1–616.

Popov VB (1933) [1932] On the palaearctic forms of the tribe Stelidini Roberts. (Hymenoptera, Megachilidae). Travaux de l'Institut Zoolgique de l'Academie des Sciences de l'URSS 1(3/4): 375–414. [In Russian]

Proshchalykin MY, Maharramov MM (2020) Additional records of osmiine bees (Hymenoptera: Megachilidae: Osmiini) from Azerbaijan. Acta Biologica Sibirica 6: 33–42. https://doi.org/10.3897/abs.6.e53095

Proshchalykin MYu, Fateryga AV, Astafurova YuV (2023) Corrections and additions to the catalogue of the bees (Hymenoptera, Anthophila) of Russia. ZooKeys 1187: 301–339. https://doi.org/10.3897/zookeys.1187.113240

Red Book of the Republic of Dagestan (2020). Dzhamaludinov MA Press, Makhachkala, 800 pp. [In Russian]

Schwarz M (1980a) Zur Kenntnis einiger von F. Morawitz beschriebener *Nomada*-Arten (Hymenoptera, Apoidea). Entomofauna 1: 1–27.

Schwarz M (1980b) Beitrag zur Kenntnis weiterer von F. Morawitz beschriebener *Nomada*-Arten (Hymenoptera, Apoidea). Entomofauna 1: 103–118.

Schwarz M (1987) Beitrag zur Klärung einiger von F. Morawitz beschriebener *Nomada*-Arten. Entomofauna 8: 237–247.

Schwarz M (2001) Revision der Gattung *Radoszkowskiana* Popov 1955 und ein Beitrag zur Kenntnis der Gattung *Coelioxys* Latreille 1809 (Hymenoptera: Apidae: Megachilinae). Linzer Biologische Beiträge 33(2): 1267–1286.

Schwarz M, Gusenleitner F (2002) Revision der von F. Morawitz 1875 aus Turkmenistan beschriebenen *Nomada*-Arten (Hymenoptera: Apidae). Stapfia 80: 457–515.

Schwarz M, Gusenleitner F (2003) Ergebnisse der Untersuchung von F. Morawitz beschriebenen *Coelioxys*-Arten, so wie weiterer von Eversmann, Friese und Radoszkowski beschriebenen Arten, nebst einigen Bemerkungen (Hymenoptera: Apidae: Megachilidae). Linzer Biologische Beiträge 35(2): 1221–1239.

Schwarz M, Gusenleitner F (2004) Weitere Beiträge zur Klärung der von Morawitz beschriebenen *Nomada*-Arten (Hymenoptera, Apidae). Denisia 13: 335–345.

van der Zanden G (1991) Systematik und Verbreitung der paläarktischen arten der Untergattung *Caerulosmia* van der Zanden 1989 (Hymenoptera, Apoidea, Megachilidae). Linzer Biologische Beiträge 23(1): 37–78.

Warncke K (1992) Die Bienengattung *Osmia* Panzer 1806, ihre Systematik in der Westpaläarktis und ihre Verbreitung in der Türkei. 11. Die Untergattung *Pyrosmia* Tkalcu 1975. Linzer Biologische Beiträge 24(2): 893–921.

Supplementary material 1

List of specimens examined

Authors: Maxim Yu. Proshchalykin, Alexander V. Fateryga

Data type: xls

Explanation note: List of all 2556 examined specimens of the megachilid bees from Dagestan.

Link: https://doi.org/10.3897/zookeys.1217.134704.suppl1

ZooKeys 1217: 119–171 (2024)
DOI: 10.3897/zookeys.1217.131730

Research Article

DNA barcode library of Portuguese water mites, with the descriptions of two new species (Acari, Hydrachnidia)

Vladimir Pešić[1], Andrzej Zawal[2], Sónia Ferreira[3,4,5], Laura Benitez-Bosco[3,4,6], Ana Cruz-Oliveira[3,4], Dinis Girão[3,4,6], Adriana Padilha[3,4,6], Paolo Turaccio[3,4,5,7], Samantha Rossini[7], Lorenzo Ballini[7], Giorgia Staffoni[7], Sara Fratini[7], Claudio Ciofi[7], Alessio Iannucci[7], Torbjørn Ekrem[8], Elisabeth Stur[8]

1 *Department of Biology, University of Montenegro, Cetinjski put b.b., 81000 Podgorica, Montenegro*
2 *Institute of Marine and Environmental Sciences, Center of Molecular Biology and Biotechnology, University of Szczecin, Wąska 13, 71–415 Szczecin, Poland*
3 *CIBIO, Centro de Investigação em Biodiversidade e Recursos Genéticos, InBIO Laboratório Associado, Campus de Vairão, Universidade do Porto, 4485-661 Vairão, Vila do Conde, Portugal*
4 *BIOPOLIS Program in Genomics, Biodiversity and Land Planning, CIBIO, Campus de Vairão, 4485-661 Vairão, Vila do Conde, Portugal*
5 *Departamento de Biologia, Faculdade de Ciências, Universidade do Porto, 4099-002 Porto, Portugal*
6 *EBM, Estação Biológica de Mértola, Praça Luís de Camões, Mértola, Portugal*
7 *Department of Biology, University of Florence, Sesto Fiorentino, Italy*
8 *Department of Natural History, NTNU University Museum, Norwegian University of Science and Technology, Trondheim, Norway*
Corresponding author: Vladimir Pešić (vladopesic@gmail.com)

Abstract

This study presents the first results from the analysis of water mites collected in Portugal as part of the Biodiversity Genomics Europe project. 307 COI DNA barcodes clustered into 75 BINs are provided, with 38 BINs being unique and deposited for the first time in the Barcode of Life Data Systems (BOLD). 65 species have been identified, of which 36 are new to the water mite fauna of Portugal. Two species, *Torrenticola soniae* Pešić, **sp. nov.** and *T. elisabethae* Pešić, **sp. nov.** (Torrenticolidae), are described as new to science. 47% of the water mite species currently known from Portugal now have reference barcodes in BOLD. High intraspecific distances were recorded for some species, suggesting the presence of cryptic diversity and species complexes that needs further study. Our results improve the DNA barcode reference database for Portuguese water mites, enhancing species identification accuracy and stimulating future investigation.

Key words: Cytochrome c oxidase subunit I (COI), DNA barcoding, Iberian Peninsula, integrative taxonomy, Portugal, systematics

Academic editor:
Fernando Jacinavicius
Received: 10 July 2024
Accepted: 17 September 2024
Published: 31 October 2024

ZooBank: https://zoobank.org/921FBCB0-D6B1-4E61-80F2-DE30167984B0

Citation: Pešić V, Zawal A, Ferreira S, Benitez-Bosco L, Cruz-Oliveira A, Girão D, Padilha A, Turaccio P, Rossini S, Ballini L, Staffoni G, Fratini S, Ciofi C, Iannucci A, Ekrem T, Stur E (2024) DNA barcode library of Portuguese water mites, with the descriptions of two new species (Acari, Hydrachnidia). ZooKeys 1217: 119–171. https://doi.org/10.3897/zookeys.1217.131730

Introduction

With nearly 7,500 species grouped into 550 genera (Smit 2020), water mites (Hydrachnidia) are the most diverse and abundant group of arachnids in freshwater habitats (Davids et al. 2007). They inhabit a wide range of aquatic habitats, including lotic, lentic, temporary, and interstitial waters (Davids et al. 2007). Despite the fact that water mites can be good indicators of ecosystem health, especially for groundwater dependent ecosystems, such as springs, the more significant involvement of this limnofaunistic group in rapid assessment programs is still limited by their often time-consuming taxonomic identification (Pešić et al. 2021a).

Knowledge of water mites in Portugal is still insufficient. The checklist published by Cantallo et al. (2022) listed 93 species from 34 genera and 16 families for Portugal and summarized all previous research on water mites in Portugal and its archipelagos (Madeira and Azores). Recently, Pešić et al. (2023b) added seven more species new for the water mite fauna of Portugal, one of which, *Atractides marizae* Pešić, 2023, was new to science.

In recent years, the use of the DNA barcode fragment of the mitochondrial cytochrome c oxidase subunit I (COI) gene has proven to be a very effective tool for the identification of water mites (e.g., Pešić et al. 2017, 2022b, 2023a; Blattner et al. 2019). A large number of regional DNA barcoding initiatives resulted in the formation of national and regional water mites DNA barcode libraries in some parts of Europe, such as, for example, Montenegro (http://dx.doi.org/10.5883/DS-MNEHYD; Pešić et al. 2021a), Corsica (http://dx.doi.org/10.5883/DS-CORHYD; Pešić and Smit 2022), Iran and Turkey (http://dx.doi.org/10.5883/DS-TRIRHYD; Pešić et al. 2023c), Norway (http://dx.doi.org/10.5883/DS-NOHYD; Gerecke et al. 2022). However, extensive sampling for DNA barcode reference library building is yet to be performed for a large part of Europe, including for countries like Portugal which have only been partially sampled (Pešić et al. 2023b).

In 2015, the Research Network in Biodiversity and Evolutionary Biology (InBIO) launched the DNA Barcoding Initiative (IBI) with the aim of forming a reference collection of DNA barcodes, focusing on Portuguese invertebrate taxa (Ferreira et al. 2020a). As a result, several datasets holding DNA barcodes of freshwater organisms have been published, namely on Megaloptera, Plecoptera and Trichoptera (Ferreira et al. 2019; Ferreira et al. 2020b; Pauperio et al. 2023). More recently the local efforts to represent countries' biodiversity in DNA barcode reference collections have been combined with wider endeavors. The implementation of the project Biodiversity Genomics Europe (BGE, https://biodiversitygenomics.eu/) aims to address the global biodiversity crisis by providing a deeper understanding of the diversity of life on Earth through genomics. Additional goals are to develop and strengthen functioning communities of practice, and to build capacity and complementarity across activities and borders. The barcode stream of the project focuses on increasing the geographic and taxonomic representation of understudied organisms in publicly accessible databases. By contributing to the DNA barcode reference library of invertebrate taxa, the project promotes improved assessment and monitoring of macroinvertebrates, including water mites. Moreover, the DNA barcode data provides valuable input for integrative taxonomic research of challenging species groups, especially of cryptic or pseudocryptic species that likely would remain undiscovered using only morphological features.

This is the first in a series of papers related to the diversity of Portuguese water mites that will present the results and ongoing public releases of the DNA barcodes in BOLD. The paper is based on specimens collected in continental Portugal in 2023 and COI records that are publicly available in the Barcode of Life Data Systems (BOLD). As a result of this investigation, we describe two new species to science, and report 36 species of water mites from Portugal for the first time.

Material and methods

Water mites were collected with kick nets and immediately preserved in 96% ethanol for the purpose of molecular analyses. Water mite specimens used for the molecular study are listed in Table 1. After non-destructive, whole-body DNA extraction, the specimen vouchers were stored in 96% ethanol and morphologically examined. Some of these vouchers were dissected and slide mounted in Faure's medium, while the rest was transferred to Koenike's fluid.

Morphological nomenclature follows Gerecke et al. (2016). The distribution data are from Cantallo et al. (2022) unless stated otherwise. The dorsal platelets of *Torrenticola* spp. were measured on both sides, therefore their dimensions were given as a range of values, rather than a single number. The holotype and paratypes of the new species are deposited in the Naturalis Biodiversity Center in Leiden (**RMNH**).

All measurements are given in μm. The photographs of selected structures were made using a camera on Samsung Galaxy smartphone. The following abbreviations are used: **Ac-1** = first acetabulum; **Cx-I** = first coxae; **Cxgl-4** = coxoglandularia 4; **dL** = dorsal length; **H** = height; **I-L-4**–**6** = fourth-sixth segments of first leg; **L** = length; **mL** = medial length; **P-1**–**P-5** = palp segments 1–5; **Vgl-1** = ventroglandularia 1; **W** = width.

Molecular and DNA barcode analyses

The molecular analysis was conducted at the University of Florence (Florence, Italy). DNA was extracted using a non-destructive protocol. Samples were digested using 95 μl of extraction buffer (100 mM Tris-HCl, 5 mM EDTA, 100 mM NaCl, 0.5% SDS, pH 8) and 5 μl of proteinase K. Dilutions (1:10) of crude digested samples were used as template for the amplification of the mitochondrial cytochrome c oxidase subunit I (COI). Amplicons were amplified and barcoded in a single-step PCR using a cocktail of two barcoded primer pairs, namely Folmer primers (LCO1490, HC02198; Folmer et al. 1994) and Lep primers (LepF1, LepR1; Hebert et al. 2004). PCR was performed using the Kapa3G Plant PCR Kit according to the manufacturer's protocol and with the following thermal profile: initial denaturation step of 3 min at 94 °C, 35 cycles of 20 s at 95 °C, annealing for 15 s at 52 °C and extension for 30 s at 72 °C, and a final extension for 1 min at 72 °C. Amplicons were checked on a 1.2% agarose gel and pooled in a single tube. The amplicon mix was used to prepare a PacBio library with the SMRTbell prep kit 3.0 according to the manufacturer's protocol. The library was sequenced on a 8M ZMW SMRT cell on a PacBio Sequel IIe platform.

Raw reads were demultiplexed using the Pacific Biosciences SMRT Link software. Consensus sequences were generated with the PacBio Amplicon Analysis (pbaa) tool. Primer trimming, translation and stop codon checking were performed using Geneious Prime 2024.0.1.

Consensus sequences were made available in the Barcode of Life Data Systems (BOLD) (Ratnasingham and Hebert 2007), and the Barcode Index Numbers (BIN) were obtained, grouping DNA sequences based on the Refined Single Linkage (RESL) analysis performed in BOLD (Ratnasingham and Hebert 2013). BINs are often considered proxies for species (e.g., Hebert et al. 2016).

Relevant voucher information, photos, and newly generated DNA barcodes are publicly accessible through the Dataset - DS-BGEPL01 BGE Biodiversity Genomics Europe: Portuguese water mites I https://www.boldsystems.org/index.php/MAS_Management_DataConsole?codes=DS-BGEPL01) in BOLD. Data related to each BIN, including the minimum *p*-distance to the nearest neighboring BIN, was estimated using BOLD tools. The dataset consists of 307 sequences generated through this study (Suppl. material 1).

Sequence alignments were performed using MUSCLE (Edgar 2004). Intra- and interspecific genetic distances were calculated based on the Kimura 2-parameter model (K2P; Kimura 1980), using MEGA X (Kumar et al. 2018). The latter software was used to calculate Neighbor-Joining (NJ) trees based on K2P distances (standard for barcoding studies) using pairwise deletion for missing data. Branch support was calculated using nonparametric bootstrap (Felsenstein 1985) with 1000 replicates and shown next to the branches. All codon positions were considered in the analyses.

Table 1. Details of DNA barcoded specimens, including localities and coordinates of sampling sites, sample codes, and the barcode index number codes (^{N} indicates a new BIN that contains only sequences from this study). BOLD data presented here was last accessed on 10 May 2024.

Taxa	Locality	Coordinates	Sample ID	Process ID	BIN
Eylaidae					
Eylais tantilla	Beja, São João dos Caldeireiros (stream)	37.625°N, 7.810°W	BGE_00110_B03	BSNTN490-23	^{N}BOLD:AFP3591
			BGE_00110_B04	BSNTN491-23	
	Beja, Herdade de Alagães (stream)	37.676°N, 7.853°W	BGE_00110_D01	BSNTN512-23	
			BGE_00110_D02	BSNTN513-23	
			BGE_00110_D03	BSNTN514-23	
	Beja, Herdade de Alagães (pond)	37.673°N, 7.848°W	BGE_00110_D08	BSNTN519-23	
	Beja, Moinho de Alferes 1	37.502°N, 7.690°W	BGE_00228_C09	BSNTN888-23	
	Beja, São Miguel do Pinheiro	37.552°N, 7.850°W	BGE_00228_G01	BSNTN928-23	
	Beja, Herdade de Alagães	37.676°N, 7.853°W	BGE_00228_H01	BSNTN940-23	
Limnocharidae					
Limnochares aquatica	Guarda, Poço do Inferno	40.373°N, 7.516°W	BGE_00227_B10	BSNTN972-23	^{N}BOLD:AFV0270
			BGE_00108_B03	BBIOP110-24	
			BGE_00108_B04	BBIOP111-24	
	Guarda, Casa do Loureiro	40.433°N, 7.701°W	BGE_00109_D05	BBIOP041-24	
Hydryphantidae					
Hydrodroma despiciens	Guarda, Covão do Forno	40.369°N, 7.638°W	BGE_00227_D11	BSNTN997-23	BOLD:ACS0426
			BGE_00108_A02	BBIOP097-24	
Protzia annularis	Faro, Parque do Barranco dos Pisões	37.333°N, 8.567°W	BGE_00228_E09	BSNTN912-23	^{N}BOLD:AFX2700
Lebertiidae					
Lebertia fimbriata	Beja, São João dos Caldeireiros	37.626°N, 7.810°W	BGE_00110_A02	BSNTN477-23	BOLD:AEI5359
			BGE_00110_B02	BSNTN489-23	
Lebertia sparsicapillata	Beja, Zambujeira do Mar	37.399°N, 8.723°W	BGE_00110_F01	BSNTN536-23	BOLD:AFN4501
	Guarda, Casais de Folgosinho	40.454°N, 7.493°W	BGE_00227_F12	BSNTN1022-23	
	Guarda, Praia fluvial de Vila Cova a Coelheira	40.379°N, 7.736°W	BGE_00228_A10	BSNTN865-23	
	Guarda, Casa do Loureiro	40.433°N, 7.701°W	BGE_00109_H05	BBIOP089-24	
Lebertia variolata	Beja, Zambujeira do Mar	37.398°N, 8.68°W	BGE_00228_D06	BSNTN897-23	BOLD:ADK0996
	Faro, Portimão	37.237°N, 8.546°W	BGE_00228_F08	BSNTN923-23	
Lebertia pilosa	Beja, Zambujeira do Mar	37.399°N, 8.723°W	BGE_00110_E11	BSNTN534-23	BOLD:AEJ2601
			BGE_00110_E12	BSNTN535-23	
			BGE_00110_F07	BSNTN542-23	
			BGE_00228_F01	BSNTN916-23	

Taxa	Locality	Coordinates	Sample ID	Process ID	BIN
Lebertia gibbosa	Guarda, Praia Fluvial de Sabugueiro	40.401°N, 7.640°W	BGE_00227_A08	BSNTN958-23	BOLD:ACR9744
			BGE_00227_B03	BSNTN965-23	
	Guarda, Ponte dos Frades	40.403°N, 7.526°W	BGE_00108_D12	BBIOP143-24	
	Guarda, Central hidroelétrica de Ponte dos Jugai	40.385°N, 7.706°W	BGE_00108_F01	BBIOP156-24	
	Guarda, Nossa Senhora do Desterro	40.395°N, 7.694°W	BGE_00108_F06	BBIOP161-24	
	Guarda, Covão da ponte	40.443°N, 7.514°W	BGE_00108_G06	BBIOP173-24	
	Guarda, Casais de Folgosinho	40.454°N, 7.493°W	BGE_00108_G11	BBIOP178-24	
	Porto, Moinho da Tapada	41.263°N, 8.307°W	BGE_00109_F05	BBIOP065-24	
Lebertia algeriensis	Guarda, Casais de Folgosinho	40.454°N, 7.493°W	BGE_00227_F07	BSNTN1017-23	^{N}BOLD:AFV0271
	Guardia, Praia fluvial de Vila Cova a Coelheira	40.379°N, 7.736°W	BGE_00228_A03	BSNTN858-23	
			BGE_00108_E09	BBIOP152-24	
Lebertia insignis	Guarda, Poço do Inferno	40.373°N, 7.516°W	BGE_00227_D05	BSNTN991-23	BOLD:AEB9107
	Porto, Moinho da Tapada	41.263°N, 8.307°W	BGE_00109_E11	BBIOP059-24	
	Guarda, Praia fluvial de Vila Cova a Coelheira	40.379°N, 7.736°W	BGE_00228_A04	BSNTN859-23	^{N}BOLD:AFW6960
Lebertia porosa aggr. sp. A	Guarda, Praia Fluvial de Sabugueiro	40.401°N, 7.640°W	BGE_00227_A10	BSNTN960-23	BOLD:ACP5319
			BGE_00109_A02	BBIOP002-24	
	Guarda, Poço do Inferno	40.373°N, 7.516°W	BGE_00227_D01	BSNTN987-23	
			BGE_00108_B08	BBIOP115-24	
	Guarda, Nossa Senhora do Desterro	40.395°N, 7.694°W	BGE_00228_C02	BSNTN881-23	
	Guarda, Praia fluvial de Vila Cova a Coelheira	40.379°N, 7.736°W	BGE_00108_E06	BBIOP149-24	
			BGE_00108_E08	BBIOP151-24	
	Guarda, Covão da ponte	40.443°N, 7.514°W	BGE_00108_F11	BBIOP166-24	
			BGE_00108_G03	BBIOP170-24	
	Guarda, Casais de Folgosinho	40.454°N, 7.493°W	BGE_00108_G10	BBIOP177-24	
Lebertia porosa aggr. sp. ACS0974	Guarda, Praia Fluvial de Sabugueiro	40.401°N, 7.640°W	BGE_00227_B07	BSNTN969-23	BOLD:ACS0974
	Guarda, Casais de Folgosinho	40.454°N, 7.493°W	BGE_00227_E12	BSNTN1010-23	
			BGE_00227_F09	BSNTN1019-23	
	Guarda, Poio do Leão	40.399°N, 7.541°W	BGE_00227_H10	BSNTN1044-23	
	Guarda, Ponte dos Frades	40.403°N, 7.526°W	BGE_00108_D10	BBIOP141-24	
	Guarda, Praia fluvial de Vila Cova a Coelheira	40.379°N, 7.736°W	BGE_00108_E05	BBIOP148-24	
	Guarda, Nossa Senhora do Desterro	40.395°N, 7.694°W	BGE_00108_F08	BBIOP163-24	
	Bragança, Torre de Dona Chama	41.665°N, 7.146°W	BGE_00109_C01	BBIOP025-24	
	Bragança, Gasparona	41.85°N, 7.013°W	BGE_00109_C12	BBIOP036-24	
	Porto, Moinho da Tapada	41.263°N, 8.307°W	BGE_00109_F01	BBIOP061-24	
Lebertia pusilla	Porto, Moinho da Tapada	41.263°N, 8.307°W	BGE_00109_E09	BBIOP057-24	BOLD:AFW6961
Oxidae					
Oxus angustipositus	Guarda, Poço do Inferno	40.373°N, 7.516°W	BGE_00227_B12	BSNTN974-23	BOLD:AET9442
	Guarda, Casa do Cantoneiro	40.418°N, 7.603°W	BGE_00227_E02	BSNTN1000-23	
			BGE_00108_H04	BBIOP183-24	
Oxus lusitanicus	Guarda, Casais de Folgosinho	40.454°N, 7.493°W	BGE_00227_E09	BSNTN1007-23	^{N}BOLD:AFX3224
			BGE_00227_E11	BSNTN1009-23	
	Beja, Moinho de Alferes 2	37.503°N, 7.687°W	BGE_00228_E05	BSNTN908-23	
			BGE_00228_E06	BSNTN909-23	
	Bragança, Torre de Dona Chama	41.665°N, 7.146°W	BGE_00109_A07	BBIOP007-24	
			BGE_00109_A08	BBIOP008-24	
	Vila Real, Noura stream	41.409°N, 7.417°W	BGE_00109_D11	BBIOP047-24	
Oxus musculus	Beja, Moinho de Alferes 1	37.502°N, 7.690°W	BGE_00228_C10	BSNTN889-23	BOLD:AFC2154
Oxus ovalis	Beja, Zambujeira do Mar	37.399°N, 8.723°W	BGE_00110_F08	BSNTN543-23	^{N}BOLD:AFP5747
			BGE_00228_F02	BSNTN917-23	
Oxus setosus	Guarda, Casais de Folgosinho	40.454°N, 7.493°W	BGE_00227_E10	BSNTN1008-23	BOLD:ACS0808
	Guarda, Covão da ponte	40.443°N, 7.514°W	BGE_00228_C03	BSNTN882-23	
Sperchontidae					
Sperchon algeriensis	Faro, Portimão	37.237°N, 8.546°W	BGE_00228_F12	BSNTN927-23	BOLD:AES2436
Sperchon clupeifer	Guarda, Casais de Folgosinho	40.454°N, 7.493°W	BGE_00227_F04	BSNTN1014-23	^{N}BOLD:AFX0389
Sperchon compactilis	Faro, Portimão	37.237°N, 8.546°W	BGE_00110_E03	BSNTN526-23	BOLD:AER7687
	Guarda, Praia fluvial de Vila Cova a Coelheira	40.379°N, 7.736°W	BGE_00228_A07	BSNTN862-23	

Taxa	Locality	Coordinates	Sample ID	Process ID	BIN
Torrenticolidae					
Monatractides madritensis	Guarda, Praia Fluvial de Sabugueiro	40.401°N, 7.640°W	BGE_00227_A12	BSNTN962-23	BOLD:AED3803
	Guarda, Poço do Inferno	40.373°N, 7.516°W	BGE_00227_C09	BSNTN983-23	
	Guarda, Poio do Leão	40.399°N, 7.541°W	BGE_00227_H07	BSNTN1041-23	
			BGE_00108_D02	BBIOP133-24	
	Bragança, Gasparona	41.850°N, 7.013°W	BGE_00109_C06	BBIOP030-24	
Monatractides stadleri	Faro, Parque do Barranco dos Pisões	37.333°N, 8.567°W	BGE_00110_G03	BSNTN550-23	BOLD:AEU1504
	Guarda, Casais de Folgosinho	40.454°N, 7.493°W	BGE_00227_F01	BSNTN1011-23	
	Guarda, Praia fluvial de Vila Cova a Coelheira	40.379°N, 7.736°W	BGE_00228_A06	BSNTN861-23	
			BGE_00108_E01	BBIOP144-24	
	Guarda, Central hidroelétrica de Ponte dos Jugais	40.385°N, 7.706°W	BGE_00228_B01	BSNTN868-23	
	Porto, Moinho da Tapada	41.263°N, 8.307°W	BGE_00109_E07	BBIOP055-24	
	Guarda, Casa do Loureiro	40.433°N, 7.701°W	BGE_00109_G11	BBIOP083-24	
Monatractides stenostomus	Beja, Corte do Pinto	37.682°N, 7.512°W	BGE_00228_G08	BSNTN935-23	^{N}BOLD:AFU3082
Torrenticola elliptica	Bragança, Gasparona	41.850°N, 7.013°W	BGE_00109_C09	BBIOP033-24	BOLD:AEI9183
Torrenticola tenuipalpis	Guarda, Casais de Folgosinho	40.454°N, 7.493°W	BGE_00227_F03	BSNTN1013-23	^{N}BOLD:AFV2021
Torrenticola soniae sp. nov.	Guarda, Praia Fluvial de Sabugueiro	40.401°N, 7.640°W	BGE_00227_A11	BSNTN961-23	^{N}BOLD:AFW5337
	Guarda, Casais de Folgosinho	40.454°N, 7.493°W	BGE_00227_F02	BSNTN1012-23	
	Guarda, Ponte dos Frades	40.403°N, 7.526°W	BGE_00108_D09	BBIOP140-24	
	Guarda, Praia fluvial de Vila Cova a Coelheira	40.379°N, 7.736°W	BGE_00108_E02	BBIOP145-24	
			BGE_00108_E07	BBIOP150-24	
	Bragança, Torre de Dona Chama	41.665°N, 7.146°W	BGE_00109_C03	BBIOP027-24	
Torrenticola elisabethae sp. nov.	Guarda, Poço do Inferno	40.373°N, 7.516°W	BGE_00227_C10	BSNTN984-23	^{N}BOLD:AFW5336
	Guarda, Poio do Leão	40.399°N, 7.541°W	BGE_00227_H06	BSNTN1040-23	
			BGE_00108_D04	BBIOP135-24	
Limnesiidae					
Limnesia acuminata	Beja, Moinho de Alferes 1	37.502°N, 7.690°W	BGE_00228_C12	BSNTN891-23	^{N}BOLD:AFU7587
	Bragança, Torre de Dona Chama	41.665°N, 7.146°W	BGE_00109_B01	BBIOP013-24	
			BGE_00109_B03	BBIOP015-24	
			BGE_00109_B04	BBIOP016-24	
Limnesia iberica	Beja, São João dos Caldeireiros	37.626°N, 7.810°W	BGE_00110_A03	BSNTN478-23	^{N}BOLD:AFN8367
			BGE_00110_A04	BSNTN479-23	
			BGE_00110_A05	BSNTN480-23	
			BGE_00110_A06	BSNTN481-23	
			BGE_00110_A11	BSNTN486-23	
			BGE_00110_A12	BSNTN487-23	
			BGE_00110_H08	BSNTN567-23	
			BGE_00110_H09	BSNTN568-23	
			BGE_00110_H11	BSNTN570-23	
Limnesia koenikei	Guarda, Covão do Forno	40.369°N, 7.638°W	BGE_00227_D09	BSNTN995-23	BOLD:ADF6559
			BGE_00108_A01	BBIOP096-24	
			BGE_00108_A03	BBIOP098-24	
	Guarda, Central hidroelétrica de Ponte dos Jugais	40.385°N, 7.706°W	BGE_00228_B02	BSNTN869-23	
Limnesia maculata	Guarda, Praia Fluvial de Sabugueiro	40.401°N, 7.640°W	BGE_00227_B05	BSNTN967-23	^{N}BOLD:AFW6935
	Guarda, Barragem do Lagoacho	40.385°N, 7.618°W	BGE_00108_C07	BBIOP126-24	
	Beja, Moinho de Alferes 2	37.503°N, 7.687°W	BGE_00228_E03	BSNTN906-23	
	Beja, Herdade de Alagães	37.673°N, 7.848°W	BGE_00228_H04	BSNTN943-23	
			BGE_00228_H06	BSNTN945-23	
Limnesia walteri	Beja, Corte do Pinto	37.682°N, 7.512°W	BGE_00110_B11	BSNTN498-23	^{N}BOLD:AFO9873
			BGE_00110_C02	BSNTN501-23	
			BGE_00228_G09	BSNTN936-23	
	Bragança, Torre de Dona Chama	41.665°N, 7.146°W	BGE_00109_B09	BBIOP021-24	
Hygrobatidae					
Atractides inflatus	Beja, Zambujeira do Mar	37.398°N, 8.680°W	BGE_00110_E05	BSNTN528-23	BOLD:AFI9009
			BGE_00228_D07	BSNTN898-23	BOLD:ACB4677
	Vila Real, Noura stream	41.409°N, 7.417°W	BGE_00109_D07	BBIOP043-24	

Taxa	Locality	Coordinates	Sample ID	Process ID	BIN
Atractides marizae	Guarda, Casais de Folgosinho	40.454°N, 7.493°W	BGE_00227_F11	BSNTN1021-23	BOLD:AER7878
	Guarda, Praia fluvial de Vila Cova a Coelheira	40.379°N, 7.736°W	BGE_00228_A08	BSNTN863-23	
	Faro, Caldas de Monchique	37.287°N, 8.554°W	BGE_00228_D12	BSNTN903-23	
	Odeceixe, Covão da Serva	37.374°N, 8.642°W	BGE_00228_E11	BSNTN914-23	
	Faro, Portimão	37.237°N, 8.546°W	BGE_00228_F07	BSNTN922-23	
Atractides nodipalpis	Guarda, Praia fluvial de Vila Cova a Coelheira	40.379°N, 7.736°W	BGE_00228_A01	BSNTN856-23	^{N}BOLD:AFV2009
Atractides robustus	Guarda, Covão da Ametade	40.328°N, 7.587°W	BGE_00227_G07	BSNTN1029-23	BOLD:AFF2463
Hygrobates balcanicus	Faro, Portimão	37.237°N, 8.546°W	BGE_00110_E01	BSNTN524-23	BOLD:AEG3198
			BGE_00110_E02	BSNTN525-23	
			BGE_00228_F06	BSNTN921-23	
	Porto, Moinho da Tapada	41.263°N, 8.307°W	BGE_00109_D12	BBIOP048-24	
			BGE_00109_E10	BBIOP058-24	
	Porto, Parque Molinológico e Florestal de Pias	41.268°N, 8.256°W	BGE_00109_F09	BBIOP069-24	
	Porto, Rio Este	41.378°N, 8.695°W	BGE_00109_G07	BBIOP079-24	
			BGE_00109_G08	BBIOP080-24	
			BGE_00109_G09	BBIOP081-24	
			BGE_00109_H11	BBIOP095-24	
Hygrobates fluviatilis	Guarda, Casa do Cantoneiro	40.418°N, 7.603°W	BGE_00227_E03	BSNTN1001-23	BOLD:ACB4846
	Guarda, Casais de Folgosinho	40.454°N, 7.493°W	BGE_00227_F10	BSNTN1020-23	
	Guarda, Praia fluvial de Vila Cova a Coelheira	40.379°N, 7.736°W	BGE_00228_A09	BSNTN864-23	
			BGE_00108_E03	BBIOP146-24	
	Guarda, Praia Fluvial de Sabugueiro	40.401°N, 7.640°W	BGE_00109_A04	BBIOP004-24	
Hygrobates longiporus complex	Guarda, Praia fluvial de Vila Cova a Coelheira	40.379°N, 7.736°W	BGE_00228_A02	BSNTN857-23	^{N}BOLD:AFV9997
		40.379°N, 7.736°W	BGE_00108_E04	BBIOP147-24	
	Guarda, Ponte dos Frades	40.403°N, 7.526 °W	BGE_00108_D11	BBIOP142-24	
	Gurad, Covão da ponte	40.443°N, 7.514°W	BGE_00108_G04	BBIOP171-24	
	Guarda, Praia Fluvial de Sabugueiro	40.401°N, 7.640°W	BGE_00109_A03	BBIOP003-24	
	Guarda, Casa do Loureiro	40.433°N, 7.701°W	BGE_00109_H07	BBIOP091-24	
			BGE_00109_H08	BBIOP092-24	
	Bragança, Torre de Dona Chama	41.665°N, 7.146°W	BGE_00109_B05	BBIOP017-24	^{N}BOLD:AFW1423
	Vila Real, Noura stream	41.409°N, 7.417°W	BGE_00109_D09	BBIOP045-24	
	Guarda, Praia Fluvial de Sabugueiro	40.401°N, 7.640°W	BGE_00227_A09	BSNTN959-23	^{N}BOLD:AFV9998
			BGE_00227_B01	BSNTN963-23	
			BGE_00227_B02	BSNTN964-23	
			BGE_00109_A01	BBIOP001-24	
	Guarda, Poço do Inferno	40.373°N, 7.516°W	BGE_00227_D03	BSNTN989-23	
			BGE_00227_D04	BSNTN990-23	
			BGE_00108_B07	BBIOP114-24	
	Guarda, Casais de Folgosinho	40.454°N, 7.493°W	BGE_00227_F06	BSNTN1016-23	
			BGE_00227_F08	BSNTN1018-23	
	Guarda, Poio do Leão	40.399°N, 7.541°W	BGE_00108_D03	BBIOP134-24	
	Gurada, Central hidroelétrica de Ponte dos Jugais	40.385°N, 7.706°W	BGE_00108_F02	BBIOP157-24	
	Guarda, Nossa Senhora do Desterro	40.395°N, 7.694°W	BGE_00108_F10	BBIOP165-24	
	Guarda, Covão da ponte	40.443°N, 7.514°W	BGE_00108_F12	BBIOP167-24	
			BGE_00108_G05	BBIOP172-24	
			BGE_00108_G07	BBIOP174-24	
			BGE_00108_G08	BBIOP175-24	
			BGE_00108_G09	BBIOP176-24	
Unionicolidae					
Neumania elliptica	Guarda, Poço do Inferno	40.373°N, 7.516°W	BGE_00227_D02	BSNTN988-23	^{N}BOLD:AFU2122
	Guarda, Nossa Senhora do Desterro	40.395°N, 7.694°W	BGE_00228_B12	BSNTN879-23	
Neumania imitata	Porto, Parque Molinológico e Florestal de Pias	41.268°N, 8.256°W	BGE_00109_G02	BBIOP074-24	^{N}BOLD:AFV0268

Taxa	Locality	Coordinates	Sample ID	Process ID	BIN
Neumania limosa	Beja, Herdade de Alagães	37.673°N, 7.848°W	BGE_00110_D06	BSNTN517-23	BOLD:ACS0551
			BGE_00110_D07	BSNTN518-23	
			BGE_00110_D09	BSNTN520-23	
			BGE_00228_H05	BSNTN944-23	
	Guarda, Lagoa	40.350°N, 7.549°W	BGE_00227_G01	BSNTN1023-23	
			BGE_00227_G02	BSNTN1024-23	
			BGE_00108_B01	BBIOP108-24	
			BGE_00108_B02	BBIOP109-24	
	Guarda, Barragem do Lagoacho	40.385°N, 7.618°W	BGE_00227_H04	BSNTN1038-23	
Neumania uncinata	Faro, Caldas de Monchique	37.287°N, 8.554°W	BGE_00228_E01	BSNTN904-23	^{N}BOLD:AFV0253
	Porto, Rio Este	41.378°N, 8.695°W	BGE_00109_G04	BBIOP076-24	^{N}BOLD:AFV0269
Neumania papillosa	Beja, Corte do Pinto	37.682°N, 7.512°W	BGE_00110_C01	BSNTN500-23	^{N}BOLD:AFO2116
			BGE_00228_G10	BSNTN937-23	
			BGE_00228_G11	BSNTN938-23	
	Guarda, Praia Fluvial de Sabugueiro	40.401°N, 7.640°W	BGE_00227_A05	BSNTN955-23	
Unionicola minor	Beja, São João dos Caldeireiros	37.626°N, 7.810°W	BGE_00110_H06	BSNTN565-23	^{N}BOLD:AFO2171
	Beja, Moinho de Alferes 2	37.503°N, 7.687°W	BGE_00228_E02	BSNTN905-23	
Pionidae					
Forelia longipalpis	Guarda, Nossa Senhora do Desterro	40.395°N, 7.694°W	BGE_00228_C01	BSNTN880-23	^{N}BOLD:AFV3893
	Guarda, Covão da ponte	40.443°N, 7.514°W	BGE_00228_C05	BSNTN884-23	
	Guarda, Barragem do Vale do Rossim	40.4°N, 7.589°W	BGE_00108_C02	BBIOP121-24	
			BGE_00108_C03	BBIOP122-24	
			BGE_00227_H02	BSNTN1036-23	
			BGE_00108_C04	BBIOP123-24	
Forelia variegator	Guarda, Central hidroelétrica de Ponte dos Jugais	40.385°N, 7.706°W	BGE_00228_B06	BSNTN873-23	^{N}BOLD:AFU5459
	Beja, São João dos Caldeireiros	37.626°N, 7.81°W	BGE_00228_H09	BSNTN948-23	
	Porto, Parque Molinológico e Florestal de Pias	41.268°N, 8.256°W	BGE_00109_F12	BBIOP072-24	
			BGE_00109_G01	BBIOP073-24	
	Porto, Rio Este	41.378°N, 8.695°W	BGE_00109_G05	BBIOP077-24	
	Guarda, Nossa Senhora do Desterro	40.395°N, 7.694°W	BGE_00108_F05	BBIOP160-24	
Hydrochoreutes krameri	Beja, Herdade de Alagães (pond)	37.673°N, 7.848°W	BGE_00110_D11	BSNTN522-23	BOLD:ACR9737
	Guarda, Covão do Forno	40.369°N, 7.638°W	BGE_00227_D12	BSNTN998-23	
Tiphys torris	Beja, Zambujeira do Mar	37.399°N, 8.723°W	BGE_00110_F02	BSNTN537-23	BOLD:ACR9977
	Guarda, Praia Fluvial de Sabugueiro	40.401°N, 7.64°W	BGE_00227_A06	BSNTN956-23	
	Guarda, Nossa Senhora do Desterro	40.395°N, 7.694°W	BGE_00228_B10	BSNTN877-23	
Nautarachna crassa	Guarda, Casa do Cantoneiro	40.418°N, 7.603°W	BGE_00227_E01	BSNTN999-23	^{N}BOLD:AFV0462
Piona carnea	Guarda, Lagoa	40.350°N, 7.549°W	BGE_00108_A10	BBIOP105-24	BOLD:ACS0622
	Beja, São Sebastião dos Carros	37.598°N, 7.754°W	BGE_00110_G05	BSNTN552-23	BOLD:ACM0527
			BGE_00110_G06	BSNTN553-23	
			BGE_00110_G07	BSNTN554-23	
			BGE_00110_G08	BSNTN555-23	
			BGE_00110_G12	BSNTN559-23	
			BGE_00228_D08	BSNTN899-23	
			BGE_00228_D10	BSNTN901-23	
	Beja, Herdade de Alagães	37.678°N, 7.848°W	BGE_00228_E08	BSNTN911-23	
	Vila Real, Noura stream	41.409°N, 7.417°W	BGE_00109_D10	BBIOP046-24	
	Guarda, Lagoa	40.350°N, 7.549°W	BGE_00108_A10	BBIOP105-24	BOLD:ACS0622
			BGE_00108_A12	BBIOP107-24	
Piona variabilis	Beja, São Sebastião dos Carros	37.598°N, 7.754°W	BGE_00110_H01	BSNTN560-23	BOLD:AAU0701
Pionopsis lutescens	Porto, Parque Torre de Vilar	41.287°N, 8.210°W	BGE_00109_F06	BBIOP066-24	^{N}BOLD:AFV3897
	Porto, Parque Molinológico e Florestal de Pias	41.268°N, 8.256°W	BGE_00109_F11	BBIOP071-24	
	Guarda, Cise	40.419°N, 7.709°W	BGE_00109_A05	BBIOP005-24	
			BGE_00109_A06	BBIOP006-24	
			BGE_00227_B08	BSNTN970-23	

Taxa	Locality	Coordinates	Sample ID	Process ID	BIN
Aturidae					
Aturus scaber	Porto, Moinho da Tapada	41.263°N, 8.307°W	BGE_00109_E03	BBIOP051-24	BOLD:ACQ9097
	Porto, Parque Molinológico e Florestal de Pias	41.268°N, 8.256°W	BGE_00109_G03	BBIOP075-24	
Mideopsidae					
Mideopsis roztoczensis	Beja, Moinho de Alferes 1	37.502°N, 7.690°W	BGE_00110_B10	BSNTN497-23	^{N}BOLD:AFP5421
	Beja, Pulo do Lobo	37.805°N, 7.633°W	BGE_00110_C08	BSNTN507-23	
			BGE_00110_C09	BSNTN508-23	
			BGE_00110_C10	BSNTN509-23	
			BGE_00110_C11	BSNTN510-23	
		37.805°N, 7.633°W	BGE_00110_C12	BSNTN511-23	
			BGE_00228_G12	BSNTN939-23	
	Vila Real, Noura stream	41.409°N, 7.417°W	BGE_00109_D08	BBIOP044-24	
	Beja, Zambujeira do Mar	37.398°N, 8.680°W	BGE_00228_D03	BSNTN894-23	
	Bragança, Gasparona	41.850°N, 7.013°W	BGE_00109_C07	BBIOP031-24	^{N}BOLD:AFU6108
			BGE_00109_C10	BBIOP034-24	^{N}BOLD:AFW3785
	Guarda, Ponte dos Frades	40.403°N, 7.526°W	BGE_00108_D06	BBIOP137-24	
	Guarda, Casa do Loureiro	40.433°N, 7.701°W	BGE_00109_D03	BBIOP039-24	^{N}BOLD:AFU6108
			BGE_00109_D04	BBIOP040-24	
			BGE_00109_G10	BBIOP082-24	
			BGE_00109_G12	BBIOP084-24	^{N}BOLD:AFW3785
			BGE_00109_H02	BBIOP086-24	^{N}BOLD:AFU6108
	Guarda, Covão da Ametade	40.328°N, 7.587°W	BGE_00108_A06	BBIOP101-24	
			BGE_00227_G05	BSNTN1027-23	^{N}BOLD:AFU6108
			BGE_00227_G09	BSNTN1031-23	
	Guarda, Poço do Inferno	40.373°N, 7.516°W	BGE_00108_B09	BBIOP116-24	
			BGE_00227_C04	BSNTN978-23	^{N}BOLD:AEV2909
			BGE_00227_C06	BSNTN980-23	
			BGE_00227_C08	BSNTN982-23	^{N}BOLD:AFU6108
	Guarda, Casais de Folgosinho	40.454°N, 7.493°W	BGE_00108_G12	BBIOP179-24	
			BGE_00227_F05	BSNTN1015-23	
	Guarda, Poio do Leão	40.399°N, 7.541°W	BGE_00108_C12	BBIOP131-24	
			BGE_00227_H08	BSNTN1042-23	
	Guarda, Central hidroelétrica de Ponte dos Jugais	40.385°N, 7.706°W	BGE_00228_B03	BSNTN870-23	
			BGE_00228_B08	BSNTN875-23	
			BGE_00228_B09	BSNTN876-23	
			BGE_00108_E10	BBIOP153-24	
			BGE_00108_E11	BBIOP154-24	
	Guarda, Nossa Senhora do Desterro	40.395°N, 7.694°W	BGE_00108_F04	BBIOP159-24	
			BGE_00108_F09	BBIOP164-24	
	Guarda, Covão da ponte	40.443°N, 7.514°W	BGE_00108_G01	BBIOP168-24	
	Guarda, Casa do Cantoneiro	40.418°N, 7.603°W	BGE_00108_H02	BBIOP181-24	
			BGE_00227_E04	BSNTN1002-23	^{N}BOLD:AFV6334
			BGE_00227_E05	BSNTN1003-23	^{N}BOLD:AFU6108
	Guarda, Praia Fluvial de Sabugueiro	40.401°N, 7.640°W	BGE_00108_H09	BBIOP188-24	
			BGE_00227_A07	BSNTN957-23	
Momoniidae					
Momonia falcipalpis	Guarda, Poço do Inferno	40.373°N, 7.516°W	BGE_00108_B10	BBIOP117-24	^{N}BOLD:AFX3396
Arrenuridae					
Arrenurus albator	Guarda, Barragem do Vale do Rossim	40.400°N, 7.589°W	BGE_00227_G11	BSNTN1033-23	BOLD:ACR9639
			BGE_00227_G12	BSNTN1034-23	
			BGE_00227_H01	BSNTN1035-23	
			BGE_00108_B11	BBIOP118-24	
	Guarda, Barragem do Lagoacho	40.400°N, 7.589°W	BGE_00108_C08	BBIOP127-24	

Taxa	Locality	Coordinates	Sample ID	Process ID	BIN
Arrenurus szalayi	Beja, Moinho de Alferes	37.502°N, 7.690°W	BGE_00110_B05	BSNTN492-23	BOLD:ACS0403
			BGE_00110_B06	BSNTN493-23	
			BGE_00228_C06	BSNTN885-23	
			BGE_00228_C07	BSNTN886-23	
			BGE_00228_C08	BSNTN887-23	
Arrenurus leuckarti	Guarda, Poço do Inferno	40.373°N, 7.516°W	BGE_00227_B11	BSNTN973-23	BOLD:ACR9670
	Guarda, Casa do Cantoneiro	40.418°N, 7.603°W	BGE_00108_H03	BBIOP182-24	
Arrenurus neumani	Beja, Moinho de Alferes 1	37.502°N, 7.690°W	BGE_00110_B07	BSNTN494-23	^{N}BOLD:AFP6143
			BGE_00110_B08	BSNTN495-23	
			BGE_00228_C11	BSNTN890-23	
			BGE_00228_H10	BSNTN949-23	
Arrenurus tricuspidator	Beja, Moinho de Alferes 1	37.502°N, 7.690°W	BGE_00228_D01	BSNTN892-23	^{N}BOLD:AFU3639
Arrenurus globator	Beja, Moinho de Alferes 1	37.502°N, 7.690°W	BGE_00110_B09	BSNTN496-23	^{N}BOLD:AFO3503
	Beja, São Sebastião dos Carros	37.598°N, 7.754°W	BGE_00110_H02	BSNTN561-23	
			BGE_00110_H03	BSNTN562-23	
			BGE_00110_H04	BSNTN563-23	
	Beja, São Miguel do Pinheiro	37.552°N, 7.850°W	BGE_00228_G02	BSNTN929-23	
			BGE_00228_G03	BSNTN930-23	
			BGE_00228_G04	BSNTN931-23	
Arrenurus zachariae	Bragança, Gasparona	41.850°N, 7.013°W	BGE_00109_C08	BBIOP032-24	^{N}BOLD:AFU0319

Results and discussion

We generated 307 DNA barcodes from 65 water mite species. The collected water mites represent 15 families of the 16 recorded in Portugal. The most sequence-rich family was Hygrobatidae with 51 sequences (16.7% of total; 10 BINs), followed by Lebertiidae wih 47 sequences (15.4%; 11 BINs), Mideopsidae with 41 sequences (13.4%; 5 BINs), Pionidae with 35 sequences (11.5%; 10 BINs), Limnesiidae with 26 sequences (8.5%; 5 BINs), Arrenuridae with 25 sequences (8.2%; 5 BINs), and Torrenticolidae with 24 sequences (7.9%; 7 BINs). Some families were rare, such as Hydryphantidae and Momoniidae, represented by a single sequence each and corresponding single BIN.

Our findings added the first records of 34 species for Portugal: *Eylais tantilla* Koenike, 1897 (Eylaidae), *Lebertia sparsicapillata* Thor, 1905, *L. variolata* Gerecke, 2009, *L. gibbosa* Lundblad, 1926, *L. algeriensis* Lundblad, 1942, *L. insignis* Neuman, 1880, *L. porosa* aggr. sp. A (Lebertiidae), *Oxus musculus* (Müller, 1776), *O. ovalis* (Müller, 1776), *O. setosus* (Koenike, 1898) (Oxidae), *Sperchon algeriensis* Lundblad, 1942, *S. compactilis* Koenike, 1911 (Sperchontidae), *Monatractides madritensis* (K. Viets, 1930), *Torrenticola elliptica* Maglio, 1909 (Torrenticolidae), *Limnesia koenikei* Piersig, 1894 (Limnesiidae), *Atractides inflatus* (Walter, 1925), *A. robustus* (Sokolow, 1940), *Hygrobates balcanicus* Pešić, 2020 (Hygrobatidae), *Neumania elliptica* Walter, 1925, *N. imitata* Koenike, 1908, *N. limosa* (Koch, 1836), *Unionicola minor* (Soar, 1900) (Unionicolidae), *Forelia longipalpis* Maglio, 1924, *Hydrochoreutes krameri* Piersig, 1896, *Nautarachna crassa* (Koenike, 1908), *Piona carnea* (Müller, 1776), *P. variabilis* (Koch, 1836) (Pionidae), *Aturus scaber* Kramer, 1875 (Aturidae), *Mideopsis roztoczensis* Biesiadka & Kowalik, 1979 (Mideopsidae), *Momonia falcipalpis* Halbert, 1906 (Momoniidae), *Arrenurus leuckarti* Piersig, 1894, *A. neumani* Piersig, 1895, *A.* cf. *tricuspidator* (Müller, 1776) and *A.* cf. *zachariae* Koenike, 1886 (Arrenuridae). Two species of the genus *Torrenticola* are described as new to science. Even though sampling was focused on certain districts (i.e., Beja, Bragança, Faro, Guarda, Porto, Vila Real), we recorded specimens from 47.4% of the Portuguese water mite fauna (65 of 137 species including 36 species new to Portugal).

The resulting sequences clustered into 75 BINs, with 38 BINs (51%) being unique and deposited for the first time in BOLD. The number of BINs per species ranged from one (58 species, 89%) to five for *Mideopsis roztoczensis* (BOLD:AFU6108, BOLD:AFP5421, BOLD:AFW3785, BOLD:AFV6334, BOLD:AEV2909). Two BINs were detected for five species, *Lebertia insignis* (BOLD:AEB9107, BOLD:AFW6960), *Atractides inflatus* (BOLD:AFI9009, BOLD:ACB4677), *Neumania uncinata* (BOLD:AFV0253, BOLD:AFV0269), *Forelia longipalpis* (BOLD:AFX2876, BOLD:AFV3893), *Piona carnea* (BOLD:ACM0527, BOLD:ACS0622), and one species, *Hygrobates longiporus* (BOLD:AFV9997, BOLD:AFW1423, BOLD:AFV9998), has three BINs.

Our study provided the first DNA barcodes for *Protzia annularis* Lundblad, 1954 (BOLD:AFX2700), *Monatractides stenostomus* (K. Viets, 1930) (BOLD:AFU3082), *Torrenticola tenuipalpis* (Lundblad, 1956) (BOLD:AFV2021), *Oxus lusitanicus* Lundblad, 1954 (BOLD:AFX3224), *Limnesia acuminata* Walter, 1925 (BOLD:AFU7587), *L. iberica* Lundblad, 1954 (BOLD:AFN8367), *L. walteri* Migot, 1926 (BOLD:AFO9873), *Neumania elliptica* (BOLD:AFU2122), *N. papillosa* (Soar, 1902) (BOLD:AFO2116), *Momonia falcipalpis* (BOLD:AFX3396) and *Arrenurus szalayi* Lundblad, 1954 (BOLD:ACS0403).

Systematics

Family Eylaidae Leach, 1815

Genus *Eylais* Latreille, 1796

Note. Only one species reported from Portugal.

Eylais tantilla Koenike, 1897

Material examined. Portugal, **Beja**: • Mértola, São João dos Caldeireiros, stream, 37.625°N, 7.81°W, 17 May 2023, leg. Ferreira, Benitez-Bosco, Ekrem, Stur & Turaccio, 1♂ (sequenced), dissected and slide mounted (RMNH); • Mértola, Moinho de Alferes 1, 37.502°N, 7.69°W, 19 May 2023, leg. Ferreira, Benitez-Bosco, Ekrem, Stur & Turaccio, 1♀ (sequenced); • Mértola, Herdade de Alagães, dry stream site 1, 37.676°N, 7.853°W, 18 May 2023, leg. Ferreira, Benitez-Bosco, Ekrem, Stur & Turaccio 1♀ (sequenced).

Remarks. As a result of the treatment during the barcoding process, all vouchered individuals except one male and two females were partly or completely destroyed. With regards to the shape of the eye bridge and gnathosoma, the specimens examined in our study matches the description of *E. tantilla* given by K. Viets (1930) for material from Spain. The sequenced specimens from Portugal form a unique BIN (BOLD:AFP3591), with the nearest neighboring BIN being BOLD:ACS1138, which includes three public sequences of specimens from Norway assigned to *E. rimosa* Piersig, 1899, and three unpublished sequences of specimens from the Netherlands, two of them assigned to *E. extendens* and one assigned to *E. setosa* Koenike, 1897. The *p*-distance between these two BINs was estimated at 14.83%.

Distribution. Palaearctic. New for Portugal.

Family Limnocharidae Grube, 1859

Genus *Limnochares* Latreille, 1796

Note. Only one species reported from Portugal.

Limnochares aquatica (Linnaeus, 1788)

Material examined. Portugal, **Guarda**: • Manteigas, Poço do Inferno, 40.373°N, 7.516°W, 1078 m a.s.l., 21 Aug. 2023, leg. Ferreira, Benitez-Bosco & Padilha, 1♀ (sequenced); • Seia, Casa do Loureiro, 40.433°N, 7.701°W, 415 m a.s.l., 19 Jul. 2023 leg. Ferreira & Padilha, 1♀ (sequenced).

Remarks. The examined specimens in our study, keyed to *L. aquatica* following Davids et al. (2007), form a unique BIN (BOLD:AFV0270). The *p*-distance between the latter BIN and its nearest neighbor, BOLD:ACS0438, which includes specimens of *L. aquatica* from the Netherlands, Norway, Montenegro, and Italy, was estimated at 11.72%, indicating the need for taxonomic revision of *L. aquatica* complex to identify possible undescribed cryptic species.

Distribution. Holarctic. In Portugal previously reported from Beira Alta and Alentejo (Lundblad 1956).

Family Hydrodromidae Viets, 1936

Genus *Hydrodroma* Koch, 1837

Note. Only one species reported from Portugal.

Hydrodroma despiciens (Müller, 1776)

Material examined. Portugal, **Guarda:** • Seia, Covão do Forno, 40.369°N, 7.638°W, 1574 m a.s.l., 19 Aug. 2023, leg. Ferreira, Benitez-Bosco & Padilha, 1♂, 1 deutonymph (sequenced).

Remarks. The sequences obtained from the specimens from Portugal fall into BOLD:ACS0426, which, in addition to the specimens used in this study for molecular analysis, includes 17 specimens of *H. despiciens* from the Netherlands, Norway, and Poland, available in the BOLD database.

Distribution. Europe. In Portugal previously reported from Alentejo (Lundblad 1956).

Family Hydryphantidae Piersig, 1896

Genus *Protzia* Piersig, 1896

Note. Only three species reported from Portugal.

Protzia annularis Lundblad, 1954

Material examined. Portugal, **Faro**: • Monchique, Ribeira de Seixe, Parque do Barranco dos Pisões, 37.333°N, 8.567°W, 480 m a.s.l., 23 May 2023, leg. Ekrem & Benitez-Bosco, 1♀ (sequenced).

Remarks. The single examined female from Ribeira de Seixe matches the description of *P. annularis*, a species known from Portugal and Spain (Lundblad 1956). The Portuguese specimen forms a unique BIN (BOLD:AFX2700), with the nearest neighboring BIN being BOLD:AEI5748, which includes specimens of *P. lata* from Corsica. The *p*-distance between these two BINs was estimated at 12.36%.

Distribution. Iberian Peninsula. In Portugal previously reported from Beira Alta (Lundblad 1956).

Family Lebertiidae Thor, 1900

Genus *Lebertia* Neuman, 1880

Note. Nine species known from Portugal, two of them, *Lebertia madericola* (Lundblad, 1942) and *Lebertia maderigena* (Lundblad, 1942), are endemic for Madeira.

Lebertia (*Lebertia*) *fimbriata* Thor, 1899

Material examined. Portugal, **Beja**: • Mértola, São João dos Caldeireiros, stream, 37.626°N, 7.81°W, 17 May 2023, leg. Ferreira, Benitez-Bosco, Ekrem, Stur & Turaccio, 1♀, 1♂ (sequenced).

Remarks. The specimens from Portugal match the description of *Lebertia fimbriata*, a species widely distributed in the Western Palaearctic (Di Sabatino et al. 2010). The Portuguese specimens were clustered within BOLD:AEI5359, which includes specimens of *L. fimbriata* from Germany, Spain and North Macedonia.

Distribution. Western Palaearctic. In Portugal previously reported from Fonte Fria in Mealhada (Buçaco mountain; Lundblad 1956).

Lebertia (*Lebertia*) *sparsicapillata* Thor, 1905

Material examined. Portugal, **Beja**: • Odemira, Ribeira de Seixe, Zambujeira do Mar, river, 37.399°N, 8.723°W, 45 m a.s.l., 23 May 2023, leg. Ekrem & Benitez-Bosco, 1♂ (sequenced). **Guarda**: • Gouveia, Rio Mondego, Casais de Folgosinho, 40.454°N, 7.493°W, 976 m a.s.l., 24 Aug. 2023, leg. Ferreira, Benitez-Bosco & Padilha, 1♂ (sequenced); • Seia, Rio Alva, Praia fluvial de Vila Cova a Coelheira, river, 40.379°N, 7.736°W, 312 m a.s.l., 23 Aug. 2023, leg. Ferreira, Benitez-Bosco & Padilha, 1♀ (sequenced); • Seia, Casa do Loureiro, 40.433°N, 7.701°W, 415 m a.s.l., 19 Jul. 2023 leg. Ferreira & Padilha, 1♀ (sequenced).

Remarks. The specimens from Portugal match the description of *L. sparsicapillata*, a species widely distributed in Europe except for the most northern and eastern parts (Di Sabatino et al. 2010). The sequenced specimens cluster within BOLD:AFN4501, which includes two specimens from Germany. The *p*-distance between the latter BIN and its nearest neighboring BOLD:ADF6063, which include specimens of *L. sparsicapillata* from Germany, was estimated at 2%.

Distribution. Europe. New for Portugal.

Lebertia (*Lebertia*) *variolata* Gerecke, 2009

Material examined. Portugal, **Beja:** • Odemira, Ribeira de Seixe, Zambujeira do Mar, 37.398°N, 8.68°W, site 32, 75 m a.s.l., 23 May 2023, leg. Ekrem & Benitez-Bosco, 1♀ (sequenced); • Faro, Portimão, 37.237°N, 8.546°W, 23 May 2023, leg. Ferreira & Turaccio 1♀ (sequenced).

Remarks. The sequences obtained from two specimens from Portugal fall into the *Lebertia variolata* cluster (BOLD:ADK0996). In addition to specimens used in this study, the BIN includes specimens from Montenegro, North Macedonia and Turkey morphologically assigned to *L. variolata*, and one private sequence of a non-identified specimen from France (GBMIN118138-1). *Lebertia variolata* is a characteristic inhabitant of streams that regularly dry up in the summer (Gerecke 2009).

Distribution. Mediterranean region. New for Portugal.

Lebertia (*Pilolebertia*) *gibbosa* Lundblad, 1926

Material examined. Portugal, **Guarda**: • Seia, Rio Alva, Praia Fluvial de Sabugueiro, river, 40.401°N, 7.64°W, 1021 m a.s.l., 24 Aug. 2023, leg. Ferreira, Benitez-Bosco & Padilha, 2♂ (sequenced); • Manteigas, Zêzere, Ponte dos Frades, 40.403°N, 7.526°W, 672 m a.s.l., 22 Aug. 2023, leg. Ferreira, Benitez-Bosco, Padilha, Andrade & Stur 1♂ (sequenced); • Seia, Rio Alva, Central hidroelétrica de Ponte dos Jugais, river, 40.385°N, 7.706°W, 555 m a.s.l., 23 Aug. 2023, leg. Ferreira, Benitez-Bosco & Padilha, 1♀ (sequenced); • Rio Alva, Nossa Senhora do Desterro, river, 40.395°N, 7.694°W, 791 m a.s.l., 23 Aug. 2023, leg. Ferreira, Benitez-Bosco & Padilha, 1♂ (sequenced); • Gouveia, Rio Mondego Casais de Folgosinho, 40.454°N, 7.493°W, 976 m a.s.l., 24 Aug. 2023, leg. Ferreira, Benitez-Bosco & Padilha, 1♀ (sequenced); • Manteigas, Mondego, Covão da ponte, 40.443°N, 7.514°W, 999 m a.s.l., 24 Aug. 2023, leg. Ferreira, Benitez-Bosco & Padilha, 1 deutonymph (sequenced). **Porto**, • Lousada, Moinho da Tapada, 41.263°N, 8.307°W, 178 m a.s.l., 1 Sep. 2023, Ferreira, Sousa, Cruz-Oliveira & Girão, 1 deutonymph (sequenced).

Remarks. This species was originally described from the island of Gotland, Sweden (Lundblad 1956), but later on synonymized with *L. porosa*. Recently Tyukosova et al. (2022) used material from Norway to redescribe *L. gibbosa* based on morphological and molecular evidence and showed that this species is widely distributed in southern Norway.

The sequenced specimens from Portugal were clustered within BOLD:ACR9744, which, in addition to the specimens from Portugal, includes specimens of *L. gibbosa* from the Netherlands, Norway, Poland, and Germany, available in BOLD.

Distribution. As this species has been widely overlooked with other species of *L. porosa* complex, the full geographical distribution of *L. gibbosa* cannot be defined without additional research.

Lebertia (*Pilolebertia*) *algeriensis* Lundblad, 1942

Material examined. Portugal, **Guarda**: • Gouveia, Rio Mondego Casais de Folgosinho, 40.454°N, 7.493°W, 976 m a.s.l., 24 Aug. 2023, leg. Ferreira, Benitez-Bosco & Padilha, 1♀ (sequenced; Table 1); • Seia, Rio Alva, Praia fluvial de Vila Cova a Coelheira, river, 40.379°N, 7.736°W, 312 m a.s.l., 23 Aug. 2023, leg. Ferreira, Benitez-Bosco & Padilha, 1♂, 1♀ (sequenced).

Remarks. The Portuguese specimens molecularly analyzed in this study match the description of *Lebertia algeriensis*. Genetic data indicate that all examined specimens form a unique BIN (BOLD:AFV0271), and the closest neighboring BIN is that of *L. inaequalis* (BOLD:AEF5683) from North Macedonia. The *p*-distance between these two BINs was estimated at 4.53%.

Distribution. Palaearctic. Gerecke (2009) mentioned that several published records of *L. inaequalis* (Koch, 1837) from the Mediterranean region could refer to similar *L. longiseta* or *L. algeriensis*. New for Portugal.

Lebertia (*Pilolebertia*) *insignis* Neuman, 1880

Material examined. Portugal, **Guarda:** • Manteigas, Poço do Inferno, 40.373°N, 7.516°W, 1078 m a.s.l., 21 Aug. 2023, leg. Ferreira, Benitez-Bosco & Padilha, 1♂ (sequenced); • Seia, Rio Alva, Praia fluvial de Vila Cova a Coelheira, river, 40.379°N, 7.736°W, 312 m a.s.l., 23 Aug. 2023, leg. Ferreira, Benitez-Bosco & Padilha, 1♂ (sequenced). **Porto**, • Lousada, Moinho da Tapada, 41.263°N, 8.307°W, 178 m a.s.l., 1 Sep. 2023, Ferreira, Sousa, Cruz-Oliveira & Girão, 1♀ (sequenced).

Remarks. The sequenced specimens from Portugal clustered within two BINs, BOLD:AEB9107, which includes specimens of *L. insignis* from Norway, Montenegro, Poland and Slovakia, and the unique BOLD:AFW6960, which includes one specimen from this study collected in Rio Alva in Guarda Province. The *p*-distance between these two BINs was estimated at 9.79%, indicating the need for taxonomic revision of *L insignis* complex to identify possible undescribed cryptic species.

Distribution. Central, Western and Northern Europe. Rare in the Mediterranean and on the Iberian Peninsula previously known only from Oviedo in Spain (Lundblad 1956). New for Portugal.

Lebertia (*Pilolebertia*) *porosa* aggr. sp. A

Material examined. Portugal, **Guarda**: • Seia, Rio Alva, Praia Fluvial de Sabugueiro, river, 40.401°N, 7.64°W, 1021 m a.s.l., 24 Aug. 2023, leg. Ferreira, Benitez-Bosco & Padilha, 2♀ (sequenced); • Manteigas, Poço do Inferno, 40.373°N, 7.516°W, 1078 m a.s.l., 21 Aug. 2023, leg. Ferreira, Benitez-Bosco & Padilha, 2♀ (sequenced); • Rio Alva, Nossa Senhora do Desterro, river, 40.395°N, 7.694°W, 791 m a.s.l., 23 Aug. 2023, leg. Ferreira, Benitez-Bosco & Padilha, 1♂ (sequenced); • Seia, Rio Alva, Praia fluvial de Vila Cova a Coelheira, river, 40.379°N, 7.736°W, 312 m a.s.l., 23 Aug. 2023, leg. Ferreira, Benitez-Bosco & Padilha, 2♀ (sequenced); • Manteigas, Mondego, Covão da ponte, 40.443°N, 7.514°W, 999 m a.s.l., 24 Aug. 2023, leg. Ferreira, Benitez-Bosco & Padilha, 2♀ (sequenced); • Gouveia, Rio Mondego, Casais de Folgosinho, 40.454°N, 7.493°W, 976 m a.s.l., 24 Aug. 2023, leg. Ferreira, Benitez-Bosco & Padilha, 1♀ (sequenced).

Remarks. The sequenced specimens from Portugal clustered within BOLD:ACP5319, which includes *porosa*-like specimens from Serbia and Spain, and specimens from Germany and Norway provisionally assigned by Tyukosova et al. (2022) to *L. porosa* aggr. sp. A.

Distribution. As this species has been widely overlooked with other species of *L. porosa* complex, the full geographical distribution of *L. porosa* aggr. sp. A. can be defined only on the basis of the records available in BOLD.

***Lebertia* (*Pilolebertia*) *porosa* aggr. sp.**

BOLD:ACS0974

Material examined. Portugal, **Guarda**: • Seia, Rio Alva, Praia Fluvial de Sabugueiro, river, 40.401°N, 7.64°W, 1021 m a.s.l., 24 Aug. 2023, leg. Ferreira, Benitez-Bosco & Padilha, 1♀ (sequenced); • Gouveia, Rio Mondego, Casais de Folgosinho, 40.454°N, 7.493°W, 976 m a.s.l., 24 Aug. 2023, leg. Ferreira, Benitez-Bosco & Padilha, 1♂, 1♀ (sequenced); • Manteigas, Poio do Leão, 40.399°N, 7.541°W, 734 m a.s.l., 22 Aug. 2023, leg. Ferreira, Benitez-Bosco & Padilha, 1♀ (sequenced); • Manteigas, Zêzere, Ponte dos Frades, 40.403°N, 7.526°W, 672 m a.s.l., 22 Aug. 2023, leg. Ferreira, Benitez-Bosco, Padilha, Andrade & Stur, 1♀ (sequenced); • Seia, Rio Alva, Praia fluvial de Vila Cova a Coelheira, river, 40.379°N, 7.736°W, 312 m a.s.l., 23 Aug. 2023, leg. Ferreira, Benitez-Bosco & Padilha, 1♀ (sequenced); • Seia, Rio Alva, Nossa Senhora do Desterro, river, 40.395°N, 7.694°W, 791 m a.s.l., 23 Aug. 2023, leg. Ferreira, Benitez-Bosco & Padilha, 1 deutonymph (sequenced). **Bragança**: • Mirandela, Torre de Dona Chama, 41.665°N, 7.146°W, 256 m a.s.l., 13 Jul. 2023, leg. Ferreira & Padilha, 1 deutonymph (sequenced); • Vinhais, Gasparona, 41.85°N, 7.013°W, 693 m a.s.l., 6 Jul. 2023, leg. Ferreira & Padilha, 1 deutonymph (sequenced). **Porto** • Lousada, Moinho da Tapada, 41.263°N, 8.307°W, 178 m a.s.l., 1 Sep. 2023, Ferreira, Sousa, Cruz-Oliveira & Girão, 1♀ (sequenced).

Remarks. The sequenced specimens from Portugal clustered within BOLD:ACS0974, which includes *porosa*-like specimens from different parts of Europe, except Fennoscandia, available in BOLD. In the phylogenetic tree, the BIN is positioned as a sister clade of *L. porosa* as defined by Tyukosova et al. (2022). The latter species was recently redefined by Tyukosova et al. (2022) based on the specimens from the type locality that were shown to belong to BOLD:ACQ9049. The taxonomic status of *L. porosa* like species of BOLD:ACS0974 needs to be clarified by resolving taxonomic status of numerous species listed as synonyms in Gerecke (2009). As emphasized by Gerecke et al. (2022), a more extensive study of *L. porosa* complex is needed to establish a stable taxonomy for this group.

Distribution. As this species has been widely overlooked with other species of *L. porosa* complex, the geographical distribution of *L. porosa* like species of BOLD:ACS0974 can be defined only on the basis of the records available in BOLD.

***Lebertia* (*Pilolebertia*) *pilosa* Maglio, 1924**

Material examined. Portugal, **Beja**: • Odemira, Ribeira de Seixe, Zambujeira do Mar, river, 37.399°N, 8.723°W, 45 m a.s.l., 23 May 2023, leg. Ekrem & Benitez-Bosco, 4♀ (sequenced), 1♀ dissected and slide mounted (RMNH).

Remarks. The sequenced specimens from Portugal were clustered within BOLD:AEJ2601, which, in addition to material from this study, include one unidentified *Lebertia* specimen from Spain. The *p*-distance between the latter BIN and its nearest neighbor, BOLD:ACS0974, which include *L. porosa* like specimens from different parts of Europe, was estimated at 12.01%.

Distribution. Europe. In Portugal previously reported from Minho River (Cantallo et al. 2021), and from São Pedro da Torre in Valença municipality (Cantallo et al. 2022).

***Lebertia* (*Lebertia*) *pusilla* Koenike, 1911**

Material examined. Portugal, **Porto**: • Lousada, Moinho da Tapada, 41.263°N, 8.307°W, 178 m a.s.l., 1 Sep. 2023, Ferreira, Sousa, Cruz-Oliveira & Girão, 1 ♂ (sequenced).

Remarks. The sequenced specimen from Moinho da Tapada cluster together with specimens collected by Pešić et al. (2023b) from Santarém, Portugal, and morphologically assigned to *L. pusilla*. These specimens form a unique BIN (BOLD:AFW6961), with a *p*-distance of 10.43% to the nearest sequence (NLACA493-15) of *L. pusilla* from the Netherlands.

Distribution. Europe.

Family Oxiidae K. Viets, 1926

Genus *Oxus* Kramer, 1877

Note. Four species known for Portugal: two of them, *Oxus hastata* (Lundblad, 1954) and *O. lusitanicus* Lundblad, 1954, originally described from Portugal. *Oxus oblongus* Kramer, 1879, reported by Lundblad (1956) from Sintra, is a possible synonym of *O. strigatus* (Di Sabatino et al. 2010; Smit and Gerecke 2010).

***Oxus* (*Oxus*) cf. *angustipositus* K. Viets, 1908**

Material examined. Portugal, **Guarda**: • Manteigas, Casa do Cantoneiro, 40.418°N, 7.603°W, 1378 m a.s.l., 24 Aug. 2023, leg. Ferreira, Benitez-Bosco & Padilha, 2♂ (sequenced); • Manteigas, Poço do Inferno, 40.373°N, 7.516°W, 1078 m a.s.l., 21 Aug. 2023, leg. Ferreira, Benitez-Bosco & Padilha, 1♀ (sequenced).

Remarks. The examined specimens cluster within BOLD:AET9442, which includes specimens from Portugal assigned by Pešić et al. (2023b) to *Oxus* cf. *angustipositus*. As emphasized by Pešić et al. (2023b) taxonomic revision of the *O. angustipositus* complex is required for identifying possibly undescribed cryptic species.

Distribution. Europe. In Portugal previously reported from Porto (Pešić et al. 2023b).

Oxus (*Oxus*) *lusitanicus* Lundblad, 1954

Material examined. Portugal, **Guarda**: • Gouveia, Rio Mondego, Casais de Folgosinho, 40.454°N, 7.493°W, 976 m a.s.l., 24 Aug. 2023, leg. Ferreira, Benitez-Bosco & Padilha, 1♀, 1 deutonymph (sequenced). **Beja** • Mértola, Moinho de Alferes 2, 37.503°N, 7.687°W, 19 May 2023, leg. Ferreira, Benitez-Bosco, Ekrem, Stur & Turaccio, 1♂, 1♀ (sequenced). **Bragança** • Mirandela, Torre de Dona Chama, 41.665°N, 7.146°W, 256 m a.s.l., 13 Jul. 2023, leg. Ferreira & Padilha, 1♂, 1♀ (sequenced). **Vila Real** • Murça, Noura stream, 41.409°N, 7.417°W, 421 m a.s.l., 12 Jul. 2023 leg. Ferreira & Padilha, 1♀ (sequenced).

Remarks. The examined specimens match the description of *Oxus lusitanicus*, a species originally described by Lundblad (1954) based on a single male collected in Côa River in Portugal. The specimens from Portugal used in this study for molecular analysis form a unique BIN (BOLD:AFX3224) with the nearest neighboring BIN being BOLD:ACL5934, which includes specimens of unidentified *Oxus* sp. from Canada, with the *p*-distance estimated at 14.34%.

Distribution. Portugal previously recorded from Beira Alta (Lundblad 1956).

Oxus (*Oxus*) *musculus* (Müller, 1776)

Material examined. Portugal, **Beja** • Mértola, Moinho de Alferes 1, 37.502°N, 7.69°W, 19 May 2023, leg. Ferreira, Benitez-Bosco, Ekrem, Stur & Turaccio, 1♀ (sequenced).

Remarks. The sequenced specimens from Portugal were clustered within BOLD:AFC2154, which includes specimens of *O. musculus* from Norway.

Distribution. Palaearctic. Widespread in Europe, but here reported for the first time for Portugal.

Oxus (*Oxus*) *ovalis* (Müller, 1776)

Material examined. Portugal, **Beja** • Odemira, Ribeira de Seixe, Zambujeira do Mar, 37.399°N, 8.723°W, 45 m a.s.l., 23 May 2023, leg. Ekrem & Benitez-Bosco, 1♂, 1♀ (sequenced).

Remarks. The sequenced specimens from Zambujeira do Mar, keyed to *Oxus ovalis* following Di Sabatino et al. (2010), form a unique BIN (BOLD:AFP5747).

Distribution. Widespread in Europe, but here reported for the first time for Portugal.

Oxus (*Gnaphiscus*) *setosus* (Koenike, 1898)

Material examined. Portugal, **Guarda**: • Gouveia, Rio Mondego, Casais de Folgosinho, 40.454°N, 7.493°W, 976 m a.s.l., 24 Aug. 2023, leg. Ferreira, Benitez-Bosco & Padilha, 1♀ (sequenced); • Manteigas, Mondego, Covão da ponte, 40.443°N, 7.514°W, 999 m a.s.l., 24 Aug. 2023, leg. Ferreira, Benitez-Bosco & Padilha, 1♀ (sequenced).

Remarks. The sequenced specimens from Portugal clustered within BOLD:ACS0808, which includes specimens of *O. setosus* from the Netherlands.

Distribution. Palaearctic. Widespread in Europe, but here reported for the first time for Portugal.

Family Sperchontidae Thor, 1900

Genus *Sperchon* Kramer, 1877

Note. Five species known from Portugal.

Sperchon (*Hispidosperchon*) *algeriensis* Lundblad, 1942

Material examined. Portugal, **Faro** • Portimão, 37.237°N, 8.546°W, 23 May 2023, leg. Ferreira & Turaccio 1♀ (sequenced).

Remarks. The single female from Portugal clusters within BOLD:AES2436, which includes one specimen of *S. algeriensis* recently collected from eastern Spain (López-Peña et al. 2022). The species was described from northern Africa (Lundblad 1942) and subsequently recorded from many sites in the central and western Mediterranean area (Di Sabatino et al. 2010). The species is considered as a characteristic species of warm Mediterranean streams that regularly dry up in the summer (Gerecke 1991). The hydrography of the sampling site where *S. algeriensis* was found in our study is characterized by summer drought.

The high genetic distance of 15.4% between Iberian populations of *S. algeriensis* and a specimen from Iran, attributed to *S. algeriensis*, suggests that the latter belongs to a further distinct species (Pešić et al. 2022a). It is likely that the latter species represents *S. beneckei* Bader & Sepasgosarian, 1982, a species proposed to be a synonym of *S. algeriensis* by Asadi et al. (2010). Therefore, the known populations of *S. algeriensis* from Eastern Mediterranean should be checked using molecular methods to see if they can be assigned to *S. beneckei*.

Distribution. North Africa, west Mediterranean. New record for Portugal.

Sperchon (*Hispidosperchon*) *clupeifer* Piersig, 1896

Material examined. Portugal, **Guarda** • Gouveia, Rio Mondego, Casais de Folgosinho, 40.454°N, 7.493°W, 976 m a.s.l., 24 Aug. 2023, leg. Ferreira, Benitez-Bosco & Padilha, 1♂ (sequenced).

Remarks. The single male from Portugal used in this study for molecular analysis matches the description of *S. clupeifer.* This specimen forms a unique BIN (BOLD:AFX0389). The *p*-distance to its nearest neighboring BIN (BOLD:ACS1100), which includes specimens of *S. clupeifer* from the Netherlands, Germany, Norway, Macedonia, Montenegro, Russia, Serbia, Austria, and Italy, was estimated at 7.06%.

Distribution. Western Palaearctic. In Portugal previously reported from Fonte Fria in Mealhada (Buçaco Mountain; Lundblad 1956).

***Sperchon* (*Hispidosperchon*) *compactilis* Koenike, 1911**

Material examined. Portugal, **Beja** • Faro, Portimão, 37.237°N, 8.546°W, 23 May 2023, leg. Ferreira & Turaccio 1♀ (sequenced). **Guarda** • Seia, Rio Alva, Praia fluvial de Vila Cova a Coelheira, river, 40.379°N, 7.736°W, 312 m a.s.l., 23 Aug. 2023, leg. Ferreira, Benitez-Bosco & Padilha, 1♀ (sequenced).

Remarks. The sequences obtained from two Portuguese specimens, keyed to *S. compactilis* following Di Sabatino et al. (2010), clustered in BOLD:AER7687, which, in addition to specimens used in this study, includes two specimens from Austria and Spain.

Distribution. Western Palaearctic. New record for Portugal.

Family Torrenticolidae Piersig, 1902

Genus *Monatractides* K. Viets, 1926

Note. So far, two species of the genus are known from Portugal.

***Monatractides* (*Monatractides*) *madritensis* (K. Viets, 1930)**

Material examined. Portugal, **Guarda**: • Seia, Rio Alva, Praia Fluvial de Sabugueiro, river, 40.401°N, 7.64°W, 1021 m a.s.l., 24 Aug. 2023, leg. Ferreira, Benitez-Bosco & Padilha, 1♂ (sequenced); • Manteigas, Poço do Inferno, 40.373°N, 7.516°W, 1078 m a.s.l., 21 Aug. 2023, leg. Ferreira, Benitez-Bosco & Padilha, 1♀ (sequenced); • Manteigas, Poio do Leão, 40.399°N, 7.541°W, 734 m a.s.l., 22 Aug. 2023, leg. Ferreira, Benitez-Bosco & Padilha, 2♀ (sequenced). **Bragança** • Vinhais, Gasparona, 41.85°N, 7.013°W, 693 m a.s.l., 6 Jul. 2023, leg. Ferreira & Padilha, 1♀ (sequenced).

Remarks. The Portuguese specimens match the description of *M. madritensis*. The specimens clustered within BOLD:AED3803, which includes specimens of *M. madritensis* from Montenegro, Serbia and Italy, available in BOLD.

Distribution. Europe. New record for Portugal.

***Monatractides* (*Monatractides*) *stadleri* (Walter, 1924)**

Material examined. Portugal, **Faro** • Monchique, Ribeira de Seixe, Parque do Barranco dos Pisões, stream, 37.333°N, 8.567°W, 23 May 2023, leg. Ekrem & Benitez-Bosco, 1♀ (sequenced). **Guarda**: • Gouveia, Rio Mondego, Casais de Folgosinho, 40.454°N, 7.493°W, 976 m a.s.l., 24 Aug. 2023, leg. Ferreira, Benitez-Bosco & Padilha, 1♀ (sequenced); • Seia, Rio Alva, Central hidroelétrica de Ponte dos Jugais, river, 40.385°N, 7.706°W, 555 m a.s.l., 24 Aug. 2023, leg. Ferreira, Benitez-Bosco & Padilha, 1♀ (sequenced); • Seia, Rio Alva, Praia fluvial de Vila Cova a Coelheira, river, 40.379°N, 7.736°W, 312 m a.s.l., 23 Aug. 2023, leg. Ferreira, Benitez-Bosco & Padilha, 1♂ (sequenced); • Seia, Casa do Loureiro, 40.433°N, 7.701°W, 415 m a.s.l., 19 July 2023 leg. Ferreira & Padilha, 1♀ (juv.) (sequenced).

Remarks. The females used in this study for molecular analysis were clustered within BOLD:AEU1504, which includes two specimens of *M. stadleri* from Belgium, one specimen from Spain (identified as *Torrenticola* sp., deposited in Taxus Medio Ambiente, Spain), and one specimen recently collected from the stream in Beja Province and assigned to *M. stadleri* by Pešić et al. (2023b).

Distribution. Europe. In Portugal previously reported from Corgo da Ponte Quebrada, Beja (Pešić et al. 2023b).

***Monatractides* (*Monatractides*) *stenostomus* (K. Viets, 1930)**

Material examined. Portugal, Beja • Mértola, Corte do Pinto, 37.682°N, 7.512°W, 19 May 2023, leg. Ferreira, Benitez-Bosco, Ekrem, Stur & Turaccio, 1♂ (sequenced), dissected and slide mounted (RMNH),

Remarks. The Portuguese specimen molecularly analyzed in this study matches the description of *M. stenostomus*. This individual forms a unique BIN (BOLD:AFU3082), with the nearest neighboring BIN being BOLD:ADZ9854, which includes three specimens of an unidentified *Monatractides* sp. from Morocco, with the *p*-distance estimated at 6.74%.

Distribution. Spain, France. In Portugal previously reported from Beira Alta (Santa Comba Dão; Lundblad 1956).

Genus *Torrenticola* Piersig, 1896

Note. So far 12 species of the genus were reported from Portugal, nine of them known from Madeira Island and four species from the mainland

***Torrenticola* (*Torrenticola*) *elliptica* Maglio, 1909**

Material examined. Portugal, **Bragança** • Vinhais, Gasparona, 41.85°N, 7.013°W, 693 m a.s.l., 6 Jul. 2023, leg. Ferreira & Padilha, 1♀ (sequenced).

Remarks. The single Portuguese specimen molecularly analyzed in this study was a juvenile female that does not allow for a confident identification to the species level. Molecular data, however, revealed that the DNA barcode of the Portuguese specimen falls into BOLD:AEI9183, which includes one specimen from Montenegro, morphologically assigned by the first author to *T. elliptica*.

Distribution. Palaearctic. New for Portugal.

***Torrenticola* (*Torrenticola*) *soniae* Pešić, sp. nov.**

https://zoobank.org/E0A41268-B54C-4366-9886-E2954F1BF00B
Figs 1, 2, 5A

Type material examined. ***Holotype*** • ♂, dissected and slide mounted (RMNH), Portugal, **Guarda**, Seia, Rio Alva, Praia Fluvial de Sabugueiro (Fig. 5D), river, 40.401°N, 7.64°W, 1021 m a.s.l., 24 Aug. 2023, leg. Ferreira, Benitez-Bosco &

Padilha, sequenced (BOLD ID: BSNTN961-23). ***Paratypes***: • 2♂ (sequenced), Portugal, **Guarda**, Seia, Rio Alva, Praia fluvial de Vila Cova a Coelheira, river, 40.379°N, 7.736°W, 312 m a.s.l., 23 Aug. 2023, leg. Ferreira, Benitez-Bosco & Padilha; • 1♂ (sequenced); Manteigas, Zêzere, Ponte dos Frades, 40.403°N, 7.526°W, 672 m a.s.l., 22 Aug. 2023, leg. Ferreira, Benitez-Bosco, Padilha, Andrade & Stur; • 1♀ (sequenced), dissected and slide mounted (RMNH), Guarda, Gouveia, Rio Mondego, Casais de Folgosinho, 40.454°N, 7.493°W, 976 m a.s.l., 24 Aug. 2023, leg. Ferreira, Benitez-Bosco & Padilha; • 1♀ (juv.; sequenced), **Bragança,** Mirandela, Torre de Dona Chama, 41.665°N, 7.146°W, 256 m a.s.l., 13 Jul. 2023, leg. Ferreira & Padilha.

Diagnosis. *Morphological*: Cx-I relatively short, anteriorly broad; suture lines of Cx-IV prominent, starting at right angle from genital field; ejaculatory complex with well-developed anterior keel and proximal arms; gnathosomal rostrum short, less than width of gnathosoma; P-3 with a subrectangular, apically serrated ventrodistal projection. ***Molecular*:** this lineage represented by a unique BIN (BOLD:AFW5337) differs from *T. brevirostris* clade by 12.27% K2P for COI.

Description. *General features.* Idiosoma roundish; dorsal shield without a color pattern as photographed in Figs 2B, 5A; area of primary sclerotization of the dorsal plate with two dorsoglandularia (Fig. 1A); frontal platelets broad, relatively short; Cx-I relatively short, anteriorly broad; gnathosomal bay U-shaped, proximally rounded; Cxgl-4 subapical; medial suture line of Cx-II+III relatively short; postgenital area extended; excretory pore and Vgl-2 away from the line of primary sclerotization, excretory pore on the level of Vgl-2; gnathosomal rostrum short, less than depth of gnathosoma (Fig. 1E); P-2 ventral margin nearly straight or slightly convex, P-2 ventrodistal protrusion bluntly pointed, apically serrated, P-3 with a subrectangular, apically serrated ventrodistal projection, P-4 with a ventral tubercle bearing one long and three shorter setae (Fig. 1C, D). **Male.** Suture line of Cx-IV evident, medially starting from posterior margin of genital field in a right angle to the main idiosoma axis; genital field large, subrectangular; ejaculatory complex conventional in shape, anterior keel, proximal and distal arms well developed (Fig. 1F). **Female.** Genital field large and pentagonal in shape, suture lines of Cx-IV extending posteriorly beyond posterior margin of genital field, laterally curved.

Measurements. Male (holotype). Idiosoma (ventral view: Fig. 1B) L 912, W 669; dorsal shield (Fig. 1A) L 756, W 581, L/W ratio 1.3; dorsal plate L 700; shoulder plate L 220–222, W 97, L/W ratio 2.27–2.29; frontal plate L 150–156, W 78–88, L/W ratio 1.8–1.9; shoulder/frontal plate L 1.42–1.47. Gnathosomal bay L 171, Cx-I total L 359, Cx-I mL 188, Cx-II+III mL 137; ratio Cx-I L/Cx-II+III mL 2.63; Cx-I mL/Cx-II+III mL 1.37. Genital field L/W 191/163, ratio 1.17; distance genital field-excretory pore 116, genital field-caudal idiosoma margin 209. Ejaculatory complex L 291.

Gnathosoma vL 331, chelicera L 375; palp total L 398, dL/H, dL/H ratio: P-1, 39/39, 1.0; P-2, 117/73, 1.59; P-3, 84/63, 1.35; P-4, 120/42, 2.86; P-5, 38/17, 2.18; L ratio P-2/P-4, 0.98. dL of I-L-4–6: 134, 150, 136; I-L-6 H 100; dL/H I-L-6 ratio 1.36.

Female (paratype from Casais de Folgosinho, BGE_00227_F02). Idiosoma (ventral view: Fig. 2C) L 1033, W 828; dorsal shield (Fig. 2A, B) L 844, W 725, L/W ratio 1.16; dorsal plate L 781; shoulder plate L 222–235, W 100–102, L/W ratio 2.2–2.3; frontal plate L 173–175, W 97–98, L/W ratio 1.79; shoulder/frontal plate L 1.28–1.34. Gnathosomal bay L 200, Cx-I total L 384, Cx-I mL 184, Cx-II+III mL 18; ratio Cx-I L/Cx-II+III mL 21.3; Cx-I mL/Cx-II+III mL 10.2. Genital field L/W 221/198, ratio 1.12; distance genital field-excretory pore 250, genital field-caudal idiosoma margin 391.

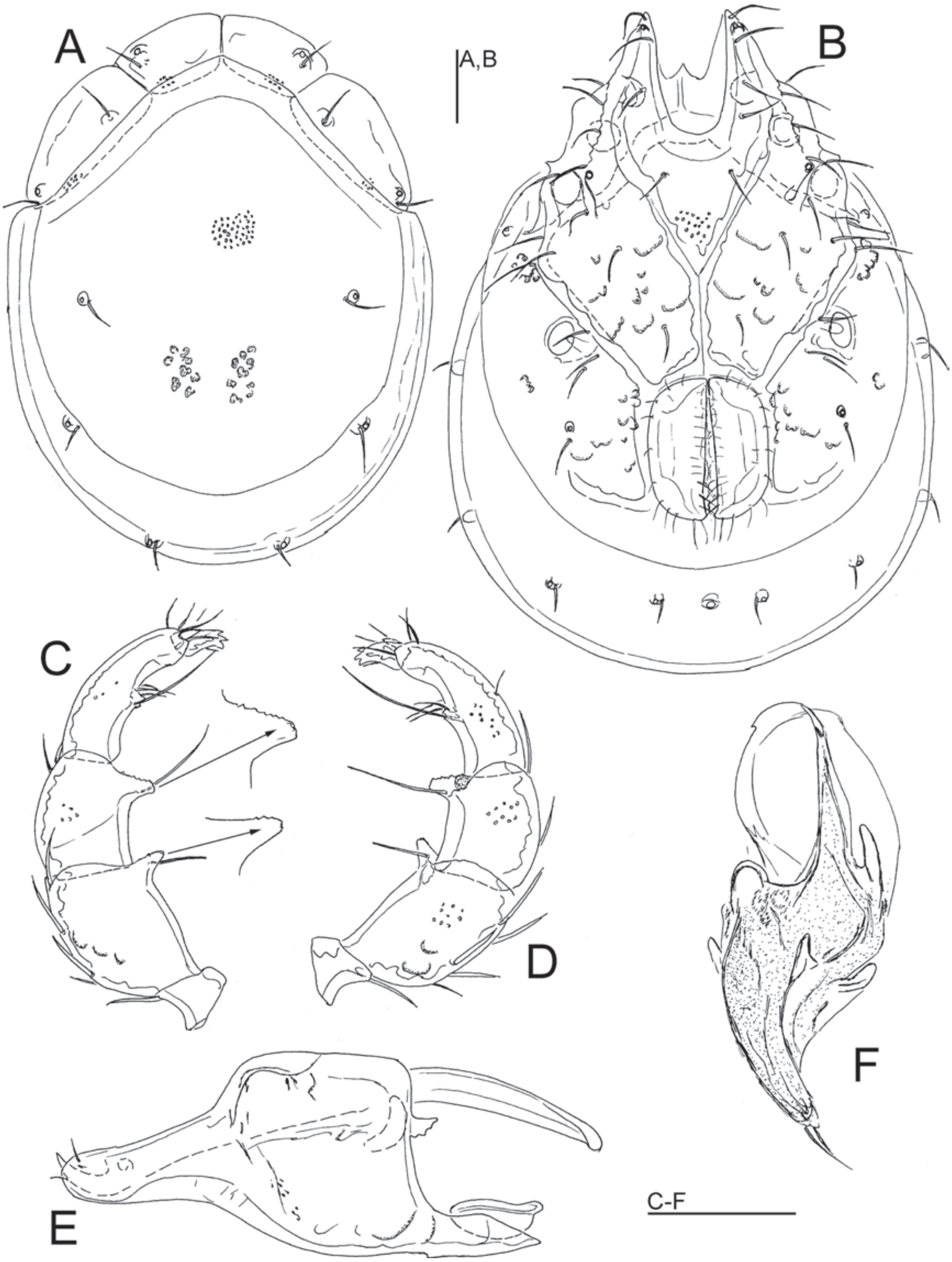

Figure 1. *Torrenticola soniae* sp. nov., ♂ holotype **A** dorsal shield **B** ventral shield **C** palp, medial view (inset: ventrodistal projections of P-2 and P-3, enlarged 2×) **D** palp, lateral view **E** gnathosoma and chelicera **F** ejaculatory complex. Scale bars: 100 µm.

Gnathosoma vL 350, chelicera L 409; palp total L 435, dL/H, dL/H ratio: P-1, 44/41, 1.08; P-2, 127/76, 1.67; P-3, 93/65, 1.44; P-4, 134/42, 3.18; P-5, 37/18, 2.0; L ratio P-2/P-4, 0.94.

Etymology. The species is dedicated to Sónia Ferreira (CIBIO, Portugal) for collecting numerous specimens used in this study and her enthusiastic support in the study of Portuguese water mites.

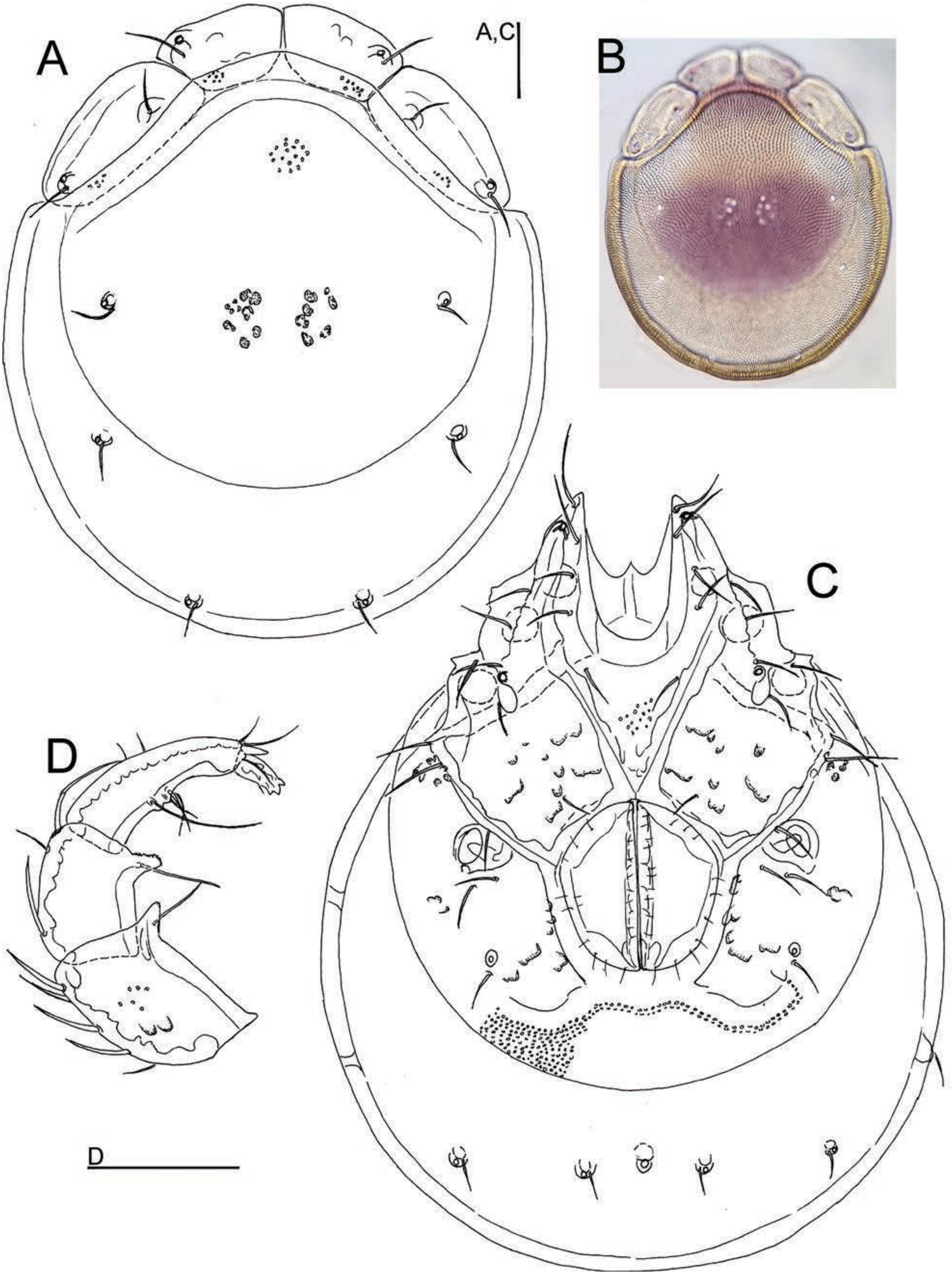

Figure 2. *Torrenticola soniae* sp. nov., ♀ paratype **A** dorsal shield **B** photograph of dorsal shield **C** ventral shield **D** palp, medial view (P-1 lacking). Scale bars: 100 µm.

Species delimitation using DNA barcodes. The final alignment for species delimitation using COI sequence data comprised 669 nucleotide positions (nps) of the 130 *Torrenticola* specimens listed in Suppl. material 2 and one outgroup, *Monatractides madritensis* from Portugal to root the tree. The NJ tree is presented in Fig. 6. The COI tree sequences retrieved from *Torrenticola* specimens from Portugal, here described as *T. soniae* sp. nov., appeared as a sister group to the cluster of sequences belonging to *T. brevirostris* (Halbert, 1911), a rhitrobiontic species widely distributed in Europe. The mean genetic distance between COI sequences of these two clusters was estimated at 12.27 ± 1.42% K2P. The genetic distance was considerably higher than the estimated barcode gap found by ASAP analyses (3–5%) of all studied *Torrenticola*, supporting the species-status of the new taxon. The mean intraspecific K2P-divergence within the cluster of the new species was 0.63 ± 0.19%.

Discussion. With regards to the presence of an anteriorly broad and short Cx-I, a robust and compact palp, and a deep gnathosoma with a short rostrum, the new species resembles *T. brevirostris*. The latter species can be separated from *T. soniae* sp. nov. by only slightly protruding ventrodistal projections of P-2 and particularly of P-3.

Distribution. Portugal (this study).

***Torrenticola* (*Torrenticola*) *elisabethae* Pešić, sp. nov.**

https://zoobank.org/354EB35B-1F5E-4FBB-9E8B-06B956A47467

Figs 3, 4, 5B, E

Type material examined. ***Holotype*** • ♂, dissected and slide mounted, Portugal, Guarda, Manteigas, Poço do Inferno (Fig. 5E), 40.373°N, 7.516°W, 1078 m a.s.l., 21 Aug. 2023, leg. Ferreira, Benitez-Bosco & Padilha, sequenced (BOLD ID: BSNTN984-23). ***Paratypes***: • 1♂, 1♀ (sequenced), Portugal, **Guarda**, Manteigas, Poio do Leão, 40.399°N, 7.541°W, 734 m a.s.l., 22 Aug. 2023, leg. Ferreira, Benitez-Bosco & Padilha, 1♀ dissected and slide mounted (RMNH).

Diagnosis. ***Morphological***: Shoulder platelets fused with dorsal plate; dorsal shield with color pattern as illustrated in Figs 4B, 5B; Cxgl–4 subapical; medial suture line of Cx-II+III in male relatively long; ejaculatory complex with poorly developed anterior keel and a relatively large proximal chamber. ***Molecular*****:** this lineage represent by a unique BIN (BOLD:AFW5336) differs from *T. lundbladi* clade by 9.8% K2P for COI.

Description. ***General features.*** Idiosoma oval; shoulder platelets fused to dorsal plate, but suture line visible; dorsal shield with a color pattern as illustrated in Figs 4B, 5B; area of primary sclerotization of the dorsal plate with four dorsoglandularia (Fig. 3A); gnathosomal bay U-shaped, proximally rounded; Cxgl–4 subapical; excretory pore and Vgl-2 on the the line of primary sclerotization, excretory pore on the level of Vgl-2; gnathosomal ventral margin curved, rostrum elongated (Fig. 3D); P-2 ventral margin nearly straight or slightly concave, P-2 and P-3 ventrodistal protrusions bluntly pointed, P-4 with a ventral tubercle bearing one long and three shorter setae (Figs 3C, 4D). **Male** — Medial suture line of Cx-II+III relatively long; genital field subrectangular; ejaculatory complex with poorly developed anterior keel, proximal chamber relatively large; Fig. 3E). **Female** — Genital field large and pentagonal in shape.

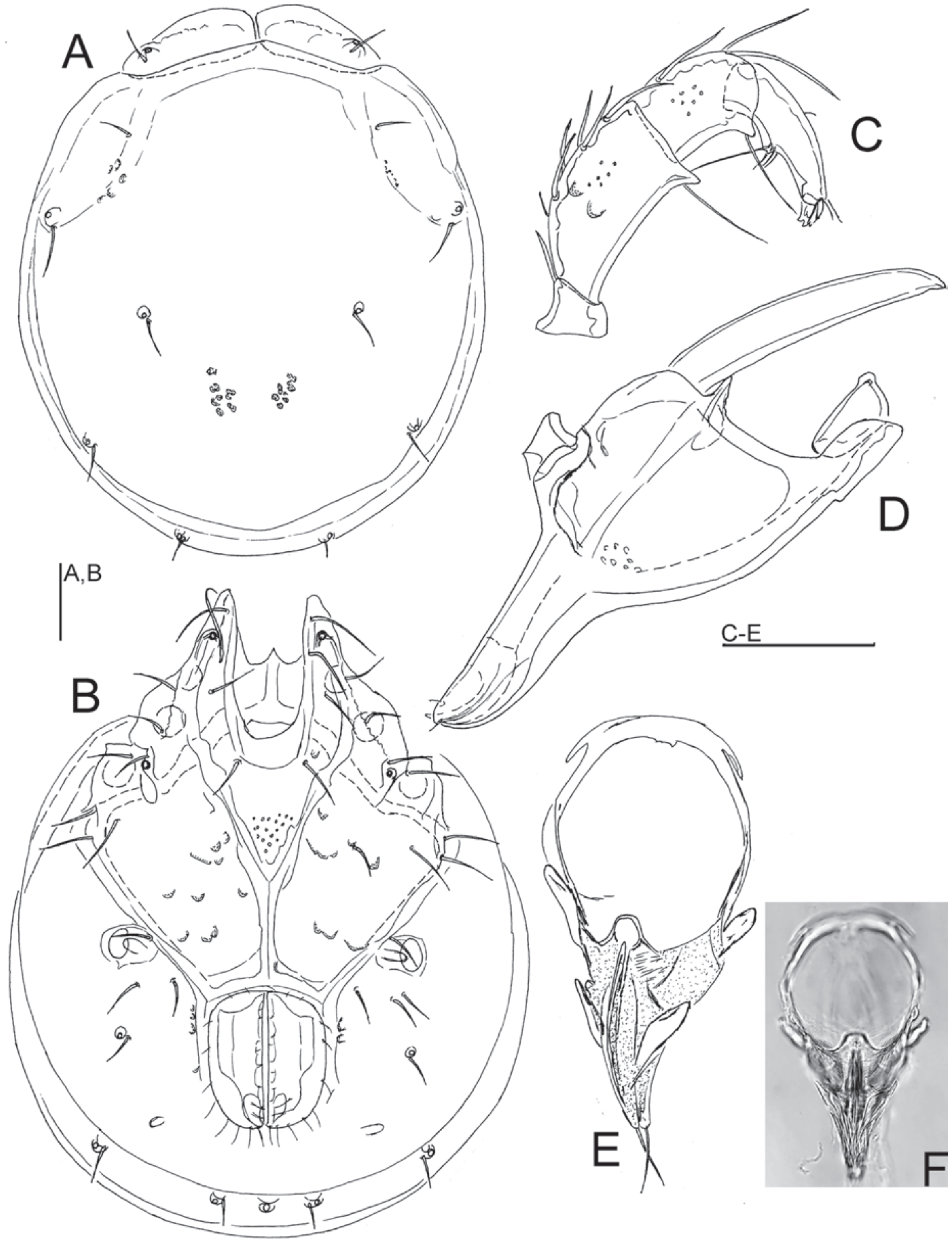

Figure 3. *Torrenticola elisabethae* sp. nov., ♂ holotype **A** dorsal shield **B** ventral shield C palp, medial view **D** gnathosoma and chelicera **E** ejaculatory complex **F** photograph of ejaculatory complex. Scale bars: 100 µm.

Measurements. Male (holotype). Idiosoma (ventral view: Fig. 3B) L 856, W 691; dorsal shield (Fig. 3A) L 731, W 619, L/W ratio 1.18; dorsal plate L 681; frontal plate L 173–183, W 64–66, L/W ratio 2.7–2.8. Gnathosomal bay L 194, Cx-I total L 383, Cx-I mL 188, Cx-II+III mL 131; ratio Cx-I L/Cx-II+III mL 2.92; Cx-I mL/Cx-II+III

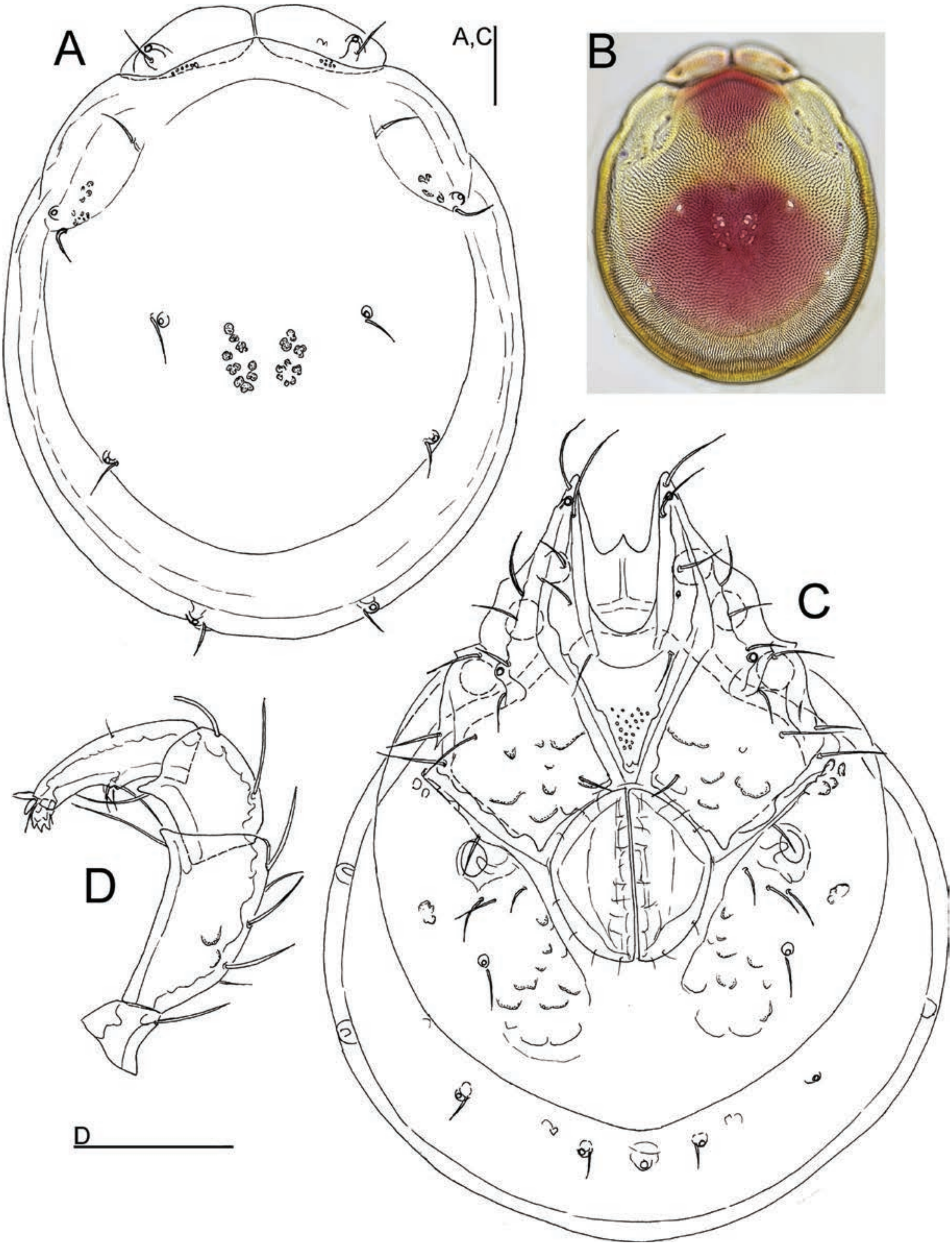

Figure 4. *Torrenticola elisabethae* sp. nov., ♀ paratype **A** dorsal shield **B** photograph of dorsal shield **C** ventral shield **D** palp, medial view. Scale bars: 100 µm.

mL 1.43. Genital field L/W 183/150, ratio 1.22; distance genital field-excretory pore 103, genital field-caudal idiosoma margin 127. Ejaculatory complex L 275.

Gnathosoma vL 367, chelicera L 448; palp total L 390, dL/H, dL/H ratio: P-1, 44/38, 1.17; P-2, 133/64, 2.08; P-3, 79/58, 1.36; P-4, 112/38, 2.98; P-5, 22/14, 1.55; L ratio P-2/P-4, 1.19. dL of I-L-4–6: 145, 160, 131; I-L-6 H 46; dL/H I-L-6 ratio 2.85.

Female (paratype from Poio do Leão, BGE_00227_H06). Idiosoma (ventral view: Fig. 4C) L 975, W 794; dorsal shield (Fig. 4A, B) L 806, W 663, L/W ratio 1.22; dorsal plate L 766; frontal plate L 172–175, W 63–68, L/W ratio 2.6–2.75. Gnathosomal bay L 203, Cx-I total L 391, Cx-I mL 188, Cx-II+III mL 0. Genital field L/W 214/204, ratio 1.05; distance genital field-excretory pore 256, genital field-caudal idiosoma margin 347. Egg (n = 1) maximum diameter 227.

Gnathosoma vL 379, chelicera L 478; palp total L 389, dL/H, dL/H ratio: P-1, 41/36, 1.15; P-2, 130/64, 2.0; P-3, 80/59, 1.35; P-4, 116/40, 2.87; P-5, 22/14, 1.55; L ratio P-2/P-4, 1.13.

Etymology. The new species is dedicated to Elisabeth Stur (NTNU University Museum Trondheim, Norway), who facilitated a number of barcoding projects on water mites in Europe.

Species delimitation using DNA barcodes. The sequences retrieved from *Torrenticola* specimens from Portugal, here described as *T. elisabethae* sp. nov., appeared as a sister group to the cluster containing sequences of *T. lundbladi* (K. Viets, 1930), a rhitrobiontic species known from Spain (Lundblad 1956; Pešić et al. 2012). The mean K2P genetic distance between COI sequences of *T. elisabethae* sp. nov. and *T. lundbladi* was estimated at 9.8 ± 1.25%. The genetic distance was also here higher than the barcode gap found for *Torrenticola* in the ASAP analysis, supporting the species-status of the new taxon. The mean intraspecific divergence within the cluster of barcodes belonging to *T. elisabethae* was relatively low (0.2 ± 0.14% K2P).

Discussion. The new species is most similar to *Torrenticola lundbladi* K. Viets, 1930, a species originally described from central Spain (K. Viets 1930). Both species have dorsal shield with the shoulder platelets partially fused with the dorsal plate, a similar color pattern of the dorsal shield, a Cxgl-4 situated subapically and a relatively long median suture line of Cx-II-III in male. *Torrenticola lundbladi* differs by the characteristic shape of the ejaculatory complex (proximal and distal arms short, proximal chamber large, proximal horns reduced, see Lundblad 1956: fig. 83E).

Distribution. Portugal (this study).

Torrenticola (*Torrenticola*) *tenuipalpis* Lundblad, 1956

Fig. 5C

Material examined. Portugal, **Guarda** • Gouveia, Rio Mondego, Casais de Folgosinho, 40.454°N, 7.493°W, 976 m a.s.l., 24 Aug. 2023, leg. Ferreira, Benitez-Bosco & Padilha, 1♀ (sequenced), dissected and slide mounted (RMNH).

Remarks. The Portuguese specimen matches the description of *Torrenticola tenuipalpis*, a species originally described by Lundblad (1956) as a “*variatio*” of *T. amplexa* based on a single female collected in a stream in Santa Comba Dão, Portugal. Recently, Cantallo et al. (2022) ranked the latter taxon as a distinct species. The sequenced specimen from Portugal forms a unique BIN (BOLD:AFV2021) with the nearest neighboring BIN (p-distance 12.2%) being BOLD:AFF4076, which consists of a single specimen of *T. ramini* from Iran.

Distribution. Portugal; known from Beira Alta (Lundblad 1956).

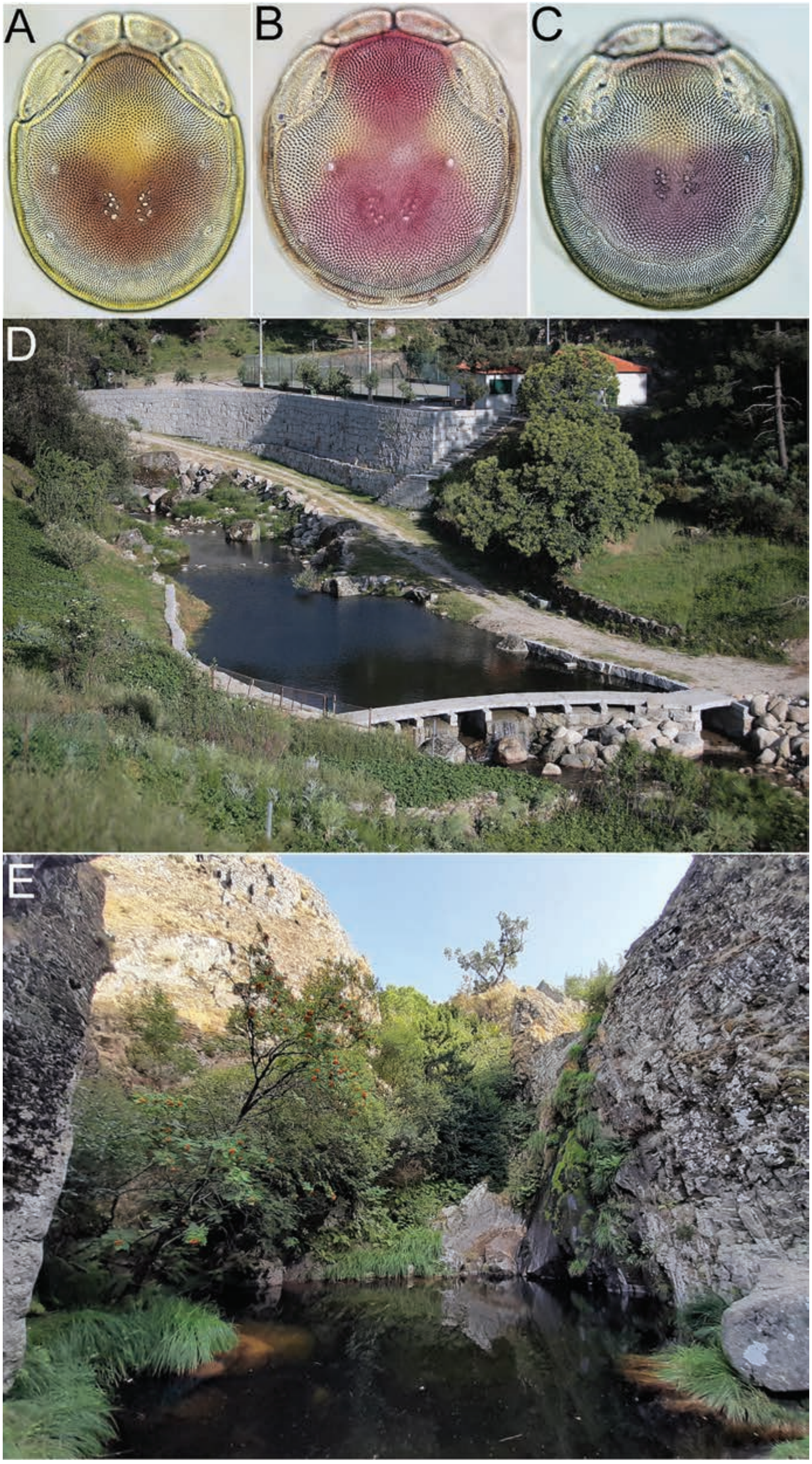

Figure 5. A–C Photographs of dorsal shield **A** *Torrenticola soniae* sp. nov., ♂ holotype **B** *T. elisabethae* sp. nov., ♂ holotype **C** *T. tenuipalpis*, ♀ (BGE_00227_F03) **D–E** Photographs of selected sampling sites **D** Praia Fluvial de Sabugueiro, *locus typicus* of *Torrenticola soniae* sp. nov. **E** Poço do Inferno, type locality of *T. elisabethae* sp. nov. Photographs by JC (5D) and SF (5E).

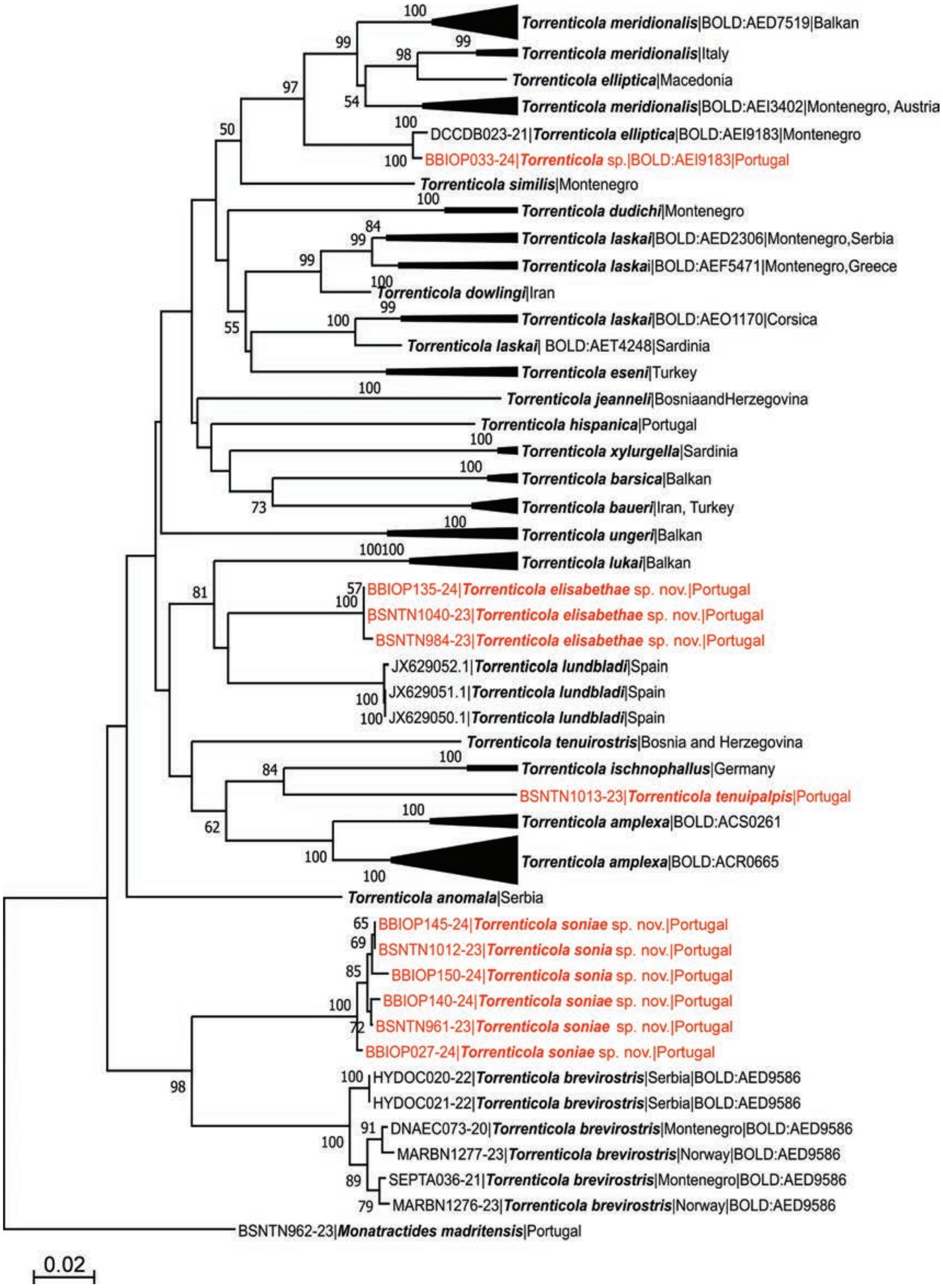

Figure 6. Neighbor-Joining tree of the genus *Torrenticola*, obtained from 130 nucleotide COI sequences. Bootstrap values > 50% from 1000 bootstrap replicates on branches.

Family Limnesiidae Thor, 1900

Genus *Limnesia* Koch, 1836

Note. In Portugal, represented by eight species, seven of them known from the mainland and one (*L. atlantica* Lundblad, 1941) known only from Madeira.

***Limnesia* (*Limnesia*) *acuminata* Walter, 1925**

Material examined. Portugal, **Beja** • Mértola, Moinho de Alferes 1, 37.502°N, 7.69°W, 19 May 2023, leg. Ferreira, Benitez-Bosco, Ekrem, Stur & Turaccio, 1♂ (sequenced). **Bragança**: • Mirandela, Torre de Dona Chama, 41.665°N, 7.146°W, 256 m a.s.l., 13 Jul. 2023, leg. Ferreira & Padilha, 2♂, 1♀ (sequenced).

Remarks. The Portuguese specimens match the description of *L. acuminata*. Genetic data indicate that specimens from Portugal form a unique cluster (BOLD:AFU7587).

Distribution. Western Mediterranean (Iberian Peninsula, southern France, Sardinia, Sicily, north Africa). In Portugal previously reported from Beira Alta, Alentejo, and Estremadura (Lundblad 1956).

***Limnesia* (*Limnesia*) *iberica* Lundblad, 1954**

Material examined. Portugal, **Beja** • Mértola, São João dos Caldeireiros, stream, 37.626°N, 7.81°W, 17 May 2023, leg. Ferreira, Benitez-Bosco, Ekrem, Stur & Turaccio, 3♂, 6♀ (sequenced).

Remarks. The specimens from Portugal morphologically matches description of *Limnesia iberica*, a species originally described by Lundblad (1956) from a stream in Beira Alta (Santa Comba Dão, Portugal). The Portuguese specimens form a distinct BIN (BOLD:AFN8367) with the closest BIN being BOLD:ACA9272, which includes specimens from Canada, United States, and Greece assigned to *L. undulata*, with the *p*-distance estimated at 14.29%.

Distribution. Portugal (Lundblad 1954, 1956; this study).

***Limnesia* (*Limnesia*) *koenikei* Piersig, 1894**

Material examined. Portugal, **Guarda**: • Seia, Covão do Forno, 40.369°N, 7.638°W, 1574 m a.s.l., 19 Aug. 2023, leg. Ferreira, Benitez-Bosco & Padilha, 1♂, 2♀ (sequenced); • Seia, Rio Alva, Central hidroelétrica de Ponte dos Jugais, river, 40.385°N, 7.706°W, 555 m a.s.l., 24 Aug. 2023, leg. Ferreira, Benitez-Bosco & Padilha, 1♂ (sequenced).

Remarks. The sequences obtained from the specimens from Portugal cluster within BOLD:ADF6559, which includes one specimen from the Netherlands assigned to *L. koenikei*. The *p*-distance from the latter BIN and its nearest neighbor BOLD:ACS0816, which includes specimens of *L. koenikei* from Norway and the Netherlands, was estimated at 2.09%.

Distribution. Holarctic; widely distributed in Europe but here reported for the first time for Portugal.

***Limnesia* (*Limnesia*) *maculata* (Müller, 1776)**

Material examined. Portugal, **Guarda**: • Seia, Rio Alva, Praia Fluvial de Sabugueiro, river, 40.401°N, 7.64°W, 1021 m a.s.l., 24 Aug. 2023, leg. Ferreira, Benitez-Bosco & Padilha, 1♀ (sequenced). **Beja** • Mértola, Moinho de Alferes 2, 37.503°N, 7.687°W, 19 May 2023, leg. Ferreira, Benitez-Bosco, Ekrem, Stur & Turaccio, 1♂ (juv.) (sequenced); • Mértola, Herdade de Alagães, pond, 37.673°N, 7.848°W, 18 May 2023, leg. Ferreira, Benitez-Bosco, Ekrem, Stur & Turaccio, 1♂, 1♀ (sequenced).

Remarks. The Portuguese specimens molecularly analyzed in this study match the description of *L. maculata*. These individuals form a unique BIN (BOLD:AFW6935), with the nearest neighboring BIN being BOLD:ACS0248, which includes specimens of *L. maculata* from Norway, the Netherlands and France. The *p*-distance between these two clusters was estimated at 4.3%.

Distribution. Holarctic. Widespread in Europe. In Portugal previously reported from Alentejo (Ribeira de Odivelas; Lundblad 1956).

***Limnesia* (*Limnesia*) *walteri* Migot, 1926**

Material examined. Portugal, **Beja** • Mértola, Corte do Pinto, 37.682°N, 7.512°W, 19 May 2023, leg. Ferreira, Benitez-Bosco, Ekrem, Stur & Turaccio, 3♀ (sequenced). **Bragança** • Mirandela, Torre de Dona Chama, 41.665°N, 7.146°W, 256 m a.s.l., 13 Jul. 2023, leg. Ferreira & Padilha, 1 ♀ (sequenced).

Remarks. The sequenced specimens from Portugal form a unique BIN (BOLD:AFO9873) with the nearest neighboring BIN being BOLD:ADZ9059 (*p*-distance 1.6%), which includes four unidentified *Limnesia* specimens from Morocco.

Distribution. North Africa, including the Sahara desert, Russia, southwestern Europe from Portugal (Lundblad 1956; Valdecasas 1988) to Greece (Gerecke et al. 2016). In Portugal previously reported from Beira Alta (Lundblad 1956).

Family Hygrobatidae Koch, 1842

Genus *Atractides* Koch, 1837

Note. Nine species known from Portugal, five of them endemic to Madeira, and *A. marizae* Pešić, 2023 endemic to mainland Portugal

***Atractides* (*Atractides*) *inflatus* (Walter, 1925)**

Material examined. Portugal, **Beja** • Odemira, Ribeira de Seixe, Herdade do Vale de Águia, river, 37.398°N, 8.68°W, 75 m a.s.l., 23 May 2023, leg. Ekrem & Benitez-Bosco, 2♀ (sequenced). **Vila Real** • Murça, Noura stream, 41.409°N, 7.417°W, 421 m a.s.l., 12 Jul. 2023 leg. Ferreira & Padilha, 1♀ (sequenced).

Remarks. The specimens from Portugal used in this study match the description of *A. inflatus*, a species widely distributed in the Mediterranean region, often very frequent in intermittent streams (Pešić et al. 2023c). The Portuguese specimens were clustered within two BINs: BOLD:AFI9009, which includes two specimens of *A. inflatus* from Italy, and BOLD:ACB4677, which includes specimens of *A. inflatus* from Iran, Morocco, Montenegro, Turkey, Greece, France, and Italy. The *p*-distance between these two BINs was estimated at 6.06%.

Distribution. Mediterranean, Iran. New for Portugal.

***Atractides* (*Atractides*) *marizae* Pešić, 2023**

Material examined. Portugal, **Guarda**: • Gouveia, Rio Mondego, Casais de Folgosinho, 40.454°N, 7.493°W, 976 m a.s.l., 24 Aug. 2023, leg. Ferreira, Benitez-Bosco & Padilha, 1♀ (sequenced); • Seia, Rio Alva, Praia fluvial de Vila Cova a Coelheira, river, 40.379°N, 7.736°W, 312 m a.s.l., 23 Aug. 2023, leg. Ferreira, Benitez-Bosco & Padilha, 1♀ (sequenced). **Faro**: • Monchique, Caldas de Monchique, 37.287°N, 8.554°W, 23 May 2023, leg. Ekrem & Benitez-Bosco, 1♀ (sequenced); • Aljezur, Ribeira de Seixe, Odeceixe, Covão da Serva, 37.374°N, 8.642°W, 100 m a.s.l., 23 May 2023, leg. Ekrem & Benitez-Bosco 1♀ (sequenced); • Portimão, 37.237°N, 8.546°W, 23 May 2023, leg. Ferreira & Turaccio 1♂ (sequenced).

Remarks. The specimens from Portugal clustered within BOLD:AER7878, which includes specimens of *Atractides marizae* Pešić, 2023, a species recently described by Pešić et al. (2023b) from Santarém, Portugal. Until now, this rhitrobiontic species was known only from the type locality (Caniceira stream), and the new findings presented in this study demonstrate that *A. marizae* is more widely distributed in Portugal.

Distribution. Portugal.

***Atractides* (*Atractides*) *nodipalpis* (Thor, 1899)**

Material examined. Portugal, **Guarda** • Seia, Rio Alva, Praia fluvial de Vila Cova a Coelheira, river, 40.379°N, 7.736°W, 312 m a.s.l., 23 Aug. 2023, leg. Ferreira, Benitez-Bosco & Padilha, 1♀ (sequenced).

Remarks. The female, which keyed to *A. nodipalpis* following Gerecke et al. (2016), forms a unique BIN (BOLD:AFV2009). The BIN is placed as sister to BOLD:ACR0209, which includes > 200 specimens of *A. nodipalpis*, available in the BOLD database. The *p*-distance between these two BINs was estimated at 4.61%.

For a long time, *A. nodipalpis* has been considered the most common species of the genus in Europe. However, in the last years, genetic data revealed that the latter species consists of several distinct lineages, some of them present in the same areas (Gerecke et al. 2022; Pešić et al. 2023d). For example, Gerecke et al. (2022) mentioned that Norwegian specimens keyed as *A. nodipalpis* belong to two different lineages, both widely distributed in Norway. The taxonomic status of most of these lineages is still unclear as a number of species have been proposed as synonyms of *A. nodipalpis* in the past. Nevertheless, Gerecke and collaborators (Gerecke pers. comm. 2022) recently clarified the correct BIN assignment of the true *A. nodipalpis* lineage. They found that specimens of *A. nodipalpis* collected near its type locality in Norway belong to the BOLD:ACR0209 cluster. After that, Pešić et al. (2023d) examined specimens from the Netherlands belonging to BOLD:ACR0209 and found that *A. nodipalpis* can be defined primarily by the shape of male genital plate which has a distinct anteromedial peg-like fissure.

Distribution. Based on the available records in BOLD, *A. nodipalpis* has a wide distribution, from SE Europe over the Fennoscandia up to Greenland. In Portugal previously reported from Beira Alta (Santa Comba Dão; Lundblad 1956).

***Atractides* (*Atractides*) *robustus* (Sokolow, 1940)**

Material examined. Portugal, **Guarda** • Manteigas, Zêzere, Covão da Ametade, 40.328°N, 7.587°W, 1431 m a.s.l., 21 Aug. 2023, leg. Ferreira, Benitez-Bosco & Padilha, 1♀ (sequenced).

Remarks. The Portuguese specimen matches the description of *A. robustus*. The specimen clusters within BOLD:AFF2463, which includes specimens from Italy, Albania and Poland. The *p*-distance from the closest neighboring BIN being BOLD:ADZ9348, which consists of specimens of *A. robustus* from Germany, Austria, Montenegro, Romania, Italy, Bosnia and Herzegovina, Albania, and Greece, was estimated at 3.15%.

Recently, Pešić et al. (2023d) showed that *A. robustus*, a species originally described from the Caucasus (the affluents of the Kuban River), consists of two distinct lineages, one which includes populations from eastern Turkey and northern Iran, and which is likely conspecific with *A. robustus*, and the second lineage, which includes *A. robustus* like specimens from central and southern Europe. The latter lineage, to which BOLD:ADZ9348 and BOLD:AFF2463 belong, possible represents a cryptic species new to science. The final decision on the taxonomic status of *A. robustus* lineages has been postponed until material of the latter species from the Caucasus is available (Pešić et al. 2023d).

Distribution. Europe. New for Portugal.

Genus *Hygrobates* Koch, 1837

Note. Five species known from mainland part of Portugal.

***Hygrobates balcanicus* Pešić, 2020**

Material examined. Portugal, **Faro** • Portimão, stream, 37.237°N, 8.546°W, 23 May 2023, leg. Ferreira & Turaccio, 2♂, 1♀ (sequenced). **Porto** • Lousada, Moinho da Tapada, 41.263°N, 8.307°W, 176 m a.s.l., 1 Sep. 2023, Ferreira, Sousa, Cruz-Oliveira & Girão, 1♂ (sequenced); • Lousada, Parque Molinológico e Florestal de Pias, 41.268°N, 8.256°W, 170 m a.s.l., 1 Sep. 2023, leg. Ferreira, Sousa, Cruz-Oliveira & Girão, 1♂ (sequenced); • Vila do Conde, Rio Este, 41.378°N, 8.695°W, 15 m a.s.l., 7 Sep. 2023, leg. Ferreira, Cruz-Oliveira & Girão, 3♂, 1 deutonymph (sequenced).

Remarks. The specimens from Portugal morphologically match the description of *Hygrobates balcanicus*. This species was originally described by Pešić et al. (2020) from Bulgaria, and later on reported from eastern Serbia (Pešić et al. 2023a). The sequenced specimens from Portugal cluster within BOLD:AEG3198, which, in addition to the specimens used in this study, includes specimens from Bulgaria, Serbia and Italy morphologically assigned to *H. balcanicus*.

Distribution. Balkans, Italy. New for Portugal.

***Hygrobates fluviatilis* (Ström, 1768)**

Material examined. Portugal, **Guarda**: • Manteigas, Casa do Cantoneiro, 40.418°N, 7.603°W, 1378 m a.s.l., 24 Aug. 2023, leg. Ferreira, Benitez-Bosco & Padilha, 1♂

(sequenced); • Gouveia, Rio Mondego, Casais de Folgosinho, 40.454°N, 7.493°W, 976 m a.s.l., 24 Aug. 2023, leg. Ferreira, Benitez-Bosco & Padilha, 1♀ (sequenced); • Seia, Rio Alva, Praia fluvial de Vila Cova a Coelheira, river, 40.379°N, 7.736°W, 312 m a.s.l., 23 Aug. 2023, leg. Ferreira, Benitez-Bosco & Padilha, 2♂ (sequenced); • Seia, Rio Alva, Praia Fluvial de Sabugueiro, river, 40.401°N, 7.64°W, 1021 m a.s.l., 24 Aug. 2023, leg. Ferreira, Benitez-Bosco & Padilha, 1♂ (sequenced).

Remarks. Genetic data indicate that Portuguese specimens belong to BOLD:ACB4846, which includes more than 300 specimens of *H. fluviatilis*, available in BOLD. The latter species was recently revised using molecular and morphological data (Pešić et al. 2017).

Distribution. Central, western, and southern Europe. In Portugal previously reported from Santa Comba Dão (Beira Alta; Lundblad 1956).

Hygrobates longiporus Thor, 1898 complex
Fig. 7

Material examined. Portugal, **Guarda**: • Seia, Rio Alva, Praia fluvial de Vila Cova a Coelheira, river, 40.379°N, 7.736°W, 312 m a.s.l., 23 Aug. 2023, leg. Ferreira, Benitez-Bosco & Padilha, 1♀, 1 deutonymph (sequenced); • Seia, Rio Alva, Praia Fluvial de Sabugueiro, river, 40.401°N, 7.64°W, 1021 m a.s.l., 24 Aug. 2023, leg. Ferreira, Benitez-Bosco & Padilha, 2♂, 1♀, 1 deutonymph (sequenced); • Manteigas, Poço do Inferno, 40.373°N, 7.516°W, 1078 m a.s.l., 21 Aug. 2023, leg. Ferreira, Benitez-Bosco & Padilha, 1♂, 1♀ (sequenced); • Manteigas, Mondego, Covão da ponte, 40.443°N, 7.514°W, 999 m a.s.l., 24 Aug. 2023, leg. Ferreira, Benitez-Bosco & Padilha, 1♂, 3♀, 2 deutonymph (sequenced); • Gouveia, Rio Mondego, Casais de Folgosinho, 40.454°N, 7.493°W, 976 m a.s.l., 24 Aug. 2023, leg. Ferreira, Benitez-Bosco & Padilha, 1♂, 1♀ (sequenced); • Manteigas, Poio do Leão, 40.399°N, 7.541°W, 734 m a.s.l., 22 Aug. 2023, leg. Ferreira, Benitez-Bosco & Padilha, 1♂ (sequenced); • Manteigas, Zêzere, Ponte dos Frades, 40.403°N, 7.526°W, 672 m a.s.l., 22 Aug. 2023, leg. Ferreira, Benitez-Bosco, Padilha, Andrade & Stur 1♂ (sequenced); • Seia, Rio Alva, Central hidroelétrica de Ponte dos Jugais, river, 40.385°N, 7.706°W, 555 m a.s.l., 23 Aug. 2023, leg. Ferreira, Benitez-Bosco & Padilha, 1♀ (sequenced); • Rio Alva, Nossa Senhora do Desterro, river, 40.395°N, 7.694°W, 791 m a.s.l., 23 Aug. 2023, leg. Ferreira, Benitez-Bosco & Padilha, 1♀ (sequenced). **Bragança**: • Mirandela, Torre de Dona Chama, 41.665°N, 7.146°W, 256 m a.s.l., 13 Jul. 2023, leg. Ferreira & Padilha, 1 ♀ (sequenced). **Vila Real** • Murça, Noura stream, 41.409°N, 7.417°W, 421 m a.s.l., 12 Jul. 2023 leg. Ferreira & Padilha, 1♂ (sequenced).

Remarks. In this study, specimens keying to *H. longiporus* in Gerecke et al. (2016) have DNA barcodes that cluster in three unique BINs (BOLD:AFV9997, BOLD:AFW1423, BOLD:AFV9998) (Fig. 7). The *p*-distance to the nearest neigbour ranged between 11.38–13.62%, far exceeding the species thresholds (6.08% K2P distance) obtained in the study on the *H. longiporus* complex by Pešić et al. (2022a).

The identity of *H. longiporus* was recently questioned by Pešić et al. (2021b, 2022a) who found that DNA barcodes of the specimens assigned to the latter species in Europe and Turkey cluster within four distinct genetic lineages. The first cluster (BOLD:AEB8359) comprises a large number of *longiporus*-like specimens from different parts of Europe, including Norway, from where the species was

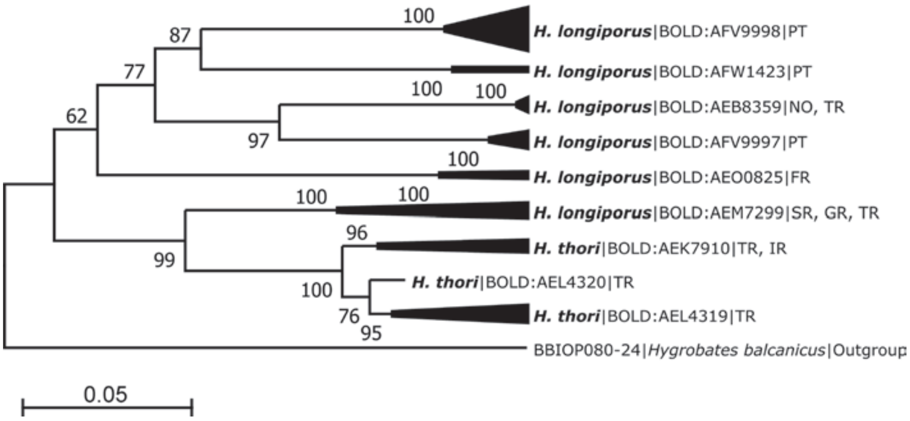

Figure 7. Neighbor-Joining tree of the *Hygrobates longiporus* complex obtained from 53 nucleotide COI sequences; 23 sequences were taken from Pešić et al. (2022a, 2023f), 26 sequences from Portugal are newly generated in this study, and four private sequences (HYDIR005-23, HYDIR006-23, HYDIR019-23, HYDIR020-23) from Turkey were directly taken from the BOLD. *Hygrobates balcanicus* from Portugal was used as outgroup. BINs are based on the barcode analysis from 16 May 2024. Country codes: FR = France, GR = Greece, IR = Iran, NO = Norway, PT = Portugal, RS = Serbia, TR = Turkey. Bootstrap values > 50% from 1000 bootstrap replicates on branches.

originally described (Thor 1898). The second cluster (BOLD:AEM7299) is restricted to SE Europe and E Turkey, while the third cluster (BOLD:AEO0825) is known only from Corsica. Most likely the latter two clusters represent a cryptic species new to science. The fourth clade, known from northern Iran and eastern Turkey, recently was described by Pešić et al. (2022a) as *H. thori* Pešić & Smit, 2022.

As emphasized by Pešić et al. (2022a), a larger-scale study of *H. longiporus* complex is needed to establish a stable taxonomy for this group. The true identity of *H. longiporus* should be morphologically redefined with material from Norway. Morphological analysis revealed that in regard to the shape of palp and genital field, Portuguese specimens match the description of *H. falcilaminatus*, a species originally described from Azrou, Morocco on the basis of a single female (Walter 1926) and later reported from a wide area in the western Mediterranean (Spain and France). The species was synonymized with *H. longiporus* by Lundblad (1956) (see also Gerecke 1991 for a discussion about this species). Further research, including a redescription of *H. falcilaminatus*, is needed to clarify taxonomic status of the Portuguese lineages and relationship with other members of *H. longiporus* complex.

Family Unionicolidae Oudemans, 1909

Genus *Neumania* Lebert, 1879

Note. Three species so far reported from Portugal.

Neumania (*Neumania*) *elliptica* Walter, 1925

Material examined. Portugal, **Guarda**: • Manteigas, Poço do Inferno, 40.373°N, 7.516°W, 1078 m a.s.l., 21 Aug. 2023, leg. Ferreira, Benitez-Bosco & Padilha, 1♂ (sequenced); • Seia, Rio Alva, Nossa Senhora do Desterro, river, 40.395°N, 7.694°W, 791 m a.s.l., 23 Aug. 2023, leg. Ferreira, Benitez-Bosco & Padilha, 1♀ (sequenced).

Remarks. The specimens from Portugal morphologically match the description of *N. elliptica*. This species was originally described from Algeria (Walter 1925) and later on reported by Pešić et al. (2007) from Corsica (France) and Italy (Sardinia and Sicily). *Neumania elliptica* is a characteristic colonizer of pools in summer-warm lowland streams with silty substrate (Pešić et al. 2007).

The sequenced specimens from Portugal form a unique BIN (BOLD:AFU2122), with the nearest neighboring BIN being BOLD:ACR9513 (*p*-distance 19.16%), which includes specimens of *N. deltoides* from the Netherlands, Macedonia and Turkey, available in BOLD.

Distribution. SW-Mediterranean. New for Portugal.

***Neumania* (*Neumania*) *imitata* Koenike, 1908**

Material examined. Portugal, **Porto** • Lousada, Parque Molinológico e Florestal de Pias, 41.268°N, 8.256°W, 170 m a.s.l., 1 Sep. 2023, leg. Ferreira, Sousa, Cruz-Oliveira & Girão, 1♂ (sequenced).

Remarks. The examined male in our study keyed to *Neumania imitata* following Gerecke et al. (2016) and forms a unique BIN (BOLD:AFV0268). The *p*-distance between this BIN and its nearest neighbour, BOLD:ADF7924, which includes specimens of *N. imitata* from the Netherlands, was estimated at 8.65%, indicating the need for taxonomic revision of this species.

Distribution. Europe; rare, reported from France, Italy, Germany, the Netherlands, Poland, and Montenegro. New for Portugal.

***Neumania* (*Neumania*) *limosa* (Koch, 1836)**

Material examined. Portugal, **Beja** • Mértola, Herdade de Alagães, pond, 37.673°N, 7.848°W, 18 May 2023, leg. Ferreira, Benitez-Bosco, Ekrem, Stur & Turaccio, 4♀ (sequenced); **Guarda**: • Manteigas, Serra de Baixo, Lagoa, 40.35°N, 7.549°W, 1431 m a.s.l., 21 Aug. 2023, leg. Ferreira, Benitez-Bosco & Padilha, 1♂, 3♀ (sequenced); • Gouveia, Ribeira do Covão do Urso, Barragem do Lagoacho, 40.385°N, 7.618°W, 1438 m a.s.l., 22 Aug. 2023, leg. Ferreira, Benitez-Bosco & Padilha, 1♂ (juv.) (sequenced).

Remarks. The specimens from Portugal cluster within BOLD:ACS0551, which includes specimens of *N. limosa* from the Netherlands. The *p*-distance between this BIN and its nearest neighbor BOLD:AEF5902, which includes specimens from Montenegro assigned to *N. limosa*, was estimated at 3.21%.

Distribution. Palaearctic. New for Portugal.

***Neumania* (*Neumania*) *uncinata* Walter, 1927**

Material examined. Portugal, **Faro** • Monchique, Caldas de Monchique, 37.287°N, 8.554°W, 23 May 2023, leg. Ferreira & Turaccio, 1♀ (sequenced). **Porto** • Vila do Conde, Rio Este, 41.378°N, 8.695°W, 15 m a.s.l., 7 Sep. 2023, leg. Ferreira, Cruz-Oliveira & Girão, 1♀ (sequenced).

Remarks. The sequenced specimens from Portugal keyed to *N. uncinata* following Gerecke et al. (2016), and cluster within two unique BINs (BOLD:AFV0253, BOLD:AFV0269). The *p*-distance between Portuguese BINs and their closest neighbor, BOLD:AER9267, which includes specimens of *N. uncinata* from Sardinia (see Pešić and Goldschmidt 2023), was estimated at 8.78% and 13.14%, respectively, indicating the need for taxonomic revision of *N. uncinata* complex from a wider geographical area.

Distribution. Western Palaearctic. In Portugal known from Estremadura (Lundblad 1956). *Neumania atlantida* Lundblad, 1962, originally described from Madeira by Lundblad (1962), was synonymized by Pešić et al. (2007) with *N. uncinata*.

***Neumania* (*Soarella*) *papillosa* (Soar, 1902)**

Material examined. Portugal, **Beja** • Mértola, Corte do Pinto, 37.682°N, 7.512°W, 19 May 2023, leg. Ferreira, Benitez-Bosco, Ekrem, Stur & Turaccio, 1♂, 2♀ (sequenced). **Guarda** • Seia, Rio Alva, Praia Fluvial de Sabugueiro, river, 40.401°N, 7.64°W, 1021 m a.s.l., 24 Aug. 2023, leg. Ferreira, Benitez-Bosco & Padilha, 1♀ (sequenced).

Remarks. The Portuguese specimens match the description of *N. papillosa*, forming a unique BIN (BOLD:AFO2116), with the nearest neighboring BIN being BOLD:ADS6560, which consists of 31 specimens of and unidentified *Neumania* sp. from South Africa. The *p*-distance between these two BINs was estimated at 14.26%.

Distribution. Europe. In Portugal previously reported from Côa River near Santa Comba Dão (Beira Alta; Lundblad 1956).

Genus *Unionicola* Haldeman, 1842

Note. Three species so far reported from Portugal.

***Unionicola* (*Hexatax*) *minor* (Soar, 1900)**

Material examined. Portugal, **Beja**: • Mértola, São João dos Caldeireiros, stream, 37.626°N, 7.81°W, 17 May 2023, leg. Ferreira, Benitez-Bosco, Ekrem, Stur & Turaccio, 1♀ (one palp dissected and slide mounted, RMNH); • Mértola, Moinho de Alferes 2, 37.503°N, 7.687°W, 19 May 2023, leg. Ferreira, Benitez-Bosco, Ekrem, Stur & Turaccio, 1♀ (sequenced).

Remarks. Specimens keying to *U. minor* in Gerecke et al. (2016) have DNA barcodes that cluster in unique BIN (BOLD:AFO2171).

Distribution. Widespread in Europe, here reported for the first time for Portugal.

Family Pionidae Thor, 1900
Subfamily Foreliinae Thor, 1923

Genus *Forelia* Haller, 1882

Note. Only one species reported from Portugal.

Forelia longipalpis Maglio, 1924

Material examined. Portugal, **Guarda**: • Gouveia, Ribeira da Fervença, Barragem do Vale do Rossim, 40.4°N, 7.589°W, 1418 m a.s.l., 22 Aug. 2023 leg. Ferreira, Benitez-Bosco, Padilha, Andrade & Stur, 3♀, 1 deutonymph (sequenced); • Seia, Rio Alva, Nossa Senhora do Desterro, river, 40.395°N, 7.694°W, 791 m a.s.l., 23 Aug. 2023, leg. Ferreira, Benitez-Bosco & Padilha, 1♀ (sequenced); • Manteigas, Mondego, Covão da Ponte, 40.443°N, 7.514°W, 999 m a.s.l., 24 Aug. 2023, leg. Ferreira, Benitez-Bosco & Padilha, 1♀ (sequenced).

Remarks. All barcoded specimens in our study were females. The shape of the genital field of specimens from Portugal morphologically match the description of *F. longipalpis* following Gerecke et al. (2016). The sequenced specimens cluster into two unique BINs (BOLD:AFX2876, BOLD:AFV3893), indicating the need for further taxonomic revision of this species. However, this revision should be postponed until males are available.

Distribution. Widespread in Europe; new record for Portugal.

Forelia variegator (Koch, 1837)

Material examined. Portugal, **Beja** • Mértola, São João dos Caldeireiros, stream, 37.625°N, 7.81°W, 17 May 2023, leg. Ferreira, Benitez-Bosco, Ekrem, Stur & Turaccio, 1♀ (sequenced). **Porto**: • Lousada, Parque Molinológico e Florestal de Pias, 41.268°N, 8.256°W, 170 m a.s.l., 1 Sep. 2023, leg. Ferreira, Sousa, Cruz-Oliveira & Girão, 2♀ (sequenced); • Vila do Conde, Rio Este, 41.378°N, 8.695°W, 15 m a.s.l., 7 Sep. 2023, leg. Ferreira, Sousa, Cruz-Oliveira & Girão, 1♂ (sequenced). **Guarda** • Rio Alva, Nossa Senhora do Desterro, river, 40.395°N, 7.694°W, 791 m a.s.l., 23 Aug. 2023, leg. Ferreira, Benitez-Bosco & Padilha, 1♀ (sequenced); • Seia, Rio Alva, Central hidroelétrica de Ponte dos Jugais, river, 40.385°N, 7.706°W, 555 m a.s.l., 23 Aug. 2023, leg. Ferreira, Benitez-Bosco & Padilha, 1♀ (sequenced).

Remarks. Regarding the shape of the genital field, the specimens from Portugal morphologically match the description of *F. variegator* following Gerecke et al. (2016). The sequenced specimens from Portugal form a unique BIN (BOLD:AFU5459), with the nearest neighboring BIN being BOLD:ACS0537, which includes specimens of *F. variegator* from the Netherlands, Norway, North Macedonia, and Russia. The *p*-distance between these two BINs is estimated at 12.82%.

Distribution. Palaearctic. In Portugal previously reported from Beira Alta and Estremadura (Lundblad 1956).

Subfamily Hydrochoreutinae K. Viets, 1942

Genus *Hydrochoreutes* Koch, 1837

Note. New genus for Portugal.

Hydrochoreutes krameri Piersig, 1896

Material examined. Portugal, **Beja** • Mértola, Herdade de Alagães, pond, 37.673°N, 7.848°W, 18 May 2023, leg. Ferreira, Benitez-Bosco, Ekrem, Stur & Turaccio, 1♀ (sequenced). **Guarda**: • Seia, Covão do Forno, 40.369°N, 7.638°W, 1574 m a.s.l., 19 Aug. 2023, leg. Ferreira, Benitez-Bosco & Padilha, 1♂ (sequenced).

Remarks. The sequenced specimens from Portugal cluster within BOLD:ACR9737. In addition to the specimen from Portugal, the BIN includes specimens of *Hydrochoreutes krameri* from Norway, the Netherlands, and North Macedonia, available in BOLD. The *p*-distance between the latter BIN and its nearest neighbor, BOLD:ADZ1025, which includes specimens of *H. ungulates*, is estimated at 15.22%.

Distribution. Palaearctic. New for Portugal.

Subfamily Pioninae Thor, 1900

Genus *Nautarachna* Moniez, 1888

Note. New genus for Portugal.

Nautarachna crassa (Koenike, 1908)

Material examined. Portugal, **Guarda** • Manteigas, Casa do Cantoneiro, 40.418°N, 7.603°W, 1378 m a.s.l., 24 Aug. 2023, leg. Ferreira, Benitez-Bosco & Padilha, 1♀ (sequenced).

Remarks. The sequenced female of *N. crassa* from Portugal forms a distinct BIN (BOLD:AFV0462). The *p*-distance between the specimen from Portugal and the barcode of a *N. crassa* specimen (MMHYD270-20) collected in Norway, is estimated at 16.7%, indicating the need for a taxonomic revision of *N. crassa* complex to identify possible undescribed cryptic species.

Distribution. Europe; widespread but here reported for the first time for the water mite fauna of Portugal.

Genus *Piona* Koch, 1842

Note. So far, two species of the genus have been reported from Portugal (Pešić et al. 2023b).

Piona carnea (Müller, 1776)

Material examined. Portugal, **Beja:** • Mértola, São Sebastião dos Carros, 37.598°N, 7.754°W, 21 May 2023, leg. Ferreira, Benitez-Bosco, Ekrem, Stur & Turaccio, 2♂, 2♀, 3 deutonymphs (sequenced); • Mértola, Herdade de Alagães, dry stream site 2, 37.678°N, 7.848°W, 18 May 2023, leg. Ferreira, Benitez-Bosco, Ekrem, Stur & Turaccio, 1 deutonymph (sequenced). **Vila Real** • Murça, Noura stream, 41.409°N, 7.417°W, 421 m a.s.l., 12 Jul. 2023 leg. Ferreira S, Padilha 1 deutonymph (sequenced). **Guarda**: • Manteigas, Serra de Baixo, Lagoa, 40.35°N, 7.549°W, 1431 m a.s.l., 21 Aug. 2023, leg. Ferreira, Benitez-Bosco & Padilha, 2 deutonymphs (sequenced).

Remarks. The specimens from Portugal morphologically match the description of *Piona carnea*. These specimens cluster within two BINs: BOLD:ACM0527, which includes three unidentified specimens from Canada and three specimens from the Netherlands assigned to *P. carnea*, and BOLD:ACS0622, which includes specimens of *P. carnea* from Norway, Finland, the Netherlands, and Germany.

Distribution. Holarctic. New record for Portugal.

Piona variabilis (Koch, 1836)

Material examined. Portugal, **Beja** • Mértola, São Sebastião dos Carros, 37.598°N, 7.754°W, 21 May 2023, leg. Ferreira, Benitez-Bosco, Ekrem, Stur & Turaccio, 1 deutonymph (sequenced; Table 1).

Remarks. The single deutonymph from Portugal cluster within BOLD:AAU0701, which includes 11 specimens from Sweden, Norway, and the Netherlands assigned to *P. variabilis*, available in the BOLD database.

Distribution. Europe. New record for Portugal.

Sunfamily Tiphyinae Oudemans, 1941

Genus *Pionopsis* Piersig, 1894

Note. One species of the genus reported from Portugal

Pionopsis lutescens (Hermann, 1804)

Material examined. Portugal, **Porto** • Lousada, Parque Torre de Vilar, 41.287°N, 8.21°W, 274 m a.s.l., 1 Sep. 2023, leg. Ferreira, Sousa & Girão 1♀ (sequenced). **Guarda** • Seia, Cise, 40.419°N, 7.709°W, fountain, 505 m a.s.l., 25 Aug. 2023, leg. Ferreira, Benitez-Bosco & Padilha, 1♂, 1♀, 1 deutonymph (sequenced).

Remarks. The examined male keyed to *Pionopsis lutescens* following Gerecke et al. (2016). The Portuguese specimens form a unique BIN (BOLD:AFV3897). The *p*-distance between the latter BIN and its nearest neighbor, BOLD:AET1848, which includes specimens of *P. lutescens* from Montenegro, was estimated at 12.34%, indicating the need for taxonomic revision of *P. lutescens* complex to identify possible undescribed cryptic species.

Distribution. Holarctic. In Portugal previously reported from Sintra-Monserrate Park and Palace, Estremadura (Lundblad 1956).

Genus *Tiphys* Koch, 1836

Note. Only one species reported from Portugal.

Tiphys torris (Müller, 1776)

Material examined. Portugal, **Beja** • Odemira, Ribeira de Seixe, Zambujeira do Mar, 37.399°N, 8.723°W, 45 m a.s.l., 23 May 2023, leg. Ekrem & Benitez-Bosco, 1♀ (sequenced). Guarda • Seia, Rio Alva, Nossa Senhora do Desterro, river, 40.395°N, 7.694°W, 791 m a.s.l., 23 Aug. 2023, leg. Ferreira, Benitez-Bosco & Padilha, 1♂ (sequenced); • Seia, Rio Alva, Praia Fluvial de Sabugueiro, river, 40.401°N, 7.64°W, 1021 m a.s.l., 24 Aug. 2023, leg. Ferreira, Benitez-Bosco & Padilha, 1♀ (sequenced).

Remarks. The sequenced specimens from Portugal form a unique BIN (BOLD:AFP3352) with the nearest neighboring BIN being BOLD:ACR9977 (*p*-distance 1.92%), which includes one specimen from the Netherlands assigned to *T. torris* and three specimens from Norway assigned to *T. lapponicus*.

Distribution. Europe. In Portugal previously reported from Estremadura (Lundblad 1956).

Family Aturidae Thor, 1900

Genus *Aturus* Kramer, 1875

Note. New genus record for Portugal.

Aturus scaber Kramer, 1875

Material examined. Portugal, **Porto**: • Lousada, Moinho da Tapada, 41.263°N, 8.307°W, 176 m a.s.l., 1 Sep. 2023, Ferreira, Sousa, Cruz-Oliveira & Girão, 1♂ (sequenced).

Remarks. The specimen from Portugal clusters within BOLD:ACQ9097, which includes > 80 specimens of *A. scaber* from Norway and Germany in BOLD.

Distribution. Western Palaearctic. New record for Portugal.

Family Mideopsidae Koenike, 1910

Genus *Mideopsis* Koenike, 1910

Note. Family and genus both new for Portugal.

Mideopsis roztoczensis Biesiadka & Kowalik, 1979
Fig. 8

Material examined. Portugal, **Beja**: • Mértola, Moinho de Alferes 1, 37.502°N, 7.69°W, 19 May 2023, leg. Ferreira, Benitez-Bosco, Ekrem, Stur & Turaccio, 1♀ (sequenced); Mértola, Pulo do Lobo, 37.805°N, 7.633°W, 18 May 2023, leg. Ferreira, Benitez-Bosco, Ekrem, Stur & Turaccio, 5♀, 1 deutonymph (sequenced); • Odemira, Ribeira de Seixe, Zambujeira do Mar, 37.398°N, 8.68°W, 75 m a.s.l., 23 May 2023, leg. Ekrem & Benitez-Bosco, 1♂ (sequenced). **Bragança** • Vinhais,

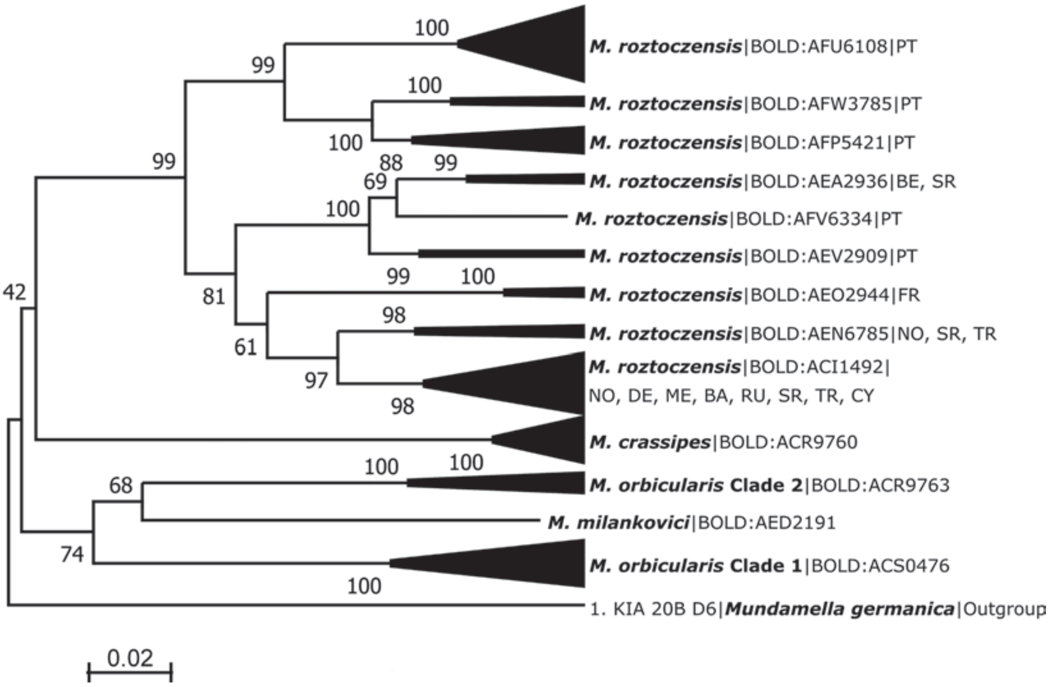

Figure 8. Neighbor-Joining tree of the genus *Mideopsis* obtained from 112 nucleotide COI sequences; 71 sequences were taken from Pešić et al. (2023a) and 41 sequences from Portugal are newly generated in this study. *Mundamella germanica* from Montenegro was used as outgroup. BINs are based on the barcode analysis from 16 May 2024. Country codes: BA = Bosnia and Herzegovina, BE = Belgium, CY = Cyprus, DE = Germany, FR = France, ME = Montenegro, PT = Portugal, RS = Serbia, RU = Russia, TR = Turkey. Bootstrap values > 50% from 1000 bootstrap replicates on branches.

Gasparona, 41.85°N, 7.013°W, 683 m a.s.l., 6 Jul. 2023, leg. Ferreira & Padilha, 1♀, 1 deutonymph (sequenced). **Guarda:** • Seia, Casa do Loureiro, 40.433°N, 7.701°W, 415 m a.s.l., 19 Jul. 2023 leg. Ferreira & Padilha, 1♂, 3♀, 1 deutonymph (sequenced); • Manteigas, Zêzere, Covão da Ametade, 40.328°N, 7.587°W, 1431 m a.s.l., 21 Aug. 2023, leg. Ferreira, Benitez-Bosco & Padilha, 1♂, 1♀, 1 deutonymph (sequenced); • Manteigas, Zêzere, Ponte dos Frades, 40.403°N, 7.526°W, 672 m a.s.l., 22 Aug. 2023, leg. Ferreira, Benitez-Bosco, Padilha, Andrade & Stur 1♀ (sequenced); • Manteigas, Poço do Inferno, 40.373°N, 7.516°W, 1078 m a.s.l., 21 Aug. 2023, leg. Ferreira, Benitez-Bosco & Padilha, 2♂, 1♀ (juv.), 1 deutonymph, 1♂ dissected and slide mounted (RMNH); • Gouveia, Rio Mondego, Casais de Folgosinho, 40.454°N, 7.493°W, 976 m a.s.l., 24 Aug. 2023, leg. Ferreira, Benitez-Bosco & Padilha, 1♂, 1♀ (sequenced); • Manteigas, Poio do Leão, 40.399°N, 7.541°W, 734 m a.s.l., 22 Aug. 2023, leg. Ferreira, Benitez-Bosco & Padilha, 2♂ (sequenced); • Seia, Rio Alva, Central hidroelétrica de Ponte dos Jugais, river, 40.385°N, 7.706°W, 555 m a.s.l., 23 Aug. 2023, leg. Ferreira, Benitez-Bosco & Padilha, 1♂, 2♀, 2 deutonymph (sequenced), 1♂ dissected and slide mounted (RMNH); • Rio Alva, Nossa Senhora do Desterro, river, 40.395°N, 7.694°W, 791 m a.s.l., 23 Aug. 2023, leg. Ferreira, Benitez-Bosco & Padilha, 2♀ (sequenced); • Manteigas, Mondego, Covão da ponte, 40.443°N, 7.514°W, 999 m a.s.l., 24 Aug. 2023, leg. Ferreira, Benitez-Bosco & Padilha, 1♂ (sequenced); • Seia, Rio Alva, Praia Fluvial de Sabugueiro, river, 40.401°N, 7.64°W, 1021 m a.s.l., 24 Aug. 2023, leg. Ferreira, Benitez-Bosco & Padilha, 2♀ (sequenced); • Manteigas, Casa do Cantoneiro, 40.418°N, 7.603°W, 1378 m a.s.l., 24 Aug. 2023, leg. Ferreira, Benitez-Bosco & Padilha, 2♂, 1♀ (sequenced). **Vila Real** • Murça, Noura stream, 41.409°N, 7.417°W, 421 m a.s.l., 12 Jul. 2023 leg. Ferreira S, Padilha 1♀ (sequenced).

Remarks. The specimens examined in our study match the description of *Mideopsis roztoczensis*, when following Biesiadka and Kowalik (1979). *Mideopsis roztoczensis* is characterized by a more elevated dorsal shield with distinctly visible anteriorly diverging lines of particularly faint fine porosity, and by the the shape of the male ejaculatory complex with the wedge-shaped anterior ramus being wider and with a characteristic arrow-shaped delimited area. Recently, Pešić et al. (2023e) showed that *M. roztoczensis* is a genetically variable species, comprising four BINs (BOLD:ACI1492, BOLD:AEN6785, BOLD:AEA2936, BOLD:AEO2944) widely distributed in Europe. In this study, we detected an additional five unique BINs (BOLD:AFU6108, BOLD:AFP5421, BOLD:AFW3785, BOLD:AFV6334, BOLD:AEV2909) within the Portuguese *M. roztoczensis*-like specimens (Fig. 8), all of them unique, and some of them present at the same sites (e.g., BOLD:AFU6108 and BOLD:AFW3785 in Casa do Loureiro, BOLD:AFU6108 and BOLD:AFV6334 in Casa do Cantoneiro).

Distribution. Europe, Turkey. New record for Portugal.

Family Momoniidae K. Viets, 1926

Genus *Momonia* Halbert, 1906

Note. Genus and family both new for Portugal.

Momonia (*Momonia*) *falcipalpis* Halbert, 1906

Material examined. Portugal, **Guarda** • Manteigas, Poço do Inferno, 40.373°N, 7.516°W, 1078 m a.s.l., 21 Aug. 2023, leg. Ferreira, Benitez-Bosco & Padilha, 1♀ (sequenced).

Remarks. The examined specimen in our study keyed to *Momonia falcipalpis* and forms a unique BIN (BOLD:AFX3396).

Distribution. Europe; rare, known from Ireland, France, Italy, and Russia. New record for Portugal.

Family Arrenuridae Thor, 1900

Genus *Arrenurus* Dugès, 1834

Note. Seven species are reported from Portugal; one of them (*Arrenurus autochthonus* Lundblad, 1941) is endemic to Madeira.

Arrenurus (*Arrenurus*) *albator* (Müller, 1776)

Material examined. Portugal, **Guarda**: • Gouveia, Ribeira da Fervença, Barragem do Vale do Rossim, 40.4°N, 7.589°W, 1418 m a.s.l., 22 Aug. 2023 leg. Ferreira, Benitez-Bosco, Padilha, Andrade & Stur, 2♂, 2♀ (sequenced); • Gouveia, Ribeira do Covão do Urso, Barragem do Lagoacho, 40.385°N, 7.618°W, 1438 m a.s.l., 22 Aug. 2023 leg. Ferreira, Benitez-Bosco, Padilha, Andrade & Stur, 1♀ (sequenced).

Remarks. The examined specimens from Portugal cluster within BOLD:ACR9639, which includes one specimen of *Arrenurus albator* from the Netherlands, available in the BOLD database.

Distribution. Western Palaearctic. In Portugal previously reported from Beira Alta (Lundblad 1956).

Arrenurus (*Arrenurus*) *szalayi* Lundblad, 1954

Material examined. Portugal, **Beja** • Mértola, Moinho de Alferes 1, 37.502°N, 7.69°W, 19 May 2023, leg. Ferreira, Benitez-Bosco, Ekrem, Stur & Turaccio, 2♂ incl. one juv., (both sequenced).

Remarks. The examined males from Moinho de Alferes match the description of *A. szalayi*, a species originally described from Ribeira d'Odivelas in Portugal (Lundblad 1956). The sequenced specimens from Portugal clustered within one BIN (BOLD:ACS0403), which in addition to the specimens from Portugal, includes a number of specimens collected from a large geographic area, from Norway to South Africa and from the Netherlands to Kyrgyzstan, and that are morphologically assigned to *A. bicuspidator* Berlese, 1885, or to *A. radiatus* Piersig, 1894. From both species, *A. szalayi*, at least morphologically, can be easily separated by the characteristic shape of the male petiole (see Lundblad 1956: fig. 161A). Further research is needed to understand the factors behind this grouping and the implication of this lack of genetic differentiation between three morphological different species.

Distribution. Portugal; previously reported from Ribeira de Odivelas, Alentejo (Lundblad 1954, 1956).

Arrenurus (*Arrenurus*) *leuckarti* Piersig, 1894

Material examined. Portugal, **Guarda**: • Manteigas, Poço do Inferno, 40.373°N, 7.516°W, 1078 m a.s.l., 21 Aug. 2023, leg. Ferreira, Benitez-Bosco & Padilha, 1♂ (sequenced); Manteigas, Casa do Cantoneiro, 40.418°N, 7.603°W, 1378 m a.s.l., 24 Aug. 2023, leg. Ferreira, Benitez-Bosco & Padilha, 1♀ (sequenced).

Remarks. The examined specimens from Portugal cluster within BOLD:ACR9670, which includes specimens of *Arrenurus leuckarti* from the Netherlands.

Distribution. Western, eastern, and central Europe. New record for Portugal.

Arrenurus (*Arrenurus*) *neumani* Piersig, 1895

Material examined. Portugal. Beja • Mértola, Moinho de Alferes 1, 37.502°N, 7.69°W, 19 May 2023, leg. Ferreira, Benitez-Bosco, Ekrem, Stur & Turaccio, 3♂, 1♀ (sequenced).

Remarks. The sequenced specimens from Portugal form a unique BIN (BOLD:AFP6143) with the nearest neighboring BIN being BOLD:ACR9801, which includes specimens of *A. neumani*, from the Netherlands, Norway and Poland in BOLD. The *p*-distance between these two BINs was estimated at 5.9%.

Distribution. Palaearctic. New record for Portugal.

***Arrenurus* (*Arrenurus*) cf. *tricuspidator* (Müller, 1776)**

Material examined. Portugal, **Beja** • Mértola, Moinho de Alferes 1, 37.502°N, 7.69°W, 19 May 2023, leg. Ferreira, Benitez-Bosco, Ekrem, Stur & Turaccio, 1 deutonymph (sequenced).

Remarks. One deutonymph from Portugal, used in this study for molecular analysis, forms a unique cluster BOLD:AFU3639, with a *p*-distance estimated at 3.21% to the closest neigbouring BIN, BOLD:ACS0825, which includes specimens of *A. tricuspidator* from the Netherlands, Norway, and Germany.

Distribution. Palaearctic. New record for Portugal.

***Arrenurus* (*Megaluracarus*) *globator* (Müller, 1776)**

Material examined. Portugal: **Beja**: • Mértola, São Sebastião dos Carros, 37.598°N, 7.754°W, 21 May 2023, leg. Ferreira, Benitez-Bosco, Ekrem, Stur & Turaccio, 2♂, 1♀ (sequenced); • Mértola, Ribeira de Carreiras, São Miguel do Pinheiro, 37.552°N, 7.85°W, 21 May 2023, leg. Ferreira, Benitez-Bosco, Ekrem, Stur & Turaccio, 1♂, 2♀ (sequenced); • Moinho de Alferes 1, 37.502°N, 7.69°W, 19 May 2023, leg. Ferreira, Benitez-Bosco, Ekrem, Stur & Turaccio, 1♀ (sequenced).

Remarks. The sequenced specimens from Portugal form a unique BIN (BOLD:AFO3503) with the nearest neighboring BIN being BOLD:ACS0765, which includes 34 specimens from the Netherlands, Norway, Poland and North Macedonia partially assigned to *A. globator* or *A. tubulator*. The *p*-distance between these two BINs was estimated at 5.45%.

Distribution. Palaearctic. In Portugal previously reported from Alentejo (Lundblad 1956).

***Arrenurus* (*Megaluracarus*) cf. *zachariae* Koenike, 1886**

Material examined. Portugal, Bragança • Vinhais, Gasparona, 41.85°N, 7.013°W, 693 m a.s.l., 6 Jul. 2023, leg. Ferreira & Padilha, 1 deutonymph (sequenced).

Remarks. One deutonymph from Portugal forms a unique cluster BOLD:AFU0319, with a *p*-distance to the closest neighboring BIN, BOLD:ADF7386, which includes mostly specimens assigned to *A. zachariae*, estimated at 2.56%.

Distribution. Europe. New record for Portugal.

Discussion

Our study provides the first DNA barcode reference library for Portuguese water mites. Our findings confirm the presence of 29 of the 101 previously recorded species; however, it also added 36 new species for the water mite fauna of Portugal, two of which are described as new to science. We found that 47.4% of the Portuguese water mites having sequences collected in Portugal were represented in BOLD. Intraspecific distances for some species were high indicating the incongruence between morphology and DNA barcodes, and therefore the need for further taxonomic revision of these species to identify possible undescribed cryptic diversity. The identity of some species in the absence of available males, for example *Forelia variegator* and *F. longipalpis*, remains questionable and needs further morphological evaluation.

Our research provided 75 BINs, 38 of which were new to BOLD. Seven species in our study were represented by multiple BINs: *Mideopsis roztoczensis* (five BINS), *Hygrobates longiporus* (three BINS), *Lebertia insignis*, *Atractides inflatus*, *Neumania uncinata*, *Forelia longipalpis*, and *Piona carnea*, each with two BINs. Furthermore, examining molecular diversity at a continental scale, we found more such cases. For example two BINs were detected within *Limnochares aquatica* (BOLD:AFV0270, BOLD:ACS0438), a species considered to be widely distributed in the Holarctic. Three BINs were also detected within *Neumania uncinata* (BOLD:AFV0253, BOLD:AFV0269, BOLD:AER9267), a species widely distributed in the Mediterranean region, and *N. imitata* (BOLD:AFV0268, BOLD:ADF7924, BOLD:AED4073), a species that is less common, but with a wide distribution from Sweden to Portugal. A high genetic divergence (16.7% *p*-distance) was found between the specimen of *Nautarachna crassa* from Portugal and a specimen of this species collected in Norway. Our study, based on the available data in BOLD suggests also that *Pionopsis lutescens*, a species common in many types of standing water in the Holarctic, includes at least four BINs in Europe. In this study we retrieved one, BOLD:AFV3897, which includes only specimens from Portugal. Two others are present in the central and northern parts of Europe, BOLD:ACS0644 in the Netherlands and Norway and BOLD:ACR9955, so far found only in the Netherlands. Finally, the fourth BIN, BOLD:AET1848, is known from Montenegro. Further research is needed to understand the taxonomic implications of these genetic divergences.

Our results show the usefulness of using BINs to detect possible cryptic species and to investigate the distribution patterns of water mite species whose presence in certain geographical areas would be difficult to confirm without molecular evidence. In this study we confirmed the presence of *Hygrobates fluviatilis* in Portugal, which represent the southernmost record of this widely distributed species. We also added the first record of *H. balcanicus*. The latter rhitrobiontic species, so far recorded from Serbia and Bulgaria, was probably previously confused with *H. fluviatilis*, but new findings from Portugal indicate that this species is widespread in the Mediterranean region.

Furthermore, our results demonstrate the efficiency of using DNA barcoding to identify preadult stages, particularly deutonymphs, whose identification to the species-level is often not possible without accompanying adult stages when using morphology. In this study, two individuals of *Arrenurus* deutonymphs were assigned to *A. tricuspidator* and *A. zachariae*, respectively, based on matching their DNA barcodes with the BINs of these species available in BOLD. Based on morphology alone, identification of these preadult stages would be difficult, if not impossible.

In summary, this study exemplifies the high molecular diversity of Portuguese water mites as well as the need to intensify international cooperation in the generation and curation of DNA barcode reference libraries.

Acknowledgements

Biodiversity Genomics Europe is funded by Horizon Europe under the Biodiversity, Circular Economy and Environment call (REA.B.3); co-funded by the Swiss State Secretariat for Education, Research and Innovation (SERI) under contract number 22.00173; and by the UK Research and Innovation under the Department for Business, Energy and Industrial Strategy's Horizon Europe Guarantee Scheme.

The authors would like to acknowledge to Estação Biológica de Mértola, to Mértola Municipality, to Lousada Municipality, to CISE and to Seia Municipality and to Faculty of Sciences – University of Porto for the logistic support during the fieldwork and to Thomas S. Ekrem, Piotr Gadawski, Roman Hodunko, José Conde, Tiago Correia, and Antonio and Luis Guilherme Sousa for the great company during fieldwork. We thank two anonymous reviewers, whose constructive comments greatly improved this work.

Additional information

Conflict of interest

The authors have declared that no competing interests exist.

Ethical statement

No ethical statement was reported.

Funding

LBB was funded by the project TROPIBIO NORTE-01-0145-FEDER-000046, supported by Norte Portugal Regional Operational Programme (NORTE2020), under the PORTUGAL 2020 Partnership Agreement, through the European Regional Development Fund (ERDF), and by a PhD fellowship (UI/BD/154733/2023) attributed by the Portuguese Foundation of Science and Technology (FCT). PT benefited from an Erasmus+ Studies Program grant (2022-1-IT02_KA131-HED-000057320). SF was funded by the FCT through the program 'Stimulus of Scientific Employment, Individual Support—3rd Edition' (https://doi.org/10.54499/2020.03526.CEECIND/CP1601/CP1649/CT0007).

Author contributions

All authors have contributed equally.

Author ORCIDs

Vladimir Pešić https://orcid.org/0000-0002-9724-345X
Andrzej Zawal https://orcid.org/0000-0002-5838-6060
Sónia Ferreira https://orcid.org/0000-0002-6884-3966
Laura Benitez-Bosco https://orcid.org/0000-0002-8863-8353
Dinis Girão https://orcid.org/0009-0008-4842-0721
Paolo Turaccio https://orcid.org/0009-0000-8627-6718
Samantha Rossini https://orcid.org/0009-0009-6881-2527
Giorgia Staffoni https://orcid.org/0009-0003-5916-1757
Torbjørn Ekrem https://orcid.org/0000-0003-3469-9211

Data availability

All of the data that support the findings of this study are available in the main text or Supplementary Information.

References

Asadi M, Pešić V, Etemadi I (2010) A revised survey of water mites (Acari: Hydrachnidia) from Iran: new synonyms and descriptions of three new species. Zootaxa 2628: 43–55. https://doi.org/10.11646/zootaxa.2628.1.3

Biesiadka E, Kowalik W (1979) A new species of Mideopsis Neuman (Hydrachnellae, Acari) from Poland. Bulletin of the Polish Academy of Sciences. Biological Sciences, Cl. II 26: 695–702.

Blattner L, Gerecke R, von Fumetti S (2019) Hidden biodiversity revealed by integrated morphology and genetic species delimitation of spring dwelling water mite species (Acari, Parasitengona: Hydrachnidia). Parasites Vectors 12: 492. https://doi.org/10.1186/s13071-019-3750-y

Cantallo H, Gomes N, Antunes C, Ribeiro T, Gomes MI, Costa DA (2021) Catalogue of aquatic mites from the Minho River (NW Iberian Peninsula). Environmental Smoke (Special Issue): 44–47. https://doi.org/10.32435/envsmoke/xibesymp.7

Cantallo H, Gomes N, Antunes C, Martins D, Costa DA (2022) Checklist of water mites from mainland Portugal and its archipelagos. Zootaxa 5213: 336–370. https://doi.org/10.11646/zootaxa.5213.4.2

Davids C, Di Sabatino A, Gerecke R, Gledhill T, Smit H, Van der Hammen H (2007) Acari: Hydrachnidia. *In*: Gerecke R (Ed.) Chelicerata: Acari I. Süßwasserfauna von Mitteleuropa (Vol. 7, 2–1). Elsevier Spektrum Akademischer Verlag, München, 241–376. https://doi.org/10.1007/978-3-662-55958-1_7

Di Sabatino A, Gerecke R, Gledhill T, Smit H (2010) Acari: Hydrachnidia II. In: Gerecke R (Ed) Chelicerata: Acari II. Süßwasserfauna von Mitteleuropa, Vol. 7, 2–2, Elsevier Spektrum Akademischer Verlag, Heidelberg, 1–234. https://doi.org/10.1007/978-3-8274-2266-8_1

Edgar RC (2004) MUSCLE: multiple sequence alignment with high accuracy and high 679 throughput. Nucleic acids research 32(5): 1792–1797. https://doi.org/10.1093/nar/gkh340

Felsenstein J (1985) Confidence limits on phylogenies: An approach using the bootstrap. Evolution 39: 783–791. https://doi.org/10.2307/2408678

Ferreira S, Paupério J, Grosso-Silva JM, Beja P (2019) DNA barcoding of Sialis sp. (Megaloptera) in Portugal: the missing tool to species identification. Aquatic Insects 40: 173–184. https://doi.org/10.1080/01650424.2019.1571612

Ferreira SA, Andrade R, Gonçalves AR, Sousa P, Paupério J, Fonseca NA, Beja P (2020a) The InBIO Barcoding Initiative Database: DNA barcodes of Portuguese Diptera 01. Biodiversity Data Journal 8: e49985. https://doi.org/10.3897/BDJ.8.e49985

Ferreira S, Tierno de Figueroa JM, Martins FMS, Veríssimo J, Quaglietta L, Grosso-Silva JM, Lopes PB, Sousa P, Paupério J, Fonseca NA, Beja P (2020b) The InBIO Barcoding Initiative Database: contribution to the knowledge on DNA barcodes of Iberian Plecoptera. Biodiversity Data Journal 8: e55137. https://doi.org/10.3897/BDJ.8.e55137

Folmer O, Black M, Hoeh W, Lutz R, Vrijenhoek R (1994) DNA primers for amplification of mitochondrial cytochrome c oxidase subunit I from diverse metazoan invertebrates. Molecular Marine Biology and Biotechnology 3: 294–299.

Gerecke R (1991) Taxonomische, faunistische und ökologische Untersuchungen an Wassermilben (Acari, Actinedida) aus Sizilien unter Berücksichtigung anderer aquatischer Invertebraten. Lauterbornia 7: 1–304.

Gerecke R (2009) Revisional studies on the European species of the water mite genus *Lebertia* Neuman, 1880 (Acari: Hydrachnidia: Lebertiidae). Abhandlungen der Senckenbergischen Naturforschenden Gesellschaft 566: 1–144.

Gerecke R, Gledhill T, Pešić V, Smit H (2016) Chelicerata: Acari III. In: Gerecke R (Ed.) Süßwasserfauna von Mitteleuropa, Bd. 7/2-3. Springer-Verlag Berlin, Heidelberg, 1–429. https://doi.org/10.1007/978-3-8274-2689-5

Gerecke R, Kjærstad G, Ekrem T, Stur E (2022) A faunistic study of water mites (Hydrachnidia and Halacaridae) from southern Norway. Norwegian Journal of Entomology 69: 243–268.

Hebert PDN, Penton EH, Burns JM, Janzen DH, Hallwachs W (2004) Ten species in one: DNA barcoding reveals cryptic species in the Neotropical butterfly *Astraptes fulgerator*. Proceedings of the National Academy of Sciences of the United States of America 101: 14812–1817. https://doi.org/10.1073/pnas.0406166101

Hebert PDN, Ratnasingham S, Zakharov EV, Telfer AC, Levesque-Beaudin V, Milton MA, Pedersen S, Jannetta P, deWaard JR (2016) Counting animal species with DNA barcodes: Canadian insects. Philosophical Transactions of the Royal Society B: 37120150333. https://doi.org/10.1098/rstb.2015.0333

Kimura M (1980) A simple method for estimating evolutionary rate of base substitutions through comparative studies of nucleotide sequences. Journal of Molecular Evolution 16: 111–120. https://doi.org/10.1007/BF01731581

Kumar S, Stecher G, Li M, Knyaz C, Tamura K (2018) MEGA X: Molecular Evolutionary Genetics Analysis across computing platforms. Molecular Biology and Evolution 35: 547–1549. https://doi.org/10.1093/molbev/msy096

López-Peña D, Gerecke R, García-Roger EM, Martin P, Jiménez-Peydró R (2022) Parasite-host relationships of water mites (Acari: Hydrachnidia) and black flies (Diptera: Simuliidae) in southeastern Spain. Parasites & Vectors 15(1): 474. https://doi.org/10.1186/s13071-022-05610-2

Lundblad O (1942) Afrikanische Hydracarinen. Entomologisk Tidskrift 63: 155–209.

Lundblad O (1954) Neue südeuropäische Wassermilben. Zoologischer Anzeiger 153: 154–159.

Lundblad O (1956) Zur Kenntnis süd- und mitteleuropäischer Hydrachnellen. Arkiv för Zoologi 10: 1–306.

Lundblad O (1962) Wassermilben von den Kanarischen Inseln. Arkiv för Zoologi, Ser. 2, 15(16): 285–300.

Pauperio J, Gonzalez LM, Martinez J, González MA, Martins FM, Veríssimo J, Puppo P, Pinto J, Chaves C, Pinho CJ, Grosso-Silva JM, Quaglietta L, Silva TL, Sousa P, Alves PC, Fonseca N, Beja P, Ferreira S (2023) The InBIO barcoding initiative database: DNA barcodes of Iberian Trichoptera, documenting biodiversity for freshwater biomonitoring in a Mediterranean hotspot. Biodiversity Data Journal 11: e97484. https://doi.org/10.3897/BDJ.11.e97484

Pešić V, Goldschmidt T (2023) New DNA-assisted records of water mites from Sardinia, with the description of a new species (Acari, Hydrachnidia). Ecologica Montenegrina 69: 24–44. https://doi.org/10.37828/em.2023.69.4

Pešić V, Smit H (2022) Water mites of Corsica: DNA barcode and morphological evidences. International Journal of Acarology 48: 418–428. https://doi.org/10.1080/01647954.2022.2086619

Pešić V, Gerecke R, Cîmpean M (2007) Water mites of the genus *Neumania* Lebert (Acari, Hydrachnidia: Unionicolidae: Pionatacinae) in the Mediterranean area. Annales de Limnologie-International Journal of Limnology 43(3): 187–198. https://doi.org/10.1051/limn:2007013

Pešić V, Valdecasas AG, García-Jimenez R (2012) Simultaneous evidence for a new species of *Torrenticola* Piersig, 1896 (Acari, Hydrachnidia) from Montenegro. Zootaxa 3515: 38–50. https://doi.org/10.11646/zootaxa.3515.1.2

Pešić V, Asadi M, Cimpean M, Dabert M, Esen Y, Gerecke R, Martin P, Savić A, Smit H, Stur E (2017) Six species in one: Evidence of cryptic speciation in the *Hygrobates fluviatilis* complex (Acariformes, Hydrachnidia, Hygrobatidae). Systematic & Applied Acarology 22: 1327–1377. https://doi.org/10.11158/saa.22.9.4

Pešić V, Jovanović M, Manović A, Zawal A, Bańkowska A, Ljubomirova L, Karaouzas I, Dabert M (2020) Molecular evidence for two new species of the *Hygrobates fluviatilis* complex from the Balkan Peninsula (Acariformes, Hydrachnidia, Hygrobatidae). Systematic & Applied Acarology 25(9): 1702–1719. https://doi.org/10.11158/saa.25.9.15

Pešić V, Zawal A, Manović A, Bańkowska A, Jovanović M (2021a) A DNA barcode library for the water mites of Montenegro. Biodiversity Data Journal 9: e78311. https://doi.org/10.3897/BDJ.9.e78311

Pešić V, Jovanović M, Manović A, Karaouzas I, Smit H (2021b) New records of water mites from the Balkans revealed by DNA barcoding (Acari, Hydrachnidia). Ecologica Montenegrina 49: 20–34. https://doi.org/10.37828/em.2021.49.2

Pešić V, Esen Y, Gülle P, Zawal A, Saboori A, Jovanović M, Bańkowska A, Smit H (2022a) New records of water mites from Turkey and Iran revealed by DNA barcoding, with the description of a new species (Acari, Hydrachnidia). Systematic & Applied Acarology 27(7): 1393–1407. https://doi.org/10.11158/saa.27.7.7

Pešić V, Esen Y, Gerecke R, Goldschmidt T, Mumladze L, Smit H, Zawal A (2022b) Evidence of cryptic speciation in the *Hygrobates calliger* complex (Acariformes, Hydrachnidia, Hygrobatidae) with the description of two new species. Ecologica Montenegrina 59: 101–122. https://doi.org/10.37828/em.2022.59.10

Pešić V, Smit H, Konopleva ES (2023a) Molecular phylogeny and description of *Hygrobates cyrnusensis* sp. nov. reveals multiple colonization of Corsica by water mites of the H. fluviatilis-complex (Acariformes, Hydrachnidia, Hygrobatidae). Acarologia 63(1): 262–274. https://doi.org/10.24349/h12f-rs8x

Pešić V, Jovanović M, Espiridiao Oliveira A, Pedro A, Freira M, Morais MM (2023b) New records of water mites (Acari, Hydrachnidia) from Portugal revealed by DNA barcoding, with the description of *Atractides marizae* sp.nov. ZooKeys 1151: 205–222. https://doi.org/10.3897/zookeys.1151.100766

Pešić V, Zawal A, Saboori A, Bańkowska A, Cakmak I, Smit H (2023c) New records of water mites (Acari, Hydrachnidia) from Iran and Türkiye based on morphology and DNA barcodes with description of one new species. Ecologica Montenegrina 66: 11–29. https://doi.org/10.37828/em.2023.66.2

Pešić V, Smit H, Zawal A (2023d) A new species of the genus *Atractides* Koch, 1837 from Montenegro (Acari: Hydrachnidia: Hygrobatidae), separated from *A. nodipalpis* (Thor, 1899), one of the most common water mite species in running waters in Europe. Systematic & Applied Acarology 28(5): 852–863. https://doi.org/10.11158/saa.28.5.7

Pešić V, Bańkowska A, Zawal A, Rewicz T, Smit H (2023e) Molecular diversity and species delimitation in the genus *Mideopsis* Neuman, 1880 in Europe (Acari, Hydrachnidia, Mideopsidae). Ecologica Montenegrina 70: 101–115. https://doi.org/10.37828/em.2023.70.12

Pešić V, Esen E, Gülle P, Zawal A, Jovanović M, Rewicz T, Smit H (2023f) An appraisal of the water mite genus *Hygrobates* Koch, 1837 from Türkiye, based on morphological and molecular data (Acariformes, Hydrachnidia, Hygrobatidae). Systematic & Applied Acarology 28(4): 742–754. https://doi.org/10.11158/saa.28.4.10

Ratnasingham S, Hebert PDN (2007) BOLD: The barcode of life data system. Molecular Ecology Notes 7: 355–364. https://doi.org/10.1111/j.1471-8286.2007.01678.x

Ratnasingham S, Hebert PDN (2013) A DNA-based registry for all animal species: The Barcode Index Number (BIN) system. PLoS ONE 8: e66213. https://doi.org/10.1371/journal.pone.0066213

Smit H (2020) Water mites of the world, with keys to the families, subfamilies genera and subgenera (Acari: Hydrachnidia). Monografieën van de Nederlandse Entomologische Vereniging 12: 1–774

Smit H, Gerecke R (2010) A checklist of the water mites of France (Acari: Hydrachnidia). Acarologia 50(1): 21–91. https://doi.org/10.1051/acarologia/20101952

Thor S (1898) Nye hydrachnideformer, fundne i Norge sommeren 1898, Forelobig meddelelse. Archiv for Mathematik og Naturvidenskab 20: 1–12.

Tyukosova V, Gerecke R, Stur E, Ekrem T (2022) Disentangling the identity of *Lebertia porosa* Thor, 1900 using integrative taxonomy (Acari: Hydrachnidia). European Journal of Taxonomy 836(1): 131–169. https://doi.org/10.5852/ejt.2022.836.1921

Valdecasas AG (1988) Lista sinonímica y bibliográfica de las Hidracnelas (Acari, Hydrachnellae) de la Península Ibérica, Islas Baleares e Islas Canarias. Lista de la flora y fauna de las aguas continentales de la Peninsula Iberica. Publicacion no 5. Asociacion Española de Limnologia, Museo Nacional de Ciencias Naturales (CSIC), Madrid, 81 pp. http://www.limnetica.net/documentos/listas/Lista_5_Hidracnelas.pdf [accessed 16 May 2024]

Viets K (1930) Zur Kenntnis der Hydracarinen-Fauna von Spanien. Archiv für Hydrobiologie 21(2): 175–240, 21(3): 359–446.

Walter C (1925) Hydracariens de l’Algerie et de la Tunisie (Collections de M. H. Gauthier), Première liste. Bulletin de la Société d’histoire naturelle de l’Afrique du Nord, Alger 16: 189–238.

Walter C (1926) Hydracariens du Maroc. Bulletin de la Société des Sciences Naturelles du Maroc 6(7–8): 129–157.

Supplementary material 1

BOLD TaxonID Tree

Authors: Vladimir Pešić, Andrzej Zawal, Sónia Ferreira, Laura Benitez-Bosco, Ana Cruz-Oliveira, Dinis Girão, Adriana Padilha, Paolo Turaccio, Samantha Rossini, Lorenzo Ballini, Giorgia Staffoni, Sara Fratini, Claudio Ciofi, Alessio Iannucci, Torbjørn Ekrem, Elisabeth Stur

Data type: pdf

Explanation note: Compact Neighbor-Joining tree of all analyzed water mite species based on Kimura 2-parameter distances. BINs are based on the barcode analysis from 16 May 2024. The analyses involved all 307 COI nucleotide sequences.

Link: https://doi.org/10.3897/zookeys.1217.131730.suppl1

Supplementary material 2

List of *Torrenticola* specimens

Authors: Vladimir Pešić, Andrzej Zawal, Sónia Ferreira, Laura Benitez-Bosco, Ana Cruz-Oliveira, Dinis Girão, Adriana Padilha, Paolo Turaccio, Samantha Rossini, Lorenzo Ballini, Giorgia Staffoni, Sara Fratini, Claudio Ciofi, Alessio Iannucci, Torbjørn Ekrem, Elisabeth Stur

Data type: doc

Explanation note: List of *Torrenticola* specimens used for building the Neighbor-Joining (NJ) tree (Fig. 6). Details on the specimens from Portugal are given in Table 1. GenBank numbers are indicated by *. BINs are based on the barcode analysis from 16 May 2024. Country codes (alpha-2 code): AT = Austria, BA = Bosnia and Herzegovina, CR = Croatia, DE = Germany, ES = Spain, FR = France, GR = Greece, IR = Iran, IT = Italy, NO = Norway, NL = the Netherlands, ME = Montenegro, MK = North Macedonia, PT = Portugal, RS = Serbia, TR = Turkey.

Link: https://doi.org/10.3897/zookeys.1217.131730.suppl2

ZooKeys 1217: 173–193 (2024)
DOI: 10.3897/zookeys.1217.129916

Research Article

Five new species and one new record of the genus *Phaenocarpa* Foerster (Hymenoptera, Braconidae, Alysiinae) from South Korea

Ju-Hyeong Sohn[1], Cornelis van Achterberg[2], Sangjin Kim[1], Hyojoong Kim[1]

1 *Animal Systematics Lab., Department of Biological Science, Kunsan National University, Gunsan, 54150, Republic of Korea*
2 *State Key Laboratory of Rice Biology and Ministry of Agriculture, Key Lab of Agricultural Entomology, Institute of Insect Science, Zhejiang University, Hangzhou, 310058, China*
Corresponding author: Hyojoong Kim (hkim@kunsan.ac.kr)

Abstract

Five new species of the genus *Phaenocarpa* Foester, 1863 (Braconidae: Alysiinae) are described and illustrated: *P. acutidentata* Sohn & van Achterberg, **sp. nov.**, *P. tacitoides* Sohn & van Achterberg, **sp. nov.**, *P. setosa* Sohn & van Achterberg, **sp. nov.**, *P. tanycauda* Sohn & van Achterberg, **sp. nov.**, and *P. angusticeps* Sohn & van Achterberg, **sp. nov.** Additionally, *P. tacita* Stelfox, 1941 is recorded for the first time from South Korea. The barcode region of mitochondrial cytochrome c oxidase I (COI) was also analyzed for the seven congeneric species including one from GenBank. In addition, an identification key for the *Phaenocarpa* species recorded in Korea is provided.

Key words: Alysiini, Hymenoptera, new species, parasitoid wasp, phylogeny, taxonomy

Academic editor: Mostafa Ghafouri Moghaddam
Received: 18 June 2024
Accepted: 17 August 2024
Published: 1 November 2024

ZooBank: https://zoobank.org/258AC9E6-CDF4-4E91-97F9-853B852A489C

Citation: Sohn J-H, van Achterberg C, Kim S, Kim H (2024) Five new species and one new record of the genus *Phaenocarpa* Foerster (Hymenoptera, Braconidae, Alysiinae) from South Korea. ZooKeys 1217: 173–193. https://doi.org/10.3897/zookeys.1217.129916

Introduction

The subfamily Alysiinae is a relatively large taxon in the family Braconidae, consisting of more than 2,440 valid species worldwide (Yu et al. 2016). Alysiinae is subdivided into two tribes, Alysiini and Dacnusini, with 76 and 31 genera, respectively. In South Korea, 270 species in 21 genera have been recorded, 132 within Alysiini and 138 within Dacnusini (NIBR 2022). These two tribes can be distinguished from each other by the presence (Alysiini) or the absence (Dacnusini) of a vein r-m on the fore wing (Shaw and Huddleston 1991). Alysiinae forms part of the Cyclostome clade and comprises exclusively koinobiont endoparasitoids of dipterous larvae (Yu et al. 2016). They use the outwardly curved or straight teeth (with 2–7 teeth) of the exodont mandible to emerge from the host puparium (Docavo et al. 2002). Several species have been utilized for biological control in *Liriomyza trifolii* (Diptera, Agromyzidae) and *Drosophila suzukii* (Diptera, Drosophilidae)(Ozawa et al. 2001; Chabert et al. 2012).

The genus *Phaenocarpa* Foerster, 1863 is a large and worldwide genus of Alysiinae, which includes 231 species in nine subgenera (Yu et al. 2016; Zhu et al. 2017). *Phaenocarpa* species are known as koinobiont endoparasitoids, mainly parasitizing larvae of diverse dipterous families, such as Anthomyiidae, Chloropidae, Clusiidae, Drosophilidae, Muscidae, Scathophagidae, Sciomyzidae, Syrphidae, and Muscidae (Wharton 1984; van Achterberg 1998, 2009). This genus can be diagnosed from other alysiine genera by the following combination of characters: the first flagellomere is shorter than the second flagellomere (rarely subequal), vein 3–SR of forewing is longer than vein 2–SR, and vein CU1b is longer than 3–CU1.

In Korea, Papp (1968, 1994) has recorded four species: *Phaenocarpa* (*Discphaenocarpa*) *angustiptera* Papp, 1968, *P.* (*Phaenocarpa*) *eunice* (Haliday, 1838), *P.* (*P.*) *picinervis* (Haliday, 1838), and *P.* (*P.*) *ruficeps* (Nees von Esenbeck, 1812). Later, Sohn et al. (2021) recorded five additional species: *Phaenocarpa* (*P.*) *artotemporalis* Sohn & van Achterberg, 2021, *P.* (*P.*) *brachyura* Sohn & van Achterberg, 2021, *P.* (*P.*) *lobata* Sohn & van Achterberg, 2021, *P.* (*P.*) *masha* Belokobylskij, 1998, and *P.* (*P.*) *fidelis* Fischer, 1970.

In this study, we used the cytochrome c oxidase I (COI), barcode region of the Korean seven *Phaenocarpa* species to confirm their pairwise genetic distances. The comparative diagnoses provides the diagnosis of each new and unrecorded species, comparing them with species that have similar characters. Descriptions, diagnoses, identification keys, and photographs of the diagnostic characters are also provided.

Materials and methods

Samples of the new species were collected using Malaise traps in South Korea at Mt. Odaesan (Gangwon-do), Mt. Kalbong (Gyeonggi-do), and Gwaneumsa Temple (Jeju-do). The sorting and preparation were performed at the Animal Systematics Laboratory (**ASL**), Department of Biological Science, Kunsan National University (**KSNU**).

Wharton et al. (1997) and Zhu et al. (2017) were used for morphological identification of generic and subgeneric levels. Morphological characters were observed with a Leica M205 C stereomicroscope. The Taxapad database (Yu et al. 2016) was used for references up to 2015. The terminology follows Wharton (2002) and van Achterberg (1993). Holotypes of the new species have been deposited in the **NIBR** (National Institute of Biological Resources, Incheon) collection. A Leica DMC2900 digital camera and a Leica M205 C stereo microscope (Leica Geosystems AG, Mannheim, Germany) were used for photography; all pictures were taken for each final photo using multi-focusing technology. LAS V4.11 (Leica Geosystems AG, St. Gallen, Switzerland) and Helicon Focus 7 (Helicon Soft, Kharkiv, Ukraine) software were used to stack the photographs. Final illustrations were created using Adobe Photoshop CS6.

For DNA analyses, whole genomic DNA was extracted from the specimens using a Labopass Tissue kit (Cosmo Genetech, Daejeon, Korea) following the manufacturer's protocol. In order to conserve morphologically complete voucher specimens, the 'non-destructive method' by Favret (2005) and the 'freezing method' by Yaakop et al. (2009) were used, with slight modification to avoid the first crushing of the sample. In the original protocol, the sample was crushed or damaged and then soaked in 180 µL of buffer ATL + 20 µL of proteinase and incubated at 55 °C for 3 h. In the slightly modified DNA extraction methods, samples were incubated in 180 µL of buffer ATL + 20 µL of proteinase K without first crushing the sample, followed by a 10-min incubation at 55 °C and then kept in a freezer at −22 °C overnight. Subsequently, a general protocol was followed for the remaining steps. The primer sets of *LCO-1490* (5'-GGTCAACAAATCATAAAGATATTGG-3') and HCO-2198 (5'-TAAACTTCAGGGTGACCAAAAAATCA-3') was used to amplify approximately 658 bp as the partial front region of the COI. The polymerase chain reaction (PCR) products were amplified by using AccuPowerH PCR PreMix (BIONEER, Corp., Daejeon) in 20 µl reaction mixtures containing 0.4 µM of each primer, 20 µM of the dNTPs, 20 µM of the $MgCl_2$, and 0.05 µg of the genomic DNA template. PCR amplification was performed using a GS1 thermo-cycler (Gene Technologies, Ltd., U.K) according to the following procedure: initial denaturation at 95 °C for 5 min, followed by 34 cycles at 94 °C for 35 sec; an annealing temperature of 48 °C for 25 sec; an extension at 72 °C for 45 sec, and a final extension at 72 °C for 5 min. PCR products were visualized using electrophoresis and a 1.5% agarose gel. A single band was observed and sequenced using an automated sequencer (ABI Prism 3730 XL DNA Analyzer, California, USA) at Macrogen Inc. (Seoul, South Korea).

Results

COI analysis

A total of 586 bp of the COI fragments were sequenced from *P. tacita* Stelfox, *P*. *acutidentata* sp. nov., *P. tacitoides* sp. nov., *P. setosa* sp. nov., *P. tanycauda* sp. nov., and *P. angusticeps* sp. nov. that were deposited in GenBank (accession numbers PP587250–PP587256) (Table 1). Pairwise distances were estimated by using the *P*-distance model with the option for pairwise deletion. Interspecific distance ranged from 0.053 to 0.268 (average 0.131) (Table 2).

Table 1. Species list for COI analysis for the present study.

No	Species	NCBI accession number	Reference
1	*P. acutidentata* Sohn & van Achterberg, sp. nov.	PP587250	this study
2	*P. angusticeps* Sohn & van Achterberg, sp. nov.	PP587255	this study
3	*P. artotemporalis* Sohn & van Achterberg, 2021	MZ318086	Sohn et al. 2021
4	*P. brachyura* Sohn & van Achterberg, 2021	MZ318087	Sohn et al. 2021
5	*P. fidelis* Fischer, 1970	MZ318083	Sohn et al. 2021
6	*P. lobata* Sohn & van Achterberg, 2021	MZ318085	Sohn et al. 2021
7	*P. masha* Sohn & van Achterberg, 2021	MW376066	Sohn et al. 2021
8	*P. ruficeps* (Nees, 1812)	MZ318084	Sohn et al. 2021
9	*P. setosa* Sohn & van Achterberg, sp. nov.	PP587252	this study
10	*P. tacita* Stelfox, 1941	PP587256	this study
11	*P. tacitoides* Sohn & van Achterberg, sp. nov.	PP587251	this study
12	*P. tanycauda* Sohn & van Achterberg, sp. nov.	PP587254	this study

Table 2. Calculated genetics distance, based on COI sequences between *Phaenocarpa* species used in the analysis.

	P. acutidentata	***P. angusticeps***	***P. artotemporalis***	***P. brachyura***	***P. fidelis***	***P. lobata***	***P. masha***	***P. ruficeps***	***P. setosa***	***P. tacita***	***P. tacitoides***	***P. tanycauda***
P. acutidentata												
P. angusticeps	0.111											
P. artotemporalis	0.162	0.140										
P. brachyura	0.106	0.108	0.123									
P. fidelis	0.104	0.108	0.125	0.072								
P. lobata	0.097	0.104	0.128	0.072	0.053							
P. masha	0.135	0.135	0.152	0.137	0.123	0.126						
P. ruficeps	0.114	0.099	0.140	0.108	0.097	0.087	0.121					
P. setosa	0.099	0.114	0.147	0.094	0.094	0.094	0.125	0.101				
P. tacita	0.119	0.113	0.109	0.118	0.106	0.108	0.121	0.104	0.108			
P. tacitoides	0.104	0.104	0.133	0.096	0.096	0.108	0.126	0.097	0.099	0.108		
P. tanycauda	0.241	0.249	0.268	0.234	0.237	0.234	0.242	0.247	0.229	0.241	0.251	

Taxonomy

Phaenocarpa Foerster, 1863

Phaenocarpa Foerster, 1863: 267. Type species (by original designation): *Alysia picinervis* Haliday, 1838.

Diagnosis. Third antennal segment shorter than fourth segment; fore wing vein 2–SR shorter than vein 3–SR, vein CU1b longer than vein 3–CU1; vein 1-M of hind wing comparatively long.

Biology. Koinobiont endoparasitoids of larvae of Dipteran species (Wharton 1984).

Distribution. Cosmopolitan.

Key to the Korean *Phaenocarpa* species

1 Temples distinctly striate ventrally; mesopleuron largely coarsely sculptured; face laterally extensively and finely striate .... ***P. angustiptera*** **Papp, 1968**
– Temples smooth ventrally; mesopleuron largely smooth, except for area of precoxal sulcus; face laterally smooth or nearly so **2**
2 Vein r-m of fore wing bordered with blackish setae, resulting in one infuscated patch; mesoscutum with metallic sheen.. .... ***P. picinervis*** **(Haliday, 1838)**
– Vein r-m of fore wing normal, not bordered with blackish setae; mesoscutum without metallic sheen **3**
3 Mandible slender, ~ 2.3 × longer than wide; vein 2-1A of fore wing of ♂ strongly widened .... ***P. eunice*** **(Haliday, 1838)**
– Mandible robust, at most 1.9 × longer than wide; vein 2-1A of fore wing of ♂ narrow **4**

4 Scutellar sulcus evenly narrowed medially, 3–5 × wider than its median length; head more or less reddish or yellowish brown .... ***P. ruficeps*** **(Nees, 1812)**

– Scutellar sulcus wide medially, 2–3 × wider than long medially; head dark brown or black **5**

5 First tooth of mandible gradually connected to second tooth, forming a straight or arcuate connection (Figs 3K, 4K) **6**

– First tooth of mandible separated from second tooth by small incision (Figs 1K, 2K, 5K, 6K) **9**

6 Ovipositor sheath approx. as long as hind tibia; first tergite 1.6–2.0 × longer than its apical width **7**

– Ovipositor sheath 1.4 × longer than hind tibia; first tergite at most 1.5 × longer than its apical width **8**

7 First flagellomere ~ 2 × longer than wide; second flagellomere 1.6 × longer than first flagellomere; notauli not reaching medio-posterior depression; vein 3-SR 1.6 × longer than 2-SR; antenna without whit segments .... ***P. fidelis*** **Fischer, 1970**

8 Second flagellomere 2 × longer than first flagellomere (Fig. 5J); mandible 1.8 × longer than wide (Fig. 4K); first metasomal tergite 1.5 × longer than its apical width (Fig. 4H) ..... ***P. tanycauda*** **Sohn & van Achterberg, sp. nov.**

– Second flagellomere 1.4 × longer than first flagellomere (Fig. 3J); madible 1.4 × longer than wide (Fig. 3K); first metasomal tergite as long as wide apically (Fig. 3H) .... ***P. setosa*** **Sohn & van Achterberg, sp. nov.**

9 First flagellomere 2.8–3.6 × longer than wide **10**

– First flagellomere 4.2–5.1 × longer than wide (Figs 1J, 2J, 5J, 6J) **13**

10 Eye in dorsal view 4.0–4.5 × as long as temple; propleuron reddish brown; notauli reduced posteriorly ... ***P. artotemporalis*** **Sohn & van Achterberg, 2021**

– Eye in dorsal view 2.0–3.0 × as long as temple; propleuron black or orange-brown; notauli usually complete (up to medio-posterior depression or nearly so) **11**

11 Mandible subparallel-sided; setose part of ovipositor sheath ~ 0.7 × as long as hind tibia; first metasomal tergite ~ 1.4 × longer than its apical width .... ***P. brachyura*** **Sohn & van Achterberg, 2021**

– Mandible distinctly widened dorsally; setose part of ovipositor sheath 1.2–1.3 × as long as hind tibia; first tergite 1.1–1.2 × longer than its apical width **12**

12 Tarsal claws slender; third and fourth antennal segments dark brown and slender; metanotum more or less tooth-shaped protruding dorsally in lateral view; pterostigma ~ 4 × longer than wide; middle tooth of mandible not widened dorsally .... ***P. masha*** **Belokobylskij, 1998**

– Tarsal claws robust; third and fourth antennal segments yellow and robust; metanotum obtuse dorsally in lateral view; pterostigma ~ 5.5 × longer than wide; middle tooth of mandible widened dorsally .... ***P. lobata*** **Sohn & van Achterberg, 2021**

13 Precoxal sulcus distinct and complete, reaching anterior and posterior edge of mesopleuron, (Fig. 1G); ovipositor sheath 1.9 × longer than hind tibia; second flagellomere 1.5 × longer than first flagellomere; propodeum entirely rugose .... ***P. acutidentata*** **Sohn & van Achterberg, sp. nov.**

– Precoxal sulcus only medially impressed, not reaching anterior and posterior edge of mesopleuron (Fig. 2J, 5J, 6J); ovipositor sheath 0.8–1.0 × as long as hind tibia; second flagellomere 1.1–1.2 × longer than first flagellomere; propodeum entirely smooth except for medio-longitudinal carina **14**

14 Mandible 1.2 × longer than its maximum width (Fig. 5K); minimum width of face (Fig. 5E) 0.9 × its height (measured from ventral rim of antennal sockets to upper margin of clypeus); first flagellomere 4.3 × longer than wide (Fig. 5J) .... ***P. angusticeps*** **Sohn & van Achterberg, sp. nov.**

– Mandible 1.6 × longer than its maximum width (Fig. 2K, 6K); minimum width of face (Fig. 2E, 6E) 1.4 × its height (measured from ventral rim of antennal sockets to upper margin of clypeus); first flagellomere 4.9–5.1 × longer than wide **15**

15 Vein r of fore wing short, ~ 1.4 × longer than wide, vein SR1 of fore wing straight (Fig. 2C); hind femur more slender, 5.6 × longer than width; first tooth of mandible lobe-shaped, widened dorsally, 1.7 × as long as third; [apical antennal segments paler than subbasal segments]........................ .... ***P. tacitoides*** **Sohn & van Achterberg, sp. nov.**

– Vein r of for wing ~ 3.0 × longer than wide, vein SR1 of fore wing slightly curved (Fig. 6C); hind femur 4.6 × longer than width. first tooth of mandible acute and as long as third tooth................................ ***P. tacita*** **Stelfox, 1941**

Phaenocarpa acutidentata Sohn & van Achterberg, sp. nov.

https://zoobank.org/7F346053-E46C-4CA6-A821-3DA7A288AE39

Fig. 1

Type material. *Holotype* • ♀ (NIBR), **South Korea**, Mt. Odae, Jinbu-myeon, Pyeongchang-gun, Gangwon-do, 37°45'54.7"N, 128°34'13.8"E, 15.IX.2020, Ju-Hyeong Sohn leg. GenBank accession no. PP587250.

Comparative diagnosis. The new species is similar with *P. telengai* Belokobylskij, 1998, but recognizable the third tooth distinctly and acutely protruding as the first one (only second tooth narrow and acute in *P. telengai*), first flagellomere 4.2 × longer than wide (2.8–3.0 × in *P. telengai*) and hind femur 4.2 × longer than wide (4.7–5.0 × in *P. telengai*).

Description. Holotype, ♀, body 2.8 mm in lateral view, fore wing 2.6 mm, ovipositor sheath 1.4 mm in lateral view, antenna 3.4 mm (apical part of antennae missing).

***Head*:** Width of head 1.5 × its median length in dorsal view (Fig. 1D). Antenna with 25 antennomeres (terminal antennomere missing), first flagellomere 4.2 × longer than wide (Fig. 1K), second flagellomere 1.5 × longer than first antennomere and 5.2 × longer than wide. Medial antennal segments (18th segment) 2.3 × longer than wide. Eye slightly oval, in lateral view 1.2 × as long as wide. Minimum width of face (Fig. 1E) 1.2 × its height; face rugose with setose. Eye in dorsal view 1.8 × as long as temple. Ocello-ocular line (OOL) 4.8 × longer than diameter of anterior ocellus; OOL: antero-posterior ocellar line (AOL): postero-ocellar line (POL) = 30: 7: 10. Vertex smooth and glabrous. Width of clypeus 2.3 × its maximum length. Mandible (Fig. 1L) 1.8 × longer than wide, wide with first tooth curved; second tooth narrow and long, 1.2 × longer than first tooth, tip of second tooth reddish brown; third tooth (as first) distinctly acutely protruding; carina on third tooth distinct.

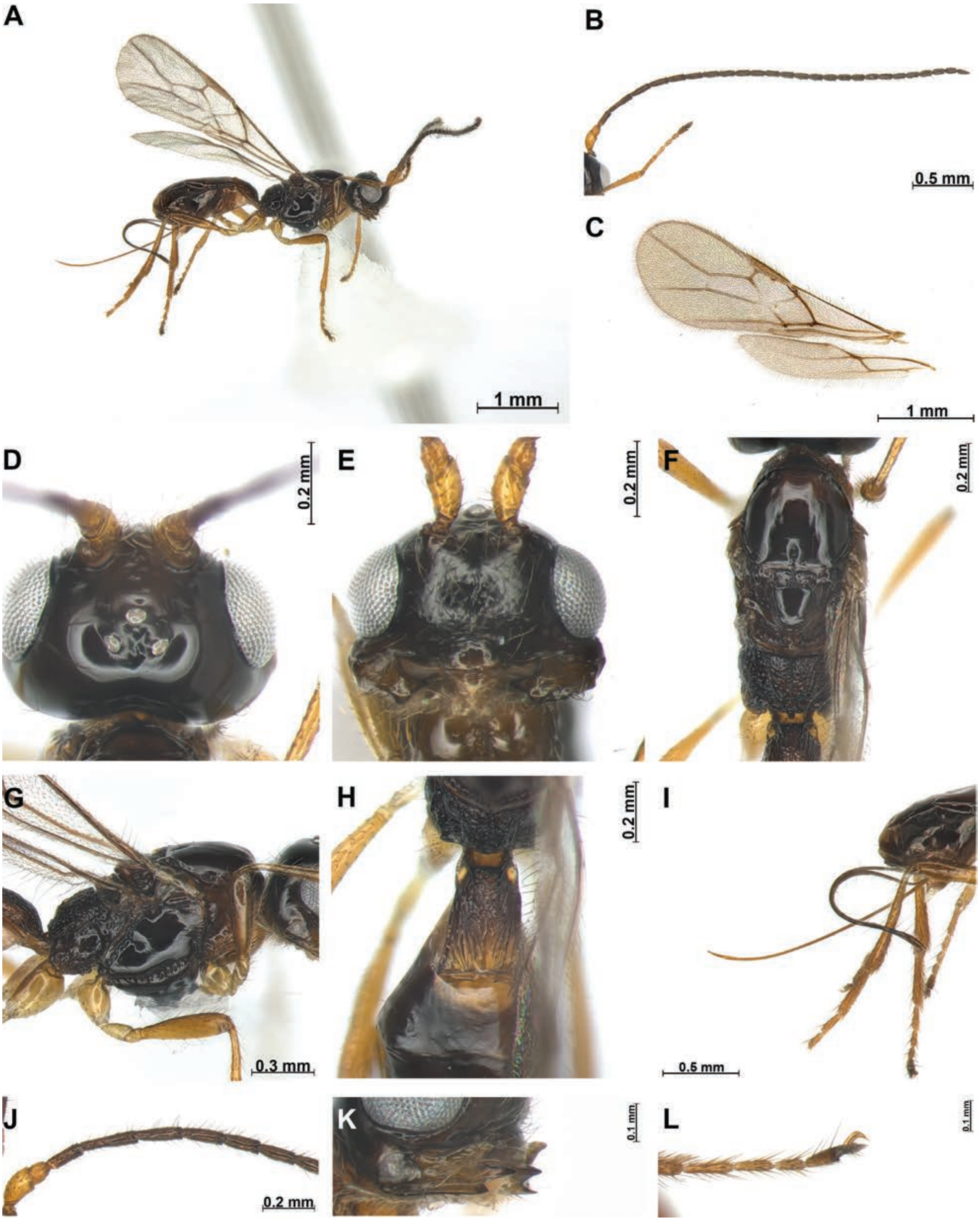

Figure 1. *Phaenocarpa acutidentata* sp. nov., ♀ **A** habitus, lateral view **B** antennae **C** wings **D** head, dorsal view **E** head, frontal view **F** mesosoma, dorsal view **G** mesosoma, lateral view **H** first metasomal tergite, dorsal view **I** ovipositor sheath, lateral view **J** proximal part of antenna **K** mandible, lateral view **L** claw, lateral view.

***Mesosoma*:** In dorsal view mesosoma 2.2 × longer than wide 1.6 × longer than high in lateral view. Mesoscutum (Fig. 1F) with small and round medio-posterior depression and glabrous; notauli impressed anteriorly, not reaching to medio-posterior depression; scutellar sulcus with one carina; apical part of mesopleuron and metapleuron without setae, posterior mesopleural groove sculpted. Precoxal sulcus distinct, reaching anterior and posterior edge of mesopleuron. Maximum length of propodeum (Fig. 1F) 0.5 × as long as its width, largely sculpted; posterior part of propodeum with small areola, not reaching middle of propodeum. Metanotum not protruding medio-dorsally in lateral view (Fig. 1G). Fore wing (Fig. 1C) 2.6 × as long as wide; pterostigma widened medially 5.1 × longer than wide; vein r of fore wing 4.0 × longer than wide; vein SR1 1.8 × longer than vein 3-SR; vein 3-SR 1.5 × longer than 2-SR; second submarginal cell long and narrow, 2.7 × longer than its medium length; 3-SR: r: SR1 = 12: 3: 22; first discal cell of fore wing 0.8 × longer than wide in median length; first discal cell of fore wing 1.1 × as longer medially than wide. Hind wing: vein M+CU+1-M: vein 1r-m = 4: 1.

***Leg*:** Hind femur 4.2 × longer than wide and 0.7 × as long as hind tibia; hind tibia 11 × longer than wide; hind tibia as long as hind tarsus.

***Metasoma*:** First tergite (Fig. 1H) sparsely rugose, 1.5 × longer than its apical width. Setose part of ovipositor sheath (Fig. 1I) 1.4 × longer than mesosoma and 1.9 × longer than hind tibia.

***Color*:** Body (Fig. 1A) dark brown, antenna dark brown, but anterior yellowish brown; metasoma dark brown; legs yellowish brown; first tergite brown.

Male. Unknown.

Biology. Unknown.

Host. Unknown.

Distribution. South Korea.

Etymology. The specific name *acutidentata* is an adjective, referring to ‘sharp teeth’ in Latin.

Phaenocarpa tacitoides Sohn & van Achterberg, sp. nov.

https://zoobank.org/AF3679A0-77B0-44DC-B3A1-1C4D994019C6

Fig. 2

Type material. ***Holotype*** • ♀ (NIBR), **South Korea**, Mt. Kalbong, Gyeongban-ri, Gapyeong-eup, Gapyeong-gun, Gyeonggi-do, 37°51'10.9"N, 127°26'27.4"E, 11.V.2020, Sohn. GenBank accession no. PP587251.

Comparative diagnosis. Differs from the other *Phaenocarpa* species by vein r of fore wing being much more distal (1.4 × longer than wide). This species similar with *P. tacita* Stelfox, 1941, but easily distinguish by apical antennal segments paler than subbasal segments, and first tooth of mandible lobe-shaped, widened dorsally, 1.7 × as long as third (first tooth of mandible acute and as long as third tooth in *P. tacita*).

Description. Holotype, ♀, body 1.7 mm in lateral view, fore wing 2.0 mm, ovipositor sheath 0.5 mm, antenna 1.5 mm.

***Head*:** Width of head 1.7 × its median length in dorsal view (Fig. 2D). Antenna with 18 antennomeres, first flagellomere slender, 4.9 × longer than wide (Fig. 2K), second flagellomere 1.2 × longer than first and 6.1 × longer than wide. Medial antennal segments 4.1 × longer than wide. Apical antennal segments paler than subbasal segments. Eye slightly oval, in lateral view 1.1 × as long as wide. Minimum width of face (Fig. 2E) 1.4 × its height; face rugose with setose. Eye in dorsal view 2.5 × as

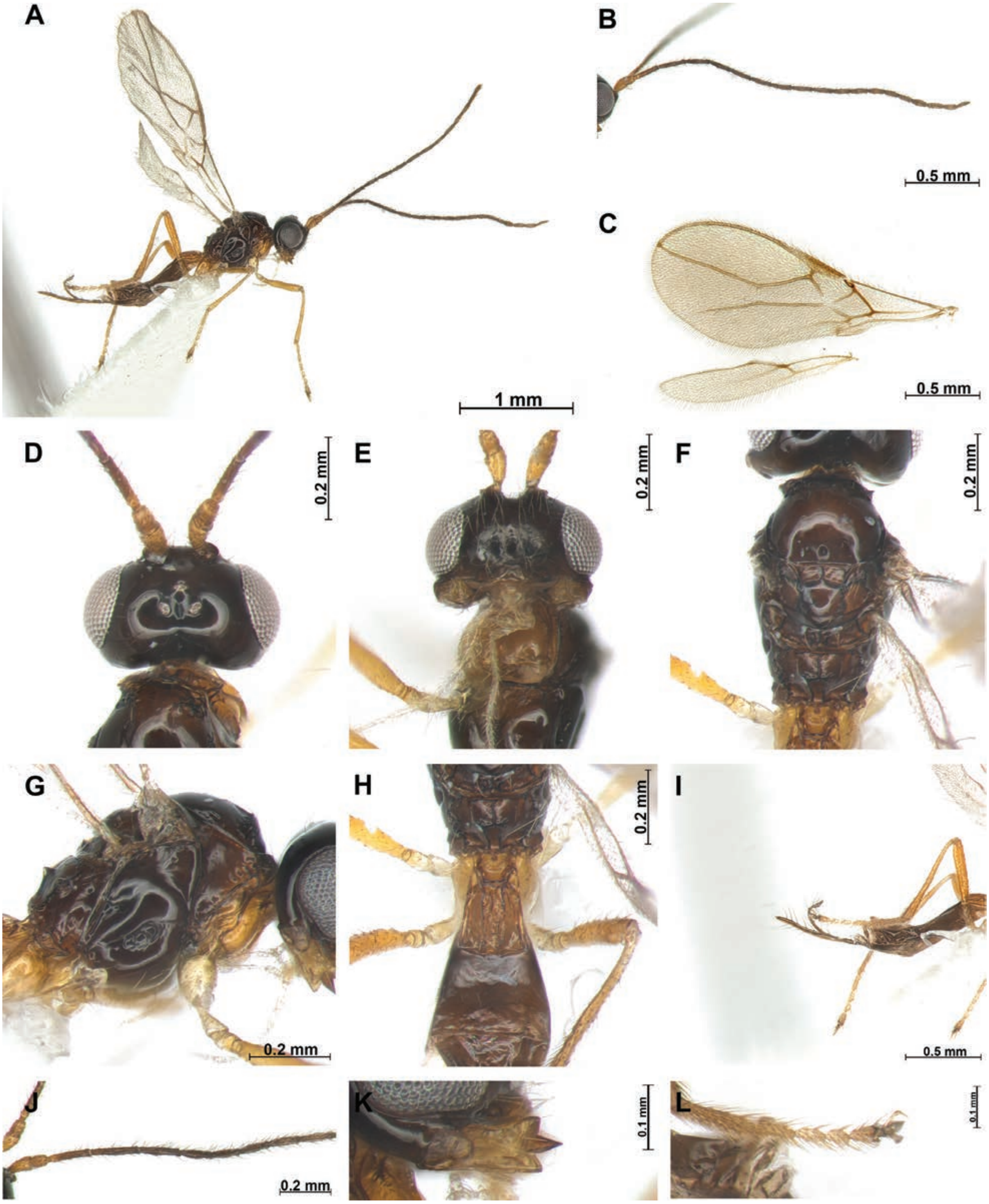

Figure 2. *Phaenocarpa tacitoides* sp. nov., ♀ **A** habitus, lateral view **B** antennae **C** wings **D** head, dorsal view **E** head, frontal view **F** mesosoma, dorsal view **G** mesosoma, lateral view **H** first metasomal tergite, dorsal view **I** ovipositor sheath, lateral view **J** proximal part of antenna **K** mandible, lateral view **L** claw, lateral view.

long as temple. Ocello-ocular line (OOL) 5.3 × longer than diameter of anterior ocellus; OOL: antero-posterior ocellar line (AOL): postero-ocellar line (POL) = 21: 5: 6. Vertex smooth and glabrous. Width of clypeus 2.2 × its maximum length. Mandible (Fig. 2L) 1.6 × longer than wide, wide with first tooth slightly curved upward; second tooth narrow and long, 1.2 × longer than first tooth, tip of second tooth reddish brown; third tooth as long as first tooth, carina on third tooth distinct.

***Mesosoma*:** In dorsal view mesosoma 1.8 × longer than wide and 1.4 × longer than high in lateral view. Mesoscutum (Fig. 2F) with small and round medio-posterior depression and glabrous; notauli impressed anteriorly, not reaching medio-posterior depression; mesoscutum without setae; scutellar sulcus with one carina; apical part of mesopleuron and metapleuron without setae, posterior mesopleuron groove smooth. Precoxal sulcus distinct, but not reaching anterior and posterior edge of mesopleuron. Maximum length of propodeum (Fig. 2F) 0.6 × its width; medio–longitudinal carina present on half of propodeum, posterior part of propodeum with areola, reaching middle of propodeum. In lateral view metanotum with acute protuberance medio-dorsally (Fig. 2G). Fore wing (Fig. 2C) 2.3 × as long as wide; pterostigma widened medially 6.2 × longer than wide; vein r of fore wing 1.4 × longer than wide; vein SR1 2.1 × longer than vein 3-SR; vein 3-SR 1.8 × longer than 2-SR; second submarginal cell long and narrow, 2.8 × longer than its medium length; 3-SR: r: SR1 = 15: 2: 33; first discal cell of fore wing ~ 1.1 × as long medially as wide. Hind wing: vein M+CU+1-M: vein 1r-m = 5: 1.

***Leg*:** Hind femur slender, 5.6 × longer than wide and 0.6 × as long as hind tibia; hind tibia 19 × longer than wide; hind tibia as long as hind tarsus.

***Metasoma*:** First tergite (Fig. 2H) medially rugose and 1.5 × longer than its apical width. Setose part of ovipositor sheath (Fig. 2I) as long as than mesosoma and as long as hind tibia.

***Color*:** Body (Fig. 2A) brown; head dark brown; first tergite yellowish brown, metasoma brown; antenna dark brown; legs yellowish brown.

Male. Unknown.

Biology. Unknown.

Host. Unknown.

Distribution. South Korea.

Etymology. The specific name *tacitoides* is an adjective, named after *P. tacita* and *-oides* added a suffix because of its similarity to this species (“oides” is Latin for “resembling”).

Phaenocarpa setosa Sohn & van Achterberg, sp. nov.

https://zoobank.org/7CB6ABB9-FEF2-4EEB-A9F1-A5980EE615C1
Fig. 3

Type material. ***Holotype*** • ♀ (NIBR), **South Korea**, Mt. Kalbong, Gyeongban-ri, Gapyeong-eup, Gapyeong-gun, Gyeonggi-do, 37°51'10.9"N, 127°26'27.4"E, 05.VI.2020, Sohn. GenBank accession no. PP587252.

Comparative diagnosis. This new species is close to *P. micula* Belokobylskij, 1998, because of sharing width of the first flagellomere (3.0–3.5 × in *P. micula*), deep and smooth notauli and width of the first tergite. However, the new species has the metanotum not protruding (tooth-like protruding in *P. micula*) (Fig. 3G), upper tooth of mandible separated from middle tooth (not separated in *P. micula*), lower tooth of mandible angulate (rounded in *P. micula*), hind tibia partly erect setose (Fig. 3A), width of head 1.7 × greater than its median length (2.0–2.2 × in *P. micula*), second flagellomere 2.0 × longer than first flagellomere (1.5–1.6 × in *P. micula*).

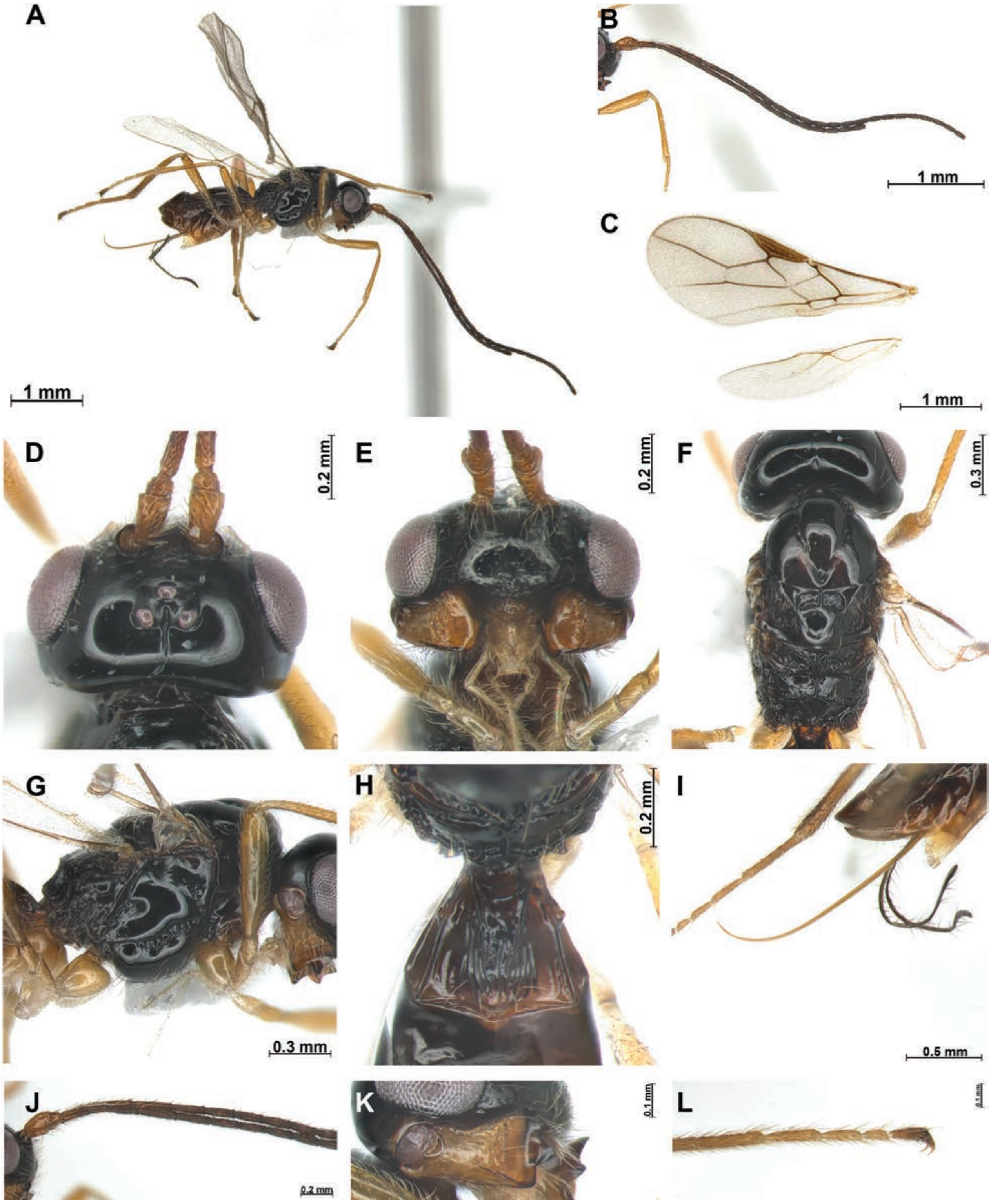

Figure 3. *Phaenocarpa setosa* sp. nov., ♀ **A** habitus, lateral view **B** antennae **C** wings **D** head, dorsal view **E** head, frontal view **F** mesosoma, dorsal view **G** mesosoma, lateral view **H** first metasomal tergite, dorsal view **I** ovipositor sheath, lateral view **J** proximal part of antenna **K** mandible, lateral view **L** claw, lateral view.

Description. Holotype, ♀, body 2.8 mm in lateral view, fore wing 2.7 mm, ovipositor sheath 1.3 mm, antenna 3.8 mm (but apical parts missing).

Head: Width of head 1.7 × its median length in dorsal view (Fig. 3D). Antenna with 23 antennomeres (but apical parts missing), first flagellomere 2.9 × longer than wide (Fig. 3K), second flagellomere 2.0 × longer than first and 7.3 × longer than wide. Medial antennal segments 2.5 × longer than wide. Eye slightly oval, in lateral view 1.2 × as long as wide. Minimum width of face (Fig. 3E) 1.6 × its height; face setose, upper part of clypeus rugose. Eye in dorsal view 1.6 × as long as temple. Ocello-ocular line (OOL) 4.8 × longer than diameter of anterior ocellus; OOL: antero-posterior ocellar line (AOL): postero-ocellar line (POL) = 14: 3: 4. Vertex smooth and glabrous, with distinct longitudinal groove. Width of clypeus 2.6 × its maximum length. Mandible (Fig. 3L) 1.4 × longer than wide, wide with first tooth curved upward and separated from second tooth, second tooth robust, 1.1 × longer than first tooth, tip of second tooth dark brown; third tooth as long as first tooth, not protruding and angulate apically, carina on third tooth distinct.

***Mesosoma*:** In dorsal view mesosoma 2.0 × longer than wide and 1.4 × longer than high in lateral view. Mesoscutum (Fig. 3F) with small and round medio-posterior depression and glabrous; notauli distinctly impressed, almost reaching medio-posterior depression; mesoscutum without setae; scutellar sulcus with one carina; apical part of metapleuron with setae, posterior mesopleuron groove sculptured. Precoxal sulcus distinct, reaching at anterior and posterior edge of mesopleuron. Maximum length of propodeum (Fig. 3F) 0.8 × its width longitudinal carina present on half of propodeum, posterior part of propodeum with areola, reaching up to half of propodeum. In lateral view metanotum obtuse curved medio-dorsally (Fig. 3G). Fore wing (Fig. 3C) 2.3 × as long as wide; pterostigma widened medially 4.5 × longer than wide; vein r of fore wing 1.3 × longer than wide; vein SR1 2.1 × longer than vein 3-SR; vein 3-SR 1.2 × longer than 2-SR; second submarginal 2.1 × longer than its medium length; 3-SR: r: SR1 = 11: 1: 25; first discal cell of fore wing ~ 1.3 × longer medially than wide. Hind wing: vein M+CU+1-M: vein 1r-m = 3: 1.

***Leg*:** Hind femur 5.7 × longer than wide and 0.8 × as long as hind tibia; hind tibia 10 × longer than wide and setae erect except basally (Fig. 3A); hind tibia as long as hind tarsus.

***Metasoma*:** First tergite (Fig. 3H) medially rugose and as long as its apical width. Setose part of ovipositor sheath 1.2 × longer than mesosoma (Fig. 3I) and 1.4 × longer than hind tibia.

***Color*:** Body (Fig. 3A) black; metasoma and antenna dark brown; legs reddish brown.

Male. Unknown.

Biology. Unknown.

Host. Unknown.

Distribution. South Korea.

Etymology. The specific name *setos*” is an adjective, named after the erect setae of the hind tibia.

Phaenocarpa tanycauda Sohn & van Achterberg, sp. nov.

https://zoobank.org/80C76B8C-AB95-48F0-A03C-5928187AA520
Fig. 4

Type material. ***Holotype*** • ♀ (NIBR), **South Korea**, Mt. Kalbong, Gyeongban-ri, Gapyeong-eup, Gapyeong-gun, Gyeonggi-do, 37°51'10.9"N, 127°26'27.4"E, 05.VI.2020, Sohn. GenBank accession no. PP587254.

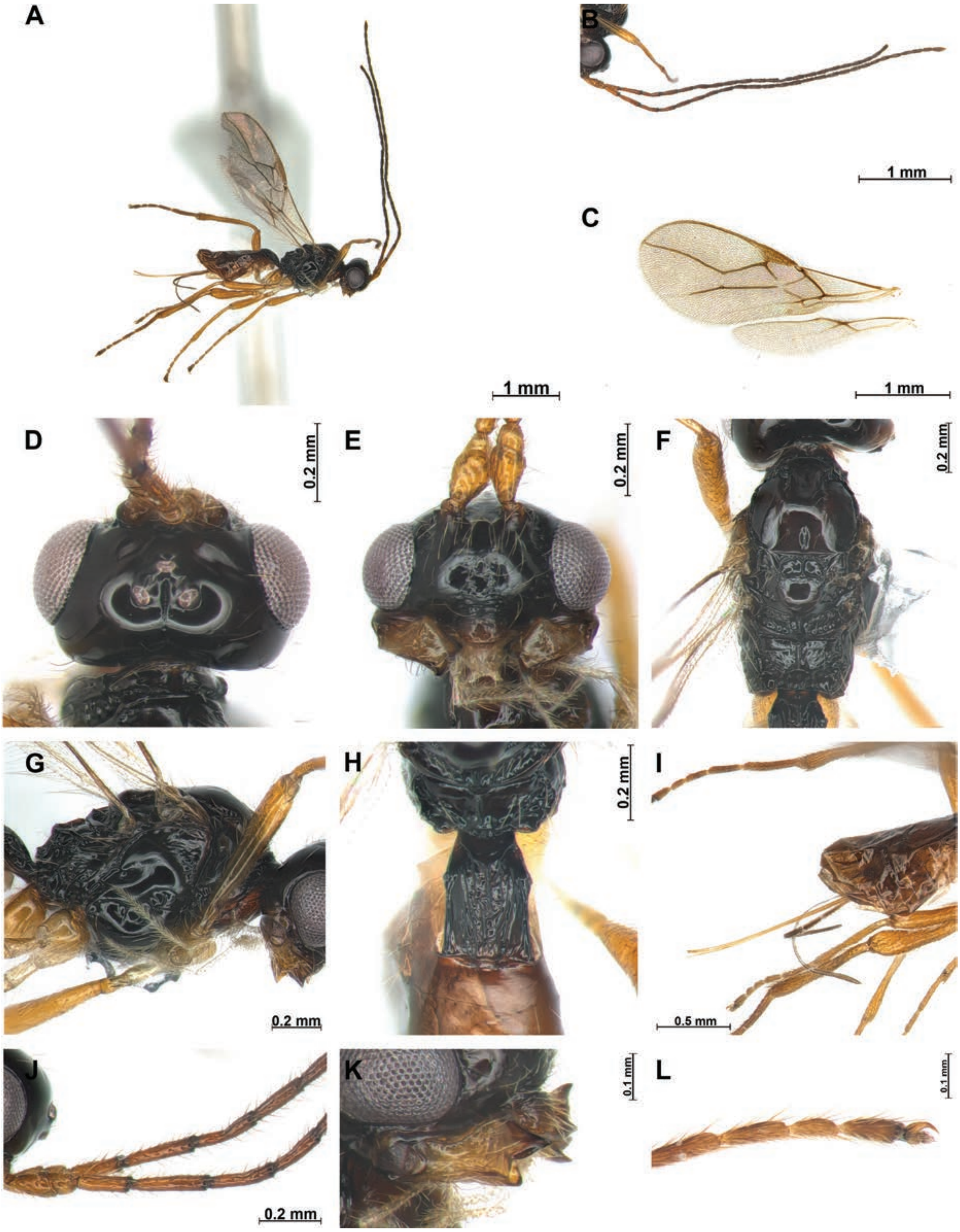

Figure 4. *Phaenocarpa tanycauda* sp. nov., ♀ **A** habitus, lateral view **B** antennae **C** wings **D** head, dorsal view **E** head, frontal view **F** mesosoma, dorsal view **G** mesosoma, lateral view **H** first metasomal tergite, dorsal view **I** ovipositor sheath, lateral view **J** proximal part of antenna **K** mandible, lateral view **L** claw, lateral view.

Comparative diagnosis. This new species is close to *P. chasanica* Belokobylskij, 1998 because of sharing second flagellomere 1.4–1.5 × longer than first flagellomere (same length in *P. chasanica*). Width of head 1.8 × its median length in dorsal view (1.8–2.0 × in *P. chasanica*). In mandible, first and second tooth not separated distinctly. Hind femur 5.0–5.5 × as long as wide. The new species differs from *P. chasanica* by head and mesosoma black (head and mesosoma yellowish brown in *P. chasanica*) and thick and short tarsal claws (tarsal claws thin and relatively long in *P. chasanica*). The new species can be recognised by its comparatively long ovipositor sheath (1.2 × longer than mesosoma and 1.4 × longer than hind tibia) and rugose median part of face rugose.

Description. Holotype, ♀, body 2.5 mm in lateral view, fore wing 2.5 mm, ovipositor sheath 1.0 mm, antenna 3.9 mm.

***Head*:** Width of head 1.8 × its median length in dorsal view (Fig. 4D). Antenna with 26 antennomeres and 1.6 × as long as fore wing or body. First flagellomere 3.2 × longer than wide (Fig. 4K). Second flagellomere 1.4 × longer than first and 4.8 × longer than wide. Middle of antenna segment 3.1 × longer than width. Eye slightly oval, in lateral view 1.1 × as long as wide. Minimum width of face (Fig. 4E) 1.3 × its height; face with setose, median part of face rugose. Eye in dorsal view 2.6 × as long as temple. Ocello-ocular line (OOL) 4.2 × longer than diameter of anterior ocellus; OOL: antero-posterior ocellar line (AOL): postero-ocellar line (POL) = 27: 8: 9. Vertex smooth and glabrous, short longitudinal groove present POL. Width of clypeus 2.6 × its maximum length. Mandible (Fig. 4L) 1.8 × longer than wide, wide with first tooth curved upward and broad; second tooth long and broad, 1.3 × longer than first tooth, tip of second tooth reddish brown; first and second tooth not separate distinctly; third tooth as long as first tooth.

***Mesosoma*:** In dorsal view mesosoma 1.9 × longer than wide and 1.4 × longer than high in lateral view. Mesoscutum (Fig. 4F) with small and round medio-posterior depression and glabrous; notauli distinct anteriorly to half of mesoscutum, not reaching to medio-posterior depression; mesoscutum few setae along notauli; scutellar sulcus with one strong carina; apical part of mesopleuron and metapleuron with few setae, mesopleural groove sculptured. Precoxal sulcus distinct, reaching anterior and posterior edges of mesopleuron. Maximum length of propodeum (Fig. 4F) 0.5 × its width; longitudinal carina present on propodeum, posterior part of propodeum with small areola, not reaching to half of propodeum. In lateral view, metanotum not protruding medio-dorsally (Fig. 4G). Fore wing (Fig. 4C) 2.4 × as long as wide; pterostigma broad, 4.3 × longer than wide; vein r of fore wing 1.7 × longer than wide; vein SR1 2.1 × longer than vein 3-SR; vein 3-SR 1.5 × longer than 2-SR; second submarginal cell 2.6 × longer than its medium length; 3-SR: r: SR1 = 13: 1: 27 first discal cell of fore wing as long as wide medially. Hind wing: vein M+CU+1-M: vein 1r-m = 4: 1.

***Leg*:** Hind femur 5.4 × as long as wide and 0.7 × as long as hind tibia; hind tibia 8.8 × longer than wide; hind tibia 0.8 × as long as hind tarsus.

***Metasoma*:** First tergite (Fig. 4H) rugose 1.4 × longer than its apical width. Setose part of ovipositor sheath (Fig. 4I) 1.2 × longer than mesosoma, 1.4 × longer than hind tibia and 0.4 × as long as fore wing.

***Color*:** Body (Fig. 4A) black; metasoma (except first tergite) and antenna dark brown but basal part of antenna and legs yellowish brown.

Male. Unknown.

Biology. Unknown.

Host. Unknown.

Distribution. South Korea.

Etymology. The specific name *tanycauda* is an adjective, named after the long ovipositor sheath; *tanyo* is Greek for stretched out, *cauda* is Latin for tail.

Phaenocarpa angusticeps **Sohn & van Achterberg, sp. nov.**

https://zoobank.org/998AAEBA-48AD-4866-BE3C-B0AFFF07A756
Fig. 5

Type material. ***Holotype*** • ♀ (NIBR), South Korea, Gwaneumsa, Sanrokbuk-ro, Jeju-si, Jeju-do, 33°25'43.9"N, 126°33'24.8"E, 06.VII.2020, Sohn. GenBank accession no. PP587255.

Comparative diagnosis. Differs from all the species of *Phaenocarpa* by having narrow face, 0.9 × from ventral rim of antennal sockets to upper margin of clypeus (1.2–1.6 × in other species). Second flagellomere 1.1 × longer than first flagellomere (1.2–2.0 × in other species).

Description. Holotype, ♀, body 2.4 mm in lateral view, fore wing 2.7 mm, ovipositor sheath 0.8 mm, antenna 3.5 mm.

Head**:** Width of head 1.8 × its median length in dorsal view (Fig. 5D). Antenna with 23 antennomeres. First flagellomere 4.3 × longer than wide (Fig. 5K), second flagellomere 1.1–1.2 × longer than first and 5.3 × longer than wide. Middle of antenna segment 3.4 × longer than wide. Eye slightly oval, in lateral view 1.2 × as long as wide. Minimum width of face (Fig. 5E) 0.9 × its height; face smooth with setose. Eye in dorsal view 2.4 × as long as temple. Ocello-ocular line (OOL) 4.9 × longer than diameter of anterior ocellus; OOL: antero-posterior ocellar line (AOL): postero-ocellar line (POL) = 28: 7: 9. Vertex smooth and glabrous, longitudinal groove present POL. Width of clypeus 2.6 × its maximum length. Mandible (Fig. 5L) 1.2 × longer than wide, wide with first tooth curved upward and broad; second tooth narrow and long, 1.2 × longer than first tooth, tip of second tooth dark brown; first and second tooth distinctly separate; third tooth as long as first tooth.

Mesosoma**:** In dorsal view mesosoma 2.0 × longer than wide and 1.4 × longer than high in lateral view. Mesoscutum (Fig. 5F) with small and round medio-posterior depression and glabrous; notauli distinct anteriorly to half of mesoscutum, not reaching to medio-posterior depression; anterior part of mesoscutum with few setae; scutellar sulcus with one carina; apical part of mesopleuron and metapleuron with few setae, mesopleuron groove sculptured in lateral view. Precoxal sulcus distinct, not reaching anterior and posterior edge of mesopleuron. Maximum length of propodeum (Fig. 5F) 0.5 × its width; longitudinal carina present on propodeum, posterior part of propodeum with small areola, not reaching up to half of propodeum, anterior part of propodeum smooth. In lateral view, metanotum curved medio-dorsally (Fig. 5G). Fore wing (Fig. 5C) 2.3 × as long as wide; pterostigma widened medially and nearly as wide as vein 1-R1; vein r of fore wing 3.8 × longer than wide; vein SR1 3.0 × longer than vein 3-SR; vein 3-SR 1.8 × longer than 2-SR; second submarginal cell 2.4 × longer than its medium length; 3-SR: r: SR1 = 5: 1: 15; first discal cell of fore wing as long as wide medially. Hind wing: vein M+CU+1-M: vein 1r-m = 4: 1.

Leg**:** Hind femur 6.0 × as long as wide and 0.7 × as long as hind tibia; hind tibia 15 × as long as wide; hind tibia 1.1 × longer than hind tarsus.

Metasoma**:** First tergite (Fig. 5H) rugose medially, 1.4 × longer than its apical width. Setose part of ovipositor sheath (Fig. 5I) 0.9 × as long as mesosoma, 0.8 × as long as hind tibia.

Color**:** Body (Fig. 5A) black; head black; first tergite reddish brown, metasoma reddish brown; antenna dark brown, anterior parts yellowish brown, apical parts brown; legs yellowish brown.

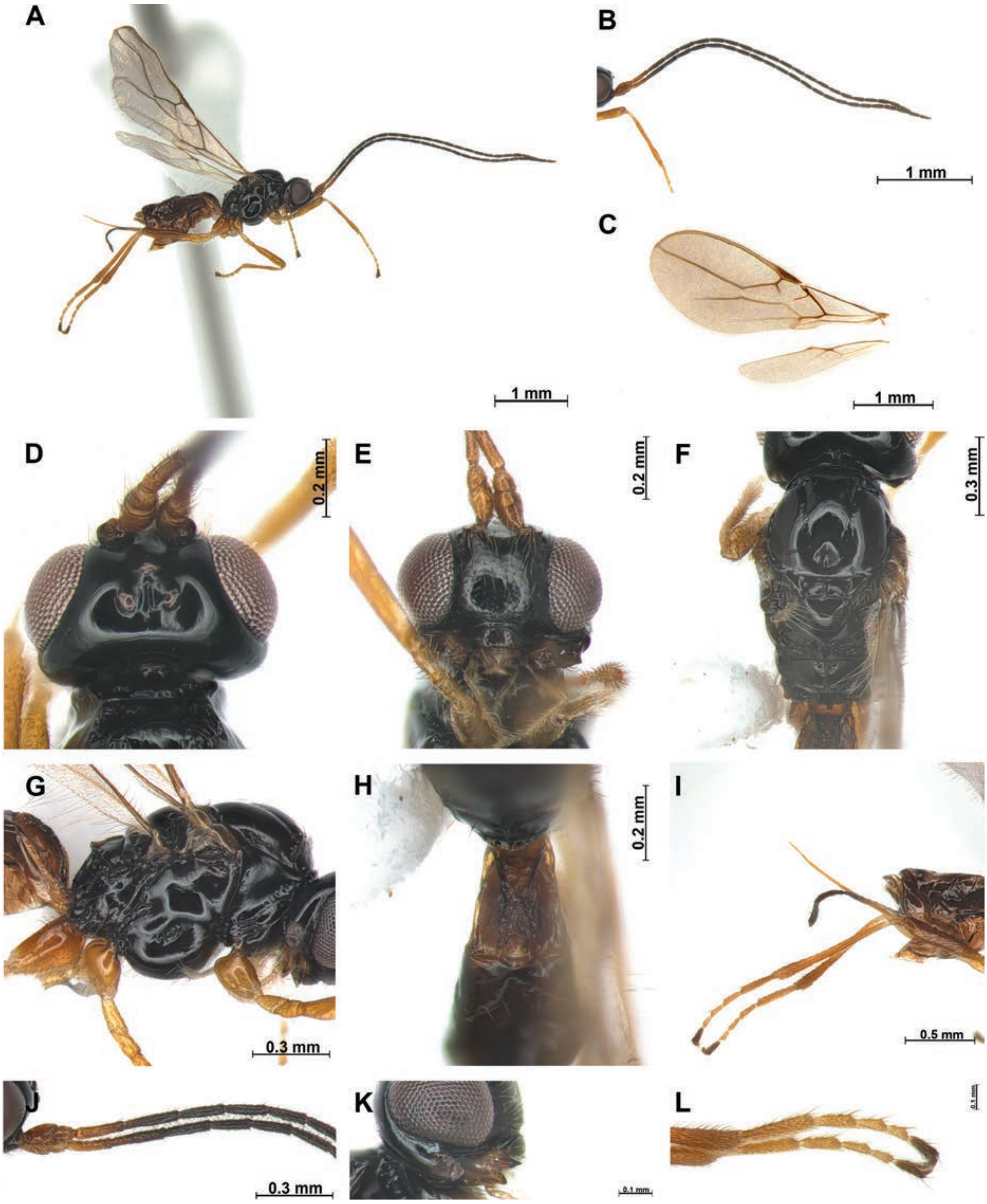

Figure 5. *Phaenocarpa angusticeps* sp. nov., ♀ **A** habitus, lateral view **B** antennae **C** wings **D** head, dorsal view **E** head, frontal view **F** mesosoma, dorsal view **G** mesosoma, lateral view **H** first metasomal tergite, dorsal view **I** ovipositor sheath, lateral view **J** proximal part of antenna **K** mandible, lateral view **L** claw, lateral view.

Male. Unknown.

Biology. Unknown.

Host. Unknown.

Distribution. South Korea.

Etymology. The specific name *angusticeps* is an adjective, *angustus* is Latin for narrow, *ceps* is Latin for head.

***Phaenocarpa tacita* Stelfox, 1941**

Fig. 6

Type material. ***Holotype*** • (NIBR), **South Korea**, Mt. Kalbongsan, Gyeongban-ri, Gapyeong-eup, Gapyeong-gun, Gyeonggi-do, 37°51'10.9"N, 127°26'27.4"E, 05.VI.2020, Sohn. GenBank accession no. PP587256.

Comparative diagnosis. According to the East Palaearctic key of Belokobylskij (1998), mandible (Fig. 6K) expanded towards the apical. Propodeum smooth, longitudinal carina present half of the propodeum. First metasomal tergite (Fig. 6H) 1.5 × longer than its apical width (1.4–1.6 × in Belokobylskij 1998). The Korean species ovipositor sheath 0.9 × as long as hind tibia (1.1–1.2 × in Belokobylskij 1998), but according to Belokobylskij (1998), it rarely equals to hind tibia.

Description. ♀. Body 1.9 mm in lateral view, fore wing 2.1 mm, ovipositor sheath 0.9 mm, antenna 2.6 mm (apical parts missing).

***Head*:** Width of head 1.8 × its median length in dorsal view (Fig. 6D). Antenna with 17 antennomeres (apical parts missing), first flagellomere 5.1 × longer than wide (Fig. 6K), second flagellomere 1.2 × longer than first and 6.1 × longer than wide. Medial antennal segments 4.6 × longer than wide. Eye slightly oval, in lateral view 1.1 × as long as wide. Minimum width of face (Fig. 6E) 1.4 × its height; face setose, upper part of clypeus rugose. Eye in dorsal view 2.3 × as long as temple. Ocello-ocular line (OOL) 4.6 × longer than diameter of anterior ocellus; OOL: antero-posterior ocellar line (AOL): postero-ocellar line (POL) = 22: 6: 7. Vertex smooth and glabrous, with distinct longitudinal groove. Width of clypeus 2.7 × its maximum length. Mandible (Fig. 6L) 1.6 × longer than wide, wide with first tooth curved upward; second tooth narrow and long, 1.3 × longer than first tooth, tip of second tooth dark brown; third tooth as long as first tooth.

***Mesosoma*:** In dorsal view mesosoma 2.0 × longer than wide and 1.3 × longer than high in lateral view. Mesoscutum (Fig. 6F) with small and round medio-posterior depression and glabrous; notauli impressed anteriorly, not reaching medio-posterior depression; mesoscutum without setae; scutellar sulcus with one carina; apical part of mesopleuron with few setae, posterior mesopleuron groove sculptured. Precoxal sulcus distinct, but not reaching anterior and posterior edge of mesopleuron. Maximum length of propodeum (Fig. 6F) 0.5 × its width; longitudinal carina present half of propodeum, posterior part of propodeum with areola, reach to half of propodeum. In lateral view, anterior part of metanotum curved medio-dorsally (Fig. 6G). Fore wing (Fig. 6C) 2.3 × as long as wide; pterostigma hardly widened medially and nearly as wide as vein 1-R1; vein r of fore wing 3.0 × longer than wide; vein SR1 1.7 × longer than vein 3-SR; vein 3-SR 2.2 × longer than 2-SR; second submarginal cell 3.3 × longer than its medium length; 3-SR: r: SR1 = 8: 1: 14; first discal cell of fore wing as long as wide medially. Hind wing: vein M+CU+1-M: vein 1r-m = 4: 1.

***Leg*:** Hind femur 4.6 × longer than wide and 0.7 × as long as hind tibia; hind tibia 15 × longer than wide; hind tibia as long as hind tarsus.

***Metasoma*:** First tergite (Fig. 6H) medially rugose 1.5 × longer than its apical width. Setose part of ovipositor sheath (Fig. 6I) 0.9 × as long as mesosoma and 0.9 × as long as hind tibia.

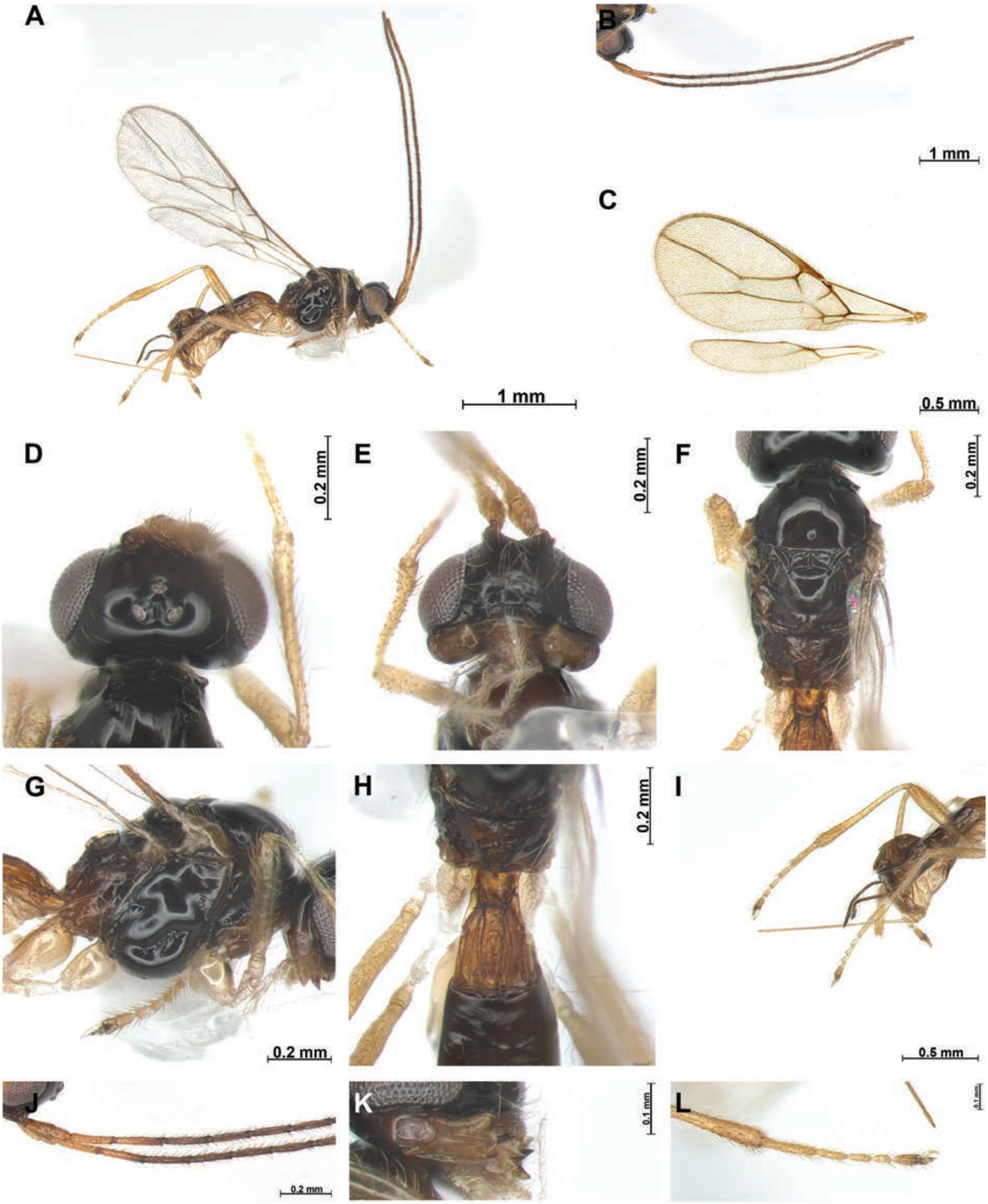

Figure 6. *Phaenocarpa tacita* Stelfox, 1941 ♀ **A** habitus, lateral view **B** antennae **C** wings **D** head, dorsal view **E** head, frontal view **F** mesosoma, dorsal view **G** mesosoma, lateral view **H** first metasomal tergite, dorsal view **I** ovipositor sheath, lateral view **J** proximal part of antenna **K** mandible, lateral view **L** claw, lateral view.

***Color*:** Body (Fig. 6A) dark brown; head dark brown; first tergite reddish brown, metasoma brown; antenna brown, apical parts pale brown; legs pale yellowish brown.

Male. Unknown.

Biology. Unknown.

Host. Unknown.

Distribution. Austria (Fischer 1970), Czechoslovakia (Lozan 2004), Hungary (Papp 2008), Ireland (Fischer 1970), Netherlands (van Achterberg 1988), Russia (Belokobylskij 1998), United Kingdom (Kloet and Hincks 1945), new to South Korea.

Discussion

The genus *Phaenocarpa* in Korea is a large group with 231 species across nine subgenera, but only nine species were recorded in Korea until now. With the addition of five new and one European species, there are now 15 species of *Phaenocarpa* in Korea. The new species and *Phaenocarpa artotemporalis* Sohn & van Achterberg, 2021, *P. brachyura* Sohn & van Achterberg, 2021, and *P. lobata* Sohn & van Achterberg, 2021 are only recorded in Korea. *Phaenocarpa masha* Belokobylskij, 1998, is recorded in Russia and Korea, and *P. fidelis* Fischer, 1970, *P. angustiptera* Papp, 1968, and *P. eunice* (Haliday, 1838), are recorded in the eastern Palearctic region (Belokobylskij 1998; Sohn et al. 2021). *Phaenocarpa picinervis* (Haliday, 1838) is recorded in both the eastern and western Palearctic regions, and *P. ruficeps* (Nees, 1812) is recorded in all regions except the Neotropic, Arctic, and Australasian regions (Yu et al. 2016).

Unfortunately, all the species used in this study are females, and records of males have not yet been confirmed. However, males could be identified later using COI barcoding and identification keys.

Additional information

Conflict of interest

The authors have declared that no competing interests exist.

Ethical statement

No ethical statement was reported.

Funding

This work was supported by a grant from the National Institute of Biological Resources (NIBR), funded by the Ministry of Environment (MOE) of the Republic of Korea (NIBR202402202 and NIBRE202404). It was also supported by Basic Science Research Program through the National Research Foundation of Korea (NRF) funded by the Ministry of Education (2022R1A2C1091308).

Author contributions

Conceptualization: HK, JHS. Data curation: JHS, SK. Formal analysis: JHS. Funding acquisition: HK. Methodology: HK, JHS, CA, SK. Project administration: HK. Resources: JHS. Software: JHS, SK. Supervision: HK. Validation: HK, JHS, CA. Visualization: JHS. Writing - original draft: JHS, CA. Writing - review and editing: JHS, HK, CA.

Author ORCIDs

Ju-Hyeong Sohn https://orcid.org/0000-0003-0976-4114
Cornelis van Achterberg https://orcid.org/0000-0002-6495-4853
Sangjin Kim https://orcid.org/0000-0001-8395-8019
Hyojoong Kim https://orcid.org/0000-0002-1706-2991

Data availability

All of the data that support the findings of this study are available in the main text.

References

Belokobylskij SA (1998) Tribe Alysiini. In: Ler PA (Ed.) Key to the Insects of Russian Far East. Dal'nauka, Vladivostok, 163–298. [In Russian]

Chabert S, Allemand R, Poyet M, Eslin P, Gibert P (2012) Ability of European parasitoids (Hymenoptera) to control a new invasive Asiatic pest, *Drosophila suzukii*. Biological control 63(1): 40–47. https://doi.org/10.1016/j.biocontrol.2012.05.005

Docavo I, Tormos J, Fischer M (2002) Three new species of *Chorebus* from Spain (Hymenoptera: Braconidae: Alysiinae). Florida Entomologist 85(1): 208–215. https://doi.org/10.1653/0015-4040(2002)085[0208:TNSOCF]2.0.CO;2

Favret C (2005) New non-destructive DNA extraction and specimen clearing technique for aphids (Hemiptera). Proceedings of the Entomological Society of Washington 107: 469–470. https://www.cabidigitallibrary.org/doi/full/10.5555/20073041183

Fischer M (1970) Zur Kenntnis der europäischen *Phaenocarpa*-Arten mit besonderer Berücksichtigung der Fauna Niederösterreichs (Hymenoptera, Braconidae, Alysiinae). Zeitschrift für Angewandte Zoologie 57: 409–498.

Foerster A (1863) Synopsis der Familien und Gattungen der Braconiden. Verhandlungen des Naturhistorischen Vereins der Preussischen Rheinlande und Westfalens 19: 225–288.

Haliday AH (1838) Essay on parasitic Hymenoptera. Entomological Magazine 5(3): 209–249.

Kloet GS, Hincks WD (1945) A check list of British Insects. 322 Wellington Road North, Heaton Chapel, Stockport, UK, 483 pp.

Lozan AI (2004) Alysiinae wasps (Hym., Braconidae) attracted by light trap in an alder carr forest of Central Europe. Entomologists Monthly Magazine, 221–241.

Nees von Esenbeck CG (1812) Icheneumonides Adesciti, in Genera et Familias Divisi. Magazin Gesellschaft Naturforschender Freunde zu Berlin 6(1812): 183–221.

NIBR (2022) National List of Species of Korea, 988 pp. National Institute of Biological Resources, Incheon. 11-1480592-001514-01. http://kbr.go.kr [accessed on 11 March 2023]

Ozawa A, Saito T, Ota M (2001) Biological control of the American Serpentine leafminer, *Liriomyza trifolii* (Burgess), on tomato in greenhouses by parasitoids. II. Evaluation of biological control by *Diglyphus isaea* (Walker) and *Dacnusa sibirica* Telenga in commercial greenhouses. Japanese Journal of Applied Entomology and Zoology 45(2): 61–74. https://doi.org/10.1303/jjaez.2001.61

Papp J (1968) A survey of the *Phaenocarpa* Foerster species of the Carpathian Basin, Central Europe (Hymenoptera, Braconidae: Alysiinae). Beiträge zur Entomologie 18(5/6): 569–603. https://doi.org/10.21248/contrib.entomol.18.5-6.569-603

Papp J (1994) Braconidae (Hymenoptera) from Korea, XV. Acta Zoologica Academiae Scientiarum Hungaricae 40(2): 133–156.

Papp J (2008) First outline of the braconid fauna of Southern Transdanubia, Hungary (Hymenoptera: Braconidae), VIII. 14 subfamilies. Sornogyi Müz. Közlm. 18: 85–100.

Shaw MR, Huddleston T (1991) Classification and biology of braconid wasps. Handbooks for the identification of British insects 7(11): 1–126.

Sohn JH, van Achterberg C, Lee G, Kim H (2021) Three new species and two new records of the genus *Phaenocarpa* Foerster (Hymenoptera, Braconidae, Alysiinae) from South Korea. Journal of Hymenoptera Research 86: 1–17. https://doi.org/10.3897/jhr.86.69998

Stelfox AW (1941) Descriptions of five new species of Alysiidae (Hymenoptera) and notes on some others. Proceedings of the Royal Irish Academy 47(B): 1–16. https://www.jstor.org/stable/20490778

van Achterberg C (1988) The genera of the *Aspilota*-group and some descriptions of fungicolous Alysiini from the Netherlands (Hymenoptera: Braconidae: Alysiinae). Zoologische Verhandelingen 247(1): 1–88. https://repository.naturalis.nl/pub/317564/

van Achterberg C (1993) Illustrated key to the subfamilies of the Braconidae (Hymenoptera: Ichneumonoidea). Zoologische Verhandelingen Leiden 283: 1–189. https://www.cabidigitallibrary.org/doi/full/10.5555/19951100799

van Achterberg C (1998) *Bobekoides* gen. n. (Hymenoptera: Braconidae: Alysiinae) from South Africa. Zoologische Mededelingen, Leiden 72(9): 105–111. https://repository.naturalis.nl/pub/215080/ZM72_105-112.pdf

van Achterberg C (2009) A new species of the genus *Phaenocarpa* Foerster from Madagascar (Hymenoptera: Braconidae: Alysiinae). Zoologische Mededelingen, Leiden 83(3): 667–671. https://repository.naturalis.nl/pub/311946/ZM83_667-672_Achterberg.pdf

Wharton RA (1984) Biology of the Alysiini (Hymenoptera: Braconidae), parasitoids of cyclorrhaphous Diptera. Texas Agricultural Experimental Station. Technical Monograph 11: 1–39.

Wharton RA (2002) Revision of the Australian Alysiini (Hymenoptera: Braconidae). Invertebrate Systematics 16: 7–105. https://doi.org/10.1071/IT01012

Wharton RA, Marsh P, Sharkey M (1997) Manual of the New World Genera of the Family Braconidae (Hymenoptera). The International Society of Hymenopterists. Washington, DC, 439 pp.

Yaakop S, van Achterberg C, Idris AB (2009) *Heratemis* Walker (Hymenoptera: Bracondae: Alysiinae: Alysiini): revision and reconstruction of the phylogeny combining molecular data and morphology. Tijdschrift voor Entomologie 152: 1–64. https://doi.org/10.1163/22119434-900000268

Yu DSK, van Achterberg C, Horstmann K. (2016) Taxapad 2016, Ichneumonoidea 2015. Database on flash-drive. www.taxapad.com, Nepean, Ontario, Canada.

Zhu JC, van Achterberg C, Chen XX (2017) An illustrated key to the genera and subgenera of the Alysiini (Hymenoptera, Braconidae, Alysiinae), with three genera new for China. ZooKeys 722: 37–79. https://doi.org/10.3897/zookeys.722.14799

ZooKeys 1217: 195–213 (2024)
DOI: 10.3897/zookeys.1217.127555

Research Article

Description of six new crab-spider species and first description of the male of *Pharta xizang* Liu & Yao, 2023 from Medog, Xizang, China (Araneae, Thomisidae)

Lu-Yu Wang[1], Yan-Nan Mu[1], Qian-Le Lu[2], Yong-Qiang Xu[3,4], Hai-Tao Bu[3,4],
Feng Zhang[5], Zhi-Sheng Zhang[1]

1 *Key Laboratory of Eco-environments in Three Gorges Reservoir Region (Ministry of Education), School of Life Sciences, Southwest University, Chongqing 400715, China*
2 *College of Life Sciences and Oceanography, Shenzhen University, Shenzhen 518000, China*
3 *Institute of Plateau Biology of Xizang Autonomous Region, Lhasa 850001, Xizang Autonomous Region, China*
4 *Medog Biodiversity Observation and Research Station of Xizang Autonomous Region, Medog, China*
5 *Key Laboratory of Zoological Systematics and Application, College of Life Sciences, Hebei University, Baoding, Hebei 071002, China*
Corresponding authors: Feng Zhang (dudu06042001@163.com); Zhi-Sheng Zhang (zhangzs327@qq.com)

Academic editor: Miquel A. Arnedo
Received: 15 May 2024
Accepted: 9 October 2024
Published: 1 November 2024

ZooBank: https://zoobank.org/B7E1DDC6-9834-42EA-A80E-77ABAADF14F1

Citation: Wang L-Y, Mu Y-N, Lu Q-L, Xu Y-Q, Bu H-T, Zhang F, Zhang Z-S (2024) Description of six new crab-spider species and first description of the male of *Pharta xizang* Liu & Yao, 2023 from Medog, Xizang, China (Araneae, Thomisidae). ZooKeys 1217: 195–213. https://doi.org/10.3897/zookeys.1217.127555

Abstract

Seven species of the crab-spider family Thomisidae from Medog, Xizang, China are described here, including six new species: *Camaricus medog* Wang, Lu & Zhang, **sp. nov.** (♂♀), *Monaeses xizang* Wang, Lu & Zhang, **sp. nov.** (♂♀), *Sinothomisus beibeng* Wang, Lu & Zhang, **sp. nov.** (♂♀), *Sinothomisus dawai* Wang, Lu & Zhang, **sp. nov.** (♂♀), *Spilosynema motuo* Wang, Lu & Zhang, **sp. nov.** (♂♀), and *Thomisus yarang* Wang, Lu & Zhang, **sp. nov.** (♂♀). The male of *Pharta xizang* Liu & Yao, 2023 is described here for the first time. Descriptions and photographs of all the species are provided.

Key words: Description, morphology, new species, taxonomy

Introduction

Medog, a county seat of Nyingchi City, located downstream of the Yarlung Zangbo River, is a key transitional zone between the Eastern Himalayas and Hengduan Mountain region. The topography of Medog is complex and with a variety of vegetation types from tropical valley monsoon rain forest to cold ice sheet between the Yarlung Zangbo Grand Canyon to the summit of Nangabawa (Wang and Peng 2022). Medog is the most northerly tropical region in the Northern Hemisphere and is affected by a subtropical humid climate due to the warm and humid airflow from the Indian Ocean. It is the lowest area of the Tibetan Plateau, with the best hydrothermal conditions and the greatest precipitation (Li et al. 2024). The unique geographical environment and climate have contributed to the rich biodiversity of Medog. However, due to the remote location, complex environment, and inconvenient transportation, the research of spider diversity in Medog has not been achieved until recently with improvements in transportation. According to preliminary statistics, only 34 species have been recorded from Medog, most of them published since 2017 (Table 1).

Our team has been investigating the spider diversity of Medog since 2018, and we have found more than 300 species, including many undescribed species. Here, seven crab-spider species are described, including six new species and the male of *Pharta xizang* new to science.

Materials and methods

All specimens are preserved in 75% ethanol and were examined, illustrated, photographed, and measured using a Leica M205A stereomicroscope equipped with a Leica DFC450 Camera and LAS software (v. 4.6). Male pedipalps and epigynes were examined and illustrated after dissection. Epigynes were cleared by immersing them in a pancreatin solution (Álvarez-Padilla and Hormiga 2007). Eye sizes were measured as the maximum dorsal diameter. Leg measurements are shown as: total length (femur, patella and tibia, metatarsus, tarsus). All measurements are in millimetres. All specimens, including the holotypes examined here, are deposited in the Collection of Spiders, School of Life Sciences, Southwest University, Chongqing, China (**SWUC**).

Terminology follows Tang and Li (2010). Abbreviations used in the text: **ALE**–anterior lateral eye; **AME**–anterior median eye; **MOA**–median ocular area; **PLE**–posterior lateral eye; **PME**–posterior median eye.

Taxonomy

Family Thomisidae Sundevall, 1833 (蟹蛛科)
Genus *Camaricus* Thorell, 1887 (顶蟹蛛属)

***Camaricus medog* Wang, Lu & Zhang, sp. nov.**
https://zoobank.org/D88E4BFE-1E8B-4050-B5CE-29730C9E751B
Figs 1A, B, 3A, B, 4, 11
Common name. 墨脱顶蟹蛛

Type material. *Holotype* • ♂ (SWUC-T-THO-01-01), China, Xizang, Medog County, Mirage observation deck, 29°20'36"N, 95°20'43"E, elev. 1297 m, 8 July 2023, Z.S. Zhang, L.Y. Wang, Q.L. Lu and X.L. Chen leg. ***Paratypes*:** • 1♂ 4♀ (SWUC-T-THO-01-02~06), same data as for holotype.

Etymology. The specific name is derived from the type locality; it is a noun in apposition.

Diagnosis. The new species resembles *C. formosus* Thorell, 1887 (Song and Zhu 1997: 173, fig. 122A–D) in having the embolus origin in the same position, but *C. medog* differs from the latter by the short and blunt ventral tibial apophysis end (vs long and sharp in *C. formosus*), a bifurcated retrolateral tibial apophysis (vs single in *C. formosus*), a broad embolus (vs slender in *C. formosus*), and a distinct copulatory atrium (vs indistinct in *C. formosus*) (Fig. 4).

Description. Male holotype (SWUC-T-THO-01-01, Figs 1A, 3A) total length 4.50. Prosoma 2.40 long, 2.09 wide; opisthosoma 2.03 long, 1.69 wide. Carapace black. Eye sizes and interdistances: AME 0.12, ALE 0.16, PME 0.05, PLE 0.12; AME–AME 0.39, AME–ALE 0.34, PME–PME 0.68, PME–PLE 0.51, ALE–PLE 0.31. MOA 0.33 long, anterior width 0.66, posterior width 0.82. Clypeus height 0.21. Chelicerae black, with 3 promarginal and 3 retromarginal teeth. Labium

Table 1. List of spider species recorded from Medog.

Family	Species	Distribution	References
Agelenidae	*Draconarius medogensis*	Medog	Zhu et al. 2017
	Draconarius subaspinatus	Medog	
Anapidae	*Sinanapis medogensis*	Medog	Zhang and Lin 2018
Araneidae	*Araneus motuoensis*	Medog	Yin et al. 1990
	Argiope beibeng	Medog	Mi et al. 2024
	Argiope caesarea	China (Xiang and Yunnan), India and Myanmar	
Clubionidae	*Clubiona medog*	Medog	Zhang et al. 2007
Corinnidae	*Apochinomma medog*	Medog	Zhang and Zhang 2023
Ctenidae	*Amauropelma medogensis*	Medog	Wang et al. 2024a
	Anahita medog	Medog, Chayu of Xizang	Chu et al. 2022
	Bowie rotundus	Medog	Wang et al. 2024a
Halonoproctidae	*Conothele medoga*	Medog	Zhang and Yu 2021
Lycosidae	*Serratacosa medogensis*	Medog	Wang et al. 2021
	Zantheres gracillimus	Medog; Bhamo of Myanmar	Wang and Zhang 2020
Oonopidae	*Ischnothyreus metok*	Medog	Tong et al. 2023
	Paramolotra metok	Medog	Cheng et al. 2021
Pholcidae	*Belisana medog*	Medog	Zhu et al. 2020
	Pholcus medog	Medog	Zhang et al. 2006
Pisauridae	*Hygropoda medogensis*	Medog	Lu et al. 2023
Psilodercidae	*Leclercera aniensis*	Medog	Chang and Li 2020
	Leclercera duandai	Medog	
	Leclercera renqinensis	Medog	
	Merizocera nyingchi	Medog	Chang et al. 2020
Salticidae	*Chrysilla yarlungzangbo*	Medog	Yang and Zhang 2024
	Hyllus qishuoi	Medog	Xiong et al. 2017
	Synagelides medog	Medog	Wang et al. 2024
Sparassidae	*Pseudopoda conica*	Medog	Zhang et al. 2023
	Pseudopoda medogensis	Medog	Jiang et al. 2018
	Pseudopoda shuo	Medog	
	Pseudopoda zhangi	Medog	Fu and Zhu 2008
Theraphosidae	*Chilobrachys jinchengi*	Medog	Lin et al. 2022
Thomisidae	*Pharta xizang*	Medog	Li et al. 2023
Zodariidae	*Asceua dawai*	Medog	Wang et al. 2024b
	Mallinella medog	Medog	

and endites brown, longer than wide. Sternum brown and scutellate. Leg measurements: I 7.65 (2.22, 2.85, 1.55, 1.03); II 7.58 (2.21, 2.83, 1.48, 1.06); III 4.39 (1.45, 1.60, 0.69, 0.65); IV 4.37 (1.44, 1.62, 0.74, 0.57). Leg formula: 1234. Opisthosoma oval, black, with a white spot at mid-anterior part. Spinnerets black.

Palp (Fig. 4A, B). Tibial as 1/2 of length cymbium, ventral tibial apophysis somewhat pediform, retrolateral tibial apophysis bifurcated: ventral arm thumb shaped, retrolateral arm hook-like in retrolateral view. Embolus originating at approximately 9-o'clock position, broad, curved along with bulb.

Female paratype (SWUC-T-THO-01-02, Fig. 3B) total length 6.60. Prosoma 3.04 long, 2.63 wide; opisthosoma 3.70 long, 3.22 wide. Eye sizes and interdistances: AME 0.11, ALE 0.21, PME 0.10, PLE, 0.19; AME–AME 0.49, AME–ALE 0.46, PME–PME 0.84, PME–PLE 0.60, ALE–PLE 0.32. MOA 0.45 long, anterior width

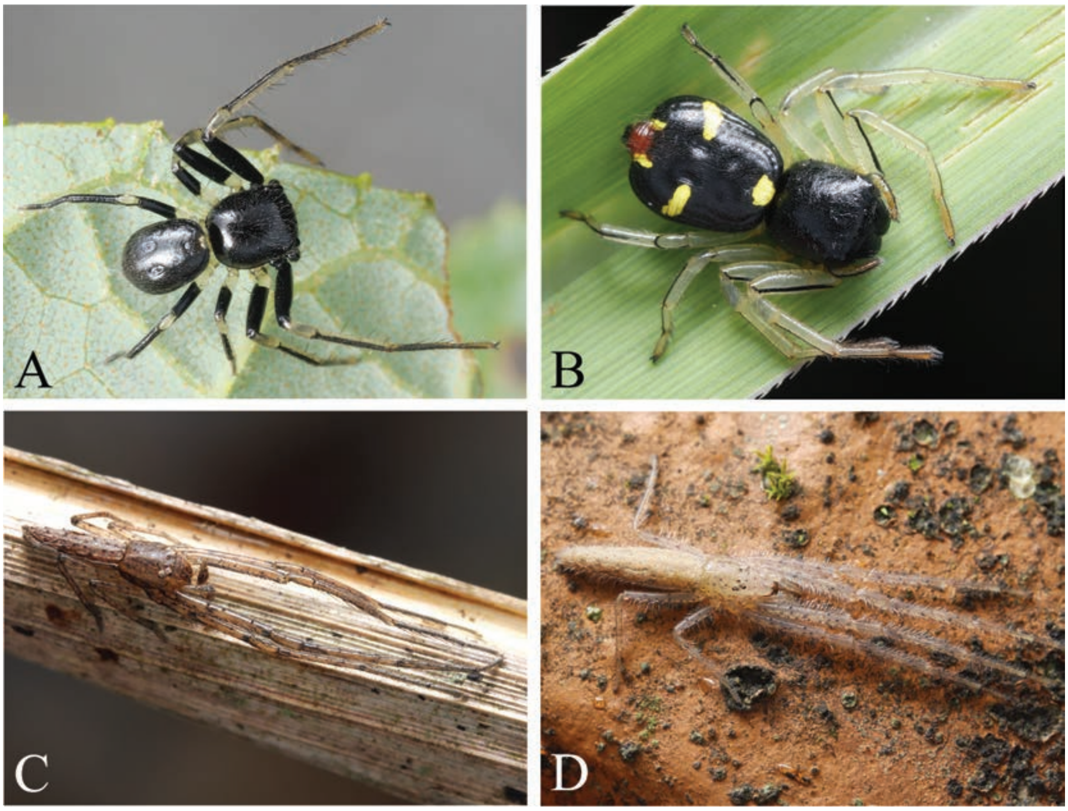

Figure 1. Living photos of crab spiders **A, B** *Camaricus medog* Wang, Lu & Zhang, sp. nov. **A** male holotype **B** female paratype **C, D** *Monaeses xizang* Wang, Lu & Zhang, sp. nov. **C** male holotype, **D** female paratype. Photographed by Qian-Le Lu.

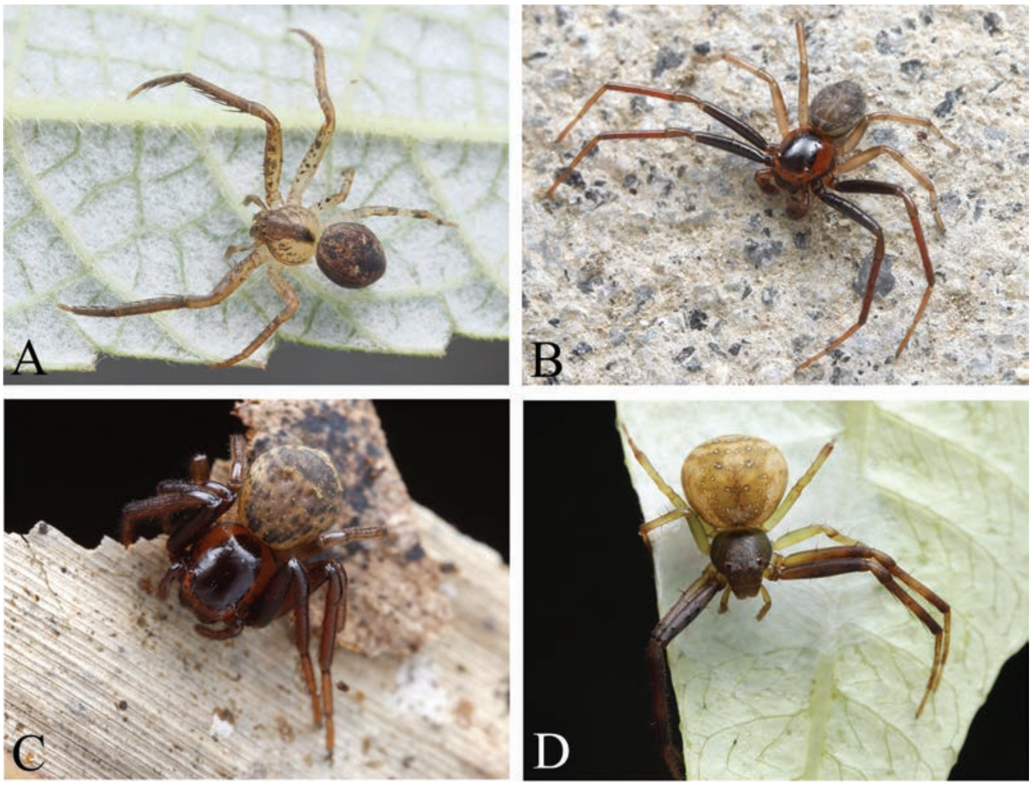

Figure 2. Living photos of crab spiders **A** *Pharta xizang* Liu & Yao, 2023, female **B, C** *Sinothomisus dawai* Wang, Lu & Zhang, sp. nov. **B** male holotype **C** female **D** *Spilosynema xizang* Wang, Lu & Zhang, sp. nov., female paratype. Photographed by Qian-Le Lu.

0.80, posterior width 1.04. Clypeus height 0.27. Leg measurements: I 7.07 (2.10, 2.55, 1.40, 1.02); II 7.16 (2.13, 2.70, 1.37, 0.96); III 4.72 (1.59, 1.77, 0.75, 0.61); IV 5.38 (1.74, 2.13, 0.87, 0.64). Leg formula: 2143. Opisthosoma oval, black, with 5 white (yellow when live) and one brown spots. Spinnerets black.

Epigyne (Fig. 4C, D). Epigynal plate longer than wide. Copulatory opening located anteriorly. Copulatory ducts transparent and C-like. Spermathecae stomach shaped. Fertilization ducts crescent-shaped.

Variation. Males (*n = 2*) total length 4.50–4.92; females (*n = 4*) total length 6.60–8.00.

Distribution. Known only from the type locality, Medog, Xizang, China (Fig. 11).

Genus *Monaeses* Thorell, 1869 (莫蟹蛛属)

Monaeses xizang Wang, Lu & Zhang, sp. nov.

https://zoobank.org/6E866803-36E5-4324-8E7A-F8F686965881
Figs 1C, D, 3M, N, 5, 11
Common name. 西藏莫蟹蛛

Type material. *Holotype* • ♂ (SWUC-T-THO-02-01), China, Xizang, Medog County, Mirage Observation Deck, 29°20'36"N, 95°20'43"E, elev. 1297 m, 8 July 2023, Z.S. Zhang, L.Y. Wang, Q.L. Lu and X.L. Chen leg. ***Paratype*:** • 1 ♀ (SWUC-T-THO-02-02), same data as for holotype.

Etymology. The specific name is derived from the type locality; it is a noun in apposition.

Diagnosis. The new species resembles *M. aciculus* (Simon, 1903) (Song and Zhu 1997: 59, fig. 35A–H) in having the ventral tibial apophysis of the same shape and spermathecae compressed, but the new species differs from *M. aciculus* in having the ventral tibial apophysis shorter than retrolateral tibial apophysis (vs as long as retrolateral tibial apophysis in *M. aciculus*), a short embolus originating at approximately 11-o'clock (vs long and originating at approximately 8-o'clock in *M. aciculus*), and comma-like copulatory ducts (vs U-shaped in *M. aciculus*) (Fig. 5).

Description. Male holotype (SWUC-T-THO-02-01, Figs 1C, 3M) total length 7.31. Prosoma 2.24 long, 1.82 wide; opisthosoma 5.33 long, 1.24 wide. Carapace yellow brown. Eye sizes and interdistances: AME 0.06, ALE 0.14, PME 0.09, PLE 0.18; AME–AME 0.17, AME–ALE 0.19, PME–PME 0.34, PME–PLE 0.29, ALE–PLE 0.31. MOA 0.40 long, anterior width 0.30, posterior width 0.51. Clypeus height 0.45. Chelicerae yellow brown. Labium and endites yellow brown, longer than wide. Sternum yellow-brown and scutellate, with brown hairs. Leg measurements: I 18.79 (5.43, 6.98, 4.57, 1.81); II 16.96 (5.06, 6.25, 3.94, 1.71); III 6.61 (2.10, 2.57, 1.09, 0.85); IV 7.81 (3.28, 2.52, 1.08, 0.93). Leg formula: 1243. Opisthosoma columnar, yellow brown. Spinnerets yellow-brown.

Palp (Fig. 5A, B). Tibia ½ length of cymbium. Ventral tibial apophysis columnar, with a curved end. Retrolateral tibial apophysis sclerous, somewhat triangular, with a sharp end. Embolus originating at approximately 11-o'clock position, slender, curved along with bulb, tip staying in cymbial furrow.

Female paratype (SWUC-T-THO-02-02, Figs 1D, 3N) total length 10.70. Prosoma 3.23 long, 2.35 wide; opisthosoma 7.28 long, 1.88 wide. Eye sizes and interdistances: AME 0.07, ALE 0.22, PME 0.11, PLE, 0.19; AME–AME 0.32, AME–ALE 0.27, PME–PME 0.52, PME–PLE 041, ALE–PLE 0.39. MOA 0.49 long,

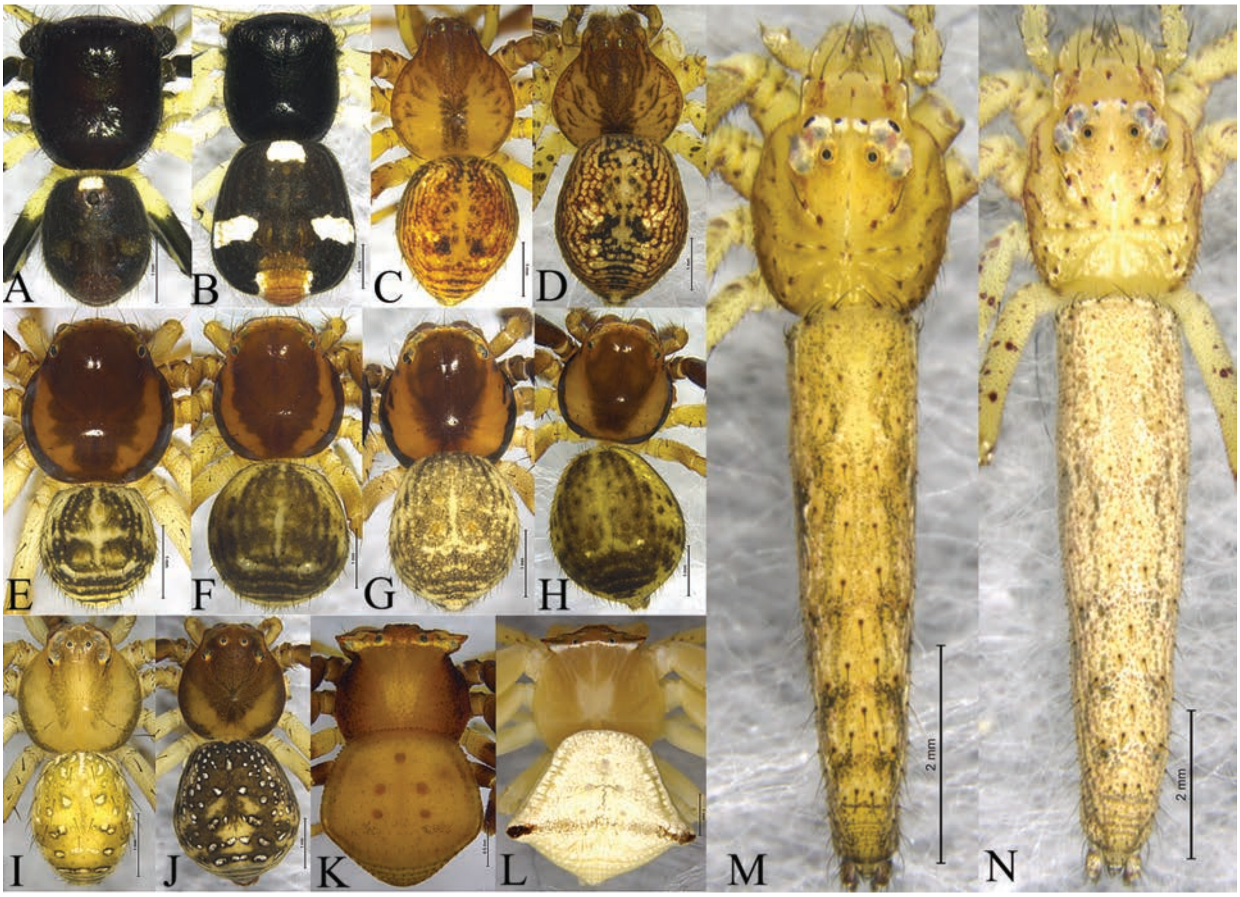

Figure 3. Habitus, dorsal view **A, B** *Camaricus medog* Wang, Lu & Zhang, sp. nov. (**A** male holotype **B** female paratype) **C, D** *Pharta xizang* Liu & Yao, 2023 (**C** male **D** female) **E, F** *Sinothomisus beibeng* Wang, Lu & Zhang, sp. nov. (**E** male holotype **F** female paratype) **G, H** *Sinothomisus dawai* Wang, Lu & Zhang, sp. nov. (**G** male holotype **H** female paratype) **I, J** *Spilosynema xizang* Wang, Lu & Zhang, sp. nov. (**I** male holotype **J** female paratype) **K, L** *Thomisus yarang* Wang, Lu & Zhang, sp. nov. (**K** male holotype, **L** female paratype) **M, N** *Monaeses xizang* Wang, Lu & Zhang, sp. nov. (**M** male holotype **N** female paratype).

anterior width 0.46, posterior width 0.74. Clypeus height 0.58. Leg measurements: I 16.12 (5.05, 6.17, 3.34, 1.56); II 14.41 (4.53, 5.52, 2.88, 1.48); III 14.30 (4.39, 5.53, 2.98, 1.40); IV 8.37 (3.57, 2.81, 1.11, 0.88). Leg formula: 1234.

Epigyne (Fig. 5C, D). Epigynal plate almost rounded. Copulatory openings slit-like, distant from each other. Copulatory ducts comma-like. Spermathecae folded. Fertilization ducts crescent-shaped.

Distribution. Known only from the type locality, Medog, Xizang, China (Fig. 11).

Genus *Pharta* Thorell, 1891 (范蟹蛛属)

Pharta xizang **Liu & Yao, 2023**
Figs 2A, 3C, D, 6, 11
Common name. 西藏范蟹蛛

Pharta xizang Liu & Yao in Li et al., 2023: 176, fig. 4A–G (♀).

Material examined. China, Xizang, Medog County: • 2 ♂, Medog Town, 29°19.470'N, 95°19.618'E, elev. 1116 m, 27 June 2018, L.Y. Wang, Z.S. Wu and Y.N. Mu leg; • 1 ♀, Beibeng Township, Damu, 29°14'51"N, 95°11'1"E, elev. 924 m,

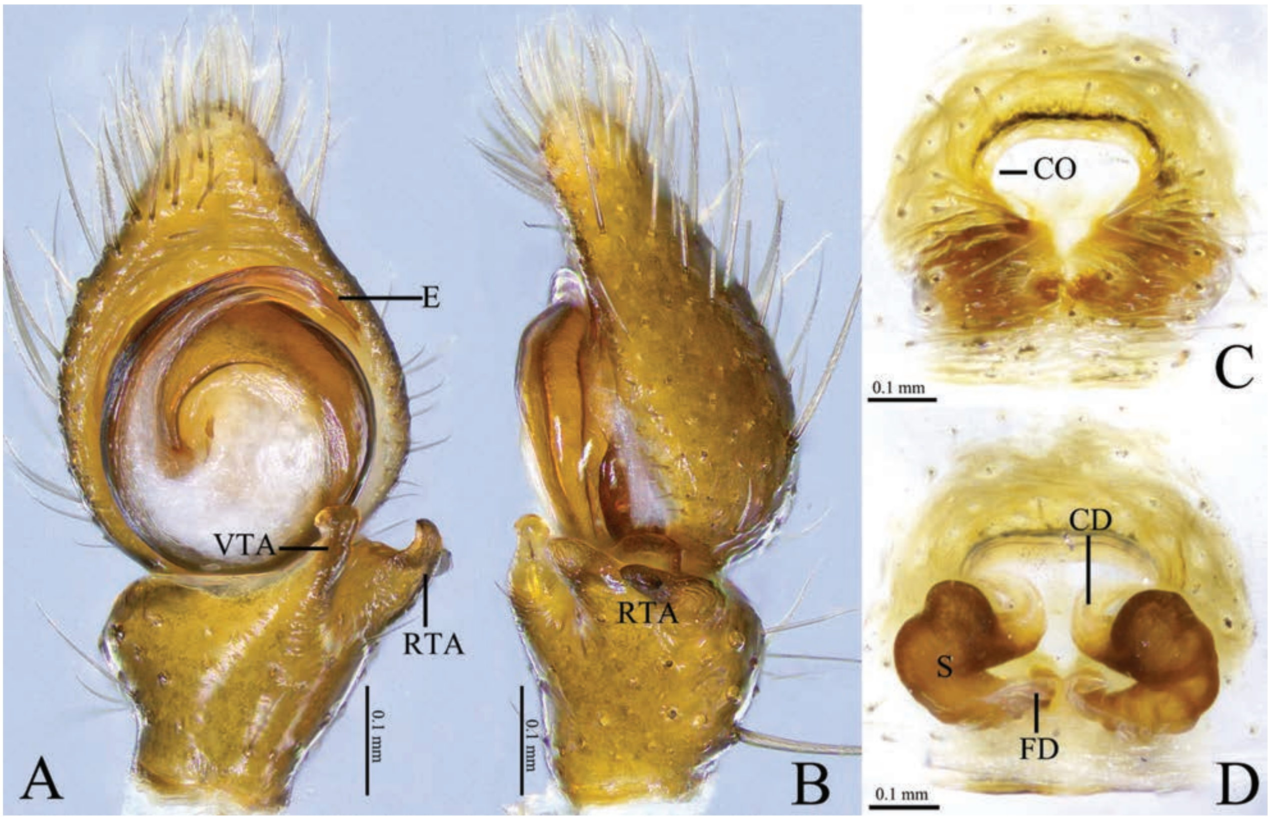

Figure 4. *Camaricus medog* Wang, Lu & Zhang, sp. nov. **A, B** holotype male **C, D** paratype female **A** male left palp, ventral view **B** same, retrolateral view. **C** epigyne, ventral view **D** same, dorsal view. Abbreviations: CD = copulatory duct; CO = copulatory opening; E = embolus; FD = fertilization duct; RTA = retrolateral tibial apophysis; VTA = ventral tibial apophysis; S = spermathecal.

28 June 2018, L.Y. Wang, Y.N. Mu and Z.S. Wu leg; • 1 ♀, Medog Town, Yarang Village, 29°17.758'N, 95°16.827'E, elev. 761 m, 22 May 2019, L.Y. Wang, T. Yuan, P. Liu and H. Wang leg; • 1 ♀, Medog Town, 23 May 2019, L.Y. Wang, T. Yuan, P. Liu and H. Wang leg; • 2 ♂ 4 ♀, Beibeng Township, Badeng Village, 29°16'28"N, 95°10'7"E, elev. 851 m, 7 July 2023, Z.S. Zhang, L.Y. Wang, Q.L. Lu and X.L. Chen leg; • 2 ♂, Mirage Observation Deck, 29°20'36"N, 95°20'43"E, elev. 1297 m, 8 July 2023, Z.S. Zhang, L.Y. Wang, Q.L. Lu and X.L. Chen leg.

Diagnosis. This species resembles *P. tangi* Wang, Mi & Peng, 2016 (Wang et al. 2016: 130, figs 1A–G, 2A–D) in having similar shaped spermathecae, but differs it from the latter by the knife-like ventral tibial apophysis (vs rhabditiform and slightly curved in *P. tangi*), the multiple spines at the base of ventral tibial apophysis (vs spine absent in *P. tangi*), the folded posterior half part of conductor (vs knife-shaped in *P. tangi*), and the kidney-shaped spermathecae (vs long oval in *P. tangi*) (Fig. 6). This new species also resembles *P. gongshan* (Yang, Zhu & Song, 2006) (Benjamin 2011: 80, figs 47A, B, D–F, 49A–F, 51A–D) in having a similar shaped bulb, but it can be distinguished by the bifurcated tip of the conductor (vs not bifurcated in *P. gongshan*) and the small copulatory openings located towards the posterior (vs large copulatory openings towards the lateral).

Description. Male (Fig. 3C) total length 5.89. Prosoma 2.74 long, 2.40 wide; Opisthosoma 3.08 long, 2.43 wide. Carapace yellow-brown, with a deep-brown spot. Eye sizes and interdistances: AME 0.07, ALE 0.20, PME 0.16, PLE 0.18; AME–AME 0.12, AME–ALE 0.07, PME–PME 0.14, PME–PLE 0.16, ALE–PLE

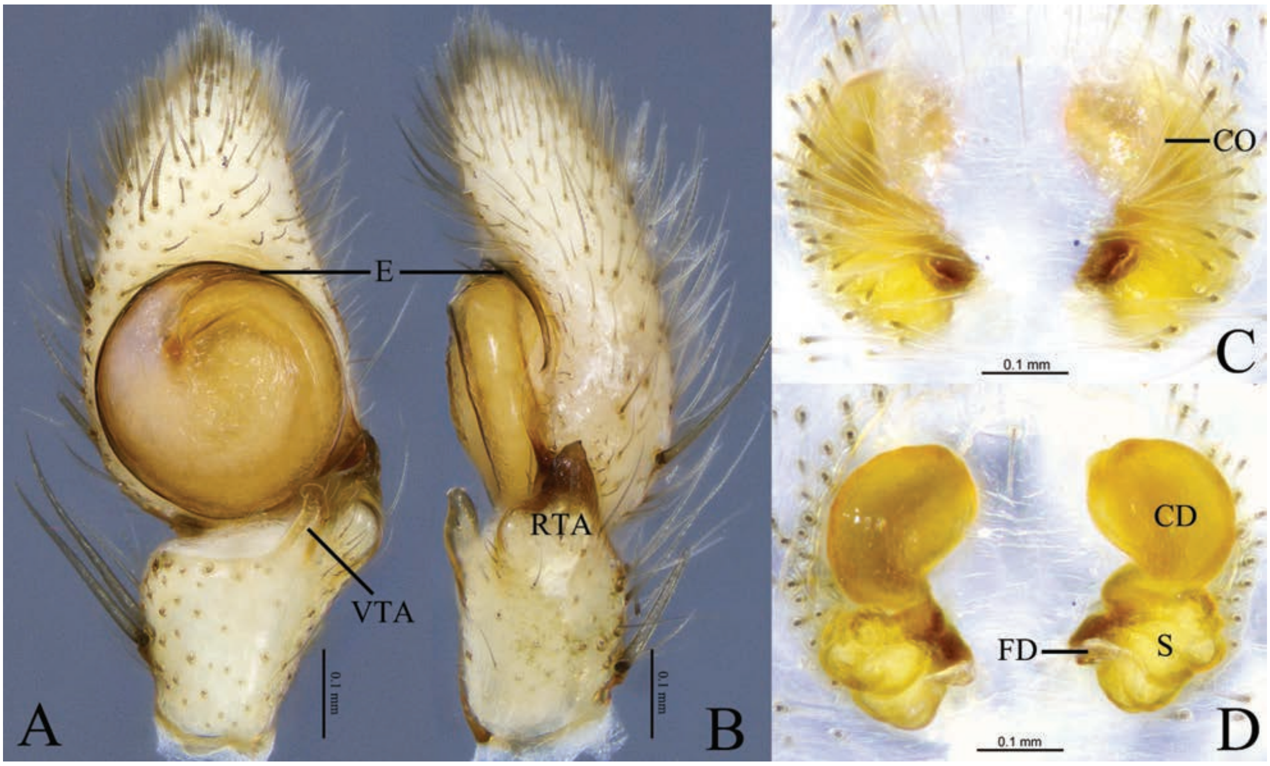

Figure 5. *Monaeses xizang* Wang, Lu & Zhang, sp. nov. **A, B** holotype male **C, D** paratype female **A** male left palp, ventral view **B** same, retrolateral view **C** epigyne, ventral view **D** same, dorsal view. Abbreviations: CD = copulatory duct; CO = copulatory opening; E = embolus; FD = fertilization duct; RTA = retrolateral tibial apophysis; VTA = ventral tibial apophysis; S = spermathecal.

0.17. MOA 0.42 long, anterior width 0.26, posterior width 0.45. Clypeus height 0.15. Chelicerae brown, with 3 promarginal and 3 retromarginal teeth. Labium and endites yellow-brown, longer than wide. Sternum yellow-brown and scutellate, with brown hairs. Leg measurements: **I** 11.47 (3.39, 4.34, 2.51, 1.23); **II** 10.92 (3.24, 4.14, 2.28, 1.26); **III** 6.16 (1.97, 2.34, 1.13, 0.72); **IV** 7.25 (2.28, 2.61, 1.58, 0.78). Leg formula: 1243. Opisthosoma oval, yellow, with a deep-red spot. Spinnerets yellow-brown.

Palp (Fig. 6A–C). Tibia longer than wide. Ventral tibial apophysis knife-like, three times longer than wide, base of ventral tibial apophysis bulging, with multiple spines. Conductor originating from centre of bulb, base wider than embolus, anterior part folded as a furrow. Embolus strong, originating at approximately 9-o'clock position, with its tip staying in conductor furrow.

Female (Fig. 3D) total length 7.20. Prosoma 3.04 long, 2.52 wide; opisthosoma 3.82 long, 3.47 wide. Eye sizes and interdistances: AME 0.06, ALE 0.19, PME 0.16, PLE, 0.19; AME–AME 0.14, AME–ALE 0.10, PME–PME 0.14, PME–PLE 0.19, ALE–PLE 0.19. MOA 0.45 long, anterior width 0.27, posterior width 0.48. Clypeus height 0.17. Leg measurements: **I** 11.07 (3.28, 4.61, 2.16, 1.02); **II** 10.28 (3.09, 4.21, 1.92, 1.06); **III** 5.90 (1.88, 2.37, 0.99, 0.66); **IV** 7.24 (2.30, 2.65, 1.55, 0.74). Leg formula: 1243.

Epigyne (Fig. 6D, E). Epigynal plate almost rounded. Copulatory openings small, rounded, far away from each other. Copulatory ducts short. Spermathecae kidney-shaped. Fertilization ducts crescent-shaped.

Distribution. China (Xizang, Medog) (Fig. 11).

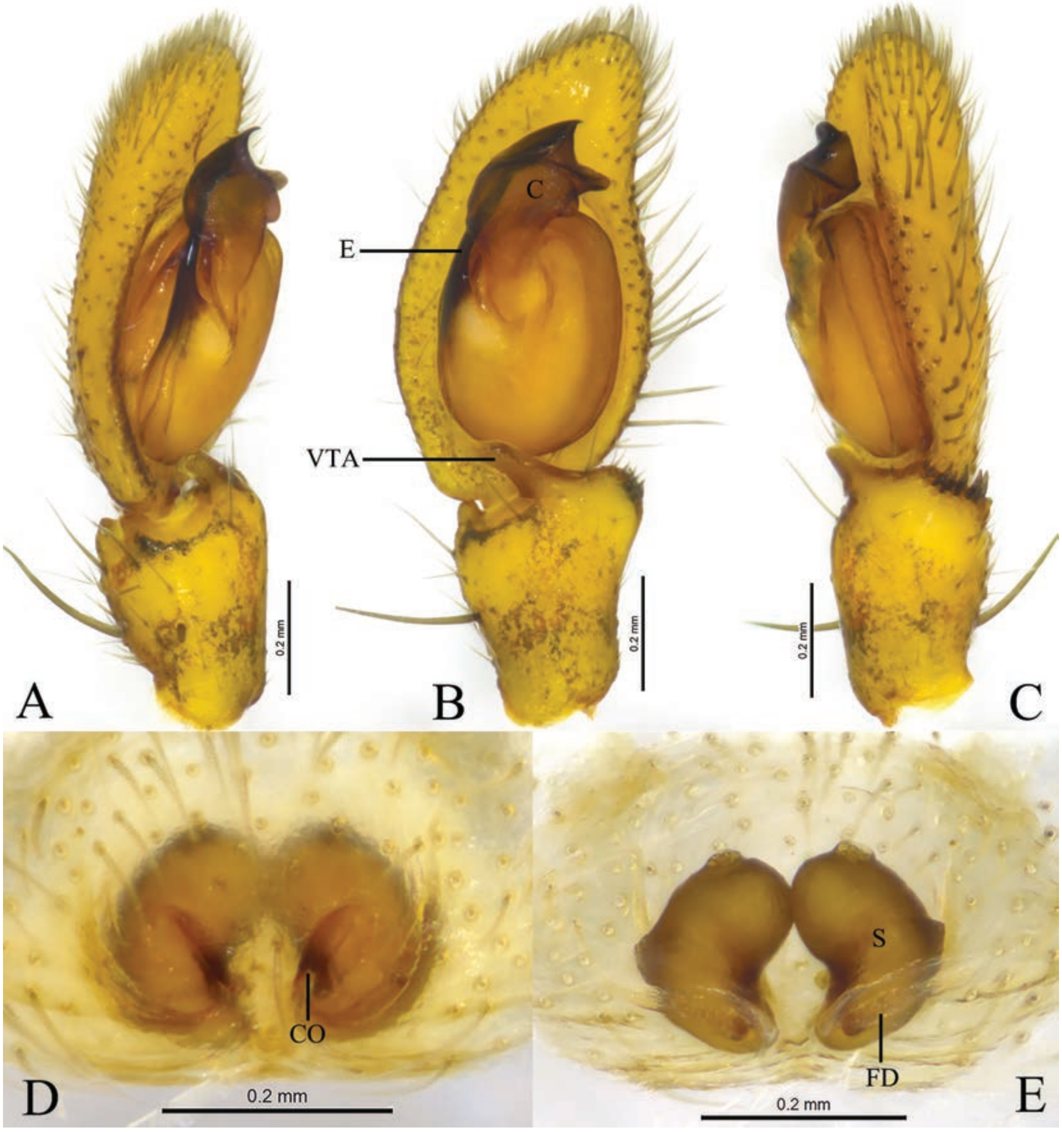

Figure 6. *Pharta xizang* Liu & Yao, 2023 **A** male left palp, prolateral view **B** same, ventral view **C** same, retrolateral view **D** epigyne, ventral view **E** same, dorsal view. Abbreviations: CD = copulatory duct; C = conductor; CO = copulatory opening; E = embolus; FD = fertilization duct; VTA = ventral tibial apophysis; S = spermathecal.

Genus *Sinothomisus* Tang, Yin, Griswold & Peng, 2006 (华蟹蛛属)

Sinothomisus beibeng Wang, Lu & Zhang, sp. nov.

https://zoobank.org/99A666E2-A89A-44A9-B224-ECA5C062D6CD
Figs 3E, F, 7, 11
Common name. 背崩华蟹蛛

Type material. ***Holotype*** • ♂ (SWUC-T-THO-03-01), China, Xizang, Medog County, Beibeng Township, Damu, 29°14'51"N, 95°11'1"E, elev. 924 m, 28 June 2018, L.Y. Wang, Y.N. Mu and Z.S. Wu leg. ***Paratype***: • 1 ♀ (SWUC-T-THO-03-02), same data as for holotype.

Etymology. The specific name is derived from the type locality; it is a noun in apposition.

Diagnosis. The new species resembles *S. liae* Tang, Yin, Griswold & Peng, 2006 (Tang et al. 2006: 65, figs 1–13) in having a similar shaped retrolateral

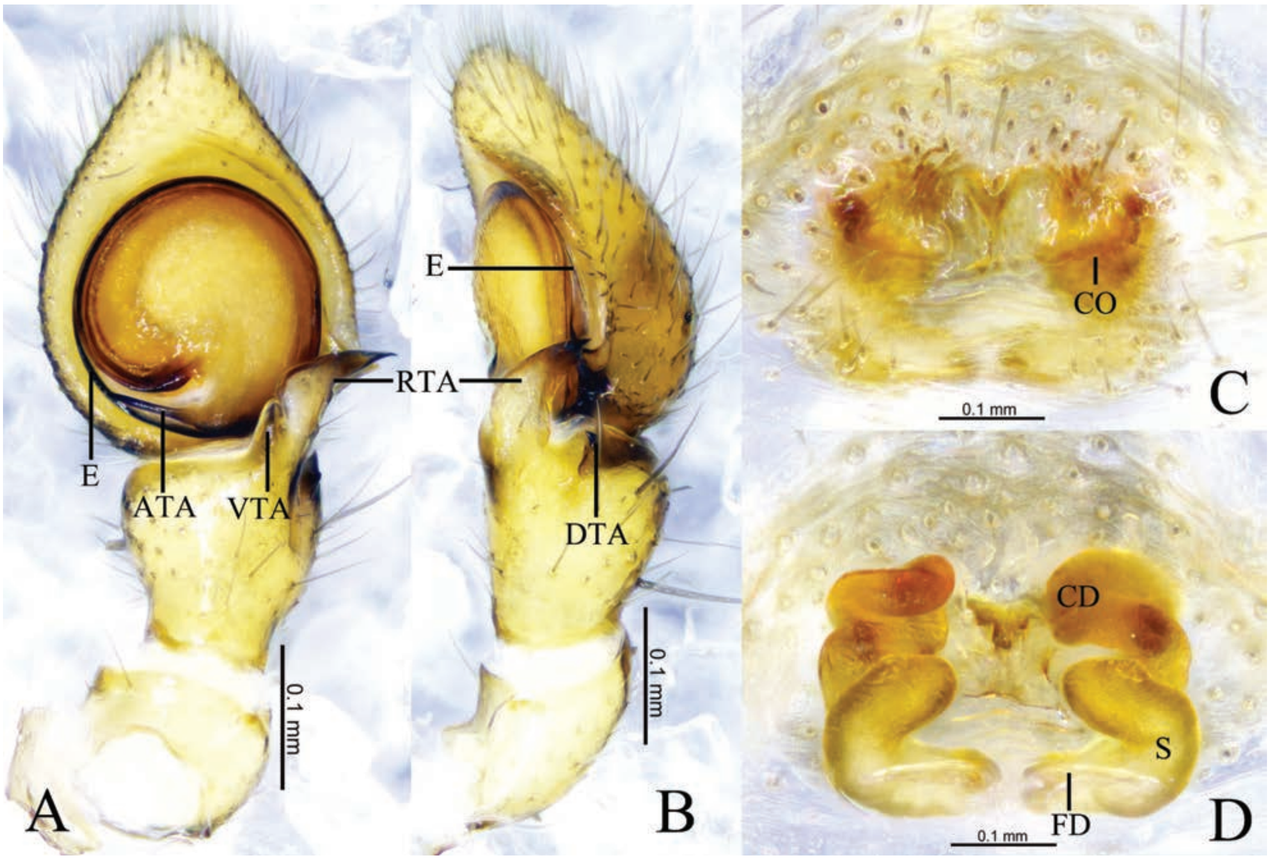

Figure 7. *Sinothomisus beibeng* Wang, Lu & Zhang, sp. nov. **A, B** holotype male **C, D** paratype female **A** male left palp, ventral view **B** same, retrolateral view **C** epigyne, ventral view **D** same, dorsal view. Abbreviations: CD = copulatory duct; CO = copulatory opening; DTA = dorsal tibial apophysis; E = embolus; FD = fertilization duct; RTA = retrolateral tibial apophysis; VTA = ventral tibial apophysis; S = spermathecal.

tibial apophysis, but it differs from the latter by the retrolateral tibial apophysis which is shorter than the bulb (vs equal in length to the bulb in *S. liae*), the long, thin apical tegular apophysis (vs short and wide in *S. liae*), and the C-like spermathecae (vs caterpillar-like in *S. liae*) (Fig. 7). This new species also resembles *S. dawai* Wang, Lu & Zhang, sp. nov.; see diagnosis for *S. dawai*.

Description. Male holotype (SWUC-T-THO-03-01, Fig. 3E) total length 4.03. Prosoma 2.19 long, 2.12 wide; opisthosoma 1.96 long, 1.56 wide. Carapace border black, with a large, deep-brown spot in the middle. Eye sizes and interdistances: AME 0.08, ALE 0.17, PME 0.02, PLE 0.16; AME–AME 0.22, AME–ALE 0.23, PME–PME 0.26, PME–PLE 0.47, ALE–PLE 0.19. MOA 0.22 long, anterior width 0.37, posterior width 0.30. Clypeus height 0.22. Chelicerae brown. Labium and endites brown, longer than wide. Sternum brown and scutellate, with brown hairs. Leg measurements: **I** 8.09 (2.39, 2.89, 1.65, 1.16); **II** 8.36 (2.46, 3.07, 1.64, 1.19); **III** 5.27 (1.70, 1.96, 0.84, 0.77); **IV** 5.25 (1.71, 1.90, 0.94, 0.70). Leg formula: 2134. Opisthosoma oval, yellow, with a black spot. Spinnerets brown.

Palp (Fig. 7A, B). Tibia longer than wide. Ventral tibial apophysis small, thumb-shaped, near retrolateral tibial apophysis. Retrolateral tibial apophysis four times longer than ventral tibial apophysis, jellyfish-shaped in retrolateral view. Dorsal tibial apophysis small, conical. Bulb flat, apical tegular apophysis thin and long. Embolus filiform, originating at approximately 6-o'clock position, curved along with bulb, tip staying in cymbial furrow.

Female paratype (SWUC-T-THO-03-02, Fig. 3F) total length 4.86. Prosoma 2.37 long, 2.17 wide; opisthosoma 2.48 long, 2.32 wide. Eye sizes and interdistances: AME 0.08, ALE 0.19, PME 0.02, PLE 0.16; AME–AME 0.23, AME–ALE 0.26, PME–PME 0.26, PME–PLE 0.52, ALE–PLE 0.23. MOA 0.26 long, anterior width 0.40, posterior width 0.32. Clypeus height 0.25. Leg measurements: I 6.90 (2.13, 2.60, 1.26, 0.91); II 7.16 (2.24, 2.62, 1.30, 1.00); III 4.85 (1.56, 1.87, 0.70, 0.72); IV 4.81 (1.60, 1.73, 0.81, 0.67). Leg formula: 2134.

Epigyne (Fig. 7C, D). Epigynal plate as long as wide. Copulatory openings slit-like, distant from each other. Copulatory ducts S-like. Spermathecae C-shaped. Fertilization ducts crescent-shaped.

Distribution. Known only from the type locality, Medog, Xizang, China (Fig. 11).

Sinothomisus dawai Wang, Lu & Zhang, sp. nov.

https://zoobank.org/36CEFA28-BE47-4CBD-8D15-BD72D8EAC7D9
Figs 2B, C, 3G, H, 8, 11
Common name. 达娃华蟹蛛

Type material. ***Holotype*** • ♂ (SWUC-T-THO-04-01), China, Xizang, Medog County, Mirage Observation Deck, 29°20'36"N, 95°20'43"E, elev. 1297 m, 8 July 2023, Z.S. Zhang, L.Y. Wang, Q.L. Lu and X.L. Chen leg. ***Paratypes*:** • 1 ♂ (SWUC-T-THO-04-02), same data as for holotype; • 1 ♀ (SWUC-T-THO-04-03), Beibeng Township, Damu, 29°14'51"N, 95°11'1"E, elev. 924 m, 28 June 2018, L.Y. Wang, Y.N. Mu and Z.S. Wu leg.

Etymology. The specific name is a patronym in honor of Mr. Dawa from the Tibet Plateau Institute of Biology in Lhasa, Xizang.

Diagnosis. The new species resembles *S. beibeng* Wang, Lu & Zhang, sp. nov. (Fig. 7) in having same shaped bulb and same position of embolus origin, but differs from the latter by the long and large retrolateral tibial apophysis (vs short and C-like in *S. beibeng*), the small spine between the retrolateral tibial apophysis and the dorsal tibial apophysis (vs absent in *S. beibeng*), the fingernail-like protuberance at epigynal plate (vs absent in *S. beibeng*) (Fig. 8).

Description. Male holotype (SWUC-T-THO-04-01, Figs 2B, 3G) total length 4.21. Prosoma 2.19 long, 2.04 wide; Opisthosoma 2.34 long, 1.92 wide. Carapace border black, with a large deep brown spot in the middle. Eye sizes and interdistances: AME 0.07, ALE 0.18, PME 0.01, PLE 0.16; AME–AME 0.24, AME–ALE 0.21, PME–PME 0.24, PME–PLE 0.45, ALE–PLE 0.21. MOA 0.24 long, anterior width 0.37, posterior width 0.29. Clypeus height 0.18. Chelicerae brown. Labium and endites brown, longer than wide. Sternum brown and scutellate, with brown hairs. Leg measurements: I 8.40 (2.54, 3.04, 1.58, 1.24); II 8.52 (2.62, 3.07, 1.63, 1.20); III 5.42 (1.81, 1.98, 0.91, 0.72); IV 5.34 (1.70, 1.99, 0.95, 0.70). Leg formula: 2134. Opisthosoma oval, yellow, with black spot. Spinnerets brown.

Palp (Fig. 8A, B). Tibia as long as wide. Ventral tibial apophysis small, thumb shaped, closing to retrolateral tibial apophysis. Retrolateral tibial apophysis middle part bulging, with a hook end. Dorsal tibial apophysis small, cone-shaped. A spine-like tubercle between retrolateral tibial apophysis and dorsal tibial apophysis. Bulb flat, apical tegular apophysis nail-shaped. Embolus filiform, originating at approximately 6-o’clock position, curved along with bulb, tip staying in cymbial furrow.

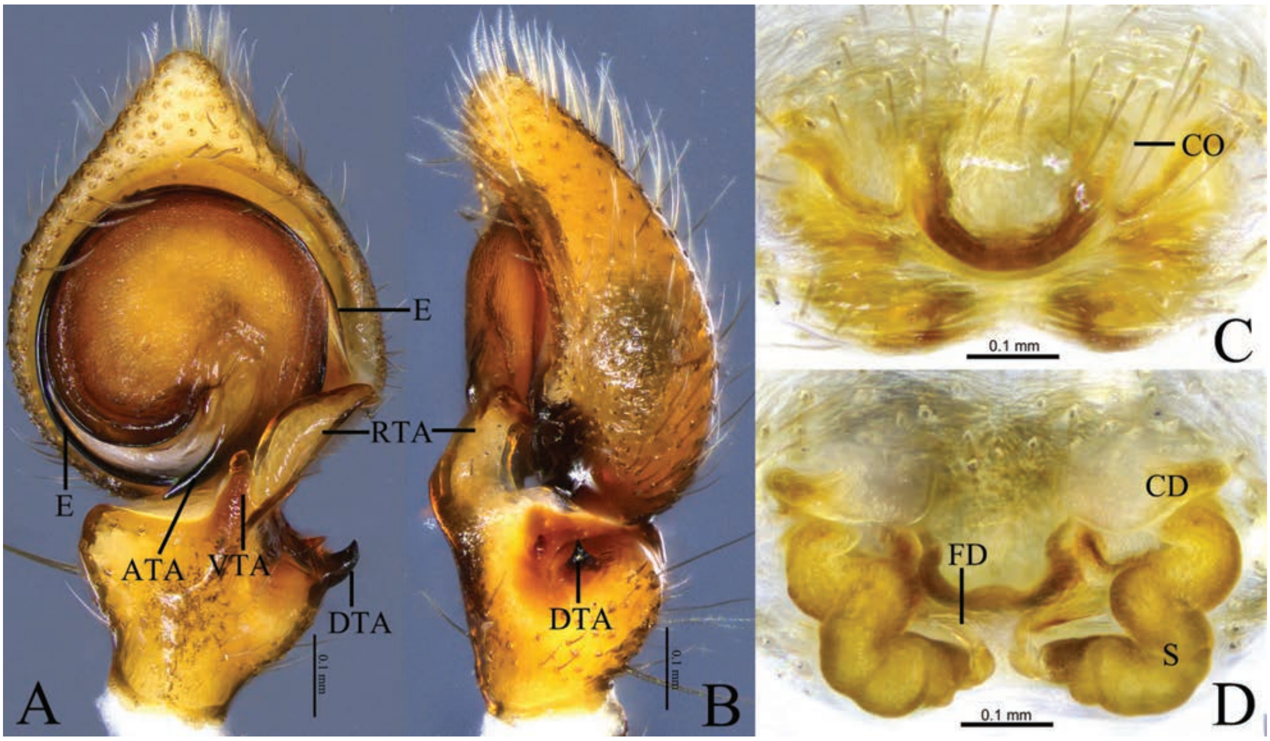

Figure 8. *Sinothomisus dawai* Wang, Lu & Zhang, sp. nov. **A, B** holotype male **C, D** paratype female **A** male left palp, ventral view **B** same, retrolateral view **C** epigyne, ventral view **D** same, dorsal view. Abbreviations: CD = copulatory duct; CO = copulatory opening; DTA = dorsal tibial apophysis; E = embolus; FD = fertilization duct; RTA = retrolateral tibial apophysis; VTA = ventral tibial apophysis; S = spermathecal.

Female paratype (SWUC-T-THO-04-03, Fig. 3H) total length 5.59. Prosoma 2.28 long, 2.25 wide; opisthosoma 3.10 long, 2.61 wide. Eye sizes and interdistances: AME 0.08, ALE 0.18, PME 0.02, PLE 0.15; AME–AME 0.28, AME–ALE 0.25, PME–PME 0.25, PME–PLE 0.54, ALE–PLE 0.25. MOA 0.26 long, anterior width 0.46, posterior width 0.33. Clypeus height 0.22. Leg measurements: **I** 7.00 (2.19, 2.56, 1.30, 0.95); **II** 7.35 (2.30, 2.79, 1.28, 0.98); **III** 5.05 (1.65, 1.90, 0.76, 0.74); **IV** 4.84 (1.44, 1.86, 0.84, 0.70). Leg formula: 2134.

Epigyne (Fig. 8C, D). Epigynal plate wider than long, with a fingernail-like protuberance at middle part. Copulatory openings slit like, far away from each other. Copulatory ducts S-like. Spermathecae C-shaped. Fertilization ducts crescent.

Variation. Males (*n* = 2) total length 4.21–5.17.

Distribution. China (Xizang, Medog) (Fig. 11).

Genus *Spilosynema* Tang & Li, 2010 (花斑蛛属)

Spilosynema motuo Wang, Lu & Zhang, sp. nov.

https://zoobank.org/C8CEDAA7-E58F-43AF-B415-3B0C06A84AE4
Figs 2D, 3I–J, 9, 11
Common name. 墨脱花斑蛛

Type material. ***Holotype*** • ♂ (SWUC-T-THO-05-01), China, Xizang, Medog County, Beibeng Township, 29°14.87'N, 95°11.02'E, elev. 924 m, 19 December 2023, Z.S. Zhang, L.Y. Wang, Q.L. Lu and Y.N. Mu leg. ***Paratypes:*** • 1 ♀ (SWUC-T-THO-05-02), Beibeng Township, Damu, 29°14'51"N, 95°11'1"E, elev. 924 m, 28

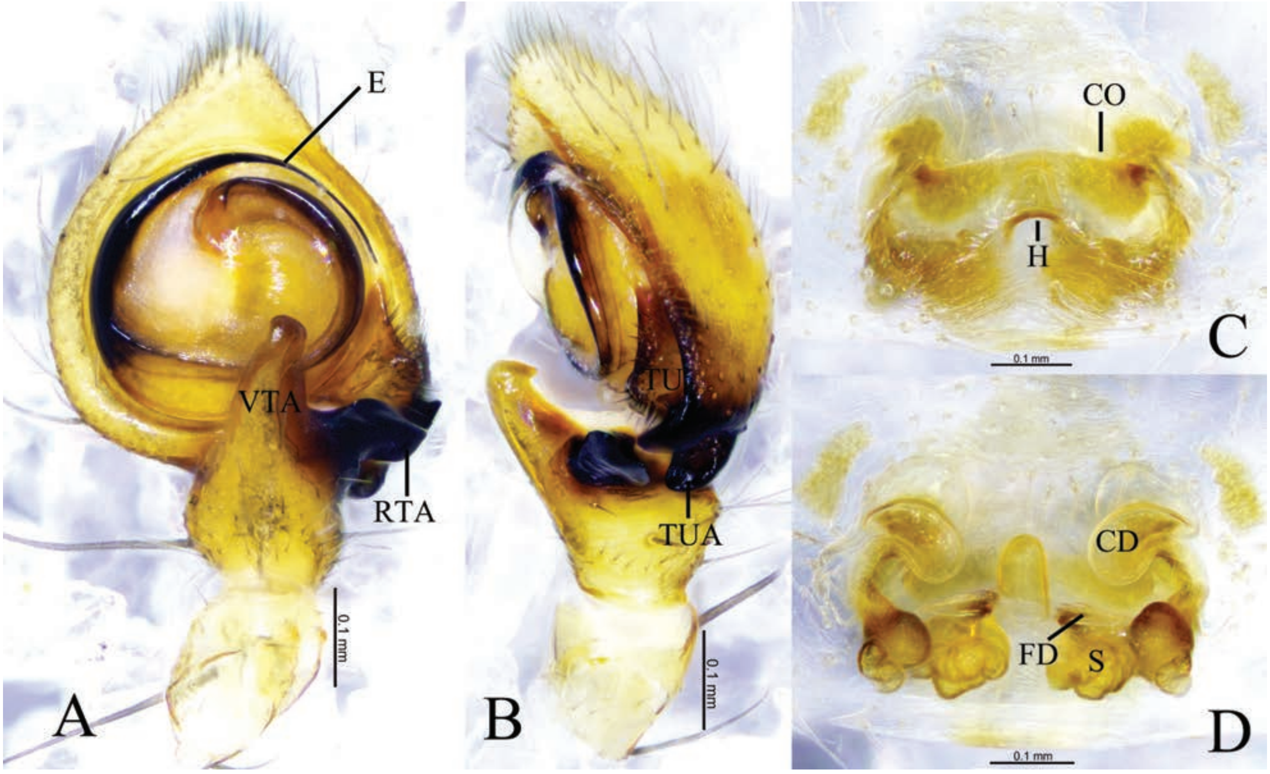

Figure 9. *Spilosynema motuo* Wang, Lu & Zhang, sp. nov. **A, B** holotype male **C, D** paratype female **A** male left palp, ventral view **B** same, retrolateral view **C** epigyne, ventral view **D** same, dorsal view. Abbreviations: CD = copulatory duct; CO = copulatory opening; E = embolus; FD = fertilization duct; H = hood; RTA = retrolateral tibial apophysis; Tu = tutaculum; TUA = tutacular apophysis; VTA = ventral tibial apophysis; S = spermathecal.

June 2018, L.Y. Wang, Y.N. Mu and Z.S. Wu leg. • 1 ♀ (SWUC-T-THO-05-03), Dexing Township, Guoguotang, 29°19.560'N, 95°16.360'E, elev.1025 m, 29 June 2018, L.Y. Wang, Y.N. Mu and Z.S. Wu leg. • 1 ♀ (SWUC-T-THO-05-04), Beibeng Township, Bayang Village, 29°12'49"N, 95°5'43"E, elev. 738 m, 7 July 2023, Z.S. Zhang, L.Y. Wang, Q.L. Lu and X.L. Chen leg. • 1 ♀ (SWUC-T-THO-05-05), Beibeng Township, Badeng Village, 29°16'28"N, 95°10'7"E, elev. 851 m, 7 July 2023, Z.S. Zhang, L.Y. Wang, Q.L. Lu and X.L. Chen leg. • 3 ♀ (SWUC-T-THO-05-06~08), Mirage Observation Deck, 29°20'36"N, 95°20'43"E, elev. 1297 m, 8 July 2023, Z.S. Zhang, L.Y. Wang, Q.L. Lu and X.L. Chen leg.

Etymology. The specific name is derived from the type locality (medog = motuo); it is a noun in apposition.

Diagnosis. The male of this new species resembles *S. comminum* Tang & Li, 2010 (Tang and Li 2010: 70, figs 52A–D, 54A, B) in the bulb of the same shape and the embolus origin in the same position, but it differs from the latter by the absence of an intermedial tibial apophysis (vs presence in *S. comminum*), the conical tutacular apophysis (vs hook-shaped in *S. comminum*) (Fig. 9A, B). The female of this new species can be distinguished from all other *Spilosynema* species in having the epigynal plate with a hood.

Description. Male holotype (Fig. 3I) total length 4.20. Prosoma 2.12 long, 1.98 wide; Opisthosoma 2.18 long, 1.65 wide. Carapace yellow brown. Eye sizes and interdistances: AME 0.11, ALE 0.21, PME 0.09, PLE 0.15; AME–AME 0.19, AME–ALE 0.18, PME–PME 0.23, PME–PLE 0.34, ALE–PLE 0.26. MOA 0.45 long, anterior width 0.40, posterior width 0.40. Clypeus height 0.19. Chelicerae brown, with 2 promarginal and 2 retromarginal teeth. Labium and endites brown, longer than wide. Sternum brown and scutellate, with brown hairs. Leg measurements: **I** 10.49 (2.89, 3.53, 2.64, 1.43); **II** 10.38 (2.88, 3.59, 2.55, 1.36); **III** 5.47 (1.72, 1.99, 0.98, 0.78); **IV** 5.96 (1.99, 2.11, 1.11, 0.75). Leg formula: 1243. Opisthosoma oval, yellow-brown, with a scaly spot. Spinnerets brown.

Palp (Fig. 9A, B). Tibia as long as wide. Ventral tibial apophysis strong, tip slightly hooked. Retrolateral tibial apophysis curved and strongly sclerotized. Cymbium base with two apophyses. Bulb flat. Embolus filiform, originating at approximately 8-o'clock position, curved along with bulb, tip staying in cymbial furrow.

Female paratype (SWUC-T-THO-05-02, Fig. 3J) total length 5.23. Prosoma 2.28 long, 2.18 wide; opisthosoma 2.93 long, 2.58 wide. Eye sizes and interdistances: AME 0.11, ALE 0.22, PME 0.10, PLE 0.14; AME–AME 0.25, AME–ALE 0.20, PME–PME 0.30, PME–PLE 0.44, ALE–PLE 0.35. MOA 0.45 long, anterior width 0.49, posterior width 0.53. Clypeus height 0.24. Leg measurements: **I** 10.10 (2.97, 3.64, 2.28, 1.21); **II** 9.98 (3.02, 3.49, 2.29, 1.18); **III** 5.10 (1.55, 1.90, 0.98, 0.67); **IV** 5.58 (1.82, 1.92, 1.10, 0.74). Leg formula: 1243.

Epigyne (Fig. 9C, D). Epigynal plate wider than long, with a hood at middle. Copulatory openings slit-like, distant from each other. Copulatory ducts S-like. Spermathecae peanut-shaped. Fertilization ducts crescent-shaped.

Variation. Females (*n* = *7*) total length 5.23–5.93.

Distribution. China (Xizang, Medog) (Fig. 11).

Genus *Thomisus* Walckenaer, 1805 (蟹蛛属)

Thomisus yarang Wang, Lu & Zhang, sp. nov.

https://zoobank.org/D3B67A42-9792-4B5D-BB7B-077186A88D48
Figs 3K–L, 10, 11
Common name. 亚让蟹蛛

Type material. ***Holotype*** • ♂ (SWUC-T-THO-06-01), China, Xizang, Medog County, Medog Town, Yarang Village, 29°17.758'N, 95°16.827'E, elev. 761 m, 28 June 2018, L.Y. Wang, Z.S. Wu and Y.N. Mu leg. ***Paratypes***: • 1 ♂ 1 ♀ (SWUC-T-THO-06-02 and SWUC-T-THO-06-02-03), same data as for holotype.

Etymology. The specific name is derived from the type locality; it is a noun in apposition.

Diagnosis. The new species resembles *T. labefactus* Karsch, 1881 (Song and Zhu 1997: 167, fig. 117A–E) in having a similar long and curved embolus, but it differs from the latter by the long, digitiform ventral tibial apophysis (vs short and conical in *T. labefactus*), the groove-shaped retrolateral tibial apophysis (vs base stretches in *T. labefactus*), and the arc-shaped copulatory ducts (vs semicircular in *T. labefactus*) (Fig. 10).

Description. Male holotype (SWUC-T-THO-06-01, Fig. 3K) total length 3.84. Prosoma 1.90 long, 1.98 wide; opisthosoma 2.24 long, 2.31 wide. Carapace brown, with a great many small denticles. Eye sizes and interdistances: AME 0.12, ALE 0.14, PME 0.11, PLE 0.10; AME–AME 0.27, AME–ALE 0.32, PME–PME 0.57, PME–PLE 0.42, ALE–PLE 0.24. MOA 0.39 long, anterior width 0.51, posterior width 0.75. Clypeus height 0.30. Chelicerae brown, with 3 promarginal and 2 retromarginal teeth. Leg measurements: **I** 5.35 (1.75, 1.87, 0.97, 0.76); **II** 5.48 (1.82, 1.93, 0.95, 0.78); **III** 2.94 (0.95, 1.06, 0.49, 0.44); **IV** 3.11 (1.04, 1.02,

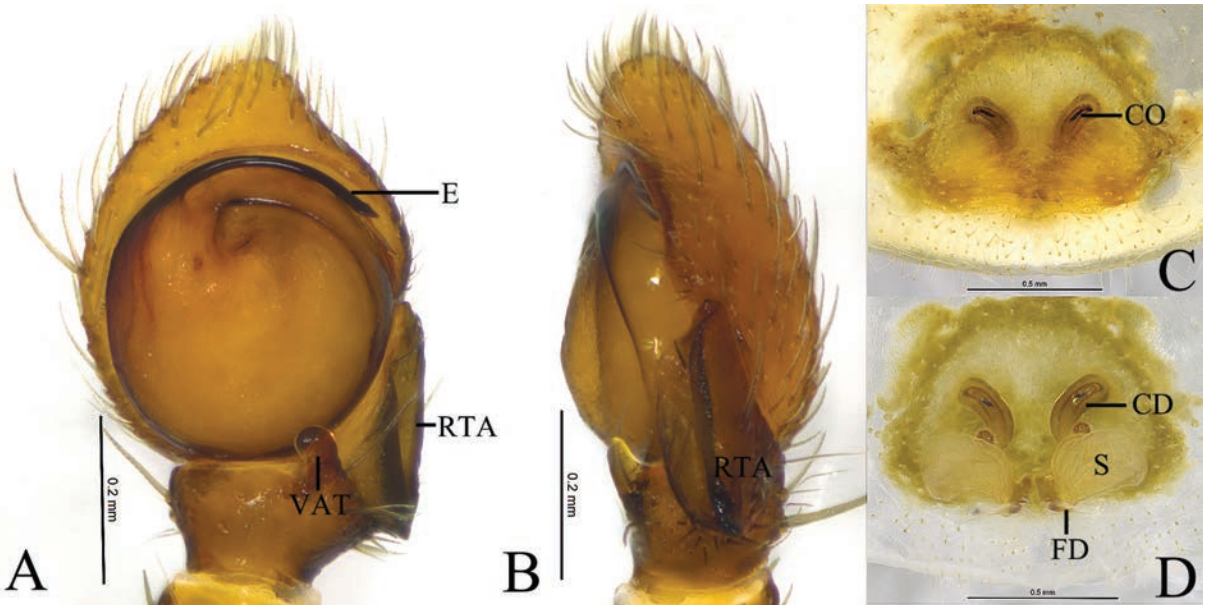

Figure 10. *Thomisus yarang* Wang, Lu & Zhang, sp. nov. **A, B** holotype male **C, D** paratype female **A** male left palp, ventral view **B** same, retrolateral view **C** epigyne, ventral view **D** same, dorsal view. Abbreviations: CD = copulatory duct; CO = copulatory opening; E = embolus; FD = fertilization duct; RTA = retrolateral tibial apophysis; VTA = ventral tibial apophysis; S = spermathecal.

0.58, 0.47). Leg formula: 2143. Opisthosoma brown, dorsum with small spines, venter yellow.

Palp (Fig. 10A, B). Tibia as long as wide. Ventral tibial apophysis blunt, digitiform. Retrolateral tibial apophysis large, wide, groove-shaped. Embolus originating at approximately 11-o'clock position, curved along with bulb.

Female paratype (SWUC-T-THO-06-03, Fig. 3L) total length 10.73. Prosoma 5.42 long, 5.19 wide; opisthosoma 5.84 long, 8.29 wide. Carapace yellowish. Eye sizes and interdistances: AME 0.20, ALE 0.23, PME 0.16, PLE 0.18; AME–AME 0.56, AME–ALE 0.71, PME–PME 1.09, PME–PLE 0.73, ALE–PLE 0.37. MOA 0.79 long, anterior width 0.95, posterior width 1.43. Clypeus height 0.65. Leg measurements: I 15.60 (4.99, 5.75, 2.81, 2.05); II 14.69 (4.74, 5.51, 2.69, 1.75); III 8.68 (2.92, 3.14, 1.62, 1.00); IV 10.14 (3.30, 3.72, 1.93, 1.19). Leg formula: 2143. Opisthosoma white, with a brown spot.

Epigyne (Fig. 10C, D). Epigynal plate oval. Copulatory openings arc-like, distant from each other. Copulatory ducts arc-like, three times longer than wide. Spermathecae transparent, spherical. Fertilization ducts crescent-shaped.

Variation. Males (*n* = 2) total length 3.29–3.84.

Distribution. Known only from the type locality, Medog, Xizang, China (Fig. 11).

Discussion

Among these seven species of crab spiders described here, only *Pharta xizang* Liu & Yao, 2023 was active at night. The rest of the species were collected during the day. All six new species were collected from flower beds along the side of a road, except *Monaeses xizang* Wang, Lu & Zhang, sp. nov. which was also collected from a road guardrail. It may be due to the abundance of precipitation, which makes the forest too dense and humid, so the crab-spider spiders go out of the forest to live at the edges.

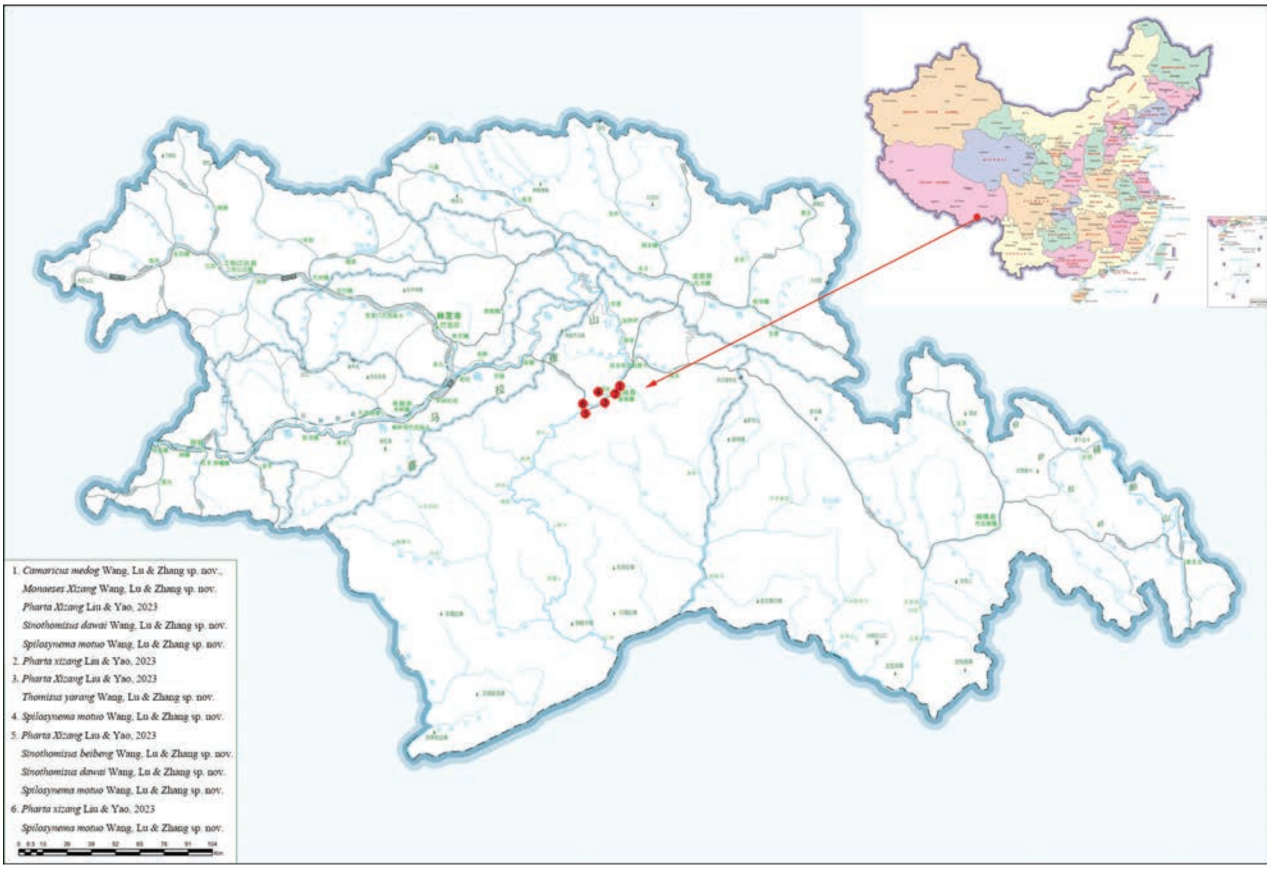

Figure 11. Distribution of crab spiders from Medog, Xizang, China.

Acknowledgements

Many thanks are given to Mr Zhi-Sun Wu, Tao Yuan, Ms Piao Liu (SWUC) and Hui Wang (College of Life Sciences, Hebei University, Baoding, China) for their assistance during fieldwork and collection. Many thanks to Miquel A. Arnedo, Renato Teixeira, and an anonymous reviewer for their valuable comments that greatly improved the manuscript.

Additional information

Conflict of interest

The authors have declared that no competing interests exist.

Ethical statement

No ethical statement was reported.

Funding

This research was supported by the Science & Technology Fundamental Resources Investigation Program (grant no. 2022FY202100), the Science Foundation of School of Life Sciences, SWU (20212020110501), and the Survey of Wildlife Resources in Key Areas of Tibet (ZL202203601).

Author contributions

All authors have contributed equally.

Author ORCIDs

Lu-Yu Wang https://orcid.org/0000-0002-5250-3473
Yan-Nan Mu https://orcid.org/0000-0002-2504-673X
Qian-Le Lu https://orcid.org/0000-0001-6291-9117
Yong-Qiang Xu https://orcid.org/0000-0002-1889-9531
Feng Zhang https://orcid.org/0000-0002-3347-1031
Zhi-Sheng Zhang https://orcid.org/0000-0002-9304-1789

Data availability

All of the data that support the findings of this study are available in the main text.

References

Álvarez-Padilla F, Hormiga G (2007) A protocol for digesting internal soft tissues and mounting spiders for scanning electron microscopy. The Journal of Arachnology 35(3): 538–542. https://doi.org/10.1636/Sh06-55.1

Benjamin SP (2011) Phylogenetics and comparative morphology of crab spiders (Araneae: Dionycha, Thomisidae). Zootaxa 3080: 1–108. https://doi.org/10.11646/zootaxa.3080.1.1

Chang WJ, Li SQ (2020) Thirty-one new species of the spider genus *Leclercera* from Southeast Asia (Araneae, Psilodercidae). ZooKeys 913: 1–87. https://doi.org/10.3897/zookeys.913.48650

ChangWJ, Yao ZY, Li SQ (2020) Twenty-eight new species of the spider genus *Merizocera* Fage, 1912 (Araneae, Psilodercidae) from South and Southeast Asia. ZooKeys 961: 41–118. https://doi.org/10.3897/zookeys.961.53058

Cheng WH, Bian DJ, Tong YF, Li SQ (2021) A new genus and two new species of oonopid spiders from Tibet, China (Araneae, Oonopidae). ZooKeys 1052: 55–69. https://doi.org/10.3897/zookeys.1052.66402

Chu C, Lu Y, Li SQ, Yao ZY (2022) Taxonomic notes on eleven species of the subfamily Cteninae (Araneae, Ctenidae) from Asia. Biodiversity Data Journal 10: e96003. https://doi.org/10.3897/BDJ.10.e96003

Fu YN, Zhu MS (2008) A new species of the genus *Pseudopoda* from China (Araneae, Sparassidae). Acta Zootaxonomica Sinica 33: 657–659.

Jiang TY, Zhao QY, Li SQ (2018) Sixteen new species of the genus *Pseudopoda* Jäger, 2000 from China, Myanmar, and Thailand (Sparassidae, Heteropodinae). ZooKeys 791: 107–161. https://doi.org/10.3897/zookeys.791.28137

Li CZ, Yao YB, Xiao YH, Liu KK (2023) Two new thomisid species (Arachnida, Araneae, Thomisidae) from China and Vietnam, with the first descriptions of the males of *Borboropactus longidens* Tang & Li, 2010 and *Stephanopis xiangzhouica* Liu, 2022. ZooKeys 1159: 169–187. https://doi.org/10.3897/zookeys.1159.102601

Li R, Wang GL, Zhang YH, Guo ZH (2024) Study on precipitation characteristics in Medog, southeastern Tibetan Plateau. Meteorololgical Monthly 50(3): 303–317. https://doi.org/10.7519/j.issn.1000-0526.2023.111801

Lin YJ, Yan XY, Li SQ (2022) Two new species of the genus *Chilobrachys* (Araneae, Theraphosidae) from China. ZooKeys 1081: 99–109. https://doi.org/10.3897/zookeys.1081.77072

Lu JZ, Wang LY, Zhang ZS (2023) A new species of *Hygropoda* from Tibet, China (Agelenidae: Pisauridae). Acta Arachnologica Sinica 32(2): 122–126. https://doi.org/10.3969/j.issn.1005-9628.2023.02.011

Mi XQ, Zhang T, Wang C (2024) Description of two species of the orb-weaver spider genus *Argiope* Audouin, 1826 (Araneae, Araneidae) from Xizang, China. Biodiversity Data Journal 12(e125601): 1–14. https://doi.org/10.3897/BDJ.12.e125601

Song DX, Zhu MS (1997) Fauna Sinica: Arachnida: Araneae: Thomisidae, Philodromidae. Science Press, Beijing, 259 pp.

Tang G, Li SQ (2010) Crab spiders from Xishuangbanna, Yunnan Province, China (Araneae, Thomisidae). Zootaxa 2703: 1–105. https://doi.org/10.11646/zootaxa.2703.1.1

Tang G, Yin CM, Griswold C, Peng XJ (2006) Description of *Sinothomisus* gen. nov. with a new species from Yunnan Province, China (Araneae, Thomisidae). Zootaxa 1366: 61–68. https://doi.org/10.11646/zootaxa.1366.1.4

Tong YF, Bian DJ, Li SQ (2023) Three new species of the genus *Ischnothyreus* Simon, 1893 and the discovery of the male of I. linzhiensis Hu, 2001 from Tibet, China (Araneae, Oonopidae). ZooKeys 1152: 119–131. https://doi.org/10.3897/zookeys.1152.100341

Wang Z, Peng JS (2022) The rich treasures of the primeval forest in Medog. Forest & Humankind 7: 62–75.

Wang LY, Zhang ZS (2020) The first record of *Zantheres* and *Z. gracillimus* Thorell, 1887 (Araneae, Lycosidae) from China. Acta Arachnologica Sinica 29(2): 99–102. https://doi.org/10.3969/j.issn.1005-9628.2020.02.004

Wang C, Mi XQ, Peng XJ (2016) A new species of *Pharta* Thorell, 1891 (Araneae: Thomisidae) from China. Oriental Insects 50(3): 129–134. https://doi.org/10.1080/00305316.2016.1197163

Wang LY, Peng XJ, Zhang ZS (2021) *Serratacosa*, a new genus of Lycosidae (Araneae) from the southern slopes of the Eastern Himalayas. European Journal of Taxonomy 762: 96–107. https://doi.org/10.5852/ejt.2021.762.1455

Wang C, Mi XQ, Li SQ (2024) Eleven species of jumping spiders from Sichuan, Xizang, and Yunnan, China (Araneae, Salticidae). ZooKeys 1192: 141–178. https://doi.org/10.3897/zookeys.1192.114589

Wang LY, Irfan M, Zhang F, Zhang Z.S (2024a) On three species of ctenids (Araneae: Ctenidae) from Tibet, China. Zootaxa 5458(1): 119–129. https://doi.org/10.11646/zootaxa.5458.1.7

Wang LY, Mu YN, Lu F, Xu YQ, Zhang ZS (2024b) Ant-eating spiders from Xizang, China (Araneae, Zodariidae). ZooKeys 1200: 183–198. https://doi.org/10.3897/zookeys.1200.120528

Xiong F, Liu ZP, Zhang ZS (2017) Review on the jumping spider genus Hyllus from China (Araneae Salticidae). Acta Arachnologica Sinica 26(1): 22–26. https://doi.org/10.3969/j.issn.1005-9628.2017.01.005

Yang ZY, Zhang JX (2024) On eight species of Chrysillini from Xizang, China (Araneae: Salticidae: Salticinae). Zootaxa 5447(2): 151–187. https://doi.org/10.11646/zootaxa.5447.2.1

Yin CM, Wang JF, Xie LP, Peng XJ (1990) New and newly recorded species of the spiders of family Araneidae from China (Arachnida, Araneae). In: Spiders in China: One Hundred New and Newly Recorded Species of the Families Araneidae and Agelenidae. Hunan Normal University Press, Changsha, 1–171.

Zhang QQ, Lin YC (2018) A review of the spider genus Sinanapis, with the description of a new species from Tibet (Araneae, Anapidae). ZooKeys 790: 45–61. https://doi.org/10.3897/zookeys.790.25793

Zhang F, Yu K (2021) Description of two species of *Conothele* Thorell, 1878 from Tibet, China (Mygalomorphae: Halonoproctidae). Journal of Hebei University, Natural Science Edition 41(5): 581–586.

Zhang L, Zhang F (2023) First report of the genus *Apochinomma* Pavesi, 1881 from China, with description of a new species (Araneae, Corinnidae, Castianeirinae). Zootaxa 5323(3): 446–450. https://doi.org/10.11646/zootaxa.5323.3.11

Zhang F, Zhu MS, Song DX (2006) A review of pholcid spiders from Tibet, China (Araneae, Pholcidae). Journal of Arachnology 34(1): 194–205. https://doi.org/10.1636/H04-22.1

Zhang F, Zhu MS, Song DX (2007) Two new species of the genus *Clubiona* from Xizang autonomous region, China (Araneae, Clubionidae). Journal of the Liaoning Normal University, Natural Science Edition 30: 90–92.

Zhang H, Zhu Y, Zhong Y, Jäger P, Liu J (2023) A taxonomic revision of the spider genus *Pseudopoda* Jäger, 2000 (Araneae: Sparassidae) from East, South and Southeast Asia. Megataxa 9(1): 1–304. https://doi.org/10.11646/megataxa.9.1.1

Zhu MS, Wang XP, Zhang ZS (2017) Fauna Sinica: Invertebrata Vol. 59: Arachnida: Araneae: Agelenidae and Amaurobiidae. Science Press, Beijing, 727 pp.

Zhu WH, Yao ZY, Zheng G, Li SQ (2020) The *Belisana* spiders (Araneae: Pholcidae) from Tibet, China. Zootaxa 4802(1): 111–128. https://doi.org/10.11646/zootaxa.4802.1.7

ZooKeys 1217: 215–246 (2024)
DOI: 10.3897/zookeys.1217.119844

Research Article

Uncovering the rich amphibian fauna of two semideciduous forest fragments in southwestern Bahia, Brazil

Carlos Augusto Souza-Costa[1], Mirco Solé[1,2], Caio Vinicius de Mira-Mendes[3,4], Antônio Jorge Suzart Argôlo[1], Iuri Ribeiro Dias[1]

1 Graduate Program in Zoology, Universidade Estadual de Santa Cruz, Rodovia Jorge Amado, km 16, 45662-900, Ilhéus, Bahia, Brazil
2 Museum Koenig Bonn (ZFMK), Leibniz Institute for the Analysis of Biodiversity Change, Adenauerallee 160, 53113 Bonn, Germany
3 Graduate Program in Tropical Aquatic Systems, Universidade Estadual de Santa Cruz, Rodovia Jorge Amado, km 16, 45662-900 Ilhéus, Bahia, Brazil
4 Department of Biology, Universidade Estadual do Maranhão, São Luís, Maranhão 65055-310, Brazil
Corresponding author: Iuri Ribeiro Dias (iurirdias@hotmail.com)

Abstract

Fauna inventories reduce biodiversity knowledge gaps by providing comprehensive data on species distribution, richness, and abundance. Furthermore, they identify undocumented species and enhance understanding of ecosystem dynamics and conservation needs. The richness and abundance of amphibian species were studied in two Semideciduous Seasonal Forest areas in the municipalities of Potiraguá (Serra Azul) and Itarantim (Serra do Mandim) in southwestern Bahia, Brazil. Active visual and acoustic surveys were conducted in 24 forest interior transects, two stream transects, and two permanent ponds investigated in the study area. Opportunistic encounters during team movements were also recorded. The richness was 46 amphibian species distributed in 14 families and 26 genera. Approximately half of the species were shared between the two areas, while 11 species were exclusive to Serra Azul and another nine were found only in Serra do Mandim. Cluster analysis for 42 locations in Atlantic Forest, Caatinga, and Cerrado, in a presence/absence matrix with 216 species, revealed that the composition of the amphibians found in Serra do Mandim and Serra Azul is similar to other sampled locations in the northeastern region of Minas Gerais, close to the study site, which are considered transitional between the Atlantic Forest and the Caatinga. Our results demonstrate that the remaining forest fragments in the region, although small and isolated, still sustain a high richness of amphibians with species restricted to the Atlantic Forest and Bahia, such as *Bahius bilineatus*, *Ololygon strigilata*, *Aplastodiscus weygoldti* and *Vitreorana eurygnatha*, and others considered typical of the Caatinga, such as *Leptodactylus troglodytes* and *Physalaemus cicada*. Additionally, we sampled potential new species, filled occurrence gaps, and expanded the geographical range of *Pseudis fusca*.

Key words: Anura, biodiversity, inventory, species distribution, species richness, transitional forest

OPEN ACCESS

Academic editor: Angelica Crottini
Received: 19 March 2024
Accepted: 10 July 2024
Published: 4 November 2024

ZooBank: https://zoobank.org/8A9A02E3-392C-49B3-9131-BF228F99ED2A

Citation: Souza-Costa CA, Solé M, Vinicius de Mira-Mendes C, Argôlo AJS, Ribeiro Dias I (2024) Uncovering the rich amphibian fauna of two semideciduous forest fragments in southwestern Bahia, Brazil. ZooKeys 1217: 215–246. https://doi.org/10.3897/zookeys.1217.119844

Introduction

Amphibians are considered good environmental indicators due to their permeable skin, exposed eggs and embryos, and generally biphasic life cycle, allowing these organisms to respond to disturbances in both terrestrial and aquatic ecosystems (Wells 2007; Da-Silva et al. 2012; Fonte et al. 2019). Additionally, climate change can affect them, and studies demonstrate that some communities in the Neotropical region are already close to their physiological temperature limits (Duarte et al. 2012; Gutiérrez-Pesquera et al. 2016; Carilo-Filho et al. 2021).

The greatest threat to amphibians and fauna in general is habitat loss and fragmentation, which reduces shelter availability, food supply, isolates populations, and affects their genetic variability (Young et al. 2004; Becker et al. 2007). Amphibians stand as the most endangered class of vertebrates, with 40.7% of their species at risk of extinction (Luedtke et al. 2023). Although the proportion of species classified as Data Deficient (DD) has decreased in the most recent Global Amphibian Assessment (from 22.5% to 11.3%), the high number of species still listed as DD poses a challenge for researchers and hinders effective conservation efforts (Hoffmann et al. 2010; Luedtke et al. 2023).

The Atlantic Forest, originally spanning approximately 1.3 million km^2, has undergone significant reduction, with estimates suggesting that only between 11.4% and 16% of its original coverage remains (Ribeiro et al. 2009). Nevertheless, the forest remnants still house an exuberant biological diversity, including endemic and threatened species, as well as species with restricted distribution to specific ecosystems (Myers et al. 2000; Haddad et al. 2013; Zappi et al. 2015).

In the southwest of Bahia, the Atlantic Forest is mainly composed of the Seasonal Forest (Deciduous and Semideciduous), which connects to interior forests, such as Caatinga and Cerrado (SOS MATA ATLÂNTICA and INPE 2018). This forest formation has physical and biological characteristics of adjacent regions, allowing faunal elements from other ecosystems to occur in these areas (Willians 1996). Nevertheless, even with the damage caused by human activities, such as pasture creation, logging, and mining (Miles et al. 2006; Silva et al. 2006), few protected areas have been established in the region, such as the REBIO (Biological reserve) Mata Escura and Alto Cariri National Park (ICMBio 2003, 2010) and the RPPN (Private Reserve of Natural Heritage) Mata do Passarinho (ICMBio 2016).

Amphibian surveys in Bahia have revealed significant species richness (e.g., Rojas-Padilla et al. 2020; Protázio et al. 2021; Bastos and Zina 2022), with records of new species (e.g., Vörös et al. 2017; Zucchetti et al. 2023; Santos et al. 2023) and expansions of the geographic distribution (e.g., Dias et al. 2010; Dias et al. 2011; Almeida et al. 2022). Interestingly, a family previously known only from the Amazon was recorded in the state of Bahia through the description of a new species (Caramaschi et al. 2013). Inventories contribute to the knowledge of species richness of a given region, as well as the understanding of the functional structure and population dynamics of amphibians (Droege et al. 1998; Haddad 1998; Camardelli and Napoli 2012). These studies are essential for planning conservation decisions and policies aimed at mitigating anthropogenic effects on species and for the creation of strategic areas for environmental protection (Silvano and Segalla 2005; IUCN 2024). Moreover, they assist in gathering information that enables the reduction of gaps in the distribution and composition of the anurofauna in the country (Rodrigues 2003; Tabarelli and Silva 2003).

Thus, the aim of this study was to conduct an inventory of the amphibians in two remaining Semideciduous Forests in the southwest of Bahia, comparing the amphibian community of these remnants with others from the Atlantic Forest, Caatinga, and Cerrado.

Materials and methods

Study area

The study was carried out in two fragments of Atlantic Forest in the Southwest region of Bahia: Fugiama farm (15°37'58"S, 39°59'01"W), with approximately 120 hectares of forest, located in the Serra do Mandim, municipality of Itarantim, and Serra Azul farm (15°52'01"S, 39°55'54"W), with about 160 hectares of forest, located in the Serra Azul, municipality of Potiraguá, both located in the state of Bahia (Figs 1, 2). While the mountains themselves reach up to approximately 1100 m in altitude, the areas accessed during the study were at around 800 m in altitude (Table 1).

The region borders the state of Minas Gerais and is located between two neighboring basins: the Pardo River basin and the Jequitinhonha River basin (IBGE 1997). Both areas are inserted in the Phytogeographic Domain of the Semideciduous Forest, characterized by the presence of climate type Am, with one to three dry months (Köppen 1936) and are ~ 28 km apart from each other. The climatic characteristics of the region encompass humid and sub-humid climates, defined by rainfall between 800 and 1100 mm and thermal averages from 23.5 to 25 °C (IBGE 1997).

The vegetation of the study area is characterized as Semideciduous Forest (SOS MATA ATLÂNTICA and INPE 2018). It occurs latitudinally parallel to the formation zone of the Ombrophilous Forest (coastal), at a distance ranging from 20 km to 140 km from the coast (Mori and Silva 1980; Argôlo 2004).

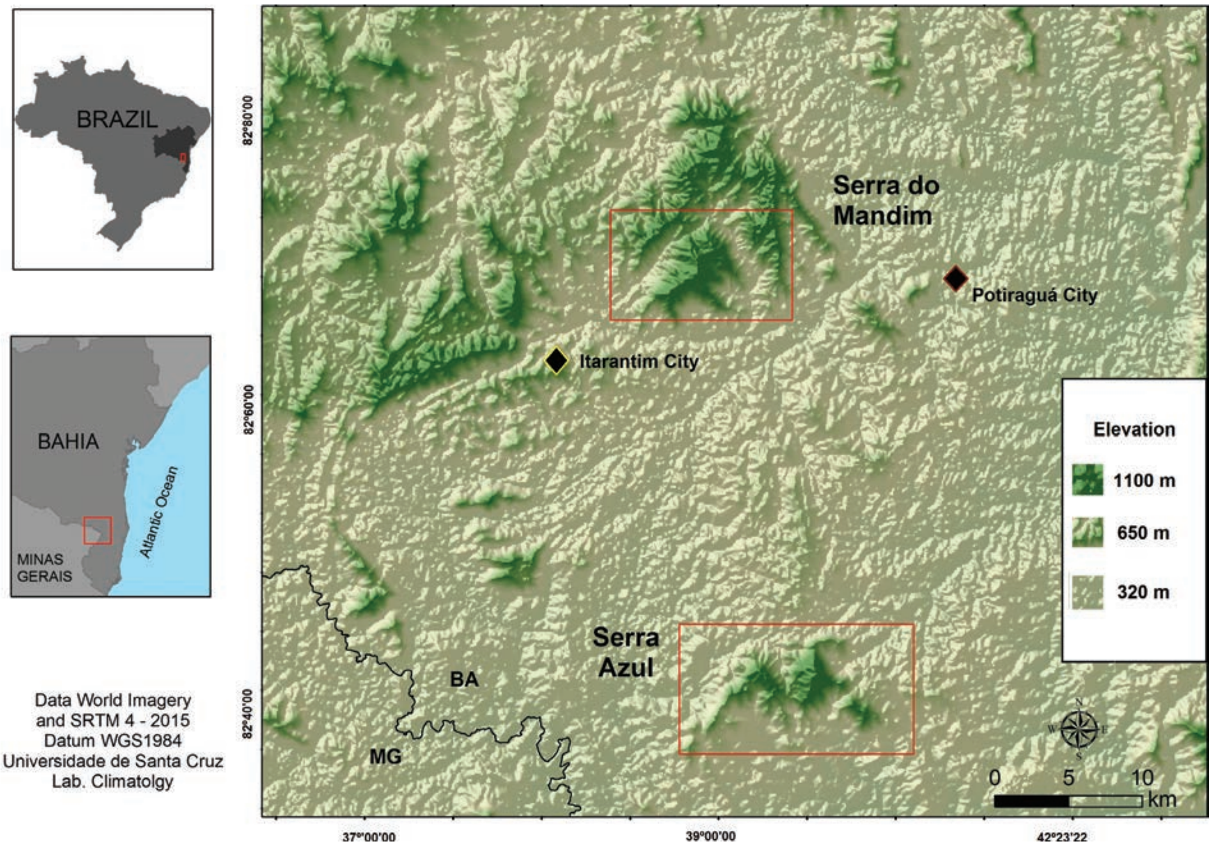

Figure 1. Study areas in the southwest region of Bahia, Brazil. Serra do Mandim belongs to the municipality of Itarantim, Bahia and Serra Azul, one of its portions inserted in the municipality of Potiraguá, Bahia.

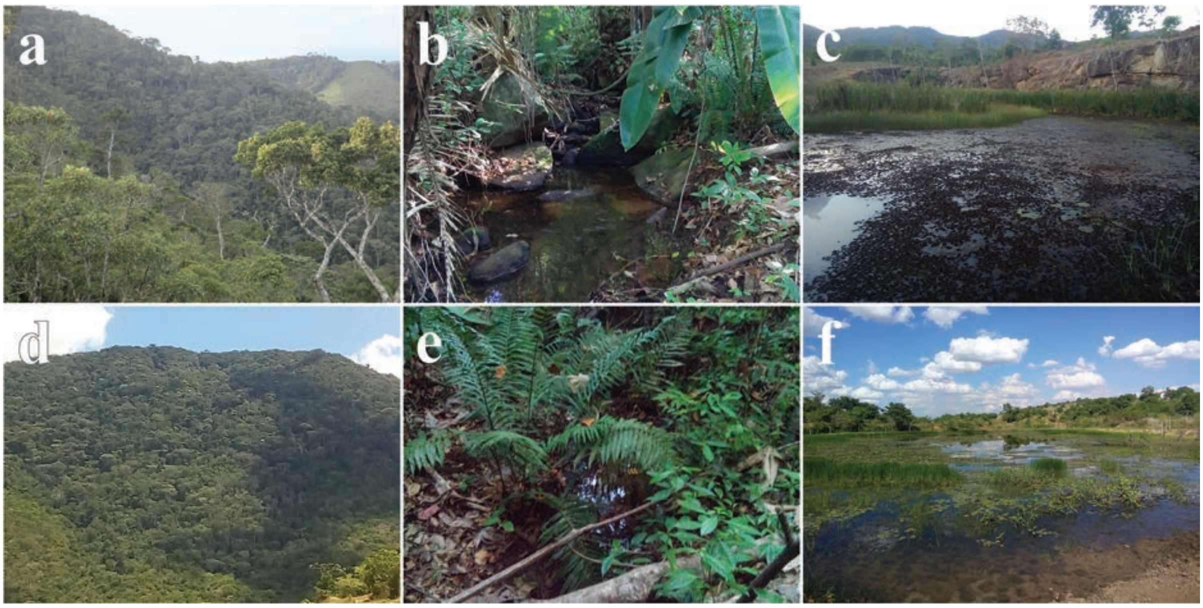

Figure 2. Study areas in the southwest region of Bahia. Fugiama farm in Serra do Mandim (**a**, **b, c**) **a** semideciduous forest fragment **b** stream **c** permanent pond. Serra Azul farm in Serra Azul (**d**, **e, f**) **d** semideciduous forest fragment **e** stream **f** permanent pond.

Table 1. Sampling points of the amphibian survey, coordinates, altitude, and sampling methods in Serra do Mandim, municipality of Itarantim and Serra Azul, municipality of Potiraguá, state of Bahia. TF = Transects in the forest; TS = Transects in the streams; P = permanent ponds.

Locality	Sampling points	Coordinates (Latitude; Longitude)	Altitude (m)	Sampling method
Serra do Mandim-BA	01	15°37'39.2"S, 39°58'41.6"W	728 m	TF
	02	15°37'38.9"S, 39°58'39.2"W	704 m	TF
	03	15°37'40.8"S, 39°58'37.5"W	672 m	TF
	04	15°37'47.9"S, 39°58'35.2"W	584 m	TF
	05	15°37'50.4"S, 39°59'02.2"W	758 m	TF
	06	15°37'49.5"S, 39°58'59.9"W	681 m	TF
	07	15°37'47.6"S, 39°58'57.9"W	635 m	TF
	08	15°37'47.8"S, 39°58'50.7"W	560 m	TF
	09	15°37'47.6"S, 39°58'48.9"W	587 m	TF
	10	15°37'47.5"S, 39°58'46.1"W	574 m	TF
	11	15°37'36.9"S, 39°58'43.5"W	755 m	TF
	12	15°37'51.4"S, 39°58'35.9"W	513 m	TF
	25	15°37'54.1"S, 39°58'34.0"W	485 m	TS
	27	15°39'15.4"S, 39°59'00.8"W	250 m	P
Serra Azul-BA	13	15°52'21.8"S, 39°54'30.6"W	731 m	TF
	14	15°52'19.7"S, 39°54'27.1"W	800 m	TF
	15	15°52'22.0"S, 39°54'22.7"W	739 m	TF
	16	15°52'24.7"S, 39°54'22.2"W	690 m	TF
	17	15°52'27.7"S, 39°54'22.5"W	672 m	TF
	18	15°52'26.3"S, 39°54'18.6"W	780 m	TF
	19	15°52'28.1"S, 39°54'10.9"W	692 m	TF
	20	15°52'25.9"S, 39°54'29.3"W	761 m	TF
	21	15°52'29.0"S, 39°54'27.7"W	650 m	TF
	22	15°52'34.5"S, 39°54'22.0"W	668 m	TF
	23	15°52'33.2"S, 39°54'25.0"W	652 m	TF
	24	15°52'29.7"S, 39°54'24.9"W	648 m	TF
	28	15°52'33.7"S, 39°54'24.2"W	658 m	TS
	26	15°51'52.5"S, 39°53'26.1"W	256 m	P

Sample design

A total of six field campaigns were carried out between December 2014 and March 2016 in Serra do Mandim and Serra Azul. Each expedition lasted approximately seven days, with approximately three or four days dedicated to active search in each mountain range.

A total of 24 transects were used between altitudes of 500–800 meters with a length of 50 meters and a width of 5 meters, spaced 100 meters apart in a forested area, two transects of 120 meters in streams, and two ponds were selected in a lowland area (Table 1). Twelve transects were sampled in forest, one in a stream, and a permanent pond in each of the areas (Figs 1, 2).

The transects in the forest were surveyed for 40 min, totaling 96 h. The streams in the forest were sampled for 90 min each, totaling 18 h. The permanent ponds were sampled for 30 min each, totaling six h. The sampling was carried out by two researchers. The total sampling effort was 44 days of sampling and 240 h/person. Amphibians were sampled using visual and acoustic active search methods (Heyer et al. 1994; Crump and Scott 1994) and by opportunistic encounters (i.e., along roads or trails outside the transects).

All animals were collected with a license from the Brazilian Institute of Environment and Renewable Natural Resources-IBAMA and/or ICMBio (No. 13708), together with the permission of the administrators of the local farms. Some specimens were euthanized through the administration of a lethal dose of 5% xylocaine to the ventral region, followed by fixation in 10% formaldehyde and preservation in 70% alcohol. All specimens were deposited in the Zoology Museum of the State University of Santa Cruz - MZUESC (Appendix 1).

Data analysis

For each species, the total number of individuals observed visually and acoustically was recorded in each sampling unit and environment. To evaluate sample sufficiency, rarefaction curves were constructed based on individuals. Four curves were made for each study area: a general curve considering all individuals sampled in the three standardized methodologies (transect in the forest, transect in the streams and ponds), and three others using individuals collected in each separate methodology. To extrapolate species richness, four non-parametric estimators were used: Chao 2, Jackknife 1, Jackknife 2, and Bootstrap (Magurran 1988; Colwell and Coddington 1994; Toti et al. 2000; Gotelli and Colwell 2001). The analysis was performed using presence/absence data for species during each sampling campaign, with 1000 randomizations.

The species richness recorded in the study area was compared to 42 locations, mostly in the northeast region of Brazil and a smaller number in the northeast region of Minas Gerais, sampled in the Atlantic Forest, Caatinga, and Cerrado (see Table 3). The information extracted from these locations was used to create a binary matrix of presence/absence with 216 amphibian species. The analysis of similarity, considering the specific composition of these areas, was performed using the Jaccard index to calculate dissimilarity and the UPMGA (Unweighted Pair Group Method with Arithmetic) linkage method. Species found in inventories with taxonomic doubts (sp., gr., and aff.) were excluded from the analyses. Subsequently, an ANOSIM (Analysis of Similarities) test was performed considering 9999 permutations, to determine whether the composition of samples recovered in the similarity analysis differs significantly among the groups (Atlantic Forest, Caatinga, and Cerrado). All analyses were conducted using the PAST 4.12 software (Hammer et al. 2001)

The species were identified based on their original descriptions, redescriptions, or recent taxonomic revisions. In addition to the original descriptions, references consulted for species identification are provided in Table 2. Additionally, the collected material was compared with specimens identified at MZUESC. For nomenclature, we followed Frost (2023), who also maintains an updated database containing all available synonyms for amphibians worldwide. Regarding *Adelophryne* spp. we follow Lourenço-De-Moraes et al. (2018). The conservation status of the species was classified according to IUCN (2024). Furthermore, we verified which species are endemic of the Atlantic Forest based on Rossa-Feres et al. (2017).

Results

A total of 1785 individuals across 46 amphibian species were recorded, encompassing one species of Gymnophiona (*Siphonops annulatus*) and 45 anuran species across 14 families (Table 2, Figs 3, 4). The majority of the identified species (*n* = 24; 53%) are endemic to the Atlantic Rainforest (Rossa-Feres et al. 2017). The Hylidae family was the most representative with 36.9% (*n* = 17), followed by the Leptodactylidae family, with 21.7% (*n* = 10) of the amphibians found. The richness identified stands among the highest ever recorded for the northeastern region of Brazil (Table 3). Furthermore, all recognized species identified are listed as Least Concern (LC) on the IUCN Red List (IUCN 2024).

The amphibian richness recorded was similar in the two analyzed areas: Serra do Mandim (*n* = 34) and Serra Azul (*n* = 37), with 25 species shared between the areas and the rest divided, with nine exclusive to Serra do Mandim and 11 to Serra Azul (Tables 2, 4). Among the total species recorded in each area, four species (*Ololygon strigilata*, *Phyllodytes luteolus*, *Trachycephalus nigromaculatus*, and *Leptodactylus* cf. *mystaceus*) were sampled exclusively through opportunistic encounters in Serra do Mandim, while another five (*Rhinella crucifer*, *Gastrotheca pulchra*, *Scinax x-signatus*, *Trachycephalus nigromaculatus* and *Dermatonotus muelleri*) also corresponded to opportunistic encounters in Serra Azul.

In Serra do Mandim most species were found in the monitored pond in the region. Although this was the smallest sampled fragment, some species considered rare and/or with restricted distribution were found only in this location, such as *Dendrophryniscus proboscideus*, and typical stream species such as *Vitreorana eurygnatha* and *Ololygon strigilata*.

The anuran richness recorded in Serra Azul was 37 species, and the only species of Gymnophiona recorded in the study was found in this area (Table 2; Fig. 4). Two species were only detected by vocalization, *Phyllodytes maculosus* and *Gastrotheca pulchra*. The first vocalized in bromeliads during forest transect sampling, while the latter was registered vocalizing in the canopy of the forest.

A higher number of individuals was recorded in Serra Azul (*n* = 868) compared to Serra do Mandim (*n* = 786). The most common species during the study were *Pristimantis vinhai* (*n* = 454), *Haddadus binotatus* (*n* = 296), and *Dendropsophus oliveirai* (*n* = 167). A total of 131 specimens were collected during opportunistic encounters, 78 at Serra Azul and 53 at Serra do Mandim (Table 2).

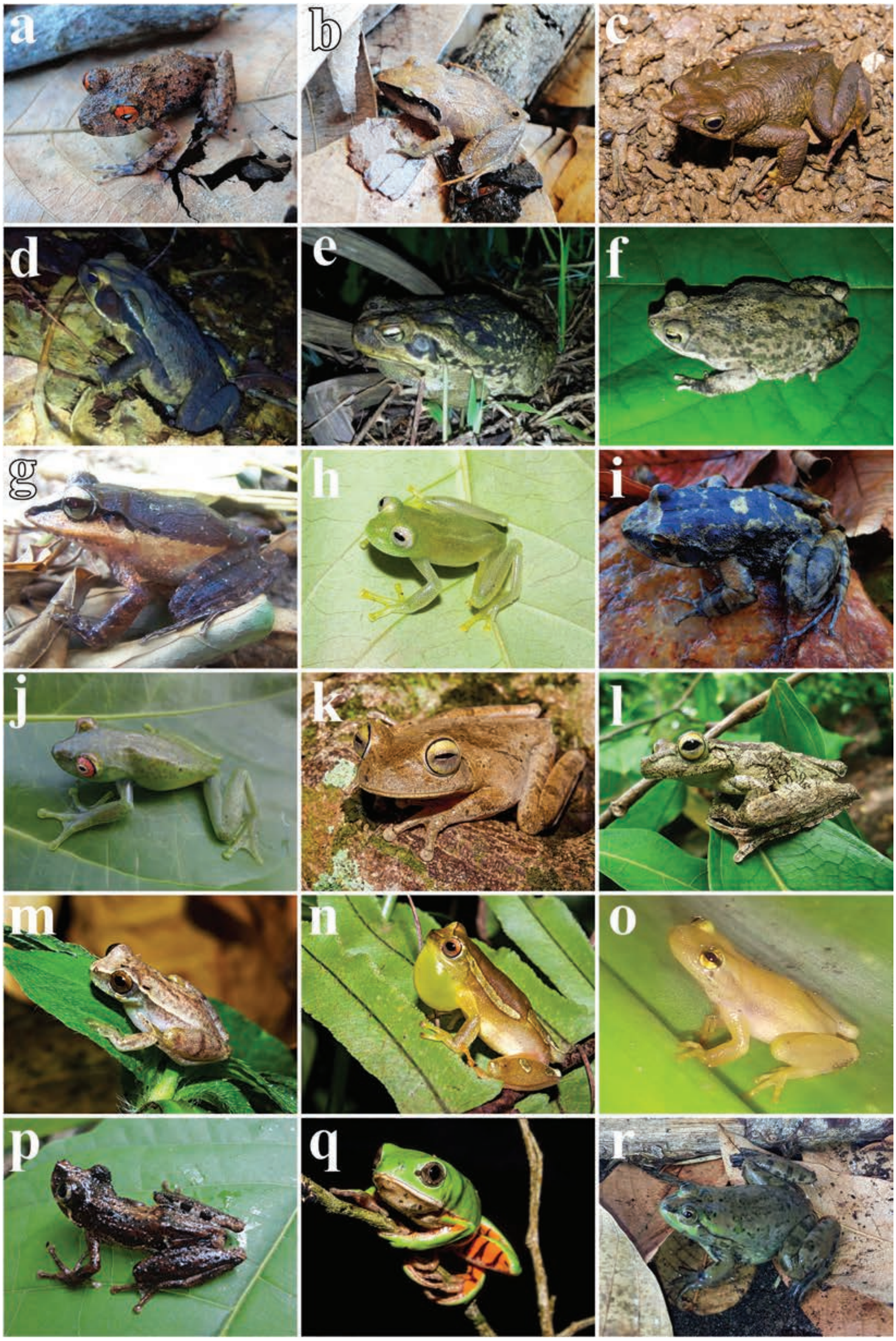

Figure 3. Amphibians registered in Serra do Mandim and Serra Azul in southwestern Bahia, Brazil. **a** *Ischnocnema verrucosa* (MZUESC 15874) **b** *Ischnocnema* sp. (gr. *parva* – MZUESC 15896) **c** *Dendrophryniscus proboscideus* (MZUESC 14688) **d** *Rhinella crucifer* (MZUESC 15148) **e** *R. diptycha* (MZUESC 15503) **f** *R. granulosa* (MZUESC 15055) **g** *Haddadus binotatus* (MZUESC 15646) **h** *Vitreorana eurygnatha* (MZUESC 14691) **i** *Thoropa miliaris* (MZUESC 15782) **j** *Aplastodiscus weygoldti* (MZUESC 15787) **k** *Boana crepitans* (MZUESC 14675) **l** *B. exastis* (MZUESC 15108) **m** *Dendropsophus branneri* (MZUESC 14683) **n** *D. elegans* (MZUESC 14679) **o** *Phyllodytes luteolus* (MZUESC 17501) **p** *Ololygon strigilata* (MZUESC 15001) **q** *Pithecopus nordestinus* (MZUESC 14682) **r** *Pseudis fusca* (MZUESC 16528).

Table 2. Species of amphibians from Serra do Mandim and Serra Azul, southwest Bahia, Brazil. Legend: **SM** = Sampling Method (**OE** = Oportunistic encounters, **TF** = Transect in the forest, **P** = Ponds, **TS** = Transect in the streams). **HAB** = Habitat (**LL** = Leaf litter or understory, **B** = Bromeliads or epiphytes, **S** = Streams, **F** = Forest, **P** = Ponds or open area). **N** = Number of registered specimens. Additional ID references = Additional references consulted to identify species. # = only acoustic record; † = species only found in the inner forests; * endemic to the Atlantic Rainforest.

Order/Family/Species	Serra do Mandim			Serra Azul			Additional ID references
	SM	HAB	N	SM	HAB	N	
ANURA							
Brachycephalidae							
Ischnocnema verrucosa (Reinhardt & Lütken, 1862)†*	TF	LL	02	TF	LL	06	Lynch 1972; Canedo et al 2010; Araújo et al. 2023
Ischnocnema sp. (gr. *parva*) †	-	-	-	TF	LL	01	Heyer et al. 1990; Silva-Soares et al. 2021
Bufonidae							
Dendrophryniscus proboscideus (Boulenger, 1882)†*	OE,TF	LL	08	-	-	-	Izecksohn 1976; Caramaschi 2012
Rhinella crucifer (Wied-Neuwied, 1821)*	TF,TS	P,LL	07	OE	P,LL	01	Baldissera et al. 2004; Oliveira et al. 2014
Rhinella diptycha (Cope, 1862)	P	P,LL	02	P	P,LL	09	Stevaux 2002; Lavilla and Brusquetti 2018
Rhinella granulosa (Spix, 1824)	-	-	-	OE,TF,P	P,LL	61	Narvaes and Rodrigues 2009; São Pedro et al. 2011
Craugastoridae							
Haddadus binotatus (Spix, 1824)†*	TF	LL	51	OE,TF,TS	LL	145	Heyer et al. 1990; Dias et al. 2012
Centrolenidae							
Vitreorana eurygnatha (A. Lutz, 1925)†*	TS	S	15	-	-	-	Heyer et al. 1990; Zucchetti et al. 2023
Cycloramphidae							
Thoropa miliaris (Spix, 1824)†*	OE,TF,TS	S,LL	10	OE,TS	S,LL	05	Feio et al. 2006a
Eleutherodactylidae							
Adelophryne sp.8†	TF	LL	08	OE,TF	LL	27	Lourenço-de-Moraes et al. 2018
Adelophryne sp.2†	TF,TS	LL	13	OE,TF	LL	29	Lourenço-de-Moraes et al. 2018
Hemiphractidae							
Gastrotheca pulchra Caramaschi & Rodrigues, 2007#†*	-	-	-	OE	B	01	Duellman 2015
Hylidae							
Aplastodiscus weygoldti (Cruz & Peixoto, 1987)†*	TS	S	06	TS	S	08	Orrico et al. 2006
Boana crepitans (Wied-Neuwied, 1824)	OE,P	P	18	OE,TF,P	P	21	Orrico et al. 2017
Boana exastis (Caramaschi & Rodriguez, 2003)†*	TF	F	01	-	-	-	Loebmann et al. 2008
Boana faber (Wied-Neuwied, 1821)*	OE,TF,P	P,F	11	OE,TF	P,F	06	Martins and Haddad 1988; Heyer et al. 1990
Dendropsophus branneri (Cochran, 1948)	OE,P	P	64	OE,P	P	83	Bastos and Pombal 1996; Nunes et al. 2007; Orrico et al. 2021
Dendropsophus elegans (Wied-Neuwied, 1824)*	OE,P	P	52	OE,P	P	24	Gomes and Peixoto 1991; Dias et al. 2017a; Pirani et al. 2022
Dendropsophus oliveirai (Bokermann, 1963)	OE,P	P	60	OEP	P	107	Santana et al. 2011; Orrico et al. 2021
Ololygon strigilata (Spix, 1824)†*	OE	S	01	-	-	-	Pimenta et al. 2007
Phyllodytes maculosus Cruz, Feio & Cardoso, 2007#†*	-	-	-	TF	B	01	Dias et al. 2020
Phyllodytes luteolus (Wied-Neuwied, 1821)*	OE	B	02	-	-	-	Bokermann 1966a; Blotto et al. 2021

Order/Family/Species	Serra do Mandim			Serra Azul			Additional ID references
	SM	HAB	N	SM	HAB	N	
Pithecopus nordestinus (Caramaschi, 2006)	OE,P	P	30	P	P	13	Vilaça et al. 2006; Vaz-Silva et al. 2020
Pseudis fusca Garman, 1883*	-	-	-	P	P	04	Caramaschi and Cruz 1998; Garda et al. 2010
Scinax eurydice (Bokermann, 1968)*	OE,TF	P,F	03	TF	P,F	01	Magrini et al. 2011; Novaes-e-Fagundes et al. 2016; Menezes et al. 2016
Scinax pachycrus (Miranda-Ribeiro, 1937a)	-	-	-	P	P	07	Carneiro et al. 2004; Novaes-e-Fagundes et al. 2016
Scinax x-signatus (Spix, 1824)	OE,P	P	07	OE	P	01	Araujo-Vieira et al. 2020a; Novaes-e-Fagundes et al. 2021
Sphaenorhynchus prasinus Bokermann, 1973*	OE,P	P	16	OE,P	P	29	Araujo-Vieira et al. 2020b
Trachycephalus nigromaculatus von Tschudi, 1838*	OE	P,F	01	OE	P,F	04	Bokermann 1966b
Leptodactylidae							
Leptodactylus fuscus (Schneider, 1799)	P	P	58	OE,P	P	28	Heyer 1978; Heyer et al. 1990; De-Sá et al. 2014
Leptodactylus latrans (Steffen, 1815)	OE,TS,P	P,S	07	P	P,S	06	Magalhães et al. 2022
Leptodactylus macrosternum Miranda-Ribeiro, 1926	TS	P,S	01	P	P,S	01	Magalhães et al. 2022
Leptodactylus cf. *mystaceus* (Spix, 1824)	OE	S	01	-	-	-	Toledo et al. 2005; De-Sá et al. 2014; Cassini et al. 2013
Leptodactylus mystacinus (Burmeister, 1861)	P	P	03	P	P	04	Abrunhosa et al. 2001; De-Sá et al. 2014; Cassini et al. 2013
Leptodactylus troglodytes Lutz, 1926	-	-	-	OE,P	P	04	De-Sá et al. 2014
Leptodactylus viridis Jim & Spirandeli-Cruz, 1973*	P	P	07	-	-	-	Magalhães et al. 2022
Physalaemus cicada Bokermann, 1966c	-	-	-	OE,P	P	05	Nascimento et al. 2005; Hepp and Pombal 2020
Physalaemus cf. *erikae* Cruz & Pimenta, 2004*	OE,P	P	18	OE,P	P	19	Nascimento et al. 2005; Hepp and Pombal 2020
Physalaemus kroyeri (Reinhardt & Lütken, 1862)	-	-	-	OE,P	P	06	Nascimento et al. 2005; Hepp and Pombal 2020; Braga et al. 2024
Microhylidae							
Dermatonotus muelleri (Boettger, 1885)	-	-	-	OE	P	02	Vaz-Silva et al. 2020; Dubeux et al. 2021
Odontophrynidae							
Proceratophrys schirchi (Miranda-Ribeiro, 1937b)†*	OE,TF,TS	S,LL	59	OE,TS	S,LL	09	Izecksohn and Peixoto 1980; Sichieri et al. 2021
Pipidae							
Pipa carvalhoi (Miranda-Ribeiro, 1937a)	P	P	04	-	-	-	Lima et al. 2020
Strabomantidae							
Bahius bilineatus (Bokermann, 1975) †*	OE,TF	LL	17	-	-	-	Dias et al. 2017b
Pristimantis vinhai (Bokermann 1975) †*	OE,TF,TS	LL	276	OE,TF,TS	LL	178	Trevisan et al. 2020
Pristimantis sp. (gr. *ramagii*)†	-	-	-	OE,TF	LL	90	Trevisan et al. 2020
GYMNOPHYONA							
Siphonopidae							
Siphonops annulatus (Mikan 1822)†	-	-	-	TF	LL	01	Maciel and Hoogmoed 2011

Table 3. The number of amphibian species (S), study duration (SD in months), and region (R) type of different study sites in northeastern Brazil, including the northeastern portion of Minas Gerais. Localities listed as RPPN are Private Natural Heritage Reserves, those labelled as APA are Environmental Protection Areas, EE represents Ecological Stations, and PN denotes National Parks. Region abbreviations include Atlantic Forest (AF), Caatinga (CA), and Cerrado (CE).

Localities, states of Brazil	S	SD	R	Source
RPPN Serra Bonita, BA	80	16	AF	Dias et al. 2014b
RE Michelin, BA	69	30	AF	Camurugi et al. 2010; Mira-Mendes et al. 2018
APA Lagoa Encantada and River Almada, BA	59	01	AF	Dias et al. 2014a
Serra da Jibóia, BA	55	~ 20 years	AF	Juncá, 2006; Freitas et al. 2018
Serra do Timbó, BA	55	12	AF	Freitas et al. 2019
PN Serra das Lontras, BA	49	07	AF	Rojas-Padilla et al. 2020
PN Grande Sertão Veredas, BA/GO/MG	47	~ 11 years	CE	Brandão et al. 2020
Serra Mandim and Serra Azul, BA	**46**	**08**	**AF**	**This study**
Middle Jequitinhonha River, MG	46	29	CA/CE	Feio and Caramaschi 1995
Chapada Diamantina, BA	44	06	CA	Juncá 2005
RPPN Frei Caneca, PE	42	12	AF	Santos and Santos 2011
Complex Limoeiro, MG	39	03	AF	Feio et al. 2006b
RPPN Estação Veracel, BA	39	01	AF	Silvano and Pimenta 2003
Complex Nossa Senhora Fatima, MG	38	02	AF	Feio et al. 2006b
Planalto de Ibiapaba, CE	38	24	AF/CA	Loebmann and Haddad 2010
Tocantins River Basin, MA/TO	38	06	CE	Brasileiro et al. 2008
Complex Cariri, BA/MG	36	03	AF	Feio et al. 2006b
Morro do Mara, BA	36	15	AF/CA	Bastos and Zina 2022
EE Serra Geral do Tocantins, TO	36	02	CE	Valdujo et al. 2011
Guaratinga, BA	34	01	AF	Silvano and Pimenta 2003
Macaíba, RN	34	14	AF/CA	Magalhães et al. 2013
Conde, BA	33	04	AF	Gondim-Silva et al. 2016
São Desiderio, BA	32	02	CE	Valdujo et al. 2009
Camamu, BA	32	01	AF	Silvano and Pimenta 2003
Serra do Brejo Novo, BA	32	19	AF/CA	Lantyer-Silva et al. 2013
PN Chapada Diamantina, BA	31	01	CA	Magalhães et al. 2015
Cruz das Almas, BA	31	39	AF	Protázio et al. 2021
Complex Bandeira, BA/MG	30	02	AF	Feio et al. 2006b
Complex Santana, MG	28	02	AF	Feio et al. 2006b
Complex Mumbuca, MG	27	02	AF	Feio et al. 2006b
RPPN Sapiranga, BA	25	05	AF	Juncá 2006
PN Descobrimento, BA	25	01	AF	Silvano and Pimenta 2003
Itapebi, BA	24	01	AF	Sivano and Pimenta 2003
EE Raso da Catarina, BA	21	13	CA	Garda et al. 2013
PN Catimbau, PE	21	01	CA	Pedrosa et al. 2014
Curimataú, PB	21	02	CA	Arzabe et al. 2005
Middle Jaguaribe River, CE	19	01	CA	Santana et al. 2015
RPPNs in Betânia and Floresta, PE	19	07	CA	Borges-Nojosa and Santos 2005
Jatobá, PE	18	04	CA	Silva et al. 2011
RPPN Serra das Almas, CE	18	02	CA	Borges-Nojosa and Cascon 2005
Paulo Afonso, BA	17	20	CA	Protázio et al. 2010
Cariri Paraibano, PB	16	23	CA	Vieira et al. 2007

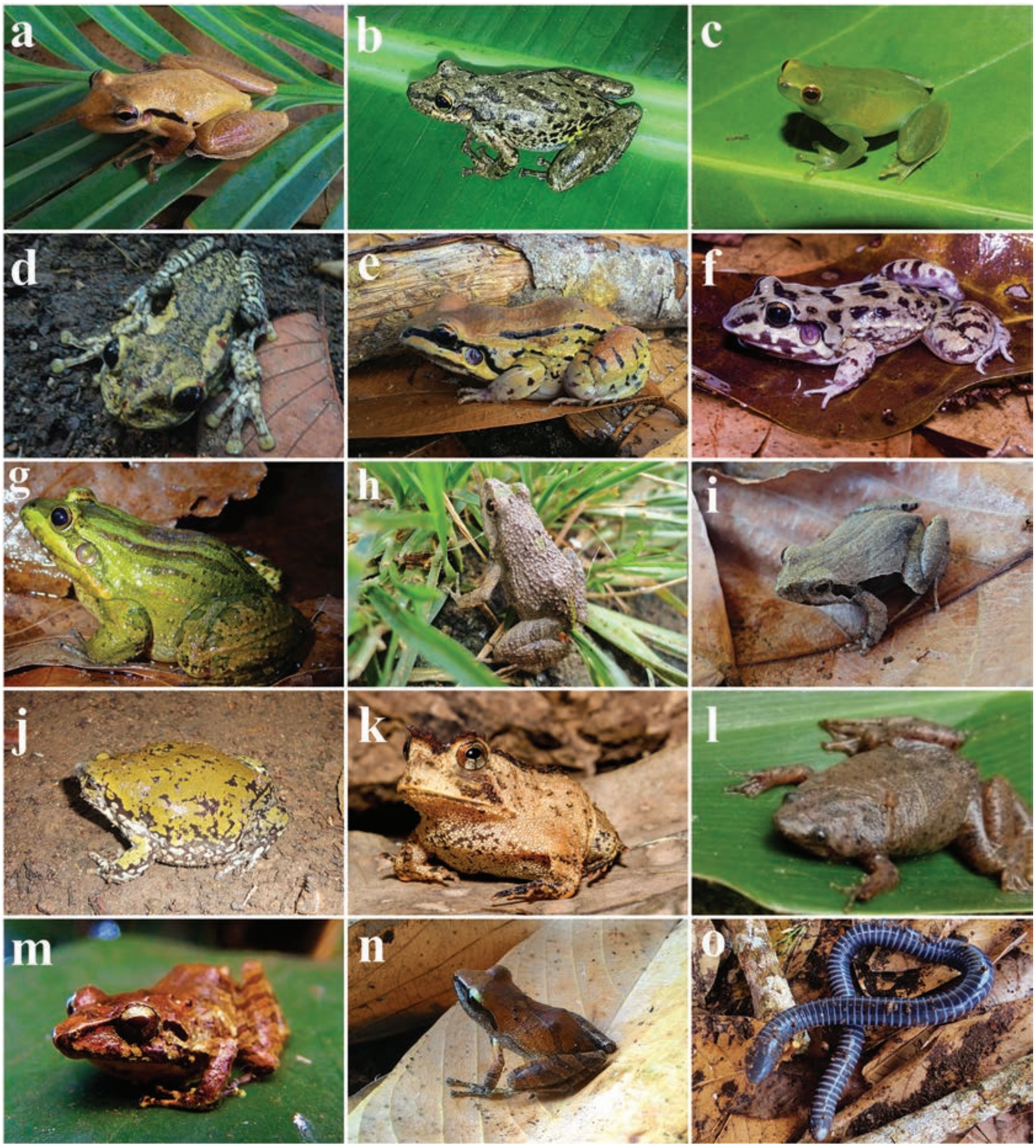

Figure 4. Amphibians registered in Serra do Mandim and Serra Azul in southwestern Bahia, Brazil **a** *Scinax pachycrus* (MZUESC 16525) **b** *S. x-signatus* (MZUESC 17503) **c** *Sphaenorhynchus prasinus* **d** *Trachycephalus nigromaculatus* (MZUESC 15064) **e** *Leptodactylus mystacinus* (MZUESC 16529) **f** *L. troglodytes* (MZUESC 15003) **g** *L. viridis* (MZUESC 15848) **h** *Physalaemus* cf. *erikae* (MZUESC 15878) **i** *P. kroyeri* (MZUESC 15784) **j** *Dermatonotus muelleri* (MZUESC 15070) **k** *Proceratophrys schirchi* (MZUESC 14689) **l** *Pipa carvalhoi* **m** *Pristimantis vinhai* (MZUESC 15642) **n** *P.* sp (gr. *ramagii* – MZUESC 16523) **o** *Siphonops annulatus* (MZUESC 15900).

Table 4. Number of species and abundance found in the study area through standardized methodologies and extrapolated richness using richness estimators. **TF**: Transect in the forest; **TS**: Transect in the streams and **P**: Ponds.

Estimators	Serra Azul				Serra do Mandim			
	TF	TS	P	Total	TF	TS	P	Total
Richness	13	5	18	32	13	9	15	30
Chao 2	15.1±2.7	5.0±0.2	25.8±7.4	39.6±6.3	15.8±3.5	9.8±1.5	15.6±1.2	35.8±6.0
Jackknife1	17.2±2.0	5.8±0.8	24.7±4.9	41.2±4.4	17.2±1.5	11.6±1.7	17.5±1.1	35.8±27
Jackknife2	18.9	5.9	28.9	45.8	19.4	12.4	17.9	39.4
Bootstrap	14.9	5.4	20.8	36.2	14.9	10.2	16.3	32.6
Abundance	433	43	392	868	350	106	330	786

The overall rarefaction curve obtained for each area showed a tendency towards stabilization but did not reach the asymptote (Fig. 5A). The curves made for the different employed methodologies did not show a stabilization trend, except for the species recorded in ponds (Fig. 5D). The richness estimators suggested the occurrence of between 39–46 species in Serra Azul and between 36–39 species in Serra do Mandim (Table 4). Thus, during field activities, between 78.2–94.4% of the estimated richness for each area was sampled. A summary of the richness estimates for each area and the employed methodologies can be found in Table 4.

Cluster analysis yielded three main groups, which are mainly based on different regions in which the samplings were carried out (Fig. 6). The ANOSIM

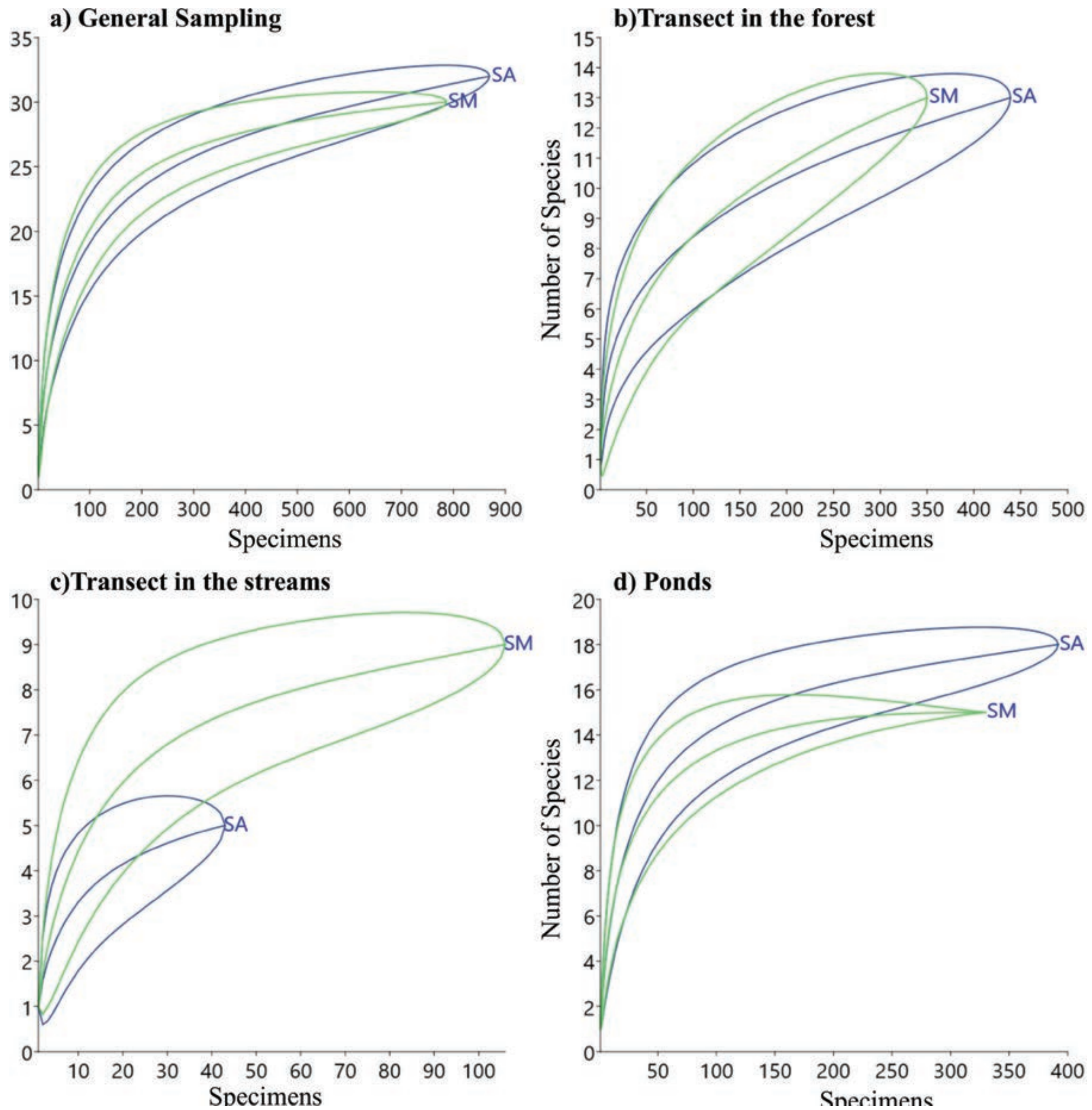

Figure 5. Rarefaction curve based on amphibian individuals for the two fragments of Semi-deciduous Seasonal Forest in Serra do Mandim and Serra Azul in southwest Bahia, Brazil **a** general sampling: Serra do Mandim and Serra Azul (without considering opportunistic records) **b** transect in the forest **c** transect in the streams and **d** ponds. The central line corresponds to the average obtained with 1000 randomizations, and the lines above and below correspond to the 95% confidence interval. The blue line represents Serra Azul (SA), and the green line represents Serra do Mandim (SM).

test demonstrates significant differences in species composition between the locations sampled in the Caatinga, Cerrado and Atlantic Forest (R = 0.662, P = 0.0001). Group 1 is formed by anuran assemblages sampled mainly in the Caatinga, where two main subdivisions can be highlighted, the first (1a) formed by localities along the middle Jequitinhonha River - MG and two localities in the Chapada Diamantina-BA, the latter hosting several endemic species (e.g., *Haddadus aramunha*, *Leptodactylus oreomantis*, *Rupirana cardosoi*) contributing to the unique anurofauna distinct from other sampled Caatinga locations (1b). Group 2 is formed by the anuran assemblages from the Cerrado.

Group 3 is comprised of anuran assemblages within the Atlantic Forest, and three main subdivisions can be highlighted. The first subdivision (3a)

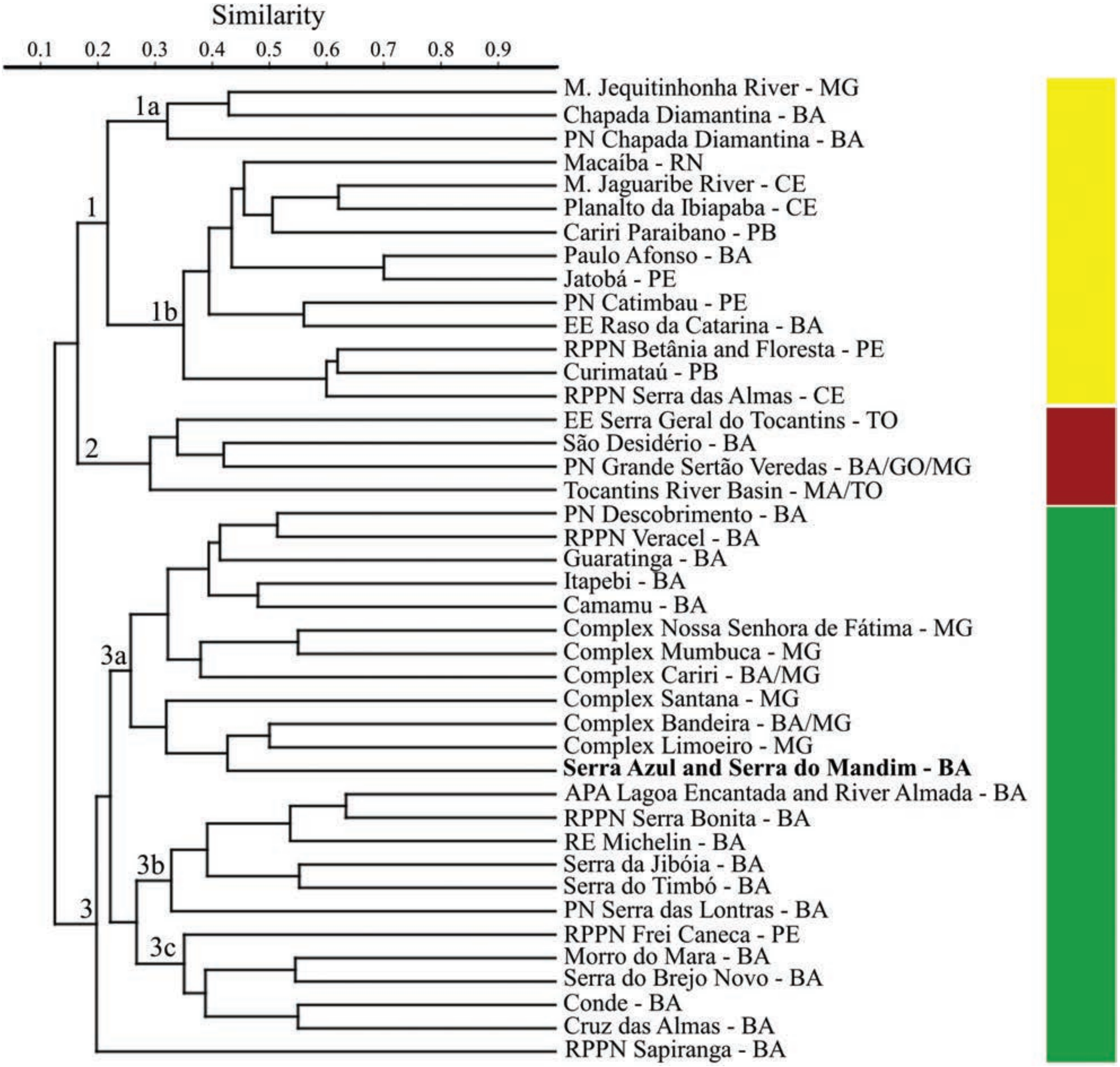

Figure 6. Similarity dendrogram for 42 locations, comparing amphibian composition primarily in the northeast region of Brazil. Jaccard index for dissimilarity calculation and UPGMA (Unweighted Pair Group Method with Arithmetic) clustering method (cophenetic correlation coefficient = 0.798). Green: locations sampled in the Atlantic Forest; Red: locations sampled in the Cerrado; Yellow: locations sampled in the Caatinga.

encompasses studies conducted in Dense Ombrophilous Forest in the extreme south of Bahia (e.g., RPPN Veracel, National Park of Descobrimento). It also includes transition areas influenced by Seasonal Forests located further inland, such as localities in the northeast of Minas Gerais (e.g., Complex Santana, Bandeira, and Limoeiro), and Serra Azul and Serra do Mandim in Bahia. The second subdivision (3b) formed by areas located in the south of the state of Bahia, primarily sampled in the Dense Ombrophilous Forest, and encompasses locations with the highest species richness in our analysis. Finally, the third subdivision (3c) encompasses transition areas between the Atlantic Forest and Caatinga (Brejo Novo, Morro do Mara), as well as Restinga areas (Conde) and Semideciduous Forest regions (RPPN Frei Caneca and Cruz das Almas).

Taxonomic remarks

Some specimens encountered during field activities posed challenges for identification. Recently, Magalhães et al. (2020) revisited the *Leptodactylus latrans* species group, employing multiple lines of evidence (DNA, acoustic, and morphological data), providing morphological diagnoses for the lineages encountered in their study. This facilitated the identification of two species from this group for the study area: *L. macrosternum* and *L. latrans*.

Physalaemus erikae was described in 2004 based on morphological and acoustic data, with the type locality in Guaratinga, Bahia (~ 100 km from the study area). This species closely resembles *P. kroyeri* but differs in having a shorter snout-vent length, a shorter advertisement call duration, and the presence of inguinal glands (Cruz and Pimenta 2004). Although our study area is close to the type locality, most specimens did not exhibit a visible inguinal gland, thus being considered as *P. kroyeri*. However, we encountered two specimens that exhibited an inguinal gland. For one of these, we recorded the advertisement call, which had a duration varying 0.37–0.46 s (MZUESC 15878). Recently, Hepp and Pombal (2020) reported that the advertisement call duration of *P. erikae* ranges from 0.478 to 0.566 s (*n* = 37 calls from four males), and for *P. kroyeri* it ranges from 0.673 to 0.759 s (*n* = 190 calls from eight males). Our data fall within the lower range of the reported variation for *P. erikae*. Braga et al. (2024) analyzed the vocalization of *P. kroyeri* from Cruz das Almas – Bahia (near the type locality) and found an advertisement call duration of 0.614 to 0.882 s (*n* = 83 calls from ten males), indicating a longer call duration in this species. However, we emphasize the need for a more comprehensive taxonomic revision of these two species, especially to increase the available data on the morphological and acoustic variation of *P. erikae*, particularly its acoustic parameters, especially those from its type locality, as well as the necessity of molecular sampling of topotypes of this species for inclusion in a phylogenetic approach.

Four species were not identified at the species level (*Adelophryne* sp. 2, *A*. sp. 8, *Ischnocnema* sp. [gr. *parva*] and *Pristimantis* sp. [gr *ramagii*]) and are considered candidate species that require further taxonomic investigation (Lourenço-De-Moraes et al. 2018; Trevisan et al. 2020; IR Dias, personal communication). Additionally, three other species (*Phyllodytes luteolus*, *Ischnocnema verrucosa* and *Vitreorana eurygnatha*) found in the area exhibit high intraspecific molecular diversity and may represent a similar case to the aforementioned (Blotto et al. 2021; IR Dias, personal communication; Zucchetti and Castroviejo-Fisher 2024).

Discussion

During the present study, 46 amphibian species were recorded in Serra Azul and Serra do Mandim in southwestern Bahia. This diversity is likely to be even greater, as the species accumulation curves have not stabilized. Thus, in these forest remnants, isolated and immersed in a matrix dominated by pastures for livestock, approximately 25% of the species that occur in Bahia can be found (Dias et al. 2014b), showing the importance of maintaining and conserving the fragments of the region. The recorded richness ranks among the top ten highest ever found in the Northeast region of Brazil, with a high proportion of species endemic to the Atlantic Rainforest. However, it is important to note that the sampling effort among the different studied areas is highly unequal, making comparisons difficult. Localities where low sampling effort was employed, such as APA (Environmental Protection Area) Lagoa Encantada and Almada River (1 month) and RPPN Veracel (1 month), have a similar richness to places where sampling effort was much higher, such as the Michelin Ecological Reserve and RPPN Frei Caneca. It is likely that the anuran fauna in these areas where low sampling effort was employed is underestimated.

Among the species found, three are restricted to the Atlantic Forest of the state of Bahia: *Bahius bilineatus*, *Physalaemus* cf. *erikae*, *Ololygon strigilata* (Juncá and Pimenta 2004; Cruz and Pimenta 2004; Pimenta et al. 2007), and five others have a geographical distribution between southern Bahia and Espirito Santo or northeastern Minas Gerais: *Ischnocnema verrucosa*, *Aplastodiscus weygoldti*, *Phyllodytes maculosus*, *Dendrophryniscus proboscideus*, and *Leptodactylus viridis* (Caramaschi and Canedo 2006; Cruz et al. 2007; Moura et al. 2009; Lantyer-Silva et al. 2011; Silva et al. 2012).

Some of the species found occur mainly in open areas, such as *Rhinella diptycha* and *Dermatonotus muelleri* (Andrade and Carnaval 2004; Feio et al. 2006b), while others are considered typical of the Caatinga, such as *Leptodactylus troglodytes*, *Scinax pachycrus*, and *Physalaemus cicada* (Feio and Caramaschi 1995; Rodrigues 2003; Peixoto and Arzabe 2004; Linares and Mello 2011). The encounter of species restricted to the Atlantic Forest, and others typical of the Caatinga, was expected since the study site is located in a transition area between these two regions. According to the similarity analysis, the composition of the anuran fauna of Serra Azul and Serra do Mandim is similar to other sampled areas in the region in ecotonal areas, which also share faunistic elements of these two morphoclimatic domains (Feio and Caramaschi 1995; Feio et al. 2006b).

Within the state of Bahia, some species found in the study area have records limited to fewer than three occurrence points, such as *Trachycephalus nigromaculatus*, and *Pseudis fusca* (Garda et al. 2010; Dias et al. 2010). *Pseudis fusca* (Fig. 3R), an aquatic species, is found in the states of Bahia, Minas Gerais, and Espírito Santo, Brazil (Garda et al. 2010). In Bahia, the species is known from two municipalities: Guaratinga and Teixeira de Freitas (Garda et al.

2010). The encounter of *P. fusca* in Serra Azul represents the third record of the species for the state of Bahia, marking an approximately 250 km straight-line increase in its geographical distribution from its type locality (Araçuaí – Minas Gerais). These new records contribute to a better understanding of the distribution patterns of these species in the region, especially for *P. fusca*, with this new occurrence point now representing the northern limit of the distribution of this species.

Amphibian inventories in southern Bahia have shown high species richness and endemism in the region (e.g., Silvano and Pimenta 2003; Camurugi et al. 2010; Rojas-Padilla et al. 2020; present study), which may be associated with the fact that the central region of the Atlantic Forest is estimated as a zone of climatic stability during the Quaternary glaciations, serving as a large refuge for amphibian species in the Atlantic Forest at the end of the Pleistocene, contributing to the maintenance of regional diversity (Carnaval and Moritz 2008; Carnaval et al. 2009).

Serra do Mandim and Serra Azul still have conserved forest fragments that form a complex network of streams that compose the Jequitinhonha river basins further south (IBGE 1997) and the Rio Pardo basin further north of the region (Pedreira 1999; Cetra et al. 2010). This great abundance of water bodies and the conservation of the study area contributed to the record of typical forest species (e.g., *Adelophryne* sp. 2, *A.* sp. 8, *Ischnocnema verrucosa*, *Pristimantis vinhai*, and *Gastrotheca pulchra*) and typical stream species (e.g., *Aplastodiscus weygoldti*, *Ololygon strigilata*, and *Vitreorana eurygnatha*). In addition, a high abundance of direct development species using leaf litter (e.g., *Pristimantis vinhai*, *P.* sp. [gr. *ramagii*] and *Haddadus binotatus*), including species that are difficult to sample such as *Ischnocnema verrucosa* and *Dendrophyrniscus proboscideus*, was found, demonstrating that the sampled forest fragments still have adequate conditions for the maintenance of these populations in the region. Despite this, no protected area has been established to ensure the conservation of these elements of the region's fauna. Actions are required to secure the preservation of these species.

Our results demonstrate that the remaining forest fragments in the region, although small and isolated, still support a high richness of amphibians with species restricted to the Atlantic Forest and Bahia, such as *Bahius bilineatus* and *Ololygon strigilata*, and others considered typical of the Caatinga, such as *Dermatonotus muelleri*, *Leptodactylus troglodytes*, and *Physalaemus cicada*.

Acknowledgments

We thank Cintia de Melo Souto Brige (in memoriam) and family (Fugiama farm) and José Cordeiro de Almeida Filho (in memoriam) and family (Serra Azul farm) for allowing the execution of the study on their properties, and Camila Souza Batista for her support in the field. We thank Kaique Brito Silva for assistance in preparing the map. CASC thanks CAPES-Coordenação de Aperfeiçoamento de Pessoal de Nível Superior and FAPESB-Fundação de Amparo à Pesquisa do Estado da Bahia, for scholarships, as well as the State University of Santa Cruz and the Zoology Graduate Program-PPGZOO for the opportunity and support granted. MS and IRD acknowledge the Brazilian National Council for Scientific and Technological Development (CNPq - PQ 309365/2019-8 and PQ:

315362/2021-9, respectively) for research scholarships. CVM-M acknowledges funding from Universidade Estadual do Maranhão (UEMA) (senior productivity grant 05/2023– PPG/UEMA).

Additional information

Conflict of interest

The authors have declared that no competing interests exist.

Ethical statement

No ethical statement was reported.

Funding

This work was supported by Conselho Nacional de Desenvolvimento Científico e Tecnológico; Coordenação de Aperfeiçoamento de Pessoal de Nível Superior; Fundação de Amparo à Pesquisa do Estado da Bahia.

Author contributions

Conceptualization: CASC, AJSA, CVMM, IRD, MS. Data curation: CASC. Formal analysis: CASC, IRD. Funding acquisition: MS. Investigation: MS, CASC. Methodology: CASC. Project administration: MS, CASC. Supervision: MS, IRD. Validation: CASC. Visualization: CASC. Writing - original draft: MS, AJSA, CVMM, IRD, CASC. Writing - review and editing: AJSA, IRD, MS, CVMM, CASC.

Author ORCIDs

Mirco Solé https://orcid.org/0000-0001-7881-6227
Caio Vinicius de Mira-Mendes https://orcid.org/0000-0002-7707-6439
Iuri Ribeiro Dias https://orcid.org/0000-0002-2825-3494

Data availability

All of the data that support the findings of this study are available in the main text.

References

Abrunhosa PA, Wogel H, Pombal Jr JP (2001) Vocalização de quatro espécies de anuros do Estado do Rio de Janeiro, Sudeste do Brasil (Amphibia, Hylidae, Leptodactylidae). Boletim do Museu Nacional do Rio de Janeiro 472: 1–12.

Almeida AP, Bastos DFO, Júnior PBA, Vila Nova MF, Dias IR, Zina J (2022) New records and geographic distribution map of *Proceratophrys sanctaritae* Cruz & Napoli, 2010 (Anura, Odontophrynidae). Check List 18(6): 1243–1247. https://doi.org/10.15560/18.6.1243

Andrade G, Carnaval AC (2004) Rhinella jimi. The IUCN Red List of Threatened Species 2004. [accessed on 29 July 2016] https://doi.org/10.2305/IUCN.UK.2004.RLTS.T54674A11184744.en

Araújo AP, Ferreira RB, Canedo C, Zocca C, Lacerda JVA (2023) After 160 years of 'silence': The advertisement call of the frog *Ischnocnema verrucosa*. Herpetological Bulletin 163(163): 31–34. https://doi.org/10.33256/hb163.3134

Araujo-Vieira K, Pombal Jr JP, Caramaschi U, Novaes-e-Fagundes G, Orrico VGD, Faivovich J (2020a) A neotype for *Hyla x-signata* Spix, 1824 (Amphibia, Anura, Hylidae). Papéis Avulsos de Zoologia 60[e20206056]: 1–30. https://doi.org/10.11606/1807-0205/2020.60.56

Araujo-Vieira K, Luna MC, Caramaschi U, Haddad CFB (2020b) A new genus of Lime Treefrogs (Anura: Hylidae: Sphaenorhynchini). Zoologischer Anzeiger 286: 81–89. https://doi.org/10.1016/j.jcz.2020.04.002

Argôlo AJS (2004) As serpentes dos cacauais do sudeste da Bahia. Editus, Ilhéus, Bahia, Brazil, 259 pp.

Arzabe C, Skuk G, Santana GG, Delfim FR, Lima YCC, Abrantes SHF (2005) Herpetofauna da área do Curimataú, Paraíba. In: Araujo FS, Rodal MJN, Barbosa MRV (Org) Análise das Variações da Biodiversidade do Bioma Caatinga: suporte a estratégias regionais de conservação. Ministério do Meio Ambiente, Brasília, 259–273.

Baldissera Jr FA, Caramaschi U, Haddad CFB (2004) Review of the *Bufo crucifer* species group, with descriptions of two new related species (Amphibia, Anura, Bufonidae). Rio de Janeiro. Arquivos do Museu Nacional. Museu Nacional (Brazil) 62(3): 255–282.

Bastos RP, Pombal Jr JP (1996) A new species of *Hyla* (Anura: Hylidae) from eastern Brazil. Amphibia-Reptilia 17(4): 325–331. https://doi.org/10.1163/156853896X00054

Bastos DFO, Zina J (2022) Amphibian fauna in an ecotonal and mountainous area in south-central Bahia State, northeastern Brazil. Herpetology Notes 15: 365–376.

Becker CG, Fonseca CR, Haddad CFB, Batista RF, Prado PI (2007) Habitat Split and the Global Decline of Amphibians. Science 318(5857): 1775–1777. https://doi.org/10.1126/science.1149374

Blotto BL, Lyra ML, Cardoso MCS, Rodrigues MT, Dias IR, Marciano-Jr E, Vechio FD, Orrico VGD, Brandão RA, Assis CL, Lantyer-Silva ASF, Rutherford MG, Gagliardi-Urrutia G, Solé M, Baldo D, Nunes I, Cajade R, Torres A, Grant T, Jungfer KH, Silva HR, Haddad CFB, Faivovich J (2021) The phylogeny of the Casque- headed Treefrogs (Hylidae: Hylinae: Lophyohylini). Cladistics 37(1): 36–72. https://doi.org/10.1111/cla.12409

Boettger O (1885) Liste von Reptilien und Batrachiern aus Paraguay. Zeitschrift für Naturwissenschaften 58: 213–248.

Bokermann WCA (1963) Nova espécie de *Hyla* da Bahia, Brasil. Atas da Sociedade de Biologia do Rio de Janeiro 7: 6–8.

Bokermann WCA (1966c) Notas sôbre três espécies de *Physalaemus* de Maracás, Bahia (Amphibia, Leptodactylidae). Revista Brasileira de Biologia 26(3): 253–259.

Bokermann WCA (1966a) O gênero *Phyllodytes* Wagler, 1830 (Anura, Hylidae). Rio de Janeiro. Anais da Academia Brasileira de Ciências 38(2): 335–344.

Bokermann WCA (1966b) Una nueva especie de *Trachycephalus* de Bahia, Brasil (Amphibia, Hylidae). Neotrópica 12(39): 124–210.

Bokermann WCA (1968) Three new *Hyla* from the Plateau of Maracás, central Bahia, Brazil. Journal of Herpetology 1(1/4): 25–31. https://doi.org/10.2307/1563259

Bokermann WCA (1973) Duas novas espécies de *Sphaenorhynchus* da Bahia (Anura, Hylidae). Revista Brasileira de Biologia 33: 589–594.

Bokermann WCA (1975) Três espécies novas de *Eleutherodactylus* do sudeste da Bahia, Brasil (Anura, Leptodactylidae). Revista Brasileira de Biologia 34(1): 11–18.

Borges-Nojosa DM, Cascon P (2005) Herpetofauna da área Reserva da Serra das Almas, Ceará. In: Araújo FS, Rodal MJN, Barbosa MRV (Org) Análise das Variações da Biodiversidade do Bioma Caatinga: suporte a estratégias regionais de conservação. Brasília, Ministério do Meio Ambiente, 243–258.

Borges-Nojosa DM, Santos EM (2005) Herpetofauna da área de Betânia e Floresta, Pernambuco. In: Araújo FS, Rodal MJN, Barbosa MRV (Org) Análise das Variações da

Biodiversidade do Bioma Caatinga: suporte a estratégias regionais de conservação. Brasília, Ministério do Meio Ambiente, 275–289.

Boulenger GA (1882) Catalogue of the Batrachia Salientia s. Ecaudata in the Collection of the British Museum. Second Edition. Taylor and Francis, London, 578 pp.

Braga HSN, Vieira MVSA, Silva TAF, Protázio AS, Protázio AS (2024) Acoustic partitioning explains the coexistence between two *Physalaemus* species (Anura, Leptodactylidae) in the Atlantic Forest in Eastern Bahia State, Brazil. Anais da Academia Brasileira de Ciências 95(1): e20211348. https://doi.org/10.1590/0001-3765202320211348

Brandão RA, Leão PF, Gedraite L (2020) Anfíbios da Trijunção dos estados da Bahia, Goiás e Minas Gerais e do Parque Nacional Grande Sertão Veredas. In: Brandão RA, Françoso RD, Machado TH, Santos NJ (Org) História Natural do Sertão da Trijunção do Nordeste, Centro–Oeste e Sudeste do Brasil. São Paulo, PerSe 1ª ed.: 88–127.

Brasileiro CA, Lucas EM, Oyamaguchi HM, Thomé MTC, Dixo M (2008) Anurans, Northern Tocantins River Basin, states of Tocantins and Maranhão, Brazil. Check List 4(2): 185–197. https://doi.org/10.15560/4.2.185

Burmeister H (1861) Reise durch die La Plata-Staaten mit besonderer Rücksicht auf die physische Beschaffenheit und den Culturzustand der Argentinischen Republik. Ausgeführt in den Jahren 1857, 1858, 1859 und 1860. Vol. 2. H. W. Schmidt, Halle, 538 pp.

Camardelli M, Napoli MF (2012) Amphibian Conservation in the Caatinga Biome and Semiarid Region of Brazil. Herpetologica 68(1): 31–47. https://doi.org/10.1655/HERPETOLOGICA-D-10-00033.1

Camurugi F, Lima TM, Mercês EA, Juncá FA (2010) Anuros da Reserva Ecológica da Michelin, Município de Igrapiúna, Estado da Bahia, Brasil. Biota Neotropica 10(2): 305–312. https://doi.org/10.1590/S1676-06032010000200032

Canedo CB, Pimenta VS, Leite FSF, Caramaschi U (2010) New species of *Ischnocnema* (Anura: Brachycephalidae) from the state of Minas Gerais, southeastern Brazil, with comments on the *I. verrucosa* species series. Copeia 2010(4): 629–634. https://doi.org/10.1643/CH-09-159

Caramaschi U (2006) Redefinição do grupo de *Phyllomedusa hypochondrialis*, com redescrição de *P. megacephala* (Miranda-Ribeiro, 1926), revalidação de *P. azurea* Cope, 1862 e descrição de uma nova espécie (Amphibia, Anura, Hylidae). Arquivos do Museu Nacional. Museu Nacional 64: 159–179.

Caramaschi U (2012) A new species of beaked toad, *Rhinella* (Anura: Bufonidae), from the State of Bahia, Brazil. Zoologia. Sociedade Brasileira de Zoologia. Curitiba 29(4): 343–348. https://doi.org/10.1590/S1984-46702012000400007

Caramaschi U, Canedo C (2006) Reassessment of the taxonomic status of the genera *Ischnocnema* Reinhardt and Lütken, 1862 and *Oreobates* Jiménez-de-la-Espada, 1872 with notes on the synonymy of *Leiuperus verrucosus* Reinhardt and Lütken, 1862 (Anura: Leptodactylidae). Zootaxa 1116(1): 43–54. https://doi.org/10.11646/zootaxa.1116.1.3

Caramaschi U, Cruz CAG (1998) Notas taxonômicas sobre *Pseudis fusca* Garman e *P. bolbodactyla* A. Lutz, com a descrição de uma nova espécie correlata (Anura, Pseudidae). Revista Brasileira de Zoologia 15(4): 929–944. https://doi.org/10.1590/S0101-81751998000400011

Caramaschi U, Rodrigues MT (2003) A new large treefrog species, genus *Hyla* Laurenti, 1768, from southern Bahia, Brazil (Amphibia, Anura, Hylidae). Rio de Janeiro. Arquivos do Museu Nacional. Museu Nacional 61(4): 255–260.

Caramaschi U, Rodrigues MT (2007) Taxonomic status of the species of *Gastrotheca* Fitzinger, 1843 (Amphibia, Anura, Amphignathodontidae) of the Atlantic Rain Forest of Eastern Brazil, with description of a new species. Boletim do Museu Nacional, Nova Serie. Zoologia 525: 1–19.

Caramaschi U, Orrico VGD, Faivovich J, Dias IR, Solé M (2013) A new species of *Allophryne* (Anura: Allophrynidae) from the Atlantic Rain Forest Biome of eastern Brazil. Herpetologica 69(4): 480–491. https://doi.org/10.1655/HERPETOLOGICA-D-13-00029

Carilo-Filho LM, Carvalho BT, Azevedo BKA, Gutiérrez-Pesquera LM, Mira-Mendes CV, Solé M, Orrico VG (2021) Natural history predicts patterns of thermal vulnerability in amphibians from the Atlantic Rainforest of Brazil. Ecology and Evolution 11(23): 16462–16472. https://doi.org/10.1002/ece3.7961

Carnaval AC, Moritz C (2008) Historical climate modelling predicts patterns of current biodiversity in the Brazilian Atlantic forest. Journal of Biogeography 35(7): 1187–1201. https://doi.org/10.1111/j.1365-2699.2007.01870.x

Carnaval AC, Hickerson MJ, Haddad CFB, Rodrigues MT, Moritz C (2009) Stability Predicts Genetic Diversity in the Brazilian Atlantic Forest Hotspot. Science 323(5915): 785–789. https://doi.org/10.1126/science.1166955

Carneiro MCL, Magalhães PS, Juncá FA (2004) Descrição do girino e vocalização de *Scinax pachycrus* (Miranda-Ribeiro, 1937) (Amphibia, Anura, Hylidae). Rio de Janeiro. Arquivos do Museu Nacional. Museu Nacional 62(3): 241–246.

Cassini CS, Orrico VGD, Dias IR, Solé M, Haddad CFB (2013) Phenotypic variation of *Leptodactylus cupreus* Caramaschi, São-Pedro and Feio, 2008 (Anura, Leptodactylidae). Zootaxa 3616(1): 073–084. https://doi.org/10.11646/zootaxa.3616.1.6

Cetra M, Sarmento-Soares LM, Martins-Pinheiro RF (2010) Peixes de riachos e novas Unidades de Conservação no sul da Bahia. Pan-American Journal of Aquatic Sciences 5(1): 11–21.

Cochran DM (1948) A new subspecies of tree frog from Pernambuco, Brazil. Journal of the Washington Academy of Sciences 38: 316–318.

Colwell RK, Coddington JA (1994) Estimating terrestrial biodiversity through extrapolation. Philosophical Transactions of the Royal Society of London. Series B, Biological Sciences 345(1311): 101–118. https://doi.org/10.1098/rstb.1994.0091

Cope ED (1862) Catalogues of the reptiles obtained during the explorations of the Parana, Paraguay, Vermejo and Uruguay Rivers, by Capt. Thos. J. Page, U.S.N.; and of those procured by Lieut. N. Michler, U.S. Top. Eng., Commander of the expedition conducting the survey of the Atrato River. Proceedings. Academy of Natural Sciences of Philadelphia 14: 346–35.

Crump ML, Scott Jr NJ (1994) Visual Encounter Surveys. In: Heyer WR, Donnelly MA, McDiarmid RW, Hayek LC, Foster MS (Eds) Measuring and monitoring biological diversity: standard methods for amphibians. Smithsonian Institution Press, Washington USA, 84–92.

Cruz CAG, Peixoto OL (1987) Espécies verdes de *Hyla*: o complexo "*albofrenata*" (Amphibia, Anura, Hylidae). Arquivos de Universidade Federal Rural do Rio de Janeiro 8: 59–70.

Cruz CAG, Pimenta BVS (2004) A new species of *Physalaemus* Fitzinger, 1826 from Southern Bahia state, Brazil (Anura, Leptodactylidae). Journal of Herpetology 38(4): 480–486. https://doi.org/10.1670/214-02A

Cruz CAG, Feio RN, Cardoso MCS (2007) Description of a new species of *Phyllodytes* Wagler, 1830 (Anura, Hylidae) from the Atlantic Rain Forest of the states of Minas Gerais and Bahia, Brazil. Arquivos do Museu Nacional. Museu Nacional 64(4): 321–324.

Da-Silva FR, Almeida-Neto M, Prado VHM, Haddad CFB, Rossa-Feres DC (2012) Humidity levels drive reproductive modes and phylogenetic diversity of amphibians in the Brazilian Atlantic Forest. Journal of Biogeography 39(9): 1720–1732. https://doi.org/10.1111/j.1365-2699.2012.02726.x

De-Sá RO, Grant T, Camargo A, Heyer WR, Ponssa ML, Stanley EL (2014) Systematics of the Neotropical genus *Leptodactylus* Fitzinger, 1826 (Anura: Leptodactylidae): Phylogeny, the relevance of non-molecular evidence, and species accounts. South American Journal of Herpetology 9(s1): 1–128. https://doi.org/10.2994/SAJH-D-13-00022.1

Dias IR, Vilaça TRA, Silva JRS, Barbosa RS, Solé M (2010) Amphibia, Anura, Hylidae, *Trachycephalus nigromaculatus* Tschudi, 1838: Distribution extension. Check List 6(3): 412–413. https://doi.org/10.15560/6.3.412

Dias IR, Medeiros TT, Solé M, Pimenta BVS (2011) Amphibia, Anura, Hylidae, *Bokermannohyla lucianae* (Napoli and Pimenta 2003): Distribution extension and geographic distribution map. Check List 7(2): 108–109. https://doi.org/10.15560/7.2.108

Dias IR, Lourenço-de-Moraes R, Solé M (2012) Description of the advertisement call and morphometry of *Haddadus binotatus* (Spix, 1824) from a population from southern Bahia, Brazil. North-Western Journal of Zoology 8(1): 107–111.

Dias IR, Mira-Mendes CV, Solé M (2014a) Rapid inventory of herpetofauna at the APA (Environmental Protection Area) of the Lagoa Encantada and Rio Almada, Southern Bahia, Brazil. Herpetology Notes 7: 627–637. http://biotaxa.org/hn/article/view/8557/10467

Dias IR, Medeiros TT, Vila Nova MF, Solé M (2014b) Amphibians of Serra Bonita, southern Bahia: A new hotpoint within Brazil's Atlantic Forest hotspot. ZooKeys 449: 105–130. https://doi.org/10.3897/zookeys.449.7494

Dias IR, Haddad CFB, Argôlo AJS, Orrico VGD (2017a) The 100th: An appealing new species of *Dendropsophus* (Amphibia: Anura: Hylidae) from northeastern Brazil. PLoS ONE 12(3): 1–20. https://doi.org/10.1371/journal.pone.0171678

Dias IR, Mira-Mendes CV, Souza-Costa CA, Juncá FA, Solé M (2017b) The advertisement call and comments on the distribution of *Eleutherodactylus bilineatus* Bokermann, 1975, an endemic frog of Bahia State, Brazil (Amphibia, Anura). ZooKeys 677(1): 151–159. https://doi.org/10.3897/zookeys.677.12309

Dias IR, Novaes-e-Fagundes G, Neto AM, Zina J, Garcia C, Recoder RS, Dal Vechio F, Rodrigues MT, Solé M (2020) A new large canopy-dwelling species of *Phyllodytes* Wagler, 1930 (Anura, Hylidae) from the Atlantic Forest of the state of Bahia, northeastern Brazil. PeerJ 8(e8642): 1–27. https://doi.org/10.7717/peerj.8642

Droege S, Cyr A, Larivée J (1998) Checklists: An under-used tool for the inventory and monitoring of plants and animals. Conservation Biology 12(5): 1134–1138. https://doi.org/10.1046/j.1523-1739.1998.96402.x

Duarte H, Tejedo M, Katzenberger M, Marangoni F, Baldo D, Beltrán JF, Martí DA, Richter-Boix A, Gonzalez-Voyer A (2012) Can amphibians take the heat? Vulnerability to climate warming in subtropical and temperate larval amphibian communities. Global Change Biology 18(2): 412–421. https://doi.org/10.1111/j.1365-2486.2011.02518.x

Dubeux MJM, Nascimento FAC, Gonçalves U, Mott T (2021) Identification key for anuran amphibians in a protected area in the northeastern Atlantic Forest. Papéis Avulsos de Zoologia 61[e20216176]: 1–10. https://doi.org/10.11606/1807-0205/2021.61.76

Duellman WE (2015) Marsupial Frogs. *Gastrotheca* & Allied Genera. Johns Hopkins University Press, Baltimore, 432 pp. https://doi.org/10.1353/book.40894

Feio RN, Caramaschi U (1995) Aspectos Zoogeográficos dos Anfíbios do Médio Rio Jequitinhonha, Nordeste de Minas Gerais, Brasil. Revista Ceres 42(239): 53–61. http://www.ceres.ufv.br/ojs/index.php/ceres/article/view/2238/272

Feio RN, Napoli MF, Caramaschi U (2006a) Considerações taxonômicas sobre *Thoropa miliaris* (Spix, 1824), com revalidação e redescrição de *Thoropa taophora* (Miranda-Ribeiro, 1923) (Amphibia, Anura, Leptodactylidae). Arquivos do Museu Nacional. Museu Nacional 64(1): 41–60.

Feio RN, Nascimento LB, Cruz CAG, Ferreira PL, Pantoja DL (2006b) Anfíbios das áreas prioritárias dos rios Jequitinhonha e Mucuri. In: Pinto LPS, Bedê L (Org) Biodiversidade e Conservação nos Vales dos Rios Jequitinhonha e Mucuri. Brasília, Ministério do Meio Ambiente 1: 94–119.

Fonte LFM, Mayer M, Lötters S (2019) Long-distance dispersal in amphibians. Frontiers of Biogeography 11(4): 1–14. https://doi.org/10.21425/F5FBG44577

Freitas MA, Abegg AD, Dias IR, Moraes EPF (2018) Herpetofauna from Serra da Jibóia, an Atlantic Rainforest remnant in the state of Bahia, northeastern Brazil. Herpetology Notes 11(1): 59–72. https://www.biotaxa.org/hn/article/view/32254/39365

Freitas MA, Silva TFS, Fonseca PM, Hamdan B, Filadelfo T, Abegg AD (2019) Herpetofauna of Serra do Timbó, an Atlantic Forest remnant in Bahia State, northeastern Brazil. Herpetology Notes 12: 245–260. https://www.biotaxa.org/hn/article/view/32254/39365

Frost DR (2023) Amphibian Species of the World: An Online Reference. Version 6.2. Electronic Database. https://amphibiansoftheworld.amnh.org/

Garda AA, Santana DJ, São-Pedro VA (2010) Taxonomic characterization of paradoxical frogs (Anura, Hylidae, Pseudae): geographic distribution, external morphology, and morphometry. Zootaxa 2666(1): 1–28. https://doi.org/10.11646/zootaxa.2666.1.1

Garda AA, Costa TB, Santos-Silva CR, Mesquita DO, Faria RG, Conceição BM, Silva IRS, Ferreira AS, Rocha SM, Palmeira CNS, Rodrigues R, Ferrari SF, Torquato S (2013) Herpetofauna of protected areas in the Caatinga I: Raso da Catarina Ecological Station (Bahia, Brazil). Check List 9(2): 405–414. https://doi.org/10.15560/9.2.405

Garman S (1883) A species of *Pseudis* from the Rio Arassuahy, Brazil. Science Observer. Journal of Science 4: 47.

Gomes MR, Peixoto OL (1991) Larvas de *Hyla* do grupo *leucophyllata* com a descrição da de *H. elegans*, 1824 e notas sobre a variação do padrão de colorido do adulto nesta espécie (Anura, Hylidae). Revista Brasileira de Biologia 51(1): 257–262.

Gondim-Silva FAT, Andrade ARS, Abreu RO, Nascimento JS, Corrêa GP, Menezes L, Trevisan CC, Camargo SS, Napoli MF (2016) Composition and diversity of anurans in the Restinga of the Conde municipality, Northern coast of the state of Bahia, Northeastern Brazil. Biota Neotropica 16(3): 1–16. https://doi.org/10.1590/1676-0611-BN-2016-0157

Gotelli NJ, Colwell RK (2001) Quantifying biodiversity: Procedures and pitfalls in the measurement and comparison of species richness. Ecology Letters 4(4): 379–391. https://doi.org/10.1046/j.1461-0248.2001.00230.x

Gutiérrez-Pesquera LM, Tejedo M, Olalla-Tárraga MÁ, Duarte H, Nicieza A, Solé M (2016) Testing the climate variability hypothesis in thermal tolerance limits of tropical and temperate tadpoles. Journal of Biogeography 43(6): 1166–1178. https://doi.org/10.1111/jbi.12700

Haddad CFB (1998) Biodiversidade dos Anfíbios no Estado de São Paulo. In: Joly CA, Bicudo CEM (Org) Biodiversidade do Estado de São Paulo, Brasil: síntese do conhecimento ao final do século XX, 6: vertebrados. São Paulo, Fapesp: 15–26.

Haddad CFB, Toledo LF, Prado CPA, Loebmann D, Gasparini JL, Sazima I (2013) Guia de Anfíbios da Mata Atlântica: diversidade e biologia. Anolisbooks, São Paulo, 544 pp.

Hammer Ø, Harper DAT, Ryan PD (2001) Past: Paleontological Statistics Software Package for Education and Data Analysis. Palaeontologia Electronica 4(1) [art. 4]: 1–9. [178kb]. http://palaeo-electronica.org/2001_1/past/issue1_01.htm

Hepp F, Pombal J (2020) Review of bioacoustical traits in the genus *Physalaemus* Fitzinger, 1826 (Anura: Leptodactylidae: Leiuperinae). Zootaxa 4725(1): 1–106. https://doi.org/10.11646/zootaxa.4725.1.1

Heyer WR (1978) Systematics of the *fuscus* group of the frog genus *Leptodactylus* (Amphibia, Leptodactylidae). Natural History Museum of Los Angeles County Science Bulletin 29: 1–85. https://doi.org/10.5479/si.00810282.301

Heyer WR, Rand AS, Cruz CAG, Peixoto OL, Nelson CE (1990) Frogs of Boracéia. Arquivos de Zoologia 31(4): 231–410. https://doi.org/10.11606/issn.2176-7793.v31i4p231-410

Heyer WR, Donnelly MA, McDiarmid RW, Hayek LC, Foster MS (1994) Measuring and monitoring biological diversity: standard methods for amphibians. Smithsonian Institution Press Washington.

Hoffmann M, Hilton-Taylor C, Angulo A, Böhm M, Brooks TM, Butchart SH, Carpenter KE, Chanson J, Collen B, Cox NA, Darwall WR, Dulvy NK, Harrison LR, Katariya V, Pollock CM, Quader S, Richman NI, Rodrigues ASL, Tognelli MF, Vié J-C, Aguiar JM, Allen DJ, Allen GR, Amori G, Ananjeva NB, Andreone F, Andrew P, Ortiz ALA, Baillie JEM, Baldi R, Bell BD, Biju SD, Bird JP, Black-Decima P, Blanc JJ, Bolaños F, Bolivar-G W, Burfield IJ, Burton JA, Capper DR, Castro F, Catullo G, Cavanagh RD, Channing A, Chao NL, Chenery AM, Chiozza F, Clausnitzer V, Collar NJ, Collett LC, Collette BB, Fernandez CFC, Craig MT, Crosby MJ, Cumberlidge N, Cuttelod A, Derocher AE, Diesmos AC, Donaldson JS, Duckworth JW, Dutson G, Dutta SK, Emslie RH, Farjon A, Fowler S, Freyhof J, Garshelis DL, Gerlach J, Gower DJ, Grant TD, Hammerson GA, Harris RB, Heaney LR, Hedges SB, Hero J-M, Hughes B, Hussain SA, Icochea M J, Inger RF, Ishii N, Iskandar DT, Jenkins RKB, Kaneko Y, Kottelat M, Kovacs KM, Kuzmin SL, La Marca E, Lamoreux JF, Lau MWN, Lavilla EO, Leus K, Lewison RL, Lichtenstein G, Livingstone SR, Lukoschek V, Mallon DP, McGowan PJK, McIvor A, Moehlman PD, Molur S, Alonso AM, Musick JA, Nowell K, Nussbaum RA, Olech W, Orlov NL, Papenfuss TJ, Parra-Olea G, Perrin WF, Polidoro BA, Pourkazemi M, Racey PA, Ragle JS, Ram M, Rathbun G, Reynolds RP, Rhodin AGJ, Richards SJ, Rodríguez LO, Ron SR, Rondinini C, Rylands AB, Sadovy de Mitcheson Y, Sanciangco JC, Sanders KL, Santos-Barrera G, Schipper J, Self-Sullivan C, Shi Y, Shoemaker A, Short FT, Sillero-Zubiri C, Silvano DL, Smith KG, Smith AT, Snoeks J, Stattersfield AJ, Symes AJ, Taber AB, Talukdar BK, Temple HJ, Timmins R, Tobias JA, Tsytsulina K, Tweddle D, Ubeda C, Valenti SV, Paul van Dijk P, Veiga LM, Veloso A, Wege DC, Wilkinson M, Williamson EA, Xie F, Young BE, Akçakaya HR, Bennun L, Blackburn TM, Boitani L, Dublin HT, da Fonseca GAB, Gascon C, Lacher Jr TE, Mace GM, Mainka SA, McNeely JA, Mittermeier RA, Reid GMG, Rodriguez JP, Rosenberg AA, Samways MJ, Smart J, Stein BA, Stuart SN (2010) The impact of conservation on the status of the world's vertebrates. Science 330(6010): 1503–1509. https://doi.org/10.1126/science.1194442

IBGE [Instituto Brasileiro de Geografia e Estatística] (1997) Diagnóstico Ambiental da Bacia do Rio Jequitinhonha: diretrizes gerais para a ordenação territorial. Salvador, Diretoria de Geociências, 1ª Divisão de Geociências do Nordeste-DIGEO 1/NE.1, 64 pp.

ICMBio [Instituto Chico Mendes de Conservação da Biodiversidade] (2003) Decretos MMA s/nº de 05 de Junho de 2003. http://www.icmbio.gov.br/portal/rebio-da-mata escura?highlight=WyJtYXRhIiwiZXNjdXJhIiwibWF0YSBlc2N1cmEiXQ [accessed on 25 March 2018]

ICMBio [Instituto Chico Mendes de Conservação da Biodiversidade] (2010) Decreto MMA s/nº de 11 de Junho de 2010. http://www.icmbio.gov.br/portal/parna-do-alto-cariri?highlight=WyJjYXJpcmkiXQ [accessed on 25 March 2018]

ICMBio [Instituto Chico Mendes de Conservação da Biodiversidade] (2016) Portaria MMA nº 110 de 22 de Dezembro de 2016. http://sistemas.icmbio.gov.br/site_media/portarias/2017/01/19/Portaria_RPPN_Mata_do Passarinho_01.pdf [accessed on 25 March 2018]

IUCN (2024) The IUCN Red List of Threatened Species. Version 2024-1. http://www.iucnredlist.org [accessed on 02 July 2024]

Izecksohn E (1976) O status sistemático de *Phryniscus proboscideus* Boulenger (Amphibia, Anura, Bufonidae). Revista Brasileira de Biologia 36(2): 341–34.

Izecksohn E, Peixoto OL (1980) Sobre a utilização do nome *Stombus precrenulatus* Miranda-Ribeiro, 1937 e a validez da espécie (Amphibia, Anura, Leptodactylidae). Revista Brasileira de Biologia 40(3): 605–609.

Jim J, Spirandeli-Cruz EF (1973) Uma nova espécie de *Leptodactylus* do Estado da Bahia, Brasil (Amphibia, Anura). Revista Brasileira de Biologia 39(3): 707–710.

Juncá FA (2005) Anfíbios e Répteis. In: Juncá FA, Funch L, Rocha W (Org) Biodiversidade e Conservação da Chapada Diamantina. Série Biodiversidade. Brasília, Ministério do Meio Ambiente 13(1): 339–376.

Juncá FA (2006) Diversidade e uso de hábitat por anfíbios anuros em duas localidades de Mata Atlântica, no norte do Estado da Bahia. Biota Neotropica 6(2): 1–8. https://doi.org/10.1590/S1676-06032006000200018

Juncá FA, Pimenta B (2004) *Ischnocnema bilineta*. In: IUCN Red List of Threatened Species (International Union for Conservation of Nature IUCN). https://doi.org/10.2305/IUCN.UK.2004.RLTS.T56462A11468784.en [accessed on 10 August 2022]

Köppen WP (1936) Das geographische System der Klimate. In: Köppen WG, Geiger RM (Eds) Handbuch der Klimatologie Band I, Teil C. Gebrüder Borntraeger, Berlin, 44 pp.

Lantyer-Silva ASF, Lourenço-De-Moraes R, Siqueira-Jr S, Solé M (2011) Amphibia, Anura, Bufonidae, *Rhinella boulengeri* Chaparro, Pramuk, Gluesenkamp and Frost, 2007: Distribution extension, state of Bahia, Brazil. Check List 7(6): 825–826. https://doi.org/10.15560/7.6.825

Lantyer-Silva ASF, Siqueira-Jr S, Zina J (2013) Checklist of amphibians in a transitional area between the Caatinga and the Atlantic Forest, central-Southern Bahia, Brazil. Check List 9(4): 725–732. https://doi.org/10.15560/9.4.725

Lavilla EO, Brusquetti F (2018) On the identity of *Bufo diptychus* Cope, 1862 (Anura: Bufonidae). Zootaxa 4442(1): 161–170. https://doi.org/10.11646/zootaxa.4442.1.9

Lima LR, Bruschi DP, Nascimento FAC, Araújo PVS, Costa LP, Thomé MTC, Garda AA, Zattera ML, Mott T (2020) Below the waterline: Cryptic diversity of aquatic pipid frogs (*Pipa carvalhoi*) unveiled through an integrative taxonomy approach. Systematics and Biodiversity 18(8): 1–13. https://doi.org/10.1080/14772000.2020.1795742

Linares AM, Mello HES (2011) *Physalaemus cicada* Bokermann, 1966 (Anura: Leiuperidae): Distribution extension with new South limit and geographic distribution map. Check List 7(6): 859–861. https://doi.org/10.15560/7.6.859

Loebmann D, Haddad CFB (2010) Amphibians and reptiles from a highly diverse area of the Caatinga domain: Composition and conservation implications. Biota Neotropica 10(3): 227–256. https://doi.org/10.1590/S1676-06032010000300026

Loebmann D, Zina J, Araújo OGS, Toledo LF, Haddad CFB (2008) Acoustic Repertory of *Hypsiboas exastis* (Caramaschi and Rodrigues, 2003) (Amphibia, Hylidae). South

American Journal of Herpetology 3(2): 96–100. https://doi.org/10.2994/1808-9798(2008)3[96:AROHEC]2.0.CO;2

Lourenço-De-Moraes R, Dias IR, Mira-Mendes CV, de Oliveira RM, Barth A, Ruas DS, Vences M, Solé M, Bastos RP (2018) Diversity of miniaturized frogs of the genus *Adelophryne* (Anura: Eleutherodactylidae): A new species from the Atlantic Forest of northeast Brazil. PLoS ONE 13(9): e0201781. https://doi.org/10.1371/journal.pone.0201781

Luedtke JA, Chanson J, Neam K, Hobin L, Maciel AO, Catenazzi A, Borzée A, Hamidy A, Aowphol A, Jean A, Sosa-Bartuano Á, Fong G A, de Silva A, Fouquet A, Angulo A, Kidov AA, Muñoz Saravia A, Diesmos AC, Tominaga A, Shrestha B, Gratwicke B, Tjaturadi B, Martínez Rivera CC, Vásquez Almazán CR, Señaris C, Chandramouli SR, Strüssmann C, Cortez Fernández CF, Azat C, Hoskin CJ, Hilton-Taylor C, Whyte DL, Gower DJ, Olson DH, Cisneros-Heredia DF, Santana DJ, Nagombi E, Najafi-Majd E, Quah ESH, Bolaños F, Xie F, Brusquetti F, Álvarez FS, Andreone F, Glaw F, Castañeda FE, Kraus F, Parra-Olea G, Chaves G, Medina-Rangel GF, González-Durán G, Ortega-Andrade HM, Machado IF, Das I, Dias IR, Urbina-Cardona JN, Crnobrnja-Isailović J, Yang J-H, Jianping J, Wangyal JT, Rowley JJL, Measey J, Vasudevan K, Chan KO, Gururaja KV, Ovaska K, Warr LC, Canseco-Márquez L, Toledo LF, Díaz LM, Khan MMH, Meegaskumbura M, Acevedo ME, Napoli MF, Ponce MA, Vaira M, Lampo M, Yánez-Muñoz MH, Scherz MD, Rödel M-O, Matsui M, Fildor M, Kusrini MD, Ahmed MF, Rais M, Kouamé NGG, García N, Gonwouo NL, Burrowes PA, Imbun PY, Wagner P, Kok PJR, Joglar RL, Auguste RJ, Brandão RA, Ibáñez R, von May R, Hedges SB, Biju SD, Ganesh SR, Wren S, Das S, Flechas SV, Ashpole SL, Robleto-Hernández SJ, Loader SP, Incháustegui SJ, Garg S, Phimmachak S, Richards SJ, Slimani T, Osborne-Naikatini T, Abreu-Jardim TPF, Condez TH, De Carvalho TR, Cutajar TP, Pierson TW, Nguyen TQ, Kaya U, Yuan Z, Long B, Langhammer P, Stuart SN (2023) Ongoing declines for the world's amphibians in the face of emerging threats. Nature 622(7982): 308–314. https://doi.org/10.1038/s41586-023-06578-4

Lutz A (1925) Batraciens du Brésil. Comptes Rendus et Mémoires Hebdomadaires des Séances de la Société de Biologie et des ses Filiales. Paris 93(2): 137–139.

Lutz A (1926) Observações sobre batrachios brasileiros/Observations on brazilian batrachians. Memorias do Instituto Oswaldo Cruz 19(2): 139–174. https://doi.org/10.1590/S0074-02761926000200001

Lynch JD (1972) Generic partitioning of the South American leptodactyloid frog genus *Eupsophus* Fitzinger, 1843 (*sensu lato*). Bulletin of the Southern California Academy of Sciences 71: 2–11.

Maciel AO, Hoogmoed MS (2011) Taxonomy and distribution of caecilian amphibians (Gymnophiona) of Brazilian Amazonia, with a key to their identification. Zootaxa 2984(1): 1–53. https://doi.org/10.11646/zootaxa.2984.1.1

Magalhães FM, Dantas AKBP, Brito MRM, Medeiros PHS, Oliveira AF, Pereira TCSO, Queiroz MHC, Santana DJ, Silva WP, Garda AA (2013) Anurans from an Atlantic Forest-Caatinga ecotone in Rio Grande do Norte State, Brazil. Herpetology Notes 6: 1–10.

Magalhães FM, Laranjeiras DO, Costa TB, Juncá FA, Mesquita DO, Rohr DL, Silva WP, Vieira GHC, Garda AA (2015) Herpetofauna of protected areas in the Caatinga IV: Chapada Diamantina National Park, Bahia, Brazil. Herpetology Notes 8: 243–261. http://www.biotaxa.org/hn/article/view/9184/13441

Magalhães FM, Lyra ML, Carvalho TR, Baldo D, Brusquetti F, Burella P, Colli GR, Gehara MC, Giaretta AA, Haddad CFB, Langone JA, López JA, Napoli MF, Santana DJ, De-Sá RO, Garda AA (2020) Taxonomic review of South American butter frogs: phylogeny, biogeographic patterns, and species delimitation in the *Leptodactylus latrans* species group (Anura: Leptodactylidae). Herpetological Monograph 34(1): 131–177. https://doi.org/10.1655/0733-1347-31.4.131

Magalhães FM, Camurugi F, Lyra ML, Baldo D, Gehara MC, Haddad CFB, Garda AA (2022) Ecological divergence and synchronous Pleistocene diversification in the widespread South American butter frog complex. Molecular Phylogenetics and Evolution 169(2): 107398. https://doi.org/10.1016/j.ympev.2022.107398

Magrini L, Carvalho-e-Silva SP, Béda AF, Giaretta AA (2011) Calls of five species of the *Scinax ruber* (Anura: Hylidae) clade from Brazil with comments on their taxonomy. Zootaxa 3066(1): 37–51. https://doi.org/10.11646/zootaxa.3066.1.3

Magurran AE (1988) Ecological Diversity and its Measurement. Springer, Dordrecht, 179 pp. https://doi.org/10.1007/978-94-015-7358-0

Martins MR, Haddad CFB (1988) Vocalizations and reproductive behaviour in the smith frog, *Hyla faber* Wied (Amphibia: Hylidae). Amphibia-Reptilia 9(1): 49–60. https://doi.org/10.1163/156853888X00206

Menezes L, Canedo C, Batalha-Filho H, Garda AA, Gehara MC, Napoli MF (2016) Multilocus phylogeography of the treefrog *Scinax Eurydice* (Anura, Hylidae) reveals a Plio-Pleistocene diversification in the Atlantic Forest. PLoS ONE 11(6): e0154626. https://doi.org/10.1371/journal.pone.0154626

Mikan JC (1822) Delectus Florae et Faunae Brasiliensis. Fasicule 2. Antonii Strauss, Vindobonae, 80 pp.

Miles L, Newton AC, DeFries RS, Ravilious C, May I, Blyth S, Kapos V, Gordon JE (2006) A global overview of the conservation status of tropical dry forests. Journal of Biogeography 33(3): 491–505. https://doi.org/10.1111/j.1365-2699.2005.01424.x

Mira-Mendes CB, Ruas DS, Oliveira RM, Castro IM, Dias IR, Baumgarten JE, Juncá FA, Solé M (2018) Amphibians of the Reserva Ecológica Michelin: A high diversity site in the lowland Atlantic Forest of southern Bahia, Brazil. ZooKeys 753: 1–21. https://doi.org/10.3897/zookeys.753.21438

Miranda-Ribeiro A (1926) Notas para servirem ao estudo dos Gymnobatrachios (Anura) brasileiros. Arquivos do Museu Nacional. Museu Nacional 27: 1–227.

Miranda-Ribeiro A (1937b) Espécies novas do gênero “*Stombus*” da série de apêndices oculares reduzidos. O Campo 8(88): 24.

Miranda-Ribeiro A (1937a) Sobre uma collecção de vertebrados do nordeste brasileiro. Primeira parte: Peixes e batrachios. O Campo 1937: 54–56.

Mori SA, Silva LAM (1980) O Herbário do Centro de Pesquisas do Cacau em Itabuna, Brasil. Comissão Executiva do Plano da Lavoura Cacaueira. Boletín Técnico 78: 1–31. https://doi.org/10.2307/2806174

Moura MRD, Santana DJ, Ferreira PL, Feio RN (2009) Amphibia, Anura, Leptodactylidae, *Leptodactylus viridis* Jim and Spirandeli-Cruz, 1979: Distribution extension, new state record, and geographic distribution map. Check List 5(4): 780–782. https://doi.org/10.15560/5.4.780

Myers N, Mittermeyer RA, Fonseca GAB, Kent J (2000) Biodiversity hotspots for conservation priorities. Nature 403(6772): 853–858. https://doi.org/10.1038/35002501

Narvaes P, Rodrigues MT (2009) Taxonomic revision of *Rhinella granulosa* species group (Amphibia, Anura, Bufonidae), with a description of a new species. São Paulo. Arquivos de Zoologia 40(1): 1–73. https://doi.org/10.11606/issn.2176-7793.v40i1p1-73

Nascimento LB, Caramaschi U, Cruz CAG (2005) Taxonomic review of the species group of the genus *Physalameus* Fitzinger, 1826 with revalidation of the genera *Engystomops* Jimenez-de-la-Espada, 1872 and *Eupemphix* Steindachner, 1836 (Amphibia, Anura, Leptodactylidae). Arquivos do Museu Nacional. Museu Nacional 63(2): 297–320.

Novaes-e-Fagundes G, Zina J (2016) Advertisement call of *Scinax camposseabrai* (Bokermann, 1968) (Anura: Hylidae), with comments on the call of three species of the *Scinax ruber* clade. Zootaxa 4084(2): 258–266. https://doi.org/10.11646/zootaxa.4084.2.5

Novaes-e-Fagundes G, Araujo-Vieira K, Entiauspe Neto OM, Roberto IJ, Orrico VGD, Solé M, Haddad CFB, Loebmann D (2021) A new species of *Scinax* Wagler (Hylidae: Scinaxini) from the tropical forests of northeastern Brazil. Zootaxa 4903(1): 001–041. https://doi.org/10.11646/zootaxa.4903.1.1

Nunes I, Santiago RS, Juncá FA (2007) Advertisment calls of four hylid frogs from the state of Bahia, northeastern Brazil (Amphibia, Anura, Hylidae). South American Journal of Herpetology 2(2): 89–96. https://doi.org/10.2994/1808-9798(2007)2[89:ACOFHF]2.0.CO;2

Oliveira RM, Ruas DS, Mira-Mendes CV, Solé M (2014) Advertisement call of *Rhinella crucifer* (Wied-Neuwied, 1821) (Anura: Bufonidae) from southern Bahia, Brazil. Zootaxa 3784(1): 97–98. https://doi.org/10.11646/zootaxa.3784.1.9

Orrico VGD, Carvalho-e-Silva AMPT, Carvalho-e-Silva SP (2006) Redescription of the advertisement call of *Aplastodiscus arildae* (Cruz & Peixoto) and description of the call of *Aplastodiscus weygoldti* (Cruz & Peixoto) with general notes about the genus in Southeastern Brazil (Anura, Hylidae). Revista Brasileira de Zoologia 23(4): 994–1001. https://doi.org/10.1590/S0101-81752006000400003

Orrico VGD, Nunes I, Mattedi C, Fouquet A, Lemos AW, Rivera-Correa M, Lyra ML, Loebmann D, Pimenta BVS, Caramaschi U, Rodrigues MT, Haddad CFB (2017) Integrative taxonomy supports the existence of two distinct species within *Hypsiboas crepitans* (Anura: Hylidae). Salamandra (Frankfurt) 53(1): 99–113.

Orrico VGD, Grant T, Faivovich J, Rivera-Correa M, Rada M, Lyra ML, Cassini CS, Valdujo PH, Schargel WE, Machado DJ, Wheeler WC, Barrio-Amorós CL, Loebmann D, Moravec J, Zina J, Solé M, Sturaro MJ, Peloso PLV, Suárez P, Haddad CFB (2021) The phylogeny of Dendropsophini (Anura: Hylidae: Hylinae). Cladistics 37(1): 73–105. https://doi.org/10.1111/cla.12429

Pedreira AJ (1999) Evolução sedimentar e tectônica da bacia metassedimentar do Rio Pardo: Uma síntese. Revista Brasileira de Geociencias 29(3): 339–344. https://doi.org/10.25249/0375-7536.199929339344

Pedrosa IMMC, Costa TB, Faria RG, França FGR, Laranjeiras DO, Oliveira TCSP, Palmeira CNS, Torquato S, Mott T, Vieira GHC, Garda AA (2014) Herpetofauna of protected areas in the Caatinga III: The Catimbau National Park, Pernambuco, Brazil. Biota Neotropica 14(4): 1–12. https://doi.org/10.1590/1676-06032014004614

Peixoto OL, Arzabe C (2004) *Scinax pachycrus*. The IUCN Red List of Threatened Species. https://doi.org/10.2305/IUCN.UK.2004.RLTS.T55984A11391526.en [accessed on 01 March 2016]

Pimenta BVS, Faivovich J, Pombal Jr JP (2007) On the identity of *Hyla strigilata* Spix, 1824 (Anura: Hylidae): redescription and neotype designation for a “ghost” taxon. Zootaxa 1441(1): 35–49. https://doi.org/10.11646/zootaxa.1441.1.3

Pirani RM, Tonini JFR, Thomaz AT, Napoli MF, Encarnação LC, Knowles LL, Werneck FP (2022) Deep genomic divergence and phenotypic admixture of the treefrog *Dendropsophus elegans* (Hylidae: Amphibia) coincide with riverine boundaries at the Brazilian Atlantic Forest. Frontiers in Ecology and Evolution 10(765977): 1–15. https://doi.org/10.3389/fevo.2022.765977

Protázio AS, Santos-Protázio A, Silva CRS, Ribeiro ES, Nogueira EMS, Moura GJB (2010) Anurofauna do Município de Paulo Afonso-BA, Bioma Caatinga, Nordeste do Brasil. Revista Nordestina de Zoologia 4(2): 31–38.

Protázio AS, Protázio AS, Silva LS, Conceição LC, Braga HSN, Santos UG, Ribeiro AC, Almeida AC, Gama V, Vieira MVSA, Silva TAF (2021) Amphibians and reptiles of the Atlantic Forest in Recôncavo Baiano, east Brazil: Cruz das Almas municipality. ZooKeys 1060: 125–153. https://doi.org/10.3897/zookeys.1060.62982

Reinhardt JT, Lütken CF (1862) Bidrag til Kundskab om Brasiliens Padder og Krybdyr. Förste Afdeling: Padderne og Öglerne. Videnskabelige Meddelelser fra Dansk Naturhistorisk Forening i Kjøbenhavn, Serie 2 3: 143–242.

Ribeiro MC, Metzger JP, Martensen AC, Ponzoni FJ, Hirota MM (2009) The Brazilian Atlantic Forest: How much is left, and how is the remaining forest distributed? Implications for conservation. Biological Conservation 142(6): 1141–1153. https://doi.org/10.1016/j.biocon.2009.02.021

Rodrigues MT (2003) Herpetofauna da Caatinga. In: Leal IR, Tabarelli M, Silva JMC (Eds) Ecologia e conservação da Caatinga. Editora Universitaria da UFPE, Recife, 181–236.

Rojas-Padilla O, Menezes VQ, Dias IR, Argôlo AJS, Solé M, Orrico VGD (2020) Amphibians and reptiles of Parque Nacional da Serra das Lontras: An importante center of endemism within the Atlantic Forest in southern Bahia, Brazil. ZooKeys 1002: 159–185. https://doi.org/10.3897/zookeys.1002.53988

Rossa-Feres DC, Garey MV, Caramaschi U, Napoli MF, Nomura F, Bispo AA, Brasileiro CA, Thomé MTC, Sawaya RJ, Conte CE, Cruz CAG, Nascimento LB, Gasparini JL, Almeida AP, Haddad CFB (2017) Anfíbios da Mata Atlântica: Lista de espécies, histórico dos estudos, biologia e conservação. In: Monteiro-Filho ELA, Conte CE (Eds) Revisões em Zoologia: Mata Atlântica. Editora UFPR, Curitiba, 237–314.

Santana DJ, Mesquita DO, Garda AA (2011) Advertisement call of *Dendropsophus oliveirai* (Anura, Hylidae). Zootaxa 2997(1): 67–68. https://doi.org/10.11646/zootaxa.2997.1.5

Santana DJ, Mângia S, Silveira-Filho RR, Barros LCS, Andrade I, Napoli MF, Juncá FA, Garda AA (2015) Anurans from the Middle Jaguaribe River Region, Ceará State, Northeastern Brazil. Biota Neotropica 15(3): 1–8. https://doi.org/10.1590/1676-06032015001715

Santos SPL, Santos EM (2011) Anurofauna da Reserva Particular do Patrimônio Natural Frei Caneca, Município de Jaqueira, Estado de Pernambuco, Brasil. In: Moura GJB, Santos EM, Oliveira MAB, Cabral MCC (Org) Herpetofauna de Pernambuco. Brasília, Ministério do Meio Ambiente: 187–198.

Santos L, Roseno RS, Solé M, Dias IR (2023) Another new species (and it's not over yet) of *Phyllodytes* Wagler, 1930 (Anura, Hylidae) from the Atlantic Forest of southern Bahia, northeastern Brazil. Zootaxa 5374(4): 519–532. https://doi.org/10.11646/zootaxa.5374.4.4

São Pedro VA, Medeiros PH, Garda AA (2011) The advertisement call of *Rhinella granulosa* (Anura, Bufonidae). Zootaxa 3092(1): 60–62. https://doi.org/10.11646/zootaxa.3092.1.4

Schneider JG (1799) Historia Amphibiorum Naturalis et Literarariae. Fasciculus Primus. Continens Ranas, Calamitas, Bufones, Salamandras et Hydros in Genera et Species Descriptos Notisque suis Distinctos. Friederici Frommann, Jenae, 264 pp. https://doi.org/10.5962/bhl.title.78757

Sichieri GRF, Cruz CAG, Pimenta BVS, Nunes I (2021) Advertisement call description of two *Proceratophrys* species (Anura: Odontophrynidae). Zootaxa 4975(2): 397–400. https://doi.org/10.11646/zootaxa.4975.2.10

Silva JF, Fariñas MR, Felfili JM, Klink CA (2006) Spatial heterogeneity, land use and conservation in the cerrado region of Brazil. Journal of Biogeography 33(3): 536–548. https://doi.org/10.1111/j.1365-2699.2005.01422.x

Silva CRS, Moura GJB, Andrade EVE, Nogueira EMS (2011) Aspectos Ecológicos da Anurofauna dos municípios de Jatobá-PE e Paulo Afonso-BA, Nordeste do Brasil. In: Moura GJB, Santos EM, Oliveira MAB, Cabral MCC (Org) Herpetofauna de Pernambuco. Brasília, Ministério do Meio Ambiente 1(1): 177–185.

Silva GR, Luna-Dias C, Hepp FSFS, Carvalho-e-Silva AMPT, Carvalho-e-Silva SP (2012) New record of *Aplastodiscus weygoldti* (Cruz & Peixoto, 1987) in the municipality of Mimoso do Sul, Espírito Santo State, southeastern Brazil (Anura, Hylidae). Herpetology Notes 5: 371–373.

Silva-Soares T, Ferreira RB, Ornellas IS, Zocca C, Caramaschi U, Cruz CAG (2021) A new species of *Ischnocnema* (Anura: Brachycephalidae) from the mountainous region of Atlantic Forest, southeastern Brazil, with a new phylogeny and diagnose for *Ischnocnema parva* series. Zootaxa 5082(3): 201–222. https://doi.org/10.11646/zootaxa.5082.3.1

Silvano DL, Pimenta BVS (2003) Diversidade de anfíbios na Mata Atlântica do Sul da Bahia. In: Prado PI, Landau EC, Moura RT, Pinto LPS, Fonseca GAB, Alger K (Eds) Corredor de Biodiversidade na Mata Atlântica do Sul da Bahia CD-ROM. IESB/CI/CABS/ UFMG/UNICAMP/ Ilhéus, Bahia, Brazil, 1–22.

Silvano DL, Segalla MV (2005) Conservação de anfíbios no Brasil. Megadiversidade 1(1): 79–86.

Sos Mata Atlântica [Fundação Sos Mata Atlântica], INPE [Instituto Nacional de Pesquisas Espaciais] (2018) Atlas dos remanescentes florestais da Mata Atlântica: período 2016–2017. Relatório Técnico, ArcPlan, São Paulo, 63 pp.

Spix JBv (1824) Animalia nova sive Species novae *Testudinum* et *Ranarum* quas in itinere per Brasiliam annis MDCCCXVII–MDCCCXX jussu et auspiciis Maximiliani Josephi I. Bavariae Regis. München, F. S. Hübschmann, ii, 53, 39 plates (numbered 1–17 and 1–22) pp.

Steffen GA (1815) De Ranis nonnullis Observationes Anatomicae quas Consensu Gratiosae Facultatis Medicae. Joannis Friderici Starckii, Berlin, 24 pp.

Stevaux MN (2002) A new species of *Bufo* Laurenti (Anura, Bufonidae) from northeastern Brazil. Revista Brasileira de Zoologia 19(suppl 1): 235–242. https://doi.org/10.1590/S0101-81752002000500018

Tabarelli M, Silva JMC (2003) Áreas e ações prioritárias para a conservação da Caatinga. In: Leal I, Tabarelli M, Silva JMC (Eds) Ecologia e Conservação da Caatinga. Editora Universitaria da UFPE, Recife, 777–796.

Toledo LF, Castanho LM, Haddad CFB (2005) Recognition and distribution of *Leptodactylus mystaceus* (Anura; Leptodactylidae) in the State of São Paulo, Southeastern Brazil. Biota Neotropica 5(1): 57–62. https://doi.org/10.1590/S1676-06032005000100006

Toti DS, Coyle FA, Miller JA (2000) A structured inventory of Appalachian grass bald and heath bald spider assemblages and a test of species richness estimator performance. The Journal of Arachnology 28(3): 329–345. https://doi.org/10.1636/0161-8202(2000)028[0329:ASIOAG]2.0.CO;2

Trevisan CC, Batalha-Filho H, Garda AA, Menezes L, Dias IR, Solé M, Canedo C, Juncá FA, Napoli MF (2020) Cryptic diversity and ancient diversification in the northern Atlantic Forest *Pristimantis* (Amphibia, Anura, Craugastoridae). Molecular Phylogenetics and Evolution 148(4): 106811. https://doi.org/10.1016/j.ympev.2020.106811

Valdujo PH, Recoder RS, Vasconcellos MM, Portella AS (2009) Amphibia, Anura, São Desidério, western Bahia uplands, northeastern Brazil. Check List 5(4): 903–911. https://doi.org/10.15560/5.4.903

Valdujo PH, Camacho A, Recoder RS, Teixeira M Junior, Ghellere JMB, Mott T, Nunes PMS, Nogueira CC, Rodrigues MT (2011) Anfíbios da Estação Ecológica Serra Geral do Tocantins, região do Jalapão, Estados do Tocantins e Bahia. Biota Neotropica 11(1): 251–261. https://doi.org/10.1590/S1676-06032011000100025

Vaz-Silva W, Maciel NM, Nomura F, Morais AR, Guerra Batista V, Santos DL, Andrade SP, Oliveira AAB, Brandão RA, Bastos RP (2020) Guia de identificação das espécies de anfíbios (Anura e Gymnophiona) do estado de Goiás e do Distrito Federal, Brasil Central. Sociedade Brasileira de Zoologia, Curitiba, 229 pp. https://doi.org/10.7476/9786587590011

Vieira WLS, Arzabe C, Santana GG (2007) Composição e distribuição espaço-temporal de anuros no Cariri Paraibano, Nordeste do Brasil. Oecologia Brasiliensis 11(3): 383–396. https://doi.org/10.4257/oeco.2007.1103.08

Vilaça TRA, Silva JES, Solé M (2006) Vocalization and territorial behaviour of *Phyllomedusa nordestina* Caramaschi, 2006 (Anura: Hylidae) from southern Bahia, Brazil. Journal of Natural History 45(29-30): 1823–1834. https://doi.org/10.1080/00222933.2011.561018

von Tschudi JJ (1838) Classification der Batrachier mit Berücksichtigung der fossilen Thiere dieser Abtheilung der Reptilien. Petitpierre, Neuchâtel, 99 pp. https://doi.org/10.5962/bhl.title.4883

Vörös J, Dias JR, Solé M (2017) A new species of *Phyllodytes* (Anura: Hylidae) from the Atlantic Rainforest of Southern Bahia, Brazil. Zootaxa 4337(4): 584–594. https://doi.org/10.11646/zootaxa.4337.4.9

Wells KD (2007) The ecology and behavior of amphibians. The University of Chicago Press Books, Chicago, 1400 pp.

Wied-Neuwied MAP (1821) Reise nach Brasilien in den Jahren 1815 bis 1817. Vol. 2. Henrich Ludwig Brönner, Frankfurt, 345 pp.

Wied-Neuwied MAP (1824) Abbildungen zur Naturgeschichte Brasiliens. Heft 8. Landes-Industrie-Comptoir, Weimar, 614 pp.

Willians PH (1996) Mapping variations in strength and breadth of biogeographic transition zones using species turnover. Proceedings. Biological Sciences 263(1370): 579–588. https://doi.org/10.1098/rspb.1996.0087

Young BE, Stuart SN, Chanson JS, Cox NA, Boucher TM (2004) Joyas que están desapareciendo: El estado de los anfibios en el Nuevo Mundo. NatureServe, Arlington, Virginia, USA, 53 pp.

Zappi DC, Filardi FLR, Leitman P, Souza VC, Walter BMT, Pirani JR, Morim MP, Queiroz LP, Cavalcanti TB, Mansano VF, Forzza RC (2015) Growing knowledge: An overview of Seed Plant diversity in Brazil. Rodriguésia 66(4): 1085–1113. https://doi.org/10.1590/2175-7860201566411

Zucchetti VM, Castroviejo-Fisher S (2024) Lost in time: unraveling the identity of *Vitreorana parvula* (Boulenger, 1895) (Anura: Centrolenidae). Zootaxa 5415(3): 351–391. https://doi.org/10.11646/zootaxa.5415.3.1

Zucchetti VM, Rojas-Padilla O, Dias IR, Solé M, Orrico VGD, Castroviejo-Fisher S (2023) An elusive giant: A new species of *Vitreorana* Guayasamin et al., 2009 (Anura: Centrolenidae) from the northern Atlantic Forest with an osteological description and comments on integumentary spicules. Zootaxa 5249(3): 301–334. https://doi.org/10.11646/zootaxa.5249.3.1

Appendix 1

List of vouchers deposited in the Museu de Zoologia da Universidade Estadual de Santa Cruz-MZUESC.

AMPHIBIANS

BRACHYCEPHALIDAE–*Ischnocnema verrucosa*: MZUESC 15874, 15875, 15885, 15886, 15895, 15898, 15899. *Ischnocnema* sp. (gr. *parva*): MZUESC 15896. BUFONIDAE–*Dendrophryniscus proboscideus*: MZUESC 14688, 15126, 15127, 15128, 15798, 15803, 15859, 16532. *Rhinella crucifer*: MZUESC 15031, 15148. *Rhinella granulosa*: MZUESC 15030, 15055, 15504, 15505, 15506, 15850. *Rhinella diptycha*: MZUESC 15503. CRAUGASTORIDAE–*Bahius bilineatus*: MZUESC 15095, 15096, 15097, 15794, 15809, 15838, 15842, 15855, 15856, 15860, 15882, 15883. *Haddadus binotatus*: MZUESC 15014, 15015, 15032, 15034, 15044, 15047, 15051, 15053, 15054, 15057, 15058, 15104, 15105, 15106, 15107, 15131, 15142, 15465, 15471, 15472, 15473, 15475, 15476, 15478, 15479, 15482, 15526, 15622, 15623, 15634, 15635, 15643, 15644, 15646, 15650, 15651, 15656, 15659, 15660, 15778, 15802. *Pristimantis vinhai*: MZUESC 15000, 15098–15103, 15109–15112, 15114, 15115, 15120, 15121, 15132, 15133, 15140, 15141, 15143, 15144, 15464, 15481, 15502, 15640, 15642, 15657, 15663, 15664, 15667, 15780, 15785, 15786, 15797, 15799–15801, 15806–15808, 15813–15815, 15837, 15840, 15841, 15843, 15853, 15854, 15857, 15858, 15861, 15879, 15897, 15889. *Pristimantis* sp. (gr. *ramagii*): MZUESC 15033, 15474, 15641, 15658, 15662, 15665, 15783, 15849, 15851, 15852, 16523. CENTROLENIDAE–*Vitreorana eurygnatha*: MZUESC 14691, 14698, 14699, 14700, 14701, 15810–15812. CYCLORAMPHIDAE–*Thoropa miliaris*: MZUESC 14674, 15130, 15477, 15782, 15789, 15845, 15846, 15872, 15873, 15880, 15881. ELEUTHERODACTYLIDAE–*Adelophryne* sp.8: MZUESC 15035, 15036, 15039, 15041, 15043, 15048, 15050, 15052, 15116, 15462, 15466, 15480, 15528–15531, 15625–15627, 15631, 15633, 15637–15639, 15647, 15652, 15661, 15796, 15830, 15834, 15835, 15839, 15862, 16522, 16530. *Adelophryne* sp.2: MZUESC 15024, 15037, 15038, 15040, 15042, 15045, 15046, 15049, 15090, 15091, 15094, 15113, 15118, 15119, 15123–15125, 15457–15460, 15467–15470, 15524, 15525, 15527, 15533, 15624, 15628, 15629, 15632, 15636, 15645, 15648, 15649, 15655, 15795, 15831, 15832, 15836. HYLIDAE–*Aplastodiscus weygoldti*: MZUESC 14690, 15787, 15788, 15844, 15887. *Boana crepitans*: MZUESC 14673, 14675, 14998, 14999, 15002, 15145, 15486. *Boana exastis*: MZUESC 15108. *Boana faber*: MZUESC 14676, 15066, 15068, 15147, 15666, 15884. *Dendropsophus branneri*: MZUESC 14683, 14684, 15022, 15023, 15509, 15510, 15512, 15818, 15824. *Dendropsophus elegans*: MZUESC 14678, 14679, 15018, 15019, 15020, 15021, 15138, 15507, 15508, 15820. *Dendropsophus oliveirai*: MZUESC 14686, 15010, 15011, 15487–15501, 15511, 15791, 15792, 15823, 15825. *Ololygon strigilata*: MZUESC 15001. *Phyllodytes luteolus*: MZUESC 17501, 17502. *Pithecopus nordestinus*: MZUESC 14680–14682, 14685, 14695, 14997, 15136, 15137, 15826, 15827, 16527. *Pseudis fusca*: MZUESC 16528. *Scinax eurydice*: MZUESC 14672, 14693, 15876, 16531. *Scinax pachycrus*: MZUESC 15790, 16525. *Scinax x-signatus*: MZUESC 14692, 14694, 15027, 15139, 15892, 15894, 17503. *Sphaenorhynchus prasinus*: MZU-

ESC 14677, 15004–15009, 15016, 15017, 15135, 15484, 15485, 15793, 15821, 15822. *Trachycephalus nigromaculatus*: MZUESC 15063, 15064, 15065, 15483, 15888. LEPTODACTYLIDAE–*Leptodactylus* cf. *mystaceus*: MZUESC 14696. *Leptodactylus fuscus*: MZUESC 15012, 15067, 15513–15516. *Leptodactylus latrans*: MZUESC 15871, 15893. *Leptodactylus macrosternum*: MZUESC 15146, 16524. *Leptodactylus mystacinus*: MZUESC 16529, 16533. *Leptodactylus troglodytes*: MZUESC 15003, 15028, 15029. *Leptodactylus viridis*: MZUESC 15848, 15869, 15870. *Physalaemus cicada*: MZUESC 15059–15062. *Physalaemus* cf. *erikae*: MZUESC 15013, 15878. *Physalaemus kroyeri*: MZUESC 15517, 15518, 15521, 15523, 15784, 15819, 15877. MICROHYLIDAE – *Dermatonotus muelleri*: MZUESC 15069, 15070. ODONTOPHRYNIDAE–*Proceratophrys schirchi*: MZUESC 14689, 14702–14705, 15071, 15072, 15122, 15134, 15779, 15781, 15804, 15816, 15817, 15833, 15847, 15863–15868. PIPIDAE–*Pipa carvalhoi*: MZUESC 15129. SIPHONOPIDAE–*Siphonops annulatus*: MZUESC 15900.

ZooKeys 1217: 247–262 (2024)
DOI: 10.3897/zookeys.1217.129707

Research Article

Two new species of *Eccoptopterus* Motschulsky, 1863 ambrosia beetle from Taiwan and Thailand (Coleoptera, Curculionidae, Scolytinae, Xyleborini)

Wisut Sittichaya[1], Ching-Shan Lin[2], Sarah M. Smith[3], Chaninan Pornsuriya[1], Anthony I. Cognato[3]

1 *Agricultural Innovation and Management Division, Faculty of Natural Resources, Prince of Songkla University, Songkhla, 90110, Thailand*
2 *Department of Entomology, National Taiwan University, Taipei 10617, Taiwan*
3 *Department of Entomology, Michigan State University, 288 Farm Lane, room 243, East Lansing, MI 48824, USA*
Corresponding author: Wisut Sittichaya (wanakorn62@hotmail.com)

Abstract

Two xyleborine ambrosia beetles, *Eccoptopterus formosanus* **sp. nov**. and *E. intermedius* **sp. nov.** are described from Taiwan and Thailand, respectively, based on DNA sequences (COI and CAD) and morphological characteristics. A key to the *Eccoptopterus* species of Southeast Asia is provided.

Key words: Ambrosia beetle, molecular, new species, Taiwan, taxonomy, Thailand, xyleborine

Academic editor:
Miguel Alonso-Zarazaga
Received: 14 June 2024
Accepted: 3 October 2024
Published: 5 November 2024

ZooBank: https://zoobank.org/541D9AC9-DD07-4435-ACA2-867C5F302D34

Citation: Sittichaya W, Lin C-S, Smith SM, Pornsuriya C, Cognato AI (2024) Two new species of *Eccoptopterus* Motschulsky, 1863 ambrosia beetle from Taiwan and Thailand (Coleoptera, Curculionidae, Scolytinae, Xyleborini). ZooKeys 1217: 247–262. https://doi.org/10.3897/zookeys.1217.129707

Introduction

Eccoptopterus Motschulsky, 1863 is one of the earliest described genera of xyleborine ambrosia beetles (Coleoptera: Curculionidae: Scolytinae). The Russian entomologist, Victor Ivanovich Motschulsky, erected the name for his monotypic genus and new species, *Eccoptopterus sexspinosus* Motschulsky, 1863, described from Burma (now Myanmar) (Motschulsky 1863) which he classified under Hylesinidae. Eichhoff (1876) later moved the genus to Xyleborini and Schedl (1963) synonymized the type species, *E. sexspinosus*, with *Scolytus spinosus* Olivier, 1800. Two other synonymous genera were later published, *Platydactylus* Eichhoff, 1886 (preoccupied by Goldfuss 1820) and its new name *Eurydactylus* Hagedorn, 1909.

Fourteen species and subspecies have been described, of which four are currently recognized: *E. drescheri* Eggers, 1940, *E. limbus* Sampson, 1911, *E. spinosus* (Olivier, 1800), *E. tarsalis* Schedl, 1936. *Eccoptopterus* is easily distinguished by the autapomorphic enlarged metatibiae and metatarsi (Hulcr et al. 2007). However, *Eccoptopterus* species are noted for their exceptional morphological variation. This continuum of variation is especially apparent with specimens collected at different altitudes and is not correlated with geographic origin (Hulcr and Cognato 2013). *Eccoptopterus spinosus* has been previously reported to be a species complex (Cognato et al. 2011; Smith et al. 2020) in need of further study. Other xyleborine species complexes have been delimited using a combination of morphological characteristics and DNA sequence data (e.g Gomez et al. 2018; Smith et al. 2020; Smith and Cognato 2022; Smith et al. 2022). Based on specimens collected as part of WS's survey of Thai xyleborine ambrosia beetles (Sittichaya et al. 2021) and CSL's collecting in Taiwan, we discovered variation in *Eccoptopterus* specimens which suggested potential new species. To test the hypothesis that these new forms represent distinct species, morphological and molecular characters were investigated.

Materials and methods

Insect collection, imaging and terminology

Specimens of a putative new species from Thailand were collected from several provinces (Chiang Mai, Lamphun, Tak, Ubon Ratchathani) between 01.i.2019–31.xii.2020 using ethanol baited traps and fallen branches. The specimens of a putative new species from Taiwan were collected from fallen branches and logs from May 2016 to October 2023. These specimens were then compared with the type specimens, images of type specimens or by examining the original descriptions (Table 1). Photographs were taken with a Canon 5D and 50D digital cameras with a Canon MP-E 65 mm Macro Photo Lens (Canon, Tokyo, Japan) and StackShot-Macrorail (Cognisys Inc, Michigan, USA). The photos were then combined with Helicon Focus ver. 6.8.0. (Helicon Soft, Ukraine); all photos were improved with Adobe Photoshop CS6 (Adobe Systems, California, USA). The antennal and pronotum types and characters follow those proposed by Hulcr et al. (2007) and subsequently elaborated on by Smith et al. (2020).

Abbreviations and terminology

CSL	Private collection of Ching Shan Lin, Taichung, Taiwan;
MFNB	Museum für Naturkunde, Berlin, Germany;
MNHN	Muséum national d'Histoire naturelle, Paris, France;
MSUC	Albert J. Cook Arthropod Research Collection, Michigan State University, East Lansing, USA;
NHMW	Naturhistorisches Museum Wien, Austria;
NMNS	National Museum of Natural Science, Taichung, Taiwan;
NMNH	National Museum of Natural History, Smithsonian Institution, Washington, D.C., USA;
NHMUK	Natural History Museum, London, UK;
NTU	National Taiwan University Insect Museum, Taipei, Taiwan;
THNHM	Natural History Museum of the National Science Museum, Pathumthani, Thailand;
UHZM	Universität Hamburg – Zoological Museum, Hamburg, Germany;
WSTC	Private collection of Wisut Sittichaya, Songkhla, Thailand;
ZMMU	Zoological Museum at Moscow State University, Moscow, Russia;

Major spines are large, regularly present in homologous positions on declivital margin; one pair for *E. limbus* at summit, and three pairs for *E. spinosus* on declivital summit, middle and apex of declivity.

Minor spines are smaller and irregularly present in some positions.

Table 1. List of *Eccoptopterus* types, repository and method of examination.

Species	Synonym	Type and repository	Method of examination
Eccoptopterus drescheri Eggers, 1940	–	Cotype (NHMW)	SMS, AIC examined
Eccoptopterus limbus Sampson, 1911	–	Holotype (NHMUK)	SMS, AIC examined
Eccoptopterus limbus Sampson, 1911	*Xyleborus squamulosus auratus* Eggers, 1923	Lectotype (NMNH)	Images; USNMENT_01547121
Eccoptopterus limbus Sampson, 1911	*Xyleborus squamulosus duplicatus* Eggers, 1923	Lectotype (NMNH)	Images; USNMENT_01547119
Eccoptopterus limbus Sampson, 1911	*Xyleborus squamulosus* Eggers, 1923	Lectotype (NMNH)	Images; USNMENT_01547120
Eccoptopterus spinosus (Olivier, 1800)	–	Holotype (MNHN)	Type not located (Hulcr and Cognato 2013)
Eccoptopterus spinosus (Olivier, 1800)	*Platydactylus gracilipes* Eichhoff, 1886	Syntypes (UHZM)	Types destroyed (Wood and Bright 1992)
Eccoptopterus spinosus (Olivier, 1800)	*Xyleborus abnormis* Eichhoff, 1869	Syntypes (UHZM)	Types destroyed (Wood and Bright 1992)
Eccoptopterus spinosus (Olivier, 1795)	*Xylebrous multispinous* Hagedorn, 1908	Syntypes (MFNB)	Original description
Eccoptopterus spinosus (Olivier, 1800)	*Eccoptopterus sagittarius* Schedl, 1939	Paratypes (NMNH)	Examined by SMS
Eccoptopterus spinosus (Olivier, 1800)	*Eccoptopterus sexspinosus pluridentatus*	Lectotype (NHMW)	SMS, AIC examined
Eccoptopterus spinosus (Olivier, 1800)	*Eccoptopterus eccoptopterus* Schedl, 1951	Lectotype (NHMW)	SMS, AIC examined
Eccoptopterus spinosus (Olivier, 1800)	*Eccoptopterus collaris* Eggers, 1923	Lectotype (NMNH)	WST examined, Images; USNMENT_01356999
Eccoptopterus spinosus (Olivier, 1800)	*Eccoptopterus sexspinosus* Motschulsky, 1863	Syntypes (ZMMU)	Original description
Eccoptopterus tarsalis Schedl, 1936	–	Holotype (NHMW)	SMS, AIC examined

DNA extraction and phylogenetic analysis

Extraction and analysis

Two specimens of an unidentified *Eccoptopterus* morphospecies (SWE01, 02) from Thailand and a specimen of another *Eccoptopterus* morphospecies from Taiwan (SWE02T) were chosen for DNA extraction. The head and pronotum of each specimen were removed and placed in 1.5 ml microfuge tube. The genomic DNA from each specimen was extracted using DNEasy Blood and Tissue Kit (Qiagen Ltd., Hilden, Germany) according to the manufacturer's protocol. PCR amplification of partial cytochrome *c* oxidase subunit I (COI) mtDNA gene and carbamoyl-phosphate synthetase 2, aspartate transcarbamylase, and dihydroorotase (CAD) was conducted by using primer pair COL6/COH6 (Schubart 2009) for COI and apCADfor4/apCADrevlmod (Danforth et al. 2006) for CAD. The PCR reaction mixtures contained DNA template, 10 *p*mol of each primer, 5x HOT FIREPol® Blend Master Mix (Thistle Scientific Ltd, Scotland) and distilled water (DW) in 25 µl tube. PCR was performed in a BIO-RAD T100™ Thermal Cycler (Hercules, CA, USA) and the PCR conditions for COI were 13 min at 95 °C, followed by 40 cycles of 95 °C for 20 sec, 55 °C for 30 sec, 72 °C for 1 min, and the final extension at 72 °C for 5 min. The annealing temperatures differed for the CAD gene with the optimum at 59 °C. PCR products were visualized by agarose gel electrophoresis and sequenced in both directions by Macrogen, Inc. (Seoul, South Korea).

Table 2. *Eccoptopterus* species and isolates used in the phylogenetic analyses, with GenBank accession numbers.

Species	Specimen/ voucher	Location	GenBank accession	
			COI	CAD
Anisandrus cristatus	SAX290	Vietnam: Cao Bang	MN619841	MN620134
Eccoptopterus limbus	Ecclim_258	Borneo	HM064081	HM064261
E. spinosus	SAX150	Vietnam: Dong Nai	MN619920	MN620195
E. formosanus sp. nov.	SAX64	Taiwan	MN619919	N/A
E. spinosus	SAX63	Indonesia: Java	MN619918	MN620194
E. spinosus	Eccspi	Papua New Guinea	HM064082	HM064262
E. spinosus (*E. gracilipes*)	Eccgra	Papua New Guinea	HM064080	HM064260
***E. formosanus* sp. nov.**	SWE02T	Taiwan	LC815914	LC815915
***E. intermedius* sp. nov.**	SWE01	Thailand: Ubon Ratchathani	LC716017	LC716015
***E. intermedius* sp. nov.**	SWE02	Thailand: Chiang Mai	LC716018	LC716016

Specimens sequenced in this study are indicated in **bold**. N/A: Not available.

Forward and reverse DNA sequences were aligned, edited and merged using MEGA X software (Kumar et al. 2018). The generated sequences were submitted to GenBank (http://www.ncbi.nlm.nih.gov) under accession numbers LC716017 and LC716018 for *COI* and LC815915, LC716015 and LC716016 for CAD sequences (Table 2). The sequences in this study were compared with sequences of *Eccoptopterus* species retrieved from GenBank. COI and CAD sequence data were concatenated, aligned with MEGA X software using ClustalW algorithm and manually adjusted as necessary. Phylogenetic tree estimation for each alignment was performed using maximum parsimony (MP), maximum likelihood (ML), and Bayesian inference (BI). The MP tree was obtained using the heuristic search option with 1000 random additions of sequences and tree bisection and reconnection (TBR) as the branch-swapping algorithm using MEGA X. The ML tree was constructed using MEGA X using the General Time Reversible (GTR) nucleotide subsitution model for tree inference and 1000 bootstrap replicates. The Bayesian tree was generated using MrBayes ver. 3.2.7a (Ronquist et al. 2012). Markov chain Monte Carlo (MCMC) runs were performed for 1,000,000 generations and sampled every 100 generations. The initial 25% of generations were discarded as burn-in, and the remaining trees were used to calculate the Bayesian inference posterior probability (BPP) values. Phylogenetic trees were visualized by using FigTree ver. 1.4.4 (http://tree.bio.ed.ac.uk/software/figtree/). DNA percent difference was measured as pairwise uncorrected “p” distance.

Species concept

We consider Xyleborini species as hypotheses of evolutionary independent lineages (Hey 2006). Monophyly of individuals, inferred from a phylogeny, demonstrates an evolutionary lineage and suggests the recognition of a species. Species recognition is based on monophyly of individuals with unique diagnostic characters similarly observed with other recognized species and a percent nucleotide difference near the threshold established for Xyleborini of >10% COI and > 2% CAD pairwise uncorrected “p” distance between sister clades (Cognato et al. 2020).

Results

Molecular evidence

The COI and CAD sequences compared between *Eccoptopterus* spp. demonstrated clear differences and confirmed the new species status of both species from Thailand and Taiwan. The sequences of SWE01 and SWE02 differ from *E. spinosus* and *E. limbus* in COI between 14.85–15.36% and in CAD between 5.64–7.65%. Similar values were found between the new species from Thailand and Taiwan 15.32–15.77% for COI and 3.88–4.0% for CAD. The percentages of both genes for both species exceed the suggested species boundary of 10% and 2% (Table 3).

Table 3. DNA percent difference of *E. formosanus* sp. nov. (SWE02T) and *E. intermedius* sp. nov. (SWE01-02) to species in the NCBI (National Center for Biotechnology Information) database.

Specimen	Gene	Species with the most related sequence	GenBank number	Difference (%)
SWE02T	COI	*Eccoptopterus spinosus* Java	MN619918	15.91
		Eccoptopterus formosanus Taiwan SAX64	MN619919	00.00
		Eccoptopterus spinosus VN Cat	MN619920	15.30
		Eccoptopterus spinosus PNG1	HM064082	14.88
		Eccoptopterus spinosus Eccgra	HM064080	17.78
		E. intermedius sp. nov. (SWE01)	LC716017	15.78
		E. intermedius sp. nov. (SWE02)	LC716018	15.33
		Eccoptopterus limbus Borneo	HM064081	15.58
	CAD	*Eccoptopterus spinosus* Java	MN620194	7.94
		Eccoptopterus spinosus Taiwan SAX64	N/A	N/A
		Eccoptopterus spinosus VN Cat	MN620195	8.81
		Eccoptopterus spinosus PNG1	HM064262	6.88
		Eccoptopterus spinosus Eccgra	HM064260	6.83
		E. intermedius sp. nov. (SWE01)	LC716015	3.88
		E. intermedius sp. nov. (SWE02)	LC716016	4.07
		Eccoptopterus limbus Borneo	HM064261	6.11
SWE01	COI	*Eccoptopterus spinosus* SAX63	MN619918	15.36
		Eccoptopterus gracilipes (*E. spinosus*)	HM064080	14.85
		Eccoptopterus spinosus	HM064082	14.90
		Eccoptopterus sp. Ecc1487_270	MN619915	15.04
	CAD	*Eccoptopterus* sp. 329	HM064259	6.36
		Eccoptopterus limbus 258	HM064261	6.55
		Eccoptopterus gracilipes 12341 (*E. spinosus*)	MK098872	6.26
		Eccoptopterus spinosus SAX331	MN620196	7.22
		Eccoptopterus gracilipes (*E. spinosus*) Eccgra	HM064260	5.69
		Eccoptopterus spinosus SAX63	MN620194	7.40
		Eccoptopterus spinosus Eccspi	HM064262	5.61
		Eccoptopterus spinosus SAX150	MN620195	7.22
SWE02	COI	*Eccoptopterus spinosus*	HM064082	15.36
	CAD	*Eccoptopterus* sp. 329	HM064259	6.57
		Eccoptopterus limbus 258	HM064261	6.77
		Eccoptopterus gracilipes 12341 (*E. spinosus*)	MK098872	6.22
		Eccoptopterus spinosus SAX331	MN620196	7.61
		Eccoptopterus gracilipes (*E. spinosus*) Eccgra	HM064260	5.64
		Eccoptopterus spinosus SAX63	MN620194	7.57
		Eccoptopterus spinosus Eccspi	HM064262	5.87
		Eccoptopterus spinosus SAX150	MN620195	7.65

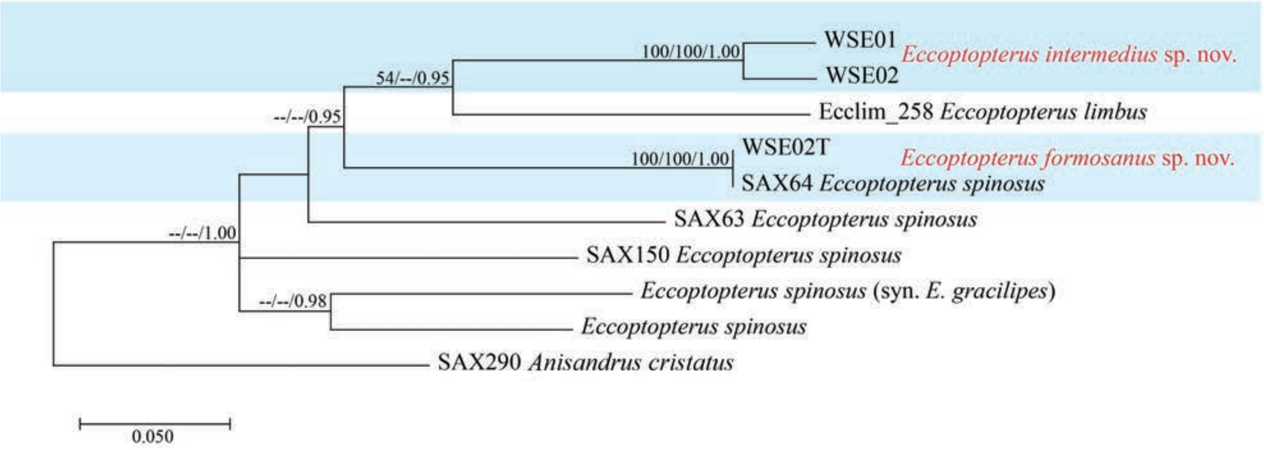

Figure 1. Phylogenetic tree generated by maximum likelihood analysis based on the combined sequences of COI and CAD sequence data of *Eccoptopterus*. Bootstrap values for maximum likelihood (ML) and maximum parsimony (MP) equal to or greater than 70% and Bayesian posterior probabilities (BPP) equal or greater than 0.95 are placed above the branches, respectively. The new species are indicated in blue area. The tree is rooted to *Anisandrus cristatus*.

The maximum likelihood (ML), maximum parsimony (MP) and Bayesian inference (BI) for phylogenetic analyses of combined sequence COI (585 characters) and CAD (376 characters) resulted in trees with similar topologies. Phylogenetic results (Fig. 1) showed that two specimens (SWE01 and SWE02), representing *E. intermedius*, clustered together and SWE02T, representing *E. formosanus* had an identical sequence to a specimen previously identified as *E. spinosus* (SAX64) from Taiwan and included in the study of Cognato et al. (2020). Each species formed a distinct lineage within *Eccoptopterus* and were recovered as sister to *E. limbus* but each can be recognized as a phylogenetically distinct species (Fig. 1).

Taxonomic treatment

Eccoptopterus Motschulsky, 1863

Eccoptopterus Motschulsky, 1863: 515.
Platydactylus Eichhoff, 1886: 25. Preoccupied by Goldfuss, 1820.
Eurydactylus Hagedorn, 1909: 733. (new name for *Platydactylus* Eichhoff, 1866 nec. Goldfuss 1820; preoccupied by Laferté-Sénectère, 1851). Synonymy: Hagedorn 1910: 110.

Type species. *Eccoptopterus sexspinosus* Motschulsky, 1863 = *Scolytus spinosus* Olivier, 1800.

Diagnosis. 1.70–5.90 mm, stout, 1.94–2.3× as long as wide; pronotum short and round, robust, broader and larger than elytra; pronotal anterior margin armed with a pair of prominently protruding denticles; pronotal base bearing a dense tuft of setae; elytra short, excavated, with denticles around its margins; declivity impressed, the impressed areas extending nearly to elytral base; metatibiae conspicuously enlarged and flattened.

Eccoptopterus formosanus **Lin, Sittichaya & Smith, sp. nov.**
https://zoobank.org/DFC6F8B0-22B2-4983-B744-411097C5F087
Fig. 2

Type material. ***Holotype:*** • female, Taiwan, Nantou county, Ren'ai Township; 24°0'0.3675"N, 121°0'34.4817"E; 969 m a.s.l.; a diameter 4.5 cm branch of *Sapium discolor* (Euphorbiaceae); 02.iv.23, (C. S. Lin) (NMNS). ***Paratypes*****:** • male, same as holotype (1, NMNS), female, (3, MSUC), 1 female, 1 male (2 NTU), 1 male, 14 females (15, CSL) • female, Nantou County (Lugu Township); 23°45'0.31"N, 120°48'59.99"E; 720 m a.s.l.; a diameter 5.2 cm branch of *Elaeocarpus sylvestris* (Elaeocarpaceae); 022.vi.23, (C. S. Lin), 1 male, 4 females (5, WSTC), female (1, NMNH), (1, NHMUK).

Diagnosis. Female, 2.56–2.64 mm long (mean = 2.61 mm; *N* = 4), 2.13–2.17× as long as wide (mean = 2.14×; *N* = 4). Medium body size, declivital armature composed of a pair of major spines on declivital summit and 2–4 minor denticles unevenly spaced on each lateral margin; protibiae slender, broadest at apical 1/3, outer margin armed with six or seven moderated socketed denticles; scutellum broadly linguiform; elytra tapering laterally.

Description. Female (Fig. 2A–E). Black brown, procoxae light brown, profemora and mesofemora paler brown, antennae, tibiae dark brown. ***Head:*** epistoma entire, transverse, with a row of hair-like setae. Frons below upper margin of eye and above epistoma flat, flattened area broadly rounded, surface subshiny, finely reticulate, sparsely punctate, punctures bearing fine, yellowish-white, hair-like setae. Eye shallowly emarginate just above antennal insertion, upper portion slightly smaller than lower portion. Submentum triangular small, moderately impressed. Antennal scape long, normal thick, slightly longer than club (12:10). Pedicel as broad as scape, as long as funicle. Funicle 4-segmented, segment 1 shorter than pedicel. Club obliquely truncate, longer than wide (10:9), type 1, segment 1 corneous, occupying basal 1/4, margin carinate, concave, encircling anterior face, segment 2 and 3 soft, visible on anterior face only. ***Pronotum:*** 0.97–1.00 (mean = 0.99, *N* = 4) × as long as wide, type 1 in dorsal view, lateral sides parallel to anterior middle, broadly rounded anteriorly; anterior margin with 4–6 serrations, median pair prominent; anterior slope strongly asperate, asperities densely spaced, rugose, lower and more transverse toward the summit; disc slightly convex, finely reticulate, dull, sparsely covered with fine punctures bearing fine short hair-like setae. Base with a tuft of short hair-like setae associated with mycangium. In lateral view short and tall, type 3, summit at middle, lateral margins obliquely costate. ***Elytra:*** 1.14–1.17 (mean = 1.16, *N* = 4) × as long as wide, 1.10–1.17 (mean = 1.12, *N* = 4) × as long as pronotum. Scutellum comparatively moderately sized, narrow, linguiform, subshiny, attached on anterior slope of elytra less visible from above. Base shallowly bisinuate, with oblique edge, humeral angles rounded, lateral side tapering from humeral angle to apex. Disc short, basal area 1/4 of disc slightly convex, apical 3/4 impressed and connecting to declivital impression; disc punctate, punctures fine confused and setose, striae and interstriae hardly marked due to irregular punctures. Declivity sulcate, with a pair of major (largest) spines on declivital summit and 2–4 much smaller denticles on declivital margin; striae and interstriae punctate, punctures small and shallow, each bearing a short,

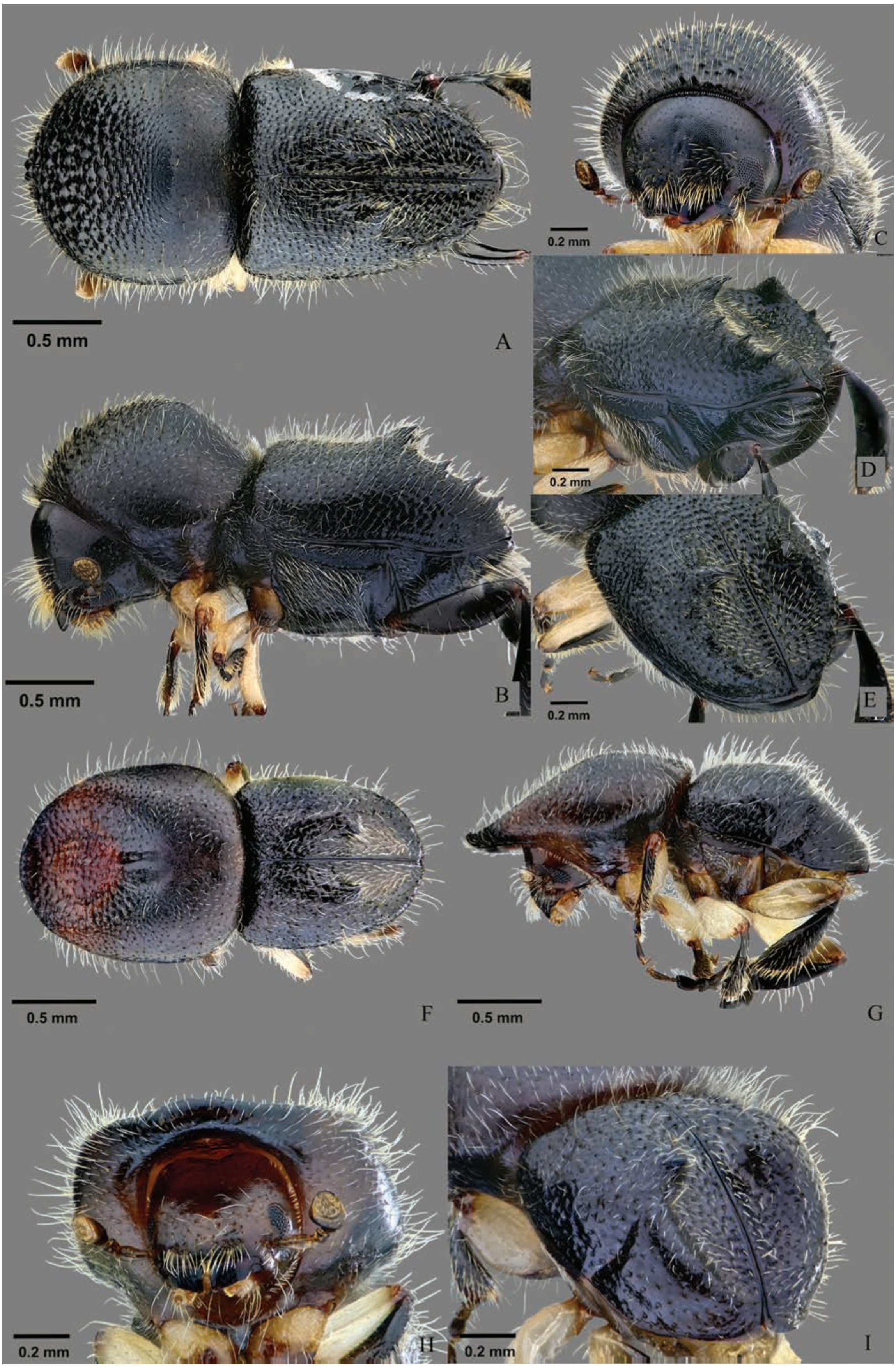

Figure 2. *Eccoptopterus formosanus* sp. nov. **A–E** holotype female **A** dorsal view **B** lateral view **C** frons **D** posterolateral view of abdomen **E** declivital face; **F–I** paratype male **F** dorsal view **G** lateral view **H** frons **I** posterolateral view of abdomen.

semi-recumbent seta. ***Legs:*** procoxae contiguous; prosternal coxal piece short, conical. Protibiae slender, broadest at middle; posterior face inflated, punctate, densely covered with long hair-like setae; outer margin armed with six or seven moderate socketed denticles. Meso- and metatibiae rounded, flat, mesotibiae armed with seven or eight smaller socketed denticles, metafemora and metatibiae enlarged, metatibiae without spines.

Male. (Fig. 2F–I). 2.18–2.30 mm (mean = 2.24 mm; *N* = 4) long, 1.81–2.04 (mean 1.95; *N* = 4) × as long as wide. Head reddish-brown, coxae light brown, femora paler brown, antennae, tibiae, pronotum and elytra dark brown in mature specimens, excepting impressed portion of pronotum is reddish-brown. ***Head***: somewhat margined laterally and concealed under the projection of pronotum. Epistoma entire, transverse, with a row of hair-like setae. Frons below upper margin of eye and above epistoma flat, the flattened area quadrate, surface subshiny, finely reticulate, sparsely shallow punctured, each bearing a short or long hair-like seta. Eye reduced, shallowly emarginate just above antennal insertion, upper portion slightly smaller than lower portion. Submentum triangular, small, slightly impressed. Antennal scape long, normal thick, slightly longer than club. Pedicel as broad as scape, as long as funicle. Funicle 4-segmented, segment 1 shorter than pedicel. Club obliquely truncate, longer than wide (7.5:5.5), type 1, segment 1 corneous, occupying basal 1/4, margin carinate, concave, encircling anterior face, segments 2 and 3 soft, visible on anterior face only. ***Pronotum***: 0.89–1.11 (mean = 0.99; *N* = 4) × as long as wide, type 1 in dorsal view, lateral sides subparallel to anterior middle, broadly rounded anteriorly; anterior margin unarmed; widely impressed on anterior slope, then gradually narrowing and slightly impressed toward disc, weakly asperate, asperities sparsely spaced, sub-rugose, becoming lower and more transverse toward the summit; slightly longitudinally impressed in middle of disc, finely reticulate, dull, sparsely covered with fine punctures bearing fine short hair-like setae. In lateral view long and tall, type 9, summit at apical 2/3, lateral margins obliquely costate. ***Elytra***: 1.00–1.05 (mean = 1.04; *N* = 4) × as long as wide, 0.80–1.00 (mean = 0.88; *N* = 4) × as long as pronotum. Scutellum small, linguiform, subshiny, attachment on anterior slope of elytra less visible from above. Base procurved, with oblique edge, humeral angles rounded, subparallel-sided in basal 1/2, then gradually incurved to broadly rounded apex. Disc short, punctate, punctures fine confused and setose, strial setae uniseriate with long, erect hair-like setae; interstrial setae uni- or biseriate with semi-recumbent hair-like setae; basal area 1/4 of disc slightly convex. Declivity somewhat steeply sloping, face weakly bisulcate, declivital face much lower than declivital margin, with a pair of major spines on declivital summit and 0–2 much smaller minor tubercles on declivital margin; striae and interstriae punctate, punctures small and shallow, each bearing a short, semi-recumbent setae. ***Legs***: procoxae narrowly separated; prosternal coxal piece short, conical. Protibiae slender, broadest at the middle; posterior face inflated, punctate, densely covered with long hair-like setae; outer margin armed with five or six moderate socketed denticles. Meso- and metatibiae rounded, flat, mesotibiae armed with six or seven smaller socketed denticles, metafemura and metatibiae enlarged, metatibiae without apical spine.

Etymology. Formosa, the former name of Taiwan island, in reference to the collection locality of types. An adjective.

Distribution. Taiwan (Nantou County).

Biology. Bred from *Elaeocarpus sylvestris* (Lour.) Poir. (Elaeocarpaceae), *Lithocarpus hancei* (Benth.) Rehder, *Quercus glauca* Thunb. ex Murray (Fagaceae), *Sapium discolor* Muell.-Arg. (Euphorbiaceae), *Trema orientale* (L.) Blume (Cannabaceae) with a diameter of about 4.8–6.2 cm in Taiwan. The radial entrance gallery leads to several branches in various planes without enlarged brood chambers (C. S. Lin pers. obs.).

Eccoptopterus intermedius **Sittichaya, Lin & Smith, sp. nov.**

https://zoobank.org/BCEE85CB-6BE4-412A-B1B7-E3096D103600
Fig. 3

Type material. ***Holotype***, • female, Thailand, Tak Province, 17°40'17.7"N, 97°51'04.2"E; 600 msl; semiagricultural area, ex. small branch of unknown tree; 08.ix.19, (W. Sittichaya) (NHMW); ***Paratypes***: • females, Ubon Ratchathani Province, Pha Taem National Park, 15°37'21.9"N, 105°36'34.7"E; 420 m a.s.l.; dry dipterocarp rainforest, ethanol baited trap; 01.v.2019, (W. Sittichaya) • Tak Province, 17°40'17.7"N, 97°51'04.2"E; 600 m a.s.l.; semiagricultural area, ex. Small branch of unknown tree; 08.ix.19 (1), (W. Sittichaya), (1 THNHM) • Lamphun Province, Maeping National Park, 17°33'29.6"N, 98°52'46.0"E; 600 m a.s.l.; Dry Dipterocarp forest, ethanol baited trap; 01.ii.19 (1), 01.iii.19 (1), 01.v.19 (1) (all W. Sittichaya) (3 WSTC) • Chiang Mai Province, Chiang Dao Wildlife Sanctuary, 17°33'29.6"N, 98°52'46.0"E; 600 m a.s.l.; mixed deciduous forest, ethanol baited trap; 01.vi.19 (W. Sittichaya) (1 MSUC).

Diagnosis. Female, 1.70–1.90 mm long (mean = 1.80 mm; *N* = 6), 2.03–2.38× as long as wide (mean = 2.13×; *N* = 6). Small body size, declivital armature composed of a pair of major spines at interstriae 3 on declivital summit and four minor spines unevenly spaced on each lateral margin, declivity covered with flattened scale-like setae; protibiae slender, broadest at apical 1/3, outer margin armed with four or five moderated socketed denticles, elytra tapering laterally.

Description. Female. Body brown, dark brown to black, impressed portion of elytral disc and declivital face paler and bearing grayish-brown scale-like setae; antennae, prolegs, middle legs and associated coxae paler brown, hind legs dark brown to black. ***Head:*** epistoma complete, margin bisinuated, with a row of hair-like setae. Frons below upper margin of eye and above epistoma impressed, without raised median line, surface reticulate, subshiny, sparsely covered with fine long setae, setal insertion shallowly punctate. Frons below upper portion of the eye slightly convex. Eye shallowly emarginate just above antennal insertion, upper portion slightly smaller than lower part. Submentum triangular small, shallowly impressed. Antennal scape long, normal thick, slightly longer than club (9:8). Pedicel as broad as scape, as long as funicle. Funicle 4-segmented, segment 1 shorter than pedicel. Club obliquely truncate, longer than wide (8:6.5), type 1, segment 1 corneous, occupying basal 1/4, margin carinate, concave, encircling in anterior face, segment 2 and 3 soft, visible on anterior face only. ***Pronotum:*** 0.93–0.97 (mean = 0.95, *N* = 6) × as long as wide, round shorter than long, type 1 in dorsal view, lateral sides parallel to anterior middle, broadly rounded anteriorly; anterior margin with 2–4 serrations, median pair prominent; anterior slope strongly asperate, asperities densely spaced, rugose, becoming lower and more transverse toward the summit; disc slightly

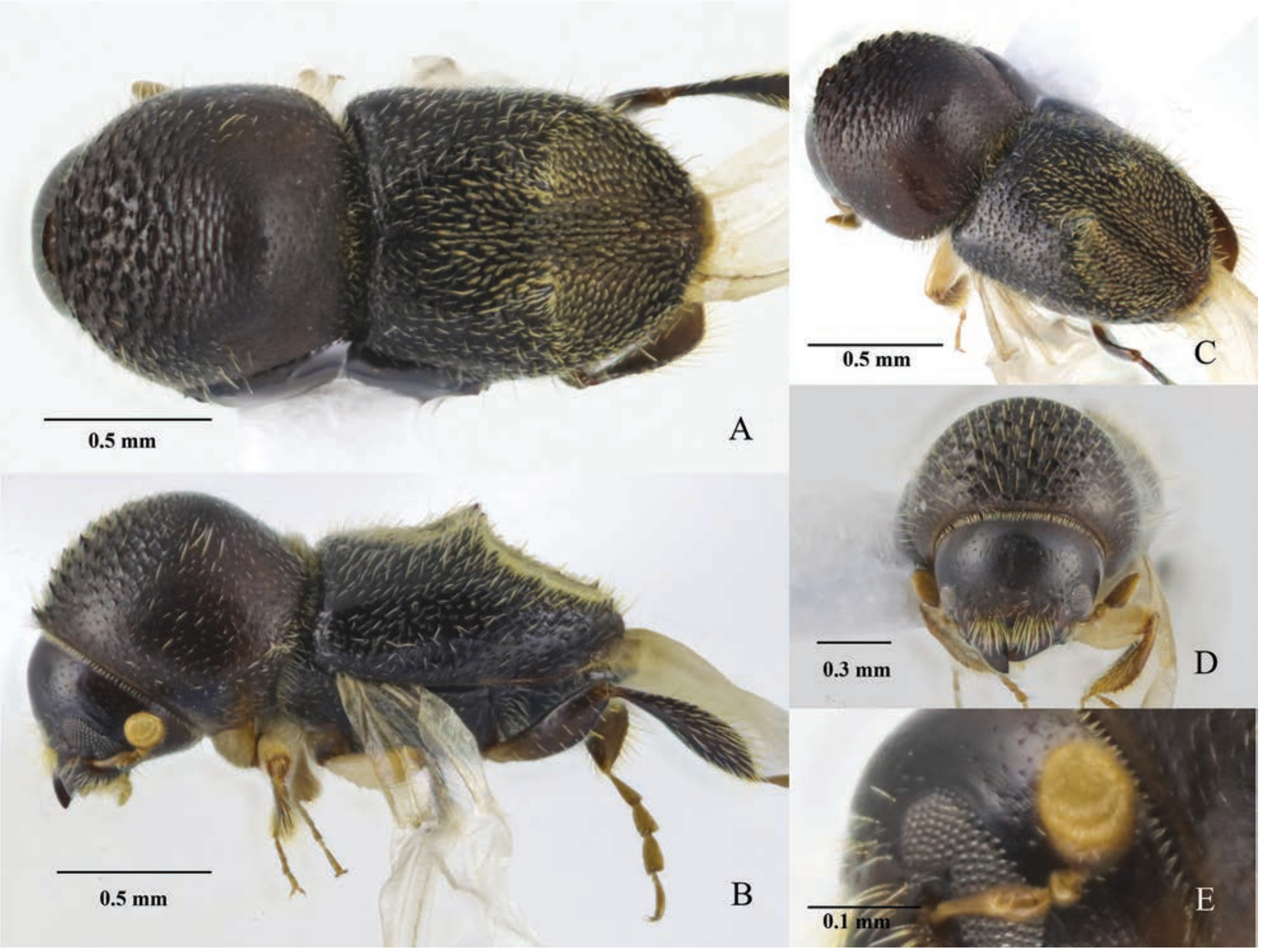

Figure 3. *Eccoptopterus intermedius* sp. nov. Holotype, female, **A** dorsal view **B** lateral view **C** posterolateral view **D** frons **E** antenna.

convex, finely alutaceous, dull, sparsely covered with fine punctures bearing fine short hair-like setae. Base with a tuft of short hair-like setae associated with mycangium. In lateral view short and tall, type 3, summit at middle, lateral margins obliquely costate. ***Elytra:*** 1.12–1.18 (mean = 1.15, *N* = 6) × as long as wide, 1.07–1.19 (mean = 1.15, *N* = 6) × as long as pronotum. Scutellum comparatively moderately sized, narrow, linguiform, finely punctate, subshiny, attachment on anterior slope of elytra less visible from above. Base shallowly bisinuate, with oblique edge, humeral angles rounded, lateral side tapering from humeral angle to apex. Disc short, basal area ¼ of disc slightly convex, apical 3/4 impressed and connecting to declivital impression; disc punctate, punctures fine confused and setose, strial setae uniseriate with long, erect hair-like setae; interstrial setae bi- or triseriate with semi-recumbent hair-like setae. Impressed portion of disc covered with leaf-like setae. Declivity sulcate, with a pair of major (largest) spines on declivital summit and four much smaller minor spines on declivital margin, first minor spine located far from the major spine; striae and interstriae punctate, punctures small and shallow; striae 1 shallowly impressed, 2–3 flattened; interstriae 1 slightly convex, 2 and 3 flattened. Striae and interstriae with flattened bristle-like setae, setae semi-recumbent, near median suture in vertical rows (3–4 rows on each side), apically pointed, near lateral margins (four or five rows per side) pointed inwardly to elytral suture, at apical margin without upwardly setae. ***Legs:*** procoxae contiguous; prosternal coxal piece short, inconspicuous. Protibiae slender, broadest at middle; posterior face inflated, punctate, densely covered with long hair-like setae; outer margin armed with four or five moderate socketed denticles. Meso- and metatibiae rounded, flat, mesotibiae armed with three or four smaller socketed denticles, metafemora and metatibiae enlarged, the latter without spine.

Male. Unknown.

Etymology. L. *inter* + *medius* = in the middle. The name refers to the morphological characters of the species which lie between those of *E. limbus* and *E. spinosus*. An adjective.

Distribution. Thailand (Chiang Mai, Lamphun, Tak, Ubon Ratchathani provinces).

Host plants. Unknown.

Key to species *of Eccoptopterus* Motschulsky, 1863 of Indochina (females only)

1 Declivity bearing one major spine on each elytral margin; declivital armature consisting of two large spines closest to suture on declivital summit and 2–8 minor, uniform-sized denticles on declivital margin **2**

– Declivity bearing three major spines on each elytral margin; largest spine near the declivital summit with or without additional 3–4 minor spines between major spines 2 and 3 .... ***E. spinosus***

2 Declivity with 2–4 minor spines, spines widely separated, unevenly spaced on interstriae; smaller size, 1.70–2.64 mm **3**

– Declivity with 6–8 minor spines, spines close together, evenly spaced on each interstriae; larger size, 3.5–4.2 mm....................................... ***E. limbus***

3 Larger body size, 2.56–2.64 mm; outer margins of protibiae with six or seven socketed denticles .... ***E. formosanus***

– Smaller body size, 1.70–1.90 mm, outer margins of protibiae with four or five socketed denticles .... ***E. intermedius***

Discussion

The differences of both COI and CAD sequences between the new species (*E. formosanus*, *E. intermedius*) and *E. limbus*, *E. spinosus* sensu lato and its junior synonym *E. gracilipes* are clearly greater than suggested species boundaries for these genes (Cognato et al. 2020). The *E. intermedius* specimens demonstrated some DNA sequence differences as illustrated by the branch lengths (Fig. 1). The morphological characters of these geographically separated individuals also exhibited slight variation in the degree of elytral tapering and declivital setal density. These also vary within the type series and are independent of locality and collection date.

The morphological features of *E. intermedius* are more similar to *E. limbus* than to *E. spinosus* but some characters are intermediary (Table 4). *Eccoptopterus intermedius* differs from *E. limbus* by the distinctly smaller size, shorter elytra (elytra: pronotum), the presence of only four minor spines on declivital margin, more slender protibiae. The species differs from *E. spinosus* by hair-like declivital setae and has only a pair of major spines and more slender protibiae.

The morphological features of *E. formosanus* are more similar to *E. spinosus* than to *E. limbus*. *Eccoptopterus formosanus* differs from *E. spinosus* by the

Table 4. Comparative morphological characters for *Eccoptopterus* species.

Species	Total length (mm)	Length/width ratio	Elytral armature on each elytral margin
E. formosanus	2.56–2.64	2.13–2.17	1 major on declivital summit, 2–4 minor spines
E. intermedius	1.70–1.90	2.03–2.38	1 major on declivital summit, 4 minor spines
E. limbus	3.5–4.2	2.1–2.3	1 major on declivital summit, many minor spines
E. spinosus	2.5–3.7	2.06–2.27	3 majors on each elytral margin, 0–4 minor spines between major spines 2 and 3

absence of second and third major spines on declivital margins and declivital face densely covered with thick, long setae. The species differs from *E. limbus* by its distinctly smaller body size, the distinctly tapered elytra, and the declivital margin with 2–4 minor denticles (Table 4).

The two major diagnostic characters used in *Eccoptopterus* species delimitation are the pattern of spines on the declivital margin and the declivital vestiture (Hulcr and Cognato 2013). Hulcr and Cognato (2013) indicated a continuum of morphological variation and geographic origin independence. *Eccoptopterus spinosus* varies greatly in both body size and declivital spine configuration. The configuration of elytral spines in *E*. *spinosus* and its junior synonym *E*. *gracilipes* is geographically extremely variable, resulting in inconsistent identifications of *E*. *spinosus* and *E*. *gracilipes* in some collections (Hulcr and Cognato 2013). Our study shows non-monophyly and long branch lengths for *E*. *spinosus* (Fig. 1). The type specimens of *E*. *spinosus* are presumed lost and the original description is not detailed enough for the comparison of species. *Eccoptopterus spinosus* is likely a species complex, and the combined use of DNA and morphological characters may be the best solution for revising this species and the entire genus (Cognato et al. 2020; Smith et al. 2020).

Acknowledgements

We are most grateful to Dr Harald Schillhammer (NHMW) for access to specimens. Special thanks to the Thai National Parks and wildlife sanctuaries staff and rangers of all field sites.

Additional information

Conflict of interest

The authors have declared that no competing interests exist.

Ethical statement

No ethical statement was reported.

Funding

This research was funded by the Faculty of Natural Resources Research Fund, Prince of Songkla University (Grant No. NAT6704088S) to WST and a Cooperative Agreement (IP00533923 to Anthony Cognato) from the United States Department of Agriculture's Animal and Plant Health Inspection Service (APHIS). It may not necessarily express APHIS' views.

Author contributions

Writing – original draft: WS, CSL. Writing – review and editing: AIC, CSL, CP, SMMS, WS.

Author ORCIDs

Wisut Sittichaya https://orcid.org/0000-0001-6200-1285
Ching-Shan Lin https://orcid.org/0009-0006-3159-697X
Sarah M. Smith https://orcid.org/0000-0002-5173-3736
Chaninan Pornsuriya https://orcid.org/0000-0002-8233-1254
Anthony I. Cognato https://orcid.org/0000-0001-6436-2447

Data availability

All of the data that support the findings of this study are available in the main text.

References

Cognato AI, Hulcr J, Dole SA, Jordal BH (2011) Phylogeny of haplo-diploid, fungus growing ambrosia beetles (Curculionidae: Scolytinae: Xyleborini) inferred from molecular and morphological data. Zoologica Scripta 40: 174–186. https://doi.org/10.1111/j.1463-6409.2010.00466.x

Cognato AI, Sari G, Smith SM, Beaver RA, Li Y, Hulcr J, Jordal BH, Kajimura H, Lin C-S, Pham TH, Singh S, Sittichaya W (2020) The essential role of taxonomic expertise in the creation of DNA databases for the identification and delimitation of Southeast Asian ambrosia beetle species (Coleoptera: Curculionidae: Scolytinae: Xyleborini). Frontiers in Ecology and Evolution 8. https://doi.org/10.3389/fevo.2020.00027

Danforth BN, Fang J, Sipes SD (2006) Analysis of family level relationships in bees (Hymenoptera: Apiformes) using 28S and two previously unexplored nuclear genes: CAD and RNA polymerase II. Molecular Phylogenetics and Evolution 39: 358–372. https://doi.org/10.1016/j.ympev.2005.09.022

Eggers H (1923) Neue indomalayische Borkenkäfer (Ipidae). Zoologische Mededeelingen 7: 129–220.

Eggers H (1940) Neue indomalayische Borkenkäfer (Ipidae) III Nachtrag (Forstsetzung). Tijdschrift voor Entomologie 83: 132–154.

Eichhoff WJ (1869) Neue exotische *Xyleborus*-Arten. Berliner Entomologische Zeitschrift 12: 273–280. https://doi.org/10.1002/mmnd.18680120213

Eichhoff WJ (1876) Synonymisches über Tomiciden. Stettiner Entomogische Zeitung 37: 378–379.

Eichhoff WJ (1886) Zwei neue ost-indische Scolytiden-Gattungen. Notes from the Leyden Museum 8: 24–26.

Goldfuss GA (1820) Handbuch der Zoologie. Zweite Abtheilung. In: Schubert GH (Ed.) Handbuch der Naturgeschichte zum Gebrauch bei Vorlesungen. Dritter Theil. Zweite Abtheilung. JL Schrag, Nürnberg, i–xxiv, 1–506.

Gomez DF, Skelton J, Steininger MS, Stouthamer R, Rugman-Jones P, Sittichaya W, Rabaglia RJ, Hulcr J (2018) Species within the *Euwallacea fornicatus* (Coleoptera: Curculionidae) complex revealed by morphometric and phylogenetic analyses. Insect Systematics and Diversity 2(6): 2, 1–11. https://doi.org/10.1093/isd/ixy018

Hagedorn M (1908) Diagnosen bisher unbeschriebener Borkenkäfer. Erste Serie. Deutsche Entomologische Zeitschrift 1908: 369–382. https://doi.org/10.1002/mmnd.48019080310

Hagedorn M (1909) Diagnosen bisher unbeschriebener Borkenkäfer (Col). Deutsche Entomologische Zeitschrift 1909: 733–746. https://doi.org/10.1002/mmnd.48019090606

Hagedorn M (1910) Ipidae. In: Schenkling S (Ed.) Coleopterorum Catalogus Auspiciis et Auxilio. Pars 4. W. Junk, Den Haag, 1–134. https://doi.org/10.1007/978-94-011-9697-0_1

Hey J (2006) On the failure of modern species concepts. Trends in Ecology and Evolution 21: 447–450. https://doi.org/10.1016/j.tree.2006.05.011

Hulcr J, Cognato AI (2013) Xyleborini of New Guinea: A Taxonomic Monograph. Thomas Say Publications in Entomology, Entomological Society of America, Lanham, 176 pp.

Hulcr J, Dole SA, Beaver RA, Cognato AI (2007) Cladistic review of generic taxonomic characters in Xyleborina (Coleoptera: Curculionidae: Scolytinae). Systematic Entomology 32(3): 568–584. https://doi.org/10.1111/j.1365-3113.2007.00386.x

Kumar S, Stecher G, Li M, Knyaz C, Tamura K (2018) MEGA X: Molecular Evolutionary Genetics Analysis across computing platforms. Molecular Biology and Evolution 35: 1547–1549. https://doi.org/10.1093/molbev/msy096

Motschulsky V (1863) Essai d’un catalogue des insectes de l’île Ceylan. (Suite). Bulletin de la Société Impériale des Naturalistes de Moscou 36: 421–532.

Olivier AG (1800) Entomologie, ou histoire naturelle des Insectes, avec leurs caractères génériques et spécifiques, leur description, leur synonymie, et leur figure enluminée. Coléoptères. Tome quatrième. Paris: de Lanneau, 519 pp [72 pls]. https://doi.org/10.5962/bhl.title.49479

Ronquist F, Teslenko M, van der Mark P, Ayres DL, Darling A, Höhna S, Larget B, Liu L, Suchard MA, Huelsenbeck JP (2012) MRBAYES 3.2: Efficient Bayesian phylogenetic inference and model selection across a large model space. Systematic Biology 61: 539–542. https://doi.org/10.1093/sysbio/sys029

Sampson FW (1911) On two new wood-boring beetles (Ipidae). The Annals and Magazine of Natural History, series 8, 8: 381–384. https://doi.org/10.1080/00222931108693046

Schedl KE (1936) Some new Scolytidae and Platypodidae from the Malay Peninsula. Journal of the Federated Malay States Museums 18: 19–35.

Schedl KE (1939) Scolytidae and Platypodidae. 47. Beitrag zur Morphologie und Systematik der Scolytoidea. Tijdschrift voor Entomologie 82: 30–53.

Schedl KE (1951) Fauna Samoanus (Scolytoides), I. 109. Contribution. Bernice P. Bishop Museum Occasional Papers 20: 131–156.

Schedl KE (1963) Scolytidae und Platypodidae Afrikas. Band II. Familie Scolytidae (Fortsetzung), Unterfamilie Ipinae (Fortsetzung). Revista de Entomologia de Moçambique 5: 1–594.

Schubart CD (2009) Mitochondrial DNA and decapod phylogenies: the importance of pseudogenes and primer optimization. In: Martin JW, Crandall KA, Felder DL (Eds) Decapod Crustacean Phylogenetics. Crustacean Issues. CRC Press, Taylor & Francis Group. Boca Raton, London, New York, 18, 47–65. https://doi.org/10.1201/9781420092592-c4

Sittichaya W, Smith SM, Beaver RA, Thaochan N (2021) Revision of the xyleborine ambrosia beetle genus *Microperus* Wood, 1980 (Curculionidae, Scolytinae, Xyleborini) of Thailand with four new species and four newly recorded species. ZooKeys 1074: 191–214. https://doi.org/10.3897/zookeys.1074.76235

Smith SM, Cognato AI (2022) New non-native pseudocryptic *Cyclorhipidion* species (Coleoptera: Curculionidae: Scolytinae: Xyleborini) found in the United States as revealed in a multigene phylogeny. Insect Systematics and Diversity 6: 1–16. https://doi.org/10.1093/isd/ixac014

Smith SM, Beaver RA, Cognato AI (2020) A monograph of the Xyleborini (Coleoptera, Curculionidae, Scolytinae) of the Indochinese Peninsula (except Malaysia) and China. ZooKeys 983: 1–442. https://doi.org/10.3897/zookeys.983.52630

Smith SM, Urvois T, Roques A, Cognato AI (2022) Recognition of the pseudocryptic species *Xylosandrus declivigranulatus* (Schedl) as distinct from *X. crassiusculus* (Motschulusky) (Curculionidae: Scolytinae: Xyleborini). The Coleopterists Bulletin 76: 367–374. https://doi.org/10.1649/0010-065X-76.3.367

Wood SL, Bright DE (1992) A catalog of Scolytidae and Platypodidae (Coleoptera), Part 2: Taxonomic index. The Great Basin Naturalist Memoirs 13: 1–1553.

ZooKeys 1217: 263–272 (2024)
DOI: 10.3897/zookeys.1217.132291

Research Article

A new species of *Proaphelinoides* Girault (Hymenoptera, Aphelinidae) from China, with a phylogenetic analysis

Yan-yan Jiang[1], Huifeng Zhao[1], Ye Chen[1]

[1] Hebei Key Laboratory of Animal Diversity, College of Life Science, Langfang Normal University, Langfang, 065000, China
Corresponding author: Ye Chen (chenye@lfnu.edu.cn)

Abstract

A new species of *Proaphelinoides* Girault, *Proaphelinoides huangi* Chen & Jiang, **sp. nov.**, is reported from China. A key to all species of the genus is provided. DNA standard barcode COI and partial nuclear ribosomal 28S-D2 from two individuals of *Proaphelinoides* were sequenced, and 28S-D2 rDNA was included in a phylogenetic analysis, confirming *Proaphelinoides* as the sister group to *Aphytis*.

Key words: Aphelininae, Chalcidoidea, parasitoid wasp, taxonomy

Academic editor: Zachary Lahey
Received: 17 July 2024
Accepted: 15 October 2024
Published: 7 November 2024

ZooBank: https://zoobank.org/A6F327F9-2946-4990-AAE3-1192E00ABDE8

Citation: Jiang Y-y, Zhao H, Chen Y (2024) A new species of *Proaphelinoides* Girault (Hymenoptera, Aphelinidae) from China, with a phylogenetic analysis. ZooKeys 1217: 263–272. https://doi.org/10.3897/zookeys.1217.132291

Introduction

Proaphelinoides Girault is a small genus in Aphelinidae, containing only seven species worldwide, with *P. elongatiformis* from Sri Lanka as the type species (Girault 1917; UCD Community 2023). Other species in the genus include *P. australis* from Australia (Girault 1922), *P. bendovi* Tachikawa (1984) from Guangdong Province of China, and the remaining four species, *P. anomalus* Hayat (1984), *P. chidambaramensis* Manickavasagam & Menakadevi (Menakadevi and Manickavasagam 2012), *P. assamensis* Hayat (2012), and *P. ematus* Hayat &Veenakumari (2016) from India. Their known hosts are diaspidid scales of the genus *Odonaspis* Leonardi (Hemiptera, Diaspididae), which are specialized plant parasites of bamboo (Tachikawa 1984; Si et al. 2019). In China, three species (*P. elongatiformis*, *P. bendovi*, *P. anomalus*) were reported prior to this study (Si et al. 2019).

Proaphelinoides is distinguished from related genera by the following combination of characters: body elongate and flattened, antenna 6-merous, pronotum dorsally long, 0.5× as long as mid lobe of mesosoma, medially divided by a suture; propodeum long, more than 3.0× as long as metanotum medially, with posterior margin transverse; linea calva bordered proximally by 1–4 lines of setae and closed posteriorly by a line of setae.

The systematic status of *Proaphelinoides* remains unclear. *Proaphelinoides* was placed in Aphytini in the subfamily Aphelininae (Hayat 1998; Kim and Heraty 2012). The parsimonious tree of Aphelininae based on 50 morphological characters recovered *Proaphelinoides* as the sister group to *Eretmocerus+Marlattiella* (Kim and Heraty 2012). However, *Eretmocerus* is now placed in Eretmocerinae (Heraty et al. 2013; Cruaud et al. 2024). Thus, analyzing the relationship between *Proaphelinoides* and other genera based on molecular data is useful for our understanding the systematic relationship of Aphelininae.

In this study, a new species, *Proaphelinoides huangi* sp. nov., is described and illustrated. The barcode region of mitochondrial cytochrome oxidase subunit I (COI) and the D2 region of the 28S ribsosomal DNA (28S-D2 rDNA) were sequenced and uploaded to GenBank. A key to all the known species of the genus is provided. In addition, phylogenetic analyses including 26 28S-D2 rDNA sequences together with our new data were carried out to assess the systematic position of the genus.

Materials and methods

Morphological study

Samples were obtained using a pyrethroid fog generated from a thermal fogger (Swingfog SN50, Germany, Model 2610E, Series 3). Samples fell into collection trays (area of each tray is 1 m^2) which were suspended 1.5 m above the ground. The collected samples were stored in 100% ethanol at 4 °C in the refrigerator.

Specimens were dissected and mounted in Canada balsam on slides following the method described by Noyes (1982). The methods of photography and measurements following Chen and Chen (2021). Scale bars in the figures are 100 μm except where otherwise indicated. All specimens listed below, including the holotype, are deposited in the collection (LFNU) of the Langfang Normal University, Langfang, China.

Terminology follows Kim and Heraty (2012). The following abbreviations are used in the text: F1–3, flagellomeres 1–3; Gt_1, Gt_2 etc., tergites 1, 2, etc. of gaster.

Phylogenetic analysis

DNA extraction, amplification, and sequencing

Genomic DNA extraction was from the entire body of female adults using the TIANGEN Genomic DNA Kit (Beijing, China) following the manufacturer's instructions. COI was amplified using the primers of LCO1490 (5'-GGTCAACAAATCATAAAGATATTGG-3') (Folmer et al. 1994), HCOout (5'-CCAGGTAAAATTAAAATATAAACTTC-3') (Carpenter 1999), and the PCR cycling profile followed the procedures in Huangfu et al. (2022). 28S-D2 rDNA was amplified using the primers of 3317F (5'-ACCCGCTGAATTTAAGCATAT-3') and 4283R (5'-TAGTTCACCATCTTTCGGGTCCC-3') (Hancock et al. 1988), and the PCR cycling profile followed the procedures in Qin et al. (2022). PCR amplifications were checked by electrophoresis in a 1% agarose gel, and the positive products were sent to Tianyi Huiyuan Biotechnology Co., Ltd (Beijing) for Sanger sequencing using an ABI 3730 automated sequencer. The raw AB1 data was corrected manually in BioEdit v. 7.0.9.0 (Hall 1999).

Phylogenetic analysis

Twenty-six sequences of 28S-D2 rDNA downloaded from GenBank, along with our two new sequences (for GenBank accession numbers see Table 1), representing 11 genera within three subfamilies of Aphelinidae were included in the analysis. Two species of *Coccophagus* (Coccophaginae) were chosen as outgroups.

Table 1. GenBank accessions for the 28S-D2 rDNA sequences used in the phylogenetic analyses.

Species	GenBank accession no.	Species	GenBank accession no.
Aphelinus albipodus	AY599361	*Eutrichosomella* sp.	AY640319
Aphelinus asychis	AY599362	*Marietta caridei*	MH455947
Aphelinus paramali	KF894417	*Marietta* sp.	AY599363
Aphytis melinus	JN623554	*Marietta* sp.	KF597646
Aphytis holoxanthus	AY635348	*Marietta leopardina*	AY635301
Aphytis nr. *africanus*	AY635347	*Marietta* nr. *marchali*	AY635300
Centrodora acridiphagus	AY635295	*Neophytis dealbatus*	AY635316
Centrodora nr. *penthimiae*	AY635297	*Neophytis melanostictus*	AY635317
Centrodora sp.	AY599366	*Neophytis* nr. *melanostictus*	AY635315
Coccophagus rusti	AY599377	*Proaphelinoides huangi* sp. nov.	PQ038115
Coccophagus sp.	AY599376	*Proaphelinoides huangi* sp. nov.	PQ038116
Eretmocerus eremicus	AY599369	*Neophytis dealbatus*	AY635316
Eretmocerus mundus	JF820004	*Neophytis melanostictus*	AY635317
Eretmocerus orchamoplati	JF750732	*Samariola* sp.	JN623552

These data were aligned with MAFFT v. 7.5 (Katoh and Standley 2013) and edited manually. Phylogenetic trees were constructed using Bayesian inference (BI) and maximum likelihood (ML). The BI analysis was performed with MrBayes v. 3.2.6 (Ronquist et al. 2012) using the best-fit model GTR+I+G which was selected by jModeltest v. 2.1.7 (Darriba et al. 2012) based on the Akaike information criterion. To ensure the average standard deviation of split frequencies was less than 0.01 in the BI analysis, two million generations were run with sampling every 1000 generations. The ML tree was obtained using RAxML v. 8.2.12 (Stamatakis 2014) with the GTRGAMMA model and the default rapid hill-climbing algorithm; support values were determined using 1000 bootstrap replicates. Both BI and ML trees were visualized and edited in Figtree v. 1.4.4 (Rambaut 2018).

Results

Key to species of *Proaphelinoides* (females)

1 Fore wing without a group of bristles below the proximal 1/3 of marginal vein; linea calva well defined, proximally bordered by 3 or 4 lines of setae............ **2**

– Fore wing with a group of bristles (Fig. 6); linea calva either absent or bordered by single line of setae...**3**

2 Antenna with scape 4.7× as long as wide; F3 (ventral length) 0.53× width, and with dorsal length equal to width; mid lobe of mesoscutum with 9 setae..***P. ematus* Hayat**

– Antenna with scape 4× as long as wide; F3 (ventral length) equal to width, and with dorsal length 1.5× as long as width; mid lobe of mesoscutum with 12–14 setae...***P. anomalus* Hayat**

3 Fore wing with linea calva defined by at least a line of setae **4**

– Fore wing with linea calva absent or not clearly defined (proximally without a complete line of setae) **7**

4 Linea calva proximally bordered by 2 lines of setae which become 3 lines in posterior third .... ***P. assamensis*** **Hayat**

– Linea calva proximally bordered by a single line of setae **5**

5 F3 clearly more than 1.2× as long as wide .... ***P. australis*** **Girault**

– F3 at most 1.2× as long as wide..**6**

6 Metasoma about as long as combined length of head and mesosoma, fore wing with a group of 7 or 8 long bristles below marginal vein, F3 and clava clearly darker than other antennomeres .... ***P. bendovi*** **Tachikawa**

– Metasoma longer than combined length of head and mesosoma, fore wing with 10–14 bristles below marginal vein, antennomeres concolorous...***P. huangi*** **sp. nov.**

7 Fore wing with a group of 15–17 long bristles below marginal vein .... ***P. elongatiformis*** **Girault**

– Fore wing with 30–35 bristles below marginal vein..................................... .... ***P. chidambaramensis*** **Manickavasagam & Menakadevi**

Proaphelinoides huangi **Chen & Jiang, sp. nov.**
https://zoobank.org/2EE3A0AC-66AC-41EC-B437-4E54733A094A
Figs 1–9

Type material. ***Holotype***: China • ♀; Yunnan Province; Xishuangbanna; Mengla County; Menglun Town; 21°53.89'N, 101°16.72'E; 568 m a.s.l.; 12 May. 2019; Z-l Bai, Z-g Chen, C Wang, H Yu leg.; LFNU Proap202405-1 [on slide]. ***Paratypes***: • 8 ♀♀ [5 ♀♀ on slides, Proap202405-2–Proap202405-7; • 2 ♀♀ destroyed for DNA extraction]; same data as holotype; LFNU.

Diagnosis. *Proaphelinoides huangi* sp. nov. can be distinguished from other species in this genus by the following combination of characters: antenna yellow, fore wing with 10–14 bristles below marginal vein, linea calva proximally bordered by a single line of setae, F3 1.0–1.2× as long as wide, the distance between posterior pair of setae of the mid lobe of mesoscutum more than the distance from a seta to later margin of the plate; the length of Gt_8 0.8× as long as the distance between two cercal plates.

Description. Female. Body length 0.9–1.2 mm (holotype, 1.2 mm).

***Colour*.** Head with face pale yellow, vertex orange, ocelli red and setae on vertex dark. Mandible brown to dark brown. Antenna yellow. Pronotum pale with brown suffusion. Dorsum of mesosoma yellow, except dark-brown posterior margin of mesoscutellum. Lateral sides of propodeum and mesopleuron brown yellow. Fore wing with following infuscate areas: two small patches below end of submarginal vein, a pale brown band below proximal third of marginal vein, a large area below stigmal vein (Fig. 6). Hind wing mostly hyaline, with slight infuscation below end of marginal vein (Fig. 7). Legs (Fig. 8) pale yellow, with metafemur infuscate dorsally. Gaster with anterior half of Gt_1, Gt_2 and Gt_8 pale, posterior half of Gt_1 pale brown, remaining tergites dark brown.

Head 0.8× as high as wide, with weakly reticulate sculpture. Vertex 0.3–0.4× the width of head, with approximately 14 setae. Ocellar triangle with apical angle obtuse. Mandible with three teeth (Fig. 3, inset). Face with 7 setae along inner margin of eyes. Antenna (Fig. 4) with scape 4.2–5.1× as long as wide; pedicle 1.4–1.8× as long as wide; F1 and F2 small and transverse, F1 0.6–0.7× as long as wide, with

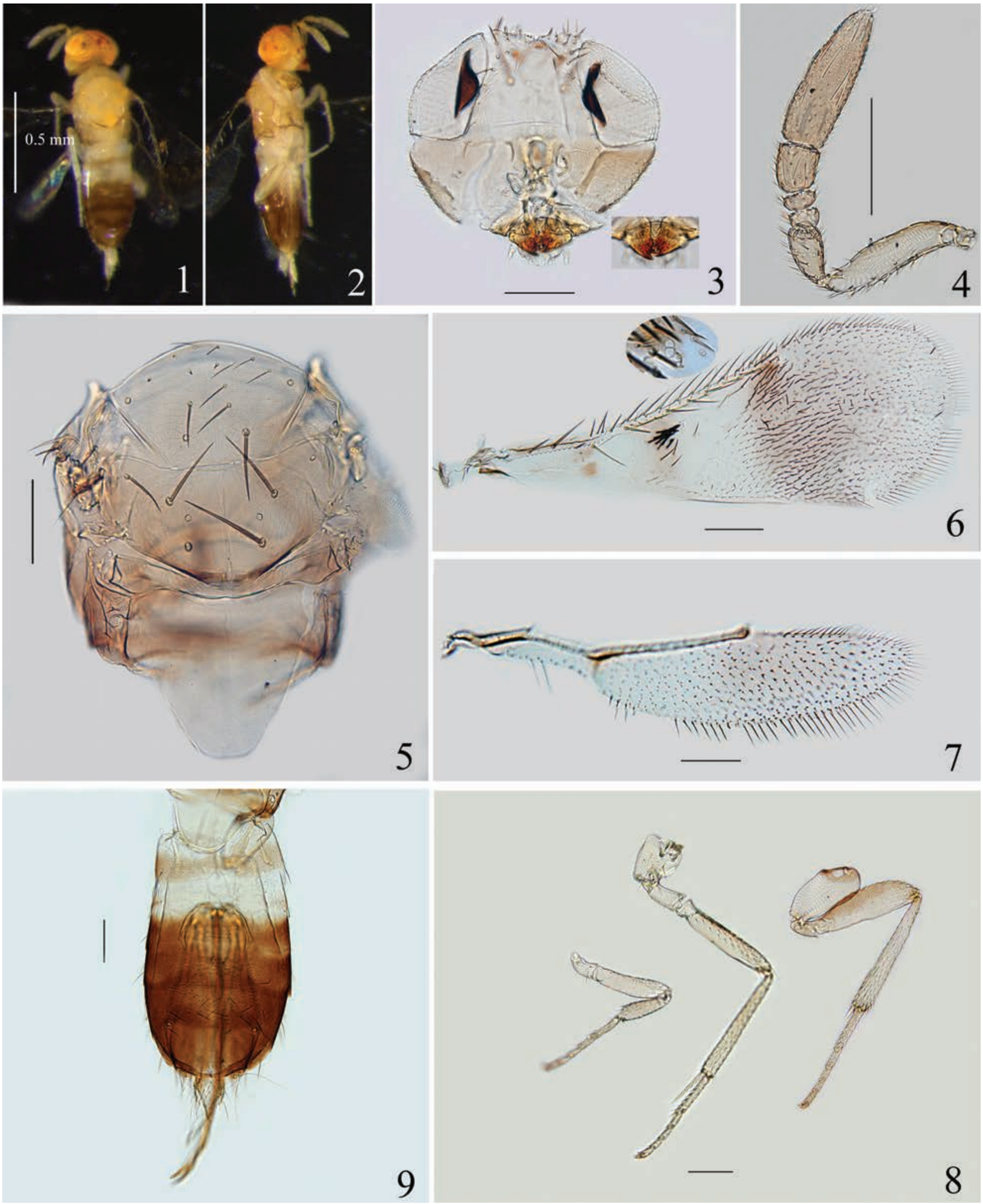

Figures 1–9. *Proaphelinoides huangi* sp. nov., holotype female (except Figs 1, 2, 5) **1** body, dorsal view **2** body, lateral view **3** head (inset: mandible) **4** antenna **5** mesosoma **6** fore wing (inset: stigmal vein) **7** hind wing **8** legs (left to right: fore-, mid- and hind-leg) **9** metasoma. Scale bars: 100 μm.

ventral margin a little longer than F2; F2 0.5× as long as wide; F3 1.0–1.2× as long as wide, with 3 longitudinal sensilla; clava 2.9× as long as wide, a little longer than combined length of pedicle and funicle, with 9–11 longitudinal sensilla.

Mesosoma. Mesoscutum with reticulate sculpture. Mid lobe of mesoscutum 0.8× as long as wide, with approximately 16 setae (Fig. 5), side lobe with 2 setae. Mesoscutellum 0.6× as long as wide, about as long as the mid lobe of mesoscutum, with 2 pairs of setae. The distance between anterior of scutellar setae 1.5× that between posterior pair. Placoid sensilla located in median region of mesoscutellum; distance between sensilla about equal to that between posterior scutellar setae. Metanotum narrow medially. Propodeum long, with median length 0.5× as long as mesoscutellum, with 3 or 4 setae proximal to each spiracle.

Wings. Fore wing (Fig. 6) 2.4–2.9× as long as wide. Costal cell 0.7× length of marginal vein, with 5 or 6 fine setae and 2 long setae distally; submarginal vein with 2 setae; parastigma with 1 seta; marginal vein with 10 setae along anterior margin; postmarginal vein short, about 0.5× as long as stigmal vein; basal cell with 2 setae below end of submarginal vein; 10–14 dark bristles present in a group below proximal third of marginal vein; linea calva proximally bordered by a single line of setae, and closed posteriorly by 1 line of setae. Hind wing (Fig. 7) 3.8–4.6× as long as wide, with longest marginal fringe 0.3× wing width.

Legs. Mesotibial spur about as long as corresponding basitarsus.

Metasoma. Metasoma about 1.5× as long as mesosoma measured from slide-mounted specimens. Gaster (Fig. 9) with setae on each tergite as follows: Gt_1–Gt_3 2 (left side) +2 (right side)), Gt_4 3+2, Gt_5 12–15 setae, arranged in 3 lines; Gt_6 1+1, Gt_7 1+1, Gt_8 with approximately 11 setae. Ovipositor originating from apex of Gt_2, clearly exerted, and 2.1–2.4× as long as mesotibia. The second valvifer 2.7–3.0× as long as third valvula, the latter 1.5× as long as mesobasitarsus.

Male. Unknown.

Host. Unknown.

Etymology. The specific name is derived from the family name of Jian Huang, in honor of his contribution to the taxonomic study of Aphelinidae from China.

Distribution. China (Yunnan).

Comments. This new species resembles *P. bendovi*, and the differences between *P*. *huangi* sp. nov. and that species are shown in the key. Also, this species is similar to *P. elongatiformis*, and the differences are as follows: (1) fore wing with 10–14 bristles below proximal third of marginal vein (15–17 setae in *P. elongatiformis*); (2) linea calva proximally bordered by a complete line of setae (Fig. 6) (not complete in *P. elongatiformis*); (3) the distance between posterior pair of setae of the mid lobe of mesoscutum more than the distance from a seta to later margin of the plate (less than in *P. elongatiformis*); (4) the length of Gt_8 0.8× as long as the distance between two cercal plates (1.2× in *P. elongatiformis*, measurements based on fig. 12 in Hayat 1984). This new species seems difficult to distinguish from *P. australis and P. assamensis*. The species differs from *P. australis* by: (1) F3 1.0–1.2× as long as wide (F3 1.5× as long as wide in *P. australis*); (2) the length of Gt_8 0.8× as long as the distance between two cercal plates (Gt_8 notably longer, 1.8× in *P. australis*); (3) ovipositor 2.1–2.4× as long as mesotibia (2.6× in *P. australis*). From *P. assamensis*, the species can be distinguished by: (1) fore wing with 10–14 dark bristles below proximal third of marginal vein (17–20 in *P. assamensis*); (2) linea calva proximally bordered by a single line of setae (bordered by 2 lines of setae which become 3 lines in posterior third in *P. assamensis*); (3) Gt_8 0.8× as long as the distance between two cercal plates (as long as in *P. assamensis*); (3) ovipositor originates from apex of Gt_2 (ovipositor originates from posterior half of Gt_1 in *P. assamensis*).

Phylogenetic analysis

The phylogenetic relationship between *Proaphelinoides* and other genera is shown in Fig. 10 (BI tree) and Suppl. material 1 (ML tree). *Proaphelinoides* was strongly supported as the sister group to *Aphytis* in both BI and ML analysis with 100 posterior probability and 92% bootstrap support, respectively. The tribe Aphytini was recovered as polyphyletic in both analyses (Fig. 10, Suppl. material 1), which is consistent with the result of Kim and Heraty (2012). In our analysis, this result of Eretmocerinae as the sister group of Aphelininae is congruous with the suggestion of Cruaud et al. (2024). More taxon and gene sampling should be added to further elucidate the systematic relationships within Aphelininae and Aphelinidae.

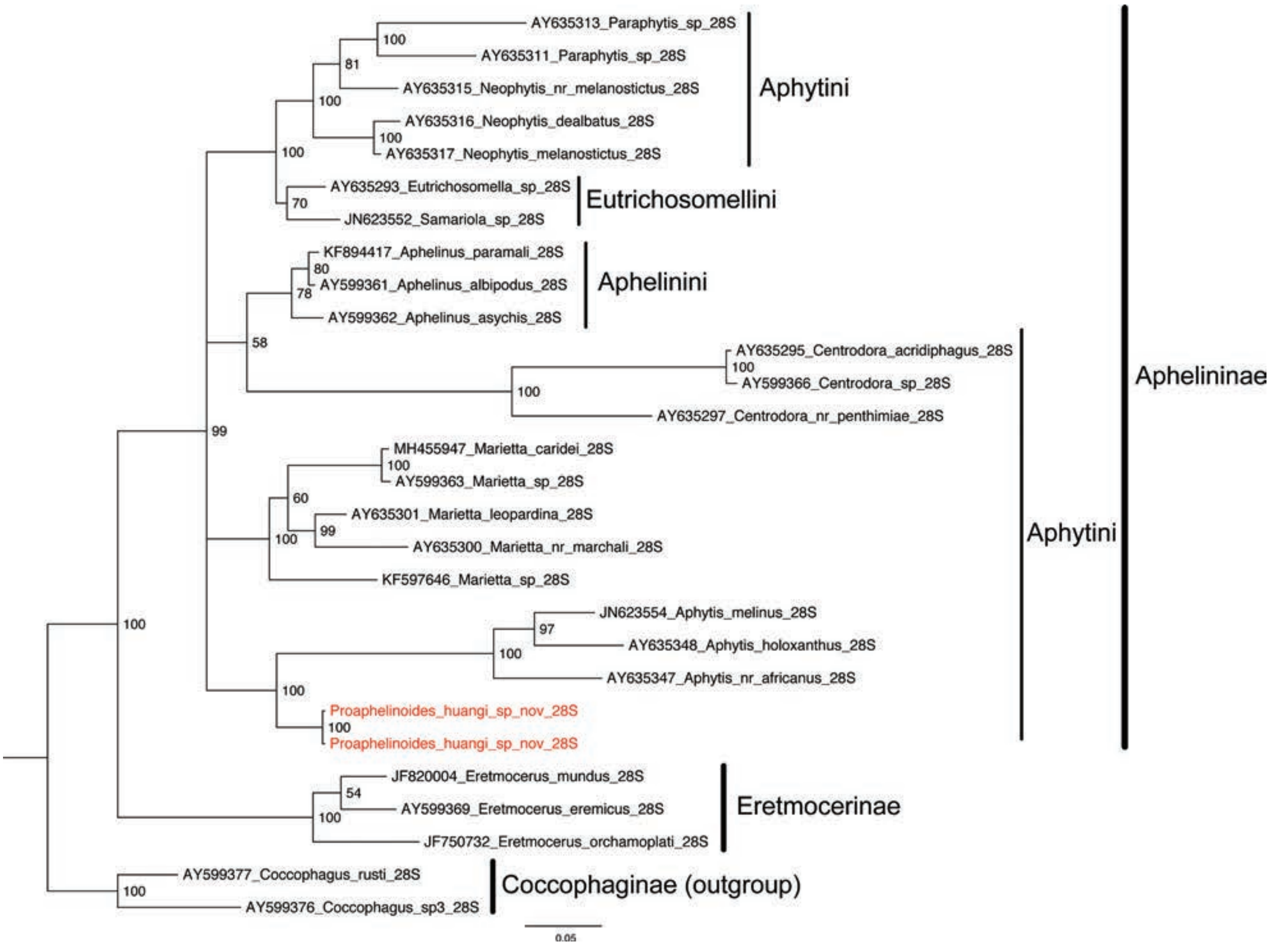

Figure 10. Bayesian phylogenetic tree of Aphelininae based on 28S-D2 rDNA. *Proaphelinoides huangi* sp. nov. is colored by red.

Acknowledgements

We thank three reviewers (Andrew Polaszek, Jason Mottern, and one anonymous reviewer) and the subject editor for providing valuable comments on earlier drafts of this manuscript. We are grateful to Professor Shu-qiang Li (Chinese Academy of Sciences, Beijing) for providing the materials. Special thanks to Professor Zhu-hong Wang (Fujian Agriculture and Forestry University) for her kind help of sending some papers by e-mail. We thank our colleague Dr Yao-guang Qin for his linguistic review.

Additional information

Conflict of interest

The authors have declared that no competing interests exist.

Ethical statement

No ethical statement was reported.

Funding

This study was supported by the Science and Technology Project of Hebei Education Department (BJK2024178), the Doctoral Scientific Research Foundation of Langfang Normal University (XBQ202034) to Ye Chen, and the Outstanding Youth Science Foundation of Langfang Normal Universtiy (JYQ202402) to Huifeng Zhao.

Author contributions

Conceptualization: YC. Formal analysis: HZ. Software: HZ. Writing - original draft: YJ. Writing - review and editing: YC.

Author ORCIDs

Huifeng Zhao https://orcid.org/0000-0003-4243-9671
Ye Chen https://orcid.org/0000-0003-0841-6775

Data availability

All of the data that support the findings of this study are available in the main text or Supplementary Information.

References

Carpenter JM (1999) Towards simultaneous analysis of morphological and molecular data in Hymenoptera. Zoologica Scripta 28: 251–260. https://doi.org/10.1046/j.1463-6409.1999.00009.x

Chen Y, Chen HF (2021) First report of *Eutrichosomella* Girault (Hymenoptera, Aphelinidae) from China, with description of a new species. ZooKeys 1071: 1–9. https://doi.org/10.3897/zookeys.1071.71909

UCD Community (2023) Universal Chalcidoidea Database Website. https://ucd.chalcid.org [accessed 13 July 2024]

Cruaud A, Rasplus JY, Zhang JX, Burks R, Delvare G, Fusu L, Fusu L, Gumovsky A, Huber JT, Janšta P, Mitroiu MD, Noyes JS, van Noort S, Baker A, Böhmová J, Baur H, Blaimer BB, Brady SG, Bubeníková K, Chartois M, Copeland RS, Dale-Skey Papilloud N, Dal Molin A, Dominguez C, Gebiola M, Guerrieri E, Kresslein RL, Krogmann L, Lemmon EM, Murray ES, Nidelet S, Nieves-Aldrey JL, Perry RK, Peters RS, Polaszek A, Sauné L, Torréns J, Triapitsyn S, Tselikh EV, Yoder M, Lemmon AR, Woolley JB, Heraty JM (2024) The Chalcidoidea bush of life: evolutionary history of a massive radiation of minute wasps. Cladistics 40 (1): 34–63. https://doi.org/10.1111/cla.12561

Darriba D, Taboada GL, Doallo R, Posada D (2012) jModelTest 2: more models, new heuristics and parallel computing. Nature Methods 9: 772. https://doi.org/10.1038/nmeth.2109

Folmer O, Black M, Hoeh W, Lutz R, Vrijenhoek R (1994) DNA primers for amplification of mitochondrial cytochrome c oxidase subunit I from diverse metazoan invertebrates. Molecular Marine Biology and Biotechnology 3: 294–299.

Girault AA (1917) Descriptiones stellarum novarum, 22 pp. [Published by the author]

Girault AA (1922) New chalcid flies from eastern Australia (Hymenoptera, Chalcididae). II. Insecutor Inscitiae Menstruus 10: 100–108.

Hall T (1999) BioEdit: a user-friendly biological sequence alignment editor and analysis program for Windows 95/98/NT. Nucleic Acids Symposium Series 41: 95–98. https://doi.org/10.1021/bk-1999-0734.ch008

Hancock JM, Tautz D, Dover GA (1988) Evolution of the secondary structures and compensatory mutations of the ribosomal RNAs of *Drosophila melanogaster*. Molecular Biology and Evolution 5: 393–414. https://doi.org/10.1093/oxfordjournals.molbev.a040501

Hayat M (1984) The genus *Proaphelinoides* from India (Hymenoptera: Aphelinidae). Oriental Insects 18: 73–78. https://doi.org/10.1080/00305316.1984.10432196

Hayat M (1998) Aphelinidae of India (Hymenoptera: Chalcidoidea): A taxonomic revision. Memoirs on Entomology, International 13: 1–416.

Hayat M (2012) Records and descriptions of some Aphelinidae (Hymenoptera: Chalcidoidea) from India. Zootaxa 3521: 39–50. https://doi.org/10.11646/zootaxa.3521.1.2

Hayat M, Veenakumari K (2016) Description of three new species of Aphelinidae (Hymenoptera: Chalcidoidea) with some records from India. Journal of Insect Systematics 2(2): 106–119. https://doi.org/10.11646/zootaxa.3990.2.6

Heraty JM, Burks RA, Cruaud A, Gibson GA, Liljeblad J, Munro JB, Rasplus JY, Delvare G, Janšta P, Gumovsky A, Huber JT, Woolley JB, Krogmann L, Heydon SL, Polaszek A, Schmidt S, Darling DC, Gates M, Mottern J, Murray E, Dal Molin A, Triapitsyn SV, Baur H, Pinto JD, Van Noort S, George JN, Yoder MJ (2013) A phylogenetic analysis of the megadiverse Chalcidoidea (Hymenoptera). Cladistics 29: 466–542. https://doi.org/10.1111/cla.12006

Huangfu N, Cao HX, Zhu CD (2022) Notes on the genus *Aceratoneuromyia* Girault (Hymenoptera: Eulophidae). Insects 13: 450. https://doi.org/10.3390/insects13050450

Katoh K, Standley DM (2013) MAFFT multiple sequence alignment software version 7: improvements in performance and usability. Molecular Biology and Evolution 30: 772–780. https://doi.org/10.1093/molbev/mst010

Kim JW, Heraty J (2012) A phylogenetic analysis of the genera of Aphelininae (Hymenoptera: Aphelinidae), with a generic key and descriptions of new taxa. Systematic Entomology 37(3): 497–549. https://doi.org/10.1111/j.1365-3113.2012.00625.x

Menakadevi C, Manickavasagam S (2012) A new species of *Proaphelinoides* Girault (Hymenoptera: Aphelinidae) with a key to world species and additional records from Tamil Nadu, India. Zootaxa 3193: 62–68. https://doi.org/10.11646/zootaxa.3193.1.4

Noyes JS (1982) Collecting and preserving chalcid wasps (Hymenoptera: Chalcidoidea). Journal of Natural History 16: 315–334. https://doi.org/10.1080/00222938200770261

Qin YG, Chen HF, Li CD, Chen Y (2022) On the genus *Coccophagus* Westwood (Hymenoptera, Aphelinidae) from Xishuangbanna Rainforest. Contribution I: Two new species of the *Coccophagus varius* group, with an identification key and phylogenetic analysis. ZooKeys 1091: 119–138. https://doi.org/10.3897/zookeys.1091.80065

Rambaut (2018) Figtree 1.4.4. http://tree.bio.ed.ac.uk/software/figtree/ [accessed 10 July 2024]

Ronquist F, Teslenko M, van der Mark P, Ayres DL, Darling A, Hohna S, Larget B, Liu L, Suchard MA, Huelsenbeck JP (2012) MrBayes 3.2: efficient Bayesian phylogenetic inference and model choice across a large model space. Systematic Biology 61: 53942. https://doi.org/10.1093/sysbio/sys029

Si Y, Huang J, Ge JQ, Zheng HN, Li PL, Wang ZH (2019) The genus *Proaphelinoides* Girault and a newly recorded species (Hymenoptera: Aphelinidae) from China. Journal of Fujian Agriculture and Forestry University (Natural Science Edition) 48(3): 291–295.

Stamatakis A (2014) RAxML version 8: a tool for phylogenetic analysis and post-analysis of large phylogenies. Bioinformatics 30: 1312–1313. https://doi.org/10.1093/bioinformatics/btu033

Tachikawa T (1984) Notes on the genus *Proaphelinoides* Girault (Hymenoptera: Chalcidoidea, Aphelinidae). Transactions of the Shikoku Entomological Society 16: 49–53.

Supplementary material 1

Maximum likelihood phylogenetic tree of Aphelininae based on 28S-D2 rDNA

Authors: Huifeng Zhao

Data type: tif

Link: https://doi.org/10.3897/zookeys.1217.132291.suppl1

ZooKeys 1217: 273–290 (2024)
DOI: 10.3897/zookeys.1217.126602

Research Article

Boreolimnus, a new leafhopper genus from northern North America, with a review of *Cribrus* Oman (Hemiptera, Cicadellidae, Deltocephalinae)

Joel H. Kits[1]

1 *Canadian National Collection of Insects, Arachnids, and Nematodes, Ottawa Research and Development Centre, Agriculture and Agri-Food Canada, Ottawa, Canada*
Corresponding author: Joel H. Kits (joel.kits@agr.gc.ca)

Abstract

The poorly known leafhopper species described as *Deltocephalus* (*Laevicephalus*) *concinnus* var. *incisurus* DeLong, 1926 previously had no accepted generic placement. It is here redescribed and placed in *Boreolimnus* **gen. nov.** in the tribe Paralimnini, as *Boreolimnus incisurus* (DeLong) **comb. nov.** *Cribrus micmac* Hamilton, 1987 is a junior **syn. nov.** of *B. incisurus*. Due to historic confusion, the species currently placed in *Cribrus* Oman, 1949 were also reviewed. *Cribrus concinnus* (Sanders & DeLong, 1917) is redescribed, and a lectotype is designated to clarify the application of the name. *Deltocephalus plagus* Ball & DeLong, 1926 and *Laevicephalus shingwauki* Beamer & Tuthill, 1934 are recognized as junior **syn. nov.** of *C. concinnus*, now the only recognized species in the genus.

Key words: COI barcodes, morphology, new genus, Paralimnini, phylogeny

Academic editor:
J. Adilson Pinedo-Escatel
Received: 30 April 2024
Accepted: 5 August 2024
Published: 7 November 2024

ZooBank: https://zoobank.org/9FEA1FAE-E60C-42FA-AB32-91E73F7D9C6B

Citation: Kits JH (2024) *Boreolimnus*, a new leafhopper genus from northern North America, with a review of *Cribrus* Oman (Hemiptera, Cicadellidae, Deltocephalinae). ZooKeys 1217: 273–290. https://doi.org/10.3897/zookeys.1217.126602

Introduction

The leafhopper taxon described by DeLong (1926) as *Deltocephalus* (*Laevicephalus*) *concinnus* var. *incisurus* has received little notice in the literature. DeLong described the taxon from a single specimen from Wisconsin. DeLong and Caldwell (1937) first treated *Laevicephalus* DeLong as a full genus, including this species as *L. concinnus* var. *incisurus*. Beamer (1938) later treated it as a full species and described the male genitalia based on additional material from Manitoba. Oman (1949) listed the species as unplaced within a broadly defined Deltocephalini. Ross and Hamilton (1972) recognized *Latalus hultus* Beirne as a junior synonym of *D. incisurus* and excluded the species from *Laevicephalus*, but they did not provide a new combination. It does not appear to have been mentioned in the literature since.

Deltocephalus incisurus belongs to the tribe Paralimnini as delimited by Zahniser and Dietrich (2013), based on the linear connective articulated with the aedeagus. This is a very diverse group of leafhoppers, with over 139 genera recognized (Zahniser and Dietrich 2013); 35 of these genera occur in the Nearctic region. There is currently no global treatment covering all genera in the tribe, but keys, descriptions, and illustrations in regional works (Oman 1949; Ribaut

1952; Ossiannilsson 1983; Anufriev and Emeljanov 1988; Emeljanov 1999; Li et al. 2011) suggest *D. incisurus* does not belong to any Nearctic or Palearctic genus as currently defined; thus, it is here placed in a new genus.

Although *D. incisurus* is clearly distinct from the Nearctic paralimnine genus *Cribrus* Oman based on male and female genitalia and wing venation, they share similar colour patterns and there has been previous confusion between the two. The holotype of *D. incisurus* is one of the two syntypes of *Cribrus concinnus* (Sanders & DeLong), and examination of the holotype and only known specimen of *Cribrus micmac* Hamilton showed that it is conspecific with *D. incisurus*. Thus, the other species currently placed in *Cribrus* were also reviewed to determine whether they are correctly placed and clarify their taxonomy.

While morphological evidence suggests that both genera examined here are distinct from other Paralimnini, molecular evidence was also examined as a further test of their status. The most comprehensive phylogeny of the Paralimnini is that of Cao et al. (2022), but neither of the taxa studied here were included. The only molecular data available for the two taxa is from the cytochrome oxidase I (COI) gene; hence, newly generated and previously published data for this gene were gathered from a number of Paralimnini in order to generate a phylogeny.

Methods

Depositories of types and other specimens examined are as follows

CNC	Canadian National Collection of Insects, Arachnids, and Nematodes (Ottawa, Ontario, Canada)
INHS	Illinois Natural History Survey Insect Collection (Champaign, Illinois, USA)
OSUC	C.A. Triplehorn Insect Collection, The Ohio State University (Columbus, Ohio, USA)
SEMC	Snow Entomological Museum Collection, University of Kansas (Lawrence, Kansas, USA)
USNM	Smithsonian National Museum of Natural History (Washington, DC, USA)

Images were taken using a Leica M205C stereomicroscope with 1.6× objective (Leica Microsystems GmbH, Wetzlar, Germany), with infinity-corrected 5× or 10× objectives (Mitutoyo Corp., Kawasaki, Japan) mounted on a Canon R10 camera (Canon Inc., Tokyo, Japan) via a Thorlabs ITL200 tube lens (Thorlabs Inc., Newton, NJ, USA), or Nikon Eclipse E800 compound microscope with 10× or 20× objectives (Nikon Corp., Tokyo, Japan). Images were stacked using Zerene Stacker (Zerene Systems, Richland, WA, USA), edited using Adobe Photoshop CS6, and assembled into plates using Adobe Illustrator CS6 (Adobe Inc., San Jose, CA, USA). Morphological terminology follows Dietrich (2005).

Additional occurrence data for mapping *Cribrus* distribution were obtained from INHS (McElrath 2023) and from Jim Bess (pers. comm. 2024). All locality data with georeferences is in Suppl. material 2. Maps were created using QGIS 3.20.0 (QGIS.org).

COI sequences from CNC specimens were generated as described by Foottit et al. (2014) and Kits (2023). Additional sequences from genera not represented in the CNC dataset were downloaded from GenBank. A sequence from

Maiestas dorsalis (Motschulsky), in the sister tribe Deltocephalini (Cao et al. 2022), was used to root the tree. Sequences were aligned using MAFFT 7.520 (Katoh and Standley 2013) and analysed using maximum likelihood in IQTREE 2.3 (Nguyen et al. 2015), with the model GTR+F+I+R5 selected by ModelFinder (Kalyaanamoorthy et al. 2017). Support values were calculated with 1000 rounds of ultrafast bootstrap (Hoang et al. 2018) and 1000 rounds of the Shimodaira-Hasegawa-like approximate likelihood-ratio test (SH-aLRT) (Guindon et al. 2010).

Results

Sequences were obtained from 44 genera and 160 species of Paralimnini (Suppl. material 3). The phylogenetic analysis resolved most included genera as monophyletic with high support where multiple species were sampled (Fig. 1, Suppl. material 1). Exceptions include *Sorhoanus* Ribaut (polyphyletic with three distantly related clades), *Laevicephalus* (paraphyletic with respect to *Giprus* Oman and *Triasargus* Novikov & Anufriev, and with *L. monticola* (Gillette & Baker) distant from the main clade), and *Flexamia* DeLong (*F. grammica* (Ball) not recovered in the main clade).

Relationships between genera were generally only moderately or poorly resolved. *Boreolimnus incisurus* was resolved as sister to *Rosenus* Oman with fairly high support (95% bootstrap, 61 SH-aLRT). *Cribrus concinnus* was resolved in a clade with *Lebradea* Remane and part of *Sorhoanus* with high support (90% bootstrap, 83 SH-aLRT), with a sister relationship to the latter weakly supported (19% bootstrap, 72 SH-aLRT).

Taxonomic treatment

***Boreolimnus* gen. nov.**

https://zoobank.org/A2032F89-FA96-4946-87CA-77064621B4A3

Type species. *Deltocephalus* (*Laevicephalus*) *concinnus* var. *incisurus* DeLong, 1926 (here designated)

Etymology. The name is derived from the Greek βορέας (north) and λίμνη (marsh), describing the habitat of the type species. The gender is masculine.

Diagnosis. Separated from other genera of Paralimnini by the following combination of characters: male subgenital plates with uniseriate macrosetae, plates as long as pygofer and tapering to a narrow rounded apex; pygofer with a process on postero-ventral margin, process nearly straight; segment X about as long as wide, broadly scerotized laterally and narrowly sclerotized dorsally; connective linear and elongate with arms fused in a stem which is about as broad as long (connective loop-shaped sensu Emeljanov (1999)); aedeagus broad and dorsoventrally flattened with subapical ventral gonopore and one pair of pre-apical processes; frontoclypeus and pronotum with longitudinal stripes; wings macropterous, fore wing with outer anteapical cell short and closed by distal fusion of veins R2+3 and R4+5 or absent.

Description. Small leafhoppers with typical Paralimnini structure. Colour generally stramineous, head and pronotum with longitudinal stripes, wing with brown infuscation around cell borders (Figs 2–5).

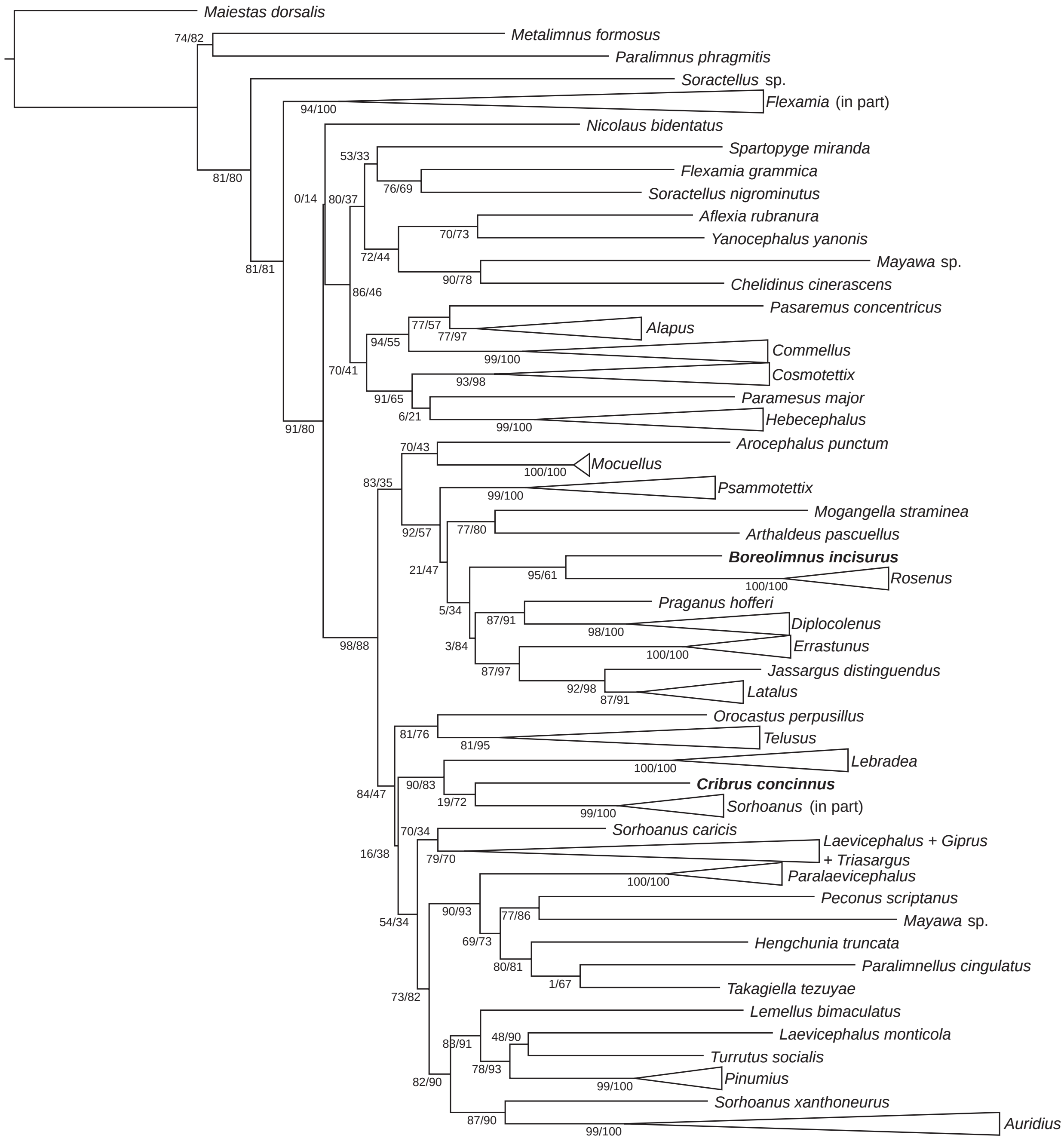

Figure 1. Maximum-likelihood tree of Paralimnini, based on 658 base pairs of cytochrome oxidase I. Selected clades collapsed to illustrate overall structure. Support values at nodes are bootstrap/SH-aLRT.

Head with crown bluntly angled, medial length about 1.5× width between eyes (Fig. 2). Crown glabrous with fine striations on basal 2/3, distal 1/3 of crown and face shagreen. Lateral frontal sutures terminating lateral of ocelli, ocelli about 2× their own diameter from eye (Fig. 5). Mesal margin of eye notched. Anteclypeus with margins nearly straight, slightly tapered pre-apically. Lorum about 3/5 width of anteclypeus, well separated from genal margin. Antennae about as long as head width.

Pronotum slightly narrower than width of head across eyes, slightly longer than medial length of head. Fore femur with AM1 near ventral margin, row IC with a few fine setae, row AV consisting of a few, widely spaced, very short setae. Fore tibia with 1 AD and 4 PD macrosetae. Hind femur with 2+2+1 macrosetae. First hind tarsomere with two rows of plantar setae, four apical platellae between a pair of normal setae. Fore wing usually with three closed anteapical cells; outer anteapical cell short and closed by distal fusion of R2+3 and R4+5 or occasionally absent.

Male abdomen with apodemes on sternite II about twice as long as wide, apical half transparent, strongly curved dorsally. Pygofer about as long as wide, with a triangular distal lobe and a sclerotized process from posteroventral corner; with a patch of long macrosetae posterodorsally and shorter fine macrosetae scattered ventrally (Figs 6, 7). Segment X about as long as wide, heavily sclerotized laterally, the sclerotized portions narrowly connected posteriorly and separated by a V-shaped unsclerotized area medially. Valve parabolic. Subgenital plates as long as pygofer, subtriangular, with a narrowly rounded apex, bearing a single row of macrosetae (Fig. 8). Connective with arms nearly parallel, slightly bowed outwards towards anterior end and fused anteriorly, stem broadened apically, wider than arms and about as long as broad. Style apophysis with lateral lobe prominent, medial lobe with rounded teeth ventrally. Aedeagus dorsoventrally flattened with subapical ventral gonopore and one pair of pre-apical processes (Figs 9, 10).

Female pygofer with moderate length macrosetae (Fig. 11). Ovipositor not projecting beyond pygofer. Gonoplac without macrosetae. First valvula slightly concave; sculpture imbricate dorsally and strigate ventrally (Fig. 13). Second valvulae evenly tapered distally, with fine irregular dorsal teeth (Fig. 14).

Remarks. *Boreolimnus* runs to *Latalus* in the keys of both Oman (1949) and Beirne (1956), but can be distinguished by several characters (alternative states in parentheses): outer anteapical cell reduced and closed by fusion of R2+3 and R4+5 (well developed and closed by crossvein s), connective narrow and nearly linear, with the posterior plate the widest part (connective broad and widest across the arms), aedeagus dorsoventrally flattened (aedeagus tubular, not flattened), frontoclypeus with longitudinal stripes (frontoclypeus with pale transverse markings separating darker areas). In Emeljanov (1999), it keys to couplet 300/307 but does not match either alternative well. In Ossiannilsson (1983) it keys best to *Lebradea*, from which is differs in the following characters: segment X about as long as wide (segment X about twice as long as wide), connective with arms connected posteriorly by a broad and long plate-like stem (connective with arms connected by a narrow bar-like stem posteriorly), stramineous with longitudinal stripes on frontoclypeus and pronotum and brown infuscation around wing cells (mostly bright yellow with black areas, no longitudinal stripes or infuscation on wing).

Boreolimnus incisurus (DeLong), comb. nov.

Figs 2–24

Deltocephalus (*Laevicephalus*) *concinnus* var. *incisurus* DeLong, 1926: 77
Laevicephalus concinnus var. *incisurus* (DeLong). Comb. DeLong and Caldwell 1937.
Laevicephalus incisurus (DeLong, 1926). Rev. stat. Beamer 1938.
= *Latalus hultus* Beirne, 1954: 123. Syn. Ross and Hamilton 1972.
= *Cribrus micmac* Hamilton in Hamilton and Langor 1987: 669. New synonym.

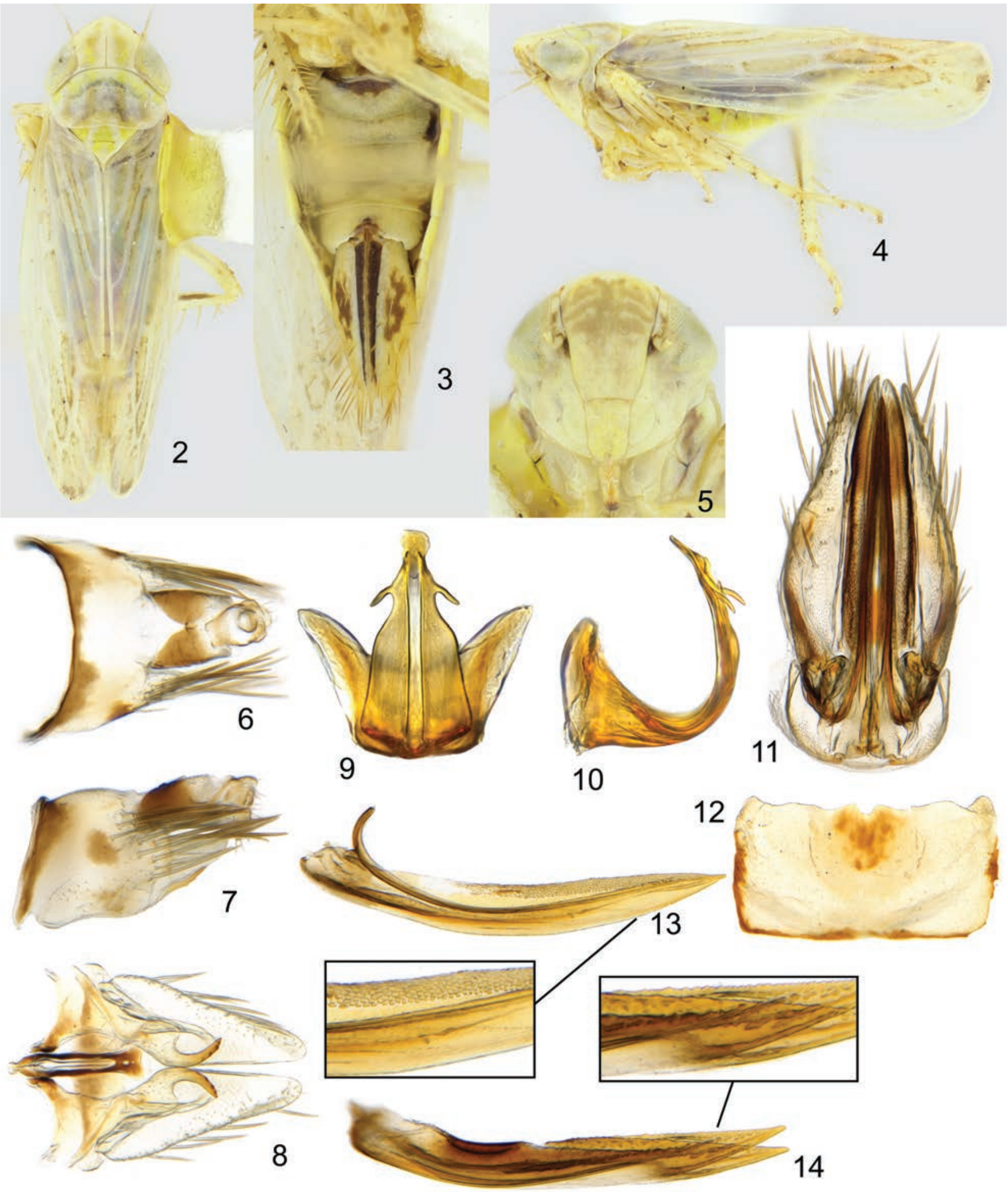

Figures 2–14. *Boreolimnus incisurus* **2** dorsal habitus **3** lateral habitus **4** abdomen ventral, female **5** face **6** male pygofer, dorsal **7** male pygofer, lateral **8** male subgenital plate, styles, connective, dorsal **9** aedeagus, caudal **10** aedeagus, lateral **11** female genital capsule, ventral **12** female sternite VII, ventral **13** first valvifer, lateral, with enlargement **14** second valvifers, lateral, with enlargement.

Description. Males 3.1–3.4 mm. Females 3.2–3.6 mm.

Colour mostly pale straw to light yellow, with two longitudinal stripes on crown and four longitudinal stripes on pronotum in a deeper yellow colour usually apparent. Palest specimens with dark colour restricted to basal tergites and spots at bases of leg macrosetae. Darker specimens may have light to dark brown markings medially on frontoclypeus (interrupted laterally by pale horizontal lines), in antennal pits, on anepisternum, medially on abdominal tergites, on base of sternite II and laterally on all sternites, and on pygofer. Fore wing milky white with brown infuscation around border of some cells.

Male pygofer process short, originating on postero-ventral margin and extending slightly dorsally. Process typically with two small teeth on ventral margin. Subgenital plates bearing a single row of approximately eight macrosetae laterally. Style with lateral lobe of apophysis quadrately rounded, medial lobe of apophysis sickle-shaped, with four or five widely spaced, rounded teeth ventrally. Aedeagus in lateral view dorsoventrally flattened, strongly curved anterodorsally, extending slightly dorsally of atrium. Atrium in posterior view with deep and broad dorsal excavation; shaft in posterior view broad, narrowing preapically, with a single pair of lateral processes just before apex, terminating in a round plate above gonopore.

Female sternite VII rectangular, posterior margin with slight, rounded projections medially and laterally and gently convex in between, medial projection with a small emargination surrounded by a dark area (Fig. 12). Gonoplac mostly dark. Base of first valvula in ventral view truncate (Fig. 11).

Material examined. ***Holotype*** of *Deltocephalus incisurus* DeLong. USA • ♀; Wisconsin, Ladysmith; 9 Aug. 1916; D.M. DeLong leg.; OSUC, OSUC 870278.

Holotype of *Latalus hultus* Beirne. CANADA • ♂; Manitoba, Birch River; 13 Aug. 1930; R.H. Handford leg.; CNC, CNC1197446.

Holotype of *Cribrus micmac* Hamilton. CANADA • ♀; Nova Scotia, Cape Breton Highlands National Park, Paquet's Lake; 27 Aug. 1983; M. Sharkey leg.; CNC, CNC#HEM403381.

Other material. CANADA – **Alberta** • 1 ♂; Beaverlodge; 1 Aug. 1961; A.R. Brooks leg.; CNC • 1 ♀; Grande Prairie; 25 Jul. 1961; A.R. Brooks leg.; CNC • 1 ♂; High Prairie; 16 Jul. 1961; A.R. Brooks leg.; CNC • 20 ♂, 12 ♀, 1 (no abdomen); same collection data as previous; 17 Jul. 1961; CNC • 18 ♂, 16 ♀, 2 (intersex); same collection data as previous; 22 Jul. 1961; CNC • 1 ♂; same collection data as previous; 25 Jul. 1961; CNC • 1 ♀; same collection data as previous; 26 Jul. 1961; CNC • 3 ♂, 1 ♀; Peace River; 12 Jul. 1961; A.R. Brooks leg.; CNC • 1 ♂, 7 ♀, 1 (intersex); Valleyview; 10 Aug. 1961; A.R. Brooks leg; CNC. – **New Brunswick** • 1; Kouchibouguac National Park; 16 Aug. 1977; S.J. Miller leg.; CNC. – **Ontario** • 1 ♀; 10 mi E Nipigon; 12 Aug. 1975; K.G.A. Hamilton leg.; CNC • 1 ♀; 4 mi S Beardmore; 12 Aug. 1975; K.G.A. Hamilton leg.; from *Calamagrostis canadensis*; CNC • 28 (unmounted specimens in a capsule); Sault Sainte Marie; 10 Aug. 1975; K.G.A. Hamilton leg.; from *Carex* sp.; CNC. – **Saskatchewan** • 4 ♀; Candle Lake; 19 Aug. 1959; A. & J. Brooks leg.; CNC. – **Manitoba** • 1 ♀; The Pas; 30 Aug. 1959; A. & J. Brooks leg.; CNC.

Remarks. The holotype of *Deltocephalus incisurus* (Figs 15–18) was not previously labelled as such in the OSUC collection. The red "paratype" label and blue "incisurus" label were both probably added by later workers. However, it seems clear this is the holotype, as it matches the locality data, description, and illustrations in DeLong (1926). This specimen is also presumably one of the two syntypes of *Deltocephalus concinnus* Sanders & DeLong, based on the labels which match the data in the original description and the fact that no other

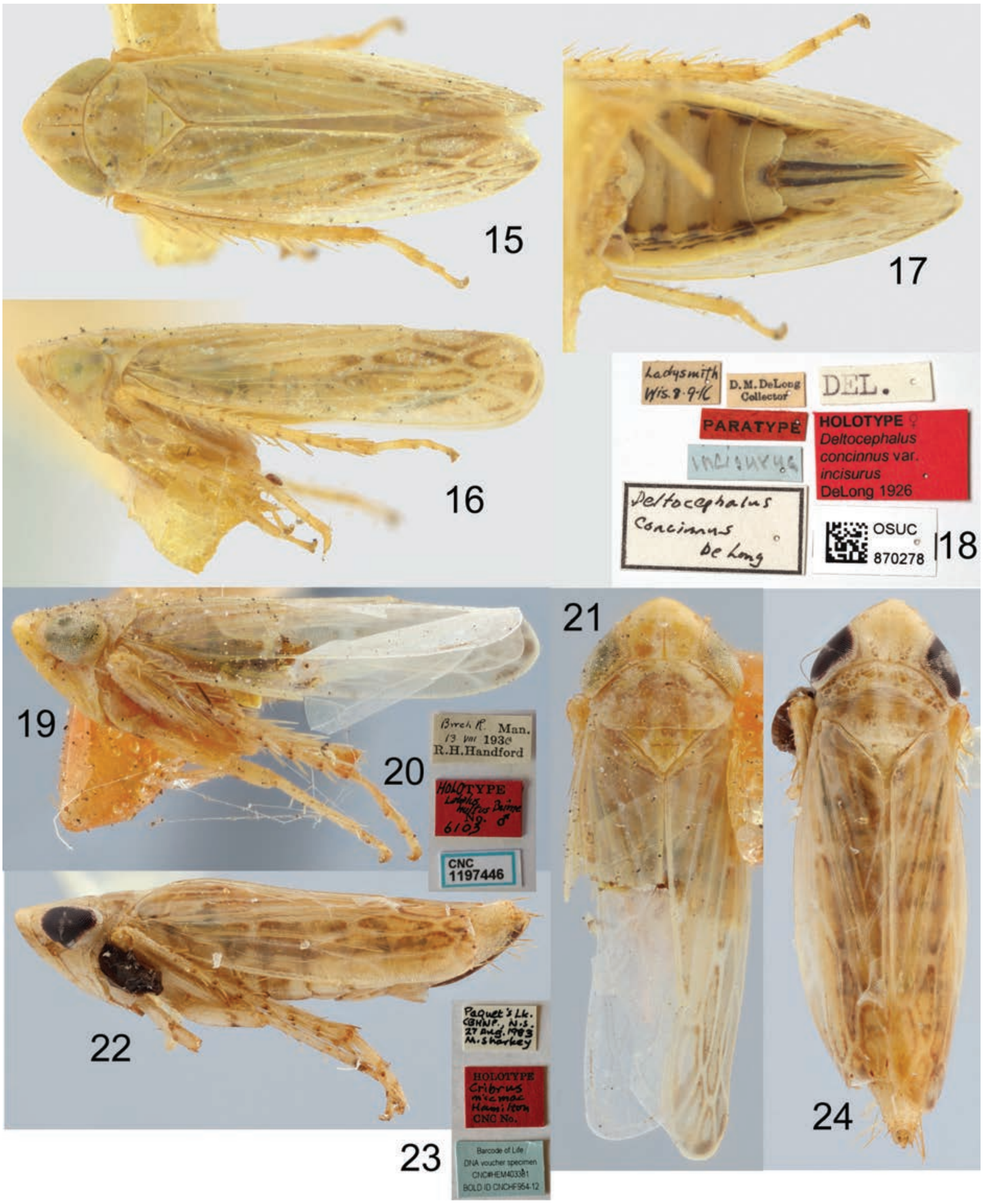

Figures 15–24. *Boreolimnus incisurus* and synonyms, primary types **15–18** *Deltocephalus concinnus* var. *incisurus* DeLong, holotype **15** dorsal habitus **16** lateral habitus **17** abdomen, ventral **18** labels **19–21** *Latalus hultus* Beirne, holotype **19** lateral habitus **20** labels **21** dorsal habitus **22–24** *Cribrus micmac* Hamilton, holotype **22** lateral habitus **23** labels **24** dorsal habitus.

potential syntypes could be located in DeLong's collection (L. Musetti pers. comm. 2022). As I am designating the other syntype as lectotype of *D. concinnus* (see below), this specimen becomes a paralectotype of the latter species.

The holotype of *Latalus hultus* (Figs 19–21) has been dissected, and matches other males of this species. The original description (Beirne 1954a) did not include collection details for the holotype; these were provided in an erratum (Beirne 1954b). The latter also mentions a paratype which could not be located in the CNC; its whereabouts are unknown.

The holotype of *Cribrus micmac* (Figs 22–24) has the fore wings reaching about the middle of the genital segment. The hind wing length is difficult to determine precisely as the wings are greasy and stuck together, but they appear to be about as long as the fore wings. In all other examined females, both wings exceed the apex of the genital segment although there is some variation in how far they exceed the apex. The holotype appears to have been parasitized, with a dark mass resembling a dryinid larval sac projecting between the first and second thoracic segments; this could have caused abnormal development of the wings. The seventh sternite also has a shallower medial emargination compared to other females, but again this may represent abnormal development due to parasitization. Otherwise, the holotype matches other examined females in structure and colour, and the small COI fragment available for the specimen (GenBank accession PP719690, 137 bp) is 100% identical to the sequence from *B. incisurus* included in the phylogenetic analysis.

Females of this species can be separated from *Cribrus* and other Nearctic Paralimnini with longitudinal stripes on the head and pronotum based on the distinctly infuscated cell borders of the fore wing, reduction of the outer anteapical cell, sternite VII with slightly projecting posterior corners and a small darkened emargination medially, and dark gonoplacs.

Distribution. Recorded from Alberta to Nova Scotia, south to Wisconsin (Fig. 25). Locations largely fall within the southern boreal forest or transition zones.

Host plants. Associated with graminoids in northern wetlands, although the specific host is unclear. The type specimen was collected from “grasses on the margin of a tamarack bog” (DeLong 1926). Beamer’s collection from Cowan, MB was probably collected from grasses along the margin of a lake (based on Beamer’s collection notes for this locality, as quoted by Whitcomb and Hicks 1988: 323). One specimen from near Beardmore, ON was collected from *Calamagrostis canadensis*, while a large series from Sault Ste. Marie, ON was collected from *Carex* sp. All three Ontario localities were wetlands with *Calamagrostis canadensis* as a dominant species (K.G.A. Hamilton field notes, unpublished) and this common wetland grass is a potential candidate for the host plant, but further fieldwork is needed.

***Cribrus* Oman, 1949**

Type species. *Laevicephalus shingwauki* Beamer & Tuthill, 1934, by original designation (Oman 1949: 166).

Diagnosis. Separated from other genera of Paralimnini by the following combination of characters: male subgenital plates with uniseriate macrosetae, plates truncate and shorter than pygofer; pygofer without processes; pygofer with a prominent pair of dorsal spots; connective linear with posterior stem about as long as wide (connective loop-shaped sensu Emeljanov (1999)); aedeagus with swollen atrium, short shaft with apical gonopore and one pair of apical processes; frontoclypeus and pronotum with longitudinal stripes; wings usually brachypterous, fore wing with three closed anteapical cells.

Figure 25. Map of localities for *Boreolimnus incisurus* (black dots) and *Cribrus concinnus* (white dots). The half-filled dot is Ladysmith, Wisconsin, type locality for both species and the only known co-occurrence.

Description. Small leafhoppers with typical Paralimnini structure. Colour generally stramineous, head and pronotum with longitudinal stripes, wing with indistinct brown infuscation around cell borders (Figs 26–31).

Head with crown bluntly angled, medial length about equal to width between eyes (Figs 26, 27). Crown glabrous at base, margin and face shagreen. Lateral frontal sutures terminating just ventral of ocelli, ocelli about their own diameter distant from eye (Fig. 30). Mesal margin of eye notched. Anteclypeus with margins slightly convex, distal third distinctly tapered. Lorum about half width of anteclypeus, well separated from genal margin. Antennae about as long as head width.

Pronotum slightly narrower than width of head across eyes, about as long as medial length of head. Fore femur with AM1 near ventral margin, row IC with a few fine setae, row AV consisting of a few, widely spaced, very short setae. Fore tibia with 1 AD and 4 PD macrosetae. Hind femur with 2+2+1 macrosetae. First hind tarsomere with two rows of plantar setae, four apical platellae between a pair of longer normal setae. Fore wing with three closed anteapical cells, although venation may be distorted due to brachyptery.

Male abdomen with apodemes on sternite II poorly developed, shorter than width. Pygofer about twice as long as wide, with a patch of long macrosetae posterodorsally and a few small macrosetae scattered ventrally (Figs 32, 33). Pygofer dorsally with a pair of heavily sclerotized spots basal to segment X. Segment X about as long as wide, completely sclerotized dorsally and laterally. Valve parabolic. Subgenital plates truncate, shorter than pygofer, bearing a single row of macrosetae laterally (Fig. 34). Connective with arms fused anteriorly, tapered towards posterior end, stem abruptly broadened apically, wider than arms. Style apophysis with lateral lobe weakly developed, medial lobe with corrugated sculpture but no distinct teeth. Aedeagus with swollen atrium, shaft very short with apical gonopore, with one pair of apical processes (Figs 35, 36).

Female pygofer with moderate length macrosetae (Fig. 37). Ovipositor not projecting beyond pygofer. Gonoplac without macrosetae. First valvula slightly concave; sculpture imbricate dorsally and strigate ventrally (Fig. 38). Second valvulae evenly tapered distally, with rounded teeth decreasing in size distally (Fig. 39).

Cribrus concinnus **(Sanders & DeLong)**

Figs 26–47

Deltocephalus concinnus Sanders & DeLong 1917: 86.
Laevicephalus concinnus (Sanders & DeLong): Comb. Beamer and Tuthill 1934.
Cribrus concinnus (Sanders & DeLong): Comb. Ross and Hamilton 1972.
= *Deltocephalus plagus* Ball & DeLong, 1926: 241. New synonym.
= *Laevicephalus shingwauki* Beamer & Tuthill, 1934: 19. New synonym.

Description. Males 2.5–2.8 mm. Females 3.3–3.6 mm.

Colour mostly light yellow, with two light brown longitudinal stripes on crown and four longitudinal stripes on pronotum. Legs with dark spots at bases of macrosetae. Abdominal tergites with four brown to black longitudinal stripes usually apparent. Abdominal sternites may have lateral brown markings. Fore wing pale brown with indistinct darker brown infuscation around border of cells. Wing length variable in females, from fully macropterous to brachypterous with fore wing reaching apex of tergite VI and hind wing reaching apex of tergite II. Males brachypterous with fore wing reaching base to midpoint of pygofer and hind wing reaching apex of tergite II to III.

Subgenital plates bearing a single row of approximately seven macrosetae laterally. Style with medial lobe of apophysis finger-shaped. Aedeagus with long apical processes curving toward base, sculptured with complex ridges.

Female sternite VII rectangular, posterior corners rounded, posterior margin straight to moderately convex, may have slight projections medially and laterally (Fig. 40). Gonoplac pale. Base of first valvula in ventral view elongate (Fig. 37).

Material examined. *Lectotype* of *Deltocephalus concinnus* Sanders & DeLong (here designated). USA • ♀; Wisconsin, Ladysmith; 9 Aug. 1916; D.M. DeLong leg.; OSUC, OSUC 0171752.

Holotype of *Deltocephalus plagus* Ball & DeLong. USA • ♀ (specimen missing from point, not examined); Wisconsin, Madison; 21 Sep. 1917; E.D. Ball leg.; USNM.

Holotype of *Laevicephalus shingwauki* Beamer & Tuthill. USA • ♂ (apparently lost, not examined); Minnesota, Aitkin; 25 Aug. 1933; P.B. Lawson leg.; SEMC.

Other material. USA – **Illinois** • 1 ♂, 3 ♀; 3 mi W Kankakee; 25 Aug. 1980; K.G.A. Hamilton leg.; CNC • 24 ♀; Fox Lake; 26 Jun. 1935; DeLong & Ross leg.; INHS • 2 ♂, 1 ♀; Fox Lake; 6 Aug. 1935; DeLong & Ross leg.; INHS • 3 ♀; Fox Lake; 26 Jun. 1936; Frison & DeLong leg.; INHS • 8 ♂, 7 ♀, 2 nymphs, approximately 20 unmounted specimens in a capsule; Iroquois Co., 7 mi NE Beaverville; 25 Sep. 1962; Ross & Ross leg.; from *Calamagrostis canadensis*; GL 177; CNC • 1 ♀; Zion; 16 Jun. 1954; Sanderson & Moore leg.; CNC. – **Wisconsin** • 1 ♂; Juneau Co., 6 mi NE Mather; 17 Jul. 1963; Smith & Stannard leg.; GL 654; CNC • 8 ♀; Wood Co.; 16 Jul. 1963; Stannard & Smith leg.; GL 666; CNC.

Remarks. All males examined are brachypterous and clearly belong to a single species with distinctive genitalia. Females differing in wing length were previously

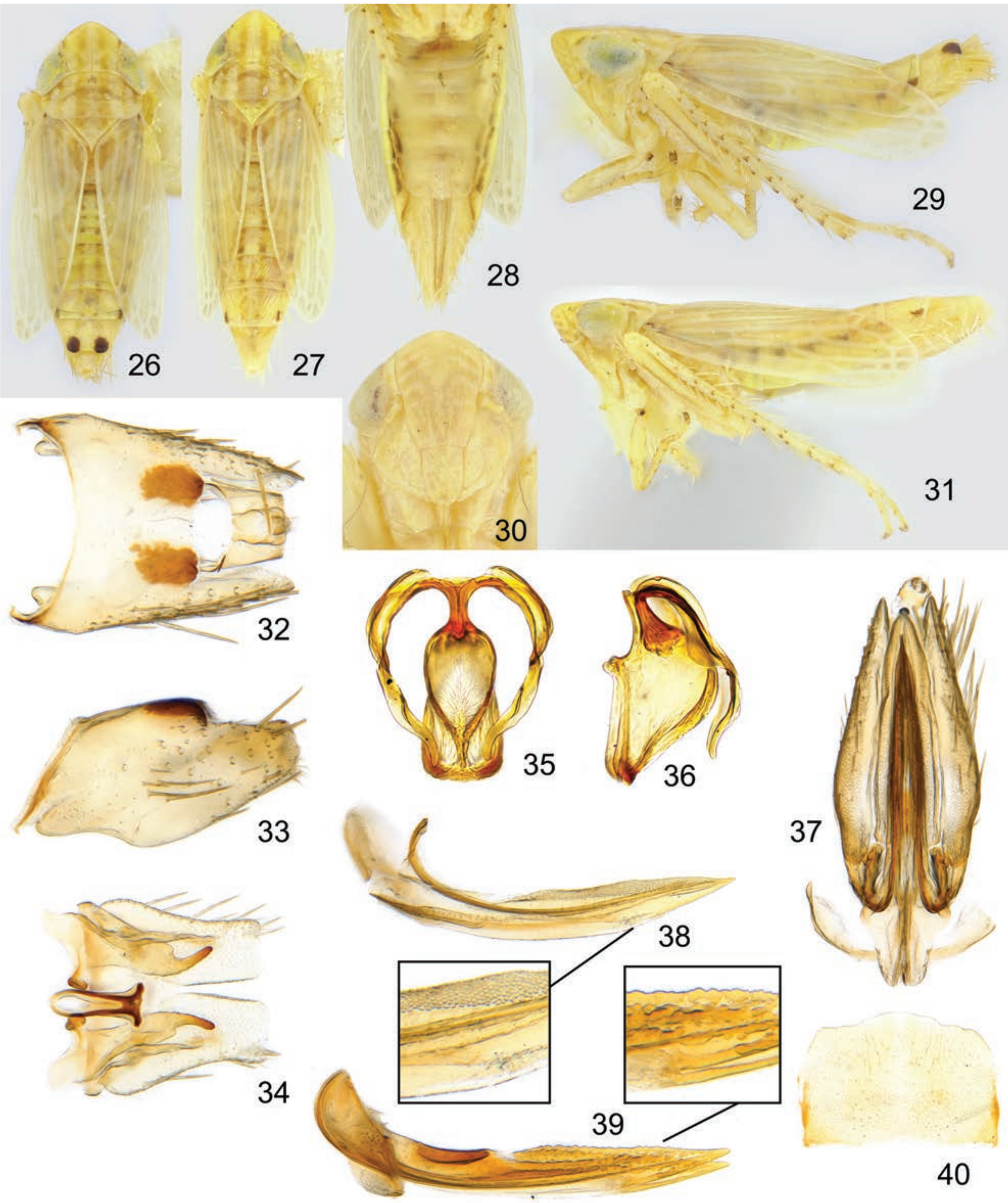

Figures 26–40. *Cribrus concinnus* **26** dorsal habitus, male **27** dorsal habitus, female **28** abdomen ventral, female **29** lateral habitus, male **30** face **31** lateral habitus, female **32** male pygofer, dorsal **33** male pygofer, lateral **34** male subgenital plate, styles, connective, dorsal 35 aedeagus, caudal **36** aedeagus, lateral **37** female genital capsule, ventral **38** first valvifer, lateral, with enlargement **39** second valvifers, lateral, with enlargement **40** female sternite VII, ventral.

treated as distinct species (e.g. DeLong 1948), but other structural features and colour pattern are consistent among specimens with different length wings. The examined series from Fox Lake, Illinois, collected on 30 June 1935, includes 23 brachypterous females with fore wing reaching the apex of tergites VI to VII and hind wing reaching the apex of tergites II to IV (all identified by D. DeLong as "*Laevicephalus shingwauki*") (Figs 41, 42) and one macropterous female with fore and hind wings both exceeding the tip of the abdomen (identified by D. DeLong as "*Laevicephalus concinnus*") (Fig. 43). The specimens are otherwise inseparable, and the best explanation for the wing length variation among females is the presence of a rare macropterous morph within a single species. Synonymies in the genus are complicated by the apparent loss of the type material of *C. plagus* and *C. shingwauki*, but the available evidence suggests both be treated as junior synonyms of *C. concinnus*. With the synonymies proposed here, *Cribrus* becomes a monotypic genus including only *C. concinnus*.

Sanders and DeLong (1917) described *D. concinnus* from two female syntypes from the same locality. One of these was apparently later designated as the holotype of *D. concinnus* var. *incisurus* as discussed above. There is no published lectotype designation for *D. concinnus*, and so I here designate the other syntype (Figs 44–47) as lectotype to stabilize the application of the name. This appears to be the specimen illustrated under this name by Sanders and DeLong (1917) and DeLong (1926). The specimen was labelled as "holotype" in DeLong's collection in OSUC. However, this label was probably added later by another worker (L. Musetti pers. comm. 2022) and is incorrect, as no holotype was originally designated. The lectotype is a macropterous specimen, but it is otherwise indistinguishable from other female specimens of the species.

The holotype of *D. plagus* is missing from the point, with only a leg remaining (S. McKamey pers. comm. 2022). The original description and illustrations are both good matches to brachypterous females of this species. Oman (1949) suggested *D. plagus* was probably a synonym of *C. shingwauki*, although he did not formally synonymize them.

The holotype and a male paratype of *Laevicephalus shingwauki* are stated in the original description to be deposited in the SEMC, but they can not be located there now (R. Osborn pers. comm. 2024). Beamer and Tuthill (1934) separated their species from *C. concinnus* based on the smaller size, shorter wings, and abdominal colouration, although they speculated it might actually be the male of the former. Ross and Hamilton (1972) later also suggested that *C. concinnus* was "close to if not the same species as *C. shingwauki*." Although the internal genitalia of the type series were not described, the description of the external characters and illustration of the external genitalia are a clear match to the present concept. The differences in size and abdominal colouration mentioned by Beamer and Tuthill (1934) both represent sexual dimorphism within the species.

Females of this species can be separated from *Boreolimnus* and other Nearctic Paralimnini with longitudinal stripes on the head and pronotum based on the longitudinal dorsal stripes on the abdomen, outer anteapical cell well developed and closed by crossvein s, sternite VII entirely pale with rounded posterior corners and without medial emargination, and pale gonoplacs.

Distribution. Found in the midwestern United States (Minnesota to Indiana), around the eastern margin of the tallgrass prairie region (Fig. 25).

Host plants. Associated with *Calamagrostis*, usually in mesic to wet prairie or wetlands (DeLong 1948; Panzer et al. 2003; J. Bess pers. comm.; examined specimens).

Figures 41–43. *Cribrus concinnus*, dorsal habitus. Females collected at Fox Lake, Illinois, 30 June 1935. Horizontal lines mark apex of hind wing **41** shorter-winged brachypter, right forewing missing **42** longer-winged brachypter **43** macropter.

Discussion

Although the Nearctic fauna of Paralimnini is fairly well known as a whole, many taxa have not yet been included in modern revisionary studies. In addition to various undescribed or unrecognized species, some currently recognized species are inadequately characterized and require more research to resolve their status. The new genus and new synonymies here resolve the status of a few of these obscure nominal species. Continued taxonomic research on other little-known taxa of Nearctic Paralimnini is needed to further advance the taxonomy of this diverse group of leafhoppers.

The phylogenetic analysis also points to potential issues in generic classification of the Paralimnini, with a few well-sampled genera recovered as non-monophyletic. However, the single gene used is insufficient for robust recovery of deeper, mostly intrageneric relationships, with low support values for most nodes near the base of the tree. Revisions to the generic classification should not be based on these results alone, but further analysis with multiple genes and dense taxon sampling should be prioritized.

Acknowledgements

I thank Tommy McElrath (INHS), Luciana Musetti (OSUC), Rachel Osborn (SEMC), and Stuart McKamey and James Zahniser (USNM) for loans of material

Figures 44–47. *Deltocelphalus concinnus* Sanders & DeLong, lectotype **44** dorsal habitus **45** lateral habitus **46** abdomen, ventral **47** labels.

and searching for types held in their collections. Jim Bess provided data on *Cribrus* occurrences in Indiana. Joanne Elsaesser provided technical support. Julie-Anne Dorval photographed primary types held at CNC. Thanks are given to Dmitry Dmitriev, James Zahniser, and an anonymous reviewer for comments on an earlier version of this manuscript.

Additional information

Conflict of interest

The author has declared that no competing interests exist.

Ethical statement

No ethical statement was reported.

Funding

This project was funded by Agriculture and Agri-Food Canada (project J-002279).

Author contributions

Conceptualization: JHK. Investigation: JHK. Writing - original draft: JHK. Writing - review and editing: JHK.

Author ORCIDs

Joel H. Kits https://orcid.org/0000-0003-2685-0567

Data availability

All of the data that support the findings of this study are available in the main text or Supplementary Information.

References

Anufriev GA, Emeljanov AF (1988) Suborder Cicadinea (Auchenorrhyncha). In: Lehr PA (Ed.) Keys to the Insects of the Far East of the USSR, Vol. 2. Nauka, Leningrad, 12–495.

Ball ED, DeLong DM (1926) Three new species of *Deltocephalus*. Journal of the New York Entomological Society 34: 241–242. https://www.jstor.org/stable/25004139

Beamer RH (1938) Miscellaneous leafhoppers with descriptions of five new species (Homoptera, Cicadellidae). The Canadian Entomologist 70: 224–230. https://doi.org/10.4039/Ent70224-11

Beamer RH, Tuthill LD (1934) Some new species and a new genus of deltocephaloid leafhoppers (Homoptera, Cicadellidae). Journal of the Kansas Entomological Society 7: 1–24. http://www.jstor.org/stable/25081372

Beirne BP (1954a) Canadian species of *Latalus* (Homoptera: Cicadellidae). The Canadian Entomologist 86: 123–127. https://doi.org/10.4039/Ent86123-3

Beirne BP (1954b) Errata. The Canadian Entomologist 86: 192. https://doi.org/10.4039/Ent86192-4

Beirne BP (1956) Leafhoppers (Homoptera: Cicadellidae) of Canada and Alaska. Memoirs of the Entomological Society of Canada 88: 5–180. https://doi.org/10.4039/entm8802fv

Cao Y, Dietrich CH, Zahniser JN, Dmitriev DA (2022) Dense sampling of taxa and characters improves phylogenetic resolution among deltocephaline leafhoppers (Hemiptera: Cicadellidae: Deltocephalinae). Systematic Entomology 2022: 1–15. https://doi.org/10.1111/syen.12540

DeLong DM (1926) A monographic study of the North American species of the genus *Deltocephalus*. The Ohio State University Studies 2(13), Contributions in Zoology and Entomology 3: 1–129.

DeLong DM (1948) The leafhoppers, or Cicadellidae, of Illinois (Eurymelinae–Balcluthinae). Bulletin of the Illinois Natural History Survey 24: 97–376. https://doi.org/10.21900/j.inhs.v24.196

DeLong DM, Caldwell, JS (1937) Check List of the Cicadellidae (Homoptera) of America, North of Mexico. The Ohio State University, Columbus, 93 pp.

Dietrich CH (2005) Keys to the families of Cicadomorpha and subfamilies and tribes of Cicadellidae (Hemiptera: Auchenorrhyncha). Florida Entomologist 88: 502–517. https://doi.org/10.1653/0015-4040(2005)88[502:KTTFOC]2.0.CO;2

Emeljanov AF (1999) A key to genera of the subfamily Deltocephalinae s.l. (Homoptera, Cicadellidae) from Kazakhstan, Middle Asia, and Mongolia with description of new genera and subgenera. Entomological Review 79: 547–562.

Foottit RG, Maw E, Hebert PDN (2014) DNA barcodes for Nearctic Auchenorrhyncha (Insecta: Hemiptera). PLoS ONE 9: e101385. https://doi.org/10.1371/journal.pone.0101385

Guindon S, Dufayard J-F, Lefort V, Anisimova M, Hordijk W, Gascuel O (2010) New algorithms and methods to estimate maximum-likelihood phylogenies: assessing the performance of PhyML 3.0. Systematic Biology 59: 307–321. https://doi.org/10.1093/sysbio/syq010

Hamilton KGA, Langor DW (1987) Leafhopper fauna of Newfoundland and Cape Breton Islands (Rhynchota: Homoptera: Cicadellidae). The Canadian Entomologist 119: 663–95. https://doi.org/10.4039/Ent119663-7

Hoang DT, Chernomor O, von Haeseler A, Minh BQ, Vinh LS (2018) UFBoot2: improving the ultrafast bootstrap approximation. Molecular Biology and Evolution 35: 518–522. https://doi.org/10.1093/molbev/msx281

Kalyaanamoorthy S, Minh BQ, Wong TKF, von Haeseler A, Jermiin LS (2017) ModelFinder: fast model selection for accurate phylogenetic estimates. Nature Methods 14: 587–589. https://doi.org/10.1038/nmeth.4285

Katoh K, Standley DM (2013) MAFFT multiple sequence alignment software version 7: improvements in performance and usability. Molecular Biology and Evolution 30: 772–780. https://doi.org/10.1093/molbev/mst010

Kits JH (2023) The genus *Errastunus* in the Nearctic region (Hemiptera, Cicadellidae, Deltocephalinae). ZooKeys 1178: 143–164. https://doi.org/10.3897/zookeys.1178.105566

Li Z, Dai R, Xing J (2011) Deltocephalinae from China (Hemiptera: Cicadellidae). Popular Science Press, Beijing, 336 pp.

McElrath T (2023). Illinois Natural History Survey Insect Collection. Illinois Natural History Survey. Occurrence dataset. https://doi.org/10.15468/eol0pe [accessed via GBIF.org on 2024-04-23]

Nguyen L-T, Schmidt HA, von Haeseler A, Minh BQ (2015) IQ-TREE: a fast and effective stochastic algorithm for estimating maximum likelihood phylogenies. Molecular Biology and Evolution 32: 268–274. https://doi.org/10.1093/molbev/msu300

Oman PW (1949) The Nearctic Leafhoppers (Homoptera: Cicadellidae): a Generic Classification and Check List. Entomological Society of Washington, Washington, DC, 153 pp.

Ossiannilsson F (1983) The Auchenorrhyncha (Homoptera) of Fennoscandia and Denmark. Part 3: the Family Cicadellidae: Deltocephalinae, catalogue, literature, and index. Scandinavian Science Press, Copenhagen, 979 pp. https://doi.org/10.1163/9789004273320

Panzer R, Derkovitz G, Gnaedinger K (2003) A survey of the leafhoppers, planthoppers, froghoppers, grasshoppers, butterflies, and moths of the Green River State Wildlife Area, Lee County, Illinois. Illinois Department of Natural Resources unpublished report, 33 pp. https://dnr.illinois.gov/content/dam/soi/en/web/dnr/grants/documents/wpfgrantreports/2001l08w.pdf

Ribaut H (1952) Homoptères Auchénorhynques. II (Jassidae). In: Faune de France, Vol. 57. Paul Lechevalier, Paris, 474 pp.

Ross HH, Hamilton KGA (1972) A review of the North American leafhopper genus *Laevicephalus* (Hemiptera: Cicadellidae). Annals of the Entomological Society of America 65: 929–942. https://doi.org/10.1093/aesa/65.4.929

Sanders JG, DeLong DM (1917) The Cicadellidae (Jassoidea–Fam. Homoptera) of Wisconsin, with description of new species. Annals of the Entomological Society of America 10: 79–97. https://doi.org/10.1093/aesa/10.1.79

Whitcomb RF, Hicks AL (1988) Genus Flexamia: new species, phylogeny, and ecology. Great Basin Naturalist Memoirs 12: 224–323. https://doi.org/10.5962/bhl.part.10987

Zahniser JN, Dietrich CH (2013) A review of the tribes of Deltocephalinae (Hemiptera: Auchenorrhyncha: Cicadellidae). European Journal of Taxonomy 45: 1–211. https://doi.org/10.5852/ejt.2013.45

Supplementary material 1

Maximum likelihood tree of Paralimnini, based on 658 base pairs of cytochrome oxidase I

Authors: Joel H. Kits
Data type: tif
Explanation note: Support values at nodes are bootstrap/SH-aLRT.

Link: https://doi.org/10.3897/zookeys.1217.126602.suppl1

Supplementary material 2

Georeferenced localities for *Boreolimnus incisurus* and *Cribrus concinnus*

Authors: Joel H. Kits
Data type: csv

Link: https://doi.org/10.3897/zookeys.1217.126602.suppl2

Supplementary material 3

Data for COI sequences used in phylogenetic analysis

Authors: Joel H. Kits
Data type: csv

Link: https://doi.org/10.3897/zookeys.1217.126602.suppl3

ZooKeys 1217: 291–307 (2024)
DOI: 10.3897/zookeys.1217.125780

Research Article

Three new species of the genus *Bambusiphaga* Huang & Ding, 1979 (Hemiptera, Fulgoroidea, Delphacidae, Tropidocephalini) from China, with an updated checklist and key to species

Sha-Sha Lv[1,2], Hong-Xing Li[3], Lin Yang[1,2], Yu-Bo Zhang[4], Xiang-Sheng Chen[1,2]

1 *Institute of Entomology, Guizhou University, Guiyang, Guizhou, 550025, China*
2 *The Provincial Special Key Laboratory for Development and Utilization of Insect Resources of Guizhou, Guizhou University, Guiyang, Guizhou, 550025, China*
3 *Guizhou Light Industry Technical College, Guiyang, Guizhou, 561113, China*
4 *Anshun University, College Agriculture, Anshun, Guizhou, 561000, China*
Corresponding author: Xiang-Sheng Chen (chenxs3218@163.com)

Abstract

In this study, three new bamboo-feeding species of the genus *Bambusiphaga* Huang & Ding, 1979 (Hemiptera, Fulgoroidea, Delphacidae, Tropidocephalini), *B. caudospina* Lv, Li & Chen, **sp. nov.**, *B. laterospina* Lv, Li & Chen, **sp. nov.** and *B. striola* Lv, Li & Chen, **sp. nov.** from Southwest China, are described and illustrated, bringing the total number of species in the genus to 34. An updated identification key and checklist to all known species of *Bambusiphaga* are provided.

Key words: Bamboo pests, Fulgoroidea, identification key, Oriental region, taxonomy, Tropidocephalini

Academic editor: Mike Wilson
Received: 19 April 2024
Accepted: 8 October 2024
Published: 8 November 2024

ZooBank: https://zoobank.org/B5222557-C6E1-49E9-A334-8C73B95C2B6D

Citation: Lv S-S, Li H-X, Yang L, Zhang Y-B, Chen X-S (2024) Three new species of the genus *Bambusiphaga* Huang & Ding, 1979 (Hemiptera, Fulgoroidea, Delphacidae, Tropidocephalini) from China, with an updated checklist and key to species. ZooKeys 1217: 291–307. https://doi.org/10.3897/zookeys.1217.125780

Introduction

The bamboo-feeding genus *Bambusiphaga* Huang & Ding, 1979 (Delphacidae, Delphacinae, Tropidocephalini) was established by Huang and Ding for six species feeding on *Neosinocalamus affinis* (Rendle) and *Phyllostachys* sp. (Poales, Poaceae), with *B. nigropunctata* Huang & Ding, 1979 as the type species from Sichuan Province, China (Huang et al. 1979). Then Kuoh et al. (1980) described two new species, *B. fascia* Huang & Tian, 1980 and *B. nigromarginata* Huang & Tian, 1980. Ding (1982) and Ding and Hu (1982) both added a new species in 1982. Asche (1983) described a new species from East Himalaya, *B. lynchi* Asche, 1983, and transferred the following two species from the genus *Columbisoga* Muir, 1921 into *Bambusiphaga*: *B. taiwanensis* (Muir, 1917) and *B. singaporensis* (Muir, 1919). Ding et al. (1986) and Yang and Yang (1986) described *B. jinghongensis* Ding & Hu, 1986 and *B. membranacea* Yang & Yang, 1986 from Yunnan and Taiwan Provinces in China, respectively. Chen et al. (2000) described two new species, *B. maculata* Chen & Li, 2000 and *B. wangmoensis* Chen & Li, 2000, attacking bamboo from Guizhou Province in China. Qin et al. (2006) transferred *Malaxa bakeri* Muir, 1919 into the genus. Chen and Liang (2007) revised *Bambusiphaga* and added two species, *B. maolanensis* Chen & Liang, 2007 and *B. pianmaensis* Chen & Liang, 2007. Since then, 11 species have been added to the genus (Hou and Chen 2010; Yang and Chen 2011; Qin et al. 2012; Li et al. 2018, 2023; Ramya and Meshram 2019). Until now, 31 species have been recorded in the genus, which is widely distributed in the Oriental region, with 28 species in China, one in the Philippines, two in Singapore, two in Malaysia, one in the North-Eastern Himalayas, and one in India (Yang and Chen 2011; Qin et al. 2012; Li et al. 2018, 2023; Ramya and Meshram 2019; Bourgoin 2024).

Herein, three new species of the genus, *B. caudospina* sp. nov., *B. laterospina* sp. nov. and *B. striola* sp. nov. from Southwest China, are described and illustrated. As a result, the number of *Bambusiphaga* species has increased to 34, with 31 recorded from China.

Materials and methods

The external morphology terminologies are as follows: male genitalia follows Yang and Yang (1986) and Bourgoin (1987), and wing venation follows Bourgoin et al. (2015). Dry male specimens were used for the descriptions and illustrations. Body measurements are from the apex of the vertex to the tip of the forewing. All measurements are in millimeters (mm). External morphology and drawings were done under the Leica MZ 12.5 stereomicroscope. Color pictures for adult habitus were obtained by the KEYENCE VHX-6000 system. The photographs and illustrations were scanned with a CanoScan LiDE 200 and imported into Adobe Photoshop 6.0 for labeling and plate composition. The dissected male genitalia are preserved in glycerin jelly in small plastic tubes pinned together with the specimens.

The type specimens examined are deposited in the Institute of Entomology, Guizhou University, Guiyang, Guizhou Province, China (IEGU).

Taxonomy

Bambusiphaga Huang & Ding, 1979

Bambusiphaga Huang & Ding, 1979: 170; Asche 1983: 211; Ding and Tian 1983 (in Kuoh et al. 1983): 49; Yang and Yang 1986: 37; Wang and Ding 1996: 22; Ding et al. 1999: 441; Ding 2006: 126; Chen and Liang 2007: 504; Hou and Chen 2010: 392; Yang and Chen 2011: 51; Li et al. 2018: 84, 2023: 143.

Type species. *Bambusiphaga nigropunctata* Huang & Ding, 1979, original designation.

Diagnosis. For the diagnosis of *Bambusiphaga* see Chen and Liang (2007: 504) and Li et al. (2023: 143).

Host plants. Bamboo (Bambusoideae).

Distribution. China, India, Malaysia, North-Eastern Himalayas, Philippines, Singapore.

Checklist and distributions of species of *Bambusiphaga* Huang & Ding, 1979

B. angulosa Li, Chen & Yang, 2023; China (Yunnan Province).
B. bakeri (Muir, 1919); China (Guangdong, Guizhou, Hainan, Shaanxi, Taiwan Provinces), Philippines (Luzón, Laguna), Malasia (Peninsula), Singapore.
B. basifusca Hou & Chen, 2010; China (Hainan Province).
B. caudospina Lv, Li & Chen, sp. nov.; China (Guizhou Province).
B. citricolorata Huang & Tian, 1979; China (Guizhou, Yunnan Provinces).
B. fascia Huang & Tian, 1980; China (Anhui, Chongqing, Gansu, Guizhou, Jiangsu, Sichuan, Taiwan, Zhejiang Provinces).
B. furca Huang & Ding, 1979; China (Fujian, Guizhou, Taiwan, Yunnan Provinces).
B. hainanensis Hou & Chen, 2010; China (Hainan Province).
B. huangi Ding & Hu, 1982; China (Yunnan Province).
B. jinghongensis Ding & Hu, 1986; China (Yunnan Province).
B. kunmingensis Yang & Chen, 2011; China (Yunnan Province).
B. lacticolorata Huang & Ding, 1979; China (Guizhou, Jiangsu, Zhejiang Provinces).
B. laterospina Lv, Li & Chen, sp. nov.; China (Yunnan Province).
B. luodianensis Ding, 1982; China (Guangxi, Guizhou, Hainan Provinces).
B. lynchi Asche, 1983; North-Eastern Himalaya.
B. maculata Chen & Li, 2000; China (Guizhou, Henan Provinces).
B. maolanensis Chen & Liang, 2007; China (Guizhou Province).
B. membranacea Yang & Yang, 1986; China (Guizhou, Taiwan Provinces).
B. mirostylis Huang & Ding, 1979; China (Yunnan Province).
B. nigrigena Li, Chen & Yang, 2023; China (Yunnan Province).
B. nigromarginata Huang & Tian, 1980; China (Jiangsu Province).
B. nigropunctata Huang & Ding, 1979; China (Guangxi, Guizhou, Gansu, Hainan, Shaanxi, Sichuan Provinces).
B. parvula Li, Chen & Yang, 2023; China (Yunnan Province).
B. pianmaensis Chen & Liang, 2007; China (Yunnan Province).
B. similis Huang & Tian, 1979; China (Yunnan Province).
B. singaporensis (Muir, 1919); Malasia (Peninsula), Singapore.
B. striola Lv, Li & Chen, sp. nov.; China (Tibet Province).
B. taibaishana Qin, Liu & Lin, 2012; China (Shaanxi Province).
B. taiwanensis (Muir, 1917); China (Fujian, Guizhou, Taiwan Provinces).
B. unispina Ramya & Meshram, 2019; India (Himachal Pradesh).
B. ventroprocessa Li, Yang & Chen, 2018; China (Hainan Province).
B. wangmoensis Chen & Li, 2000; China (Guizhou Province).
B. yangi Yang & Chen, 2011; China (Yunnan Province).
B. yingjiangensis Li, Yang & Chen, 2018; China (Yunnan Province).

Key to species of *Bambusiphaga* Huang & Ding, 1979

Modified from Li et al. 2018.

1 Vertex dark brown or with dark brown spots **2**
– Vertex light, without dark brown spots **4**

2 Vertex yellowish-brown, middle part of basal compartment with a black oval spot; anal segment without a process; pygofer without medioventral processes (Huang et al. 1979: figs 2, 4) .... ***B. nigropunctata*** **Huang & Ding, 1979**

– Vertex brownish-black, middle part of basal compartment without a black oval spot; anal segment with a thick and long process; pygofer with a pair of medioventral processes **3**

3 Anal segment with process distinctly divided into 2 processes at apex; apical part of aedeagus without two unciform processes (Chen and Liang 2007: figs 46, 53) .... ***B. pianmaensis*** **Chen & Liang, 2007**

– Anal segment with process distinctly divided into 3 processes at apex (Fig. 6C, E); apical part of aedeagus with two unciform processes (Fig. 6J) .... ***B. striola*** **Lv, Li & Chen, sp. nov.**

4 Mesonotum with dark brown markings **5**

– Mesonotum without dark brown markings **17**

5 Lateral areas of pronotum with dark brown markings **6**

– Lateral areas of pronotum without dark brown markings **15**

6 Forewings with a large irregular pale brown stripe along transverse vein, hence bending along posterior margin to apex (Li et al. 2018: fig. 8) .... ***B. yingjiangensis*** **Li, Yang & Chen, 2018**

– Forewings with basal ⅓ black or with black markings at basal half **7**

7 Forewings with basal ⅓ black **8**

– Forewings with large black markings at base **12**

8 Anal segment without a process on ventral margin (Yang and Chen 2011: fig. 6) .... ***B. kunmingensis*** **Chen & Yang, 2011**

– Anal segment with a very long process on ventral margin **9**

9 Anal segment with a spiny process at right lateroapical angle (Hou and Chen 2010: fig. 14) .... ***B. basifusca*** **Hou & Chen, 2010**

– Anal segment with a spiny process at left lateroapical angle **10**

10 Pygofer without medioventral process; apical half of aedeagus without two processes (Ding 2006: fig. 54c, f) .... ***B. fascia*** **Huang & Tian, 1980**

– Pygofer with medioventral process; apical half of aedeagus with two processes **11**

11 Pygofer with a short medioventral process, without lateroventral process; genital styles without process at middle part (Qin et al. 2012: figs 12, 16, 17) .... ***B. taibaishana*** **Qin, 2012**

– Pygofer with a pair long medioventral and a lateroventral processes (Fig. 4C, D); inner margin of genital styles with a toothed process at middle part (Fig. 4C, G) .... ***B. laterospina*** **Lv, Li & Chen, sp. nov.**

12 Forewings with two large black markings at base; anal segment without process on ventral margin (Li et al. 2018: figs 29, 31) .... ***B. ventroprocessa*** **Li, Yang & Chen, 2018**

– Forewings with one large black marking at base; anal segment with a long process on ventral margin **13**

13 Anal segment with a long ventral process medially; pygofer without medioventral process (Li et al. 2023: fig. 6C, F) .... ***B. nigrigena*** **Li, Chen & Yang, 2023**

– Anal segment with a long ventral process at left lateroapical angle; pygofer with medioventral process **14**

14 Genital styles branched at apical part; medioventral process forked near base (Chen et al. 2000: figs 4, 7, 8) .... ***B. maculata*** **Chen & Li, 2000**

– Genital styles unbranched at apical part (Fig. 2G–I); medioventral process forked near apical 1/2 (Fig. 2C, F) ..... ***B. caudospina*** **Lv, Li & Chen, sp. nov.**

15 Mesonotum without black marking in middle (Ramya and Meshram 2019: fig. 3) .... ***B. unispina*** **Ramya & Meshram, 2019**

– Mesonotum with black markings in middle **16**

16 Forewings somewhat reddish-orange, costal margin dark brown; genital styles relatively broad and short (Kuoh et al. 1980: fig. 8c, f) .... ***B. nigromarginata*** **Huang & Tian, 1980**

– Forewings somewhat yellowish-brown, costal margin yellowish-brown; genital styles relatively slender (Yang and Yang 1986: fig. 20c, e) .... ***B. taiwanensis*** **(Muir, 1917)**

17 Anal segment with a process on ventral margin **18**

– Anal segment without a process on ventral margin **22**

18 Pygofer with medioventral process (Ding 2006: fig. 62c)........................... .... ***B. bakeri*** **(Muir, 1919)**

– Pygofer without medioventral process **19**

19 Anal segment with the process long and extends to ventral margin of pygofer **20**

– Anal segment with the process short **21**

20 Body small, about 3.5–3.6 mm; genital styles with a process at base, apex rounded (Ding et al. 1986: figs 1(5–6)) ..... ***B. jinghongensis*** **Ding & Hu, 1986**

– Body slightly larger, about 4.3 mm; genital styles without a process at base, apex forked (Huang et al. 1979: fig. 18)... .... ***B. mirostylis*** **Huang & Ding, 1979**

21 Tegula dark brown at apical ½; hind margin of pygofer produced at an acute angle medially; genital styles slender; aedeagus without phallobase (Ding and Hu 1982: figs 1–4) .... ***B. huangi*** **Ding & Hu, 1982**

– Tegula yellowish-brown; hind margin of pygofer not produced medially; genital styles broad and short; aedeagus with developed phallobase (Chen and Li 2000: figs 11, 13, 15–16) .... ***B. wangmoensis*** **Chen & Li, 2000**

22 Ventral margin of pygofer with a spine **23**

– Ventral margin of pygofer without a spine.. **25**

23 Caudal side of genital styles with an inversed spine near apex; aedeagus with three spines subapically (Yang and Chen 2011: figs 20–22) .... ***B. yangi*** **Chen & Yang, 2011**

– Caudal side of genital styles with an angular or tooth-like process near apex; aedeagus without spines subapically **24**

24 Genital styles asymmetrical; aedeagus with an inversed process on right side near apical ⅓ (Muir 1919: fig. 8) .... ***B. singaporensis*** **(Muir, 1919)**

– Genital styles symmetrical; aedeagus without any processes (Ding 1982: figs 3, 5).. ***B. luodianensis*** **Ding, 1982**

25 Basal part of genital styles with a fingerlike process **26**

– Basal part of genital styles without a fingerlike process **27**

26 Genital styles with a fingerlike process subapically; aedeagus curved medially (Chen and Liang 2007: figs 20–22).......... ***B. maolanensis*** **Chen & Liang, 2007**

– Genital styles with a lamellate process subapically; aedeagus almost straight (Hou and Chen 2010: figs 9–10) .... ***B. hainanensis*** **Hou & Chen, 2010**

27 Genital styles forked apically..**28**

– Genital styles unforked apically..**30**

28 Frons longer at midline than maximum width, about 2.0: 1; basocaudal part of genital styles in profile produced at a right angle (Yang and Yang 1986: fig. 22b, h)................................***B. membranacea* Yang & Yang, 1986**

– Frons longer at midline than maximum width, about 2.5: 1; basocaudal part of genital styles in profile not produced at a right angle..................**29**

29 Middle part of genital styles granulate (Huang et al. 1979: figs 8–11) ....***B. furca* Huang & Ding, 1979**

– Middle part of genital styles not granulate (Asche 1983: fig. 4) ....***B. lynchi* Asche, 1983**

30 Ventral margin of anal segment incised medially; genital styles short (Huang et al. 1979: fig. 20) ....***B. lacticolorata* Huang & Ding, 1979**

– Ventral margin of anal segment not incised medially; genital styles slender **31**

31 Genital styles with a spinous process near apex **32**

– Genital styles without a spinous process near apex.................................**33**

32 Aedeagus with some small teeth near apex, not forked at apex (Li et al. 2023: fig. 2H–I)...***B. parvula* Li, Chen & Yang, 2023**

– Aedeagus without small teeth near apex, forked at apex (Li et al. 2023: fig. 4H–I) ....***B. angulosa* Li, Chen & Yang, 2023**

33 Apex of vertex obviously broadened, frons widest at base; apex of genital styles without small teeth; aedeagus short and stout (Huang et al. 1979: fig. 17) ....***B. similis* Huang & Tian, 1979**

– Apex of vertex unbroadened, frons widest at apex; apex of genital styles with several small teeth; aedeagus relatively long (Huang et al. 1979: figs 13–15)..***B. citricolorata* Huang & Tian, 1979**

***Bambusiphaga caudospina* Lv, Li & Chen, sp. nov.**

https://zoobank.org/374EE33D-FD7B-4ED4-8736-4E84E8D058A3
Figs 1–2

Type material. ***Holotype*:** CHINA • ♂: Guizhou Province, Weining County, Xueshan Town; 27°4'N, 104°7'E; sweeping, 4 August 2023; Hong-Xing Li leg.; IEGU. ***Paratypes*:** CHINA • 8 ♂♂, 12 ♀♀; Guizhou Province, Weining County, Xueshan Town; 27°4'N, 104°7'E; sweeping, 4 August 2023; Hong-Xing Li and Jie Wang leg.; IEGU.

Diagnosis. The salient features of the new species include: vertex (Fig. 1A, C) light, without dark brown spots; lateral areas of pronotum (Fig. 1A, C) with dark brown markings; mesonotum (Fig. 1A, C) with dark brown markings; forewings (Fig. 1F) with one large black marking at basal 1/3; medioventral process of pygofer (Fig. 2C, F) forked near apical 1/2; dorsolateral margin of aedeagus (Fig. 2J) with three spinous processes at apical part, ventrolateral margin with four spinous processes of similar length. This species is similar to *B. maculata* Chen & Li, 2000, but differs from the latter in: (1) forewings MP_{1+2} fully commingled (forewings MP_{1+2} commingled at base in *B. maculata*); (2) apical part of genital styles not forked (apical part of genital styles forked in *B. maculata*); and (3) apical part of aedeagus with some spinous processes on both sides (apical part of aedeagus with some spinous processes on only one side in *B. maculata*).

Figure 1. *Bambusiphaga caudospina* Lv, Li & Chen, sp. nov., male **A** habitus, dorsal view **B** habitus, lateral view **C** head and thorax, dorsal view **D** head and thorax, lateral view **E** frons, ventral view **F** forewing.

Description. *Measurements*. Total length: male 4.6–4.9 mm (*N* = 9), female 5.0–5.3 mm (*N* = 12).

***Coloration*.** General color yellowish-white to black (Fig. 1A–F). Vertex and frons yellowish-white, rostrum blackish-brown at apex. First segment of antennae yellowish-white at dorsal and ventral sides, lateral sides dark brown, second segment yellowish-white. Eyes reddish-brown. Pronotum yellowish-white, outer sides of lateral carinae with black broad stripes, inner sides with two dark brown round spots. Mesonotum black, lateral margins yellowish-brown, apex of scutellum opalescent. Outer part of tegula black brown, inner part yellowish-white. Forewings milky-white, hyaline, basal 1/3 with a dark brown, wide transverse marking. Legs yellowish-white, except coxae of fore and median legs dark brown.

***Head and thorax*.** Vertex (Figs 1C, 2A) shorter in middle line than wide at base (1: 1.11), width at apex narrower than at base (1: 1.19), middle part of anterior margin convex, lateral margins widened towards the end, lateral and submedian carinae distinct, Y-shaped carina indistinct. Frons (Figs 1E, 2B) longer in middle line than wide at widest portion (about 2.12: 1), widest at apex,

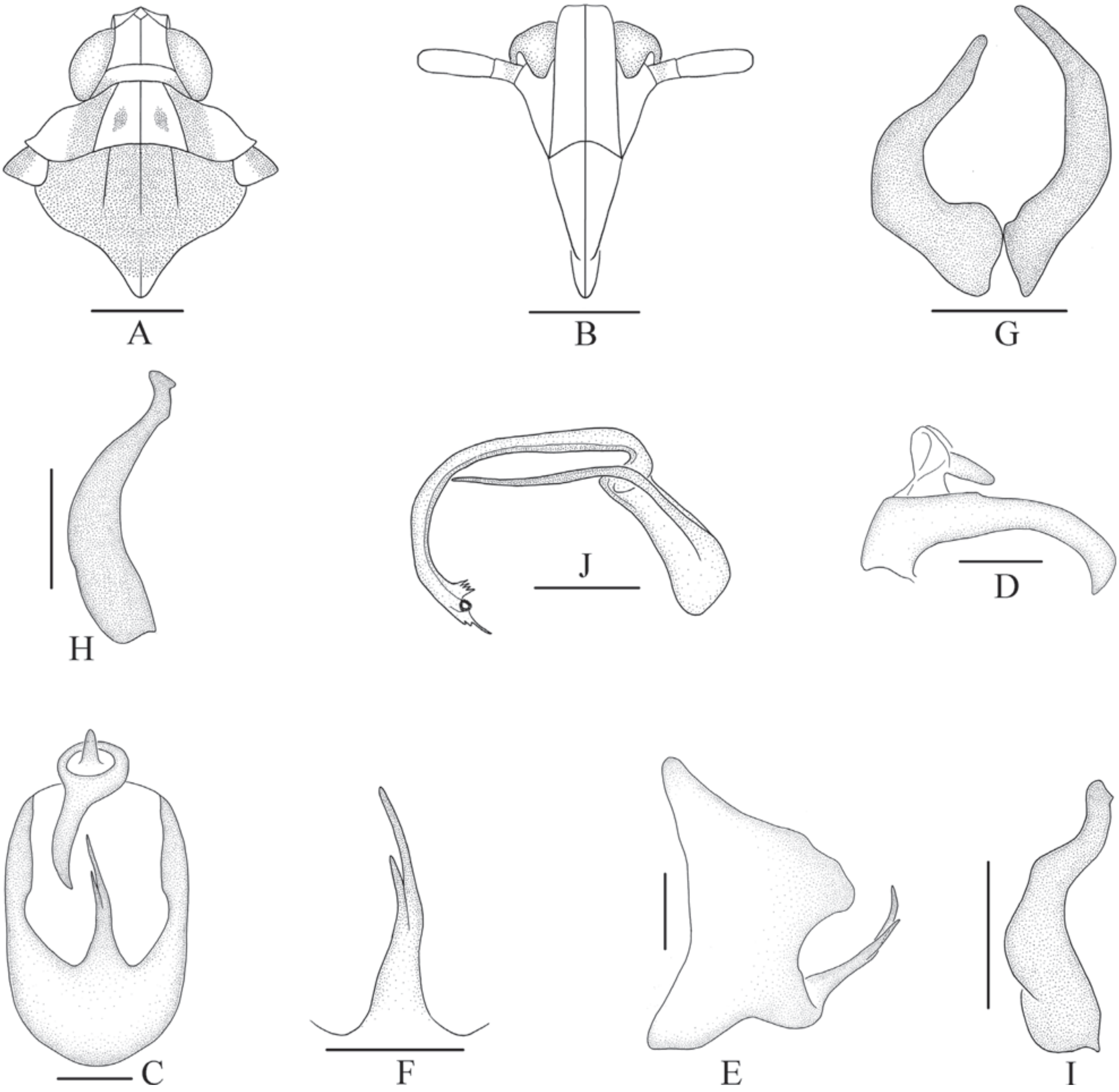

Figure 2. *Bambusiphaga caudospina* Lv, Li & Chen, sp. nov., male **A** head and thorax, dorsal view **B** frons, ventral view **C** male genitalia, posterior view **D** anal segment, lateral view **E** pygofer, lateral view **F** medioventral process of pygofer, posterior view **G** genital style, posterior view **H** left genital style, lateral view **I** right genital style, lateral view **J** aedeagus, lateral view. Scale bars: 0.5 mm (**A, B**); 0.2 mm (**C–J**).

median carina simple. Base of postclypeus (Figs 1E, 2B) as wide as apex of frons. Antennae (Figs 1E, 2B) with first segment longer than wide, shorter than second segment (1: 3.33). Pronotum (Figs 1C, 2A) longer than vertex in midline (1.14: 1). Mesonotum (Figs 1C, 2A) longer than 1.17 times pronotum and vertex combined. Forewings (Fig. 1F) slender, longer than maximal width (2.81: 1).

***Male genitalia*.** Pygofer ventral margin distinctly longer than dorsal margin in lateral view (Fig. 2E), in posterior view (Fig. 2C) with opening longer than wide, ventral margin with long medioventral process, forked near apical 1/2, right branch longer than left one. Anal segment (Fig. 2C, D) ring-like, with a thick and long anal process at left lateroapical angle, taper the end and bend to the right. Genital styles (Fig. 2G–**I**) moderately long, wide at base, tapering at the end, in posterior view asymmetrical, in lateral view apex truncated. Aedeagus (Fig. 2J) with phallobase, phallus tubular, basal part thick, apical part thin, ventrally curved at basal 1/3; dorsolateral margin of apical part with three spinous processes, inner one much longer than the other two, ventrolateral margin with four spinous processes of similar length; gonopore located at apex of phallus, node-like; phallobase slender and long, arched medially.

Host plant. Bamboo.

Distribution. China (Guizhou Province).

Etymology. The species name is a combination of the Latin word "*caudo*-" and "*spina*", referring to apical part of aedeagus with spinous processes.

Bambusiphaga laterospina Lv, Li & Chen, sp. nov.

https://zoobank.org/077D3B46-9854-4474-B64E-C8DE09459674
Figs 3–4

Type material. ***Holotype*:** China • ♂; Yunnan Province, Lushui City; 25°50'N, 98°54'E; sweeping, 8 August 2023; Yong-Jin Sui and Feng-E Li leg.; IEGU. ***Paratypes*:** China • 13 ♂♂, 6 ♀♀; same collection data as for holotype; IEGU.

Diagnosis. The salient features of the new species include: vertex (Fig. 3A, C) light, without dark brown spots; lateral areas of pronotum (Fig. 3A, C) with dark brown markings; mesonotum (Fig. 3A, C) with dark brown markings; forewings (Fig. 3F) with basal ⅓ black; pygofer (Fig. 4C, D) with long medioventral and lateroventral processes; inner margin of genital styles (Fig. 4C, G) with a toothed process at middle part; apical part of aedeagus (Fig. 4H) with two slender spinous processes. This species is similar to *B. taibaishana* Qin, 2012, but differs from the latter in: (1) outer part of tegula black brown, inner part yellowish-white (tegula black brown in *B. taibaishana*); (2) pygofer with a pair long medioventral and a lateroventral processes (pygofer with a short medioventral process, without lateroventral process in *B. taibaishana*); and (3) inner margin of genital styles with a toothed process at middle part (genital styles without process at middle part in *B. taibaishana*).

Description. ***Measurements*.** Total length: male 4.7–4.9 mm (N = 14), female 4.9–5.1 mm (N = 6).

***Coloration*.** General color yellowish-white to black (Fig. 3A–F). Vertex, frons and clypeus yellowish-white. Genae dark brown at base, yellowish-white at apex. Eyes and ocelli reddish-brown. First segment of antennae yellowish-white except for dorsal side dark brown. Pronotum with lateral carinae yellowish-white at inner side, with two dark brown triangular spots, outer side black. Mesonotum black, lateral margins yellow, apex of scutellum yellowish-white. Outer part of tegula black brown, inner part yellowish-white. Forewings pale yellowish-white, hyaline, blackish-brown at basal 1/3. Legs yellowish-white, except coxae of fore and median legs dark brown.

***Head and thorax*.** Vertex (Figs 3C, 4A) shorter in middle line than wide at base (0.90: 1), width at apex narrower than at base (0.82: 1), middle part of anterior margin convex, lateral margins widened towards the end, lateral and submedian carinae distinct, Y-shaped carina distinct. Frons (Figs 3E, 4B) longer in middle line than wide at widest portion (about 2.80: 1), widest at apex, median carina simple. Base of postclypeus (Figs 3E, 4B) as wide as apex of frons. Antennae (Figs 3E, 4B) with first segment longer than wide, shorter than second segment

Figure 3. *Bambusiphaga laterospina* Lv, Li & Chen, sp. nov., male **A** habitus, dorsal view **B** habitus, lateral view **C** head and thorax, dorsal view **D** head and thorax, lateral view **E** frons, ventral view **F** forewing.

(1: 2.0). Pronotum (Figs 3C, 4A) equal in length to vertex in midline (1.14: 1). Mesonotum (Figs 3C, 4A) longer than 2.08 times pronotum and vertex combined. Forewings (Fig. 3F) slender, longer than maximal width (2.57: 1).

***Male genitalia*.** Pygofer ventral margin longer than dorsal margin in lateral view (Fig. 4D), in posterior view (Fig. 4C) with opening longer than wide, ventral margin with long medioventral process, forked near apical 1/2, lateral margins each with a lateroventral process. Anal segment (Fig. 4C–E) ring-like, with a thick and long anal process at left lateroapical angle, taper the end. Genital styles (Fig. 4C, D, G) moderately long, hogged, wide at base, tapering at the end, inner margin with a toothed process near the middle. Aedeagus (Fig. 4H) with phallobase, phallus tubular, curved ventrally, basal part thick, apical part thin, apical part with two slender spinous processes; gonopore located at apex of phallus; phallobase slender and long, arched near basal 1/3.

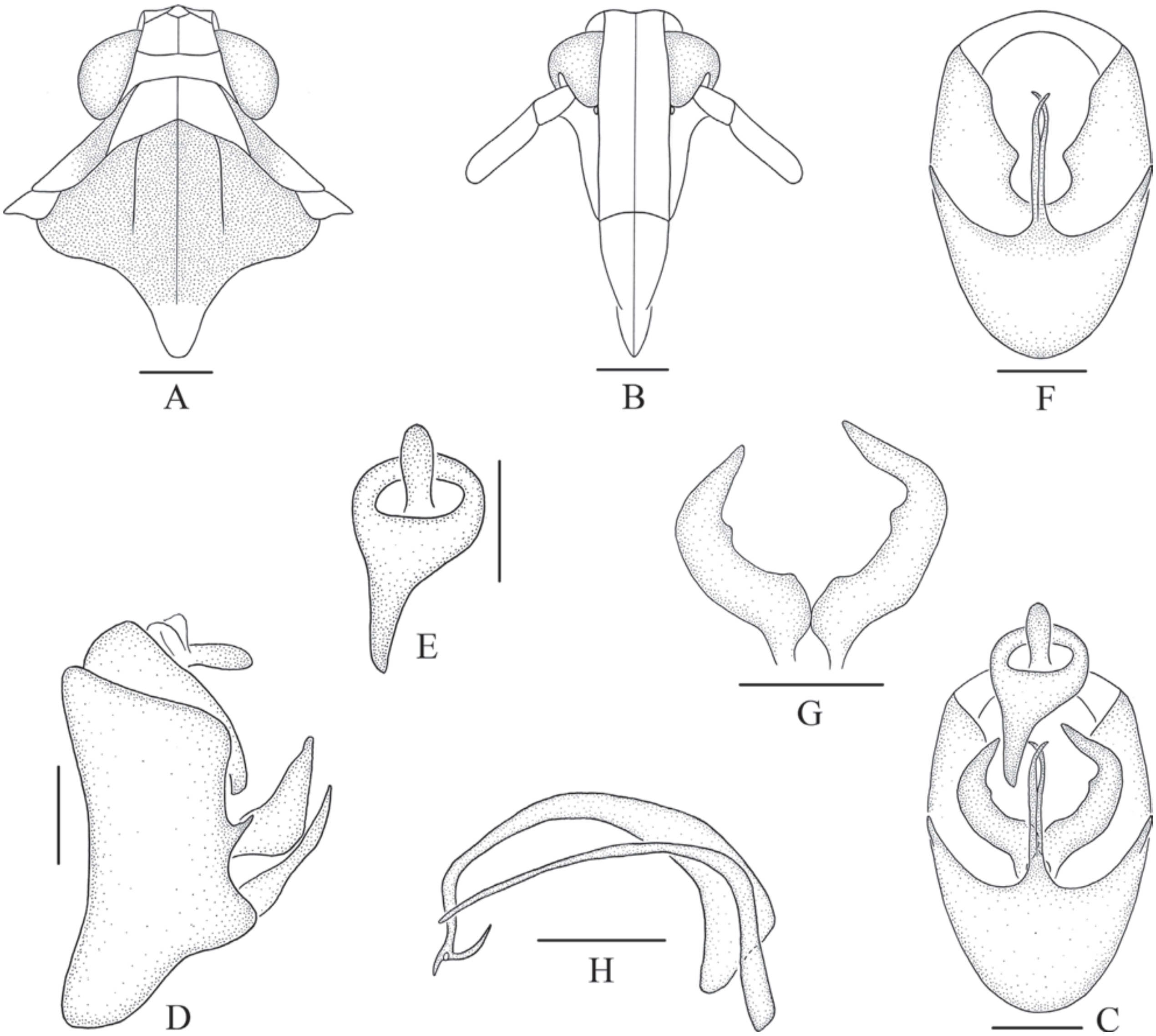

Figure 4. *Bambusiphaga laterospina* Lv, Li & Chen, sp. nov., male **A** head and thorax, dorsal view **B** frons, ventral view **C** male genitalia, posterior view **D** male genitalia, lateral view **E** anal segment, posterior view **F** pygofer, posterior view **G** genital style, posterior view **H** aedeagus, lateral view. Scale bars: 0.5 mm (**A, B**); 0.2 mm (**C–H**).

Host plant. Bamboo.

Distribution. China (Yunnan Province).

Etymology. The species name is a combination of the Latin word "*latero-*" and "*spina*", referring to lateral margins of pygofer, each with a latero-ventral process.

Bambusiphaga striola **Lv, Li & Chen, sp. nov.**

https://zoobank.org/4C51A91E-4402-4A2A-B7C2-BD3564D53DA3
Figs 5–6

Type material. ***Holotype*:** China • ♂; Tibet Province, Milin County, Milin Town; 29°13'N, 94°13'E; sweeping, 22 August 2022; Yong-Jin Sui leg.; IEGU. ***Paratypes*:** China • 13 ♂♂, 15 ♀♀; same collection data as for holotype; IEGU.

Figure 5. *Bambusiphaga striola* Lv, Li & Chen, sp. nov., male **A** habitus, dorsal view **B** habitus, lateral view **C** head and thorax, dorsal view **D** head and thorax, lateral view **E** frons, ventral view **F** forewing.

Diagnosis. The salient features of the new species include: vertex (Fig. 5A, C) brownish-black, basal compartment milky-white; tegula (Fig. 5A, C) milky-white; forewings (Fig. 5F) with a dark brown longitudinal band from anterior margin of basal part to posterior margin of apical part along the CuP and MP; pygofer (Fig. 6C, G) with a pair of medioventral processes; anal segment (Fig. 6C, E) with the process distinctly divided into 3 processes at apex; apical part of aedeagus (Fig. 6J) with two unciform processes, basal and middle parts each with a dentate processes. This species is similar to *B. pianmaensis* Chen & Liang, 2007, but differs from the latter in: (1) posterior margin of pronotum milky-white at middle part (posterior margin of pronotum blackish-brown at middle part in *B. pianmaensis*); (2) apical part of anal segment divided into 3 processes at apex (apical part of anal segment divided into 2 processes at apex in *B. pianmaensis*); and (3) basal and middle parts of aedeagus each with a dentate process (basal and middle parts of aedeagus without a dentate process in *B. pianmaensis*).

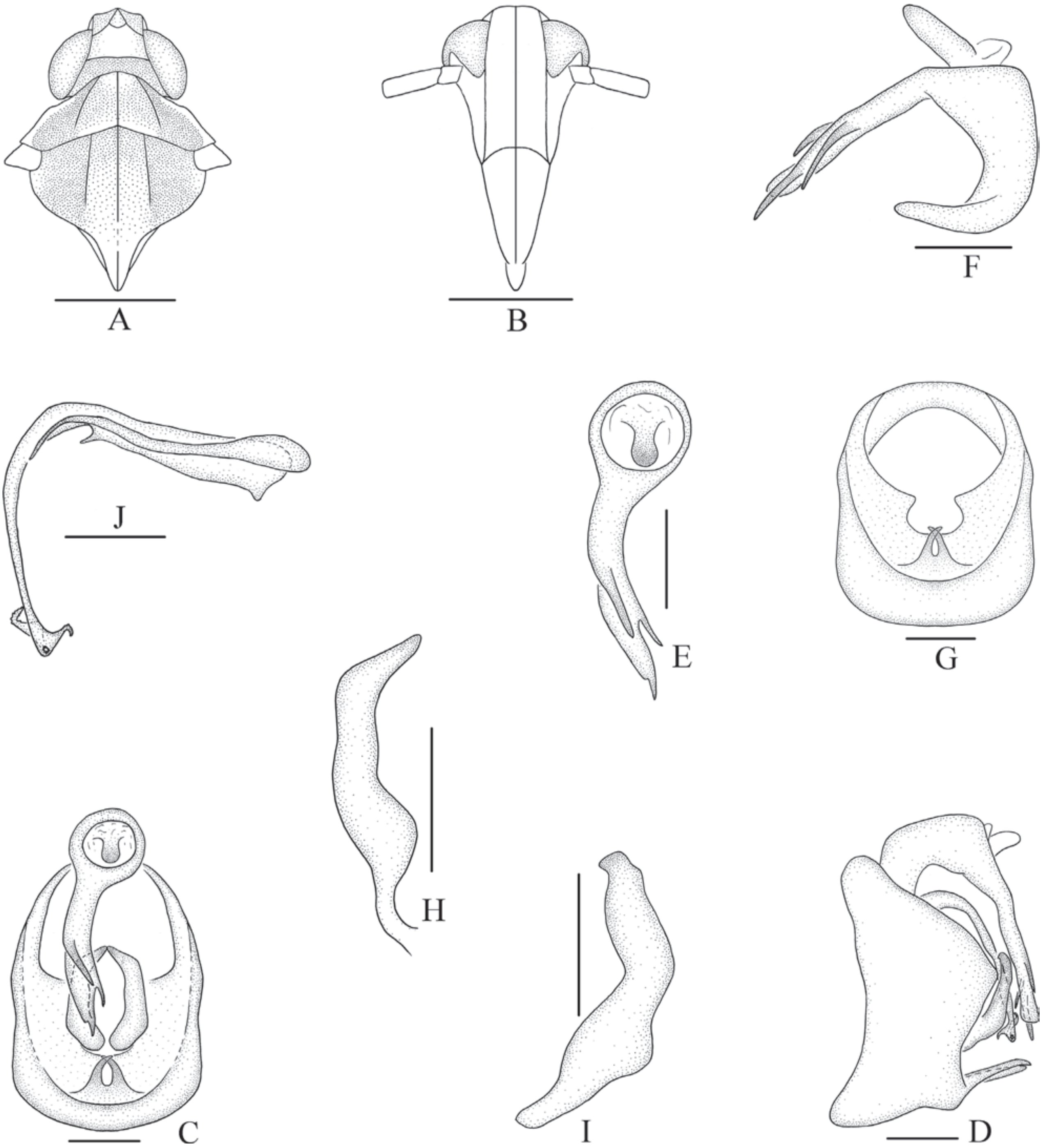

Figure 6. *Bambusiphaga striola* Lv, Li & Chen, sp. nov., male **A** head and thorax, dorsal view **B** frons, ventral view **C** male genitalia, posterior view **D** male genitalia, lateral view **E** anal segment, posterior view **F** anal segment, lateral view **G** pygofer, posterior view **H** genital style, posterior view **I** genital style, lateral view **J** aedeagus, lateral view. Scale bars: 0.5 mm (**A, B**); 0.2 mm (**C–J**).

Description. ***Measurements*.** Total length: male 4.8–5.0 mm (*N* = 14), female 5.3–5.6 mm (*N* = 15).

***Coloration*.** General color milky-white to dark brown (Fig. 5A–F). Vertex blackish-brown, basal compartment milky-white. Frons milky-white, basal part with two blackish-brown spots. Clypeus milky-white. Genae basal 1/4 dark brown, rest milky-white. Antennae light brown. Pronotum with lateral carinae yellowish-white at inner side, with two dark brown spots, outer side black, lateral margins yellowish-white. Mesonotum pale yellowish-brown, lateral sides with two blackish-brown spots, lateral margins yellow, apex of scutellum yellowish-white. Tegula milky-white. Forewings translucent, with a dark brown longitudinal band from anterior margin of basal part to posterior margin of apical part along CuP and MP. Legs yellowish-white, except coxae of fore and median legs dark brown.

***Head and thorax*.** Vertex (Figs 5C, 6A) shorter in middle line than wide at base (1: 1.30), width at apex narrower than at base (1: 1.31), middle part of anterior margin convex, lateral margins widened towards the end, lateral and submedian carinae distinct, Y-shaped carina indistinct. Frons (Figs 5E, 6B) longer in middle line than wide at widest portion (about 2.06: 1), widest at apex, median carina simple. Base of postclypeus (Figs 5E, 6B) as wide as apex of frons. Antennae (Figs 5E, 6B) with first segment longer than wide, shorter than second segment (1: 2.41). Pronotum (Figs 5C, 6A) nearly equal in length to vertex in midline (1.10: 1). Mesonotum (Figs 5C, 6A) longer than 1.40 times pronotum and vertex combined. Forewings (Fig. 5F) slender, longer than maximal width (3.41: 1).

***Male genitalia*.** Pygofer ventral margin longer than dorsal margin in lateral view (Fig. 6D), ventral margin slightly concave, posterior margin convex medially, in posterior view (Fig. 6C) with opening longer than wide, oval, ventral margin with a relatively short medioventral process, forked medially. Anal segment (Fig. 6C–F) ring-like, with a thick and long anal process at left lateroapical angle, taper the end, distinctly divided into 3 processes at apex. Genital styles (Fig. 6C, D, H–I) short, hogged, apical part pointed, curved inward. Aedeagus (Fig. 6J) with phallobase, phallus tubular, basal part thick, curved ventrally in the middle, basal and middle parts each with a dentate process, apical part with two unciform spinous processes; gonopore located at apex of phallus; phallobase slender and long, curved at apex.

Host plant. Bamboo.

Distribution. China (Tibet Province).

Etymology. The species name is derived from the Latin word “*striola*”, referring to forewing with a dark brown stripe.

Discussion

Host plant information is rarely recorded in Fulgoroidea and even in Delphacidae; most of the host information is recorded in Tropidocephalini. Species of the Tropidocephalini feed on Poaceae, with most reported plant associations involving bamboo. Many of these species are important or potential pests of bamboo (Chen 2003; Ding 2006; Chen and Tsai 2009). In *Bambusiphaga*, all species are known to exclusively feed on bamboo (Bambusoideae), of which *B. luodianensis* Ding, 1982, *B. citricolorata* Huang & Tian, 1979, *B. furca* Huang & Ding, 1979, *B. taiwanensis* (Muir, 1917) were reported to be one of the main stinging pests on bamboo (Yang et al. 1999; Liu and Chen 2008; Li et al. 2010; Hou and Chen 2013), occurring in 3~5 generations every year. It feeds on the tender parts of plants and has a significant impact on bamboo growth, making it one of the most important pests in bamboo forest production.

Based on data from published information and our field surveys, all species of *Bambusiphaga* were known from the Oriental region, and are especially species-rich in China, where 31 species are now recorded. However, at present, the genus is mainly distributed in Central China, East China, South China and Southwest China, and most species are known only from their type locality. Only 10 species have been reported outside their type locality and we believe that the actual distribution range of most species remains unclear. Therefore, further collection and investigation remain necessary to identify other undiscovered species and populations to better understand their ecological impacts and enhance the taxonomy of the group.

Acknowledgements

The authors are grateful to the specimen collectors for their hard work in the field.

Additional information

Conflict of interest

The authors have declared that no competing interests exist.

Ethical statement

No ethical statement was reported.

Funding

This work was supported by the National Natural Science Foundation of China (No. 32460397, 32470479, 32060343, 32260399, 32360131), and the Program of Planting Management Department of the Ministry of Agriculture and Rural Affairs (grant no. 152407055).

Author contributions

SSL, LY and YBZ conceived the original idea. SSL and HXL carried out the experiment. SSL wrote the manuscript with support from LY, YBZ and XSC. SSL and HXL offered great in data analysis.

Author ORCIDs

Sha-Sha Lv https://orcid.org/0000-0001-5353-5082
Hong-Xing Li https://orcid.org/0000-0002-6427-8875
Lin Yang https://orcid.org/0000-0002-7841-5156
Yu-Bo Zhang https://orcid.org/0000-0002-6118-6190
Xiang-Sheng Chen https://orcid.org/0000-0001-9801-0343

Data availability

All of the data that support the findings of this study are available in the main text.

References

Asche M (1983) *Bambusiphaga lynchi* nov. spec., a new delphacid from northeastern Himalaya, and some contributions to the genus *Bambusiphaga* Huang & Ding, 1979 (Homoptera Auchenorrhyncha Fulgoromorpha Delphacidae). Marburger Entomologische Publikationen 1: 197–210.

Bourgoin T (1987) A new interpretation of the homologies of the Hemiptera male genitalia, illustrated by the Tettigometridae (Hemiptera, Fulgoromorpha). Proceedings 6th Auchenorrhyncha Meeting, Turin, Italy, 7–11 September, 113–120.

Bourgoin T (2024) FLOW (Fulgoromorpha Lists On the Web): A knowledge and a taxonomy database dedicated to planthoppers (Insecta, Hemiptera, Fulgoromorpha, Fulgoroidea). Version 8, updated 06 September 2024. https://flow.hemiptera-databases.org/flow/ [Accessed on: 19 April 2024]

Bourgoin T, Wang RR, Asche M, Hoch H, Soulier-Perkins A, Stroiński A, Yap S, Szwedo J (2015) From micropterism to hyperpterism recognition strategy and standardized homology-driven terminology. Zoomorphology 134(1): 63–77. https://doi.org/10.1007/s00435-014-0243-6

Chen XS (2003) Key to genera of the tribe Tropidocephalini from the People's Republic of China with description of a new genus. The Canadian Entomologist 135: 811–821. https://doi.org/10.4039/n02-097

Chen XS, Liang AP (2007) Revision of the Oriental genus *Bambusiphaga* Huang & Ding (Hemiptera: Fulgoroidea: Delphacidae). Zoological Studies 46: 503–519.

Chen XS, Tsai JH (2009) Two new genera of Tropidocephalini (Hemiptera: Fulgoroidea: Delphacidae) from Hainan Province, China. Florida Entomologist 92(2): 261–268. https://doi.org/10.1653/024.092.0210

Chen XS, Li ZZ (2000) Descriptions of two new species of Delphacidae attacking bamboo from Guizhou Province, China (Homoptera: Delphacidae). Acta Zootaxonomica Sinica 25(2): 178–182.

Chen XS, Li ZZ, Jiang SN (2000) Descriptions of two new species of Delphacidae attacking bamboo from China (Homoptera: Fulgoroidea). Scientia Silvae Sinicae 36: 77–80.

Ding JH (1982) Two new species of the tribe Tropidocephalini (Homoptera: Delphacidae). Journal of Nanjing Agricultural College 4: 42–45.

Ding JH (2006) Fauna Sinica Insecta Vol. 45. Homoptera Delphacidae. Beijing, China: Science Press.

Ding JH, Hu GW (1982) A new species of the genus *Bambusiphaga* from Yunnan (Homoptera: Delphacidae). Acta Entomologica Sinica 25: 443–444.

Ding JH, Yang LF, Hu CL (1986) Descriptions of new genera and species of Delphacidae attacking bamboo from Yunnan Province, China. Acta Entomologica Sinica 29: 415–425.

Ding JH, Zhou WX, Huang BK (1999) Delphacidae of Fujian (Homoptera: Fulgoroidea). In BK Huang (Ed) Fauna of insects in Fujian Province of China. Vol. 2. Fuzhou, China: Fujian Science and Technology Press, 432–464.

Hou XH, Chen XS (2010) Oriental bamboo planthoppers: two new species of the genus *Bambusiphaga* (Hemiptera: Fulgoroidea: Delphacidae) from Hainan Island, China. Florida Entomologist 93: 391–397. https://doi.org/10.1653/024.093.0311

Hou XH, Chen XS (2013) Molecular identification of bamboo planthoppers (Hemiptera: Delphacidae) based on mitochondrial *16S rDNA* gene sequences. Forest Research 26(1): 65–69.

Huang CL, Tian LX, Ding JH (1979) A new genus and some new species of Delphacidae attacking bamboo in China. Acta Zootaxonomica Sinica 4(2): 170–181.

Kuoh CL, Ding JH, Tian LX, Huang CL (1983) Economic insect fauna of China, Fasc. 27, Homoptera: Delphacidae. Beijing, China: Science Press.

Kuoh CL, Huang CL, Tian LX, Ding JH (1980) New species and new genus of Delphacidae from China. Acta Entomologica Sinica 23(4): 413–426.

Li HR, Yang L, Chen XS (2010) The fauna and biogeography of bamboo-feeding planthoppers (Hemiptera: Fulgoroidea: Delphacidae) in the world. Acta Zootaxonomica Sinica 35(4): 806–818.

Li HX, Yang L, Chen XS (2018) Two new species of the bamboo-feeding planthopper genus *Bambusiphaga* Huang & Ding from China (Hemiptera, Fulgoromorpha, Delphacidae). ZooKeys 735: 83–96. https://doi.org/10.3897/zookeys.795.28036

Li HX, Chen XS, Yang L (2023) Three new species of the bamboo-feeding planthopper genus *Bambusiphaga* Huang & Ding from China (Hemiptera: Fulgoroidea: Delphacidae). European Journal of Taxonomy 875: 142–158. https://doi.org/10.5852/ejt.2023.875.2145

Liu MH, Chen XS (2008) Occurrence and harm of planthoppers in bamboo grove in Guiyang. Guizhou Agricultural Sciences 36(1): 87–89.

Muir F (1919) Some Malayan Delphacidae (Homoeptera). The Philippine Journal of Science 15: 521–531.

Qin DZ, Zhang YL, Ding JH (2006) A taxonomic study of the genus *Bambusiphaga* (Hemiptera, Fulgoroidea, Delphacidae). Acta Zootaxonomica Sinica 31(1): 148–151.

Qin DZ, Liu TT, Lin YF (2012) A new species in the *Bambusiphaga fascia* group (Hemiptera, Fulgoroidea, Delphacidae) from Shaanxi, China, with a key to all species in the group. Acta Zootaxonomica Sinica 37(4): 777–780.

Ramya N, Meshram NM (2019) New record of the genus *Bambusiphaga* (Hemiptera: Delphacidae: Tropidocephalini) from India with description of a new species. Zootaxa 4658(1): 197–200. https://doi.org/10.11646/zootaxa.4658.1.13

Wang JC, Ding JH (1996) Delphacidae fauna of Gansu Province, China (Homoptera: Fulgoroidea). Lanzhou, China: Gansu Science and Technology Press, 1–163.

Yang L, Chen XS (2011) The Oriental bamboo-feeding genus *Bambusiphaga* Huang & Ding, 1979 (Hemiptera: Delphacidae: Tropidocephalini): a checklist, a key to the species and descriptions of two new species. Zootaxa 2879: 50–59. https://doi.org/10.11646/zootaxa.2879.1.5

Yang JT, Yang CT (1986) Delphacidae of Taiwan (I). Asiracinae and the tribe Tropidocephalini (Homoptera: Fulgoroidea). Taiwan Museum Special Publication 6: 1–79.

Yang L, Chen XS, Chen HM (1999) Notes on planthoppers infesting bamboo in Guizhou. Journal of Mountain Agriculture and Biology 18(3): 154–161.

ZooKeys 1217: 309–326 (2024)
DOI: 10.3897/zookeys.1217.130397

Research Article

A new *Trychopeplus* species (Phasmatodea, Diapheromerinae, Cladomorformia) discovered from Ecuador's enigmatic Chocó ecoregion

Oskar V. Conle[1], Pablo Valero[2], Frank H. Hennemann[3]

1 *The Bavarian State Collection of Zoology, Munich, Germany*
2 *University of Murcia, Murcia, Spain*
3 *Zoologische Staatssammlung München, Munchen, Germany*
Corresponding author: Pablo Valero (pvr230286@gmail.com)

Academic editor: Sven Bradler
Received: 24 June 2024
Accepted: 11 September 2024
Published: 12 November 2024

ZooBank: https://zoobank.org/B16FEDFF-50D6-4C41-869C-F00BDABC4B62

Citation: Conle OV, Valero P, Hennemann FH (2024) A new *Trychopeplus* species (Phasmatodea, Diapheromerinae, Cladomorformia) discovered from Ecuador's enigmatic Chocó ecoregion. ZooKeys 1217: 309–326. https://doi.org/10.3897/zookeys.1217.130397

Abstract

This study presents a description of a new stick insect species belonging to the genus *Trychopeplus* Shelford, 1909, discovered by the authors in the Chocó ecoregion of northwestern Ecuador. *Trychopeplus mashpiensis* **sp. nov.** is described and illustrated based on males, females, and eggs. The distinctive features of this new species, such as its unique body ornamentation and the morphology of its egg structure without fringes, clearly differentiate it from other known species within the genus. Photographs of the new species are provided, along with an updated key and distribution map for all *Trychopeplus* species. These findings enhance our understanding of the genus's diversity.

Key words: Identification key, Insecta, stick insects, taxonomy, morphology

Introduction

Trychopeplus Shelford, 1909, is a genus of Neotropical stick insects (order Phasmida Leach, 1815) known for its remarkable morphological adaptations that allow it to blend almost perfectly with the epiphytic mosses in its habitat. These adaptations make *Trychopeplus* one of the most cryptic stick insect genera (Hennemann and Conle 2024).

The genus was described by Shelford in 1909 to distinguish Neotropical species from *Pericentrus* Redtenbacher, 1908, based on morphological differences and distinct geographic distributions compared to the type species *Pericentrus moewisi* Redtenbacher, 1908. The known distribution of *Pericentrus* is confined to East and South Asia, while *Trychopeplus* is endemic to the Neotropics (Zompro 2001; Brock and Büscher 2022; Hennemann and Conle 2024).

Traditional taxonomic revisions by Zompro (1998) and more recent work by Hennemann and Conle (2024) have confirmed the classification of *Trychopeplus* within the subfamily Diapheromerinae Kirby, 1904. Additionally, molecular phylogenetic studies, such as those by Bank and Bradler (2022) and Forni et al. (2022), have supported this classification, positioning *Trychopeplus* as closely related to *Phanocles* Stål, 1875. Despite this phylogenetic relationship, *Trychopeplus* is morphologically distinct due to several specialisations, including irregularly foliaceous lobes, spines, and teeth on the head, body, and limbs, adaptations that enhance its ability to camouflage effectively in its natural habitat of moist, mossy forests (Hennemann and Conle 2024).

Until now, the only eggs described from the genus were those of the type species *Trychopeplus laciniatus* (Westwood, 1874), which were characterised by being entirely covered with long fringes, a trait previously considered a potential autapomorphy of the genus (Hennemann and Conle 2024).

This study aims to describe a new species, *Trychopeplus mashpiensis* sp. nov., based on specimens collected from the Chocó forests in northwestern Ecuador. Through a comprehensive morphological analysis of males, females, and eggs, distinctive features are described and illustrated, which not only distinguish this new species from its congeners but also provide crucial insights into intrageneric variability. Furthermore, an updated key to all known *Trychopeplus* species is presented, along with a distribution map for the genus.

Material and methods

The material used in this study was collected through nocturnal direct sampling on trails near Mashpi Lodge, located in the parish of Pacto, northwest of the Ecuadorian province of Pichincha. Samplings took place from 1–4 October, 2023, under the collection permit MAATE–ARSFC–2023–3348.

The adult females collected were kept in a terrarium for several days to lay eggs. Euthanasia was performed by immersing the specimens in 96% ethanol for a few minutes. Both adults and eggs were stored dry, with adult specimens pinned. Insects and eggs were examined using a stereoscope (Zeiss Stemi SV6). Measurements were taken with a digital caliper at a precision of 0.1 mm. All eggs examined were fully developed and already laid. The terminology used for the descriptions of egg structures follows that of Clark-Sellick (1997, 1998). The terminology for the description of the genital morphology follows Bradler (2009). Photographs of live and dry specimens were taken with a Sony A7RIII camera fitted with a Tamron 90 mm f/2.8 DI VC USD macro lens. Lighting was provided by a Godox V350 flash with a diffuser. In photographs with a white background, backlighting was provided by a 24W 6000K LED light panel. Sample depositories and type status are abbreviated as follows:

ZSFQ	Museo de Zoología de la Universidad San Francisco de Quito, Quito, Ecuador;
ZSM	Zoologische Staatssammlung München, Munich, Germany.

Results

Diapheromeridae
Diapheromerinae Kirby, 1904
Cladomorformia

***Trychopeplus* Shelford, 1909**

Type species. *Pericentrus multilobatus* Redtenbacher, 1908: 352 (= *Ceroys laciniatus* Westwood, 1874: 174), by original monotypy.

Trychopeplus Brunner v. Wattenwyl, in litt. Shelford 1909: 354, 356 & pl. 6: 5 (♂). Hebard 1922: 358, pl. 15: 5 & 6 (♀ & egg). Hebard 1924: 148, pl. 6: 8 & 9 (♀). Campos 1926: 15 & plate (♀). Zompro 2001: 230. Otte and Brock 2005: 338. Conle, Hennemann and Gutiérrez 2011: 56. Brock and Büscher 2022: 515. Hennemann and Conle 2024: 283.

Ceroys Westwood, 1874: 174, pl. 32: 4 (♀).

Parobrimus Kirby, 1904: 344.

Pericentrus Redtenbacher, 1908: 352 (in part). Shelford, 1909: 356.

Trichopeplus Bradley and Galil 1977: 180 (misspelling).

Species included. *Trychopeplus laciniatus* (Westwood, 1874: 174, pl. 32: 4) [Nicaragua, Costa Rica, Panama]
= *Pericentrus multilobatus* Redtenbacher, 1908: 352
Trychopeplus spinosolobatus (Redtenbacher, 1908: 353) [Venezuela]
= *Pericentrus appendiculatus* Redtenbacher, 1908: 353.
Trychopeplus thaumasius Hebard, 1924: 148, pl. 6: 8 & 9 [Colombia, Ecuador]
= *Trychopeplus ortho-lamellatus* Campos, 1926: 15 & pl.
Trychopeplus mashpiensis Conle, Valero & Hennemann sp. nov. [Ecuador]

***Trychopeplus mashpiensis* Conle, Valero & Hennemann, sp. nov.**

https://zoobank.org/F2317335-BBE0-4CBF-8A42-3363832F8965
Figs 2–7

Material examined. ***Holotype*** • ♂; Ecuador: Prov. Pichincha, Parroquia de Pacto, Mashpi Lodge; 0°09'58.0"N, 78°52'38.4"W; 800–1000 m; leg. Cisneros, Conle, Valero & Hennemann 1–4.10.2023. [ZSFQ]. ***Paratype*** • 1 ♂, 3 ♀♀; 10 eggs: Ecuador: Prov. Pichincha, Parroquia de Pacto, Mashpi Lodge; 0°09'58.0"N, 78°52'38.4"W; 800–1000 m; leg. Cisneros, Conle, Valero & Hennemann 1–4.10.2023. [ZSFQ]. ***Paratype*** • 2 ♂♂, 2 ♀♀; 10 eggs: Ecuador: Prov. Pichincha, Parroquia de Pacto, Mashpi Lodge; 0°09'58.0"N, 78°52'38.4"W; 800–1000 m; leg. Cisneros, Conle, Valero & Hennemann 1–4.10.2023. [ZSM].

Differential diagnosis. *T. mashpiensis* sp. nov. is clearly distinguishable from *T. laciniatus* and *T. thaumasius* by the shape of its ornamentation, which is spiny in the new species and consists of irregular foliar lobes in *T. laciniatus* and *T. thaumasius*. Additionally, the distribution of *T. laciniatus* appears to be restricted to Central America (Fig. 1). Furthermore, the eggs of *T. laciniatus* and *T. thaumasius* have capsules densely covered with long, hair-like yellowish fringes, whereas in *T. mashpiensis* sp. nov. the capsule surface is smooth (Fig. 2).

The female of the new species is similar to *T. spinosolobatus*, of which the male and egg are unknown. However, they can be easily differentiated by the shape of the spines, the ornamentation of the femora, and the length of the subgenital plate. In *T. mashpiensis* sp. nov., the tips of the body spines are acute, while in *T. spinosolobatus* they are clearly rounded. The femoral ornamentation of *T. mashpiensis* sp. nov. consists only of two pairs of foliar lobes (Figs 3D, 4D),

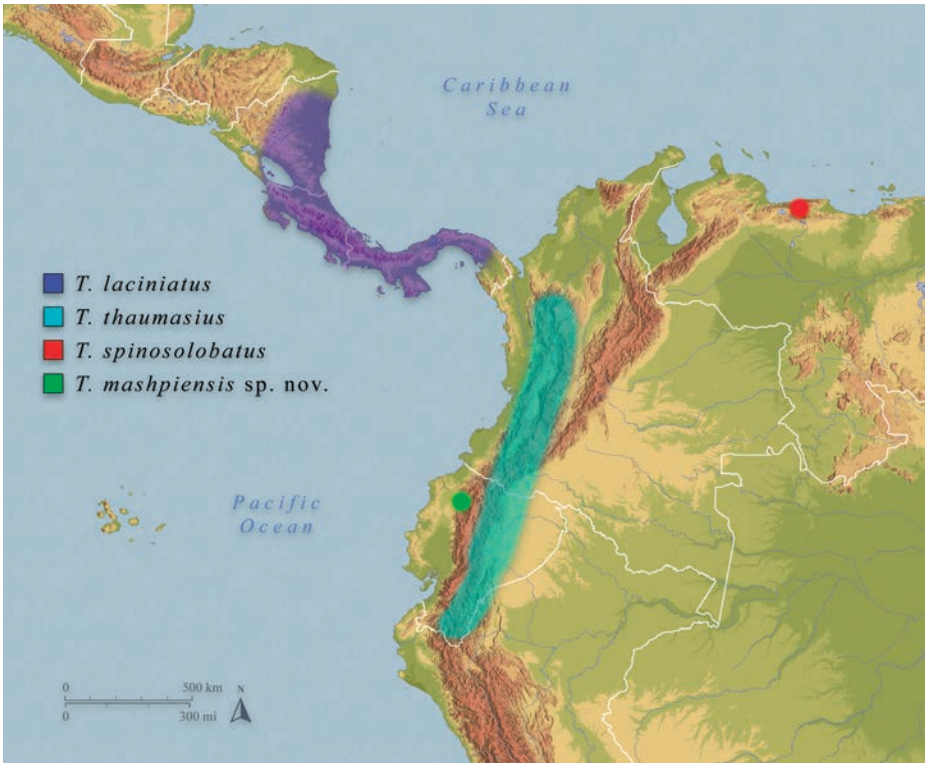

Figure 1. Approximate known distribution of four species of *Trychopeplus* Shelford, 1909 based on available literature.

whereas *T. spinosolobatus* has four, which are also larger. As for the subgenital plate, in *T. mashpiensis* sp. nov. it is approximately 1.2 times the length of the last three tergites combined, whereas in *T. spinosolobatus* it is much longer, measuring about 1.7 times the length of the last three tergites. Additionally, the distribution of *T. spinosolobatus*, although somewhat uncertain, seems to encompass Venezuela and Colombia (Hennemann and Conle 2024), while the new species is only known from the northwest of Ecuador (Fig. 1).

Description. The colouration is described mostly from photographs of live specimens. Table 1 presents the detailed measurements of the Holotype, as well as the measurement ranges of the Paratypes deposited in two official collections.

♀♀ (Figs 3, 5, 6). Of medium size for the genus (body length 79.6–85.6 mm), it features numerous spines of varying sizes across the head, thorax, and abdomen; and a relatively short subgenital plate for the genus. Its overall body and limb colouration range from medium to dark brown and olive green, with an irregular pattern occasionally speckled with small white or cream marks. Lime green eyes exhibit irregular dark brown lines. Antennae can be divided into a pattern formed out of groups of antennomeres, gradually darkening towards the apex of each group of antennomeres. The pronotum displays a thin, black, dorsolongitudinal line that gradually fades or even disappears towards its posterior half. In dorsal view, the metanotum displays two cream-coloured diagonal bands arranged in a "V" shape, with the apex touching the posterior margin of the metanotum.

Head. The head is ovoid, with the occiput strongly convex, approximately 1.4 times longer than wide. The vertex features two dorsolateral formations of spines or conical protuberances, arranged more or less in line, two of which

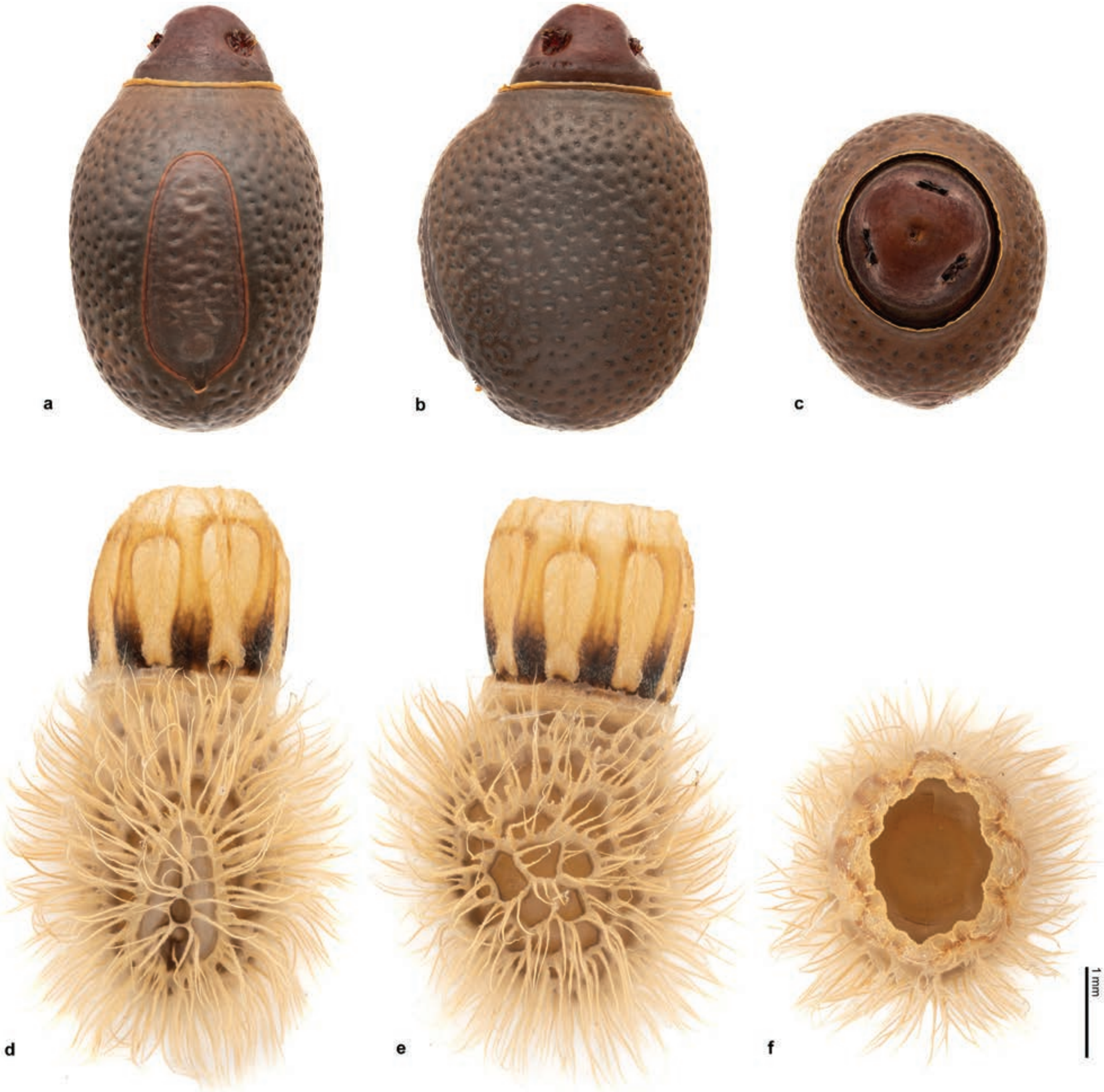

Figure 2. Egg of *Trychopeplus mashpiensis* sp. nov. in dorsal (**a**), lateral (**b**) and anterior (**c**) view. Egg of *Trychopeplus laciniatus* (Westwood, 1874) in dorsal (**d**), lateral (**e**) and anterior (**f**) view.

are prominently larger and slightly pointing towards the posterior. Additionally, irregular and much smaller conical protuberances are present between these formations, as well as on the genae. The eyes are medium-sized, nearly circular in shape, projecting almost hemispherically, and their diameter is approximately twice the length of the genae. The antennae are filiform and reach the posterior margin of abdominal segment V. The scape is dorsoventrally compressed, with the outer lateral margin gently concave and approximately 2.1 times longer than wide. The pedicel is round in cross-section and somewhat constricted apically.

Thorax. The entire thorax is densely covered with spine-like protuberances, varying in size and generally exhibiting a degree of bilateral symmetry. The pronotum is approximately 0.75 times the length of the head and 0.9 times its width, with a basically rectangular shape and a slight premedial narrowing.

Table 1. Measurements (mm) of *Trychopeplus mashpiensis* sp. nov. HT = holotype; PT = paratype.

	♂, HT [ZSFQ]	**♂♂, PT [ZSFQ]**	**♀♀, PT [ZSFQ]**	**♂♂, PT [ZSM]**	**♀♀, PT [ZSM]**
Body (incl. subgen. pl.):	–	–	81.5–87.4	–	83.6–85.7
Body:	73.3	72.3–74.3	79.6–85.6	72.6–73.9	82.1–83.0
Pronotum:	2.5	2.7–3.1	3.7–4.5	2.7–2.8	4.1–4.3
Mesonotum:	14.1	14.5–14.7	18.0–19.4	14.1–14.3	17.7–19.0
Metanotum:	4.1	3.6–4.3	5.6–6.2	3.0–4.4	6.2–7.4
Median segment:	10.5	10.7–10.9	6.4–7.1	9.4–10.3	4.4–6.4
Tegmina:	5.8	6.3–6.5	–	5.6–5.7	–
Alae:	35.7	34.5–37.7	–	34.9–36.8	–
Profemora:	27.6	27.2–28.0	23.9–26.2	26.4–28.2	24.6–26.3
Mesofemora:	21.3	22.1–22.4	17.8–18.8	22.3–23.0	19.1–20.6
Metafemora:	25.2	26.1–26.9	22.1–22.3	26.5–27.6	23.3–24.5
Protibiae:	30.5	30.9–31.0	25.4–28.0	30.6–31.1	26.1–29.2
Mesotibiae:	22.3	22.6–22.9	19.7–21.3	22.6–22.8	19.9–23.1
Metatibiae:	27.8	28.3–28.9	26.0–28.8	28.9–29.0	26.3–32.0
Antennae:	74.1	74.5–75.2	23.8–61.1	74.2–75.3	62.1–70.6

The anterior margin is somewhat elevated. The transverse median sulcus is moderately distinct, curved, and nearly expanding across the entire width of the segment. It features several dorsal spines, arranged approximately parallel to each other; the first pair of spines are simple and small, located just before the transverse median sulcus; the second pair is situated near the posterior margin of the pronotum, larger in size and appearing paired, almost as if forming a single bifurcated structure. The mesothorax is approximately 4.3 times longer than the prothorax and of uniform diameter except for a slight anterior narrowing. Among the spines of the mesonotum, the most prominent are located approximately at the distance of the first and second quarters of its total length. The metanotum is approximately one-third the length of the mesonotum. The posterior margins of the meso- and metanotum exhibit two dorsal spines each, parallel-sided and of medium size, slightly directed backwards.

***Abdomen*.** The abdomen (excluding the subgenital plate) is approximately the same length as the combination of the head and thorax (including the median segment). The median segment is roughly the same size as the metanotum and is more or less quadrangular. Segments II–IX feature prominent dorsoventrally flattened lobes, with rounded margins on the posterior sides of each segment. These lobes gradually increase in size from segment II to VI, and then gradually decrease until segment IX. Segment II is slightly shorter than the median segment and slightly longer than wide. Segments II–V have approximately the same length and width, while from VI to IX, they gradually decrease in length and width. Sternites II–VII exhibit small blunt spines and a medial protuberance on the posterior margin of each segment, covered by small setae. The preopercular organ is barely distinguishable and consists simply of a small, wart-like swelling near the posterior margin of sternite VII; the entire area is dark reddish-brown. The anal segment is slightly longer than tergum IX and has a generally rounded outline, except for a small posterior medial incision and two triangular lateral projections near the base. The epiproct is very

Figure 3. Female of *Trychopeplus mashpiensis* sp. nov. **a** habitus in lateral view **b** head and thorax in dorsolateral view **c** head, pro- and mesothorax in dorsal view **d** mesofemora in dorsal view **e** end of the abdomen in dorsal view **f** end of the abdomen in lateral view **g** end of the abdomen in ventral view.

small and almost completely hidden beneath the anal segment. The cerci are of similar length to the anal segment, thin, and circular in cross-section; extending clearly beyond the posterior margin of the anal segment. The gonapophyses are moderately enlarged, keeled, and almost reaching the base of the cerci.

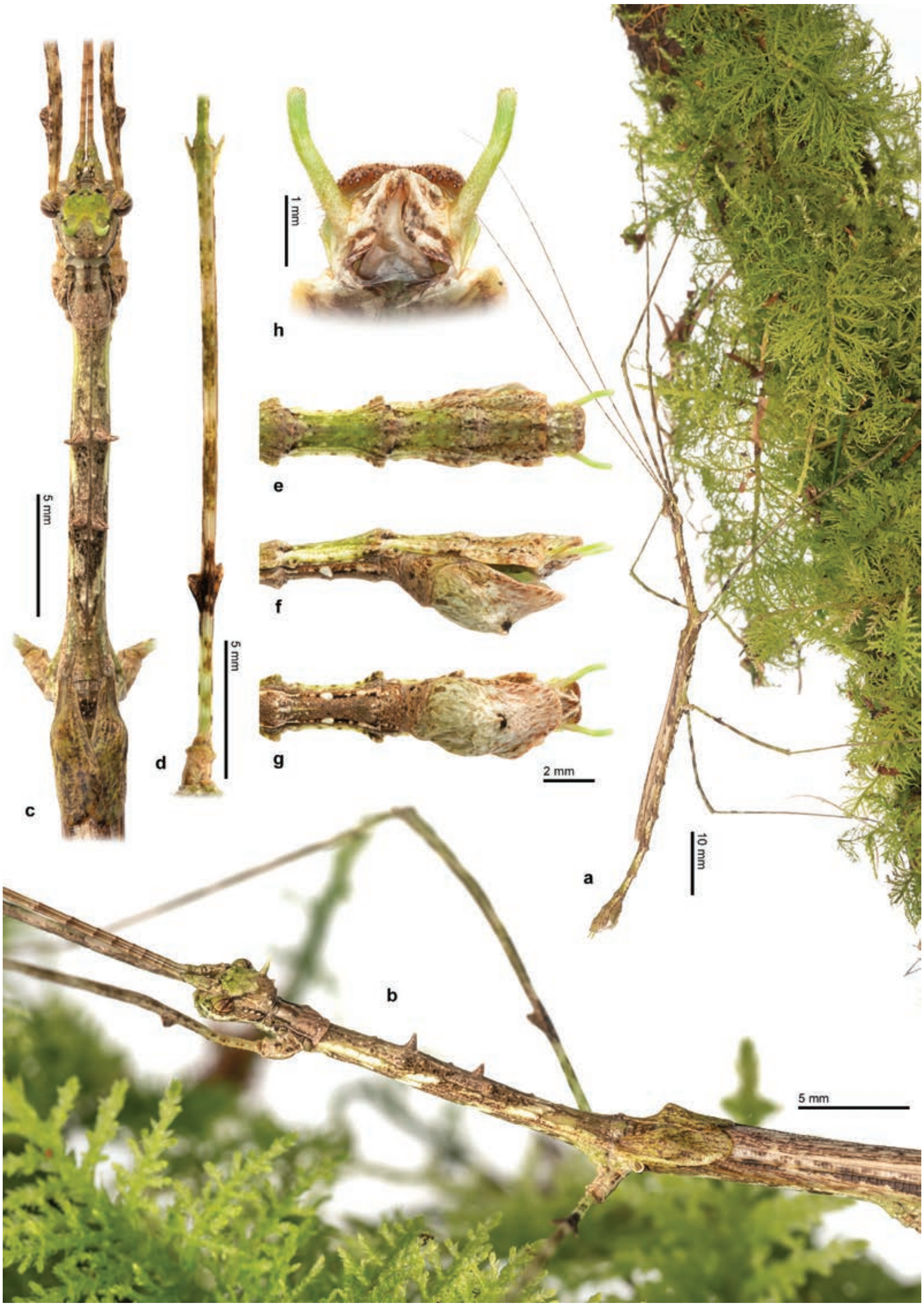

Figure 4. Male of *Trychopeplus mashpiensis* sp. nov. **a** habitus in lateral view **b** head and thorax in dorsolateral view **c** head, pro- and mesothorax in dorsal view **d** mesofemora in dorsal view **e** end of the abdomen in dorsal view **f** end of the abdomen in lateral view **g** end of the abdomen in ventral view **h** detail of the vomer.

Gonapophysis VIII is relatively long and slightly curved upwards, reaching approximately the posterior margin of the anal segment or even slightly surpassing it, but never reaching the apex of the subgenital plate. The subgenital plate is shovel-shaped, slightly longitudinally keeled, and projecting approximately 20% of its total length over the apex of the anal segment; the lateral margins are undulated and the apex is slightly curved downwards.

Figure 5. Habitus of *Trychopeplus mashpiensis* sp. nov. in dorsal view **a** male holotype **b** female paratype.

Legs**.** All legs are long and slender. Both femora and tibiae are trapezoidal in cross-section, with the two dorsal carinae closely spaced. All femora are strongly curved. Additionally, the profemora are also strongly curved at the base to accommodate the head when aligned in line with the body. The meso- and metafemora feature two pairs of foliaceous lobes on the ventral carinae, one on the outer ventral carina and another on the inner, with rounded edges. The first pair is located approximately at one-third from the base, consisting of semicircular lobes. The second pair is positioned at the posterior end of the profemora, and they are at least twice as long as they are wide. In the profemora, the lobes are similarly

Figure 6. Females of *Trychopeplus mashpiensis* sp. nov. in their natural habitat.

arranged but only present on the outer ventral carina. All femora are longer than the mesothorax. All tibiae are slender, more or less straight, slightly longer than the corresponding femur, and lack ornamentation. The basitarsi are slightly shorter than the combined remaining tarsomeres and also lack ornamentation.

♂♂ (Figs 4, 5, 7). Of medium size for the genus (body length 72.3–74.3 mm), has spines on the head and part of the body, although they are less numerous and smaller compared to those of the female. Similar to other known males of the genus, it has fully developed tegmina and alae.

Figure 7. Males of *Trychopeplus mashpiensis* sp. nov. in their natural habitat.

The general colouration is similar to that of the female, though usually with less green. The tegmina and the costal area of the alae follow the same colouration pattern as the rest of the body, while the anal area of the wings is uniformly translucent ochre. The cerci are light green.

Head. The head is very similar to that of the female, but with smaller ornamentation. However, the eyes are proportionally larger, with a diameter approximately 1.4 times the length of the genae. Ocelli absent. The antennae, although similar to those of the female, are proportionally longer, reaching and even slightly exceeding the total body length.

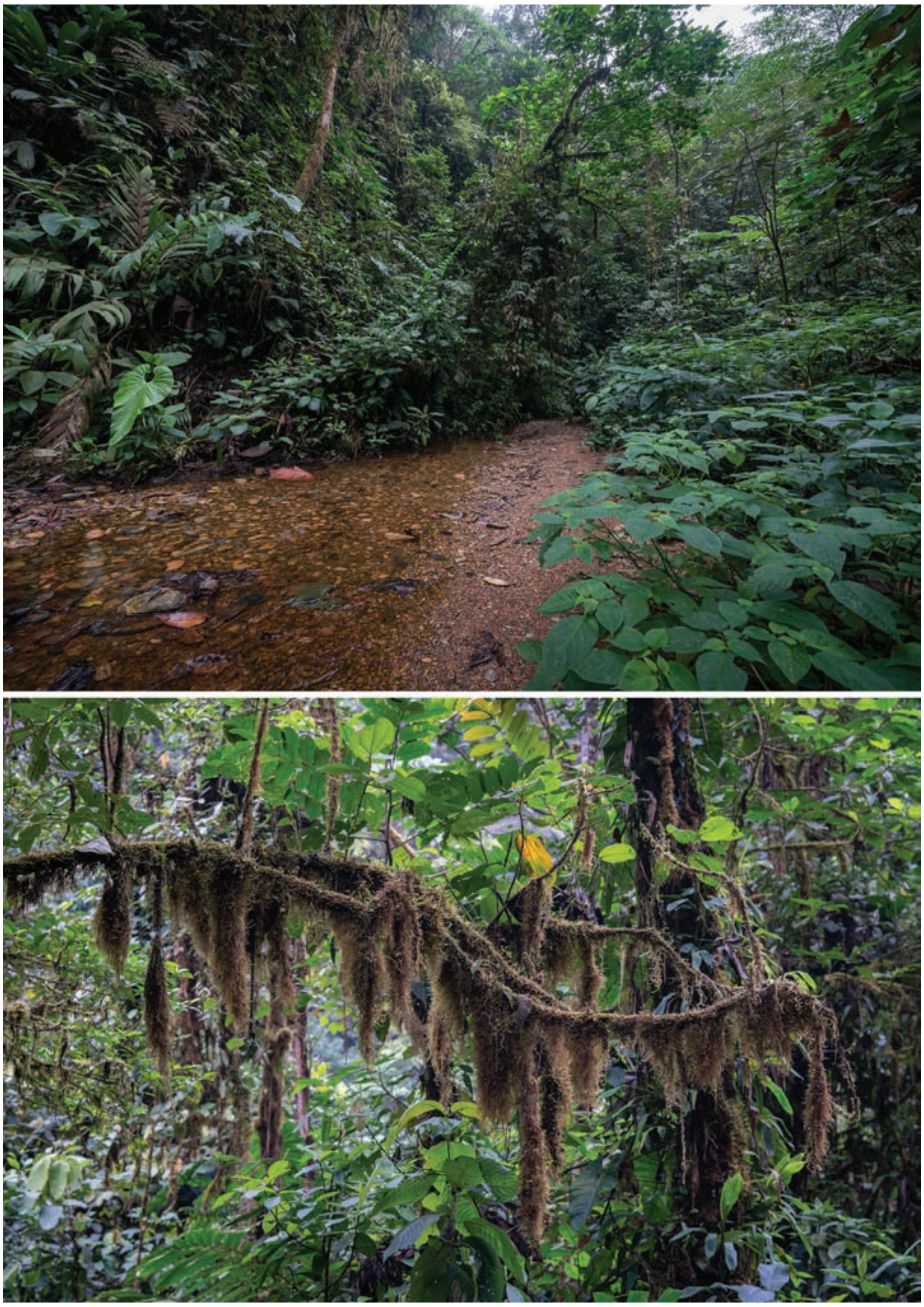

Figure 8. Natural habitat of *Trychopeplus mashpiensis* sp. nov. (Top), including an example of a microhabitat with concentrations of epiphytic mosses (Bottom) where they are commonly found resting.

Thorax. The thorax ornamentation is very similar to that of the female in terms of the number and position of spines, but these are much smaller, with the smallest considered as small protuberances rather than spines. The pronotum is approximately 0.75 times the length and width of the head, similar in shape to that of the female but with small protuberances instead of spines. The mesothorax is approximately 4.6 times longer than the pronotum and uniformly wide throughout its length. As in the female, the most prominent spines on the mesonotum are arranged in the first and second quarters of its total length; however, they are smaller than in the female, and the remaining spines appear as small protuberances. The metanotum is approximately one-third the length of the mesonotum and, unlike the female, does not have spines on the posterior margins. The tegmina are simple, with a slight elevation at the base of the wings to accommodate them; they are approximately 3.2 times longer than wide and cover a little more than one-third of the total length of the metathorax. The wings are approximately twice as long as they are wide and reach the abdominal segment VI.

Abdomen. The abdomen is approximately the same length as the combined head and thorax (including the median segment). The median segment is 2.7 times longer than the metanotum. As in the female, segments II–IX have flattened lateral lobes near the posterior margin of each segment, but in the males, these are very small and uniformly sized across all segments. Abdominal segment II is approximately 0.5 times the length of the median segment and about three times longer than wide. Segments II–VII are all the same width, while VIII and IX are slightly wider. Segment III is the same length as segment II. From segment IV onwards, the length of each segment gradually decreases slightly. The median segment and tergites II–IX have a smooth surface without ornamentation.

Sternites II–VII have small blunt spines and a medial protuberance on the posterior margin of each segment. The anal segment is approximately 0.6 times the length of tergite IX and, as in the female, has a generally rounded outline, except for a small posterior medial incision and two triangular lateral projections near the base. The cerci are approximately 1.5 times longer than the anal segment, clearly extending beyond its posterior margin; they are slender and circular in cross-section. The vomer is shaped like a sharp spine and dorsoventrally flattened, with the basal half broadly widened. The poculum is shaped like an elongated scoop, with a small basal protuberance in the centre. In ventral view, it is asymmetrical, as the right outer margin presents a small expansion. The posterior margin is rounded and reaches halfway up the anal segment.

Legs. The legs have similar morphology and ornamentation to those of the females, although they are longer, slender, and with less curved femora. All femora are longer than the combined head, pro-, and mesothorax. All tibiae are thin, more or less straight, slightly longer than the corresponding femur, and lack ornamentation. The basitarsi are slightly longer than the remaining tarsomeres combined and also lack ornamentation.

Eggs (Fig. 2). Of medium size and atypical appearance for the genus (length 2.9–3.4 mm). The capsule is chestnut brown in colour, ovoid in shape, slightly higher than wide and longer than high. Its surface is adorned with numerous small crater-like pits arranged irregularly. There are no ornamental features such as hairs or fringes. The operculum rises prominently, forming a cone with a strongly rounded apex. The interior of the operculum is hollow and divided into three cavities by a thin, transparent membrane. Three openings in the walls of the operculum connect each of these cavities to the exterior, each surrounded by an irregularly elevated crown-like structure. A fourth opening, lacking an outer crown, is located at the vertex and seemingly provides access to the three cavities. The function of these structures remains unknown to the authors. The micropylar plate is outlined by a contour of reddish-brown colour. It resembles the silhouette of an avocado, approximately a little over half the length of the capsule. It is roughly twice as long as it is wide and is slightly shifted towards the polar area.

Measurements [mm]. Length including operculum 3.6–4.2, length 2.9–3.4, height 2.5–2.8, width 2.2–2.4, length of micropylar plate 1.9–2.1.

Distribution. So far, the species is known only from the type locality, in the northwest of Pichincha Province, Ecuador.

Etymology. The epithet *mashpiensis* refers to the Mashpi Reserve, where the species was discovered, in appreciation for the excellent treatment received from the lodge staff and the scientific team, as well as their significant conservation efforts.

Key to species of *Trychopeplus* Shelford, 1909

Note. The males of *T. spinosolobatus* and *T. thaumasius* remain undescribed.

♀♀ && ♂♂

1 Prominent head and mesonotum ornamentation in the form of simple spines; mesofemora lobes simple with rounded margins.......................... **2**

– Prominent head and mesonotum ornamentation in the form of foliate lobes or branched spines; at least the medial pair of mesofemora lobes are compound and have irregular margins... **3**

2 Subgenital plate 1.6× longer than combined tergites VIII–X; femora with four pairs of rounded foliate lobes, one at the apex and the rest in the first, second, and third quarter of the corresponding femur length; Venezuela .... ***Trychopeplus spinosolobatus***

– Subgenital plate 1.2× longer than combined tergites VIII–X; femora with two pairs of rounded foliate lobes, one at the apex and another in the first third of the corresponding femur length; NW Ecuador .... ***T. mashpiensis* sp. nov.**

3 Body length > 100 mm; pronotum without ornamentation; gonapophyses shorter than the subgenital plate; Ecuador, Colombia........... ***T. thaumasius***

– Body length < 100 mm; pronotum with small spines; gonapophyses distinctly longer than the subgenital plate; Nicaragua, Costa Rica, and Panama .... ***T. laciniatus***

Discussion

The inclusion of *Trychopeplus mashpiensis* sp. nov. within the genus *Trychopeplus* Shelford, 1909, is based on a careful evaluation of morphological and ecological criteria. Despite clear differences from the type species *Trychopeplus laciniatus* (Westwood, 1874), particularly in egg ornamentation, *T. mashpiensis* sp. nov. shares a suite of characteristics consistent with the typical morphology and ecology of the genus. According to Hennemann and Conle (2024), the distinctive morphological traits of *Trychopeplus* include large, numerous appendages and excrescences on the head and mesothorax, prominent lateral lobes on the abdominal tergites, as well as irregularly foliaceous lobes and teeth on the limbs.

Morphologically, *Trychopeplus spinosolobatus* (Redtenbacher, 1908) is the most similar species within the genus, as it exhibits appendages and excrescences on the head and thorax in the form of spines rather than foliaceous lobes, which distinguishes it from *T. laciniatus* and *T. thaumasius* Hebard, 1924.

Unfortunately, only the female of *T. spinosolobatus* is known, leaving the morphology of its eggs uncertain, whether they resemble those of *T. laciniatus*, *T. mashpiensis* sp. nov., or are distinct to both of them.

One of the most significant findings of this study is the morphological differentiation between the eggs of *T. mashpiensis* sp. nov. and those of *T. laciniatus*, the only species in the genus whose eggs had been previously documented (Hebard 1922; Hennemann and Conle 2024). While the eggs of *T. laciniatus* are covered with long fringes (a feature previously suggested as a potential autapomorphy of the genus (Hennemann and Conle 2024)) the eggs of *T. mashpiensis* sp. nov. lack these fringes entirely (Fig. 2). This observation suggests a greater diversity in egg morphology within *Trychopeplus*, potentially indicating adaptive ecological diversification within the genus.

Hennemann and Conle (2024) hypothesised that the fringes on the eggs of *T. laciniatus* might aid in their attachment to moss or lichens, providing protection during embryonic development. However, this hypothesis is not applicable to *T. mashpiensis* sp. nov., given the absence of fringes on its eggs. Recent observations by one of the authors, during a short period of captivity (10 days), revealed that despite the presence of moss in the terrarium, females of *T. laciniatus* did not deposit their eggs on it, but instead threw them forcefully in random directions, a common behaviour among Diapheromerinae (Goldberg et al. 2015; Hennemann and Conle 2024). This egg-laying method makes it unlikely that the eggs would adhere to surrounding moss, especially considering that the fringes on the eggs of *T. laciniatus* remain retracted at the time of laying and for several hours afterwards (Hennemann and Conle 2024), preventing immediate adhesion. Büscher et al. (2024) examined the eggs of *T. laciniatus* using electron microscopy and observed that the egg hairs are, in fact, porous. Based on this finding, they suggested that these hairs might serve to absorb water, thereby preventing the egg from dehydration. Additionally, they proposed other hypotheses regarding the potential functions of these hairs, such as trapping air between them to prevent the embryo from drowning if submerged, or even playing a role in thermoregulation.

Despite the absence of long fringes on the eggs of *T. mashpiensis* sp. nov., this new species retains other characteristic features of the genus, such as the ovoid egg capsule, which is slightly longer than it is tall and wide; a pear-shaped micropyle plate displaced towards the polar area, sculpted similarly to the capsule; and an almost circular operculum with a prominently elevated outer margin, forming a hollow structure. The discovery of *T. mashpiensis* sp. nov.. highlights the need to reassess the characteristics used to define autapomorphies at the genus level, as the absence of fringes in the eggs of *T. mashpiensis* sp. nov. challenges the notion that this feature is diagnostic for the genus, as suggested by Hennemann and Conle (2024). Nevertheless, this intrageneric diversity is not entirely surprising, given the known interspecific variability observed in the eggs of related genera such as *Phanocles* Stål, 1875 and *Phanocloidea* Zompro, 2001 (Hennemann and Conle 2024).

The habitat, behaviour, and distribution of *T. mashpiensis* sp. nov. are consistent with those known for the genus (Fig. 8). All specimens, both nymphs and adults, were found at night in montane humid forests, at a height of 1.5 to 4 metres on trees with abundant epiphytic mosses. Similar habitats were observed by one of the authors during previous surveys, where *T. laciniatus* was found in Panama and *T. thaumasius* in Tungurahua Province, Ecuador.

In Monteverde, Costa Rica, *T. laciniatus* is known to feed exclusively on orchids such as *Prosthechea campylostalix* (Rchb.f.) W.E.Higgins and *Oncidium* spp. (Orchidaceae; Kenji Nishida, pers. comm.). Additionally, one of the authors observed specimens of the same species feeding on *Maxillaria egertoniana* (Bateman ex Lindl.) Molinari in Chagres National Park, Panama. This is noteworthy, as there appear to be no other reports of Diapheromerinae feeding on orchids, suggesting this might be a unique characteristic of the genus. Nevertheless, although various types of epiphytic orchids were observed in the natural habitat of *T. mashpiensis* sp. nov., it was not possible to confirm whether any of them served as host plants, as no feeding specimens were observed during the surveys.

Conclusions

The inclusion of *Trychopeplus mashpiensis* sp. nov. within the genus *Trychopeplus* Shelford, 1909 underscores the importance of taxonomic exploration and morphological revision in understanding Neotropical biodiversity. This study not only increases the number of known species within the genus to four, but also provides new insights into the morphological variability of eggs, which has significant implications for future identification and classification within the genus. The close phylogenetic relationship between *Trychopeplus* and *Phanocles* highlights the need for further research to clarify evolutionary relationships within the subfamily Diapheromerinae and to address the complexity of diversity within the genus.

Acknowledgements

We would like to express our gratitude to Mateo Roldán, Director of Research and Biology at Mashpi Reserve, and Estuardo Lima, guide at Mashpi Lodge, for their invaluable assistance and guidance, which allowed us to quickly familiarise ourselves with the area, facilitating the planning of our samplings. We also wish to extend our sincere thanks to Diego F. Cisneros-Heredia and Emilia Peñaherrera-Romero, from the Department of Biology at the University San Francisco de Quito (USFQ) for their unwavering support. Thanks to their collaboration, the authors have been able to realise an ambitious national research project aimed at studying and cataloguing the little-known diversity of phasmids in Ecuador.

Additional information

Conflict of interest

The authors have declared that no competing interests exist.

Ethical statement

No ethical statement was reported.

Funding

No funding was reported.

Author contributions

Funding acquisition: OVC. Resources: PV, OVC, FHH. Writing - original draft: PV. Writing - review and editing: PV, OVC, FHH.

Author ORCIDs

Oskar V. Conle https://orcid.org/0000-0001-5609-5107
Pablo Valero https://orcid.org/0000-0002-5471-3458
Frank H. Hennemann https://orcid.org/0000-0002-6547-4704

Data availability

All of the data that support the findings of this study are available in the main text.

References

Bank S, Bradler S (2022) A second view on the evolution of flight in stick and leaf insects (Phasmatodea). BMC Ecology and Evolution 22: 62. https://doi.org/10.1186/s12862-022-02018-5

Bradler S (2009) Die Phylogenie der StaB- und Gespenstschrecken (Insecta. Phasmatodea). Species Phylogenie and Evolution 2: 3–139. https://doi.org/10.17875/gup2009-710

Bradley JC, Galil BS (1977) The taxonomic arrangement of the Phasmatodea with keys to the subfamilies and tribes. Proceedings of the Entomological Society of Washington 79: 176–208.

Brock, PD, Büscher TH (2022) Stick and Leaf Insects of the World – Phasmids. N.A.P. Editions, Verrières-le-Buisson, 611 pp.

Büscher TH, Reck LM, Gorb SN (2024) Functional surface structures on the eggs of stick and leaf insects (Insecta: Phasmatodea). Zoologica 166: 1–278.

Campos F (1926) Una nueva especie del genero Trychopeplus (Ortóptero de la fam. Phasmidae, subfam. Phibalosominae). Revista del Colegio Nacional Vicente Rocafuerte, Guyaquil 23/24: 15–18.

Clark-Sellick JT (1997) Descriptive terminology of the phasmid egg capsule, with an extended key to the genera based on egg structure. Systematic Entomology 22: 97–122. https://doi.org/10.1046/j.1365-3113.1997.d01-30.x

Clark-Sellick JT (1998) The micropylar plate of the eggs of Phasmida, with a survey of the range of plate form within the order. Systematic Entomology 23: 203–228. https://doi.org/10.1046/j.1365-3113.1998.00056.x

Conle OV, Hennemann FH, Gutiérrez Y (2011) The Stick Insects of Colombia. A catalogue and bibliography with the descriptions of four new genera and 74 new species. Books on Demand GmbH, Norderstedt, 406 pp.

Forni G, Martelossi J, Valero P, Hennemann FH, Conle OV, Luchetti A, Mantovani B (2022) Macroevolutionary analyses provide new evidence of phasmid wing evolution as a reversal process. Systematic Biology 2022 (syac038): 1–16. https://doi.org/10.1093/sysbio/syac038

Goldberg J, Bresseel J, Constant J, Kneubühler B, Leubner F, Michalik P, Bradler S (2015) Extreme convergence in egg-laying strategy across insect orders. Scientific Reports 5: 1–7. https://doi.org/10.1038/srep07825

Hebard M (1922) Studies in the Mantidae and Phasmidae of Panama. Transactions of the American Entomological Society 48: 327–362.

Hebard M (1924) Studies in Dermaptera and Orthoptera of Equador. Proceedings of the Academy of Natural Sciences of Philadelphia 76: 109–248.

Hennemann FH, Conle OV (2024) Studies on Neotropical Phasmatodea XXVI: Taxonomic review of Cladomorformia tax. n., a lineage of Diapheromerinae stick insects, with the descriptions of seven new genera and 41 new species (Phasmatodea:

Occidophasmata: Diapheromerinae). Zootaxa 5444(1): 001–454. https://doi.org/10.11646/zootaxa.5444.1.1

Kirby WF (1904) A Synonymic Catalogue of Orthoptera, 1. Orthoptera Euplexoptera, Cursoria et Gressoria. (Forficulidae, Hemimeridae, Blattidae, Mantidae, Phasmidae). British Museum, London, 501 pp.

Otte D, Brock P (2005) Phasmid Species File. Catalog of Stick and Leaf Insects of the World. The Insect Diversity Association and the Academy of Natural Sciences, Philadelphia, 414 pp.

Redtenbacher J (1908) Die Insektenfamilie der Phasmiden, III. Phasmidae Anareolatae (Phibalosomini, Acrophyllini, Necrosciini). Leipzig, 341–589.

Shelford R (1909) Family Phasmidae. In: Biologia Centrali-Americana; or, Contributions to the knowledge of the Fauna and Flora of Mexico and Central America. Insecta, Orthoptera Vol. 2: 343–377.

Westwood JO (1874) Thesaurus Entomologicus Oxoniensis; or, illustrations of new, rare, and interesting insects, for the most part contained in the collections presented to the University of Oxford by the Rev. F.W. Hope. Clarendon Press, Oxford, 205 pp. https://doi.org/10.5962/bhl.title.14077

Zompro O (1998) Revision nearktischer und neotropischer Genera der Insektenordnung Phasmatodea, insbesondere der Familie Heteronemiidae sensu Bradley & Galil [Unpublished PhD Thesis]. Universität zu Kiel, 95 pp.

Zompro O (2001) A generic revision of the insect order Phasmatodea: The New World genera of the stick insect subfamily Diapheromeridae: Diapheromerinae = Heteronemiidae: Heteronemiinae sensu Bradley & Galil, 1977. Revue suisse de Zoologie 108(1): 129–255. https://doi.org/10.5962/bhl.part.79626

ZooKeys 1217: 327–342 (2024)
DOI: 10.3897/zookeys.1217.122695

Research Article

A new species of the genus *Dryadaula* Meyrick (Lepidoptera, Dryadaulidae) from Japan, with a redescription of *D. epischista* (Meyrick, 1936)

Jinhyeong Park[1], Sadahisa Yagi[2,3], Shigeki Kobayashi[4], Toshiya Hirowatari[2,3]

1 *Entomological Laboratory, Graduate School of Bioresource and Bioenvironmental Sciences, Kyushu University, 744 Motooka, Nishi-ku, Fukuoka, 819-0395, Japan*
2 *Entomological Laboratory, Faculty of Agriculture, Kyushu University, 744 Motooka, Nishi-ku, Fukuoka, 819-0395, Japan*
3 *Insect Science and Creative Entomology Center, Kyushu University, 744 Motooka, Nishi-ku, Fukuoka, 819-0395, Japan*
4 *Environmental Entomology and Zoology, Graduate School of Agriculture, Osaka Metropolitan University, Sakai, Osaka, 599-8531, Japan*
Corresponding author: Jinhyeong Park (parkjinhyeong19990929@gmail.com)

Abstract

Dryadaula epischista (Meyrick, 1936), initially described from a single male specimen in Japan, is herein redescribed based on newly collected specimens from the type locality. Furthermore, we describe *Dryadaula orientalis* Park & Yagi, **sp. nov.**, a new species from Japan that closely resembles *D. epischista*. The adults and genitalia of the two species are illustrated. The genitalia of *D. epischista* from a specimen collected at the type locality are shown for the first time. DNA barcodes of the two *Dryadaula* species and the genetic distances of barcode regions among them and other congeners are provided.

Key words: Cytochrome *c* oxidase subunit I, molecular phylogeny, morphology, taxonomy

Academic editor: José Luis Yela
Received: 15 March 2024
Accepted: 30 September 2024
Published: 12 November 2024

ZooBank: https://zoobank.org/6DB61E4E-2D7F-4C91-AC64-1A8E8EFA66D1

Citation: Park J, Yagi S, Kobayashi S, Hirowatari T (2024) A new species of the genus *Dryadaula* Meyrick (Lepidoptera, Dryadaulidae) from Japan, with a redescription of *D. epischista* (Meyrick, 1936). ZooKeys 1217: 327–342. https://doi.org/10.3897/zookeys.1217.122695

Introduction

The family Dryadaulidae was recently established for two genera, *Dryadaula* and *Brachydoxa*, based on molecular phylogenetic analysis, although these two genera were, in the past, included within Tineidae. Three genera, *Eschatotypa*, *Eugennaea*, and *Sagephora*, have been suggested to belong to Dryadaulidae based on asymmetrical male genitalia (Regier et al. 2015). However, details of the morphology, including wing venation, mouth parts, and female genitalia, have not been examined (Robinson and Nielsen 1993; Regier et al. 2015).

The genus *Dryadaula* currently has 50 described species (Yang and Li 2021; Lee et al. 2023) and has a pan-global distribution. Fourteen species occur in the Palearctic, 16 in the Neotropics, one in the Nearctic, two in the Afrotropics, four in Indomalaya, 12 in Australia, and two in Oceania, while *Dryadaula pactorlia* Meyrick, 1901, has been recorded in New Zealand and Europe (Yang and Li 2021; Lee et al. 2023). Only two species of *Dryadaula* species are described from Japan: *D. epischista* (Meyrick, 1936) and *D. trapezoides* (Meyrick, 1935) (Sakai 2013).

Dryadaula epischista was described by Meyrick (1936) as *Thermocrates epischista* based on a single male specimen obtained in “Japan, Kyûsyû, Mozi

(=Moji ward)”. Later, Robinson (1988) transferred it to the genus *Dryadaula* based on its genital morphology. The abdomen of the holotype was missing, but Robinson (1988) described the male genitalia of a specimen collected from Hong Kong as *D. epischista*. Before Zagulajev (1970), most species in this genus were described based only on external features. However, several species that are difficult to distinguish using external morphology were discovered recently, for example, *Dryadaula auriformis* Yang & Li, 2021, *D. flavostriata* Yang & Li, 2021, *D. hirtiglobosa* Yang & Li, 2021, and *D. securiformis* Yang & Li, 2021. These facts suggest that the species diversity of this genus is underestimated, and that Hong Kong specimens identified as *D. epischista* by Robinson (1988), based on their appearance, were doubtfully conspecific to the holotype specimen from Moji, Fukuoka, Japan.

We conducted field surveys at the type locality to determine the true genital morphology of *D. epischista*. We successfully obtained specimens of *D. epischista* from the type locality and compared their morphology and DNA with those of specimens from other Japanese localities with similar appearances. In the course of the study, we observed that “*D. epischista*” from Hong Kong in Robinson (1988) is not representative of true *D. epischista* and discovered another unknown species from Japan. In this study, we describe a new species, *D. orientalis* Park & Yagi, sp. nov. and provide a redescription of *D. epischista* (Meyrick, 1936) with illustrations of adults and genitalia.

Materials and methods

Sampling and dissection

Specimens were collected by sweeping nets during the day and using an LED UV lamp (LTMW20S-BL, Iida shomei) at night (light trap: LT) and a Malaise trap. The material newly collected in this study is deposited in the Entomological Laboratory, Kyushu University (ELKU). We examined specimens deposited at the following universities and museums:

NHMUK	The Natural History Museum, Department of Zoology, Cromwell Road, London SW7 5BD, United Kingdom;
OMU	Environmental Entomology and Zoology, Osaka Metropolitan University (formerly Osaka Prefecture University, OPU), Sakai, Osaka, Japan;
ELKU	Entomological Laboratory, Kyushu University, Fukuoka, Japan.

Images of adults were obtained using a SONY α7R IV digital camera (SONY, Tokyo, Japan) fitted with a CANON MP-E 65 mm macro lens (CANON, Tokyo, Japan). To examine male and female genitalia, the abdomens of specimens were removed and boiled in a 10% KOH solution for approximately 10 min. After washing with 70% ethanol, the genitalia were dissected in 70% ethanol and stained with a Chlorazol Black E solution. After dehydration by soaking in different concentrations of ethanol, from 70% to 99% for at least one hour, the genitalia were mounted in Euparal on glass slides. The specimens were dissected and observed under a Nikon stereomicroscope (SMZ-U). Images of genitalia were obtained using an EOS Kiss X5 digital camera connected to a Leica S8APO stereomicroscope and a Canon EOS 90D digital camera connected to a Nikon ECLIPSE Ci-L stereomicroscope. Photographs were processed using Adobe Photoshop 2022 and Adobe Photoshop 2023 processing software.

The terminology of genital morphology follows Robinson (1988).

DNA extraction, PCR amplification, and sequencing

DNA analysis was performed to clarify male/female correspondence and genetic divergence in the partial mitochondrial cytochrome *c* oxidase subunit I (COI) region (DNA barcode region).

Adult specimens of *D. epischista* and *D. orientalis* sp. nov. were used for the extraction of DNA using a DNeasy Blood and Tissue Kit (Qiagen, the Netherlands). DNA was extracted from the abdomens of the moths using a kit protocol. To obtain the partial COI gene, the sequences were amplified using the primers LCO1490 (GGTCAACAAATCATAAAGATATTGG) and HCO2198 (TAAACTTCAGGGTGACCAAAAAATCA) (Folmer et al. 1994). The composition of the PCR reaction mixture used was as follows: 5 μL of KOD One® PCR Master Mix -Blue- (TOYOBO, Japan), 0.3 μL (10 pmol/μL) of each of the forward and reverse primers, and 1.0 μL of template DNA, with Milli-Q water added to a final volume of 10 μL. PCR amplification was performed using the following program: an initial denaturation at 98 °C for 10 s, followed by 35 cycles at 98 °C for 10 s, 50 °C for 5 s, and 68 °C for 5 s. The amplified products were purified using ExoSAP-IT™ Express (Thermo Fisher Scientific Inc., USA), and sequencing was conducted using the pre-mixed option at Sanger Sequencing Services (Azenta, USA). The alignment and deletion of ambiguous sites resulted in a COI of 658 bp.

Phylogenetic analyses were conducted using MEGA v.11.0.13 (Tamura et al. 2021). For constructing maximum likelihood (ML) trees and maximum parsimony (MP) trees for the partial COI mitochondrial genes, five *Dryadaula* species and two additional outgroup species [*Infurcitinea captans* (Meessidae) and *Doleromorpha porphyria* (Tineidae)] were downloaded from the Bold Systems (Ratnasingham and Hebert 2007) and GenBank (Sayers et al. 2021). In summary, 17 OTUs, including specimens of *D. epischista* (two specimens) and *D. orientalis* sp. nov. (eight specimens), were analyzed using the General Time Reversible model. Branch support was calculated using 1000 bootstrap replicates. The uncorrected pairwise distances (p-distances) were calculated using *Dryadaula* species to construct the phylogenetic tree.

Results

In the phylogenetic analysis, eight specimens of *D. orientalis* sp. nov. formed a sister group to two specimens of *D. epischista* (Meyrick, 1936) with high support (ML 99%, MP 100%; Fig. 1). The two Japanese species formed a single clade with *D. heindeli* Gaedike & Scholz, 1998 from Germany and *D. terpsichorella* (Busck, 1910) from the United States (bootstrap support = 91 in the ML analysis).

The results of pairwise distances (Table 2) indicated that interspecific distances between *D. epischista* (*N* = 2) and *D. orientalis* (*N* = 8) ranged from 1.52 to 1.83%, and intraspecific distances ranged from 0.15% in *D. epischista*, and 0.00 to 0.30% in *D. orientalis* sp. nov.

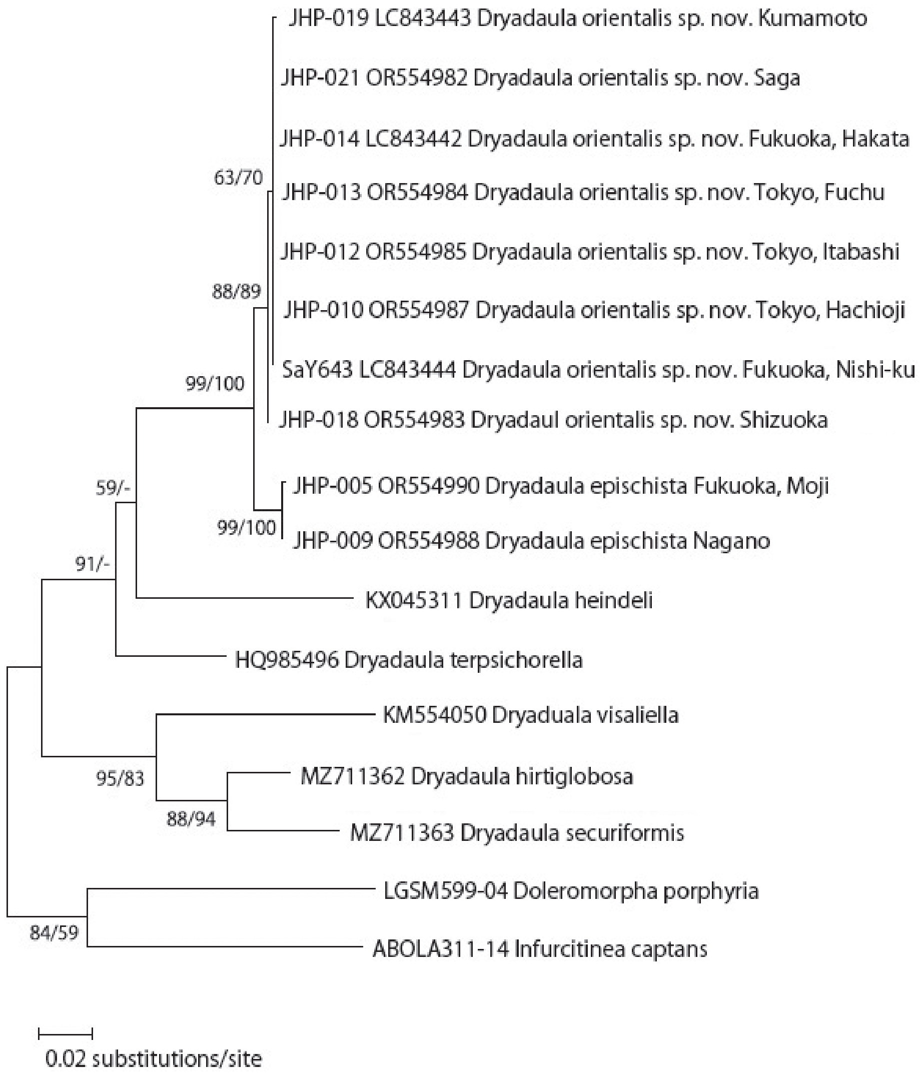

Figure 1. Maximum likelihood (ML) tree of *Dryadaula* constructed by MEGA 11 based on the partial COI region. The number near the node is the bootstrap value (ML/MP). Nodes annotated by "–" indicate a mismatch in the topology between the ML and MP methods.

Taxonomic accounts

Dryadaula epischista **(Meyrick, 1936)**
Figs 2, 3, 12, 16, 18–29, 45–48

Thermocrates epischista Meyrick, 1936: 621.
Thermocrates epischista: Moriuti 1982, 1: 170, 2: pl. 233-2.
Dryadaula epischista: Robinson 1988: 70 (nec Meyrick 1936).
Dryadaula koreana Roh & Byun, 2020: Roh et al. 2020: 221. syn. nov.

Type material. ***Holotype*****:** JAPAN: • 1♂ (Fig. 2); Mozi [=Moji], Japan; 2. VII. 1934; S. Issiki leg.; *THERMOCRATES* Meyr.; *epischista* Meyr.; *Thermocrates epischista* 1/1 Meyr. E. Meyrick det. in Meyrick Coll.; abdomen missing; NHMUK 014045892; NHMUK.

Other material. JAPAN: [Fukuoka] • 3♂; Kitakyushu, Moji, Mt. Tonoue-yama (33°54'00.2"N, 130°57'02.4"E); 153 m; LT (light trap); 22. VII. 2022; J.-H. Park

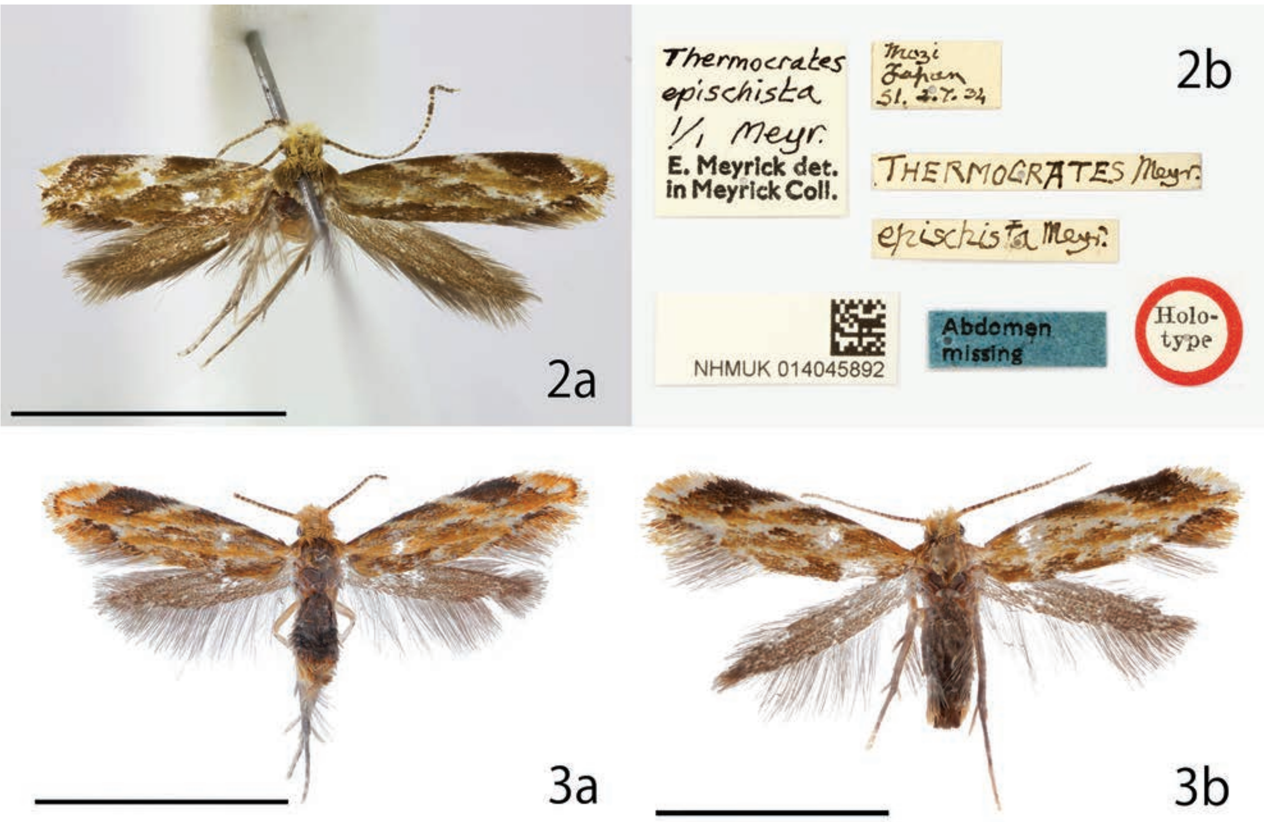

Figures 2, 3. *Dryadaula epischista* (Meyrick, 1936), adults **2a** holotype, male **2b** labels of holotype **3** Fukuoka, Moji, J.-H. Park leg. **3a** male, Museum ID ELKU-I-L-000043 **3b** female, ELKU-I-L-000044. Scale bars: 3 mm.

leg. • 1♂ (Fig. 3a); same data; genitalia slide No. JP-025; DNA sample JHP-005; Museum ID ELKU-I-L-000043 • 1♂; same data; genitalia slide No. JP-044 • 1♂; same data; genitalia slide No. JP-023 • 4♂1♀; same locality; LT; 6. VIII. 2022; J.-H. Park leg. • 1♀ (Fig. 3b); same data; genitalia slide No. JP-051; DNA sample JHP-006; Museum ID ELKU-I-L-000044 • 1♂; same data; Museum ID ELKU-I-L-000042 • [Nagano] 5♂; Matsumoto, Arigase, Joyama Park (33°14'44.7"N, 137°57'15.2"E); LT; 5. IX. 2022; J.-H. Park leg. • 1♂; same data; DNA sample JHP-009; Museum ID ELKU-I-L-000045.

Diagnosis. This species has an orange ground color on the forewing with a brown and white pattern and can be easily distinguished from other congeners by these characteristics. For the differences between *D. orientalis* sp. nov., which has a very similar color and forewing pattern, see Diagnosis of the latter species.

Redescription. Male (Figs 2a, 3a): Forewing length 2.9 mm in holotype, 2.7–3.0 mm (*N* = 18); antenna length 1.6–2.1 mm (*N* = 9). Head small. Vertex and frons covered with yellowish-orange hair. Labial palpus spatulate, covered with cream yellow bristles; a few dark brown bristles arising laterally along second palpomere; third palpomere spatulate. Antenna filiform; scape and pedicel simple short columnar, flagellum dorsally covered with yellow scales, outer surface of flagellomere striped with blackish-brown and yellow, from the center to the tip, the blackish-brown parts fuse together to form four strips. Prothorax, mesothorax, and tegula covered with yellow and light-brown scales. Forewing costal and posterior margin straight, and gently curved toward apex. Forewing ground color orange, with brown and white pattern. Costa brown with three white lines at 1/4, 1/2 and apical part; the white line located at 1/2 of the costa connects to the tornal margin but is interrupted at center. Dorsum brown. Tornal area outer margin with brown line. Cilia orange, white basally; brown at tornus. Hind wing narrow trapezoidal, grayish brown. Abdomen covered with dark brown scales.

Male genitalia. (Figs 12, 18–29, 45–48) Asymmetrical (Fig. 12). Uncus elongated and weakly curved to tip, and weakly twisted at subapically. Tegumen twisted to the left and slightly wider in the center, fused with vinculum. Vinculum narrowly arched; saccus equipped with obtuse triangle lobe at middle (Figs 18, 19). Gnathos absent. Right and left valva clearly asymmetrical (Figs 20–23, 29). Right valva flat; basal half with broad triangular lobe; apical half densely covered with relatively long setae; basally with small setose rod-shaped projection (Figs 20, 21). Left valva thick, but slenderer than right valva, tip paddle-like shaped, with lobate process and three spines: spines at the base short; spines on the left side of the center twice as long as spines at the base; spines on the right side of the center about the same length as spines on the left side, but they curve ventrally in the middle, in some cases, a single spine protrudes from the curved part; lobate process near apical part bearing spinose setae on dorsal surface (Figs 22, 23, 29). Sternite VIII hollow and curved claw- shaped; apical spine long and slender; ventral margin with two projections: central projection protruding trapezoidal, basal projection slender, longer than central projection (Figs 24, 25). Juxta rounded triangle and connected to left valva and phallus (Figs 12, 26). Phallus asymmetrical elliptical with two thick and sharp spines apically; rounded projection attached to juxta; cornuti absent (Figs 27, 28). Intersegmental membrane between seventh and eight tergite with a pair of free sclerites laterally; right free sclerite broad U-shaped, sometimes wider (Figs 45, 46); left free sclerite V-shaped (Figs 47, 48).

Female (Fig. 3b): Forewing length 2.8–3.2 mm (*N* = 3). Almost all same as male, but white spot of subapical part of costal margin narrowed and connected to white line of costal margin in female.

***Female genitalia*.** (Fig. 16) Sternite VIII covered with bristles, strongly sclerotized, right side markedly swollen posterolateral; terminal swelling weakly sclerotized and does not reach the ventral edge; ostium bursae opening the posterior end of swelling. Right side of "seventh segment" with ball-shaped bulge. Right side of "sixth segment" with posteriorly protruded bulge. Median dent deeply concave between right side of sixth and seventh segments. Papillae analis slender and short, 1.1× length of the apophyses posterioris. Apophysis posterioris relatively short, half the length of the eighth abdominal segment. Ductus bursae and corpus bursae membranous. Ductus bursae thin tubular, 5× as long as apophysis posterioris. Corpus bursae elliptical, densely wrinkled throughout (Fig. 16a).

Distribution. Japan (Honshu, Kyushu), Korea.

Biology. Unknown. Adults are observed from July to September.

DNA barcode. Three DNA barcodes from two males and one female were generated and deposited in the International Nucleotide Sequence Database (INSD) and BOLD Systems (accession number/process ID): OR554990/JHP001-23, OR554989/JHP002-23, and OR554988/JHP003-23 (Table 1).

Remarks. Moriuti figured the "female" adult as the second specimen of this species; this specimen lacks the abdomen and the hindwings (Robinson 1988: 71). The specimen is not currently in OMU collection, missing.

The morphology of this species differs from that of the Hong Kong specimen identified as *D. epischista* by Robinson (1988) in the following characteristics: the left valva has three spines; the phallus has two apical spines; sternite VIII

Table 1. Names and collection localities for taxa used in the phylogenetic analyses.

Species	Country	Site	Accession No. (sequence ID)	Sample ID
Dryadaula epischista	Japan	Fukuoka, Moji	OR554990	JHP-005
D. epischista	Japan	Nagano, Matsumoto	OR554988	JHP-009
D. orientalis sp. nov.	Japan	Tokyo, Itabashi	OR554985	JHP-012
D. orientalis sp. nov.	Japan	Tokyo, Fuchu	OR554984	JHP-013
D. orientalis sp. nov.	Japan	Tokyo, Hachioji	OR554987	JHP-010
D. orientalis sp. nov.	Japan	Shizuoka	OR554983	JHP-018
D. orientalis sp. nov.	Japan	Fukuoka, Hakata	LC843442	JHP-014
D. orientalis sp. nov.	Japan	Fukuoka, Nishi-ku	LC843444	SaY643
D. orientalis sp. nov.	Japan	Saga, Arita	OR554982	JHP-021
D. orientalis sp. nov.	Japan	Kumamoto, Matsubase	LC843443	JHP-019
D. heindeli	Germany	Bavaria	KX045311	BC ZSM Lep 53186
D. hirtiglobosa	China	Zhejiang	MZ711362	DNAYLL18170
D. securiformis	China	Hainan	MZ711363	DNAYLL18122
D. terpsichorella	United States	Florida	HQ985496	BIOUG<CAN>: 10BBLEP -01124
D. visaliella	Canada	Ontario	KM554050	BIOUG03835-H04
Doleromorpha porphyria	United States	Tennessee	(LGSM599-04)	DNA-ATBI-0599
Infurcitinea captans	Austria	Tyrol	(ABOLA311-14)	TLMF Lep 15333

Table 2. Genetic distances of the partial cytochrome *c* oxidase subunit I (COI) gene sequences of the two *Dryadaula* species. Genetic distances (%) were calculated with the p-distances model using MEGA 11.

	1	2	3	4	5	6	7	8	9	10
1. *Dryadaula orientalis* sp. nov. JHP-010/OR554987/Tokyo, Hachioji										
2. *Dryadaula orientalis* sp. nov. JHP-012/ OR554985/Tokyo, Itabashi	0.00									
3. *Dryadaula orientalis* sp. nov. JHP-013/OR554984/Tokyo, Fuchu	0.00	0.00								
4. *Dryadaula orientalis* sp. nov. JHP-014/LC843442/Fukuoka, Hakata	0.00	0.00	0.00							
6. *Dryadaula orientalis* sp. nov. SaY643/LC843444/Fukuoka, Nishi-ku	0.00	0.00	0.00	0.00						
5. *Dryadaula orientalis* sp. nov. JHP-021/OR554982/Saga	0.00	0.00	0.00	0.00	0.00					
7. *Dryadaula orientalis* sp. nov. JHP-018/OR554983/Shizuoka	0.15	0.15	0.15	0.15	0.15	0.15				
8. *Dryadaula orientalis* sp. nov. JHP-019/LC843443/Kumamoto	0.15	0.15	0.15	0.15	0.15	0.15	0.30			
9. *Dryadaula epischista* JHP-005/OR554990/Fukuoka, Moji	1.82	1.82	1.82	1.82	1.82	1.83	1.67	1.67		
10. *Dryadaula epischista* JHP-009/OR554988/Nagano	1.67	1.67	1.67	1.67	1.67	1.68	1.52	1.52	0.15	

has longer elongated projections; and the basal half of the right valva is broadly triangular. However, we observed that *D. koreana* Roh & Byun, 2020 was identical to *D. epischista* based on its appearance and male genitalia. Therefore, here we synonymize *D. koreana* with *D. epischista*. We observed some variation in the apical spines protruding midway on the left valva occur in a few individuals within the same location.

Dryadaula orientalis Park & Yagi, sp. nov.

https://zoobank.org/18075FB2-38B0-41A3-8DC0-7A7CA03F50B0
Figs 4–11, 13–15, 17, 30–44, 49, 50

Dryadaula epischista: Sakai 2013: 129, fig. 3-12-13 (nec Meyrick 1936) [examined]; Jinbo et al. 2014: fig. 8 (nec Meyrick 1936).

Type material. ***Holotype*:** Japan: • 1♂ (Fig. 4); Tokyo, Itabashi, Akatsuka Park (35°47'05.4"N, 139°38'35.9"E); 26–27. VIII. 2022; J.-H. Park leg.; genitalia slide No. JP-028; DNA sample JHP-012; Museum ID ELKU-I-L-000048; deposited in ELKU. Materials were preserved in ELKU and OMU. ***Paratypes*:** Japan: [Tokyo] • 1♂ (Fig. 5); Tokyo, Fuchu, Sengenyama Park (35°40'48.3"N, 139°30'01.5"E), 28. VIII. 2022; J.-H. Park leg.; genitalia slide No. JP-024; DNA sample JHP-013; Museum ID ELKU-I-L-000049 • 1♂1♀; Tokyo, Hachioji, Hatsuzawa, Mt. Hatsuzawa-yama; 1–2. X. 2022; J.-H. Park & T. Hirowatari leg.; (ELKU) • 1♀ (Fig. 9); same data; Museum ID ELKU-I-L-000041 • 1♂; same data; genitalia slide No. JP-047; DNA sample JHP-037; Museum ID ELKU-I-L-000052 • 1♀; same data; genitalia slide No. JP-039; DNA sample JHP-011; Museum ID ELKU-I-L-000047 • 1♂(Fig. 6); same data; DNA sample JHP-010; Museum ID ELKU-I-L-000046 • [Shizuoka] 1♂; Shizuoka, Kamo, Shimoda, Toji; 10. IX. 2022; LT; S. Yagi leg.; genitalia slide No. JP-035; DNA sample JHP-018; Museum ID ELKU-I-L-000050 • [Kyoto] 1♀; Kyoto, Higashiyama-ku, Seikanji, Yamanouchi-cho; 21. VI. 2014; H. SHIMIZU leg.; genitalia slide No. SK978; Museum ID OPU-IN-LE 2018XII0195; (OMU) • [Osaka] 1♀; Higashiosaka, Rokumanji-cho; 14. IX. 2014; H. SHIMIZU leg.; genitalia slide No. SK969; Museum ID OPU-IN-LE 2018XII0196; (OMU) • 1♀; Yao-shi, Kodachi Jusan Toge, Fumin no mori; 26. VIII. 2016; H. SHIMIZU leg.; genitalia slide No. SK979; Museum ID OPU-IN-LE 2018XII0197; (OMU) • 1♂; Hiraoka; 16. VI. 1995; S. KOSINO (leg.); Museum ID OPU-IN-LE 2018XII0193; (OMU) • 1♂; same data; genitalia slide No. SK968; Museum ID OPU-IN-LE 2018XII0194; (OMU) • [Ehime] 1♂ (Fig. 7); Matsuyama, Marunouchi, Matsuyama castle; 30. VIII. 2016; J. Oku leg.; genitalia slide No. JP-026; DNA sample JHP-022; Museum ID ELKU-I-L-000130 • [Fukuoka] 1♂; Fukuoka, Motooka, Kyushu Univ. (33.597N 130.214E); alt. 48 m; 4–18. IX. 2019; Malaise trap; Ent. Lab. Kyushu Univ. leg.; Museum ID ELKU-I-L-000040 • 1♂; Fukuoka, Hakata, Higashi-hirao Park; 19. VIII. 2022; LT; J.-H. Park leg.; genitalia slide No. JP-030; DNA sample JHP-014; Museum ID ELKU-I-L-000053 • 1♀ (Fig. 10); Fukuoka, Nishi-ku, Kuwabara, Kyushu Univ.; 1. VIII. 2020; S. Yagi leg.; genitalia slide No. JP-032; DNA sample SaY643; Museum ID ELKU-I-L-000054 • 1♂; same locality; 1. VIII. 2020; S. Yagi leg.; genitalia slide No. JP-027; DNA sample JHP-007; (ELKU) • [Saga] 1♂ (Fig. 8); Matsuura-gun, Arita-cho, Hiroseyama; 29. V. 2021; Yu Hisasue leg.; genitalia slide No. JP-029; DNA sample JHP-021; Museum ID ELKU-I-L-000051 • [Kumamoto] 1♀ (Fig. 11); Matsubase, Natl. Agricultural Res. Center; 6.VII.2022; K. Goto leg.; DNA sample JHP-019; Museum ID ELKU-I-L-000055.

Other materials. [Fukuoka] • 1♂1♀; Fukuoka, Motooka, Kyushu Univ. (33.597°N, 130.214°E); alt. 48 m; 22. VIII–4. IX. 2019; Malaise trap; Ent. Lab. Kyushu Univ. leg; (ELKU) • 23♂26♀; Fukuoka, Motooka, Kyushu Univ. (33.597°N, 130.214°E); alt. 48 m; 4–18. IX. 2019; Malaise trap; Ent. Lab. Kyushu Univ. leg.; (ELKU) •1♂; same data; genitalia slide No. JP-042; (ELKU) • 1♀; same data; genitalia slide No. JP-034; (ELKU) • 1♀; (Fukuoka Pref.,) same locality (33.597°N, 130.214°E); alt. 48 m; 18. IX–2. X. 2019; Malaise trap; Ent. Lab. Kyushu Univ.

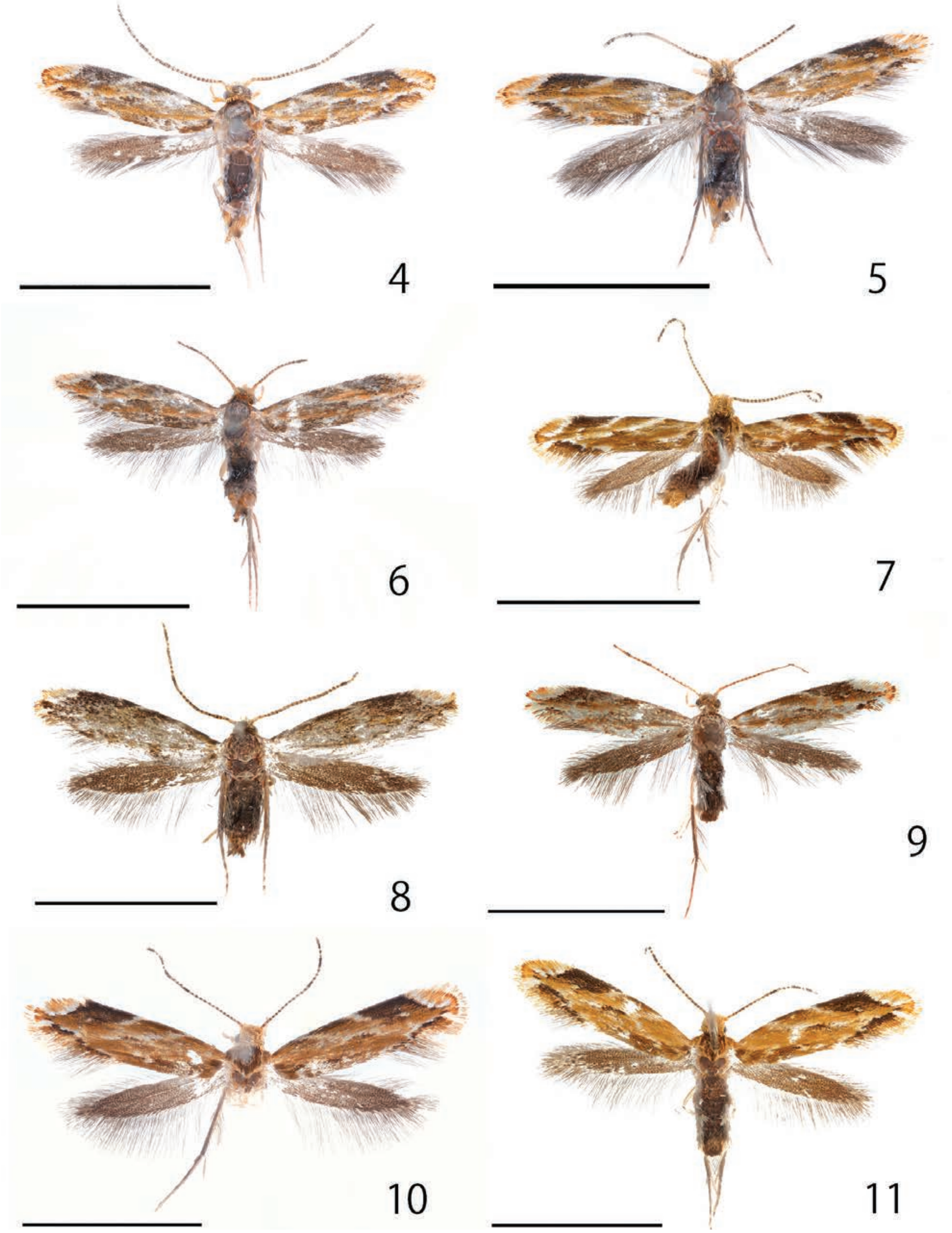

Figures 4–11. *Dryadaula orientalis* sp. nov., adults **4** holotype, male, Tokyo, Itabashi, J.-H. Park leg., Museum ID ELKU-I-L-000048 **5–8** paratypes, male **5** Tokyo, Fuchu, J.-H. Park leg., ELKU-I-L-000049 **6** Tokyo, Hachioji, T. Hirowatari & J.-H. Park leg., ELKU-I-L-000046 **7** Ehime, J. Oku leg., ELKU-I-L-000130 **8** Saga, Yu Hisasue leg., ELKU-I-L-000051 **9–11** paratype, female **9** Tokyo, Hachioji, T. Hirowatari & J.-H. Park leg., ELKU-I-L-000041 **10** Fukuoka, Nishi-ku, S. Yagi leg., ELKU-I-L-000054 **11** Kumamoto, K. Goto leg., ELKU-I-L-000055. Scale bars: 3 mm.

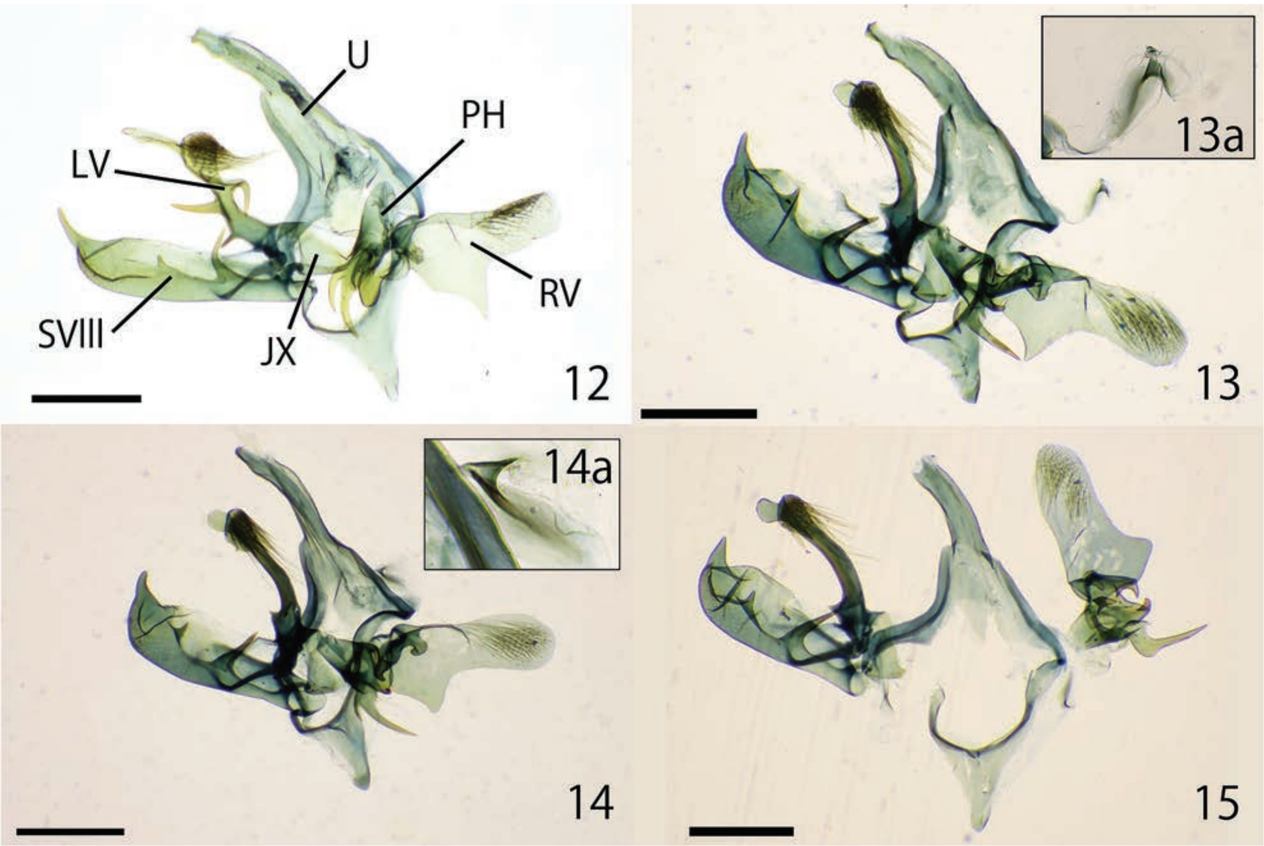

Figures 12–15. Overview of male genitalia **12** *Dryadaula epischista* (Meyrick, 1936), Fukuoka, Moji, J.-H. Park leg., genitalia slide No. JP-044; SVIII = sternite VIII; U = uncus; PH = phallus; JX = juxta; LV = left valva; RV = right valva **13–15** *Dryadaula orientalis* sp. nov. **13** holotype, Tokyo, Itabashi, J.-H. Park leg., genitalia slide No. JP-028 **13a** right free sclerite **14** paratype, Tokyo, Koganei, J.-H. Park leg., JP-024 **14a** right free sclerite **15** paratype, Fukuoka, Hakata, J.-H. Park leg., JP-030. Scale bars: 0.3 mm.

leg.; (ELKU) • 1♀; (Fukuoka Pref.,) same locality (33.597°N, 130.214°E); alt. 48 m; 16–30. X. 2019; Malaise trap; Ent. Lab. Kyushu Univ. leg.; (ELKU).

Diagnosis. The color of the general habitus is very similar to *D. epischista*, but the new species can be distinguished by the following characteristics of the male and female genitalia: in the male genitalia, spines in the left valva are absent (present in *D. epischista*); in the female genitalia, a larger lateral abdominal swelling reaches the end of the abdomen in the eighth segment (smaller and not reaching the end of the abdomen in *D. epischista*).

Description. Male (Figs 4–8): Forewing length 3.0 mm, antenna length 2.4 mm in holotype, Forewing length 2.7–3.7 mm (*N* = 11); antenna length 1.9–2.6 mm in paratypes (*N* = 9). Similar to *D. epischista* except forewing ground color varies from bright orange to dull brown.

Male genitalia (Figs 13–15, 30–44, 49, 50) Asymmetrical (Figs 13–15). Uncus elongated and weakly curved to tip, and weakly twisted at middle. Tegumen twisted to the left and slightly wider in the center, fused with vinculum. Vinculum narrowly arched; saccus equipped with an obtuse triangle lobe at middle (Figs 30, 31). Gnathos absent. Right and left valva clearly asymmetrical (Figs 32–35). Right valva flat; basal half with broad triangular lobe, protrusions varied from sharp to rounded; apical half densely covered with relatively long setae; basally with small setose curved rod-shaped projection. (Figs 32, 33). Left valva thick, but slenderer than right valva, tip paddle-like shaped, with

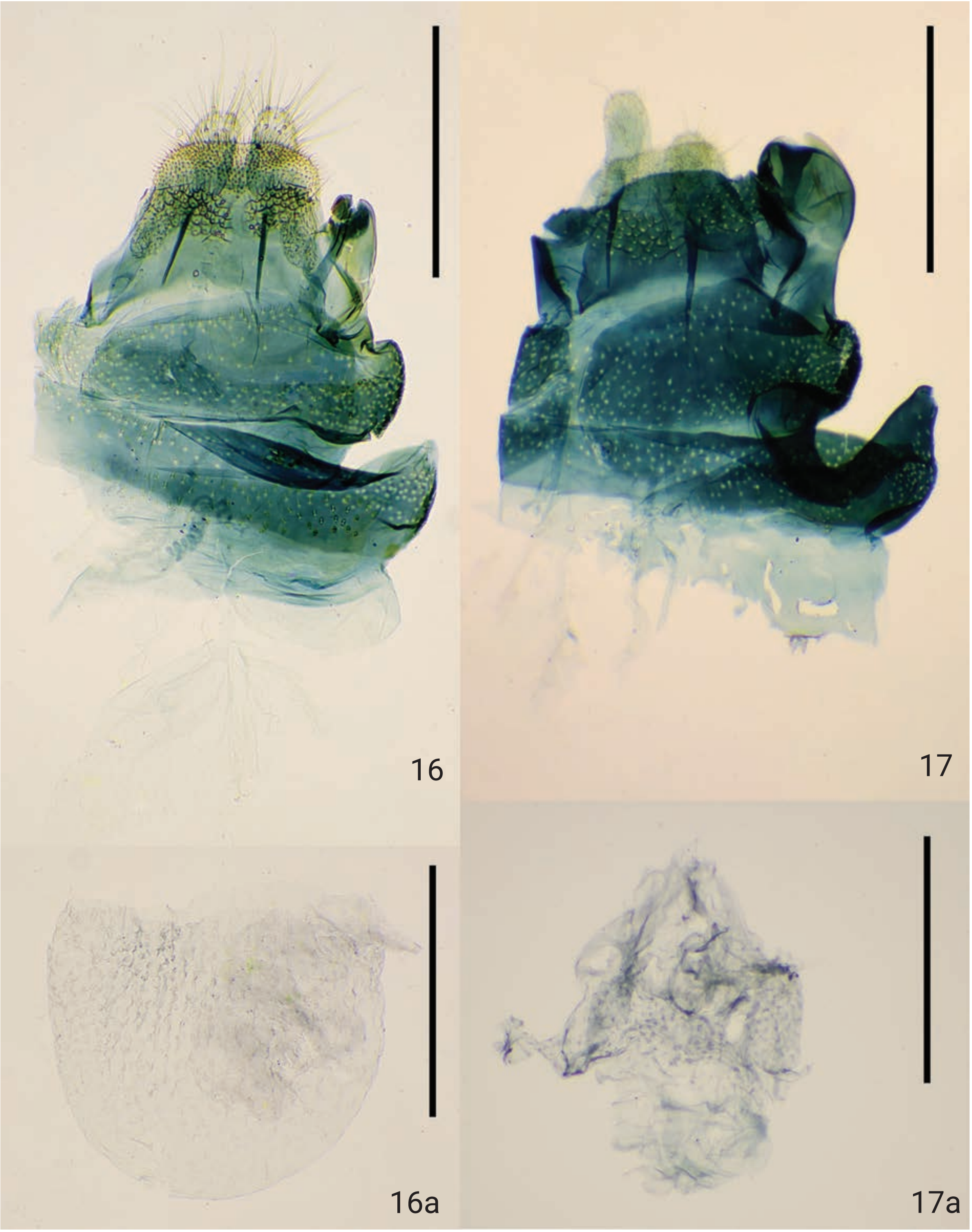

Figures 16, 17. Overview of female genitalia, ventral view **16** *Dryadaula epischista* (Meyrick, 1936), Fukuoka, Moji, J.-H. Park leg., genitalia slide No. JP-051 **16a** corpus bursae **17** *Dryadaula orientalis* sp. nov., paratype, Tokyo, Hachioji, T. Hirowatari & J.-H. Park leg., JP-050 **17a** corpus bursae. Scale bars: 0.3 mm.

lobate process; lobate process near apical part bearing spinose setae on dorsal surface (Figs 34, 35). Sternite VIII hollow and curved claw-like shaped; apical spine short and thick; ventral margin with two slender projections, basal projection longer than central projection (Figs 36, 37). Juxta rounded triangle and connected to left valva and phallus (Figs 13–15, 38). Phallus asymmet-

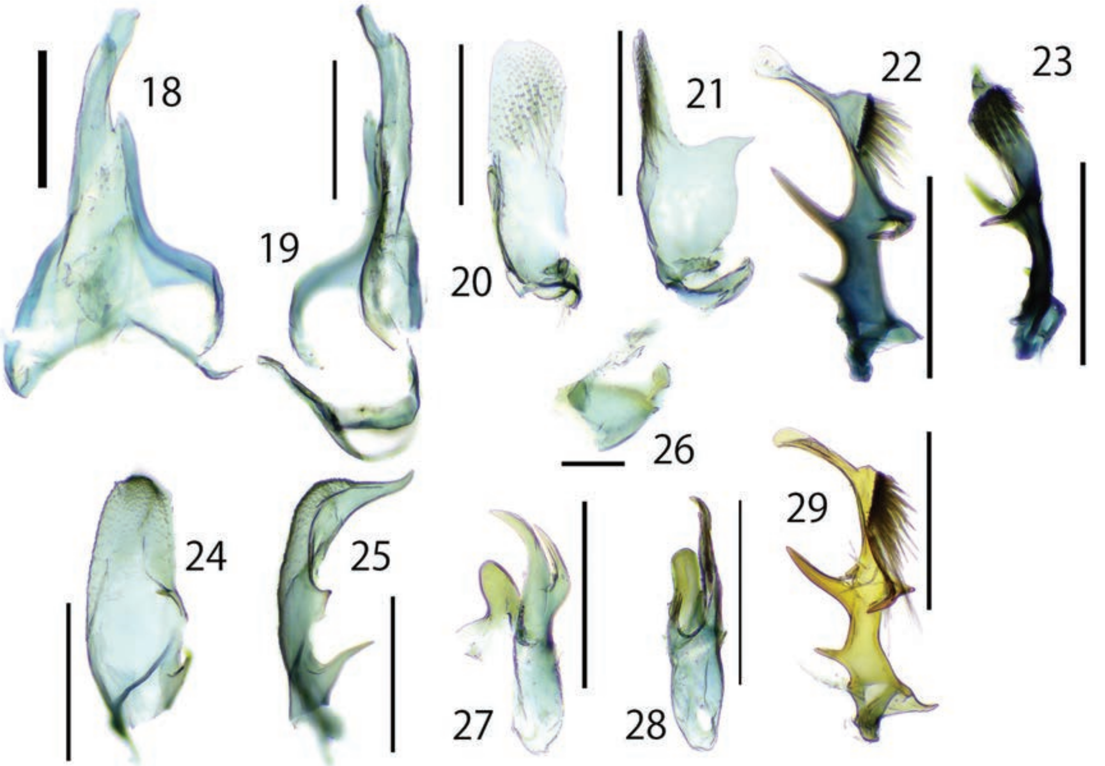

Figures 18–29. Details of the male genitalia of *Dryadaula epischista* (Meyrick, 1936) **18**–**28** Fukuoka, Moji, J.-H. Park leg., genitalia slide No. JP-023 **18, 19** uncus, tegmen, vinculum **18** dorsal view **19** lateral view **20, 21** right valva **20** internal view **21** lateral view **22, 23** left valva **22** lateral view **23** dorsal view **24, 25** VIII sternites **24** lateral view **25** dorsal view **26** juxtae, dorsal view **27, 28** phallus **27** dorsal view **28** lateral view **29** left valva lateral view, Nagano, Matsumoto, J.-H. Park leg., Museum ID ELKU-I-L-000131. Scale bars: 0.3 mm (**18–25, 27–29**); 0.1 mm (**26**).

rical elliptical with a curved, thick, and sharp spine apically; and with basal side of projection with or without a straight or curved thin projection; rounded projection attached to juxta; cornuti absent (Figs 39–44). Intersegmental membrane between seventh and eight tergite with a pair of free sclerites laterally; right free sclerite broad U-shaped (Figs 13a, 14a, 49); left free sclerite V-shaped (Fig. 50).

Female (Figs 9–11): Forewing length 3.0–3.6 mm in paratypes (*N* = 7), Antenna length 2.2–2.3 mm in paratypes (*N* = 4). Almost all same as male, but white spot of subapical part of costal margin narrowed and connected to white line of costal margin in female.

Female genitalia. (Fig. 17) Sternite VIII covered with bristles, strongly sclerotized, right side markedly swollen posterolateral; terminal swelling passing the ventral edge; ostium bursae opening the posterior end of swelling. Right side of "seventh segment" slightly bulged. Right side of "sixth segment" with posteriorly protruded bulge. Median dent spherically and strongly concaves between right side of sixth and seventh segments. Papillae analis slender and short, same length as the apophyses posterioris. Apophysis posterioris relatively short, slightly longer than eighth abdominal segment. Ductus bursae and corpus bursae membranous. Ductus bursae thin tubular, 4× as long as apophysis posterioris. Corpus bursae elliptical, densely wrinkled from ductus bursae side to the end (Fig. 17a).

Distribution. Japan (Honshu, Shikoku, Kyushu).

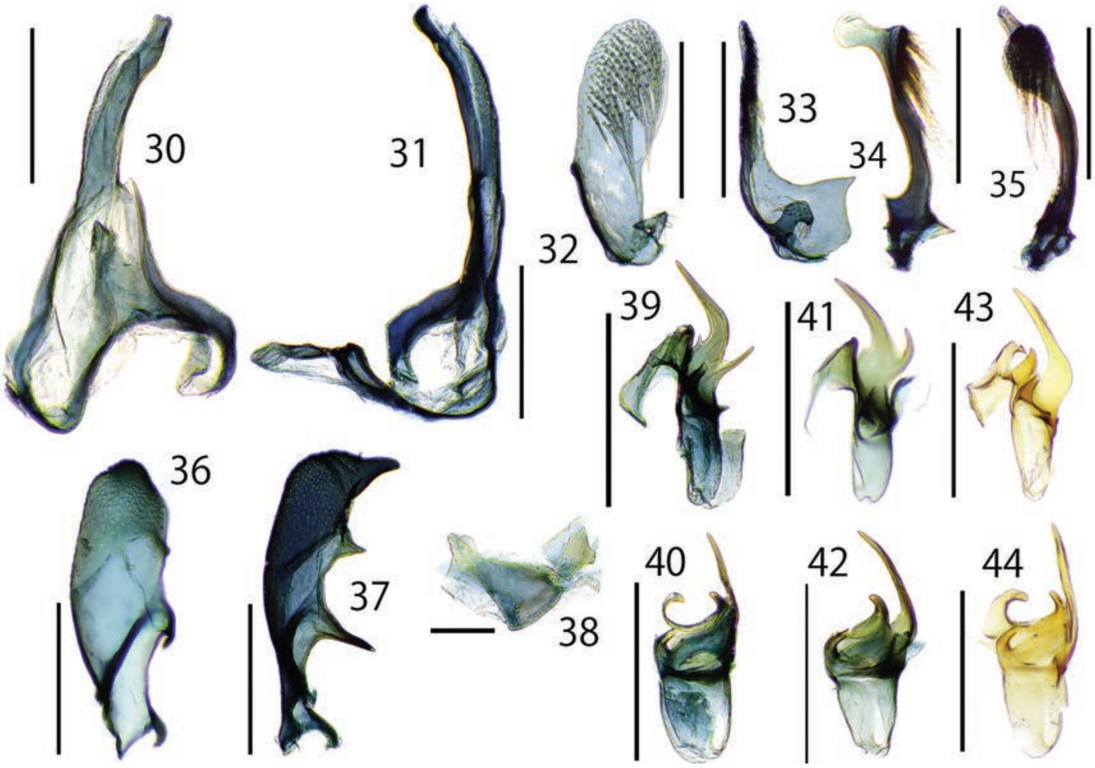

Figures 30–44. Details of male genitalia of *Dryadaula orientalis* sp. nov. **30–40** Tokyo, Hachioji, T. Hirowatari & J.-H. Park leg., Museum ID ELKU-I-L-000046 **30, 31** uncus, tegmen, vinculum **30** dorsal view **31** lateral view **32, 33** right valva **32** internal view **33** lateral view **34, 35** left valva **34** lateral view **35** dorsal view **36, 37** sternite VIII **36** lateral view **37** dorsal view **38** juxta, dorsal view **39, 40** phallus **39** dorsal view **40** lateral view **41, 42** phallus, Fukuoka, Nishi-ku, Ent. Lab. Kyushu Univ. leg., ELKU-I-L-000040 **41** dorsal view **42** lateral view **43, 44** Osaka, Hiraoka, S. Kosino leg., Museum ID OPU-IN-LE 2018XII0194 **43** dorsal view **44** lateral view. Scale bars: 0.3 mm (**30–37, 39–44**); 0.1 mm (**38**).

Biology. The adults were observed between May and September. Adult females laid flat eggs on the dead leaves of monocotyledonous plants (*Sasa* sp.) during plastic rearing.

Etymology. The new species name is derived from the Latin ‘Orient’ (east) because the distribution of this species is restricted to eastern Asia.

DNA barcode. Seven DNA barcodes from seven males and three females were generated and deposited in INSD and BOLD Systems (accession number/process ID (or sample ID)): OR554987/JHP004-23 (for holotype), OR55486/JHP005-23, OR554985/JHP006-23, OR554984/JHP007-23, OR554983/JHP008-23, OR554982/JHP009-23, OR554981/JHP010-23, LC843442/(JHP-014), LC843443/(JHP-019), LC843444/(SaY643) (for paratypes) (Table 1).

Remarks. The phallus, right valva, and body color of this species exhibit marked geographical variation. Morphological variation was continuous, and there was little or no genetic distance between the specimens.

Many specimens of this species were collected in Malaise traps set at the forest margins in the forest of Kyushu University (26♂, 30♀).

Discussion

The maximum likelihood tree suggested that *D. epischista* and *D. orientalis* sp. nov. were nested in a clade including *D. heindeli* and *D. terpsichorella*, but the former two species treated in this study differed in many characteristics,

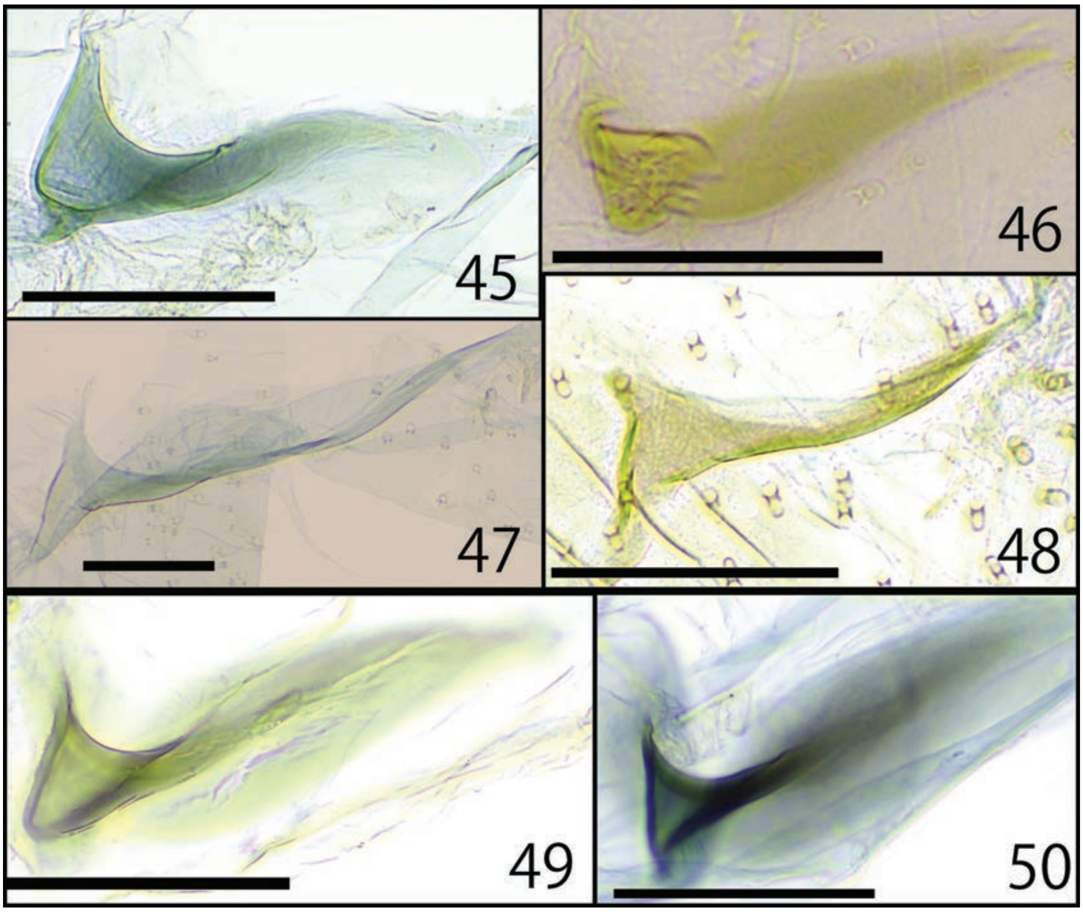

Figures 45–50. Free sclerites **45–48** *D. epischista* (Meyrick, 1936) **45, 47** Fukuoka, Moji, J.-H. Park leg., genitalia slide No. JP-025 **45** right free sclerite **47** left free sclerite **46, 48** Nagano, Matsumoto, J.-H. Park leg., Museum ID ELKU-I-L-000045 **46** right free sclerite **48** left free sclerite **49, 50** *D. orientalis* sp. nov. **49** right free sclerite, Fukuoka, Nishi-ku, Ent. Lab. Kyushu Univ. leg., JP-042 **50** left free sclerite, Tokyo, Hachioji, T. Hirowatari & J.-H. Park leg., ELKU-I-L-000046 Scale bars: 0.05 mm.

including narrow trapezoidal wings, flat right valva, and curved, twisted, and elongated uncus, whereas most species in this genus have broad trapezoidal hind wings. The South American species of this genus, *D. metrodoxa* (Meyrick 1919) and *D. amentata* (Meyrick, 1919), have narrow trapezoidal wings (Clarke, 1970: pl. 34, figs 1, 2), but DNA analysis has not been conducted, and additional research is needed to discuss their phylogenetic relationships in this genus.

Robinson (1988) considered the free sclerites to be the abdominal seventh and/or eighth tergites. Free sclerites are a character only observed in *D. epischista* (Meyrick, 1936), *D. orientalis* sp. nov., and "*D. epischista*" from Hong Kong in Robinson (1988). The other external morphologies, including the genital characteristics of these species, are similar, and these species may be grouped together in future studies.

The results of this study indicate that the two closely related species are widely distributed in the southern part of Honshu and Kyushu but were never collected from the same locality (the closest point is approximately 50 km away in a straight line). The distribution of the two different species in geographically contiguous areas suggests that other factors, including host differences and interspecific competition, rather than geographic isolation, may influence the distribution of each species.

Acknowledgments

The authors express their gratitude to Dr D.C. Lees (NHMUK) for capturing a photograph of the holotype of *Thermocrates epischista*. We would like to express our cordial thanks to Drs N. Hirai and S. Ueda (OMU) for permitting us to examine the OMU collection and to Drs J. Oku, Y. Hisasue, Mr S. Tomura, and K. Goto (ELKU) for providing us with adult samples. The first author thanks the members of ELKU for their technical guidance and valuable advice in preparing this paper.

Additional information

Conflict of interest

The authors have declared that no competing interests exist.

Ethical statement

No ethical statement was reported.

Funding

This research was supported by the JSPS KAKENHI Grant Number 23K26929 (Grant-in-Aid for Scientific Research B) to TH and SY.

Author contributions

All authors have contributed equally.

Author ORCIDs

Jinhyeong Park https://orcid.org/0009-0005-3121-9990
Sadahisa Yagi https://orcid.org/0000-0002-4261-1219
Shigeki Kobayashi https://orcid.org/0000-0002-1336-4730
Toshiya Hirowatari https://orcid.org/0000-0002-6839-2229

Data availability

All of the data that support the findings of this study are available in the main text.

References

Busck A (1910) New Central-American Microlepidoptera introduced into the Hawaiian Islands. Proceedings of the Entomological Society of Washington 12: 132–135. https://biostor.org/reference/65281

Clarke JFG (1970) Catalogue of the type specimens of Microlepidoptera in the British Museum (Natural History) described by Edward Meyrick. The Trustees of the British Museum (Natural History), London 8: 1–261. https://www.biodiversitylibrary.org/item/137718#page/7/mode/1up

Folmer O, Black M, Hoeh W, Lutz R, Vrijenhoek R (1994) DNA primers for amplification of mitochondrial cytochrome c oxidase subunit I from diverse metazoan invertebrates. Molecular Marine Biology and Biotechnology 3: 294–299.

Gaedike R, Scholz A (1998) *Dryadaula heindeli* sp. n. aus Bayern (Lepidoptera, Tineidae). Nachrichtenblatt der bayerischen Entomologen 47(3/4): 106–114. https://biostor.org/reference/116788

Jinbo S, Arita Y, Nakajima H, Kishida Y, Yago M, Owada M (2014) Moths of Gardens in the Imperial Palace, Tokyo (2009–2013). Memoirs of the National Museum of Nature and Science 50: 129–237.

Lee GE, Hoare RJB, Yang LL (2023) A new species of *Dryadaula* (Tineoidea, Dryadaulidae) with a discussion of male genital structures and *Eudarcia dentata* (Tineoidea, Meessiidae) new to Korea. Journal of Asia-Pacific Entomology 23: 1–13. https://doi.org/10.1016/j.aspen.2023.102124

Meyrick E (1919) Exotic Microlepidoptera 2(9): 225–288. https://www.biodiversitylibrary.org/item/37719#page/263/mode/1up

Meyrick E (1936) Exotic Microlepidoptera 4: 621. https://www.biodiversitylibrary.org/item/286856#page/627/mode/1up

Moriuti S (1982) Tineidae. In: Inoue H, Sugi S, Kuroko H, Moriuti S, Kawabe A, Owada M (Eds) Moths of Japan. Kodansha, Tokyo, 162–171. [in Japanese]

Ratnasingham S, Hebert PD (2007) BOLD: The Barcode of Life Data System (http://www.barcodinglife.org). Molecular ecology notes 7(3): 355–364. https://doi.org/10.1111/j.1471-8286.2007.01678.x

Regier JC, Mitter C, Davis DR, Harrison TL, Sohn JC, Cummings MP, Zwick A, Mitter KT (2015) A molecular phylogeny and revised classification for the oldest ditrysian moth lineages (Lepidoptera: Tineoidea), with implications for ancestral feeding habits of the mega-diverse Ditrysia. Systematic Entomology 40(2): 409–432. https://doi.org/10.1111/syen.12110

Robinson GS (1988) The systematic position of *Thermocrates epischista* Meyrick (Lepidoptera: Tineidae) and the biology of the Dryadaulinae. Nota Lepidopterologica 11(1): 70–79. http://biostor.org/reference/116935

Robinson GS, Nielsen ES (1993) Tineid genera of Australia (Lepidoptera). Monographs on Australian Lepidoptera 2. CSIRO Publishing, Melbourne, 344 pp. https://doi.org/10.1071/9780643105102

Roh SJ, Shin YM, Lee DJ, Byun BK (2020) The first record of Dryadaulidae (Lepidoptera, Tineoidea) from Korea with the description of a new species, *Dryadaula koreana* sp. nov. Nota Lepidopterologica 43: 221–22. https://doi.org/10.3897/nl.43.51564

Sakai M (2013) Tineidae. In: Hirowatari T, Nasu Y, Sakamaki Y, Kishida Y (Eds) The Standard of Moths in Japan III: Zygaenidae, Sesiidae, Limacodidae. Gakken Educational Publishing, Tokyo, 118–135. [In Japanese]

Sayers EW, Cavanaugh M, Clark K, Pruitt KD, Schoch CL, Sherry ST, Karsch-Mizrachi I (2021) GenBank. Nucleic Acids Research 49: 92–96. https://doi.org/10.1093/nar/gkaa1023

Tamura K, Stecher G, Kumar S (2021) MEGA 11: Molecular Evolutionary Genetics Analysis Version 11. Molecular Biology and Evolution 38(7): 3022–3027. https://doi.org/10.1093/molbev/msab120.

Yang LL, Li HH (2021) The genus *Dryadaula* Meyrick (Lepidoptera, Tineoidea, Dryadaulidae) in China, with descriptions of four new species and a world checklist. Zookeys 1074: 61–81. https://doi.org/10.3897/zookeys.1074.73067

Zagulajev AK (1970) Two new primitive species of lichenophagous moths (Lepidoptera, Tineidae) from the damp forests of Azerbaidzhan. Entomologicheskoe Obozrenie 49(3): 657–663. [In Russian]

ZooKeys 1217: 343–351 (2024)
DOI: 10.3897/zookeys.1217.134940

Research Article

Clarifying the phylogenetic placement of Eupoinae Maddison, 2015 (Araneae, Salticidae) with ultra-conserved element data

Junxia Zhang[1,2], Yi Ni[1,2], Kiran Marathe[3,4], Yaozhuo Wang[1,2], Wayne P. Maddison[5]

1 *Key Laboratory of Zoological Systematics and Application, College of Life Sciences, Hebei University, Baoding, Hebei 071002, China*
2 *Hebei Basic Science Center for Biotic Interaction, Hebei University, Baoding, Hebei 071002, China*
3 *Department of Zoology and Beaty Biodiversity Museum, University of British Columbia, 6270 University Boulevard, Vancouver, British Columbia, V6T 1Z4, Canada*
4 *National Centre for Biological Sciences, Tata Institute of Fundamental Research, GKVK 11 Campus, Bengaluru, 560065, India*
5 *Departments of Zoology and Botany and Beaty Biodiversity Museum, University of British Columbia, 6270 University Boulevard, Vancouver, British Columbia, V6T 1Z4, Canada*
Corresponding author: Junxia Zhang (jxzhang1976@163.com)

Abstract

The subfamily Eupoinae Maddison, 2015 is an enigmatic group of minute leaf-litter-dwelling jumping spiders from Southeast Asia. Although previous molecular phylogenetic studies have suggested that it is one of the basal (non-salticine) lineages within jumping spiders, its exact placement remains unclear. In this study, ultra-conserved element data were collected from major salticid lineages to investigate the phylogenetic relationships of all salticid subfamilies, with a special focus on the placement of Eupoinae. The results provide a well-supported phylogeny for jumping spider subfamilies, and suggest a sister relationship of Eupoinae with Spartaeinae Wanless, 1984, a basal lineage of jumping spiders with relatively high species diversity and morphological and behavioural diversity. With the placement of Eupoinae, we have resolved the relationships of all salticid subfamilies, supplying a robust framework for evolutionary studies of jumping spiders.

Key words: Basal lineages, Eupoines, jumping spiders, phylogenomics, UCE

Academic editor: Shuqiang Li
Received: 17 August 2024
Accepted: 11 October 2024
Published: 12 November 2024

ZooBank: https://zoobank.org/C376ECBC-A3FB-4835-8373-628FD04CFD4B

Citation: Zhang J, Ni Y, Marathe K, Wang Y, Maddison WP (2024) Clarifying the phylogenetic placement of Eupoinae Maddison, 2015 (Araneae, Salticidae) with ultra-conserved element data. ZooKeys 1217: 343–351. https://doi.org/10.3897/zookeys.1217.134940

Introduction

Salticidae Blackwall, 1841 (jumping spiders) comprises seven subfamilies: Asemoneinae Maddison, 2015, Eupoinae Maddison, 2015, Hisponinae Simon 1901, Lyssomaninae Blackwall, 1841, Onomastinae Maddison, 2015, Spartaeinae Wanless, 1984, and Salticinae Blackwall, 1841 (Maddison 2015). Among them, the subfamily Eupoinae Maddison, 2015 was erected to include an enigmatic group of leaf-litter dwelling jumping spiders known from southern China, Vietnam, Thailand, Malaysia, Laos, and India (Maddison 2015; Fig. 1). Currently 43 species of four genera (*Corusca* Zhou & Li, 2013, *Eupoa* Żabka, 1985, *Megaeupoa* Lin & Li, 2020, and *Sinoinsula* Zhou & Li, 2013) have been described in this subfamily (World Spider Catalog 2024). They are mostly minute spiders, with body size ranging from 1.5 to 5.6 mm, but they possess highly complex genitalic structures, especially the male palps (Żabka 1985; Zhou and Li 2013; Lin and Li 2020).

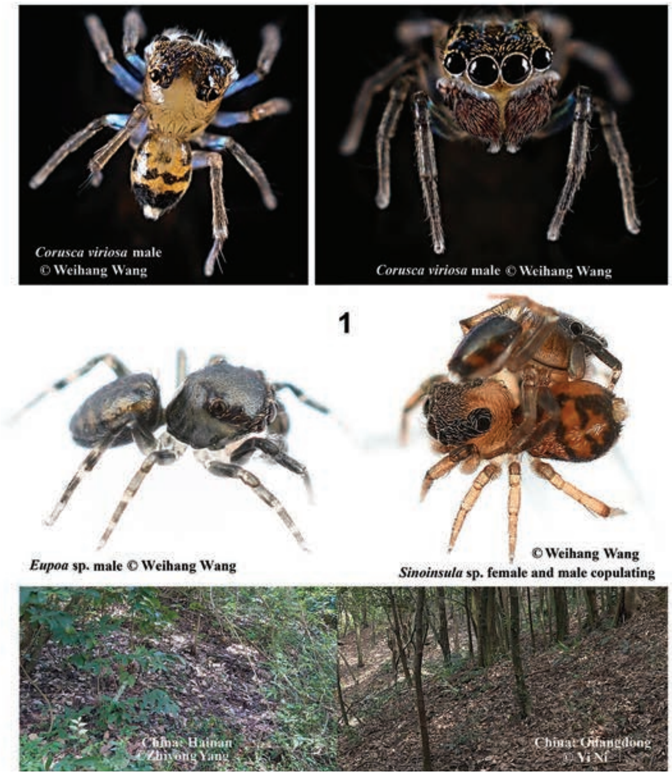

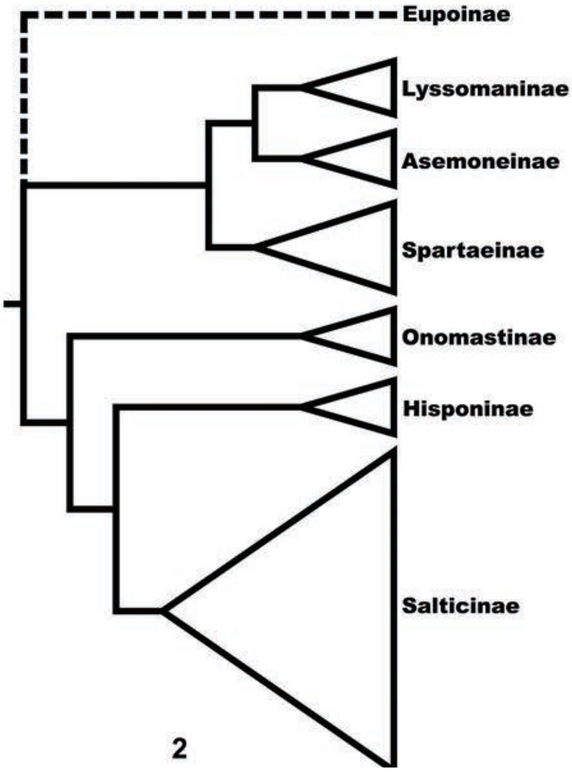

Figures 1, 2. Eupoinae and summary phylogeny of Salticidae **1** photos of living spiders of eupoines and microhabitats **2** summary phylogeny of salticid subfamilies (modified from Maddison et al. 2017).

So far, the phylogenetic relationships of all salticid subfamilies except Eupoinae have been clarified (Maddison et al. 2014, 2017; Fig. 2). Even though previous studies of morphology and molecular phylogeny have suggested that Eupoinae belongs to the basal (non-salticine) lineages of jumping spiders, its placement was unstable in analyses with only a few genes, and thus its exact position on the phylogeny remained uncertain (Maddison et al. 2007, 2014; Maddison 2015). Here we investigate the phylogenetic placement of Eupoinae using ultra-conserved element (UCE) data to fulfill the subfamily-level phylogeny of jumping spiders.

Materials and methods

All specimens are preserved in 85–100% ethanol and stored at −20 °C in the Museum of Hebei University, Baoding, China (MHBU) and the Spencer Entomological Collection at the Beaty Biodiversity Museum, University of British Columbia, Vancouver, Canada (UBCZ). The ultra-conserved elements (UCEs) were obtained for 70 taxa that include 68 salticids covering all seven subfamilies and two outgroups (one each of Cheiracanthiidae and Philodromidae). Among them, data were newly collected for 57 taxa in this study, while data for an additional 13 taxa were obtained from previous publications (Zhang et al. 2023; Lin et al. 2024; Yu et al. 2024; Marathe et al. 2024a, 2024b; see Suppl. material 1: table S1 for detailed information). Genomic DNA was extracted using the QIAGEN DNeasy Blood & Tissue Kit. The library preparation was performed with the NEXTFLEX Rapid DNA-Seq Kit 2.0 and the NEXTFLEX Unique Dual Index

Barcodes (Set C) (Bioo Scientific) following the protocols described in Zhang et al. (2023). UCE enrichment followed the myBaits protocol 5.01 (Daicel Arbor Biosciences) using a modified version of the RTA probes, the "RTA_v3" probe set (42,213 probes targeting 3818 UCE loci; Zhang et al. 2023). The enriched UCE libraries were then sequenced using the Illumina NovaSeq platform with 150-bp paired-end reads. The UCE loci were extracted from the empirically enriched and sequenced raw reads following the protocols applied in Zhang et al. (2023) with the PHYLUCE (Faircloth 2016) workflow. For seven species with whole genome sequencing data, the genomes were first assembled using the Phylogenomics from Low-coverage Whole-genome Sequencing (PLWS) pipeline (Zhang et al. 2019), and then the UCEs were harvested using the "RTA_v3" probes and the PHYLUCE workflow (see Zhang et al. 2023 for details).

The UCEs extracted from genomes and target enrichment data were combined and organized by locus, and then aligned using Mafft v. 7.313 (Katoh and Standley 2013) with the L-INS-I strategy. Poorly aligned regions were initially trimmed by the heuristic method "-automated1" in trimAl v. 1.4.1 (Capella-Gutiérrez et al. 2009). We then applied Spruceup v. 2020.2.19 (Borowiec 2019) to convert the remaining obviously misaligned fragments to gaps in each alignment (cutoff as 0.7). The gappy regions in each alignment were later masked using Seqtools (PASTA; Mirarab et al. 2014) with "masksites = 35". An individual gene tree was constructed for each alignment using RAxML v. 8.2.12 (Stamatakis 2014) with the GTRGAMMA model. Gene trees were then inspected using TreeShrink v. 1.3.1 (Mai and Mirarab 2018) to detect and remove sequences that resulted in abnormally long branches on the gene tree. Loci with a length less than 150 bp or less than 50% of taxon occupancy were removed, which resulted in 2685 loci in the final dataset for phylogenetic inference. All remaining UCE loci were concatenated by FASconCAT v. 1.0 (Kück and Meusemann 2010). The maximum-likelihood (ML) analyses were conducted in IQ-TREE v. 2.0.6 (Minh et al. 2020) with the best-fitting model and optimized partition scheme inferred using the option "-m MF+MERGE". Twenty independent ML tree searches (ten with random starting trees and ten with parsimonious starting trees) were run with the optimized model and partition scheme, and 5000 replicates of ultrafast bootstrap analysis were conducted to assess the node supports. The coalescent-based species-tree method to account for potential gene tree heterogeneity and discordance was also applied. First, the ML tree and 1000 ultrafast bootstrap replicates were inferred in IQ-TREE v. 2.0.6 for each of the remaining UCE loci using the best-fitting model selected by ModelFinder (Kalyaanamoorthy et al. 2017). For each gene tree, the branches with bootstrap ≤ 50% were collapsed by Newick Utils v. 1.6 (Junier and Zdobnov 2010). The Accurate Species Tree Algorithm (ASTRAL-III v. 5.7.1; Zhang et al. 2018) was then applied to estimate the species tree with 100 replicates of bootstrapping to assess the node support.

Data resources

The sequenced raw reads were submitted to the GenBank with accession numbers provided in Suppl. material 1: table S1. The alignments of UCE loci, the final concatenated UCE dataset, and the resulting phylogenetic trees are deposited in the Dryad Data Repository at https://doi.org/10.5061/dryad.z08kprrph.

Results

The final concatenated dataset of 2685 UCE loci contained 1,109,833 bp and 354,024 parsimony-informative sites. The ML tree is presented in Fig. 3, and the ASTRAL tree is shown in Suppl. material 2: fig. S1. Both results are congruent in the relationships of the salticid subfamilies and strongly support the sister relationship of Eupoinae with Spartaeinae (Fig. 3, Suppl. material 2: fig. S1). Most nodes on the phylogenies gain full support (bootstrap = 100%), with only a few exceptions among the relatively shallower relationships, such as the node with *Salticus scenicus* (Clerck, 1757), *Evarcha proszynskii* Marusik & Logunov, 1998, and *Bianor maculatus* (Keyserling, 1883) (ML bootstrap = 99%, ASTRAL bootstrap = 92%; Fig. 3, Suppl. material 2: fig. S1). The ML and species trees only show minor differences in the relationships of species within *Brettus* Thorell, 1895 and *Onomastus* Simon, 1900 (Fig. 3, Suppl. material 2: fig. S1).

Discussion

Since the establishment of the genus *Eupoa* by Żabka (1985), resolving its phylogenetic position has been particularly intriguing due to the unusual male palpal structures observed in this group. Based on two morphological characteristics, the presence of a median apophysis in the male palp and of a tarsal claw in the female palp, *Eupoa* was suggested to be excluded from the clade Salticinae, which contains the bulk of jumping spider diversity (Maddison et al. 2007). Sequences of nuclear and mitochondrial genes (28S, 18S, *wingless*, 16S–ND1, CO1) were obtained for *Eupoa nezha* Maddison & Zhang, 2007 to investigate its position on the jumping spider phylogeny (Maddison et al. 2007, 2014). Analyses of these gene regions tended to place *Eupoa* among basal (non-Salticinae) salticids, but they failed to find a clear placement (Maddison et al. 2007, 2014), with *Eupoa* usually outside Salticinae, but occasionally attaching to the long-branched agorines among Salticinae. This may reflect an unusual compositional bias in eupoines (Maddison et al. 2014), or perhaps simply that the limited number of markers that could not resolve the recalcitrant phylogenetic relationships resulting from the rapid radiation of jumping spiders. Later, the genome-wide sequence data were applied to clarify jumping spider phylogeny using the anchored hybrid enrichment (AHE) method. However, no eupoine was included due to a lack of material (Maddison et al. 2017). In this study, seven species from three genera (*Corusca*, *Eupoa*, and *Sinoinsula*) of Eupoinae, along with other major lineages of Salticidae (Suppl. material 1: table S1, Fig. 3), were sampled in the UCE-based phylogenomic analyses. The UCE phylogeny (Fig. 3) recovered the same relationships for the six salticid subfamilies as the AHE result (Maddison et al. 2017; Fig. 2). Unlike previous implications that eupoines may represent a deep-branching lineage long separate from lyssomanines, spartaeines, and other basal groups (Maddison et al. 2007), the UCE phylogenomic results strongly support a sister relationship of Eupoinae with Spartaeinae, which show considerable diversity in morphology and behavior (Wanless 1984; Su et al. 2007).

Although this study did not aim to solve the phylogeny within Eupoinae, the UCE results strongly support a relationship of (*Eupoa* (*Corusca*, *Sinoinsula*)) (Fig. 3, Suppl. material 2: fig. S1). Due to the lack of material, the genus

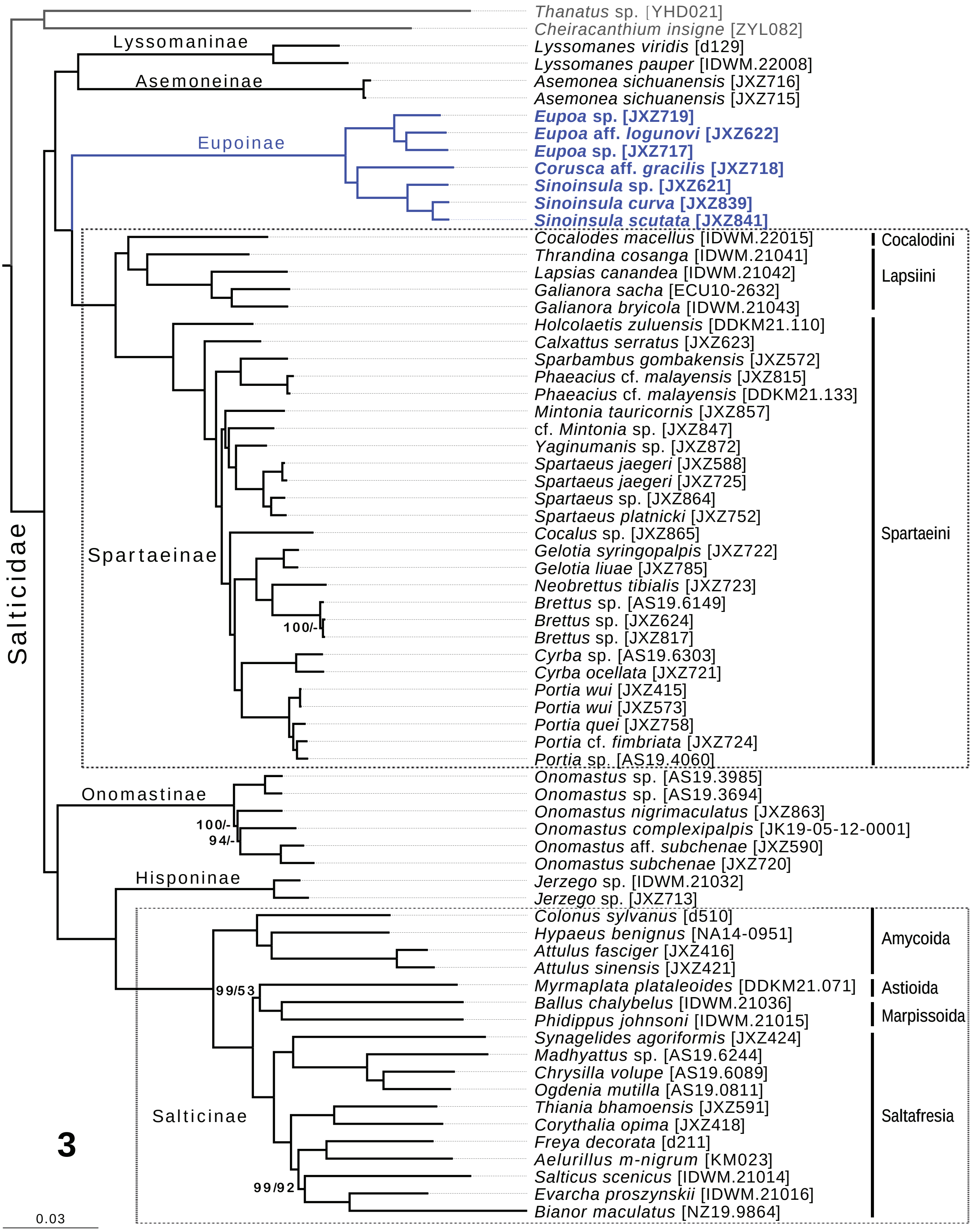

Figure 3. Phylogenetic results. Tree shown is the maximum-likelihood tree from the UCE dataset; numbers along the branches indicate bootstrap support values from the ML (before "/") and ASTRAL (after "/") analyses, only numbers lower than 100% are shown; "-" indicates this node is not recovered in the ASTRAL analysis.

Megaeupoa was not sampled in the UCE phylogenomic analyses. Species of *Megaeupoa* also have perplexing male palpal structures like other eupoines, but show significant differences in the somatic characteristics, such as their rather large body size (almost twice as large as species of the other three genera), the presence of a fovea (absent in the other three genera), and the absence of typical eupoine markings (paired paled-colored spots on the abdomen) (Żabka 1985; Maddison et al. 2007; Zhou and Li 2013; Maddison 2015; Lin and Li 2020). Therefore, whether the *Megaeupoa* indeed belongs to Eupoinae or represents an independent lineage in the basal salticids requires further investigation.

It is worth mentioning that although the known species diversity of Eupoinae has dramatically increased in the past decade (Zhou and Li 2013; Logunov and Marusik 2014; Lin and Li 2020; Ying et al. 2021; Wang and Li 2022; Wang et al. 2023; Logunov 2024), we expect that many more species remain to be discovered. Future thorough comparative morphological studies, especially on the genitalic organs, will help to pinpoint the synapomorphies for the clade containing Eupoinae and Spartaeinae, as well as different lineages within Eupoinae.

Acknowledgements

We thank Weihang Wang and Zhiyong Yang for providing photographs of eupoines and microhabitat, the Hebei Basic Science Center for Biotic Interaction, and the National Animal Collection Resource Center of China for support. We also thank the three reviewers, Dr Tamás Szűts, Cheng Wang, and Dmitri V. Logunov, and the subject editor, Dr Shuqiang Li for their valuable comments that helped to improve the manuscript.

Additional information

Conflict of interest

The authors have declared that no competing interests exist.

Ethical statement

No ethical statement was reported.

Funding

This work was funded by the National Natural Science Foundation of China (grant no. 32070422), and the Natural Science Foundation of Hebei Province (grant no. C2024201017) to Junxia Zhang.

Author contributions

Conceptualization: JZ, WP. Data acquirement: JZ, YW, KM. Formal analysis: JZ. Resources: JZ, WP, KM. Visualization: YN. Writing – original draft: JZ, YN. Writing – review and editing: JZ, WP, KM.

Author ORCIDs

Junxia Zhang https://orcid.org/0000-0003-2179-3954
Yi Ni https://orcid.org/0009-0003-3239-3697

Kiran Marathe https://orcid.org/0000-0002-7364-3475
Yaozhuo Wang https://orcid.org/0009-0007-3252-1838
Wayne P. Maddison https://orcid.org/0000-0003-4953-4575

Data availability

All of the data that support the findings of this study are available in the main text or Supplementary Information.

References

Borowiec ML (2019) Spruceup: Fast and flexible identification, visualization, and removal of outliers from large multiple sequence alignments. Journal of Open Source Software 4(42): 1635. https://doi.org/10.21105/joss.01635

Capella-Gutiérrez S, Silla-Martínez JM, Gabaldón T (2009) trimAl: A tool for automated alignment trimming in large-scale phylogenetic analyses. Bioinformatics (Oxford, England) 25(15): 1972–1973. https://doi.org/10.1093/bioinformatics/btp348

Faircloth BC (2016) PHYLUCE is a software package for the analysis of conserved genomic loci. Bioinformatics (Oxford, England) 32(5): 786–788. https://doi.org/10.1093/bioinformatics/btv646

Junier T, Zdobnov EM (2010) The Newick utilities: Highthroughput phylogenetic tree processing in the UNIX shell. Bioinformatics 26(13): 1669–1670. https://doi.org/10.1093/bioinformatics/btq243

Kalyaanamoorthy S, Minh BQ, Wong TKF, von Haeseler A, Jermiin LS (2017) ModelFinder: Fast model selection for accurate phylogenetic estimates. Nature Methods 14(6): 587–591. https://doi.org/10.1038/nmeth.4285

Katoh K, Standley DM (2013) MAFFT multiple sequence alignment software version 7: Improvements in performance and usability. Molecular Biology and Evolution 30(4): 772–780. https://doi.org/10.1093/molbev/mst010

Kück P, Meusemann K (2010) FASconCAT: Convenient handling of data matrices. Molecular Phylogenetics and Evolution 56(3): 1115–1118. https://doi.org/10.1016/j.ympev.2010.04.024

Lin Y, Li S (2020) Two new genera and eight new species of jumping spiders (Araneae, Salticidae) from Xishuangbanna, Yunnan, China. ZooKeys 952: 95–128. https://doi.org/10.3897/zookeys.952.51849

Lin L, Yang Z, Zhang J (2024) Revalidation of the jumping spider genus *Cheliceroides* Żabka, 1985 based on molecular and morphological data (Araneae, Salticidae). ZooKeys 1196: 243–253. https://doi.org/10.3897/zookeys.1196.117921

Logunov DV (2024) Jumping spiders (Araneae: Salticidae) of the Bidoup–Nui Ba National Park, Lam Dong Province, Vietnam. Arachnology 19(8): 1074–1099. https://doi.org/10.13156/arac.2024.19.8.1074

Logunov DV, Marusik YM (2014) Taxonomic notes on the genus *Eupoa* Żabka, 1985 (Arachnida, Araneae, Salticidae). ZooKeys 410: 63–93. https://doi.org/10.3897/zookeys.410.7548

Maddison WP (2015) A phylogenetic classification of jumping spiders (Araneae: Salticidae). The Journal of Arachnology 43(3): 231–292. https://doi.org/10.1636/arac-43-03-231-292

Maddison WP, Zhang JX, Bodner MR (2007) A basal phylogenetic placement for the salticid spider *Eupoa*, with descriptions of two new species (Araneae: Salticidae). Zootaxa 1432(1): 22–33. https://doi.org/10.11646/zootaxa.1432.1.2

Maddison WP, Li D, Bodner M, Zhang J, Xu X, Liu Q, Liu F (2014) The deep phylogeny of jumping spiders (Araneae, Salticidae). ZooKeys 440: 57–87. https://doi.org/10.3897/zookeys.440.7891

Maddison WP, Evans SC, Hamilton CA, Bond JE, Lemmon AR, Lemmon EM (2017) A genome-wide phylogeny of jumping spiders (Araneae, Salticidae), using anchored hybrid enrichment. ZooKeys 695: 89–101. https://doi.org/10.3897/zookeys.695.13852

Mai U, Mirarab S (2018) TreeShrink: Fast and Accurate Detection of Outlier Long Branches in Collections of Phylogenetic Trees.” BMC Genomics 19 (S5): 272. https://doi.org/10.1186/s12864-018-4620-2

Marathe K, Maddison WP, Kunte K (2024a) *Ghatippus paschima*, a new species and genus of plexippine jumping spider from the Western Ghats of India (Salticidae, Plexippini, Plexippina). ZooKeys 1191: 89–103. https://doi.org/10.3897/zookeys.1191.114117

Marathe K, Tripathi R, Sudhikumar AV, Maddison WP (2024b) Phylogenomic placement and revision of *Iranattus* Prószyński, 1992 jumping spiders (Salticidae, Plexippini, Plexippina). Zoosystematics and Evolution 100(2): 531–542. https://doi.org/10.3897/zse.100.122034

Minh BQ, Schmidt HA, Chernomor O, Schrempf D, Woodhams MD, Von Haeseler A, Lanfear R (2020) IQ-TREE 2: New models and efficient methods for phylogenetic inference in the genomic era. Molecular Biology and Evolution 37(5): 1530–1534. https://doi.org/10.1093/molbev/msaa015

Mirarab S, Nguyen N, Warnow T (2014) PASTA: Ultra-large multiple sequence alignment. In: Sharan R (Ed.) Research in Computational Molecular Biology. RECOMB 2014. Lecture Notes in Computer Science. Springer, Cham, 177–191. https://doi.org/10.1007/978-3-319-05269-4_15

Stamatakis A (2014) RAxML version 8: A tool for phylogenetic analysis and post-analysis of large phylogenies. Bioinformatics 30(9): 1312–1313. https://doi.org/10.1093/bioinformatics/btu033

Su KF, Meier R, Jackson RR, Harland DP, Li D (2007) Convergent evolution of eye ultrastructure and divergent evolution of vision-mediated predatory behaviour in jumping spiders. European Society for Evolutionary Biology 20(4): 1478–1489. https://doi.org/10.1111/j.1420-9101.2007.01335.x

Wang C, Li S (2022) On eleven species of jumping spiders from Xishuangbanna, China (Araneae, Salticidae). ZooKeys 1116: 85–119. https://doi.org/10.3897/zookeys.1116.82858

Wang C, Li S, Pham DS (2023) Thirteen species of jumping spiders from northern Vietnam (Araneae, Salticidae). ZooKeys 1148: 119–165. https://doi.org/10.3897/zookeys.1148.98271

Wanless FR (1984) A review of the spider subfamily Spartaeinae nom. n. (Araneae: Salticidae) with descriptions of six new genera. Bulletin of the British Museum of Natural History (Zool.) 46: 135–205. https://doi.org/10.5962/bhl.part.15964

World Spider Catalog (2024) World Spider Catalog. Version 25.5. Natural History Museum Bern. https://doi.org/10.24436/2 [Accessed on 9 September 2024]

Ying Y, Yuan S, Sun W, Xiao Y, Liu K (2021) A new *Eupoa* Żabka, 1985 species from south China (Araneae: Salticidae). Acta Arachnologica Sinica 30(1): 41–52. https://doi.org/10.3969/j.issn.1005-9628.2021.01.007

Yu K, Zhang F, Wang Y, Maddison WP, Zhang J (2024) Robust phylogenomics settles controversies of classification and reveals evolution of male embolic complex of the Laufeia clade (Araneae, Salticidae, Euophryini). Cladistics. https://doi.org/10.1111/cla.12597

Żabka M (1985) Systematic and zoogeographic study on the family Salticidae (Araneae) from Viet-Nam. Annales Zoologici 39(11): 197–485.

Zhang C, Rabiee M, Sayyari E, Mirarab S (2018) ASTRAL-III: Polynomial time species tree reconstruction from partially resolved gene trees. BMC Bioinformatics 19(S6): 15–30. https://doi.org/10.1186/s12859-018-2129-y

Zhang F, Ding Y, Zhu CD, Zhou X, Orr MC, Scheu S, Luan YX (2019) Phylogenomics from low-coverage whole-genome sequencing. Methods in Ecology and Evolution 10(4): 507–517. https://doi.org/10.1111/2041-210X.13145

Zhang J, Li Z, Lai J, Zhang Z, Zhang F (2023) A novel probe set for the phylogenomics and evolution of RTA spiders. Cladistics 39(2): 116–128. https://doi.org/10.1111/cla.12523

Zhou Y, Li S (2013) Two new genera of jumping spiders from Hainan Island, China (Araneae, Salticidae). Zootaxa 3712(1): 1–84. https://doi.org/10.11646/zootaxa.3712.1.1

Supplementary material 1

Specimen information and summary of harvested UCE loci

Authors: Junxia Zhang, Yi Ni, Kiran Marathe, Yaozhuo Wang, Wayne P. Maddison

Data type: xlsx

Link: https://doi.org/10.3897/zookeys.1217.134940.suppl1

Supplementary material 2

Phylogenetic result from the ASTRAL analysis

Authors: Junxia Zhang, Yi Ni, Kiran Marathe, Yaozhuo Wang, Wayne P. Maddison

Data type: pdf

Explanation note: Numbers along the branches indicate bootstrap support values, only numbers lower than 100% are shown; clades with different relationships from the maximum-likelihood tree are marked in red.

Link: https://doi.org/10.3897/zookeys.1217.134940.suppl2